University of Bath

UNIVERSITY OF BATH

PHD

The design, synthesis and application of a novel electrochemical DNA gene sensor

Hillier, Stephen

Award date:
2005

Awarding institution:
University of Bath

[Link to publication](#)

UNIVERSITY OF

BATH

The Design, Synthesis and Application of a Novel

Electrochemical DNA Gene Sensor

Submitted by Stephen Hillier

for the degree of PhD

of the University of Bath

2005

COPYRIGHT

.... (signed)

......3./7./05.... (date)

UMI Number: U193583

UMI

Dissertation Publishing

ProQuest

Abstract

The detection of specific DNA gene sequences allows the diagnosis of both genetic diseases and of disease causing pathogens. Electrochemical detection offers significant advantages, including cost, simplicity and ease of miniaturisation over established sensing protocols which are based on fluorescent labelling and detection.

The electrochemical gene sensor described here uniquely utilises enzymatic digestion to generate ferrocenylated oligonucleotide fragments in a matched (gene sequence present) sensor assay. These small fragments give a characteristically high response on electrochemical analysis using Differential Pulse Voltammetry (DPV). The mismatched assay (no gene sequence present) inhibits enzymatic digestion, resulting in no fragment generation and a lower electrochemical signal. Hence, discrimination and therefore gene sensing is obtained

Three distinct studies are described. Initially novel, ferrocene based molecules were designed and synthesised. These linker molecules can be used to label the oligonucleotide gene probes, to allow electrochemical detection. Control is achieved over the electropotential of the ferrocene label, based on the structure of the linker molecule. In the next study, the oligonucleotide probes are labelled with selected linker molecules and gene sensing is developed, which ultimately uses the T7 exonuclease enzyme. The gene sensor is shown to be successful for four different synthetic gene sequences and for a PCR (Polymerase Chain Reaction) amplicon gene sequence. The simplicity of this work, using an unmodified electrode is unusual and makes it well suited for commercial exploitation. Finally, since surface modification is justified if it greatly improves the sensitivity of the sensor, the development work is given for the use of a novel sensor system, which exploits surface modification.

Acknowledgements

I would like to thank everyone who has helped me over the course of my PhD. Special mentions must go to the following:

Firstly I would like to thank my brother, John, for invaluable proof-reading and advice with writing the thesis and also for discussions and camaraderie throughout the PhD. I probably owe you a drink!

I would also like to thank Chris, in Sweden, for proof-reading beyond the call of duty and also Dave and Hayley for all their comments.

Dr Steve. Thanks for sharing all of the joy and the pain! Thanks for all the discussions and proof-reading.

Thanks are also due to Dr Geoff Syms, for his help with styling and structuring this thesis.

Thanks also go to the people from Molecular Sensing (Helen, John and Russell) who have helped me develop this project and provided invaluable support. Good luck in your new jobs.

In addition, I'd like to mention all the other PhD students who have made my time at Bath enjoyable. Thanks for the memories!
Thanks especially go to: Dawn, Diane, Duncan, Gan, Jon, Kelly, Marcus, Mike, Phil, Rachel, Stav and Suvi.

I also want to thank my supervisors, Dr Jenkins and Dr Frost.

I must also thank Prof. Takenaka and his entire research group at Kyushu University, Japan, for allowing me to work with them for two months.

To my parents: thanks for all your help, advice and proof-reading. In particular for the supply of tea and cake which enabled me to finish the thesis. To my sister: thanks for the enthusiasm and optimism - it's infectious.

Finally, and most importantly, I would like to thank Jen for all her love and support.

Table of Contents

Abbreviations

bp	base pair
CE	Counter Electrode
Cp	cyclopentadienyl
CV	Cyclic Voltammetry
D	diffusion coefficient
dA	adenine
DCC	dicyclohexylcarbodiimide
DCM	dichloromethane
DMF	dimethylformamide
DMSO	dimethylsulfoxide
DPV	Differential Pulse Voltammetry
dsDNA	double stranded DNA
E	potential (Volts)
ECD	Electrochemical Detector
EDCI	1-(3-dimethylaminopropyl)-3-ethyl carbodiimide hydrochloride
Ep	electropotential
F	Faraday constant
Fc	ferrocene
Fc^+	ferrocenium ion
FRET	Fluorescence Resonance Energy Transfer
HPLC	High Performance Liquid Chromatography
i	current (Amps)
K	Kelvin
Kd	Equilibrium dissociation constant
LSV	Linear Sweep Voltammetry
MCE	mercaptoethanol
MCH	mercaptohexanol
Pa	Pascal
PCR	Polymerase Chain Reaction
PMA	Phosphomolybdic acid
RE	Reference Electrode
SNP	Single Nucleotide Polymorphism
ssDNA	single stranded DNA
SV	Sinusoidal Voltammetry
TLC	Thin Layer Chromatography
V	voltage
WE	Working Electrode

Chapter 1: Introduction

1 Introduction

1.1 Overview

The detection of specific DNA gene sequences allows the diagnosis of both genetic diseases and of disease causing pathogens. Established sensing technologies approach this using fluorescence based detection. As electrochemical detection offers significant advantages over the use of fluorescence, the work described in this thesis concerns the design, synthesis and application of novel electrochemical DNA probes for gene sensing. Typically DNA sensing technology interrogates a DNA sample whose concentration has been enzymatically amplified, through Polymerase Chain Reaction (PCR). The novel sensing approach, detailed here, utilises enzymatic digestion, during or after this amplification. In the presence of the target gene sequence enzymatic digestion occurs, increasing the electrochemical response of the sample and thus facilitating gene detection.

This introductory chapter puts the work contained within this thesis into context. It gives the necessary detail to allow the "development of electrochemical gene sensors", described in section 1.10, to be fully understood.

DNA and its behaviour are central to the work and therefore DNA is introduced, with emphasis on its structure and function. Discussing the function of DNA allows the importance of genes and genetic disease to be understood. This culminates by detailing the achievements of the Human Genome Project.

DNA hybridisation is integral to the sensor work as this is used as the recognition event. The physical chemistry of DNA hybridisation is therefore introduced, in terms of DNA helix formation and DNA melting temperature. The main issues concerning DNA hybridisation probes are then discussed in detail, including a summary of all the available detection techniques.

The two main areas of application for DNA hybridisation sensors, gene sequencing and the detection of specific DNA sequences, are described, of which the latter is of direct interest. Importantly, established fluorescent techniques are then compared with existing electrochemical methods. Once the advantages of electrochemical detection are emphasised, electrochemical DNA hybridisation sensors are then discussed in detail. Three distinct approaches for electrochemical detection exist: direct analysis; methods using non-covalent labelling and methods using covalent labelling. These dictate the approach used and are discussed in separate sections, using prominent examples from the literature. This justifies the development of electrochemical gene sensors using covalent labelling. To conclude the chapter, the aims of the thesis are stated and the structure of the thesis is given.

1.2 Introduction to DNA

The elucidation of the structure of DNA by Watson and Crick in 1953 was a profound scientific breakthrough (Watson et al. 1953). The existence of DNA molecules as a complementary double helix completely transformed what had been previously thought of as a simple polymeric molecule, a molecule consisting of a sequence of only four subunits, into a structure complex enough to convey genetic information (Alberts et al. 1994).

In this section, the structure of DNA will be initially described, followed by a discussion of its function. As genetic material, DNA must be able to effectively replicate. The theory behind this replication is discussed, followed by the mechanism involved. The storage of genetic information in DNA as gene sequences is introduced, followed by a description of how these genes code for the structure of the proteins which are synthesised. The effect of errors in the DNA gene sequence on protein synthesis is introduced, with a subsequent focus on genetic disease. Finally genetic sequencing is introduced and concluded with a discussion of the Human Genome Project.

1.2.1 DNA structure

Although widely known, the structure of DNA should be introduced. DNA consists of a chain of deoxyribonucleotides (deoxyribose sugars with base substituents) linked together through phosphodiester covalent bonds, which join the 5' carbon of one nucleotide to the 3' carbon of the next, as shown in Figure 1.1 (Neidle 2002). The terminal groups at each end of the DNA strand, labelled as 5' and 3', are different; therefore the sequence (order of bases) of a DNA strand must always be described with direction (i.e. the 5' and 3' ends are assigned).
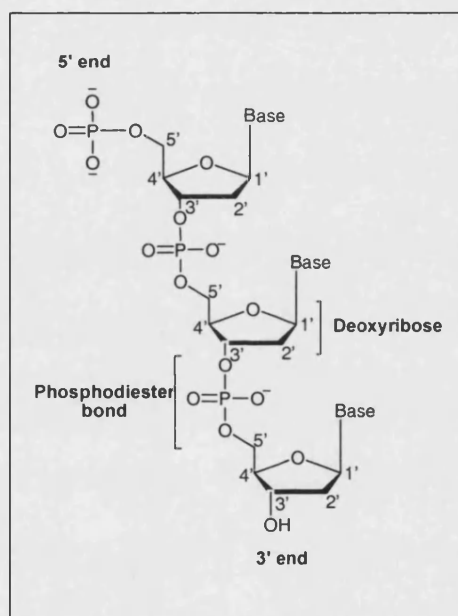
Figure 1.1 – Illustration DNA strand.
DNA nucleotides consist of a deoxyribose sugar with a base substituent. The carbon atoms in the sugar are numbered from the base (1') to the alcohol (5'). Consecutive nucleotides are linked together through phosphodiester bonds which covalently join the 5' carbon of one nucleotide to the 3' carbon of the next. The structures of the bases are described in Figure 1.3).

DNA contains four different bases: adenine (A); cytosine (C); guanine (G) and thymine (T) and equivalent proportions of A:T and G:C are always found (Neidle 2002). The model building by Watson and Crick elucidated the double helix structure, which located complementary base pairs together on the inside of the helix and with phosphate groups on the outside (Watson et al. 1953). The complementary base pairs are able to form strong hydrogen bonds to each other. The direction of the strands is important. A 3' to 5' strand is able to bond to (hybridise with) a complementary strand of the opposite direction (5' to 3') but not with one of the same direction (3' to 5'), therefore

the two strands run in opposite directions, which is described as being anti-parallel, Figure 1.2. The most common form of duplex DNA, in aqueous solution, is the B form (Blackburn et al. 1996; Bustamante et al. 2003). In this form, DNA is a right handed helix, with 10 bases per turn of the helix. The bases are 0.34 nm apart and as they are planar and are able to lie flat (stack) over each other.
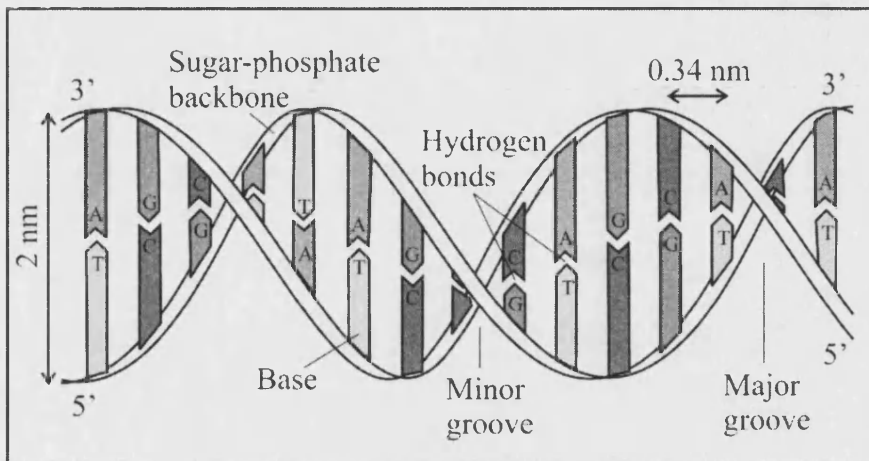
Figure 1.2 - DNA double helix.
Two DNA strands are shown in a double helix. This is a B form, right handed helix, which has a minor groove and a major groove. Each DNA strand consists of a sugar-phosphate backbone (white strip) on the outside and bases (shaded boxes) on the inside. The two strands run in opposite directions. Each base forms hydrogen bonds with its complementary base on the opposite strand (shown as short gap). The four bases (A,C,G,T) are labelled and shaded differently. GC and AT base pairs are formed. The bases are 0.34 nm apart and the helix is 2 nm in diameter.

The molecular detail of the DNA bases is important and is described in Figure 1.3. The G:C base pair contains 3 hydrogen bonds whilst the A:T base pair contains only 2 hydrogen bonds. The G:C base pair is therefore stronger (Alberts et al. 1994).
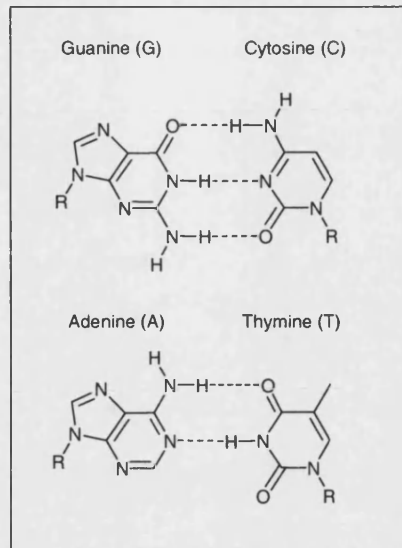
Figure 1.3 – Structure of the DNA bases.
Hydrogen bonding (dotted line) is shown between the base pairs. This is a bond between a hetero atom (oxygen or nitrogen) and a hydrogen atom of the other base. Guanine (G) forms 3 hydrogen bonds with Cytosine (C). Adenine (A) forms 2 hydrogen bonds with Thymine (T). The R group is the nucleotide, described in Figure 1.1). Only the hydrogen atoms involved in the bonding are shown.

1.2.2 DNA function

In a living organism genetic information must be precisely copied from one cell to its progeny (daughter cells) and this information must be readily conveyed to allow production of the genetic material in the cell. Genetic information is stored in DNA through genes, each of which code for the production of a specific protein (Alberts et al. 1994).

Replication

DNA replication is a complex biological process. Simplistically, the parent DNA is unwound and DNA polymerase synthesises complementary strands for each parent strand. This synthesis is described in Figure 1.4 (Alberts et al. 1994).
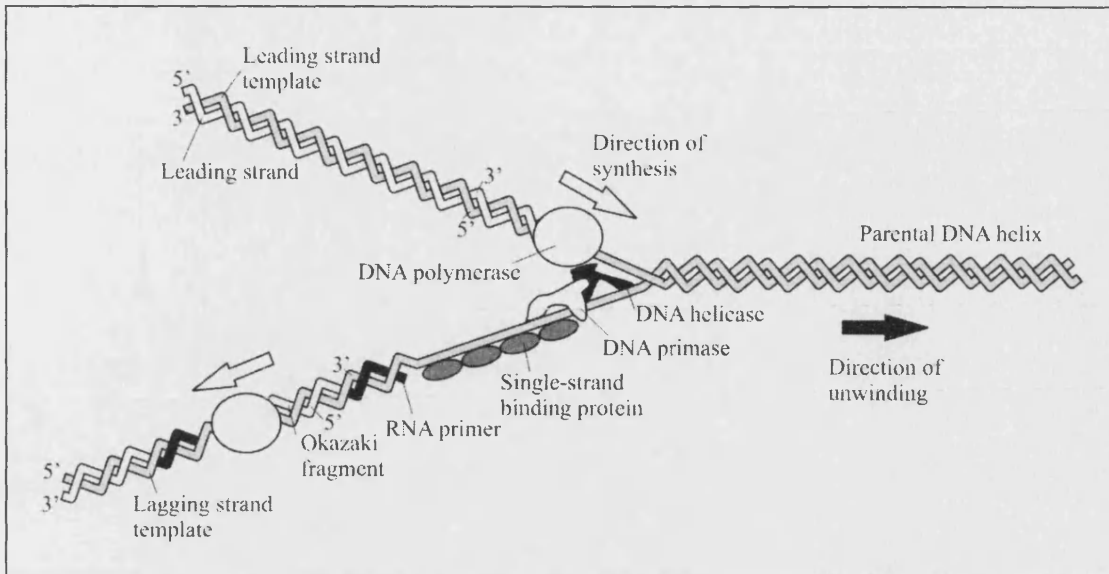
Figure 1.4 – Biological DNA replication.
The parent DNA (grey double helix) is unwound (black arrow, left to right) into a leading strand template (top, 3' to 5' left to right) and a lagging strand template (bottom, 5' to 3' left to right). This process is done by the DNA helicase molecule in concert with the DNA polymerase enzyme on the leading strand template. The single stranded DNA is straightened by single strand binding proteins (dark grey circles). The DNA polymerase enzyme (white circle) reads along the leading strand template (3' to 5' direction) and synthesises a complementary leading strand (white strand) in the 5' to 3' direction (white arrow), using deoxyribonucleoside triphosphates as building blocks (not shown). The enzyme works in the same way, in the same direction on the lagging strand template (bottom grey strand), which takes it away (right to left) from the opening helix. To overcome this problem the DNA primase molecule lays down RNA primers (short black sequences) at regular intervals. These allow the DNA polymerase to synthesise short complementary fragments (Okazaki fragments, short white sequences), from the primers to fill the gaps between the primers. In the illustration the enzyme is just finishing an Okazaki fragment. When the enzyme has finished the fragment it falls off the strand. The RNA primers are subsequently erased by a repair enzyme, the gap filled by DNA polymerase and sealed by a DNA ligase enzyme.

Mechanism of replication

The mechanism of the replication is given in Figure 1.5. The DNA polymerase enzyme uses deoxyribonucleoside triphosphates molecules to extend the DNA strand in the 5' to 3' direction. The appropriate deoxyribonucleoside triphosphate is selected through interaction with the base on the complementary strand. The driving force for the addition of bases is the loss of the pyrophosphate and its hydrolysis (Blackburn et al. 1996).
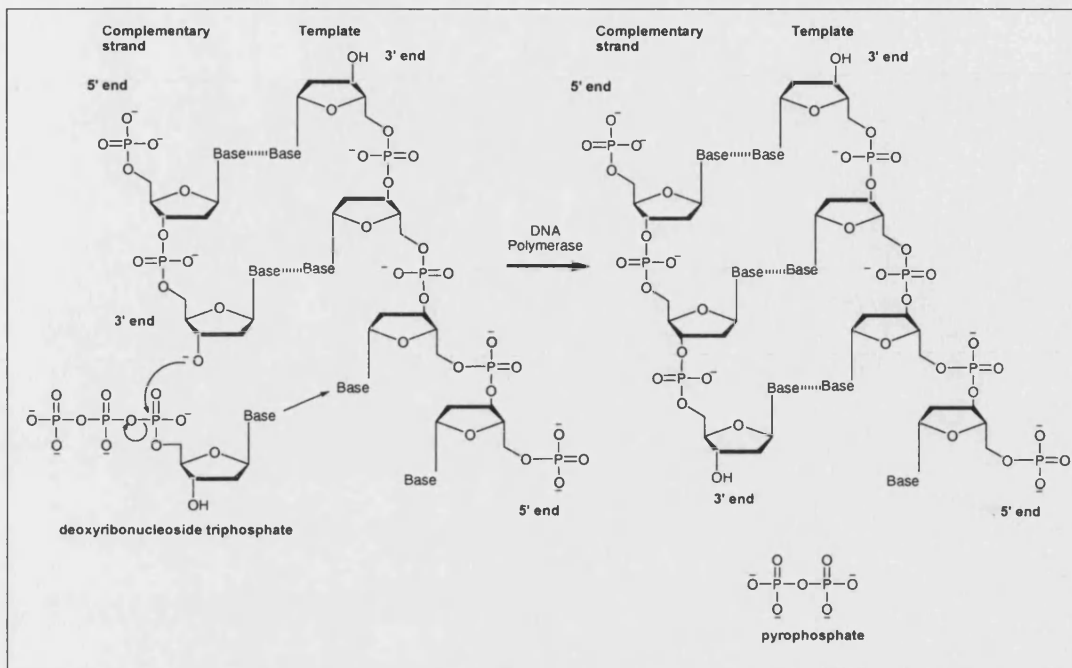
Figure 1.5 - Mechanism of biological DNA replication.
The complementary strand (left hand side) is extended along the template by the DNA polymerase enzyme (not shown) in a 5' to 3' direction (downwards). The deoxyribonucleoside triphosphate required to form a base pair with the template base, is selected and the enzyme mediates the addition of the deoxyribonucleoside, releasing a molecule containing two phosphate groups (pyrophosphate). The mechanism shown is a simplification of reality and does not show the enzyme mediated transition state (Steitz 1999). The next deoxyribonucleoside is added in an identical way. Hydrogen bonding between complementary bases is shown as a dotted line.

The DNA polymerase is a very effective DNA replication enzyme, but makes mistakes approximately once every 10^9 nucleotides (Alberts et al. 1994). This accuracy is very good as the enzyme can correct many of its own mistakes and it is aided by proof reading enzymes, which also have the ability to correct mistakes. When errors do occur the enzyme uses a C instead of a T or an A instead of a G. It is also possible for it to add on or skip a few nucleotides.

There are several different consequences of a genetic mistake (mutation). If the gene inactivates an important protein, which is essential for cell viability, then cell death will occur and the mutation is lost. If the gene mutation impairs the action of an alternative protein, or does not affect protein function (silent mutation), it will be faithfully copied and the mistake will propagate. In rare cases the mutation will give an improved or novel function to a protein, which gives the organism a survival advantage, which propagates through natural selection (Alberts et al. 1994).

Genes and protein synthesis

It has been illustrated above that DNA can be effectively copied and it will now be shown how the genetic information in the DNA genes is utilised for protein synthesis.

A DNA gene (sequence of bases), which specifies the structure of the protein, is a finite linear sequence of amino acids.   After synthesis, the protein folds into a complex 3D structure on synthesis, due to intramolecular bonding, which generally gives the protein its functionality.

The protein synthesis is now discussed to show the effect that genetic mutations can have on a protein structure, which may affect its function.

The DNA genes are first transcribed to RNA and then translated for protein formation, as shown in Figure 1.6 (Watson et al. 1992).

DNA $\xrightarrow{\text{Transcription}}$ RNA $\xrightarrow{\text{Translation}}$ Protein
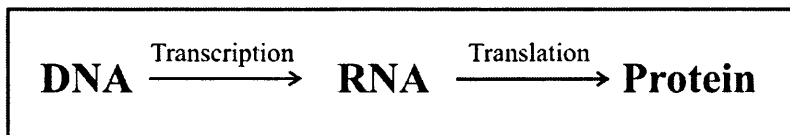
Figure 1.6 – Protein formation.

The transcription process is similar to the DNA replication process.   Using the double stranded DNA (dsDNA) as a template, RNA polymerase moves along one of the strands synthesising a complementary RNA strand, from ribonucleoside triphosphates building blocks, as it progresses.   Unlike DNA replication, described in Figure 1.4, the dsDNA closes just behind where the synthesis of the RNA occurs releasing the RNA chain.   At the end of the RNA synthesis the dsDNA has reformed and the RNA is a separate single stranded molecule.   This is messenger RNA (mRNA) (Alberts et al. 1994).

RNA, illustrated in Figure 1.7, is structurally different from DNA, illustrated in Figure 1.1.   The differences occur as RNA is synthesised from ribonucleosides rather than deoxyribonucleosides.
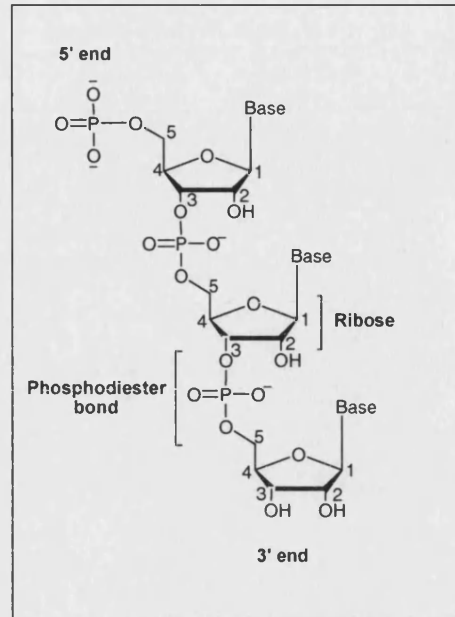
Figure 1.7 - RNA structure.
RNA nucleotides consist of a ribose sugar with a base substituent, this differs from DNA by an alcohol substituent on the 2' carbon. The carbon atoms in the sugar are numbered from the base (1') to the alcohol (5'). Consecutive nucleotides are linked together through phosphodiester bonds which covalently join the 5' carbon of one nucleotide to the 3' carbon of the next.

Three of the RNA bases are the same as in DNA, but the thymine (T) base is replaced by uracil (U), which are contrasted in Figure 1.8. The only difference between these two bases is a methyl group, so the hydrogen bonding is the same as for DNA bases, which was shown in Figure 1.3. Hence on transcription the DNA bases (ATGC) produce the complementary RNA bases (UACG).
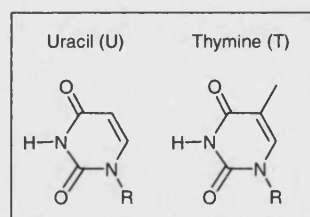
Figure 1.8 – Comparison between the structure of Uracil and Thymine bases.

RNA production is turned on and off by regulatory proteins in the cell. RNA sequences are short and generally only code for one or two proteins (Alberts et al. 1994).

Codons

It is necessary to understand the genetic information in mRNA. The sequence of the mRNA nucleotides is read 5' to 3' as sequential sets of three nucleotides, which are called codons. As the order of the nucleotides is important, and there are four different nucleotides, the number of possible codons is $4^3 = 64$. The codons code for 20 different amino acids and a stop signal. Many of the 64 codons are degenerate and code for the same amino acid. There is no set start position for reading the sequence, but if the initial reading position (described as a frame) is wrong, a stop codon is invariably quickly reached and the synthesis stops.

After the DNA gene is transcribed into mRNA, the mRNA codes for a finite sequence of amino acids, which constitute the protein (the gene contains three bases per amino acid). The mRNA codon does not have the ability to recognise the amino acid which it specifies. To afford the translation of the information in each codon, an adapter is needed which recognises both the codon and amino acid. This adapter constitutes small, 80 nucleotide, folded transfer RNA (tRNA) molecules. The tRNA is held in place by a protein complex of over 50 proteins called a ribosome. The ribosome moves along the mRNA and the peptide is subsequently produced one amino acid at a time. At the stop codon the ribosome falls off releasing the protein and separating into its component parts.

Replication and errors

It can now be clearly seen that the mutation of one base in a DNA gene directly relates to the change in a codon of the mRNA and potentially a change of an amino acid residue in the protein that it codes for. Figure 1.9 shows an example of a DNA base mutation and the effect that it can have, potentially leading to a genetic disease.
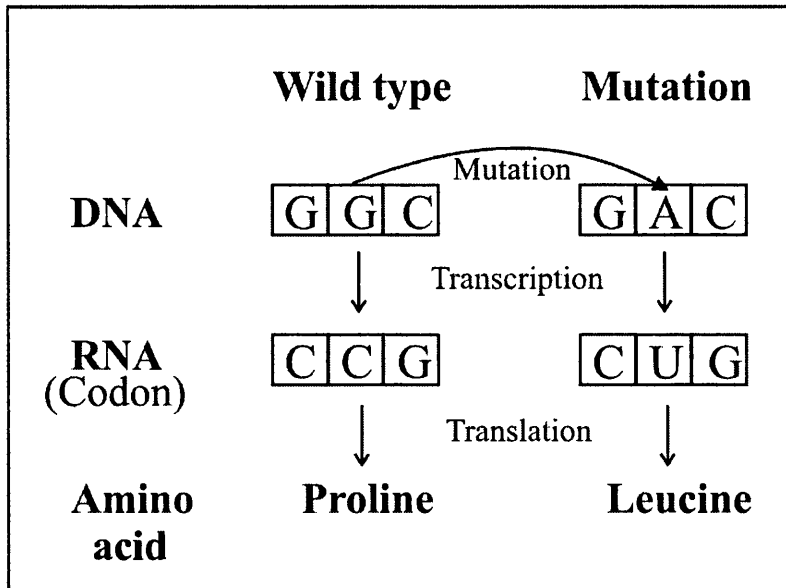
Figure 1.9 – An example of the effect of DNA base mutation.
A single base mutation in the wild type DNA base sequence (G mutates to A) results in a different sequence of the RNA codon on transcription. The different codons can code for different amino acids in the protein. In this example the wild type codon codes for proline and the mutation codes for leucine. It should be noted that in this case any mutation of the third base (C) would, however, not affect the coding for proline.

Genetic disease

Mutations in the genes can result in genetic diseases. In humans over 3000 genetic diseases are attributed to the mutation of a single base (single nucleotide polymorphisms, SNPs) (Alberts et al. 1994) and often the exact mutation is known. In sickle-cell anaemia, for example, there is a mutation from GAG to GTG of a section of the gene which codes for haemoglobin (Alberts et al. 1994). Most genetic diseases are recessive, namely a child must receive the mutant gene from both parents to acquire the disease.

Detection of genes will be discussed later in section 1.6. To allow detection of the genes the sequence of DNA which contains the gene must be first elucidated, by using genetic sequencing. The results of this elucidation are verified using proteomics, which is the study of proteins and their formation.

Genetic sequencing

The two main DNA sequencing methods were developed in the 1970s, and are the chemical degradation method of Maxam and Gilbert (Maxam et al. 1977) and the enzymatic method of Sanger and Coluson (Sanger 1977), which later became the method of choice (Brown 1995a). The techniques are summarised here.

The chemical degradation method involves the radiolabelling (with ^{32}P) of the unknown DNA, a chemical is then used to degrade a specific base (for example adenine, A). The degradation is done under mild conditions in order that only one of the specific bases is degraded per DNA strand. This procedure generates a range of DNA fragments of different sizes, depending on the position of the adenine residues which are degraded in the sequence. Gel electrophoresis, a technique introduced in section 2.3, separates the fragments by size and quantifies the size of the fragments (i.e. number of bases). This procedure is then repeated for the other 3 bases in turn. Fragments are therefore obtained for every cleavage site and the sequence can be elucidated by considering the fragments of increasing size.

The enzymatic approach uses a DNA polymerase and a radiolabelled (^{32}P) primer. The polymerase extends the primer (as discussed in the biological DNA synthesis, Figure 1.4) using deoxyribonucleoside triphosphate precursors. However, for one base (for example adenine) some triphosphates are added which omit the 3' OH group (dideoxyribonucleoside triphosphates). If these are used by the enzyme the lack of the alcohol group prevents further synthesis and terminates the chain. Fragments are therefore obtained which terminate randomly at A bases in the unknown sequence. This process is repeated for the other three bases in turn. Gel electrophoresis is then used, as above, to determine the sequence.

Alternatively, methods exist to sequence large genomes genetically. A common method maps restriction fragment length polymorphisms (RFLPs) between family groups. Restriction enzymes recognise specific DNA sequences and then cut the DNA helix in a specific position. Differences in the gene sequence will affect the fragments produced and this change can be used to detect mutations (Alberts et al. 1994).

Human Genome Project

In humans the total genetic DNA, or genome, is split over 24 chromosomes (22 autosomes and 2 sex chromosomes). Knowledge of the complete human genome would greatly assist the identification of genes which contribute to disease, using methods such as classifying genes via function (Jimenez-Sanchez et al. 2001).

The aims of the Human Genome Project included the identification all the human DNA genes, the determination of the entire sequence, the storage of all the information in a valuable accessible way and the development of the scientific techniques and methodology to achieve this effectively (The Human Genome Project 2005).

Research specifically to sequence the human genome was initiated in 1988 (Roberts 2001) and a comprehensive draft sequence was published in simultaneously in 2001 by the public Human Genome Project (The International Human Genome Mapping Consortium 2001) and by a private research group (The Celera Genomics Sequencing Team 2001). Owing to the magnitude of these results the above references were included in special issues of Science and Nature and complemented with many other papers. The sequence was completed in 2003 (Collins et al. 2003).

The human genome contains over 3 billion base pairs, specifically 3164.7 million, and around 20,000 to 25,000 genes. In 2003 over 15,000 genes had been characterised (Collins et al. 2003). There were originally thought to be many more genes but a high level of degeneracy (repeats) results in a lower actual number. The function of over half of these genes is not yet known.

The sequencing techniques are thought to be very accurate (1 error per 100,000 bases) and these show that the genome is 99.9% the same in all humans. These differences, however, are significant. In 2001 1.4 million SNPs were known (The International SNP Map Working Group 2001) which had increased to 3.7 million in 2003 (Collins et al. 2003) and may increase further.

Summary

The knowledge of the location of the SNPs and the genes which cause disease, gives the opportunity for sensing technologies to be developed which can detect them.

1.3 Physical chemistry of DNA

The physical chemistry of DNA is considered in more detail. The reasons for the double helix formation are described in more detail and the strength of this double helix formation, is then discussed in relation to the melting temperature (Tm).

1.3.1 DNA helix formation

Under suitable physiological conditions two complementary DNA strands, of sufficient length, will hybridise together to form a double helix. To appreciate the physical behaviour of the DNA the reasons behind this must be understood. Spontaneous chemical reactions are described by the Gibbs function, Equation 1.1 (Atkins 1990).

$$\Delta G = \Delta H - T\Delta S \qquad\qquad (1.1)$$

ΔG = change in Gibbs free energy, ΔH = change in reaction enthalpy = H(bonds broken) – H(bond formation), T = temperature and ΔS = change in reaction entropy = S(reactants) – S(products).

For a spontaneous reaction to occur there must be a reduction (negative change) of Gibbs free energy (ΔG). The change in reaction enthalpy (ΔH) concerns the change of heat energy in the reaction. Energy is required to break bonds and released on bond formation. The bases on the ssDNA H-bond with the solvating water and then H-bond with their complementary base on hybridisation, which gives no net enthalpy change. Electron delocalisation is, however, possible between the base pair and the neighbouring base pairs, which are stacked above and below it in the duplex. This reduces the enthalpy of the duplex and favours the duplex formation reaction. It follows that the sequence of the DNA helix will affect its stability.

Considering a DNA duplex that has formed, the major stabilising force is actually an increase in entropy, due to the hydrophobic effect (Blackburn et al. 1996). Superficially

the hybridisation appears to give a decrease in order as two unconstrained ssDNA molecules hybridise to give one constrained dsDNA duplex, which is 50 times more rigid (Bustamante et al. 2003). This is not the case. Before hybridisation there is an ordered interaction between water molecules and the DNA molecules, including the bases. On hybridisation the hydrophobic bases (all of ATGC) are able to minimise their interactions with water, by H-bonding at the centre of the helix, and the water molecules are expelled to the disordered bulk solution. This gives a decrease in order (ΔS = positive). With a negative enthalpy change and a positive entropy change, the Gibbs free energy decreases (Equation 1.1) making the hybridisation spontaneous.

It should be noted that although the hybridisation is thermodynamically feasible (as described above), it may be kinetically not favoured. The rate of hybridisation (k) decreases if the temperature is reduced (Equation 1.2) and can be slowed to a prohibitively slow rate (Morris 1987).

$$k = Ae^{-E/RT}$$ (1.2)

Arrhenius equation: k = rate of hybridisation, A = constant, E = activation energy, R = gas constant and T = temperature.

1.3.2 DNA melting temperature

The DNA melting temperature is a measure of the stability of the DNA duplex.

A sequence of ssDNA will hybridise to its fully matched complement, but its ability to do this is affected by its base sequence and length, together with the hybridisation conditions. These include: temperature; pH; ionic strength; DNA concentration and the presence of denaturants, such as DMSO (Watterson et al. 2002). Mismatches on the complementary target also affect the hybridisation.

The effect of the base sequences and length of the ssDNA will be discussed first. The longer the ssDNA sequence (more bases and therefore more hydrogen bonding) and the higher the proportion of GC bases pairs in the duplex (more hydrogen bonds per base) the stronger the hybridisation bonding of the duplex (Sigma Genosys 2004). For short

oligonucleotides, under specific conditions the Wallace rule, Equation 1.3, applies (Wallace et al. 1979), whereby the dissociation temperature (Td) can be determined (Sigma Genosys 2004). This is the temperature at which 50% of the ssDNA has formed a duplex with its exact complement.

$$T_d = 2(nA + nT) + 4(nC + nG) \qquad (1.3)$$

Wallace rule: Td = dissociation temperature (°C) and n(A, T, C or G) = the number of DNA bases of that type. The equation is valid for short DNA strands of 14-20 bases hybridising to membrane bound complementary strands in 0.9M NaCl. Note the Td is 7-8 °C lower (and called Tm, as described in Equation 1.4) if the duplex is formed in solution.

Commercial oligonucleotide (ssDNA) suppliers, such as Sigma Genosys, use a more complex equation, which gives a more useful result. They use the "Nearest-Neighbour" method developed by Breslauer (Breslauer et al. 1986) to calculate a melting temperature (Tm) at which 50 % of the oligonucleotide is hybridised, which is described by Equation 1.4. This equation utilises the changes in enthalpy and entropy when each base pair hybridises, these values are affected by the base's immediate neighbour.

$$Tm = \frac{\Delta H}{A} + \Delta S + R \ln\left(\frac{C}{4}\right) - 273.15 + 16.6 \log[Na^+] \qquad (1.4)$$

Tm = melting temperature (°C), ΔH = the sum of the nearest-neighbour enthalpy change on hybridisation (calmol^{-1}), A = helix initiation constant, ΔS = the sum of the nearest-neighbour entropy change on hybridisation (cal/mol), R = gas constant = 1.99 cal K^{-1}mol^{-1}), C = oligonucleotide concentration and [Na$^+$] = concentration of sodium ions (salt concentration). The nearest-neighbour entropy and entropy changes are available (Sigma Genosys 2004).

The nearest neighbour equation (Equation 1.4) includes a term for salt concentration (in this case sodium, Na^+). The negatively charged polyphosphate backbone of DNA constitutes a repulsive barrier to hybridisation. The presence of cations (M^+) is essential to reduce the repulsive action of these charges. Increasing the salt concentration, or increasing the charge on the cation, for example from sodium (Na^+) to magnesium (Mg^{2+}), decreases repulsion and increases the Tm (Blackburn et al. 1996).

DNA hybridisation is typically undertaken at physiological pH, or at pH conditions tailored to suit the enzyme present in the assay. pH will have a large effect on hybridisation as acid conditions (low pH) will protonate the DNA, whilst basic

conditions (high pH) will deprotonate it. Hybridisation is not considered practical below pH = 3 or above pH = 10 (Watson et al. 1992).

Commercially produced oligonucleotides, such as those produced by Sigma Genosys, have a Tm quoted for typical Polymerase Chain Reaction (PCR, see Chapter 2) buffer containing 50 mM monovalent salt and 500 nM oligonucleotide.

It should be noted that whilst the nearest neighbour approach gives an approximation for the Tm, it is not exact. The exact value is measured experimentally by UV spectroscopy. dsDNA absorbs UV light at $\lambda = 260$ nm and the absorbance at this wavelength increases by up to 30% on denaturation, due to the hyperchromic effect (Blackburn et al. 1996). The absorption at this wavelength ($\lambda = 260$ nm) is measured, and increases to a maximum, as temperature is increased, since absorption is directly proportional to the amount of ssDNA present. The Tm is the temperature at which the absorption has increased by 50%.

The presence of denaturants, such as DMSO, reduces the Tm of the duplex.

If the two DNA strands in the duplex do not have perfectly complementary sequences, the mismatched bases will destabilise the duplex. The mismatched bases do not H-bond together and disrupt the base stacking and therefore electron delocalisation of the rest of the duplex. The destabilising effect of a single mismatch decreases as the duplex length increases. Typically 1% of mismatched bases in a duplex of less than 100 base pairs reduces its Tm by 1 °C. The stringency of duplex formation is the ability of that duplex to tolerate mismatches. Under high stringency experimental conditions several mismatched based will be tolerated and the duplex will form.

Peptide nucleic acids (PNA) actually form more stable DNA·PNA duplexes, with higher Tm values, through H-bonding with complementary bases, than DNA does (Wang, J. 1998). This is because the uncharged PNA backbone, illustrated in Figure 1.10, does not repel the negatively charged DNA backbone.
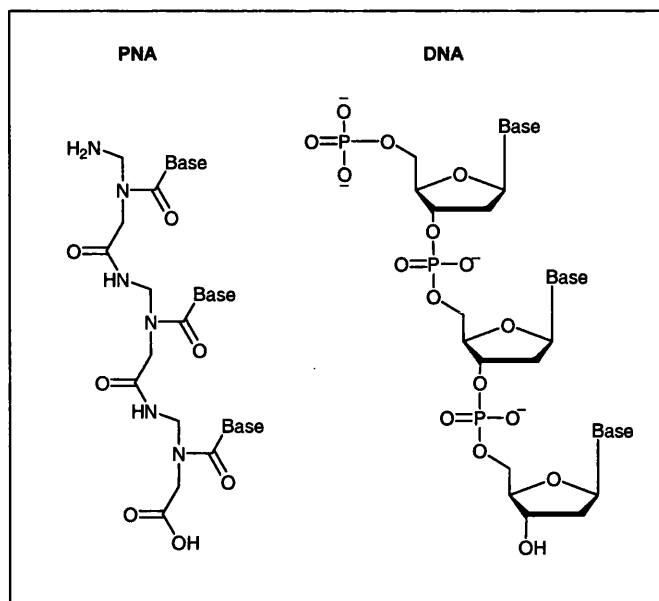
Figure 1.10 – Comparison between the structure of DNA and PNA.

1.4 DNA hybridisation probes

An effective sensor should be both sensitive and specific. Namely, it would be able to detect a low concentration of the target analyte and only that analyte, from a mixture (assay).

DNA hybridisation sensors involve a hybridisation event between a probe and target sequence, defined below in section 1.4.1, followed by a detection event. ssDNA is an ideal probe sequence for a sensor, as the specificity of the DNA hybridisation can be controlled by the stringency, defined in section 1.4.5, of the experimental conditions and the resultant DNA duplex can be very stable. This hybridisation can be detected by a variety of highly sensitive techniques.

1.4.1 Terminology

In the context of DNA sensing the DNA target is the DNA sequence, either known or unknown, which is being sequenced or detected. The DNA probe is usually a shorter DNA sequence (often termed oligonucleotide) which can bind (hybridise) to a specific (complementary) region on the target, as shown in Figure 1.11 (Wang, J. 2002).
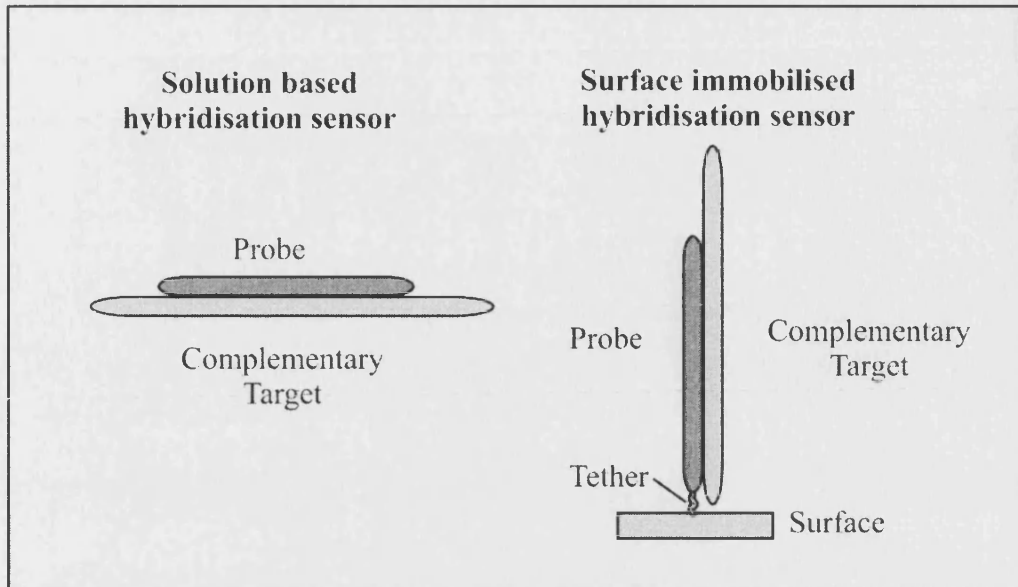
Figure 1.11 – Terminology for DNA hybridisation sensors.
The probe DNA (dark grey) strand hybridises with a complementary sequence on the larger target
DNA (light grey) strand. A duplex is formed, but this is drawn as parallel strands for clarity. The
hybridisation can occur with the probe in solution (left hand side) or when the probe is immobilised
on a surface (right hand side). In this case the immobilised probe is tethered to the surface by one
end.

1.4.2 Practical considerations

The probe oligonucleotides are typically synthetic oligonucleotides, which can be
custom synthesised with the desired sequences and often with a label. Labelling is
introduced in section 1.4.6. The oligonucleotides are supplied with high purity and
relatively low cost. The probe may be used free in solution or immobilised on a
surface, as shown in Figure 1.11.

The probe oligonucleotides have a typical length of 25-40 nucleotides (Wang, J. 2002).
Longer oligonucleotides form more stable duplexes but take longer to hybridise.

Work using PNA probe sequences has been undertaken (Wang, J. et al. 1996c; Wang, J.
1998; Aoki et al. 2000; Ozkan et al. 2002) but they are much more expensive to
synthesise than DNA (ten to over a hundred fold more) and for this reason will not be
discussed further here.

1.4.3 The hybridisation event

For a given ssDNA sequence it has been described, in section 1.2.2, that the assay conditions can be optimised to achieve a low stringency, such that the sequence will hybridise with its fully matched complementary sequence, but not a sequence containing mismatches. In a sensor this selected duplex formation is then detected by an appropriate technique. Figure 1.12 describes the high and low stringency approaches. Such selective hybridisation is the basis for the majority of DNA hybridisation probes (de-los-Santos-Alvarez et al. 2004).

Techniques have also been developed which utilise a high stringency, whereby both the fully matched complementary sequence and sequences containing some base mismatches hybridise. Discrimination is then obtained through the different responses of the fully complementary duplex and imperfect, mismatched duplex to the visualisation technique.
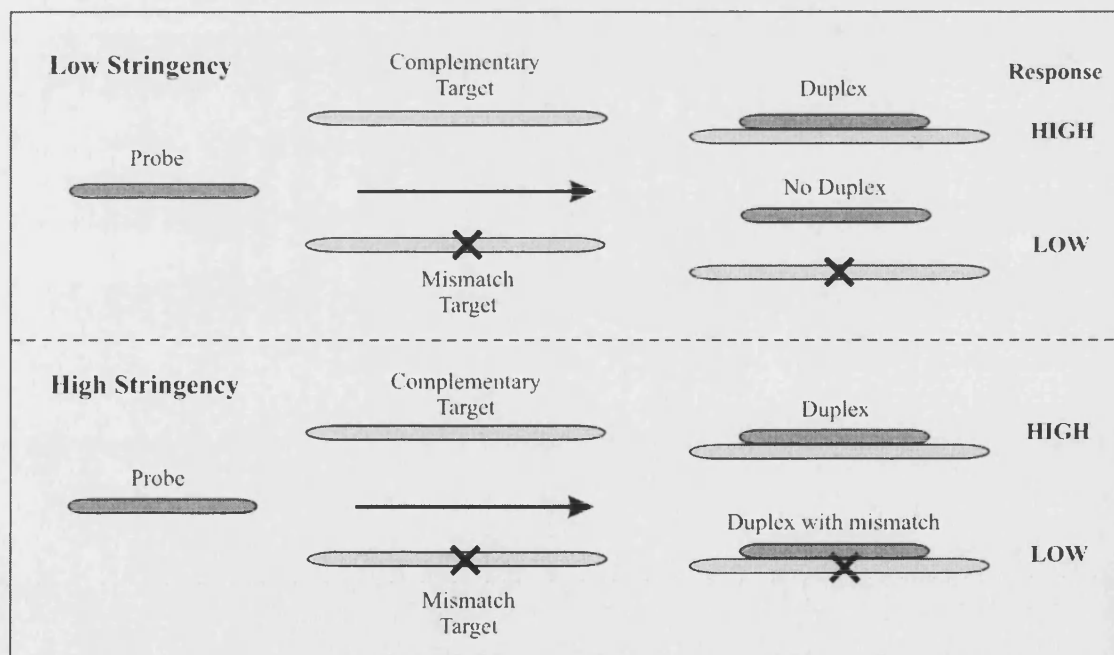
Figure 1.12 – Stringency in DNA hybridisation.
Under low stringency conditions (top scheme) the probe (dark grey) strand will hybridise to the complementary target (light grey) strand to form a duplex. The probe will not hybridise to a target containing a mismatch (X) and no duplex is formed. Discrimination is obtained as the detection protocol selected gives a high response for duplex formation and a low response for no duplex. Under high stringency conditions (bottom scheme) the probe (dark grey) strand will hybridise to the complementary target (light grey) and the mismatch target to form a duplex. Discrimination is obtained as the detection protocol selected gives a high response for a fully complementary duplex and a low response for a mismatched duplex.

Reviews show that the vast majority of recent sensing technologies involve the use of modified sensing surfaces (Wang, J. 1999; Palecek et al. 2001; Palecek 2002; Popovich et al. 2002b; Wang, J. 2002; Drummond et al. 2003; de-los-Santos-Alvarez et al. 2004). The probe is typically immobilised at the surface, a solution containing the target is introduced and hybridisation occurs at the surface. The location of the analysis is therefore typically also at the surface and a low stringency hybridisation approach is also usually used. This is shown diagrammatically in Figure 1.13. as part of the range of possible approaches.
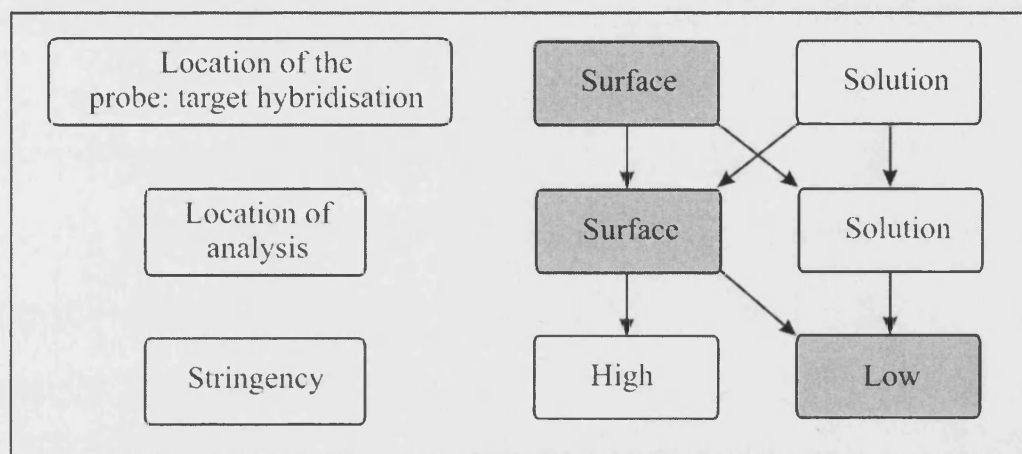
Figure 1.13 – Diagrammatic overview of DNA hybridisation techniques.
The most common DNA hybridisation sensor systems involve: (i) probe/ target immobilisation at the surface; (ii) detection at the surface and (iii) a low stringency approach. This common approach is shaded. The combinations which have been used in literature techniques are linked (arrows).

1.4.4 Surface hybridisation

The use of surface hybridisation is discussed here. If the ssDNA capture probe is immobilised on a surface, it will still hybridise with the target from the solution, providing that that probe is sufficiently accessible and has adequate freedom of movement. Under optimised conditions the stability of the duplex (Tm) can be higher at the surface than in solution (Takenaka, pers. comm, 2004).

Surface hybridisation requires surface immobilisation. Surface immobilisation is practical to use and concentrates the duplex DNA at the surface. It is very important in DNA sensing applications as it allows control over the properties of the sensing surface, thus allowing the sensitivity and selectivity of the approach to be optimised. This

approach has the ability to give improved sensitivity and selectivity over the use of unmodified surfaces (Peterson et al. 2002). Surface immobilisation allowed the development of chip based sensors, discussed in section 1.5.1, as it enabled different probe sequences to be attached to different areas of the sensor chip.

Surface modification introduces a level of complexity and additional cost to the sensor system. The DNA immobilisation requires good experimental design, as the modified surface must retain good binding affinity to the target DNA. The surface must also be stable, reasonably straightforward to prepare and give reproducible results. It has been shown experimentally that there is a trade off between the surface coverage of probe DNA and hybridisation efficiency (Herne et al. 1997; Watterson et al. 2002). More complex modelling, using the experimental data, has also been undertaken (Hagan et al. 2004).

1.4.5 Practical surface immobilisation

A range of different approaches for immobilising the probe DNA have been developed, depending on the choice of surface. These include: direct physical adsorption of DNA onto the surface; direct adsorption onto films and membranes covering the surface; covalent attachment to the surface; affinity binding and chemisorption onto gold electrodes (i.e. surfaces) through thiol linkages (de-los-Santos-Alvarez et al. 2004). All the direct adsorption techniques rely on electrostatic interaction between the surface and the DNA (Brett et al. 1993; Zhao et al. 1997; Wang, J. et al. 2000; Xu, J. et al. 2001) and although they are reasonably straightforward to produce, the control over the structure and hence properties of the surface is limited. In contrast the remaining three approaches produce stable sensing surfaces and give control over orientation and density of DNA packing. This allows their binding capacity for the complementary target sequence to be optimised and the amount of non-specific adsorption (i.e. adsorption of the target, without hybridisation, and of other material) to be limited. The 3 latter approaches are now discussed individually.

Covalent attachment

Covalent attachment involves the functionalisation of the electrode surface. Most commonly functionalisation uses carbodiimide reagents, which are used synthetically in section 3.3.2, to couple the probe oligonucleotide to the surface through carboxylate groups on a carbon paste surface (Millan et al. 1993; Millan et al. 1994) and amino groups on a gold surface (Sun et al. 1998) and a graphite surface (Liu et al. 1996). Two approaches for covalent attachment of oligonucleotides to the surface are shown in Figure 1.14.
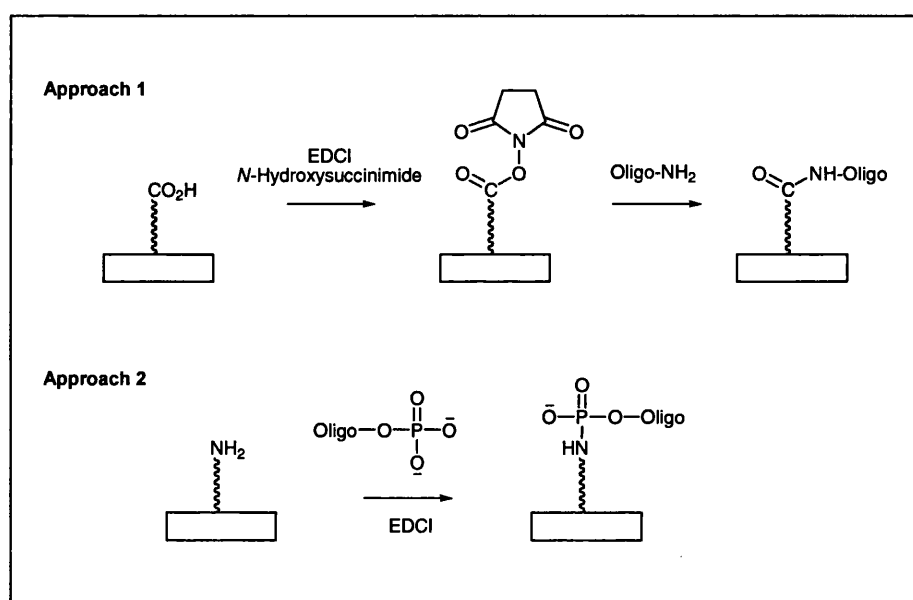
Figure 1.14 - Covalent attachment of oligonucleotides to the surface.
Approach 1: immobilised carboxylate groups (Millan et al. 1994). Stearic acid (shown as wavy line-CO_2H) is incorporated into the surface (shown as a box). The acid is converted to an activated ester using 1-(3-Dimethylaminopropyl)-3-ethyl carbodiimide hydrochloride (EDCI) and N-Hydroxysuccinimide. The activated ester reacts with the amine groups of terminal guanine residues of an oligonucleotide (Oligo-NH₂), forming a covalent amide bond. Approach 2: immobilised amine groups. The surface is either directly functionalised (Liu et al. 1996) or functionalised with an amino thiol (Sun et al. 1998). The amine is coupled with the 5' phosphate group of the oligonucleotide using EDCI, forming a covalent phosphoramide bond.

Whilst covalent attachment works well, it is more complex and has a higher cost than chemisorption techniques, discussed below, and is therefore not as attractive for development as a commercial sensor.

Affinity binding

Affinity binding is primarily based on the very strong interaction between the streptavidin protein and biotin. Immobilisation techniques use affinity binding in two approaches, shown in Figure 1.15, whereby the biotin labelled oligonucleotide is immobilised on the surface by streptavidin (Wojciechowski et al. 1999; Gau et al. 2001). This type of biotin labelled oligonucleotides is widely commercially available (Sigma Genosys). In terms of electrochemical detection, whilst the physical bulk of the streptavidin should afford good hybridisation to the immobilised oligonucleotide, it also limits the surface coverage and introduces a physical barrier between the duplex and the electrode causing potential probes for electrochemical detection.
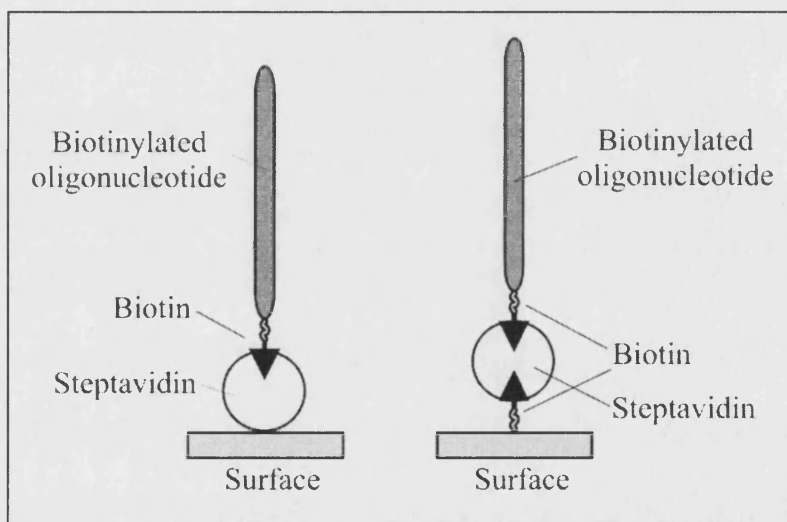
Figure 1.15 - Affinity binding using surface immobilised streptavidin.
The figure shows two approaches for immobilising a biotin labelled oligonucleotide on a surface. The oligonucleotide (grey strand) is labelled at one end by biotin (black triangle). The biotin strongly binds to streptavidin (white circle). The streptavidin is either directly attached to the surface (left hand side) or is bound to a biotin protein which is itself directly attached to the surface (right hand side).

Chemisorption

The chemisorption approach involves the chemisorption of thiol modified oligonucleotides onto gold surfaces (Herne et al. 1997; Peterson et al. 2002; Wolf et al. 2004), as shown in Figure 1.16. The major advantage of this approach is that these oligonucleotides are able to self assemble onto gold electrodes, through the terminal thiol end group. No modification of the electrode is required to achieve this and the

thiolated oligonucleotides are commercially available and relatively inexpensive. Ihara has achieved the same result using oligonucleotides 5' labelled with phosphorothioate units (Ihara 1997; Nakayama et al. 2002), which are also commercially available. In an alternative approach, work by Barton (Drummond et al. 2003) involves the immobilising of a thiolated duplex.
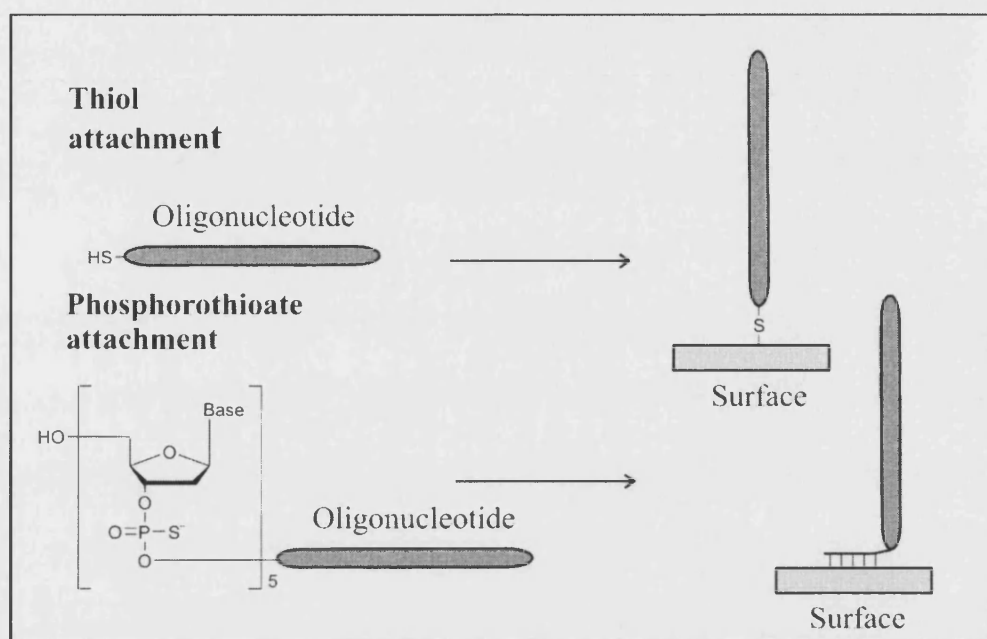
Figure 1.16 - Chemisorption onto gold surfaces.
The figure shows two methods of attachment of oligonucleotides to a gold surface by chemisorption. In thiol attachment (top) the oligonucleotide (grey strand) has a terminal thiol group (SH), through which it can chemisorb onto the gold surface. In phosphorothioate attachment, the oligonucleotide (grey strand) has five repeating phosphorothioate groups through which it can chemisorbe to the gold surface.

This self assembly approach allows the use of other thiolated molecules, such as alkyl thiols, to act as blocking layers or conductors, to improve the sensing layer.

Summary

In summary, the ideal sensing surface is one that can be produced easily, cheaply and reproducibly. It should be robust and stable. If hybridisation occurs at the surface, the binding efficiency (i.e. duplexes successfully formed per unit area with the target sequence) should be high and preferably the hybridisation should be reversible and reproducible enabling multiple uses of the sensor. As a general rule, the higher the

binding efficiency the higher the sensitivity of the sensor irrespective of the detection method.

1.4.6 Detection techniques for DNA hybridisation

A general overview of the techniques which have been developed to detect DNA hybridisation between a DNA strand and its complement is given here for clarity. Further details are given later in sections 1.5, 1.6 and 1.9.

DNA hybridisation procedures are generally classified first by their detection technique (e.g. electrochemistry) and then by the application for which they are used (e.g. hybridisation probe for SNP detection).

Different detection techniques require different labels (often called reporter molecules) which are discussed below. There are three categories of labelling: covalent labelling (typically of the probe oligonucleotide); non-covalent binding of reporter molecules and direct (unlabelled) detection (de-los-Santos-Alvarez et al. 2004).

Covalent labelling involves the covalent attachment of a reporter molecule. This can be electrochemically active (de-los-Santos-Alvarez et al. 2004), fluorescent (Epstein et al. 2002) or radioactive (Brown 1995b). In a successful sensor there is a change in analytical response of the reporter molecules on hybridisation.

Similarly in the non-covalent labelling there is preferential binding of reporter molecules, typically electrochemical or fluorescent, to dsDNA over ssDNA. This binding behaviour gives a difference in the analytical response on hybridisation which is detected.

In contrast the direct detection techniques use the formation of the duplex itself. Quartz crystal microscopy (QCM) is used to measure the mass change at the detection surface on hybridisation (Han et al. 2001; Willner et al. 2002). Other approaches measure the change in optical properties at the detection surface such as surface plasmon spectroscopy (SPR) (Peterlinz et al. 1997; Georgiadis et al. 2000). Alternatively a

change in the electrochemical properties of the DNA bases (e.g. G) can be directly measured (Popovich et al. 2002a).

The use of techniques which label the DNA, as opposed to label-free approaches, introduces an extra level of complexity to the detection system. This is often justified as they can afford better sensitivity and selectivity, often with more straightforward detection (Drummond et al. 2003).

Applications

DNA hybridisation probes have been applied to both genetic sequencing and to the detection of genetic disease or specific DNA sequences. The aims of these two applications are different and therefore the analytical techniques which use DNA hybridisation probes are often very different.

1.5 Genetic sequencing

Genetic sequencing is an important sensing technology and will be discussed with an emphasis on commercialised technologies. The aim of genetic sequencing is to determine the base pair sequence of a sample of DNA. This can range from a short gene sequence (e.g. human β-globin gene: 2010 base pairs (Alberts et al. 1994)) to an entire genome (e.g. human genome: 3164.7M base pairs (Collins et al. 2003)). Given the large amount of base pairs to be sequenced, the method must have a high throughput, preferably with the ability to simultaneously detect different sequences, but it must also be robust and have a very high accuracy. In a commercial context a method must also cost effective and this necessitates that it allows rapid analysis, minimising both operator time and overall running time. The technique will enable the full sequence of the target DNA to be determined, allowing specific genes or mutations to be detected if required.

1.5.1 Sequencing technology

The development of technologies that allowed the fast and accurate sequencing of DNA to be achieved arose largely to fulfil the rapid parallel screening requirements for genomic DNA in the Human Genome Project. The original gel based sequencing techniques of Sanger and Coluson (Sanger 1977) and Maxam and Gilbert (Maxam et al. 1977) have already been introduced (section 1.2.2). These original techniques were automated and more modern techniques, based on capillary gel electrophoresis, (Brazill et al. 2001) can sequence 1000 bp over several hours. Further advances have made these reliable methods faster and cheaper. At the end of the Human Genome Project [2002], it was possible to sequence over 1,400 M bp per year at a cost of $US 0.09 per base (Collins et al. 2003).

The development of DNA chips could provide an alternative sensing protocol, which should allow DNA sequencing to be further improved and eliminate the use of radioactive labels or toxic DNA binding dyes (such as ethidium bromide) (Brown 1995a). DNA chips involve the immobilisation of thousands of different DNA probes, of known sequences, on a surface. Such chips are then exposed to the biological assay under low stringency conditions and only fully complementary sequences hybridise to the probes. The duplexes formed are then visualised using a duplex specific fluorescent dye, followed by fluorescence plate analysis. The first commercialised chips of this type were developed by Affymetrix (Foreman et al. 1998). These chips have great potential as they can rapidly interrogate DNA sequences. As the chips can be directly integrated into computerised systems, the data they produce can also be readily analysed and stored. Problems with the DNA chip approach do exist as it is often difficult to maintain low stringency conditions across the chip (for many different sequences) and this can cause sensitivity issues, typically through a lack of discrimination between fully matched and SNP mismatched sequences binding to the same probe (King et al. 2001). These difficulties are dismissed by Affymetrix (Foreman et al. 1998).

Improved discrimination is obtained with better probe design, both through practical approaches (size, sequence and mismatch position) (Letowski et al. 2004) and through improved modelling of the hybridisation (Hagan et al. 2004; Halperin et al. 2004).

29

DNA chips using fluorescent molecular beacon probes, as opposed to the duplex specific fluorescent labels, have been developed (Steemers et al. 2000) and give good sensitivity (the use of these probes in solution is described in section 1.6.2).

All of the above sequencing technology relies on Polymerase Chain Reaction (PCR, see section 2.2) to increase the concentration of the DNA sample before analysis (King et al. 2001).

Routine genetic sequencing is still based on the reliable capillary gel electrophoresis techniques developed for the Human Genome Project. The fluorescent chip technology, however, is likely to be established as a viable alternative in the near future.

1.6 Detection of specific DNA sequences: genetic disease and pathogens

The second application for DNA hybridisation probes is the detection of specific DNA sequences. This will be introduced with an emphasis on commercialised technologies and both surface and solution based approaches will be discussed.

In the post-genomic era the location and sequences of the genes which cause some specific genetic diseases are known. These are typically caused by SNP mismatches in gene sequences (The International SNP Map Working Group 2001). The gene sequences of some specific viral or bacterial pathogens are also known (Wang, D. et al. 2002a) and the detection of characteristic gene sequences allows the detection of the pathogen.

Both applications are diagnostic tools, which aim to detect a specific gene sequence, either a pathogen or gene mutation, quickly and accurately (Umek, R.M 2001). Simultaneous detection of a small number of different SNPs is sometimes required for the detection of complex genetic diseases (Drummond et al. 2003). The simultaneous analysis of a control sample is also highly beneficial. A commercialised product must also be simple to use, reliable and as cheap as possible.

PCR, see section 2.2, is often used to increase the concentration of the DNA sample before analysis. However, this approach is time consuming, with a typical PCR taking over an hour and it is often desirable to develop techniques which are sensitive enough to analyse the original sample. Such techniques must not compromise accuracy.

1.6.1 Surface based detection

For the application to sensing technology, DNA chips or sensors have been developed which are optimised to detect only one, or a low number, of sequences at the surface. This is typically achieved by immobilising only one probe sequence on the sensor surface. The fluorescence chips, introduced in section 1.5, have the potential to be applied to this detection.

Using electrochemical detection Motorola have developed the CMS eSensor^{TM} for SNP detection (Farkas 1999; Umek, R.M 2001). This is described in detail in section 1.9.3. Alternative chip design based upon the use of flow channels, allows electrochemical or fluorescent based approaches to be used with techniques that detect hybridisation, whilst the DNA strands are in solution (Lenigk et al. 2002).

1.6.2 Solution based detection

Well established, fluorescence based, technologies exist for the solution based detection of specific sequences. The most important examples are Molecular Beacons (Tyagi et al. 1996), TaqMan$^{®}$ (Applied Biosystems) (Bassler et al. 1995; Livak et al. 1995; Fujii et al. 2000; Guiver et al. 2000) and Invader (New Wave Technology) (Kwiatkowski et al. 1999; Olivier et al. 2002) technologies. The general structure of the three technologies is described in Figure 1.17.

The three DNA hybridisation technologies all rely on fluorescent quenching through Fluorescence Resonance Energy Transfer (FRET, section 2.6.1). After the hybridisation recognition event between the probe and the target (usually a PCR product), FRET is stopped and an increased fluorescent response is recorded.
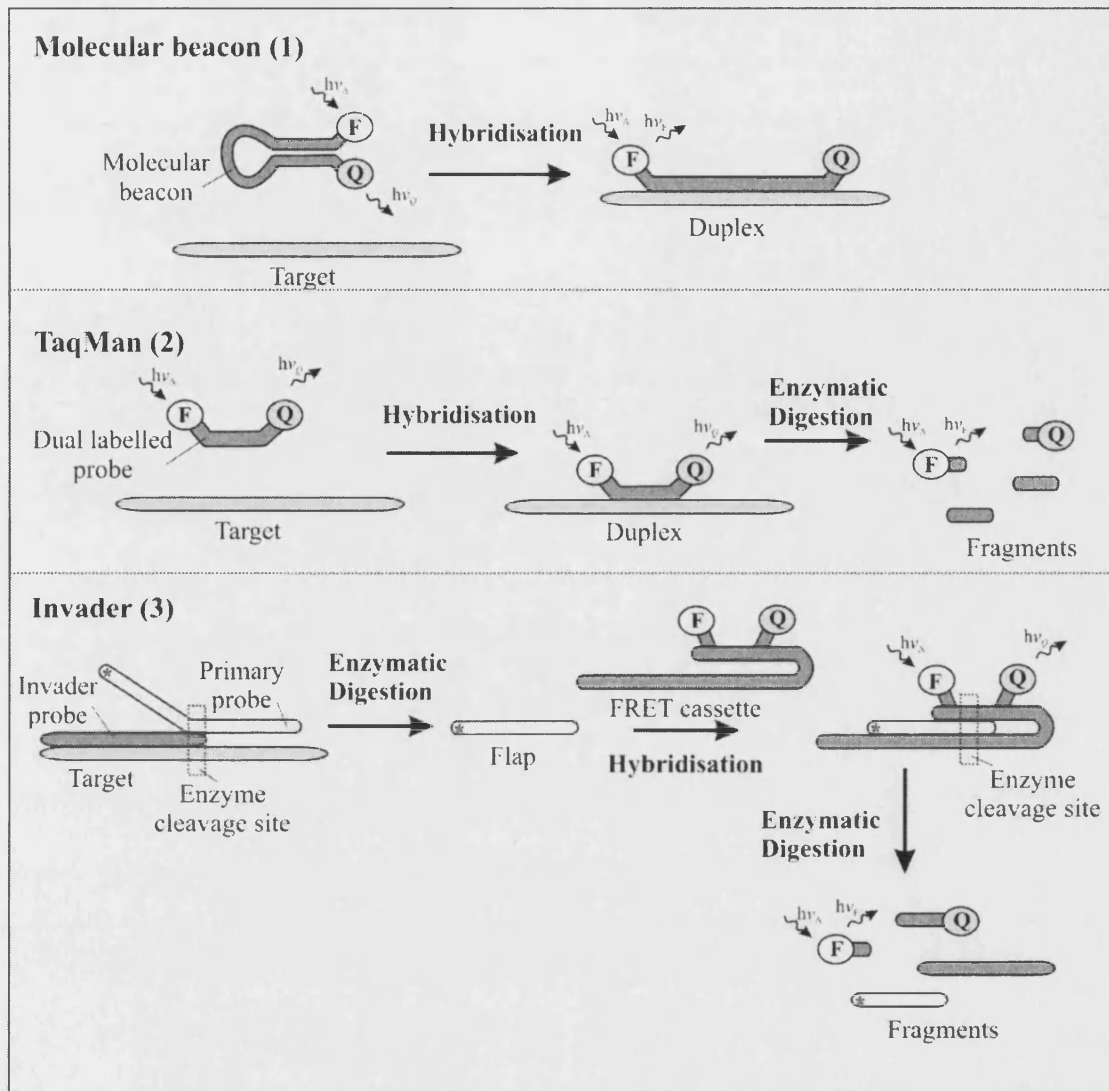
Figure 1.17 - Fluorescent solution based sensor systems.
Molecular beacon approach (method 1). The molecular beacon probe (dark grey) contains a hairpin section (the oligonucleotide contains a self complementary sequence which can hybridise together). The fluorophore (F) and quencher molecule (Q) are in close proximity. The fluorescence of F is quenched by Q through FRET, see section 2.6.1. Hybridisation of the molecular beacon to the complementary target (light grey strand) spatially separates F and Q. F is no longer quenched by Q and its fluorescence is detected. Hence the hybridisation event is detected. TaqMan[R] approach (method 2). A short dual labelled probe (dark grey) has F and Q at separate ends. F and Q are close enough together for FRET quenching and the fluorescence of F is quenched. The dual labelled probe hybridises to the complementary target sequence (light grey strand). FRET still occurs. The Taq enzyme digests the probe, generating oligonucleotide fragments (short grey strands). F and Q are no longer covalently joined and can move apart. F is no longer quenched by Q and its fluorescence is detected. Hence the hybridisation event is detected. The full technique is described in Chapter 2. Invader approach (method 3). The Invader probe (dark grey strand) and primary probe (white strand) hybridise to the complementary target (light grey strand). A Cleavase[R] enzyme digests the triplex at the cleavage site (dotted box) generating a flap fragment (short white strand labelled with *). The flap fragment can hybridise with the FRET cassette which is also present in solution. The FRET cassette contains F and Q close together at one end, the fluorescence of F is quenched by FRET. The FRET cassette: flap fragment triplex is also digested by the Cleavase[R] enzyme at the cleavage site (dotted box), generating fragments. As in method 2, F can now fluoresce and the hybridisation event has been detected.

Specifically the TaqMan® approach is actually a PCR assay, which allows the amplification of a gene sequence (known or unknown) to be followed. A detailed discussion of the TaqMan® approach and its application is given in section 1.7. The Molecular Beacon approach has also been adapted to monitor PCR (Tyagi et al. 1998; Vet et al. 1999; Whitcome et al. 1999). The Invader approach does not require PCR.

Although routine detection of specific genetic sequences is primarily based on the established fluorescence based technology, electrochemical chips are commercially available and may soon be in widespread use.

1.7 *In situ* monitoring of PCR

Polymerase chain reaction (PCR, see section 2.2) is routinely used in biological applications to amplify a desired DNA sequence (the amplicon) from a biological assay, prior to analysis or further manipulation. If PCR is used diagnostically to determine if a gene sequence is present, it can be considered to be a gene sensor. To optimise the efficiency of the technique, sensitive real-time analysis is required, which allows the progress of the PCR to be followed and the end point (the point at which the desired concentration of amplicon has been produced, or at which the target gene has been definitely detected) to be determined. This allows the process to be halted as soon as possible, saving both time and money (Mullis et al. 1994).

The most well established, commercialised technique for real-time analysis of PCR assays is the patented, fluorescence based, TaqMan® system (Applied Biosystems) (Bassler et al. 1995; Livak et al. 1995; Applied Biosystems et al. 2004), shown in Figure 1.18. The TaqMan® approach should be considered as identical to PCR, but with the addition of a dual labelled probe, which allows the progress of the PCR to be followed.
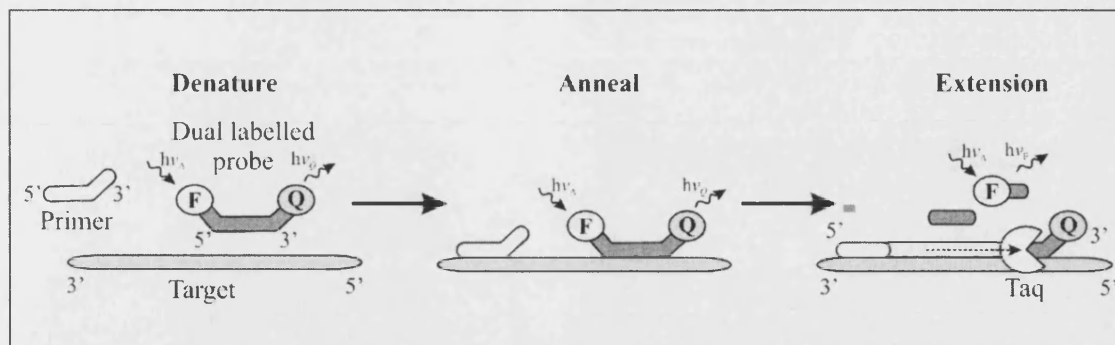
Figure 1.18 – Detail of the TaqMan® sensor (Molecular Probes 2004).
A PCR cycle involves three stages which are repeated: Denature, Anneal and Extension (see section 2.2). In the TaqMan® approach a short dual labelled probe (dark grey), with a fluorophore (F) and quencher (Q) at separate ends, is used in combination with a primer (short white sequence). Initially (denature step) the primer and dual labelled probe are not annealed to the target, but they anneal on cooling (anneal step) to complementary sequences on the target (light grey strand). In both steps the F and Q of the dual labelled probe are close enough together for FRET quenching to occur (see section 2.6.1) and the fluorescence of F is quenched. In the extension step the Taq polymerase enzyme (large white circle) recognises the primer sequence and synthesises a new complementary stand (white strip) in the 5' to 3' direction (direction of dotted arrow). The enzyme digests the dual labelled probe, generating oligonucleotide fragments (short, dark grey strands) and separating F and Q. Separating F and Q which can move apart. F is no longer quenched by Q and its fluorescence is detected. Hence the synthesis of a new complementary strand is detected.

In the TaqMan® system the reporter fluorophore on the dual labelled probe (F) is initially quenched by a quenching fluorophore (Q) also on the probe through Fluorescence Resonance Energy Transfer (FRET). Once the primer and probe have annealed to the ssDNA, the DNA polymerase enzyme (Taq) recognises the primer and moves from it along the strand, laying down a complementary strand and digesting the probe when it reaches it. The separated fluorophore is no longer quenched and fluorescence is seen. As the PCR progresses and the amount of DNA increases exponentially, the fluorescent intensity increases a direct relation to the amount of DNA which has been produced.

This technique is highly effective (Mullis et al. 1994) and since it is solution based, there are no compatibility issues with a sensing surface, which might be experienced with electrochemical sensing.

1.8   Contrasting fluorescence and electrochemical detection

The fluorescent based TaqMan® system works well, but optical (fluorescent) detection has a number of disadvantages. The main issue is that it requires costly, large and sophisticated equipment (de-los-Santos-Alvarez et al. 2004) and consequently, there are commercial opportunities for any technique than can deliver the comparable results more cheaply. Fluorescence is also susceptible to photobleaching (inactivation) of the fluorophore which can affect the sensitivity of the technique (Umek, R. M. et al. 2000; Umek, R.M 2001; Fryer 2002). Electrochemistry also has other potential advantages, which include the ease of miniaturisation, direct electrical read-out and the ability to tolerate opaque samples (Wang, J. 1999; 2002; Drummond et al. 2003).

1.9   Electrochemical DNA hybridisation sensors

The work described in this thesis centres on the development of an electrochemical DNA hybridisation gene sensor, based on enzymatic digestion, which is conceptually similar to the TaqMan® approach. This work must be put into context by the discussion of existing electrochemical DNA hybridisation sensors.

Electrochemical DNA sensing is a wide-ranging and diverse field, which has been most recently reviewed by Drummond and Barton (Drummond et al. 2003), de-los-Santos-Alvarez (de-los-Santos-Alvarez et al. 2004) and Wang (Wang, J. 2002). The following section will discuss, with prominent recent examples, the different approaches with which DNA hybridisation can be detected through electrochemical methods. The approaches are categorised according to the method of electrochemical labelling: direct analysis (no labelling); analysis of non covalent labels and analysis of covalent labels. The labelling categories were introduced, in section 1.4.6, in a general context.

Electrochemical detection requires an electrochemical cell and electrodes, including a Working Electrode (WE, see section 2.5.8). The surface of the WE is often modified with a probe oligonucleotide or alternative materials. The hybridisation event is detected by a change in electrochemical response from the sensing system.

1.9.1 Detection: direct analysis

It was reported by Palecek in 1960 (Palecek 1960) that discrimination, between ssDNA and dsDNA, could be obtained with electrochemical analysis. It is possible to directly measure the oxidation of adenine (de-los-Santos-Alvarez et al. 2002) and guanine (Wang, J. et al. 1995; Wang, J. et al. 1996a; Popovich et al. 2002a) bases of ssDNA immobilised at an electrode surface. When the ssDNA probe is hybridised with its complementary target, the bases are now inside the duplex and the oxidation signal is reduced, which indicated hybridisation (Wang, J. et al. 1996b; de-los-Santos-Alvarez et al. 2002; Meric et al. 2002). However, as there can be up to double the amount of DNA present at the surface, if the hybridisation of the probe and target is totally efficient, this can give sensitivity problems due to high background (hybridisation) responses and non-linear calibration curves (de-los-Santos-Alvarez et al. 2004).

The sensitivity issue has been addressed in a number of ways. Firstly the guanine on the probe can be replaced by inosine bases (guanine without the amine group), which still hybridise with cytosine (Wang, J. et al. 1998; Wang, J. et al. 2001; Meric et al. 2002). As the electrochemical signal for inosine is resolved from that of guanine, the sensitivity is much higher. Secondly, extensive work by Thorp on both ssDNA (Yang, I. V. et al. 2001a) and dsDNA (Johnston et al. 1995; Napier et al. 1997; Yang, I. V. et al. 2001b; Yang, I. V. et al. 2002a) has shown that the guanine oxidation can be mediated (facilitated) by ruthenium complexes. This improves the sensitivity to the extent that SNP mismatch detection is possible. A final approach involves the immobilisation of the probe on a magnetic bead (Palecek et al. 2002; Wang, J. et al. 2002b). After hybridisation with the target, the beads are removed from the solution and treated with acidic solution, this hydrolyses the DNA leaving only the guanine and adenine bases intact. This can then be analysed by voltammetry, see section 2.5, with sensitive results.

1.9.2 Detection: non covalent labelling

Non covalent labelling is based on redox intercalators, which are described below.

Intercalators

Electrochemical hybridisation intercalators are small electroactive molecules which have preferential binding affinities to dsDNA over ssDNA (Wang, J. 1999). The most successful of these intercalators bind into the groove of dsDNA (de-los-Santos-Alvarez et al. 2004).

The properties required for good intercalators have been summarised by de-los-Santos-Alvarez (de-los-Santos-Alvarez et al. 2004). The properties are: the affinity to dsDNA must be very high, with the affinity to ssDNA being as low as possible; the redox potential, detailed in section 2.5.1, should be away from the responses of the nucleobases; the electron transfer must be fast and reversible, see section 2.5.2; both the oxidised and reduced forms of the intercalator must be stable and the intercalator must have low toxicity and cost.

With intercalators discrimination between dsDNA and ssDNA by electrochemical detection is possible as a higher binding affinity of the intercalator to dsDNA results in more of the intercalator being bound. A higher concentration of intercalator is therefore present at the surface and a higher signal is obtained. Discrimination can be aided by a change in the redox potential of the intercalator on hybridisation (Hashimoto 1994; Hashimoto et al. 1998). The exception is methylene blue, whose electrochemical response falls on hybridisation (Erdem et al. 2000; Yang, W. et al. 2002b) as its interaction with guanine is reduced.

A wide range of intercalator molecules have been used and these are comprehensively summarised by de-los-Santos-Alvarez (de-los-Santos-Alvarez et al. 2004). Initial work by Mikkelesen (Mikkelesen 1996) demonstrated that a cobalt complex [Co(bpy)$_3^{3+}$] was an effective intercalator for DNA hybridisation and it enabled the detection of a gene deletion sequence (ΔF508) common to 70% of cystic fibrosis patients (Millan et al.

1994). SNP detection has been demonstrated with $[Co(bpy)_3^{3+}]$ (Wang, J. et al. 1997) and using other intercalators such as Hoecht 33258 (Hashimoto 1994) and daunomycin (Hashimoto 1994; Wang, J. et al. 1996c; Ozkan et al. 2002).

The main advantage of intercalators is that no labelling is required of the target or probe strands. Unfortunately the discrimination obtained between the responses before and after DNA hybridisation is often not good enough for DNA sensing (de-los-Santos-Alvarez et al. 2004). The two exceptions to this are the work by Takenaka (2000), using ferrocenylated intercalators, and the work by Barton (Kelley et al. 1999b), using methylene blue. These will be discussed in detail.

Takenaka: ferrocenylated intercalators

Ferrocene based intercalators have been developed by Takenaka (Takenaka et al. 2000) and successfully applied to SNP detection (Miyahara et al. 2002; Yamashita et al. 2002; Nojima et al. 2003). The first of these was ferrocenylnapthalene diimide (FND), illustrated in Figure 1.19.
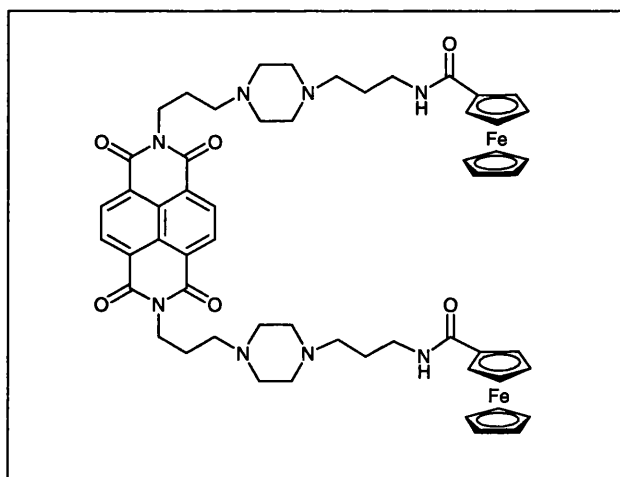
Figure 1.19 - Ferrocenylnaphthalene diimide intercalator (FND) (Takenaka et al. 2000).

The response of the intercalator (FND) is measured with an immobilised probe sequence and then on duplex formation, after the addition of the target, as shown in Figure 1.20. A difference current (response of DNA duplex with intercalator – response of ssDNA probe with intercalator) is reported. As more FND binds to the duplex than the ssDNA the difference increases on duplex formation. SNP detection is possible as

the presence of a SNP in the duplex reduces the amount of FND that binds. The use of difference current is very effective as it takes into consideration the differences in the capture probe surfaces and gives the technique very good reproducibility, by negating systematic bias.
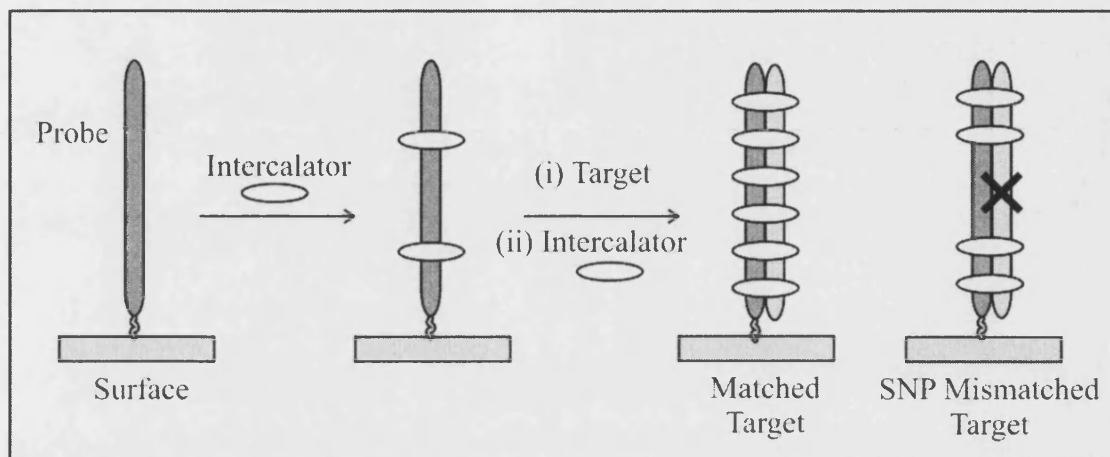
Figure 1.20 - SNP detection by Takenaka.
The thiolated probe oligonucleotide (dark grey strand, left hand side) is immobilised on a gold surface. A short thiol (mercaptohexanol or mercaptoethanol) is added (not shown) to ensure the probe "stands up" into the solution. The intercalator (FND, white disc) is then added to the probe sequence and a response is measured by differential pulse voltammetry (DPV, see section 2.5.7). The target sequence (light grey strand) is introduced and hybridisation occurs, forming the duplex. The intercalator (white disc) is added again and the DPV response is measured. As the intercalator has stronger binding to dsDNA, more FND will bind to the duplex giving an increase in signal. If a SNP mismatch (X) is present in target sequence and hence the duplex (right hand side), fewer FND will be able to bind and the signal will be lower. The difference current (current dsDNA − current ssDNA) is reported.

As the mode of electron transfer to the electrode surface can have a significant effect on the electrochemical response, it will be discussed. Further work by Takenaka using glucose oxidase (Takenaka et al. 1998; Takenaka 2001) proposed the theory that the electron transfer is mediated by the ferrocene moieties. This idea is explained in Figure 1.21. Electron transfer is shown between ferrocene, glucose oxidase and glucose. This cycle is only possible if electron transfer can occur through the ferrocene moieties of the bound FND intercalators in the duplex. If a SNP is present this electron transfer is greatly reduced. Control experiments using FND without the ferrocene moieties also give a low current. By implication the electron transfer occurs in the same way in the earlier experiments.
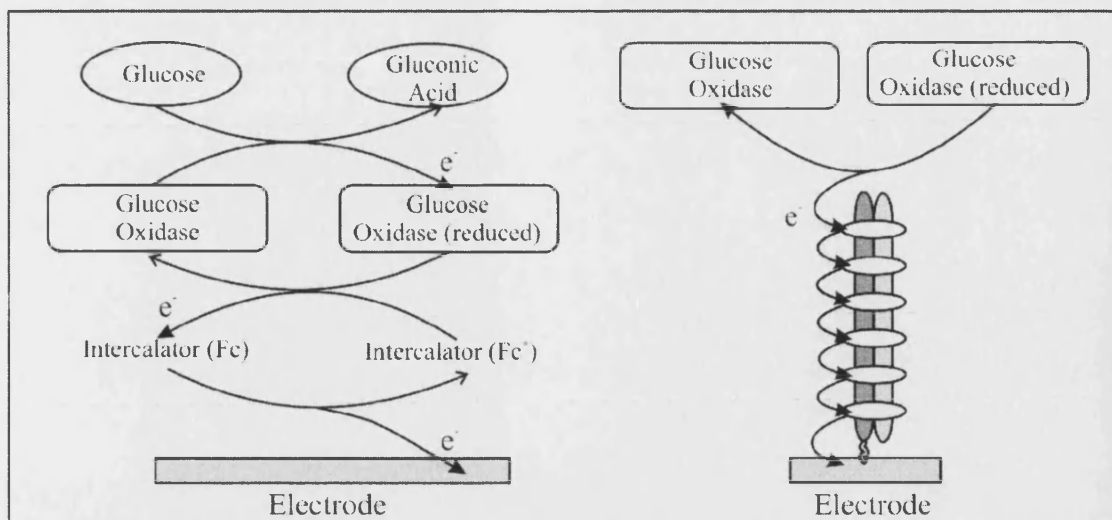
Figure 1.21 – Use of glucose oxidase with FND.
The electron transfer for oxidation (removal of electron) of the ferrocene moieties (Fc) in FND is shown diagrammatically (left hand side). The electron (e⁻) moves in the direction of the full head arrow, whilst the corresponding change of state of the species in solution is shown by the open head arrow. At a high (positive) electrode potential the ferrocene moieties (Fc) in FND are oxidised to ferrocenium ions (Fc⁺). The Fc⁺ is reduced (gain electron) back to Fc, by oxidising the reduced glucose oxidase to glucose oxidase, which in turn allows the reduction of glucose to gluconic acid. If the FND is at the top of the duplex (right hand side) Takenaka suggests that the electron transfer can occur down through the ferrocene of the stacked FND intercalators. This electron transfer is inhibited if SNP mismatches are present in the duplex. The system is analysed using cyclic voltammetry (CV, see section 2.5.3).

Takenaka's work is currently being commercialised into a DNA hybridisation sensor.

Barton: methylene blue intercalator

Barton uses a completely different approach to Takenaka, exploiting the fact that electron transfer can occur through the stacked bases in a DNA helix. The crucial difference between the two approaches is the density of the packing of the DNA film at the surface: Barton uses a tightly packed film, whilst Takenaka does not.

Extensive work by Barton (Kelley et al. 1999a; Kelley et al. 1999b; Drummond et al. 2003) shows that electron transfer readily occurs along dsDNA in a tightly packed film, but is significantly disrupted if SNP mismatches are present, which is shown in Figure 1.22. Under high stringency conditions in different experiments a thiolated probe can hybridise with a complementary target or a SNP mismatched target. Films of these duplexes are then formed on the electrode surface, for each duplex. An intercalator (methylene blue, MB⁺) is introduced to the duplex. Reduction of the MB⁺ (addition of an electron) and the subsequent oxidation of a ferricyanide reporter molecule is only

possible for the fully matched duplex, where the electrical current can flow unhindered to the MB^+. Thus, a detectable signal only occurs for a fully matched duplex and not when a SNP mismatch is present.
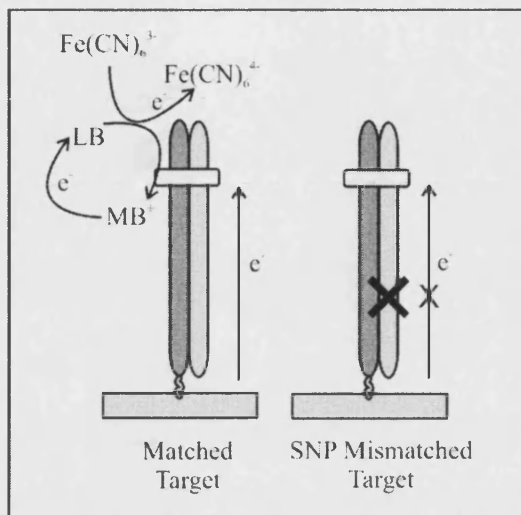
Figure 1.22 - SNP detection by Barton.
A probe oligonucleotide (dark grey strand) containing a terminal thiol group is hybridised in solution with a target (light grey strand). The hybridisation is not shown. High stringency conditions are used which allow the probe to also hybridise with a SNP mismatched target (light grey strand, X is the SNP) in a separate experiment. The duplexes are immobilised onto a gold surface in a buffer containing a high salt concentration, to allow a very tightly packed dsDNA film to form. They are tethered by a terminal thiol group to the surface. The figure shows the fully matched duplex (left hand side) and the film containing the SNP mismatched duplex (right hand side). An intercalator (methylene blue, MB^+, white box) is introduced and due to steric hindrance it can only bind to the top of the dsDNA. When a low voltage is applied to the fully matched duplex current can flow along the DNA reducing the methylene blue (MB^+) to leucomethylene blue (LB), which in turn can reduce ferricyanide in solution, giving a high electrochemical response. The presence of a SNP in the DNA duplex greatly reduces the conductivity of the DNA and therefore a significantly lower current is observed for the ferricyanide reduction.

Good discrimination can therefore be achieved by this technique but there are potential problems. The necessity of duplex formation in solution means the sensing surface cannot be modified in advance. Perhaps more significantly for commercial applications, the use of a tightly packed film prevents the surface being reused. Heating will remove the target, but rehybridisation to form a sufficient duplex density, is not possible due to steric hindrance.

The work by Takenaka and Barton has demonstrated that the use of intercalators can achieve good discrimination for SNP detection. The work highlights issues with surface preparation and electron transfer; the latter is not widely discussed in the literature.

1.9.3 Detection: covalent labelling

Covalent reporter molecules

Covalent reporter molecules are redox active species which are covalently bound to one of the oligonucleotides (typically the target and not the probe), which allow an electrochemical response to be obtained on hybridisation. They must fulfil the same criteria as the intercalators, which were discussed in section 1.9.2, except instead of good intercalation they must be able to readily label the oligonucleotide.

To the author's knowledge, only 5 different types of redox active reporter molecules have been covalently bound to ssDNA oligonucleotide probes, although many derivatives of ferrocene are used. These five reporter molecules are illustrated in Figure 1.23. Particle based labels are discussed later.
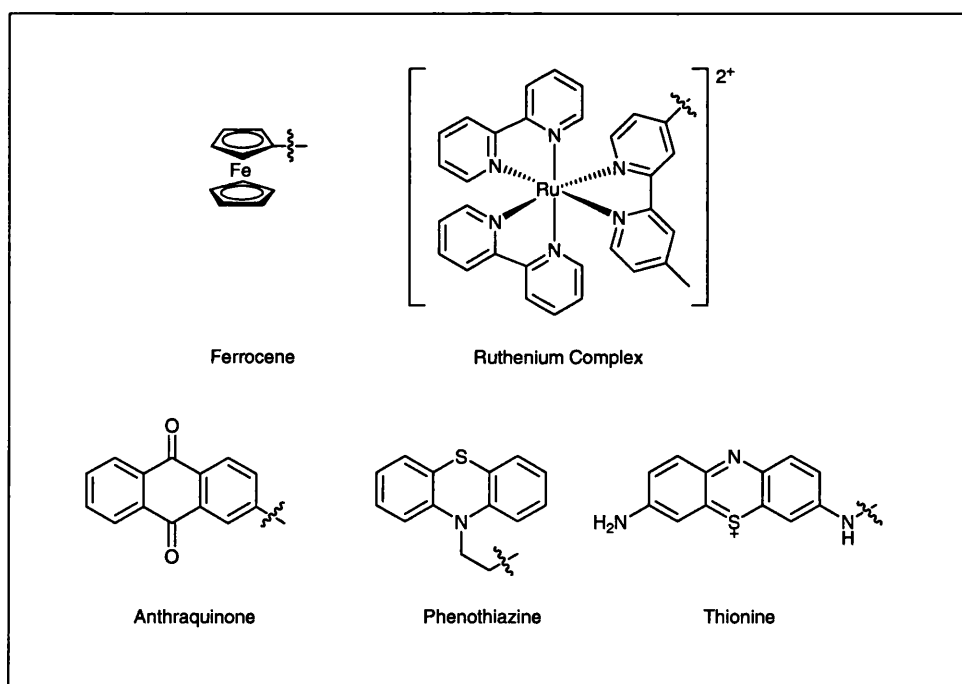
Figure 1.23 – Redox active reporter molecules for covalent labelling.
The reporter molecules are linked to the oligonucleotide through assorted linker molecules with different molecular structures. The wavy line through the bond signifies the start of the linker molecule.

Ferrocene is by far the most widely used reporter molecule and is ideal due to its well understood, robust electrochemistry and convenient synthetic chemistry (Yu et al. 2000). Ruthenium complexes are also very stable and undergo reversible one-electron

oxidations (Verheijen et al. 2000). Grinstaff *et al.* have done significant work on ruthenium labels (Khan et al. 1999; Hu et al. 2000). Metal-free redox active labels have also been developed which use anthraquinone (Kertesv 2000; Tierney et al. 2000a; 2000b), phenothiazine (Tierney et al. 2000b; 2000a) and thionine (Mao et al. 2003).

Oligonucleotides have been labelled in the same way as reporter molecules with redox active particles, which include gold nanoparticles (Cai et al. 2001; Cai et al. 2002; Ozsoz et al. 2003) and metal sulfides (Wang, J. et al. 2003). Techniques have also been developed which precipitate silver on gold nanoparticle labels (Park et al. 2002; Li et al. 2003; Urban et al. 2003).

Covalent labelling will now be discussed for target oligonucleotides and probe oligonucleotides. Covalent labelling of reporter oligonucleotides will then be introduced in sandwich complexes. Finally the use of enzyme labelling will be summarised.

Target labelling

The simplest use of covalent labels is with target labelling. The labelled target hybridises with an immobilised probe, as represented in Figure 1.24, and an electrochemical response can then be detected. The use of low stringency conditions allows this technique to be used for SNP detection; however, covalent labelling of the target is cumbersome and inconvenient for sensor systems. Target labelling, with ferrocene labels, is currently used in studies into the optimisation and understanding of sensor surfaces (Herne et al. 1997; Peterson et al. 2002; Yamashita et al. 2002; Long et al. 2003). It has also been used to demonstrate the possibilities for multiplexing, whereby different target sequences contain different ferrocene labels, whose electrochemical responses can be resolved, allowing them to be detected in the same assay (Mukumoto et al. 2003).
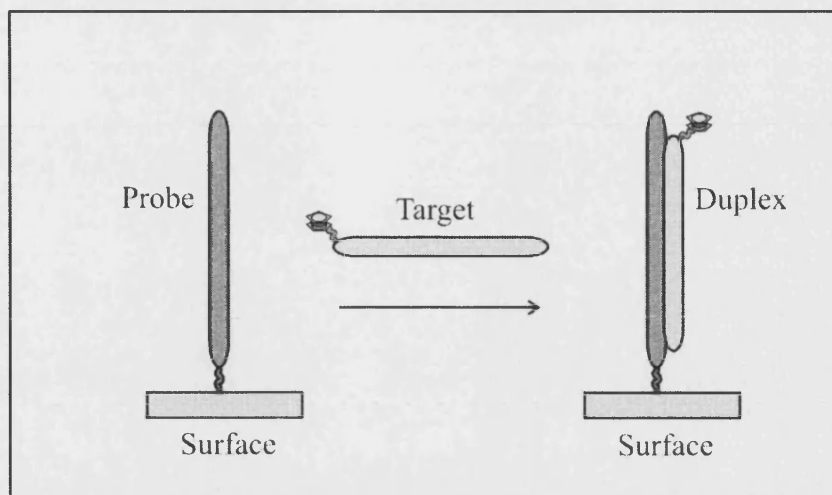
Figure 1.24 - Target labelled hybridisation probes.
The probe (dark grey strand, left hand side) is immobilised on the surface at one end. A complementary target (light grey strand), labelled with ferrocene at one end, hybridises with the probe to form a labelled duplex at the surface (right hand side).

Probe labelling

The use of labelled probes is based on the concept of molecular beacons (Tyagi et al. 1996) which has been introduced in section 1.6.2. Figure 1.25 details the use of a hairpin probe oligonucleotide, which is immobilised on a surface at one end with other end labelled with an electroactive moiety. Hybridisation of the hairpin probe with a complementary target oligonucleotide removes the electroactive moiety from the surface, greatly reducing its signal. This has been illustrated with ferrocene (Fan et al. 2003) and thionine (Mao et al. 2003) electroactive labels.
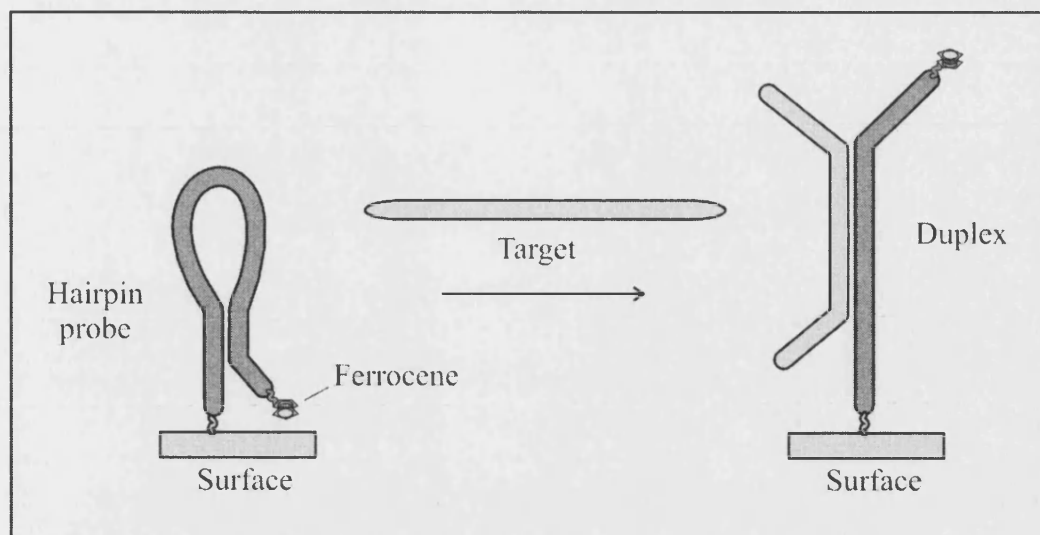
Figure 1.25 - Electrochemical hairpin probe (Fan et al. 2003).
The hairpin probe (dark grey loop) is immobilised onto the surface at one end and ferrocene labelled at the other. The complementary sequence (bottom) is shorter then the length of the loop. Electrochemical analysis with Cyclic Voltammetry (CV, see section 2.5.3) gives a high response for the ferrocene label as it is held near the surface. Hybridisation of the target (light grey strand) with the loop section of the probe, breaks the hairpin to form the more stable duplex (right hand side). In the duplex the ferrocene label is moved much further from the electrode surface and the CV response is greatly reduced.

Whilst the probe labelling approach has the advantage that it does not require any labelling of the target oligonucleotide, care must be taken experimentally as reduction of electrochemical response indicates a positive result (i.e. that hybridisation has occurred). Hence problems with the surface or fouling could give a false positive response.

Sandwich complexes

Sandwich complexes involve the use of a surface immobilised probe oligonucleotide, which is able to hybridise with a target oligonucleotide/reporter oligonucleotide duplex. Electrochemical sandwich complexes were developed by Ihara (Ihara 1997; Nakayama et al. 2002) and are described in Figure 1.26.

In Ihara's approach, the gold surface is modified with a thiolated ssDNA capture probe. The complementary target oligonucleotide is not directly labelled, but is first hybridised with a small ferrocenylated reporter oligonucleotide in solution. Hence, when the complementary target hybridises with the capture probe at the surface this event can be detected through electrochemical analysis (Differential Pulse Voltammetry, DPV, see

section 2.5.7). With a mismatched sequence the bulky mismatched target/reporter oligonucleotide duplex does not hybridise and therefore the ferrocene moiety cannot reach the surface, due to electrochemical repulsion and steric bulk. Despite the added complexity of requiring two successive hybridisation steps the high discrimination between the samples has been argued to justify the approach (Nakayama et al. 2002).
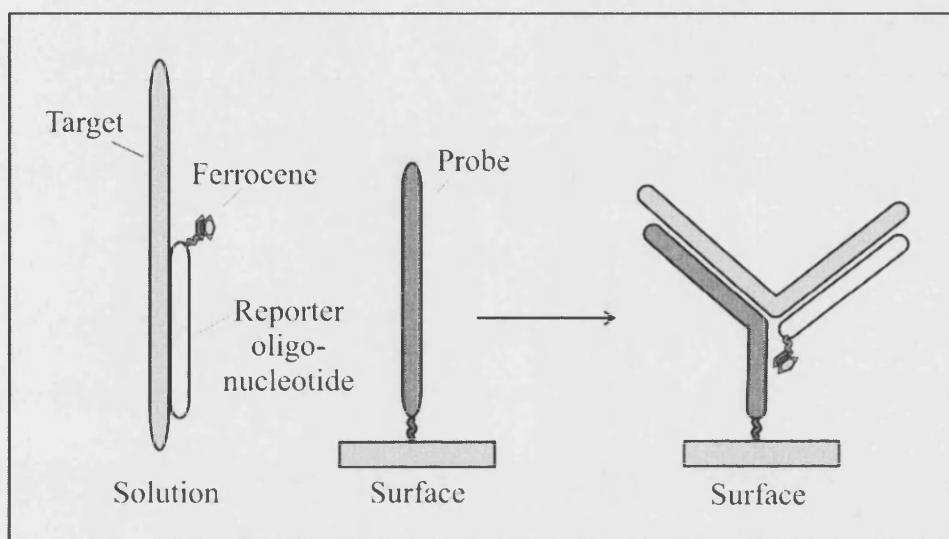
Figure 1.26 - Ferrocenylated reporter molecules.
The target oligonucleotide (light grey strand) hybridises with the smaller, ferrocene labelled reporter oligonucleotide (white strand) in solution. The probe oligonucleotide (dark grey stand) is immobilised on a gold surface through a thiol linkage. The target/ reporter oligonucleotide duplex is introduced to the probe modified surface. The probe hybridises with another sequence on the target. The ferrocene on the reporter oligonucleotide is now held at the surface and can be detected by electrochemical detection. In this work (Nakayama et al. 2002) the target/ reporter oligonucleotide duplex is only 7 bp long, but discrimination is obtained between a matched and SNP mismatched target sequence at cool temperatures (5 to 10 $^\circ$C).

This work was developed by the CMS group from Motorola (Yu et al. 2000; Umek, R.M 2001; Yu et al. 2001) who made a number of improvements. The first of these improvements was to introduce compounds called molecular wires, which are illustrated in Figure 1.27, to the sensor surface. A range of these wires have been studied by Creager (Creager et al. 1999) and Cygan (Cygan et al. 1998). As the name suggests, these are long molecular chains which are able to easily conduct electricity, therefore improving the ease with which the ferrocene moieties on the reporter moieties can be oxidised. Without these wires the ferrocene must either reach the surface of the electrode, which is unlikely, or the electron transfer is inefficiently mediated along the oligonucleotide probe.
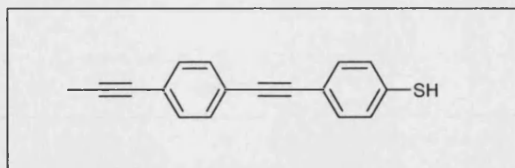
Figure 1.27 - Thiol terminated oligophenylethynyl molecular wire.

The Motorola CMS eSensor™ chip, which uses molecular wires in combination with a thiol terminated polyethylene glycol blocking layer, is shown in Figure 1.28.
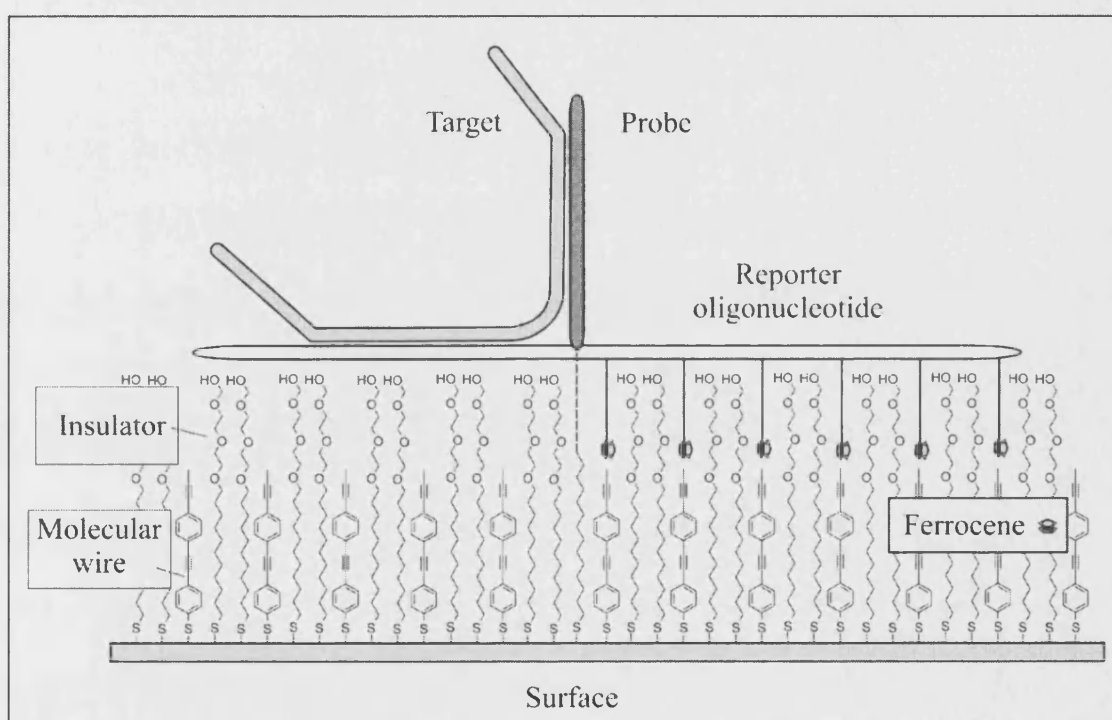
Figure 1.28 - Motorola CMS eSensor™ chip.
The chip uses a sandwich complex. The reporter oligonucleotide (white strand) and target (light grey strand) hybridise in solution. The probe oligonucleotide (dark grey strand) is immobilised on the surface (dotted line to alkyl chain, with thiol end group). The surface also contains insulator molecules and molecular wires. The target/ reporter oligonucleotide duplex is introduced to the probe modified surface and the probe hybridises with another sequence on the target. The multiple ferrocene labels on the reporter oligonucleotide now have access to the surface, via the molecular wires, and can be detected by electrochemical detection. If the probe/ target hybridisation does not occur, the reporter oligonucleotide is not brought close to the surface and the ferrocene moieties are insulated from the surface.

To optimise the sensitivity the reporter oligonucleotide was synthesised with multiple ferrocene labels through the incorporation of ferrocenylated phosphoramidite nucleobases. This approach is discussed in section 3.2.3.

47

The selectivity of the eSensor^{TM} chip is also sufficient for SNP detection (Yu et al. 2001). This SNP detection is illustrated in Figure 1.29 by using two reporter oligonucleotides, one of which is fully complementary to the oligonucleotide sequence of the matched target sequence, whilst the other is fully complementary to the SNP sequence. The two reporter oligonucleotides have different ferrocene labels, which give a response at different electropotentials (electropotential is described in section 2.5.7). Due to this, the addition of a matched, or SNP mismatched, target sequence gives a different electrochemical response, which will allow discrimination to be possible between the two sequences.
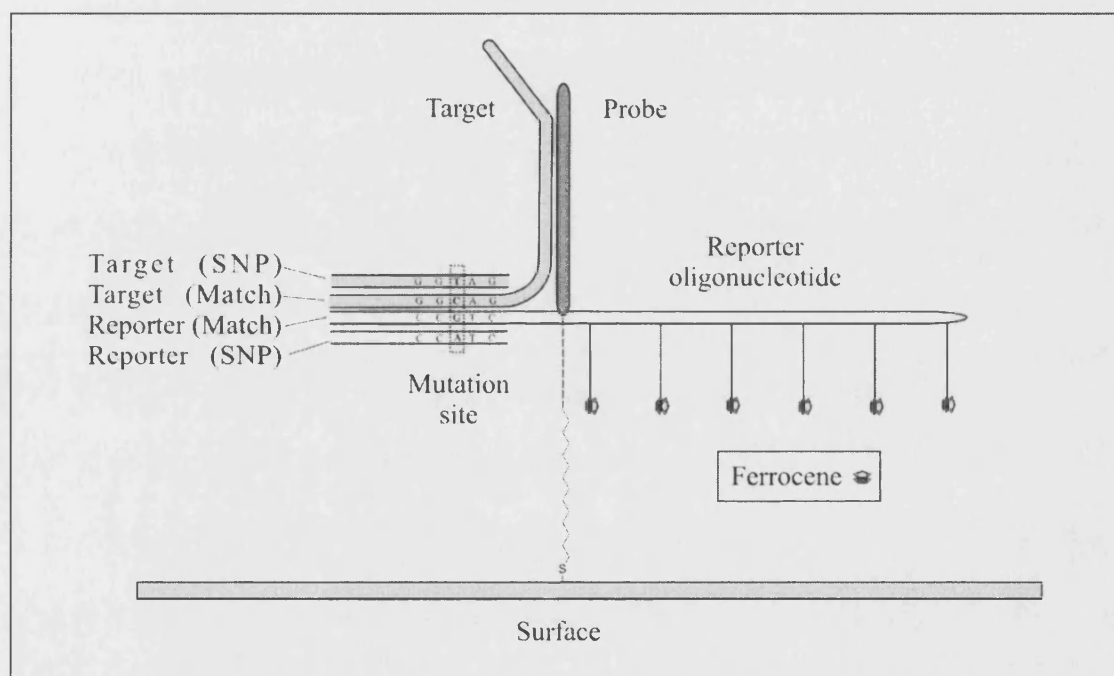
Figure 1.29 - SNP detection with the Motorola CMS eSensor^{TM} chip.
This is a simplified diagram of the chip illustrated in Figure 1.28, with the surface modifications omitted for clarity. Detection of matched target: the matched target (light grey strand) is added to a 50:50 mixture (in 5 to 10 fold excess) of the matched and SNP mismatched reporter molecules (white strands). Only a section of the SNP reporter strand is shown. The reporter molecules have different ferrocene labels. The target binds to the matched reporter molecule. The sample is then allowed to hybridise for 4 hours at the sensor surface and on electrochemical analysis only a response from the matched reporter molecule is obtained. Detection of SNP mismatched target: use of the SNP mismatched target is the same procedure exclusively gave a response from the SNP reporter molecule. No wash step was needed in either case. SNP detection is possible. It should be emphasised that the target oligonucleotides (Match and SNP) are identical apart from the base at the SNP mutation site (dotted box).

The ability of the chip to provide SNP detection can be rationalised by considering the relatively stability of the matched and SNP mismatched target/ reporter oligonucleotide duplexes. The mismatched duplex has a lower Tm (less stable) and therefore the

matched duplex will form in preference. As the reporter oligonucleotides are in excess of the target, no SNP/ target duplex will remain and therefore it will not be detected.

The chip technology is being commercialised by Motorola as CMS eSensor™ (Umek, R.M 2001). It has the ability to detect 48 different sequences in simultaneously.

Nanoparticle sandwich complexes

Ozsoz has developed a sandwich sensor complex, using a colloidal gold nanoparticle label on a reporter molecule (Ozsoz et al. 2003). The high number of gold atoms in the nanoparticle gives a high response for the gold oxidation with Differential Pulse Voltammetry (DPV, see section 2.5.7) and gives the technique high sensitivity.

An alternative approach uses metal sulfide (ZnS, PdS or CdS) nanoparticle labelled reporter molecules (Wang, J. et al. 2003). The probe sequence is immobilised on a magnetic bead and then allowed to hybridise with first the target and then the reporter oligonucleotide. The beads can then be magnetically removed from solution and dissolved. The reduction of the metal ions (M^{2+}) to the metal (M) is then measured. The three labels allow three sequences to be simultaneously detected.

Gold nanoparticles have been used to label reporter oligonucleotides (Park et al. 2002; Li et al. 2003). Probe oligonucleotides are immobilised on a surface between two electrodes. After target and reporter molecule hybridisation, silver is precipitated on the gold nanoparticles. The silver causes a connection to be formed between the two electrodes, giving a detectable decrease in resistance. This is being commercialised (Urban et al. 2003).

Enzyme labelling

It is also possible to covalently bind an enzyme, such as horseradish peroxidase (HRP), to the reporter oligonucleotide (deLumley et al. 1996; Alfonta et al. 2001). The enzyme can then either be used to directly to measure the hybridisation, through its reduction (deLumley et al. 1996), whereby hydrogen peroxide is used to oxidise the enzyme

which is then electrochemically reduced, or indirectly whereby the enzyme is used to oxidise a soluble molecule, causing its precipitation on the electrode, which changes the electrochemical properties of the system (Alfonta et al. 2001). A full discussion of this work is outside the scope of this thesis.

Generally, it has been shown that there are three broad categories of methods for electrochemical DNA detection and that these categories each contain a range of different approaches. The choice of method is determined by the exact aims and constraints of a project.

1.10 Development of electrochemical gene sensor

The TaqMan® technique (introduced in section 1.6.2) can, in theory, be directly adapted for electrochemical detection by interchanging the fluorophore for a redox active moiety, as shown in Figure 1.30.
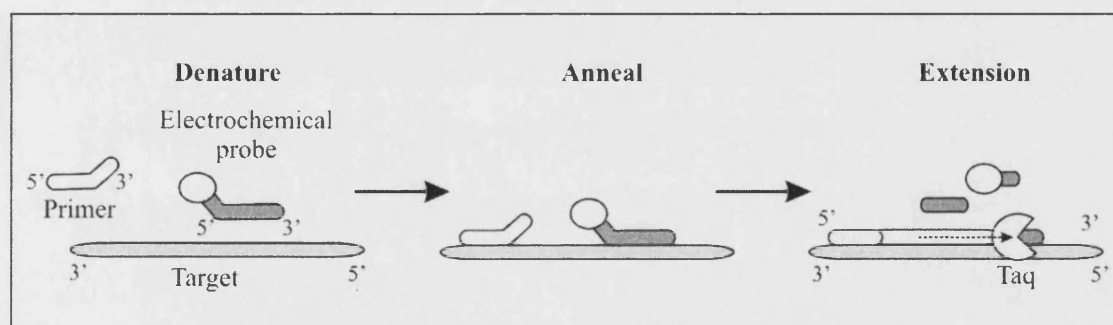
Figure 1.30 - Proposed electrochemical PCR probe.
The PCR cycle has been described in Figure 1.18. In this case the probe (dark grey strand) contains an electroactive label (white circle). In the extension stage (right hand side) the enzyme digests labelled probe, generating oligonucleotide fragments (short, dark grey strands; only two are shown) one of which contains the electroactive label.

Under PCR conditions, both primer and probe anneal to the complementary target DNA and the DNA polymerase enzyme (Taq) digests the probe whilst synthesising the complementary strand, producing digestion fragments. The digestion fragment containing the electrochemical label, as shown in Figure 1.30, is clearly shorter, and hence contains fewer oligonucleotides, than both the undigested probe (denature step) and the hybridised probe (duplex, anneal step). If this difference alters the

electrochemical signal of the electroactive label, then it should be possible to follow the progress of the PCR electronically and realise the project aims.

1.10.1 Choice of electrochemical labelling approach

The fluorescent TaqMan® method and the analogous electrochemical approach, introduced above, both use covalent labelling of a probe oligonucleotide with a reporter molecule. For completeness the direct and non-covalent methods of electrochemical detection, introduced in section 1.9, should be discussed before they are dismissed.

No direct methods have been reported as they rely on the hybridisation event and in the course of the PCR there is repeated cycling between ssDNA and dsDNA in solution. It is also likely that electrode fouling and poor sensitivity, amongst other factors, would inhibit this approach.

No non-covalent labelling methods have been reported as they also rely directly on the hybridisation event, with the intercalators binding preferentially to dsDNA over ssDNA. The repeated cycling between ssDNA and dsDNA would also be a major problem. Even if a difference could be engineered, the unbound reporter molecule would be able to readily reach the electrode surface giving a high background response, which would swamp any effect.

Hence the use of electroactive labels covalently bound to the probe DNA appears to be the only viable approach for this technique, as enzymatic digestion irreversibly generates small labelled fragments which can be electrochemically detected.

1.10.2 Choice of electrochemical label

The requirements for the electrochemical probe for this research project are:

- Novel (to avoid patent restrictions).

- Sensitivity to electrochemical detection.

- Robust synthetic route with good yield.

- Variation in electropotential of labels (preferably from analogues when a synthetic route has been developed).

- Stable under PCR conditions.

- Inexpensive.

It was thought that the use of a ferrocene label should allow these requirements to be fulfilled.

To be a covalent label the ferrocene moiety is attached to the oligonucleotide by a linker molecule, shown in Figure 1.31. In this work the labelled oligonucleotide is called a probe oligonucleotide.
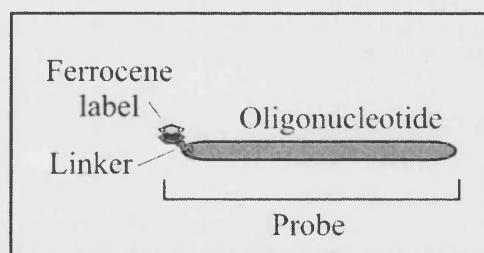
Figure 1.31 - Component parts of a probe oligonucleotide.

It is useful to consider a linker molecule covalently labelled with ferrocene as a ferrocene derivative instead. This is because a synthesis of the ferrocenylated linker molecule will usually be based around a ferrocene derivative, rather than synthesising the linker molecule and coupling it with ferrocene in the final step.

1.10.3 Ferrocene based biosensors: justification of the use of ferrocene

Ferrocene has the potential to fulfil all the criteria for a reporter molecule given in section 1.10.2. The following are discussed in detail in later sections: the sensitivity of ferrocene to electrochemical detection in section 3.1.2, the synthetic routes to the ferrocene derivatives in section 3.3 and the control over the electropotential of the ferrocene through synthetic variation in section 3.1.3.

The proven applicability of ferrocene derivatives to biological sensor systems must be illustrated. Their use in DNA sensors, through incorporation in intercalators has been described in section 1.9.2, followed by their use as covalent labels for DNA probes, which is introduced in section 1.9.3 and discussed in greater detail in section 3.2.

In a more general sense ferrocene and its derivatives have been used in biosensor systems as enzyme mediators, in particular for glucose sensors. Glucose sensors are important as the blood glucose levels of diabetes sufferers must be determined rapidly. Accurately and precision are paramount as is the need for a convenient approach to allow the condition to be managed. Typically this was achieved by following the oxidation of glucose, which is shown in Scheme 1.1 and catalysed by the glucose oxidase (GOD) enzyme (Wingard 1983). Glucose levels are determined through the electrochemical oxidation of the hydrogen peroxide which is generated.

$$\text{Glucose} + O_2 \longrightarrow \text{gluconic acid} + H_2O_2$$
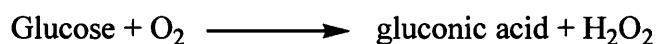
Scheme 1.1 - Oxidation of glucose by oxygen.

Variation of the oxygen concentration in whole blood sample produces fluctuation in the electrode response, which often necessitates dilution of the sample with an oxygenated buffer (Cass et al. 1984). To avoid this additional step further amperometric detection methods were developed which were not dependent on the oxygen concentration.

Oxygen is a mediator in electron transfer to the GOD enzyme and therefore alternative mediators were investigated. Ferricyanide [$Fe(CN)_6^{3-}$] (Schlapfe et al. 1974) and organic dyes (Aleksandrovskii et al. 1981) were initially used but the dyes often have problems due to rapid autoxidation, cytotoxicity, instability in their reduced form and pH dependant redox potential (Cass et al. 1985). The high solubility of the ferricyanide made it difficult to immobilise with the enzyme at the electrode and control was not possible over its electropotential. Ferrocene derivatives in contrast have well behaved electrochemistry and control is possible over both the physical properties and electropotential of the mediators (Cass et al. 1985).

The mechanism of action of the mediators is described in Figure 1.32. The mediators serve to activate the reduced form of the enzyme, by oxidising it.
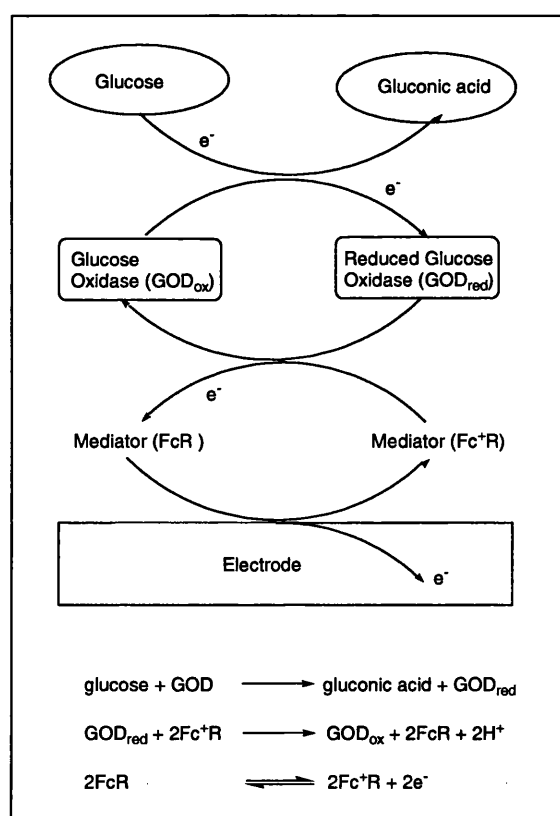
Figure 1.32 - Action of mediators in glucose sensing

This mediation was shown to be successful for ferrocene and 5 derivates (Cass et al. 1984) and these are illustrated in Figure 1.33. Incorporation of the enzymes and 1,1'-dimethylferrocene at the electrode surface allowed a successful glucose sensor to be fabricated.
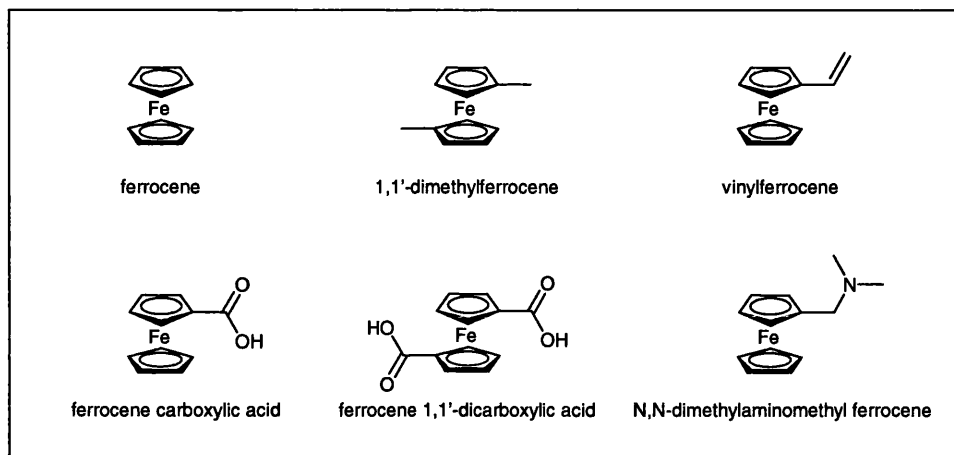
Figure 1.33 - Ferrocene and ferrocene based mediators

Substantial work has been undertaken to continue the development and optimisation of the ferrocene mediated glucose sensors (Sakakida et al. 1993; Sha et al. 1993; Mizutani et al. 1994; Padeste et al. 2003; Ghica et al. 2005). Furthermore the use of ferrocenylated mediators can be applied to other oxido-reductase enzymes (Cass et al. 1985; Boujtita et al. 2000; Padeste et al. 2003) and other sensor systems, including immunoassays (Gleria et al. 1986).

1.10.4 Enzymatic digestion

The TaqMan® approach to generate small ferrocene labelled oligonucleotide fragments involves the complexity of a PCR assay. The approach will be developed sequentially from less complex assays, using alternative enzymes: ssDNA specific S1 nuclease and dsDNA specific T7 exonuclease. These enzymes are described in section 5.4.

1.11 Aims of thesis

The aim of the thesis is the development of an electrochemical DNA hybridisation gene sensor, based on enzymatic digestion, which if successful, could be applied to *in situ* PCR (Polymerase Chain Reaction) detection. To realise this aim, the following must be achieved:

- Synthesis of novel ferrocenylated linker molecules to label probe oligonucleotides (Chapters 3 and 4).

- Labelling of probe oligonucleotides with linker molecules and the successful use of these probes as gene sensors (Chapters 5 and 6).

After the gene sensor has been developed the following will be undertaken:

- Surface modification of the electrode surface to improve the sensitivity of the sensor (Chapters 7 and 8).

Specific aims for the attainment of these goals are given, in detail, at the start of each of the theory chapters (Chapters 3, 5 and 7).

1.12 Structure of thesis

The thesis describes the development of a DNA hybridisation gene sensor based on enzymatic digestion. The background is given in Chapter 1, followed by the experimental theory and methods in Chapter 2. There then follow three distinct studies, each of which is presented as a specific theory chapter followed by a results chapter. These are: "Probe design and synthesis" in Chapters 3 and 4; "Development of DNA hybridisation probes" in Chapters 5 and 6 and "Surface supported DNA hybridisation probes" in Chapters 7 and 8. Specific conclusions and future work are given in each of the results chapters, with overall conclusions in Chapter 9. In more detail the structure of the thesis is as follows:

- **Chapter 1** introduces the concept of electrochemical DNA hybridisation gene sensors. The structure and function of DNA are described to highlight the role and importance of DNA genes. The hybridisation properties of DNA are detailed and these can be harnessed by hybridising a target gene sequence with a complementary probe sequence. Existing DNA hybridisation probes are discussed in detail, together with their application to genetic sequencing and gene detection. Much existing technology is based on fluorescence detection and this is discussed with emphasis on the enzymatic digestion methods, especially TaqMan[®]. As electrochemical detection is considered a viable alternative to fluorescence a detailed evaluation of existing electrochemical detection methods is given. This allows the potential for an enzyme based detection system, similar to TaqMan[®], to be realised, which utilises electrochemical detection together with ferrocene labelled DNA probes.

- **Chapter 2** details the experimental methods and theory used the thesis. Specific details are given of the organic synthesis and biological assays, together with the theory behind all of the techniques used.

- **Chapter 3** gives theory and rationale behind the design and synthesis of novel linker molecules. These are ferrocenylated molecules which will be used to label probe oligonucleotides. Different labelling approaches exist and two types of linker

molecules are synthesised. The majority of the linker molecules are designed for post-labelling and the characteristic electropotentials of these linkers were measured. A phosphoramidite linker molecule was also synthesised. The results for this work are given in **Chapter 4**.

- **Chapter 5** gives specific theory behind electrochemical DNA hybridisation probes based on enzymatic digestion. Selected linker molecules (from Chapter 4) are used to label probe oligonucleotides and are subjected to enzymatic digestion assays of increasing complexity, until a DNA hybridisation gene sensor has been developed. A progression of digestion assays are used to validate the hybridisation gene sensor, which is a TaqMan® mimic. The mode of action of the enzymes used in this work is also studied. The results for this work are given in **Chapter 6**.

- **Chapter 7** gives the theory and rationale behind an alternative approach to increase the sensitivity of the gene sensor, by using a surface modified electrode. Work is undertaken with a fluorescent based system to validate this approach. The results for this work are given in **Chapter 8**.

- **Chapter 9** provides an overview of the development of the gene sensor technology and gives the overall conclusions to the work.

Chapter 2: Experimental theory and methods

2   Experimental theory and methods

2.1   Overview

This chapter details the experimental theory (part A) and detailed experimental methods (part B) which were utilised during the course of this study.

The understanding of Polymerase Chain Reaction (PCR) is ultimately very important to this work and is discussed first. The analytical techniques used in the development of the gene sensor are then described: gel electrophoresis; UV spectroscopy; electrochemical detection and fluorescence. Electrochemical detection using voltammetry is the main detection technique and the theory behind it is discussed in section 2.5. This allows a clear understanding to be gained of Differential Pulse Voltammetry (DPV), which is the main analytical technique used in this work and is specifically described in section 2.5.7. Fluorescent analytical techniques are used in sensor systems to corroborate the results observed from electrochemical detection. Common fluorescent techniques are introduced together with the necessary theory concerning the quantification of fluorescence and the exploitation of Fluorescent Resonance Quenching (FRET). In short, all the relevant experimental techniques are introduced and explained.

The synthetic methods are given for the synthesis of the novel linker molecules, together with their characterisation. The specific details are given as Protocols for the determination of electropotentials, in section 2.9, for the biological assays used for gene sensing, in section 2.10, and for the surface supported work, in section 2.11.

PART A: Experimental theory

2.2   Polymerase Chain Reaction (PCR)

PCR is a routine biological technique that is used to make a huge number of copies of a desired gene sequence (Mullis et al. 1986). Its mode of action is well described in standard biology textbooks (Alberts et al. 1994; Mullis et al. 1994; Brown 1995a) and will be summarised here.
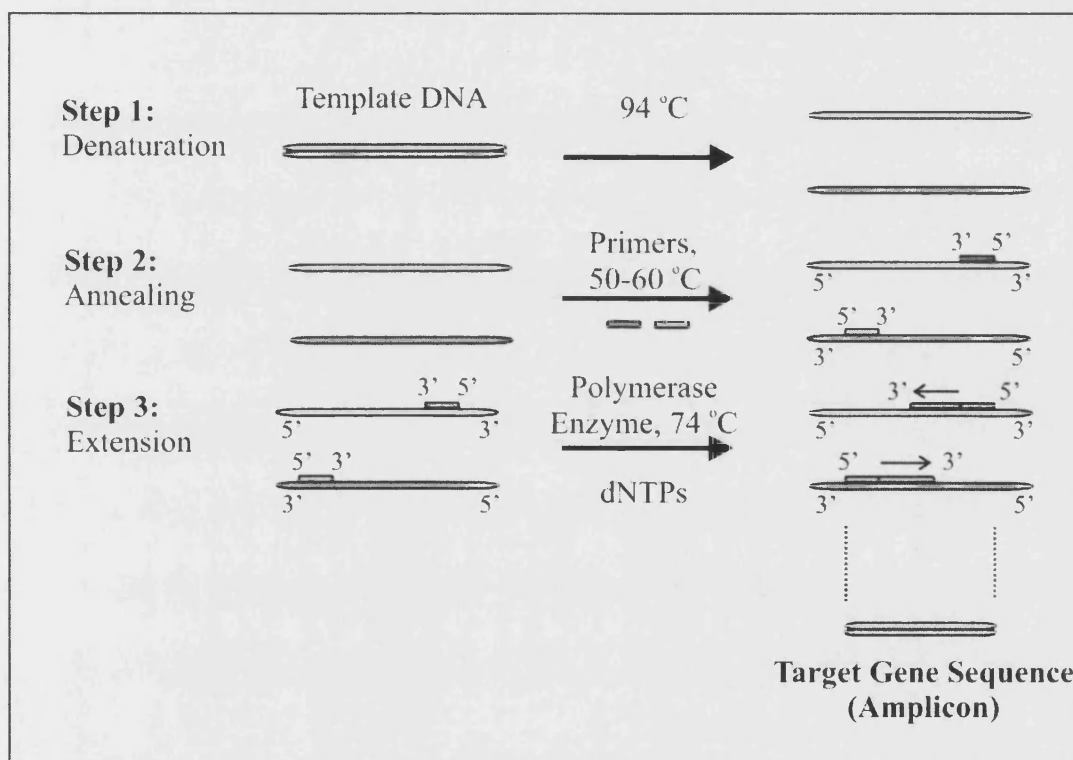
Figure 2.1 – Polymerase Chain Reaction (PCR).
The PCR contains three consecutive steps which are repeated (cycled) by a variation of assay temperature. Step 1 - Denaturation: template DNA is heated and denatures. The light grey strand is fully complementary to the dark grey strand. Step 2 - Annealing: at a lower temperature primer sequences (short grey strands) anneal to fully complementary sequences on the denatured template DNA. The light grey primer is fully complementary to a section of the dark grey denatured template. Step 3 - Extension: the DNA polymerase enzyme extends the complementary strand from the primer, using the dNTPs (deoxyribonucleoside triphosphates) 5' to 3' direction, until the end of the template sequence. This occurs for both template strands. One template DNA sequence produces two copies of the gene sequence. The temperatures given for each step are typical (Brown 1995a), but can be varied. The annealing temperature should be 1-2 °C lower than the melting temperature (Tm) of the primer/template duplex.

The technique involves three steps which are repeated (cycled) until the desired amount of the gene sequence has been synthesised. These steps are detailed in Figure 2.1. A

61

PCR assay contains the template DNA (the DNA which contains the gene sequence to be amplified), two primers (these short oligonucleotide sequence define the edges of the gene to be amplified, there is one for each template strand), the four different deoxyribonucleoside triphosphates (dNTPs; these are building blocks for DNA, one for each DNA base) and DNA Polymerase (the enzyme which extends the DNA strand from the primers, this is from a thermophilic bacterium so that it doesn't denature on heating).

Repeating the thermal cycling repeats the cycle. Each cycle exponentially increases the amount of the target gene sequence, as shown in Figure 2.2, allowing a large amount of the sequence to be rapidly produced.
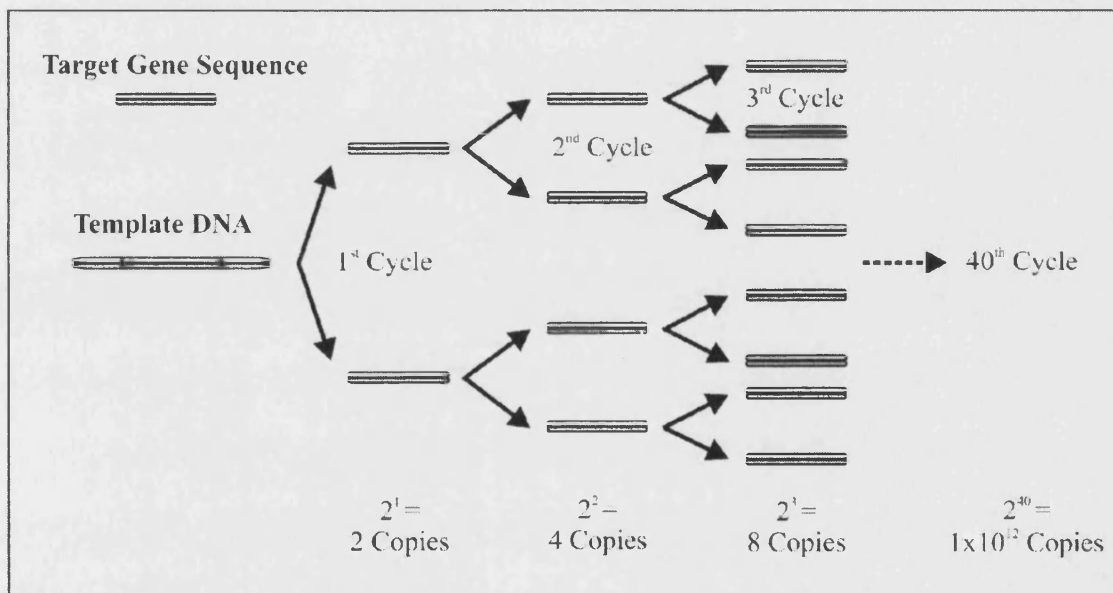
Figure 2.2 - PCR target gene sequence amplification.
The target gene sequence is shown as a short duplex, which is present in the template DNA. Each cycle of PCR doubles the number of target gene sequences present. Hence after n cycles there are 2^n copies of the gene sequence. This is an exponential increase. Typically a maximum of 40 cycles of PCR are undertaken.

It should be noted that in the extension step the polymerase continues extending the complementary strand until the template strand finishes. Therefore in the early cycles of PCR many of the amplicons produced will be duplexes larger than, but containing, the target gene sequence. By the third cycle exact target sequence duplexes are synthesised and these quickly swamp the others in the following cycles.

In terms of size, the oligonucleotide primers are short (15 to 20 nucleotides) and the amplified gene sequences are substantially longer (20 to 2000 nucleotides). The template DNA must incorporate the gene sequence, but can be significantly larger than it, for example human genomic DNA can be used, which has 50×10^6 to 250×10^6 nucleotides per chromosome (Alberts et al. 1994) and a total of 3×10^9 nucleotides overall (Brown 1995a).

Problems can occur with PCR and therefore PCR assays must be analysed to ensure that the desired gene sequence has been amplified. No product can be obtained if the quality of the DNA is poor, if one (or both) of the primers is badly designed and does not fit or if there is too much of the initial template. Alternatively, if one of the primers can anneal to the wrong place, such as an alternative complementary sequence too close the second primer, then the amplicon can be too short. If both primers can anneal to different locations then a range of amplicons, including the desired amplicon, can be produced.

Primer design will not be discussed here as only established protocols are followed in this work. However, for human genomic DNA a 17 bp primer is the shortest primer which should not, on average, give any duplicate primer sites. Duplicate attachment sites occur every 4^n bases (n = number of bases in primer), which is 17×10^9 for the 17 bp primer, over 5 times the length of the template DNA (Brown 1995a).

Gel electrophoresis is a common, well established, method for the analysis of PCR products.

2.3 Gel electrophoresis

Gel electrophoresis is a technique which has the ability to separate DNA sequences by size and then to quantify the length of these sequences, by comparison against a standard (ladder). This has applications for the analysis of PCR products and the study of enzymatic digestion of DNA samples (Alberts et al. 1994; Brown 1995a).

Theory

Electrophoresis involves the migration of a charged species, through solution, when an electric field is applied. The rate of migration depends on the shape and charge to mass ratio of the species involved. However, as most DNA molecules have a very similar shape and charge to mass ratio, molecules of different sizes will not be separated.

Separation by size is possible in gel electrophoresis, whereby the sample DNA migrates through a gel, rather than solution. The gel is typically agarose or polyacrylamide and contains a complex network of pores, through which the DNA has to pass. The smaller DNA molecules are less hindered by the pores and able to migrate more readily, affording size separation from the larger molecules. The composition and size of the gel determines which DNA molecules can be readily separated. Increasing the amount of agarose or polyacrylamide in the gel, decreases the pore size and allows smaller DNA samples to be separated (Brown 1995a).

Practical considerations

The technique has three stages: preparation and loading of the gel; running of the electrophoresis and visualisation of the DNA.

- Preparation and loading of the gel

This study uses agarose gels. The agarose solid is dissolved in a hot aqueous buffer solution and poured into a tank to set (Figure 2.3). A comb at one end of the gel forms wells in the gel, which remain when it is removed.
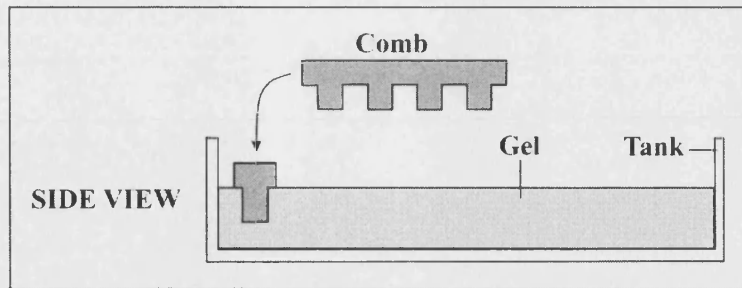
Figure 2.3 – Schematic preparation of an agarose gel.
A solution of agarose solidifies in a tank, containing a comb, to form the gel. The comb shown forms 4 adjacent wells.

- Running of the electrophoresis

The gel is placed in the electrophoresis tank and immersed in buffer (Figure 2.4), which must be the same buffer as was used to make the gel. Each DNA sample is prepared by the addition of a "loading buffer" which contains a small, charged dye molecule (such as bromophenol blue, New England Biolabs) to allow the progress of the electrophoresis to be seen. A detergent (such as SDS, sodium dodecylsulfate) ensures that all the DNA strands are ssDNA and a heavy substance, typically glycerol, to prevent the sample from floating out of the well. The DNA samples are now injected (loaded) to the bottom of separate wells and a DNA ladder is also loaded in a well at the edge. The ladder contains DNA fragments of known sizes to allow the size of the sample DNA to be determined.
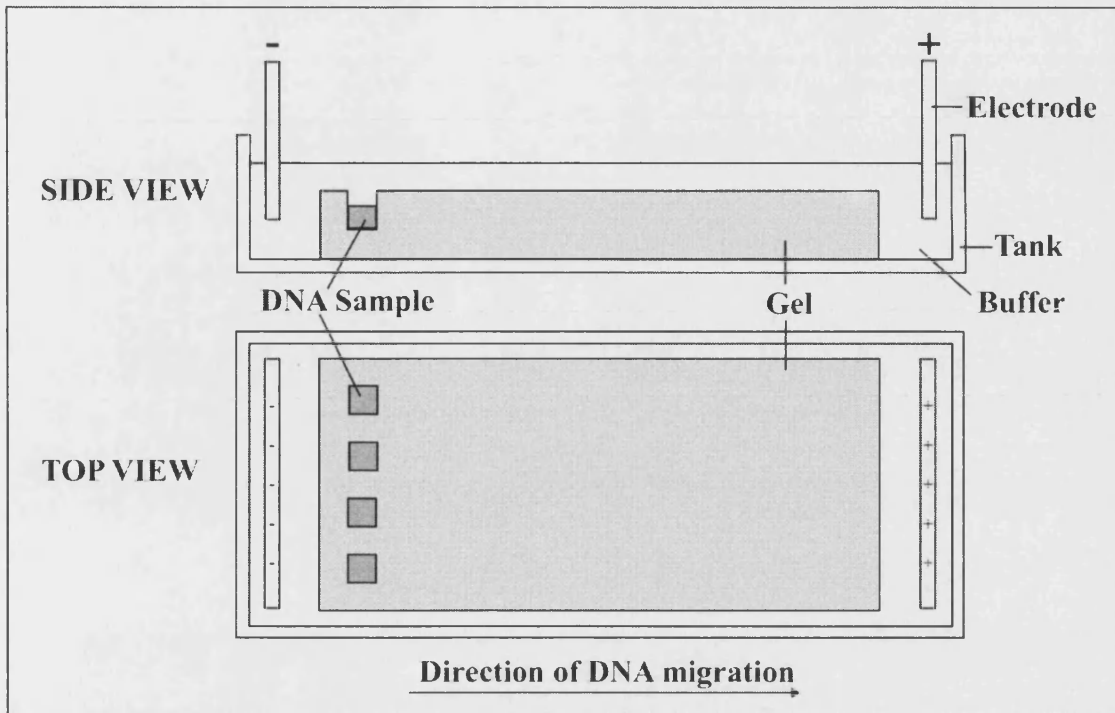
Figure 2.4 - Gel electrophoresis (before application of electric field).
The agarose gel (light grey) is immersed in buffer. DNA samples (dark grey) have been loaded into each well. The two electrodes are shown at either end of the tank. On the application of the electric field the DNA will migrate (left to right) towards the anode (positive electrode).

A potential is applied to the gel and the DNA samples migrate through the gel towards the positive electrode, as shown in Figure 2.5. The DNA cannot be visualised at this stage, so the progress of the dye along the gel is followed. The electrophoresis is stopped before the dye reaches the edge of the gel.
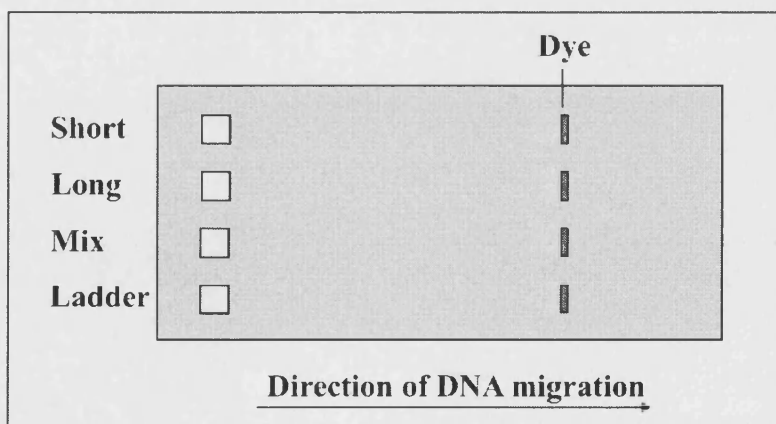
Figure 2.5 - DNA separation by electrophoresis.
On the application of the electric field, the DNA migrates through the gel (left to right), leaving the wells (white boxes) empty. The DNA cannot be seen, but the small dye molecules (dark bands) move the faster than the DNA through the gel and allow the progress of the gel to be followed. The gel is stopped before the dye reaches the edge of the gel

• Visualisation of the DNA

On completion of the electrophoresis the DNA must be visualised. The most straightforward way to visualise the gel is to stain it using a molecule which binds non-specifically to DNA. Ethidium bromide is traditionally used, but newer assays, such as SYBR Gold (Molecular Probes), have been developed which claim to work more effectively. Other methods of visualisation, such as using radioactive labelling of DNA before analysis, are also used (Brown 1995a).

After staining the gel is washed and the bands of DNA are then visualised under ultraviolet irradiation. The presence of different band indicates different sizes of the DNA molecules in the sample and these can be approximated by comparison to the DNA ladder, as shown in Figure 2.6.
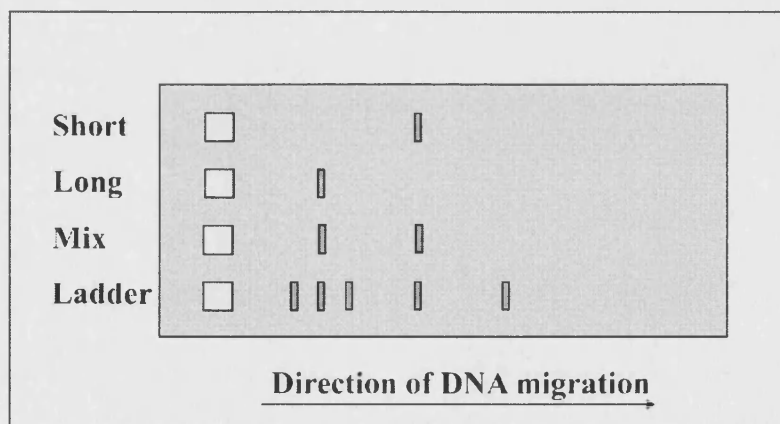
Figure 2.6 – Visualisation of the gel.
The DNA is visualised (grey bands) under ultraviolet irradiation, using an indicator. The shorter DNA molecules (top well) were able to move more quickly and therefore moved further through the gel than the longer DNA molecules (top middle well). The two sizes of DNA molecules can be resolved (bottom middle well). A ladder containing DNA molecules of different (known) lengths (bottom well) allows the size of the DNA molecules in the above wells to be quantified.

For a successful standard PCR one DNA band of the desired gene size is obtained. For an enzymatic digestion of DNA the initial large strand of DNA should disappear.

Gel electrophoresis is an effective method for determining the success of PCR and the success of enzymatic digestion reactions.

2.4 UV spectroscopy of DNA

As ssDNA absorbs UV light at $\lambda = 260$ nm the concentration of ssDNA oligonucleotides in solution can be determined by UV spectroscopy (Blackburn et al. 1996).

After synthesis the oligonucleotides supplier (Sigma Genosys, UK) measures the weight and UV absorbance (OD, optical density) of the oligonucleotide sample in a 1 mL cuvette using a 1 cm light path length. Hence, the weight per optical density (μg/ OD) is reported. The concentration of the oligonucleotide after labelling is then readily determined using the same experimental set-up, by using Equation 2.1.

$$[\text{Oligonucleotide}] = \text{OD} \cdot \frac{\mu g}{\text{OD}} \cdot \frac{1}{\text{MWt}} \cdot \frac{1}{1000} \tag{2.1}$$

Determination of oligonucleotide concentration: [Oligonucleotide] = oligonucleotide concentration (μM); OD = optical density and (μg/OD) = mass per OD and MWt = molecular weight.

2.5 Electrochemical detection: voltammetry

The electrochemical analysis in this study is undertaken using voltammetry; specifically differential pulse voltammetry (DPV), with ferrocenylated oligonucleotides. The electrochemical cell is described, followed by the theory behind voltammetry.

2.5.1 Voltammetry: the electrochemical call

Voltammetry concerns the interrogation of a redox active species, through the measurement of electrode current as a function of voltage applied to the cell.

Voltammetry will be discussed in relation to the analysis of ferrocene. A redox couple contains an oxidised and a reduced form of a redox active species. The redox couple between ferrocene (Fc) and the ferrocenium ion (Fc^+) is shown in Figure 2.7.
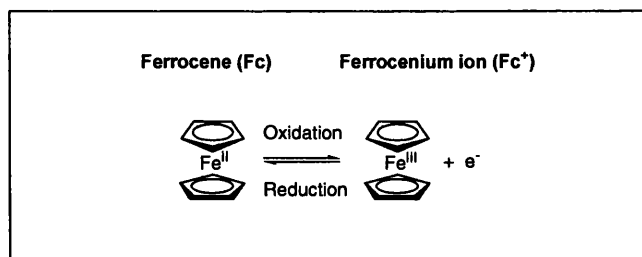
Figure 2.7 – Ferrocene redox couple.

The electrochemical cell

A three electrode electrochemical cell was used for the electrochemical measurements and is illustrated in Figure 2.8. The cell contains two electrodes through which the current flows, which each have opposite polarity (charge). The measured potential is the sum of the electrochemical reactions occurring at the two electrodes. For electrochemical sensing the electrode of interest is the one at which the ferrocene oxidation or reduction occurs (working electrode: WE) but any variation in the electrochemical behaviour at the other electrode (counter: CE) will cause the cell potential (i.e. the measured potential) to vary. To overcome this, the CE is made of an inert material (typically platinum). A self contained electrode, with an invariant (constant) cell potential (reference electrode: RE) is held near the WE. The potentiostat is then able to vary the current applied to the CE to ensure that the potential between the WE and RE is maintained at the desired value. The RE does not draw any current.
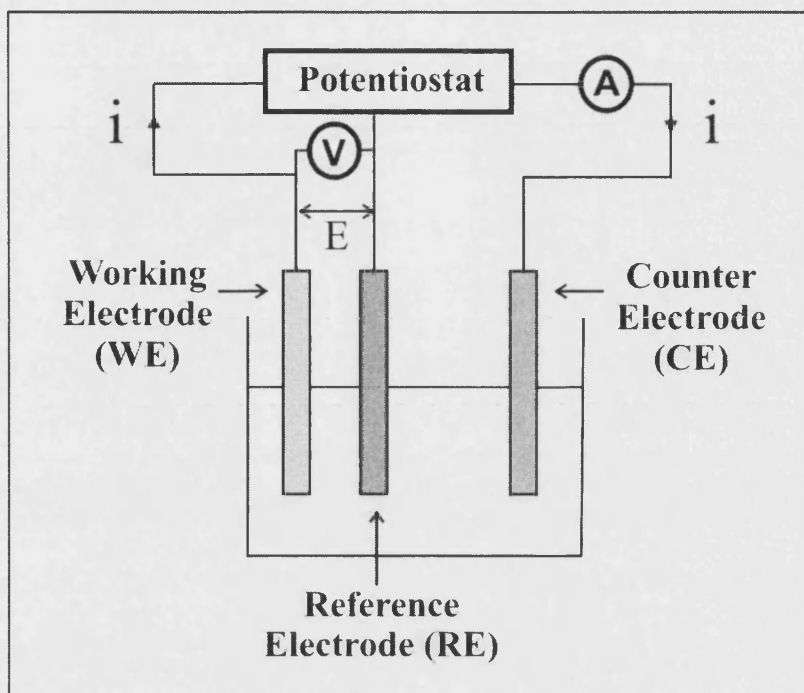
Figure 2.8 – A three electrode electrochemical cell.
The cell contains three electrodes: Working Electrode (WE); Reference Electrode (RE) and Counter Electrode (CE). These are placed in a solution containing the analyte and a background electrolyte. The potentiostat is a device which is able to vary the potential (E) applied to the WE in relation to the RE. The potential is measured with a voltmeter (V). Varying the potential of the WE causes a current (i) to flow from the WE to the CE. The current is measured by the ammeter (A).

Reference electrode

Historically the Standard Hydrogen Electrode (SHE) RE was used which has the potential (by definition) of 0 V, under standard conditions (298.15 K, 10^5 Pa H_2(g), 1M HCl) (Atkins 1990). The reduction potential of a redox active species is the applied voltage which is required to reduce it (i.e. add electron(s) to it). The SHE is cumbersome to use, so an alternative silver/silver chloride RE is often used which is + 0.196 V relative to SHE (298.15K, 3M KCl) (Bard et al. 2001). The relationships are schematically summarised in Figure 2.9.

Standard Hydrogen Electrode

$Pt|H_2(g)|H^+(aq)$

$2H^+(aq) + 2e^- \rightarrow H_2(g) \qquad E^\theta = 0\ V$

Silver/Silver Chloride Electrode

$Pt|H_2(g)|H^+(aq)||Cl^-(aq)|AgCl(s)|Ag(s)$

$AgCl + e^- \rightarrow Ag + Cl^-$

$E = + 0.196\ V\ (298.15\ K,\ 3\ M\ KCl)$
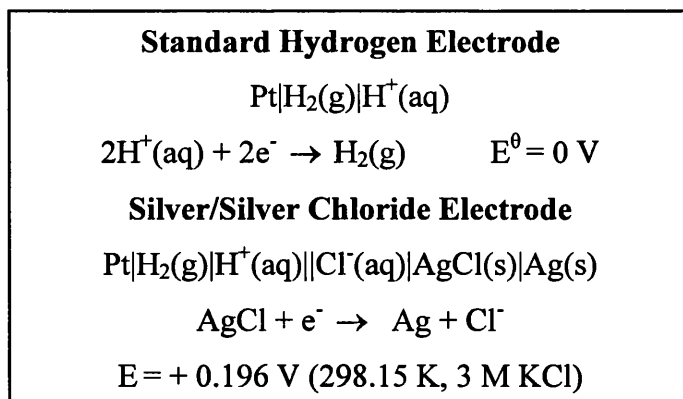
Figure 2.9 – Reduction potentials.

2.5.2 Voltammetry: theory

The theory behind voltammetry can now be considered. Voltammetry concerns the interrogation of a redox active species, through the measurement of electrode current as a function of voltage applied to the cell.

For analysis to occur, the redox active species must first reach the working electrode (WE), through mass transport, before it can undergo electron exchange, as shown in Figure 2.10. Three different mass transport mechanisms are possible, which are: diffusion; migration and convection (Fisher 1996). Diffusion involves the movement of the species, towards lower concentration, along a concentration gradient. Migration is the transport of a charged species in an electric field and convection is the transport of species by hydrodynamic transport, such as thermal motion and stirring. The effect of migration is routinely suppressed by using a background electrolyte, such as an inactive salt, which is present at higher concentrations (at least one or two magnitudes) than the redox active species. The effect of convection is minimised if the potential of the system is quickly changed, whilst the solution is kept at a constant temperature and not stirred or agitated. The electron transfer kinetics are determined by the quality and type of the electrode and should be much faster than the mass transport. In this instance the system is said to be under diffusion control.
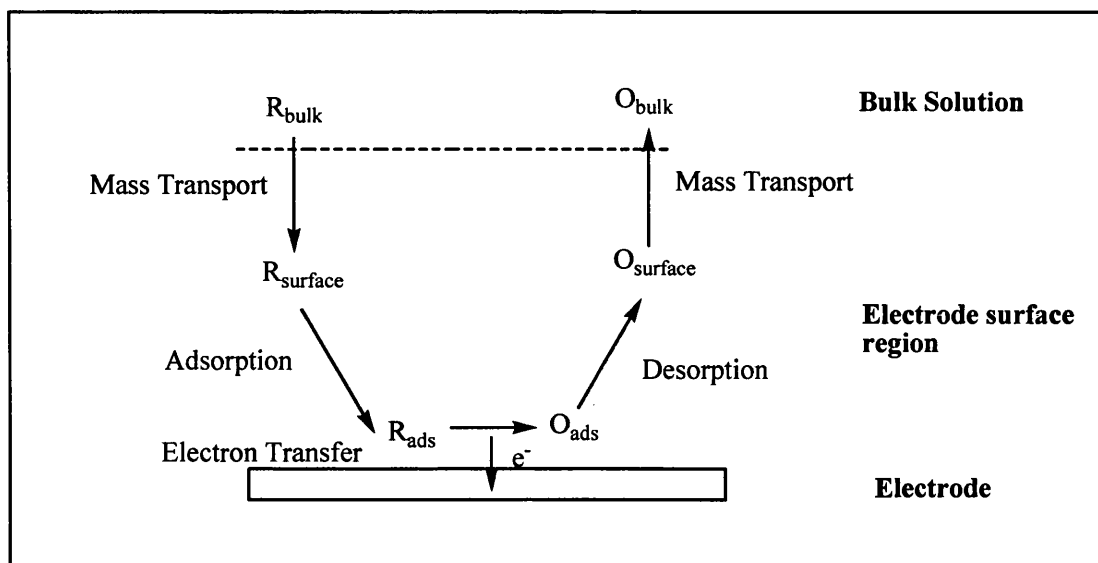
Figure 2.10 - Electrode oxidation pathway.
The reduced species in the bulk solution (R_{bulk}) undergoes mass transport to reach the electrode surface region ($R_{surface}$). $R_{surface}$ is adsorped onto the electrode surface (R_{ads}). R_{ads} is oxidised through electron transfer to the electrode, generating the adsorped oxidised species (O_{ads}). O_{ads} is desorped into the electrode surface region ($O_{surface}$) and undergoes mass transport into the bulk solution (O_{bulk}).

2.5.3 Linear Sweep Voltammetry (LSV)

The oxidation of a ferrocene species, in a diffusion controlled system, is considered. When the voltage is swept between V1 (low potential, no electrode reaction) and V2 (potential higher than oxidation potential, fast ferrocene oxidation) a characteristic trace is produced, as described in Figure 2.11 (Bard et al. 2001).
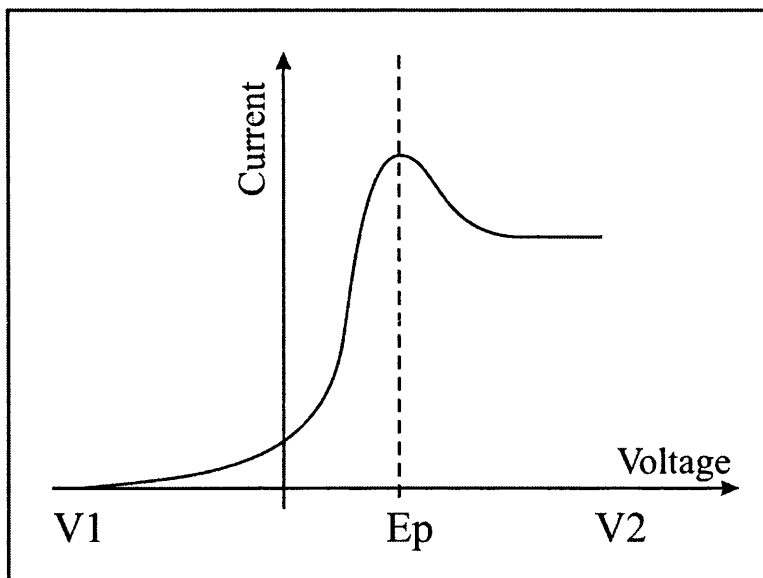
Figure 2.11 - Linear Sweep Voltammetry.
The voltage is swept from the initial voltage (V1) to a final (more positive) voltage (V2) and the current response is measured. A characteristic electropotential peak (Ep) is obtained when the ferrocene is oxidised.

The shape of the graph is explained by considering the behaviour of the ferrocene close to the electrode, which is shown in Figure 2.12. At potentials close to V1 there is a high concentration of ferrocene at the electrode, but it is oxidised very slowly. As the potential is increased the ferrocene is oxidised more quickly, whilst the distance over which depletion occurs increases slowly. At the Electropotential (Ep) all the ferrocene at the electrode is oxidised very quickly and a current spike is seen. As the voltage is increased further the depletion distance increases and the current falls. When the diffusion layer thickness reaches a constant value, diffusion limited current is obtained. Cyclic voltammetry (CV) is a variation of this technique where the potential is swept in one direction and then in the reverse direction.
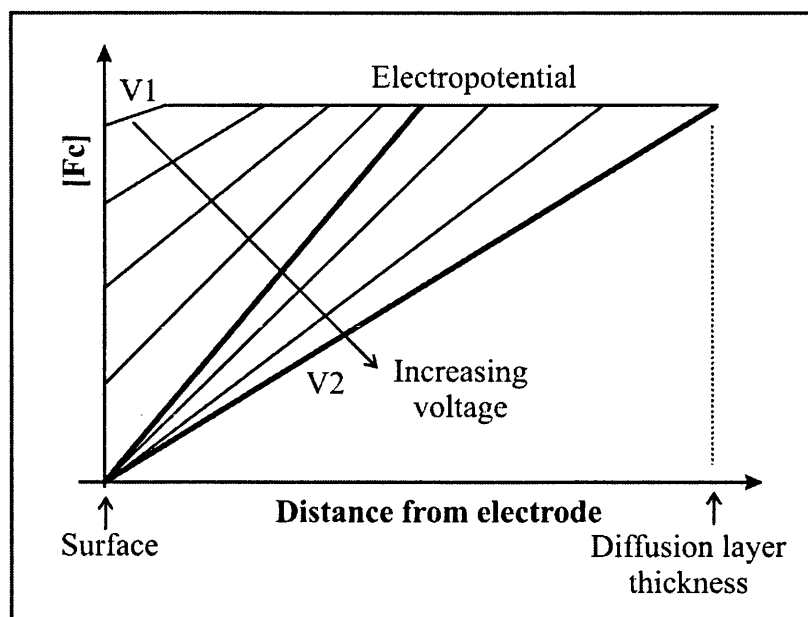
Figure 2.12 – Explanation of LSV peak shape.
The figure shows the variation in the concentration of ferrocene [Fc] as a function of distance from the electrode surface, for different voltages (8 separate graphs are shown). The gradient of the graph is very important as a high gradient indicates rapid diffusion (mass transport) of ferrocene to the electrode surface. In the LSV voltage sweep the voltage is increased from V1 (top left hand graph) to V2 (right hand side, bold graph). Initially the voltage (V1) is low and the surface concentration of ferrocene is high. The ferrocene is not readily oxidised and the current is very low (kinetic control). As the voltage increases the ferrocene at the surface is oxidised more rapidly than the solution is depleted of ferrocene, hence the concentration gradient and therefore the LCV current increases. At the electropotential (middle bold graph) the potential is sufficiently high that any ferrocene at the surface is oxidised (hence zero surface concentration) and the concentration gradient is at its highest. This gives the maximum peak current. As the potential is increased the solution continues to be depleted of ferrocene faster than it can be replenished and the concentration gradient falls, causing a fall in the LSV current. Throughout the voltage sweep ferrocene depletion has occurred further into solution. At the diffusion layer thickness (dotted line, right hand side), the rate of depletion along the concentration gradient equals the rate at which the ferrocene is replenished from bulk solution. This gives a constant diffusion limited current.

For any sensing technology reproducibly high sensitivity and selectivity are crucial. Sensitivity is defined as the ability to resolve an analyte peak from the background current, whilst the selectivity is the discrimination between the response for the positive and control assays.

The Faradaic peak current (i_p) for ferrocene in LSV is given in Equation 2.2 (Fisher 1996).

$$i_p = 0.4663^{3/2} AFD^{1/2} v_s^{1/2} [Fc]_{bulk} \left(\frac{F}{RT}\right)^{1/2} \qquad (2.2)$$

i_p = Faradaic peak current, A = electrode area, F = Faraday constant, D = diffusion coefficient, v_s = sweep rate, $[Fc]_{bulk}$ = ferrocene concentration in bulk solution, R = gas constant and T = temperature.

Hence the peak current (i_p) is proportional to sweep rate (v_s) ($i_p \propto v_s^{1/2}$) and can be increased by increasing the sweep rate, as shown in Figure 2.13.
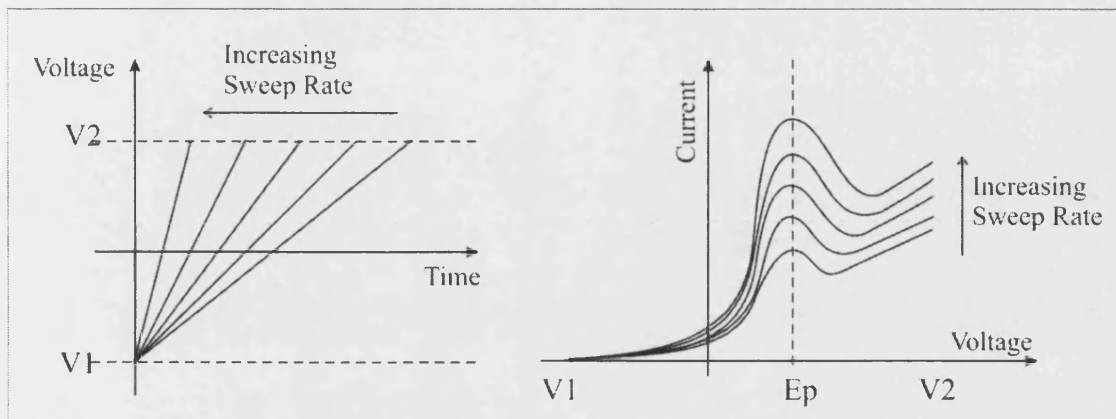
Figure 2.13 – Variation of Linear Sweep Voltammetry trace with sweep rate.
Increasing the sweep rate between the initial voltage (V1) and the final voltage (V2) is shown in relation to time (LHS graph). Increasing the sweep rate increased the current peak intensity at Electropotential (Ep) (RHS graph) (Fisher 1996).

However, the sensitivity will only increase to a certain point as a capacitive charging current (see section 2.5.4), from the background electrolyte, will also increase and swamp the signal.

The peak current is also directly proportional to the electrode area, as shown in Equation 2.2, but again increasing the area also increases the capacitive charging current, limiting the maximum sensitivity.

2.5.4 Development of voltammetry

To improve the sensitivity of the system the capacitive charging current should be understood and minimised. To achieve this, the capacitive double layer will be introduced and explained.

Modelling the interface

The existence of the capacitive charging current can be explained by the formation of a charge Double Layer at the electrode interface. When an electrode is polarised (i.e. when a potential is applied at the start of a voltammetry sweep) ions of an opposite

charge will line up at the surface. The Double Layer is defined as the entire array of charged species and orientated dipoles existing at the electrode/solution interface (Bard et al. 2001). The description is misleading as it only loosely resembles two layers.

The Double Layer was initially modelled by Helmholtz at the start of the 20th century and his model was refined by Gouey and Chapman and then later by Stern (Fisher 1996). These methods give a good understanding of the Double Layer and modern methods, which use statistical mechanics, will not be discussed.

The Double Layer can be modelled using solvated ions, in Figure 2.14 (Bard et al. 2001). In this model, illustrated with a negatively charged electrode, solvated cations are non-specifically adsorbed at the solvated electrode surface, at a position described by the Outer Helmholtz Plane (OHP). There is a sharp potential drop from the electrode surface to the OHP. The remaining potential drop occurs more slowly to solvated cations in solution.
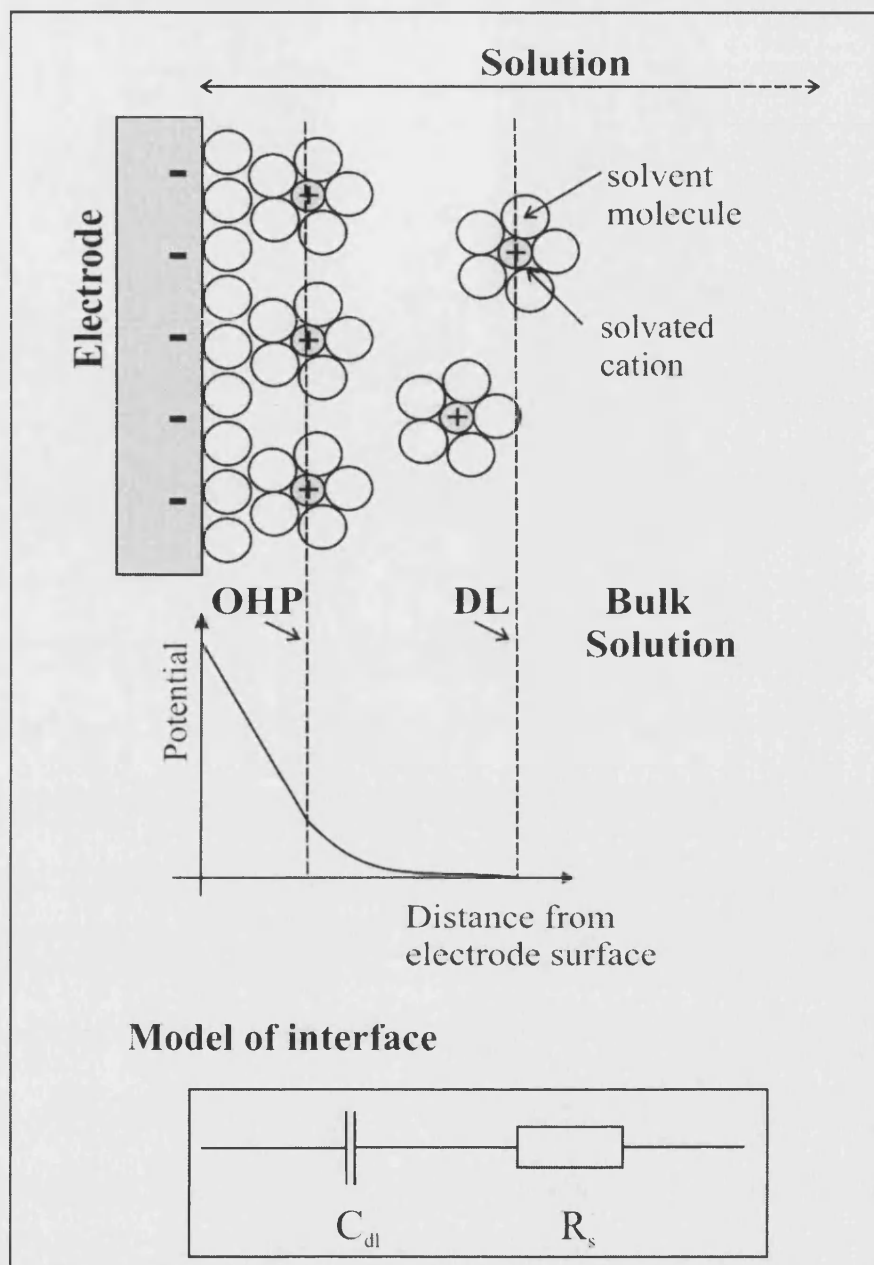
Figure 2.14 – Model of the Double Layer at the electrode surface.
The Double layer describes the entire region from the electrode surface to the end of the Diffuse Layer (DL). The figure describes the drop of potential from a charged electrode surface across the Double Layer. The electrode surface (grey shaded area) has a negative charge (5 unit charges in this figure) and it is solvated by a layer of solvent molecules (white circles), one molecule thick. Cations (positive charge, grey shaded circles) are solvated by 5 solvent molecules and are attracted to the surface. Some solvated cations reach the surface (3 in this figure) and the distance of them from the surface is described by Outer Helmholtz Plane (OHP). There is a drop of potential, directly proportional to distance, between the electrode surface and the OHP. Other solvated anions are required to neutralise the electrode surface potential, but they are unable to reach the surface. These anions (2 in this figure) remain mobile in the diffuse layer and the potential drops more slowly. When electroneutrality is achieved the edge of the DL has been reached. NOTES: This figure is not to scale and the DL is much larger than the OHP. The size of the DL is determined by the salt concentration of the buffer. There will be some anions in the DL, which extend the size of the layer. These are not shown for clarity. An electrical circuit modelling the electrode interface (bottom box) is shown. It has a solution resistance (R_s) and the double layer capacitance (C_{dl}) in series.

This model was advanced by Grahame (Fisher 1996) as other species (both ions and molecules) can sometimes be specifically adsorbed through the solvent layer, directly onto the electrode. This can affect the initial voltage drop by introducing an Inner Helmholtz Plane (IHP). A discussion of this work is not required.

To summarise, in the model described in Figure 2.14, there is a potential difference across the Double Layer region, between the electrode and the bulk electrolyte. However, the majority of charge is dropped across the OHP, between the solvated cations and the electrons on the metal surface. These form two layers of opposite charge which are separated by a layer of solvent molecules two molecules thick. As pure water is a dielectric (very poor electrical conductor) the interface can therefore be modelled as a capacitor.

Modelling the interface as a Capacitor

A capacitor consists of two charged interfaces separated by a dielectric insulator: a dielectric. The maximum charge (q) that can be stored on a capacitor depends on its capacitance (C) and the potential difference between the charged interfaces (E). This is described below in Equation 2.3.

$$q = CE \qquad (2.3)$$

q = Maximum charge, C = capacitance and E = potential across the interface

The capacitance depends on the overlap area (A), between the charged interfaces, the distance (d) between them and the dielectric permitivity (also called the dielectric constant) of the dielectric material (ε_r). ε_0 is the permitivity of free space.

$$C = \frac{\varepsilon_0 \varepsilon_r A}{d} \qquad (2.4)$$

C = capacitance, ε_0 = permitivity of free space = 8.854×10^{-12} $C^2 N^{-1} m^{-2}$, ε_r = permitivity of dielectric material, A = overlap area of interfaces and d = distance between interfaces

If LSV is considered, an oxidation sweep (a positive increase of potential) charges the double layer capacitor, as described in Equation 2.3. The current (i) is defined as the rate of flow of charge in Equation 2.5.

$$i = \frac{dq}{dt}$$ (2.5)

i = current and dq/dt = rate of flow of charge

Therefore the current which flows to charge the double layer capacitor can be described in Equation 2.6.

$$i = C\frac{dE}{dt}$$ (2.6)

i = current, C = capacitance and dE/dt = LSV voltage sweep rate

The total current which flows in a LSV trace is therefore the sum of the Faradaic current from the redox active species, which was discussed above Equation 2.2, and the capacitive charging current, which is given in Equation 2.6. This is summarised below in Equation 2.7.

$$i_{total} = i_{Faradaic} + i_{capacitive}$$ (2.7)

It is not possible to resolve the Faradaic current from the charging current, therefore to improve sensitivity the contribution from the charging current must be limited or eliminated.

2.5.5 Potential step amperometry

The contribution of the charging current can be greatly reduced if the LSV technique is subtly changed. If a potential step is applied to a diffusion controlled solution containing a redox active ferrocene, from a potential below its electropotential to a potential above it, all the ferrocene at the electrode surface will be oxidised and a

current flows (Figure 2.15). This is a combination of the Faradaic current and charging current.
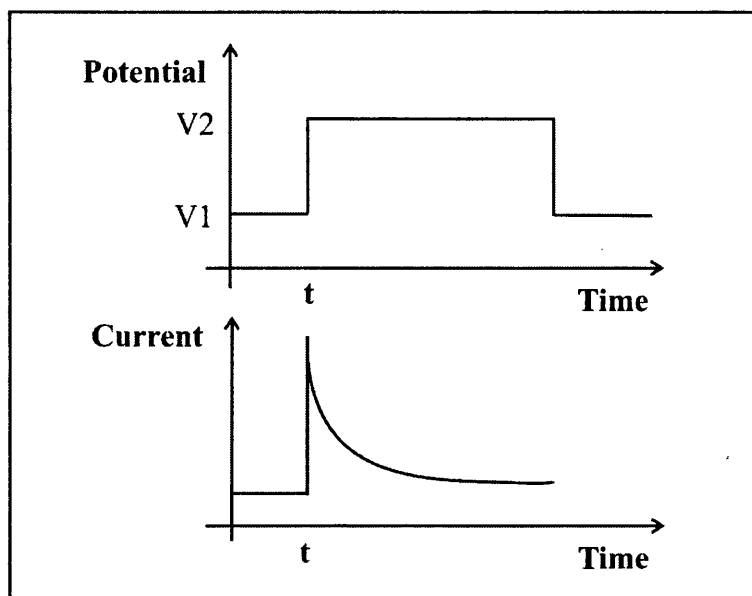
Figure 2.15 - Potential step amperometry.
At time t the potential of the electrode is stepped from V1 (below ferrocene oxidation potential) to V2 (above ferrocene oxidation potential) (top graph). A current spike is generated which decays with time (bottom graph)

The decay of the Faradaic current with time is described by the Cottrell equation (Equation 2.8). The Faradaic current decays at a rate proportional to $1/t^{1/2}$.

$$|i| = \frac{nFA\sqrt{D}C_\infty}{\sqrt{\pi t}}$$

(2.8)

Cottrell Equation: i = current, n = number of electrons transferred in redox couple, F = Faraday constant, A = electrode area, D = diffusion coefficient, C_∞ = bulk concentration of reactant and t = time.

The decay of the capacitive charging current can also be modelled after the potential step (Bard et al. 2001). The electrode interface can be modelled as a solution resistance (R_s), between the RE and WE, in series with a double layer capacitor (C_{dl}) as shown in Figure 2.16.
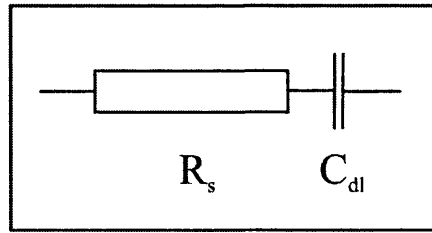
Figure 2.16 – Electrical circuit describing the electrode interface
A solution resistance (R_s) and the double layer capacitance (C_{dl}) are in series.

The potential difference across the interface therefore has two components, shown by Equation 2.9.

$$E = E_{R_s} + E_{C_{dl}}$$ (2.9)

E = total potential difference, E_{R_s} = potential across resistor and $E_{C_{dl}}$ = potential across capacitor.

For a resistor, potential is related to current by Ohm's law (Equation 2.10), where R is the resistance.

$$E_{R_s} = iR_s$$ (2.10)

Ohm's Law: E_{R_s} = potential across resistor, i = current and R_s = resistance.

Therefore, the potential drop across the interface can be described by substituting Equations 2.3 and 2.10 into Equation 2.9, to give Equation 2.11.

$$E = iR_s + \frac{q}{C_{dl}}$$ (2.11)

Equation 2.11 can be rearranged in terms of i, to give Equation 2.12. i has been defined previously in Equation 2.5.

$$i = \frac{E}{R_s} - \frac{q}{R_s C_{dl}} \Rightarrow \frac{dq}{dt} = \frac{-q}{R_s C_{dl}} + \frac{E}{R_s}$$ (2.12)

Integrating the equation (assuming that the capacitor is initially uncharged: q = 0 at t = 0) gives Equation 2.13, which describes the charge.

$$q = EC_{dl}[1 - e^{-(t/R_sC_{dl})}]$$ (2.13)

Differentiating with respect to time gives the capacitive charging current, shown in Equation 2.14.

$$i = \frac{E}{R_s}e^{-t/R_sC_{dl}}$$ (2.14)

The above equations show that, in relation to time, the potential step the capacitive charging current decays exponentially (i α e^{-t}), whilst the Faradaic current decays proportionally to the square root of time (i α t$^{-1/2}$). If these currents are considered together, as illustrated in Figure 2.17, it can be seen that the Faradaic current decays more slowly and at the "Sample time" shown it contributes all the peak current. Hence at this point the charging current has been eliminated.
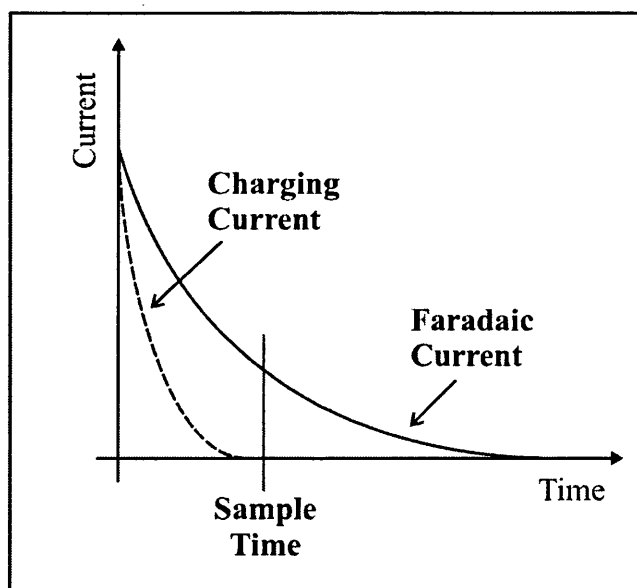
Figure 2.17 - Measurement of Faradaic current.
The figure shows the Charging current (dotted line) and Faradaic current (solid line) which are generated with a potential step. The Charging current decays more rapidly (exponentially) than the Faradaic current (t$^{-1/2}$). At the sample time the Charging current has decayed, but most of the Faradaic current remains.

Practical considerations

At the low concentrations of electroactive species used in this work, the charging current can be considered to be virtually independent of the concentration of the

electroactive species. In contrast the Faradaic current is directly proportional to the concentration of the electroactive species, shown in Equation 2.2. This can cause problems on occasions. If the surface of the WE is very rough, the real surface area will be very high, hence the capacitance will be very high, due to Equation 2.4, as will be the capacitive charging current, given in Equation 2.14. In contrast the effective area for the diffusion remains close to the cross sectional area as the diffusion occurs many μm from the electrode surface. In this case the capacitive current can swamp the Faradaic current. This can also occur if the concentration of electroactive species is lower than approximately 100 μmol dm^{-3}.

2.5.6 Pulse Voltammetry (PV)

Pulse Voltammetry (PV) is an adaptation of LSV which was developed to eliminate most of the charging current. The voltage sweep involves a succession of pulses of increasing potential and the Faradaic current is measured at the end of each pulse when the capacitive charging current has decayed, which is illustrated in Figure 2.18 (Bard et al. 2001).
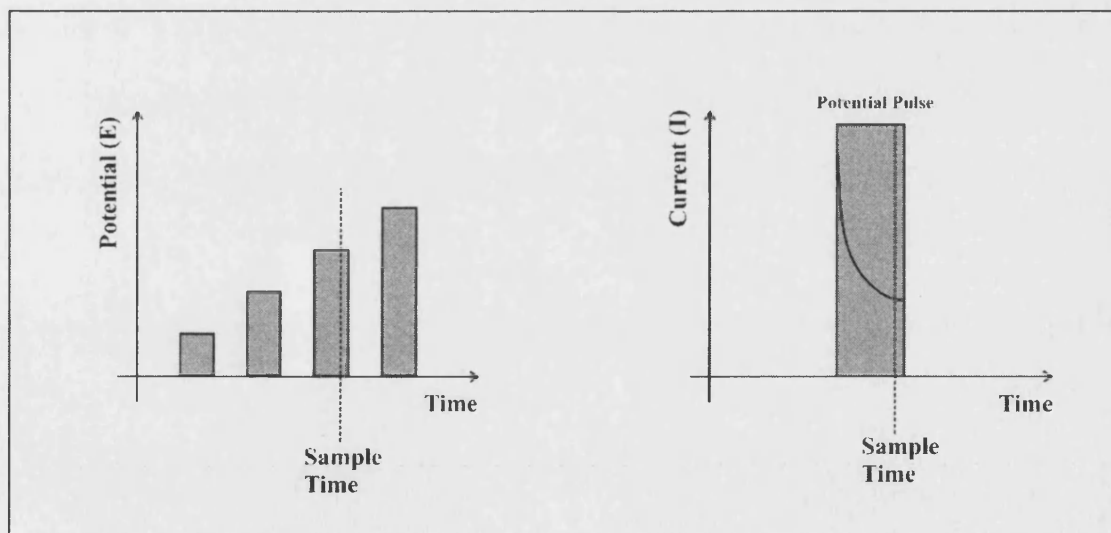
Figure 2.18 – Pulse Voltammetry.
Potential pulses (grey shaded areas) are applied to a sample (LHS graph). The magnitude of these pulses increases with time. Detail is shown for one of these potential pulses (RHS graph). After the pulse is applied a current spike (solid line) is observed, which decays with time. The current is sampled at the end of the pulse (dotted line).

Plotting the current against applied potential gives the pulse voltammogram, shown in Figure 2.19, from which the characteristic half potential ($E_{1/2}$) and maximum current (I_{max}) are obtained.
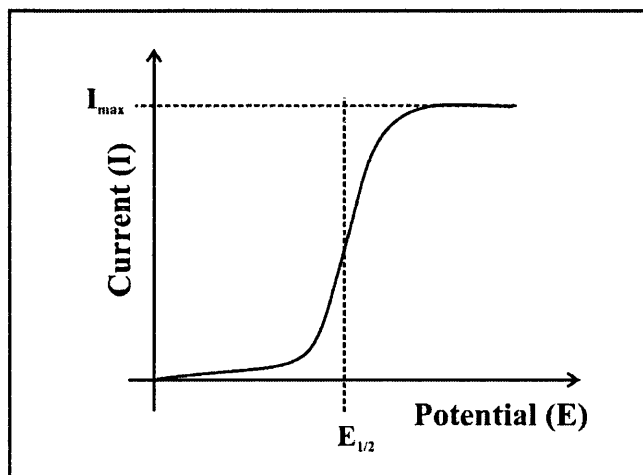
Figure 2.19 – Pulse Voltammogram.
The current is measured as the pulse potential is increased. At high potential a constant maximum current (I_{max}) is obtained. The potential required to obtain half the maximum current is the half potential ($E_{1/2}$).

Summary

PV affords an improvement in sensitivity over LSV, by the reduction of the influence of the charging current. However, this sensitivity can be improved further.

2.5.7 Differential Pulse Voltammetry (DPV)

Differential Pulse Voltammetry (DPV) is designed have higher sensitivity than PV, by minimising the response from the charging current still further (Ihara 1997). DPV measures the electropotential (Ep) of the redox active species. This is related to the half potential ($E_{1/2}$) as shown below in equation 2.15.

$$Ep = E_{1/2} - \Delta E/2 \qquad\qquad (2.15)$$

$E_{1/2}$ = half potential and ΔE = Change in pulse amplitude.

The variation of potential during DPV is described in Figure 2.20. A constant potential pulse is superimposed on a stepped base potential, and the current is measured before the application of the pulse (time = τ') and just before the end of the pulse (time = τ).
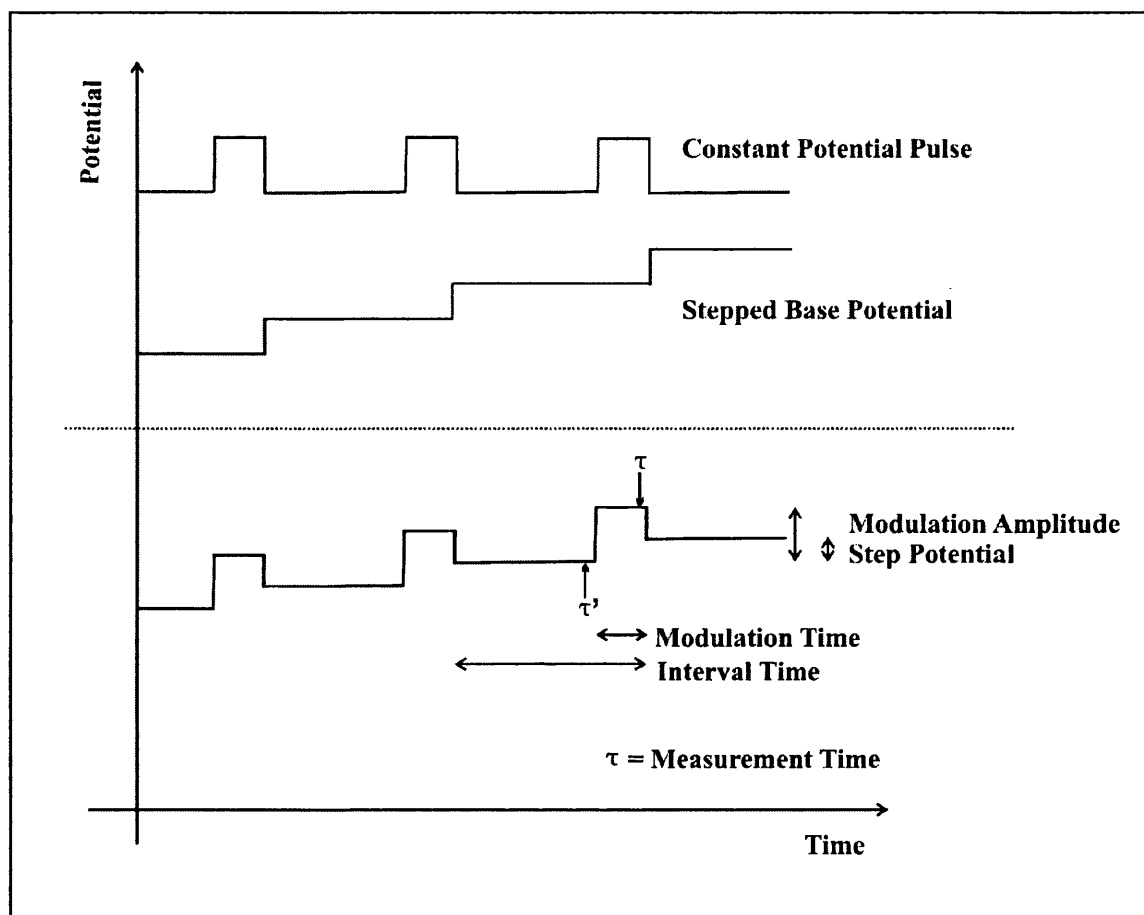
Figure 2.20 - Differential Pulse Voltammetry.
The figure describes the variation of potential with time in a DPV trace. A constant potential pulse and a stepped base potential (shown at the top of the graph) are superimposed to give the DPV trace (shown at the bottom of the graph). During the Interval Time one complete pulse occurs and this is repeated. The Modulation Time and Amplitude describe the shape of the pulse. The Step Potential describes the increase in the baseline potential at the end of the pulse. The current is measured before the application of the pulse (time = τ', current = $i_{\tau'}$) and just before the end of the pulse (time = τ, current = i_{τ}).

The differential current (δi) is the difference between the current at the two points ($i_{\tau} - i_{\tau'}$). This is calculated for each step and plotted against potential, allowing the E_p to be determined, as shown in Figure 2.21.
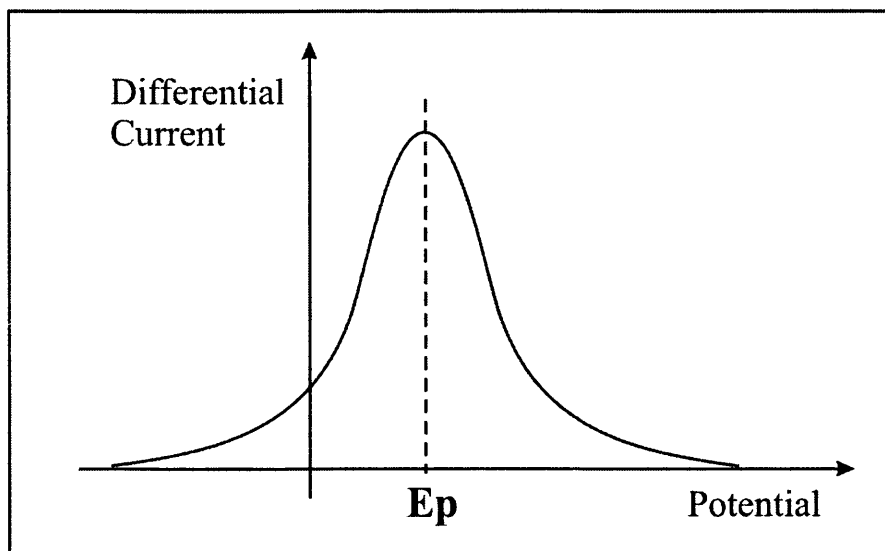
Figure 2.21 - DPV: determination of Ep.
Plotting the differential current (δi) against potential for the DPV traces allows the electropotential (Ep) to be determined.

The maximum differential peak current, $(\delta i)_{max}$, is described in Equation 2.16.

$$(\delta i)_{max} = \frac{nFAD^{1/2}[Fc_{bulk}]}{\pi^{1/2}(\tau - \tau')^{1/2}}\left(\frac{1-\sigma}{1+\sigma}\right)$$

(2.16)

$(\delta i)_{max}$ = maximum DPV differential peak current, n = number of electron transferred = 1, F = Faraday constant, A = electrode area D = diffusion coefficient, $[Fc]_{bulk}$ = ferrocene concentration in bulk solution, τ - τ' = modulation time. $(1 - \sigma)/(1 + \sigma)$ = a quotient which depends on the number of electrons transferred in the oxidation and the size of the modulation amplitude. For a 1 electron transfer with a modulation amplitude of 50 mV this is 0.453 (Bard et al. 2001).

Evaluation

A combination of smaller changes in potential together with the measurement of differential current is an improvement in eliminating the capacitive charging current (Bard et al. 2001), which allows measurements of electroactive molecules at very low concentrations (de Castro et al. 2003). DPV is a versatile technique which is more sensitive than PV.

Determination of DPV electropotentials: practical considerations

Electropotentials measured by DPV for ferrocenylated species will be comparable if the assay and external conditions remain constant. For reproducibility the experimental setup should also remain the same.

The variation of the electropotential (Ep) of a redox couple from its standard potential (Ep$^\theta$) is described by Equation 2.17, the Nernst equation (Fisher 1996).

$$E_p = E^\theta + \frac{RT}{nF} \ln \frac{[Fc^+]}{[Fc]}$$

                                                                                          (2.17)

Nernst equation: Ep = electropotential, Ep$^\theta$ = standard potential, R = gas constant, T = temperature, n = the number of electrons exchanged = 1, F = Faraday constant, [Fc$^+$] = concentration of ferrocenium species and [Fc] = concentration of ferrocene species. The equation assumes that the activity of both the species in the redox couple is unity (i.e. 1). The activity is the "effective concentration" of each species (Atkins 1990) and at low concentrations it is usually approximately unity as the solute behaves ideally, but it can be affected by the solvent used and other species in the solution. Even if the activities are not unity for all of the ferrocenylated species studied the relative electropotentials will still be valid and comparable.

The electropotentials are affected by temperature and increased temperature increases electropotential. Therefore the temperature should be kept constant and it was kept at 20 °C. Small variations in the absolute concentration of the ferrocenylated species will not affect the measured electropotential as this is dependent on the ratio between the two ferrocenylated species.

A freshly polished gold working electrode was used, together with the electrochemical cell which is described in the next section (2.5.8). The specific DPV details are given in section 2.10.2.

Interpretation of DPV traces: practical considerations

The Autolab potentiostat is run using the GPES (General Purpose Electrochemical System) software. The DPV traces routinely show a peak on a sloping baseline. To allow the peaks to be readily compared the baseline correction options on the GPES software are used to generate peaks, with a flat baseline at zero current. The software shows a dotted fit of the proposed baseline before the data is manipulated and this allows the most appropriate correction method to be used. The first option is the fitting of a user defined polynomial baseline curve to the data, which involves the selection of 3 or 5 data points for the curve. This approach was extensively used for the early work. However, it became apparent that this baseline correction could generate false peaks for both the solvent and control (undigested oligonucleotide) assays. This was a particular problem at low concentrations of analyte, as the background DPV current trace is typically "U" shaped and the peak of interest can actually lie around the minimum of this trace. To reduce this problem the "moving average" baseline correction was adopted and all the DPV traces were reinterpreted. This technique is fully described (AutoLab 2001) and summarised below. It was developed to resolve peaks which appear as shoulders on sloping baselines.

The number of data points in the DPV trace is initially reduced by defining a "Voltage Step Window". The data points are reduced to one point at the average current for the "Voltage Step Window". Each point is then compared to the average of its two neighbours, as shown in Figure 2.22. If the data point is greater than the average, then its value is replaced by the average value. This process continues iteratively until no more points are replaced and the final curve is the baseline, which can then be subtracted.
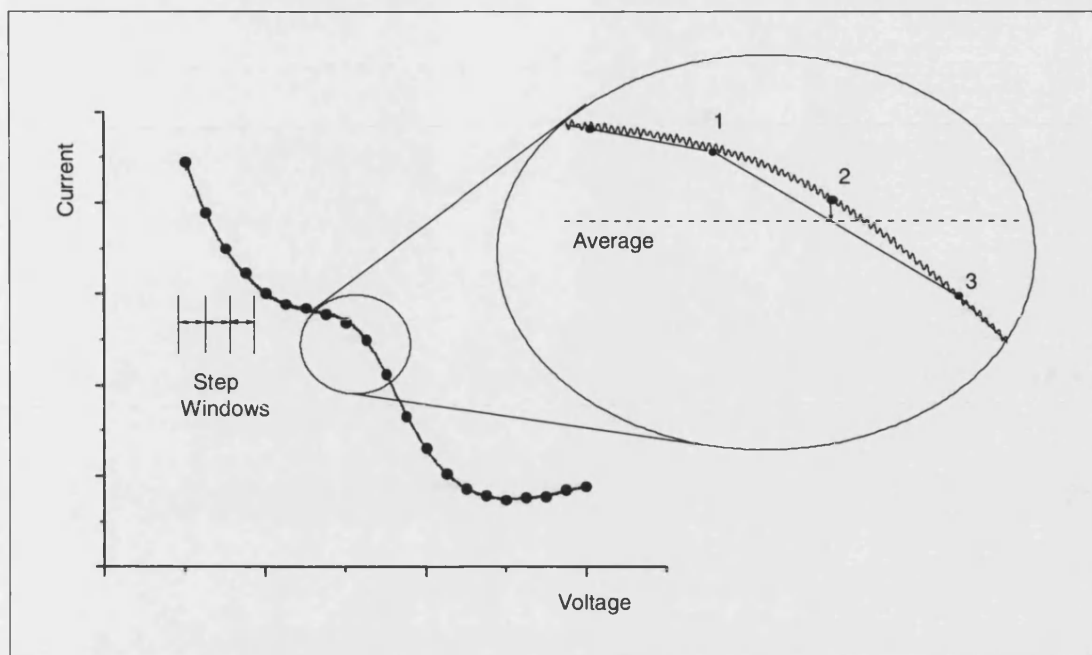
Figure 2.22 - Moving average baseline correction.
The DPV trace shown (thick black curve on main graph) consists of many data points, which are not individually shown. The voltage axis is then divided into consecutive sections of equal voltage called "voltage step windows" (three are shown). The average of the data points in the step window is calculated and the DPV trace is replotted using only these average data points (black circles). Each average data point is then compared to the average of its two neighbours: in the detail (magnified circle) point 2 is compared to the average of points 1 and 3, which is shown as a dotted line. If the data point (point 2) is higher than the average, it is replaced by the average value (shown by the downwards arrow). This process continues iteratively until no more points are replaced and the final curve is the baseline which can then be subtracted from the original DPV trace (thick black curve).

Even when the "moving average" correction is used common sense must also be applied. The approach should only be used to quantify peak height when real peaks (i.e. peaks visible to the eye) are present.

2.5.8 Electrochemical cell and electrodes: practical considerations

The theory behind electrochemical detection methods for the analysis of ferrocene has been introduced above. The choice of a suitable electrochemical cell and working electrode will ensure that the electrochemical techniques will give the best possible sensitivity and selectivity. If the choice of cell or electrode is poor even the best, well suited, electrochemical analysis technique will not be able to give good results. The preparation of the electrodes is also important to allow reproducible results to be obtained. These practical considerations will also be introduced here.

Electrochemical Cell

All the electrochemical analysis of the ferrocenylated species was undertaken using a standard electrochemical cell set-up (BAS, UK). Using an established commercial set-up is of value as it should improve reproducibility of results and their applicability to future work. Analysis of low volumes of analyte was required and this necessitated using the working electrode in a low volume (200 μL) cell, shown in Figure 2.23. The analyte sample was separated from a platinum counter electrode and an Ag|AgCl reference electrode by a electrically conducting Vycor^TM polymer frit. Where necessary the temperature was regulated by an external water bath. A potentiostat (Autolab PGstat12, Windsor Scientific, U.K.) was used for all the electrochemical measurements.
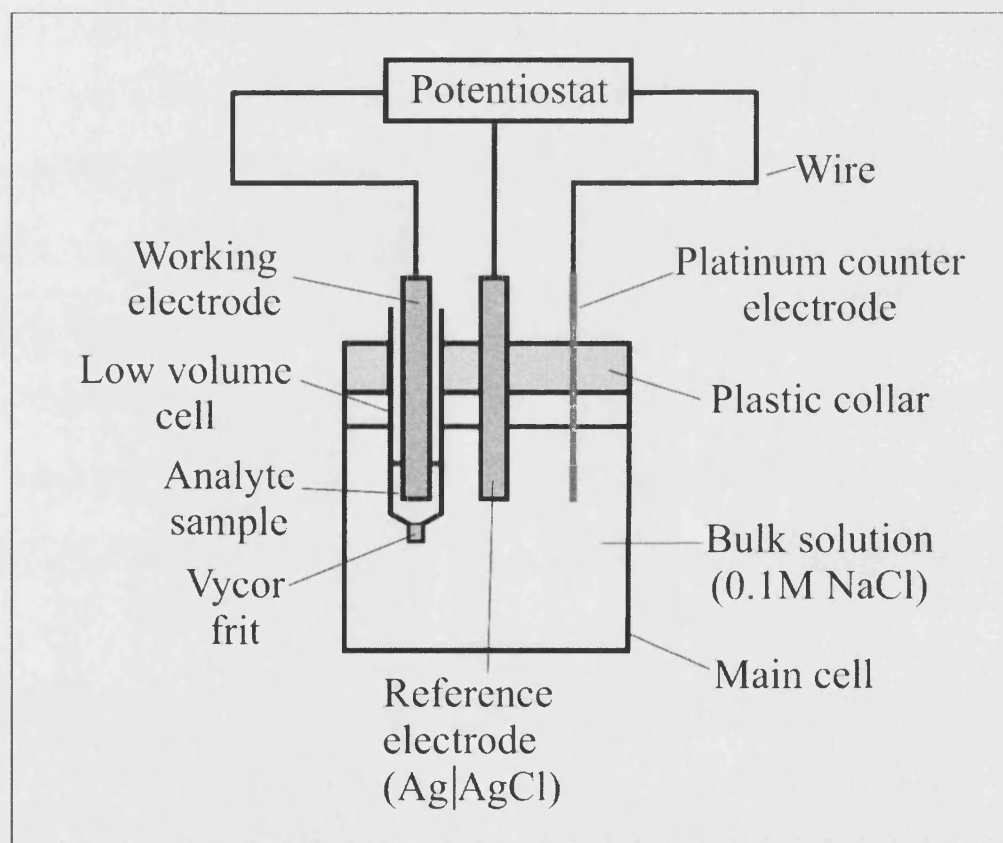
Figure 2.23 - Electrochemical setup.
The main glass cell contains a bulk solution of conducting electrolyte (0.1 M NaCl). A plastic collar (light grey box) containing three holes is placed at the top of the main cell. The platinum counter electrode (right hand side) and Ag | AgCl reference electrode (centre) are placed in two of the holes and connected to the potentiostat with wires (thick black lines). The analyte sample (200 μL) is added to the glass low volume cell and this is placed in the remaining hole (left hand side). There is a conducting polymer (Vycor) frit (small grey box) at the bottom of the low volume cell. The working electrode is then positioned in a low volume cell and connected to the potentiostat with a wire.

Working electrodes

An ideal electrode is one that gives reproducible, sensitive results. Sensitivity should be addressed first. The pathway of a general electrode oxidation reaction is shown below for a diffusion controlled system, in Figure 2.24 (Bard et al. 2001). An ideal material will allow the redox active species to readily adsorbed onto the electrode surface, the electron transfer to the electrode should then be very rapid and unhindered, before the reduced species is desorbed. Any electrode material which has poor electron transfer properties should be avoided. Electrode fouling caused by poor desorption of the oxidised species will clearly reduce the electrode area and cause a reduction in the measured current.
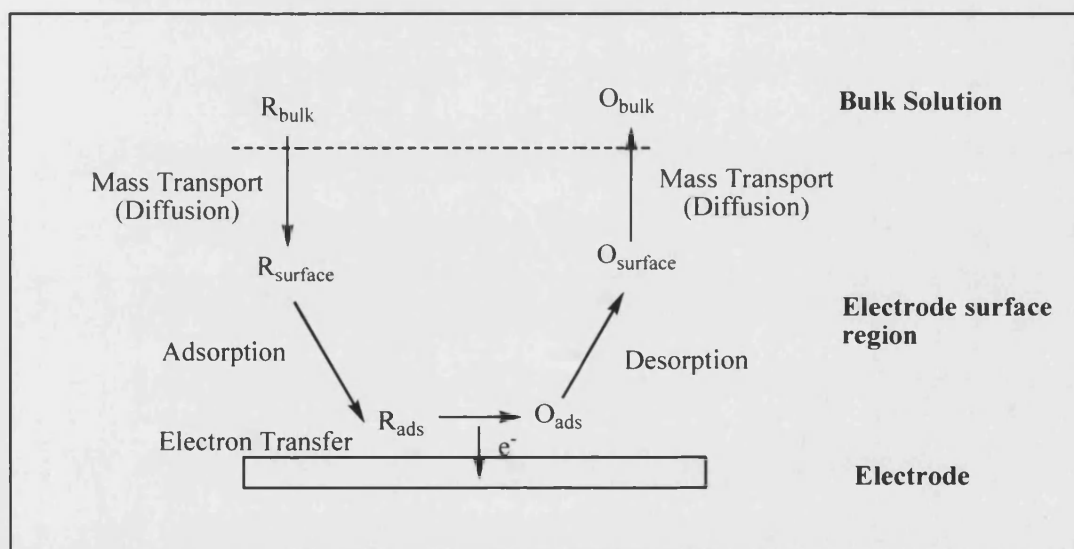
Figure 2.24 - Electrode oxidation pathway in a diffusion controlled system.
The reduced species in the bulk solution (R_{bulk}) diffuses into the electrode surface region ($R_{surface}$). $R_{surface}$ is adsorbed onto the electrode surface (R_{ads}). R_{ads} is oxidised through electron transfer to the electrode, generating the adsorbed oxidised species (O_{ads}). O_{ads} is desorbed into the electrode surface region ($O_{surface}$) and diffuses into the bulk solution (O_{bulk}). This is a specific form of Figure 2.10.

Three working electrodes were used in the analysis: Glassy Carbon (GC, 3.0 mm diameter, BAS, UK); Gold (Au, 1.6 mm diameter, BAS, UK) and Boron Doped Diamond (BDD, 3.0 mm diameter, Windsor Scientific, UK). These are common electrode materials, which have fast electron transfer properties and are easy to handle and polish (BAS 2004).

To ensure a smooth, reproducible surface, the electrodes should be freshly polished, with aluminium oxide slurry, and the electrochemical analysis should be done on the first analytical trace, as electrode fouling can affect the response of subsequent traces. The method of electrode polishing is recommended by BAS (Bott 1997). A coarse grade of slurry is initially used followed by progressively finer slurries (down to 0.05 μm) until the electrode is visually smooth and shiny. The choice of the grade of the coarsest slurry is dependent on the initial roughness of the electrode.

The different electrodes inherently have different surface characteristics and may give appreciably different responses for the same sample, for reasons that may not be clear without extensive further study. It is common practice to use different electrodes in exploratory work.

2.6 Fluorescence

The use of fluorescent molecules in analytical detection methods is widespread due to the high sensitivity of fluorescence and the speed of the fluorescent response. Fluorescent techniques are used in this study to complement the electrochemical detection.

2.6.1 Theory

Fluorescent emission occurs due to the emission of a photon from the excited state of a fluorophore (F*) as the excited electron falls back down to the ground state. This is described schematically in Figure 2.25.

$$F + h\nu_A \xrightarrow{\text{Absorption}} F^* \xrightarrow{\text{Fluorescence}} F + h\nu_F$$
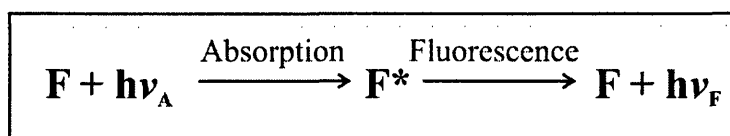
Figure 2.25 – Fluorescence.
The fluorophore (F) absorbs radiation ($h\nu_A$) to promote an electron to an excited state (F*). The exited state decays back to the ground state (F) releasing fluorescent radiation ($h\nu_F$).

The theory behind fluorescence can be understood by considering the energy levels of the electron in the fluorescence process (Christian 1994). These are described by a

Jablonsky diagram, illustrated in Figure 2.26. From the ground state (F, S_0) the electron can absorb radiation (hν_A) and be promoted into an excited state (F*, S_1). Normally the electron is promoted to the lowest vibrational state, but it can reach higher vibrational states. In these cases there is a rapid vibrational relaxation of the electron to the lowest state, through loss of energy to solvent molecules. The electron can now decay back to the ground state, releasing fluorescent radiation (hν_F). Decay to the lowest vibrational level of the ground state is often favoured, but decay can also occur to other vibrational states, giving rise to a range of frequencies of fluorescent emission. The action of a quenching molecule can compete with fluorescence reducing the fluorescent intensity.
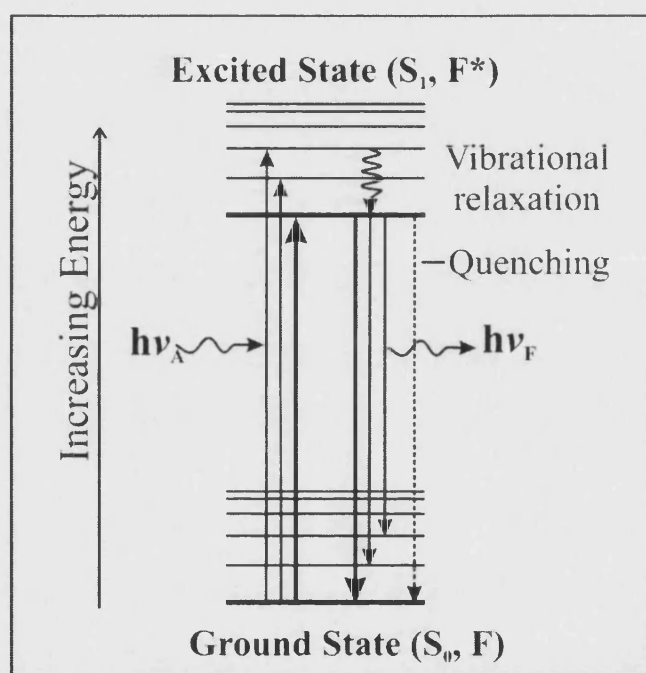
Figure 2.26 – Representation of fluorescence using the Jablonsky diagram.
An electron in the ground state (F, S_0) of the fluorescent molecule is excited (vertical arrow) by the absorption of electromagnetic radiation (hν_A) to an excited state (F*, S_1) of higher energy. The length of the arrow directly relates to the energy absorbed. The ground state and the excited state each contain several energy levels (horizontal lines). The lowest energy level (thick line) corresponds to the lowest vibrational energy levels of that state. Higher energy levels (thin lines) are due to vibrational levels of increasing energy. Electrons can be excited to different vibrational levels, but they will rapidly undergo vibrational relaxation (curved arrow) to the lowest energy level. The electron can now decay (vertical arrow) to the ground state and fluorescent emission (hν_F) occurs. Decay to different vibrational levels is possible, hence a range of frequency of fluorescent emission is observed. The "0-0" transitions (thick, central vertical arrows) are the excitation and the fluorescence between the lowest vibrational states of the ground and excited state. Quenching molecules are able to adsorb energy from the excited state electron, returning the electron to the ground state (dotted arrow) without any fluorescent emission occurring.

It is apparent that the "0-0" transitions between the ground state (S_0) and excited state (S_1) occur at the same energy and therefore have the same wavelength (λ) for both the absorption and fluorescence. This energy can be described by Equation 2.18.

$$E = hc/\lambda \qquad\qquad (2.18)$$

E = energy of radiation, h = Plank's constant, c = speed of light and λ = wavelength

As the energy of the radiation is inversely proportional to the wavelength of the radiation, the "0-0" is the longest wavelength (lowest energy) of absorption and the shortest wavelength (highest energy) of emission. Hence, the fluorescent emission spectrum occurs at a longer wavelength (lower energy) than the absorption spectrum, although the two overlap, as shown in Figure 2.27. In practice the "0-0" for the fluorescent emission is shifted to a higher wavelength than for the absorption, by differences in the heat of solvation energies between the excited and ground state fluorophore. The absorption spectrum is obtained by varying the excitation wavelength, whilst measuring the fluorescent emission at a constant wavelength. In contrast, the emission spectrum is obtained by exciting the molecule at a constant wavelength and measuring the fluorescent emission at a range of wavelengths.
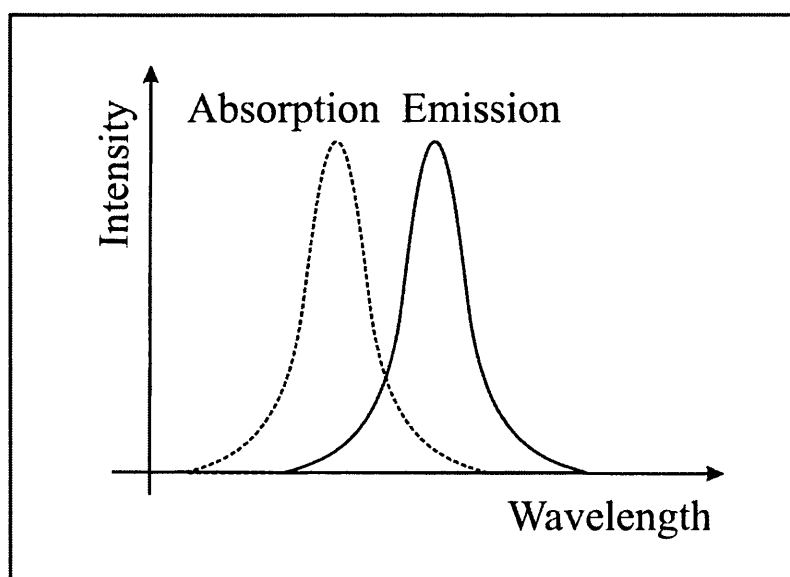
Figure 2.27 – Fluorescence spectra.
The absorption spectrum for a fluorophore (dotted graph) occurs at a lower wavelength than the emission spectrum (line graph).

Quantifying fluorescence

In fluorescence the rate of electron transfer occurs rapidly. Absorption is very fast (rate constant = 10^{-15} s) as is vibrational relaxation (rate constant = 10^{-12} s). Fluorescence is slower (k_F, rate constant = 10^{-6} to 10^{-9} s), but is still a rapid process. To reduce the

observed fluorescent intensity the competing processes must also be rapid (Christian 1994).

The efficiency of fluorescence, from the excited state (S_1, F*), is defined in terms of quantum yield, in Equation 2.19 (Rendell 1987; Christian 1994).

$$\phi = \frac{\text{Intensity of fluorescence}(I_F)}{\text{Intensity of absorption}(I_A)} = \frac{k_F}{(k_F + k_0)} \qquad (2.19)$$

ϕ = quantum yield, k_F = rate of fluorescence and k_0 = rate of non radiative decay (k_Q + k_{ET} + k_{ISC} + k_{IC})

The non radiative decay (k_0) is due to quenching processes, which can be separated into general quenching (k_Q), through collisions or of the formation of complexes with other molecules, and resonance energy transfer (k_{ET}), which will be discussed later. Intersystem crossing (k_{ISC}) of the electron to a triplet orbital (T_1) and internal conversion (k_{IC}) to a very high vibrational level of the ground state, will not be discussed.

A good fluorophore will have a low loss of fluorescence through intra-molecular non-radiative decay (k_{IC} and k_{ISC}) and any loss of fluorescence will occur through inter-molecular quenching (k_Q and k_{ET}), which is influenced by experimental conditions. With low levels of quenching an ideal fluorophore has a quantum yield close to 1 (Rendell 1987).

For analytical purposes the intensity of the fluorescence must be related to the concentration of the fluorophore in solution. This relationship is given in Equation 2.20 (Rendell 1987).

$$I_F = \phi I_0 (1 - e^{-\kappa cd}) \qquad (2.20)$$

I_F = fluorescent intensity ϕ = quantum yield, I_0 = intensity of excitation source, κ = proportionality coefficient, c = concentration, d = cell path length

The fluorescence is not linearly proportional to concentration. However, at low concentration e^{-x} approximates to $(1 - x)$ and the fluorescence is proportional to concentration, as shown in Equation 2.21.

$$I_F = \phi I_0 \kappa cd \qquad (2.21)$$

Fluorescent intensity (I_F) at low concentration: ϕ = quantum yield, κ = proportionality coefficient, c = concentration, d = cell path length

This can be rewritten in terms of molar absorbtivity, in Equation 2.22.

$$I_F = 2.303\phi I_0 \varepsilon cd \qquad (2.22)$$

Fluorescent intensity (I_F) at low concentration: ϕ = quantum yield, ε = molar absorption coefficient, c = concentration, d = cell path length

The low concentration approximations are valid for concentrations of less than 2.4 µM (Rendell 1987). In this instance fluorescent intensity is directly proportional to concentration and can be used for sensing.

Calibration of the fluorimeter used to measure the fluorescence against known concentrations of fluorophore, combined with the use of control samples ensures the accuracy of the detection technique and would allow higher concentrations of fluorophore to be measured.

Fluorescence Resonance Energy Transfer (FRET) quenching

FRET has been introduced (as k_{ET} on the previous page) as a route of radiationless decay of an electron in an excited state (S_1, F*). It allows selective quenching of a fluorophore and can be exploited.

In FRET an electron in an excited state (F*) transfers energy to quencher molecule (Q), exciting it (Q*). Subsequently the quencher molecule fluoresces, whilst the fluorophore does not, as illustrated in Figure 2.28.

$$\text{F} + \text{h}\nu_A \xrightarrow{\text{Absorption}} \text{F}^* \xrightarrow[\text{Q}]{\text{Energy Transfer}} \text{F} + \text{Q}^* \xrightarrow{\text{Fluorescence}} \text{Q} + \text{h}\nu_Q$$
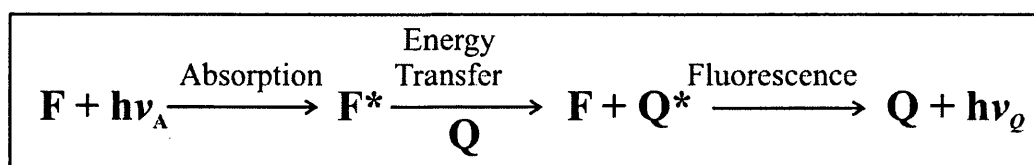
Figure 2.28 – Schematic description of FRET.
The excited fluorophore (F*) transfers energy to the quencher molecule (Q) when it decays to its ground state (F). This promotes an electron in the quencher to an excited state (Q*). The exited state (Q*) decays back to the ground state (Q) releasing fluorescent radiation ($h\nu_Q$).

To understand the theory behind FRET the energy levels of the electrons from the fluorophore and quencher must be discussed. This is most clearly described using a Jablonsky diagram, drawn in Figure 2.29. An electron in the excited state (S_1, F*) of a fluorophore decays to the ground state (S_0, F) releasing energy. No fluorescence is seen as a second fluorescent molecule (quencher) is able to absorb the energy and promote its own electron to an excited state (S_1, Q*). Fluorescent emission can then occur ($h\nu_Q$) but this is at a longer wavelength (lower energy) than that of the original fluorophore.
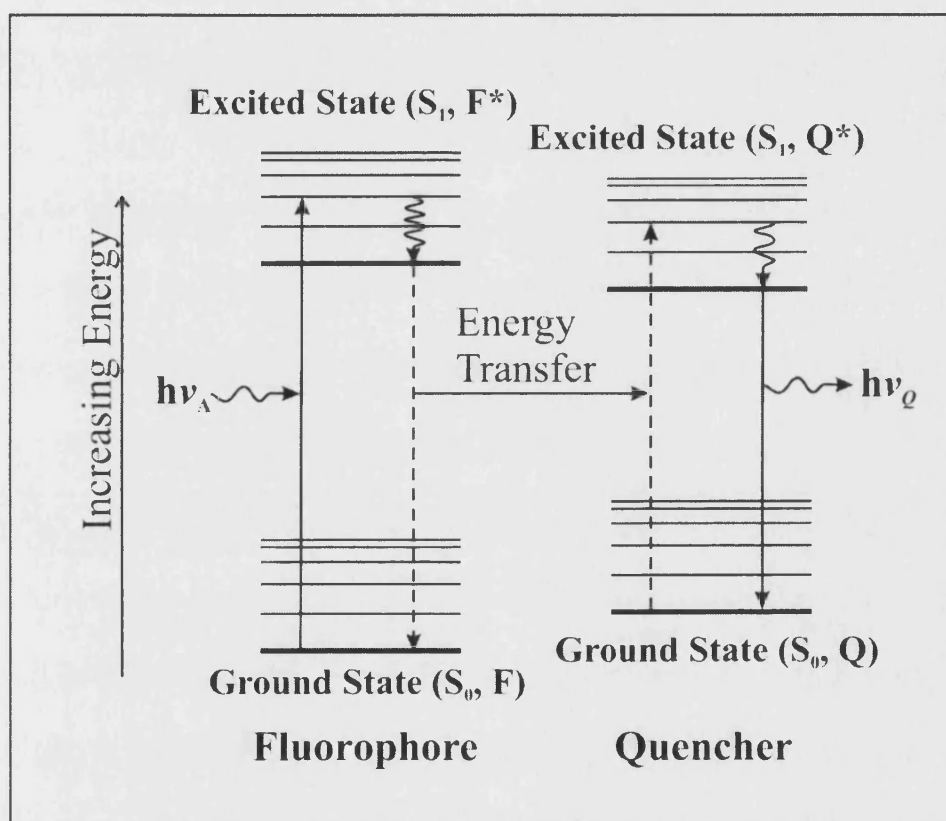
Figure 2.29 – FRET: Jablonsky diagram.
Jablonsky diagrams have been described earlier in Figure 2.28. An electron in the ground state (S_0, F) of the fluorophore molecule is excited (vertical arrow) by the absorption of electromagnetic radiation ($h\nu_A$) to an excited state (S_1, F*) of higher energy. If it is excited to a high vibrational level, it rapidly undergoes vibrational relaxation (curved arrow) to the lowest energy level. The electron can now decay (dotted downwards arrow) to the ground state by releasing energy. Fluorescence is not seen as the energy is absorbed by the quencher molecule (dotted upwards arrow), which promotes an electron to an excited state (S_1, Q*). The energy transferred remains constant (the dotted arrows are the same length). The quencher electron can decay (vertical line) to the ground state (S_0, Q) and fluorescent emission ($h\nu_Q$) occurs.

For clarity a practical example of FRET is given in Figure 2.30. Initially both the fluorophore and quencher can fluoresce when excited at their own absorption wavelengths, although the fluorophore absorbs and fluoresces at a lower wavelength. When the two molecules are brought spatially together by covalent bonding, the

fluorescence band of the fluorophore overlaps with the absorption band of the quencher. Hence, exciting the fluorophore at its absorption wavelength leads to fluorescent emission of the quencher. If the covalent bond between the fluorophore and quencher was broken, FRET would not be possible and fluorescence from the fluorophore would only be seen.
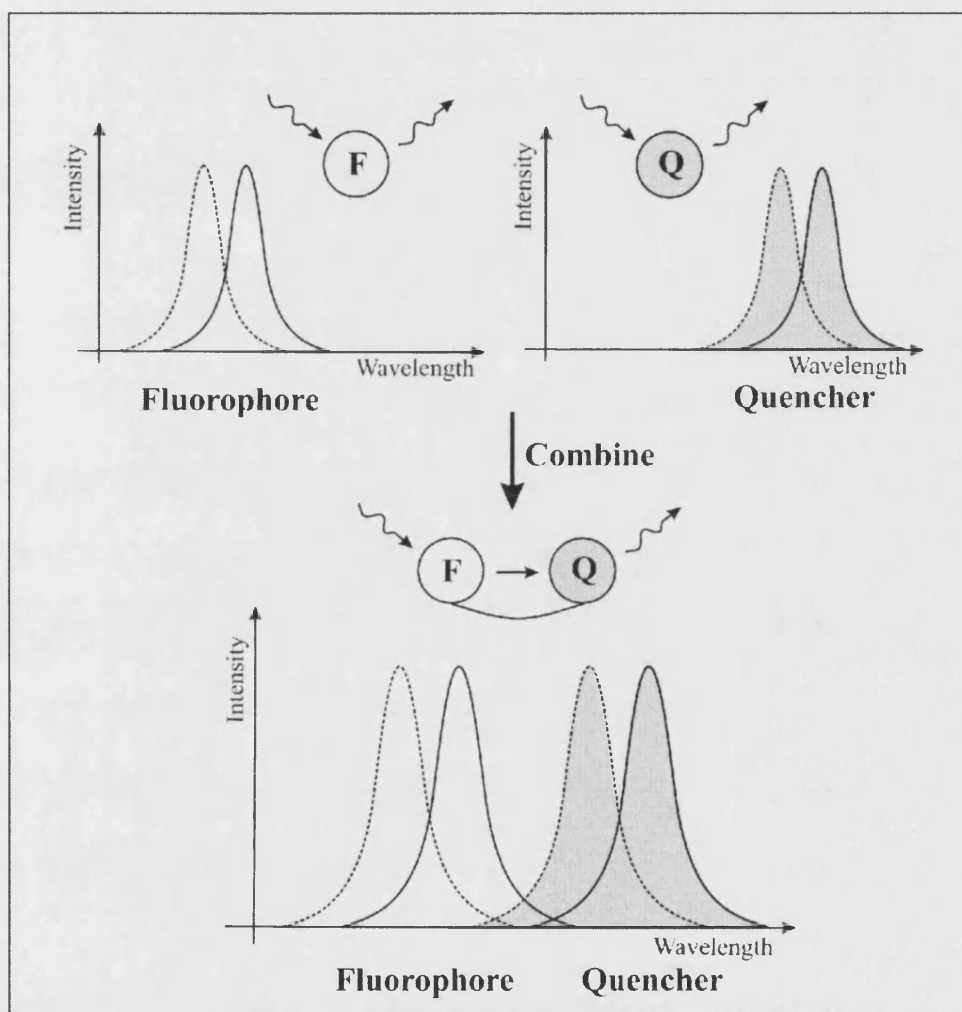
Figure 2.30 – Illustration of FRET.
This figure describes FRET quenching of a fluorophore. The fluorophore (F, white circle) and quencher (Q, shaded circle) are both fluorescent molecules. Individually both molecules absorb radiation (dotted line) and fluoresce (full line). These processes occur at lower wavelength (higher energy) for the fluorophore. Covalently linking F and Q (bottom half of diagram), brings the molecules spatially close together and allows FRET to occur. Overlap (dark shading) between the fluorescent emission band of F (white line graph) and the absorption band of Q (shaded, dotted graph) allows non radiatative transfer from F to Q. Therefore on excitation of F ($h\nu_A$) fluorescent emission is only seen from Q ($h\nu_Q$).

2.6.2 Fluorescent analysis

The two instruments used for fluorescent analysis in this work will be described. Fluorescence is measured relative to the intensity of the excitation radiation.

Light Cycler (Roche)

Individual samples (20 µL) are loaded into small, thin glass capillaries. These are then loaded into a carousel and their fluorescence is measured in turn. Computer control allows the analysis to be tailored for the experiment.

Figure 2.31 – External view of LightCycler (Roche).
The instrument is open, with a carousel placed at the bottom left. The white cylinders seen on the carousel and the plastic tops to the glass capillaries.

Plate fluorimeter (FARCyte)

The FARCyte™ fluorescence plate reader is designed to sequentially measure fluorescence of multi-well plates (typically 200 µL). The depth in the well at which the fluorescence is measured is initially optimised. Computer control allows the analysis to be tailored for the experiment.

99

Figure 2.32 – External view of the plate fluorimeter (FARCyte).

2.7 Accuracy

An indication of the accuracy of the analytical results is given by considering the standard deviation of the data samples. The Q test can be used to determine if data points in a sample are valid.

2.7.1 Standard deviation

The standard deviation is commonly used to determine the precision of analytical results and is described, for a finite set of experimental data, in Equation 2.23 (Christian 1994). If the experimental data is normally distributed, then 68% of the individual values fall within $\overline{x} \pm s$ and 95% of the values fall within $\overline{x} \pm 2s$.

$$s = \sqrt{\frac{\Sigma(x_i - \overline{x})^2}{(N-1)}} \qquad\qquad (2.23)$$

s = standard deviation for a finite set of experimental data, x_i = data point, $\overline{x}$ = sample mean and N = number of measurements

2.7.2 Q test

If a data point appears to differ markedly from the others, its validity can be determined by using the Q test, equation 2.24 (Christian 1994). The Q value is determined for the data point and compared to tabulated values, which correspond to the number of data

points and the desired confidence level. If the Q value is greater than the tabulated value, the data point can be discarded.

$$Q = a/w \qquad \qquad (2.24)$$

Q = reaction quotient, a and w are defined in Figure 2.33
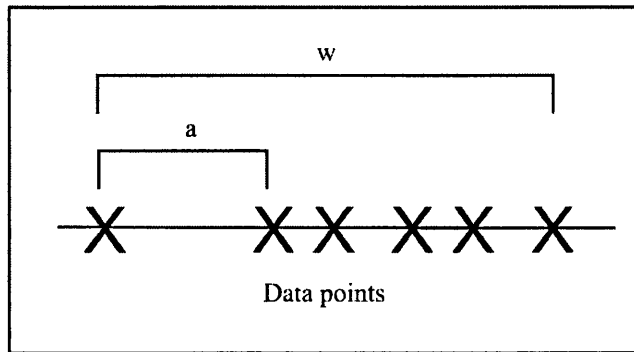
Figure 2.33 - Illustration of Q test parameters.

PART B: Experimental methods

2.8 Synthetic methods

2.8.1 General experimental

Reactions requiring the use of anhydrous, inert atmosphere techniques were carried out under an atmosphere of nitrogen, or argon. In all cases, apparatus was thoroughly oven-dried at 100 °C or 250 °C and then swept with nitrogen for at least 15 minutes before use. All solvents were distilled before use and stored in the presence of 4Å molecular sieves.

Diethyl ether and hexane were distilled from sodium wire. DCM and DMF, were distilled from CaH_2. DMSO was distilled without prior drying. 1,4-Dioxane was obtained in anhydrous form from Aldrich.

TLC using aluminium backed plates coated with Merck Kieselgel 60 GF_{254} neutral (Type E) silica monitored all reactions. Visualisation of these plates was by 254 nm UV light and/or PMA followed by gentle warming. Organic portions were routinely dried with anhydrous magnesium sulfate and evaporated using a Büchi evaporator. Where necessary, further drying was obtained by exposure to high vacuum in a 50 °C oven. Flash chromatography was carried out using Kieselgel 60H silica (0.04-0.063 nm), pore diameter *ca.* 6 nm obtained from Acros Organics.

Proton (^1H) NMR spectra were run in $CDCl_3$ or d_6-DMSO at 300 MHz using a Bruker AM (300 MHz) instrument. Chemical shifts are reported in parts per million (ppm) relative to $SiMe_4$ (δ_H = 0.00ppm) as internal standard, or to the residual solvent peak. Coupling constants (*J*) are given in Hz and multiplicities denoted as singlet (s), doublet (d), triplet (t), quartet (q), unresolved multiplet (m) or broad (b). Carbon (^{13}C) NMR spectra were run in $CDCl_3$ or d_6-DMSO at 75.5 MHz using a Bruker AM (300 MHz) instrument, using the residual solvent peak as the internal standard.

IR Spectra were recorded using a Perkin-Elmer 1600 series FT-IR spectrophotometer in the range 600-4000 cm^{-1} as liquid films, KBr discs or Nujol mulls, with internal background scan. Absorption maxima are recorded in wavenumbers (cm^{-1}) and classified as strong (s), medium (m), weak (w) or broad (br.).

Mass spectra, including high-resolution spectra, were recorded on a Micromass Autospec Spectrometer using Fast Atom Bombardment (FAB+) ionisation at the University of Bath or at the EPSRC Mass Spectroscopy Centre, Swansea.

Unless preparative details are provided, all chemicals were commercially available and purchased from either: Acros; Aldrich; Avocado; Fluka: Lancaster: Sigma or Strem chemical companies.

Where necessary, to allow clear assignment of peaks in NMR spectra, the protons in the novel compounds synthesised are labelled alphabetically in sequence and the carbon atoms are labelled numerically in sequence.

The numbering of the compounds corresponds to the order to which they occur in the text; from Chapter 3 onwards.

2.8.2 Synthesis of linker molecules

Azido(ferrocenyl)methanone 21
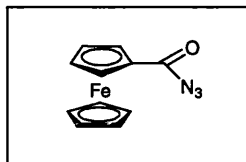
To a nitrogen purged flask was added oxalyl chloride (1.29 g, 10.0 mmol, 1.00 equiv.) and dichloromethane (20 mL), which was cooled to 5 °C. Ferrocene carboxylic acid **1** (2.30 g, 10.0 mmol, 1.00 equiv.), partially dissolved to a blood-red slurry in dichloromethane (65 mL), was added dropwise over 20 minutes, whilst maintaining the temperature at 5 °C. The mixture was stirred for 45 minutes, after which it was allowed to warm to room temperature resulting in an intense red solution. The solvent and residual oxalyl chloride were removed by rotary evaporation, to give an intense red oil which crystallised on standing. The crystals were dissolved in acetone (40 mL) and the solution was cooled to 5 °C, to which sodium azide (1.37 g, 20.0 mmol, 2.00 equiv.) in water (4 mL) was added dropwise. The solution changes to a red/orange colour. The solution was warmed to room temperature, stirred for 1 hour, poured into water (280 mL), which precipitated orange solid. The solid was separated by Buchner filtration. Drying in a vacuum oven yielded the *azide* **21** as orange crystals (1.81 g, 71%). R_f (5:1 ethyl acetate / petroleum ether (bp 40-60 °C) = 0.73. Mp 83.5-84.5 °C. ^{1}H-NMR δ (300MHz, CDCl$_3$) 4.26 (5H, s, Cp), 4.52 (2H, t, J = 2.1, Cp*), 4.83 (2H, t, J = 2.3, Cp*). ^{13}C-NMR δ (100.5MHz, CDCl$_3$) 70.4 70.5 72.0 73.3 (Cp,Cp*), 176.6 (CO). IR (nujol) ν (cm^{-1}) 2150 (RN$_3$), 1674 (RCON$_3$).

Known molecule (Van Berkel et al. 1998).

4-(3-ferrocenyl-ureido)-benzoic acid 32
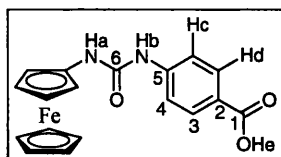
Azide **21** (300 mg, 1.18 mmol, 1.00 equiv.), 4-aminobenzoic acid **29** (244 mg, 1.78 mmol, 1.50 equiv.) and 1,4-dioxane (40 mL) were added to a nitrogen purged round-bottom flask. The reaction mixture was stirred under nitrogen in a 100 °C oil bath for 2 hours 50 minutes and then allowed to cool to room temperature. 2M hydrochloric acid (100 mL) was added to the reaction mixture and the product extracted into ethyl acetate (150 mL). The organic phase was washed with 2M hydrochloric acid (100 mL), dried with sodium sulphate and concentrated *in vacuo* at 50 °C, to afford the desired *acid* **32** as orange crystals in 96% yield (413 mg). ^{1}H-NMR δ (300MHz, d_6-DMSO) 3.96 (2H, b, Cp*), 4.14 (5H, s, Cp), 4.53 (2H, b, Cp*), 7.54 (2H, app d, J = 8.7 Hz, Hc), 7.85 (2H, app d, J = 8.7 Hz, Hd), 7.98 (1H, s, Ha), 8.87 (1H, s, Hb) 12.57 (1H, s, He). ^{13}C-NMR δ (100MHz, d_6-DMSO) 60.5 (Cp*), 63.5 (Cp*), 68.5 (*Cp*), 95.9 (Cp*), 116.5 (C4), 122.9 (C2), 130.2 (C3), 143.8 (C5), 152.0 (C6), 167.6 (C1). IR (KBr)v (cm^{-1}) 3315, 3093, 1680 (*CO*OH), 1593 (NH*CO*), 1540 (*NH*CO), 1412, 1308, 1288, 1245, 1175, 1120, 941, 856, 788, 697, 611. MS (FAB+) *m/z* 364.1 [M]. HRMS (FAB+): $C_{18}H_{16}FeN_2O_3$ requires 364.0510 found 364.05013 [M].

3,5-di(3-ferrocenyl-ureido)benzoic acid 37
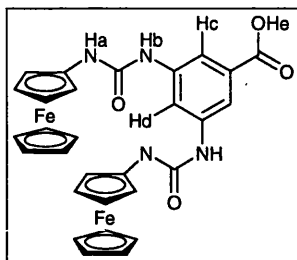
To a purged round-bottom flask was added *azide* **21** (800 mg, 3.14 mmol, 2.5 equiv.), 3,5-diaminobenzoic acid **35** (194 mg, 1.25 mmol, 1.00 equiv.) and 1,4-dioxane (60 mL) under nitrogen. The reaction mixture was stirred under nitrogen in a 100 °C bath for 1 hour and then allowed to cool to room temperature. Water (300 mL) and ethyl acetate (150 mL) were added to the reaction mixture. To improve separation the aqueous phase was acidified with hydrochloric acid. The organic phase was washed with water (100 mL) and on standing solid began to precipitate. The solution was concentrated *in vacuo* to afford the crude product as an orange oil, which was dried with a toluene azeotrope (100 mL), to yield a light orange solid. This was purified using silica flash chromatography and a gradient solvent system from dichloromethane 90/ methanol 10 to dichloromethane 50/ methanol 50. Drying *in vacuo* at 50 °C yielded the *acid* **37** as orange crystals (205 mg, 27%). ^{1}H-NMR δ (300MHz, d6-DMSO) 3.95 (4H, b, Cp*), 4.14 (10H, s, Cp), 4.54 (4H, b, Cp*), 7.69 (2H, s, Hc), 7.81 (1H, s, Hd), 8.08 (2H, s, Ha), 8.94 (2H, s, Hb). MS (FAB+ m/z) 607.07 [M+H]. **37** was considered an intermediate and full characterisation was completed for the *ester* **71**.

4-((3-ferrocenyl-ureido)methyl)benzoic acid 49
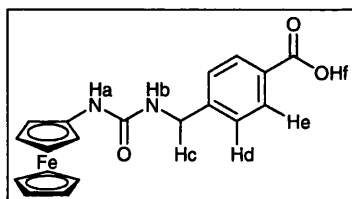
To a purged round-bottom flask was added *azide* **21** (250 mg, 0.980 mmol, 1.00 equiv.), 4-(aminomethyl)benzoic acid **52** (402 mg, 2.58 mmol, 2.60 equiv.) and 1,4-dioxane (10 mL). Due to poor solubility anhydrous DMSO (100 mL) was added and the mixture was sonnicated at 40 °C for 15 minutes, forming a suspension of white solid in orange solution. The reaction mixture was stirred under nitrogen in a 90 °C bath for 1 hour 15 minutes, forming a yellow/brown solution, with some brown/black solid. This was allowed to cool to room temperature. The solid was removed by filtration and discarded. 1M aqueous HCl (50 mL) and ethyl acetate (100 mL) were added to the reaction mixture. The phases were separated and the aqueous was washed with ethyl acetate (2x100 mL). The organic phases were combined, dried with anhydrous magnesium sulphate and concentrated *in vacuo* to afford the crude product. The product was purified using silica flash chromatography using a gradient of ethyl acetate 50/ petroleum ether (bp 40-60 °C) 50 eluent to ethyl acetate. Drying *in vacuo* at 50 °C yielded the *acid* **49** as light orange crystals (78 mg, 21%). A 2% impurity of *amide* **52** was also present. ^{1}H-NMR δ (300MHz, d$_6$-DMSO) 3.89 (2H, t, J = 2.1Hz, Cp*), 4.08 (5H, s, CP), 4.33 (2H, d, J = 6.0Hz, Hc), 4.45 (2H, t, J = 1.5Hz, Cp*), 6.49 (1H, t, J = 6.0Hz, Hb), 7.39 (2H, app d, J = 8.4 Hz, Hd), 7.74 (1H, s, Ha), 7.91 (2H, app d, J = 8.1 Hz, He). ^{13}C-NMR δ (75MHz, d$_6$-DMSO) 42.7, 60.0, 63.2, 68.4, 97.7, 126.8, 129.2, 145.9, 155.6 – 2 tertiary carbons are not seen. IR (KBr)ν (cm^{-1}) 3093, 2927, 1699 (*CO*OH), 1635 (NH*CO*), 1569 (*NH*CO), 1419, 1250, 1105.

4-((ferrocenyl-carbamoyl)methyl)benzoic acid 50
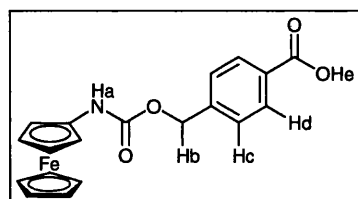
To a purged round-bottom flask was added *azide* **21** (100 mg, 0.390 mmol, 1.00 equiv.), 4-(hydroxymethyl)benzoic acid **47** (40.2 mg, 0.261 mmol, 0.67 equiv.) and 1,4-Dioxane (5 mL). The reaction mixture was stirred under nitrogen in a 90 °C bath for 30 min. Additional 4-(hydroxymethyl)benzoic acid **47** (89.9 mg total, 0.585 mmol, 1.5 equiv.) was added and the reaction mixture was stirred under nitrogen in a 90 °C bath for 30 minutes. Additional 4-(hydroxymethyl)benzoic acid was added **47** (189.9 mg total, 1.25 mmol, 3.2 equiv.) and the reaction mixture was stirred under nitrogen in a 95 °C bath for 1 hour. Triethylamine (0.90 mL, 5.6 mmol, 14 equiv.) and 1,4-Dioxane (1.5 mL) were added and reaction mixture was stirred under nitrogen in a 95 °C bath for 1 hour. NOTE: The boiling point of triethylamine is 89 °C, so the reaction mixture must be allowed to cool before the addition. Ethyl acetate (40 mL) and brine (40 mL) were added to the reaction mixture. The phases were separated and the aqueous was washed with ethyl acetate (3x 40 mL). The organic phases were combined, washed with 2M hydrochloric acid (2x 100 mL) and dried with anhydrous magnesium sulfate. The organic phase was then washed with 1M sodium hydroxide (50mL) to remove residual 4-(hydroxymethyl)benzoic acid, which caused an exotherm. It was then concentrated *in vacuo* to afford the crude product. The product was purified using silica flash chromatography using a gradient of ethyl acetate 30/ petroleum ether (bp 40-60 °C) 70 eluent to ethyl acetate. Drying *in vacuo* at 50 °C yielded the *acid* **50** as orange crystals (92 mg, 62%). ^{1}H-NMR δ (300MHz, d$_6$-DMSO) 3.93 (2H, b, Cp*), 4.09 (5H, s, Cp), 4.47 (2H, b, Cp*), 5.18 (2H, s, Hb) 7.50 (2H, app d, J = 8.1 Hz, Hc) 7.96 (2H, app d, J = 8.4 Hz, Hd) 9.08 (1H, s, Ha). IR (KBr)ν (cm^{-1}), 3223, 1714 (*COOH*), 1648 (NH*COO*), 1616 (*NH*CO), 1406, 1337, 1277, 1128, 1093, 756, 722. HRMS (FAB+): C$_{19}$H$_{17}$FeNO$_4$ requires 379.0507 found 380.0582 [M+H].

4-((ferrocenyl-carbamoyl-sulfonylmethyl)benzoic acid 51
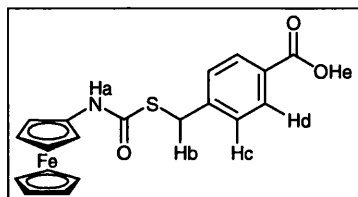
To a purged round-bottom flask was added *azide* **21** (100 mg, 0.390 mmol, 1.00 equiv.), 4-(mercaptomethyl)benzoic acid **48** (99 mg, 0.59 mmol, 1.5 equiv.) and 1,4-Dioxane (10 mL). The substrates readily dissolve. Hunig's base (200 μL, 1.18 mmol, 3.0 equiv.) was added turning the solution deep red. The reaction mixture was stirred under nitrogen in a 100°C bath for 2 hours, resulting in an orange solution containing a small amount of solid. The solution was allowed to cool to room temperature and the solid was removed by filtration and discarded. Ethyl acetate (50 mL) and 2M aqueous hydrochloric acid (100 mL) and were added to the reaction mixture. The phases were separated and the ethyl acetate phase was washed with 2M hydrochloric acid (2x 50 mL) and water (2x 50 mL). The organic phase was dried with anhydrous magnesium sulphate and concentrated *in vacuo* to afford the crude product. The product was crystallised from hot ethyl acetate using cyclohexane. Drying *in vacuo* at 50 °C yielded the *acid* **51** as light orange crystals (96 mg, 62%). ^{1}H-NMR δ (300MHz, d$_6$-DMSO) 3.84 (2H, b, Cp*), 3.97 (5H, s, Cp), 4.18 (2H, s, Hb), 4.50 (2H, b, Cp*), 7.47 (2H, app d, J = 7.8, Hc), 7.88 (2H, app d, J = 8.4, Hd), 9.76 (1H, s, Ha), 12.90 (1H, s, He). ^{13}C-NMR δ (75MHz, d$_6$-DMSO) 31.5, 59.6, 62.9, 67.8, 127.8, 128.3, 128.4, 143.3, 166.0, 172.5. IR (KBr)ν (cm^{-1}) 3010, 1684 (*C*OOH), 1646 (NH*C*O), 1559 (*NH*CO), 1481, 1425, 1321, 1292, 1260, 1183, 1106, 736, 668. HRMS (FAB+): C$_{19}$H$_{17}$FeNO$_3$S requires 395.0279 found 395.0274 [M].

Methyl (3-ferrocenyl-ureido)ethanoate 58
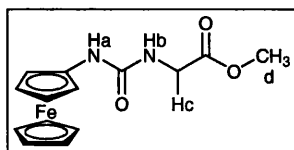
To a purged round-bottom flask was added *azide* **21** (100 mg, 0.392 mmol, 1.00 equiv.), glycine methyl ester hydrochloride **55** (97 mg, 0.784 mmol, 2.00 equiv.) and DMSO (6 mL) under nitrogen. The reaction mixture was stirred under nitrogen in a 100 °C bath for 3 hours 10 minutes and then allowed to cool to room temperature. Diethyl ether (100 mL) was added to the reaction mixture resulting in a yellow solution with brown oil. The diethyl ether phase was decanted and the oil was extracted again with diethyl ether (100 mL). The diethyl ether phases were combined and washed with water (200 mL). The aqueous wash was extracted with diethyl ether (100 mL) and the diethyl ether phases were combined. This solution was concentrated *in vacuo* to afford the crude product. The product was purified using silica flash chromatography using ethyl acetate 70/ petroleum ether (bp 40-60 °C) 30 eluent. Drying *in vacuo* at 50 °C yielded the *ester* **58** as light yellow/orange crystals (39 mg, 31%). ^{1}H-NMR δ (300MHz, CDCl$_3$) 3.77 (3H, s, Hd), 4.06 (2H, d, J= 5.4 Hz, Hc), 4.10 (2H, m, Cp*), 4.25 (5H, s, Cp), 4.35 (2H, m, Cp*), 5.71 (1H, s, Ha), 5.87 (1H, s, Hb). IR (KBr)ν (cm^{-1}) 3288, 3364, 1750 (*C*OO), 1636 (NH*C*O), 1592 (*NH*CO), 1489, 1437, 1410, 1389, 1284, 1229, 1104, 1022, 805, 695. HRMS (FAB+) *m/z*: C$_{19}$H$_{17}$FeNO$_3$S requires 316.0510 found 316.0534 [M].

Methyl phenyl(3-ferrocenyl-ureido)ethanoate 59
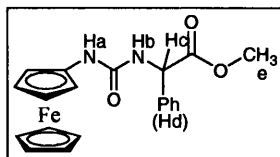
To a purged round-bottom flask was added *azide* **21** (250 mg, 0.980 mmol, 1.00 equiv.), *R*-2-phenylglycine methyl ester hydrochloride **62** (245 mg, 1.17 mmol, 1.2 equiv.) and DMSO (10 mL) under nitrogen. The reaction mixture was stirred under nitrogen in a 100 °C bath for 1hour and then allowed to cool to room temperature. Diethyl ether (100 mL) was added to the reaction mixture resulting in a yellow solution with brown oil. The diethyl ether phase was decanted and the oil was extracted again with diethyl ether (100 mL). The diethyl ether phases were combined and washed with water (2x 50 mL). The aqueous wash was extracted with diethyl ether (2x 100 mL) and the diethyl ether phases were combined. This solution was dried with sodium sulphate and concentrated *in vacuo* to afford the crude product. The product was recrystallised from hot ethanol and yielded the *ester* **59** as orange crystals (48 mg, 12%). ^{1}H-NMR δ (300MHz, CDCl$_3$) 3.68 (3H, s, Hc), 4.05 (2H, m, Cp*), 4.13 (5H, s, Cp), 4.27 (2H, m, Cp*), 5.51 (1H, d, J = 7.5 Hz, Hc), 5.68 (1H, s, Ha), 6.27 (1H, d, J = 6.0 Hz, Hb), 7.31 (5H, m, Hd). ^{13}C-NMR δ (75.5MHz, CDCl$_3$) 51.7, 56.2, 126.2, 127.5, 128.0, 136.0, 171.3. IR (Nujol)v (cm^{-1}) 3379, 1740 (*CO*OMe), 1628 (NH*CO*), 1551 (*NH*CO), 1206, 1172, 1103, 1024, 997, 936, 804, 722. HRMS (FAB+) *m/z*: C$_{19}$H$_{17}$FeNO$_3$S requires 393.0901 found 393.0898 [M+H].

Methyl (3-ferrocenyl-carbamoyl)ethanoate 64
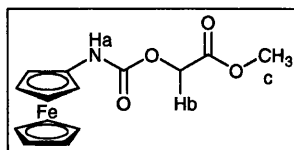
To a purged round-bottom flask was added *azide* **21** (129 mg, 0.51 mmol, 1.00 equiv.), 1,4-dioxane (10 mL) and crushed 4 Å molecular sieves under nitrogen. The reaction mixture was stirred for 30 minutes to allow traces of water to be removed. Methylglycolate **62** (237mg, 2.53 mmol, 5.00 equiv.) and Hunig's base (0.13mL, 0.77 mmol, 1.5 equiv.) were added under nitrogen and the flask was heated in a 100 °C bath for 1 hour 35 minutes and then allowed to cool to room temperature. Gravity filtration was used to remove the molecular sieves. Ethyl acetate (100 mL) was added to the solution and this was washed with water (50 mL and 2x 100 mL). The organic phase was dried with anhydrous magnesium sulphate and filtered. The solution was concentrated *in vacuo* to afford the crude product, which was purified using recrystalisation from diethyl ether. Drying *in vacuo* yielded the *ester* **64** as light orange crystals (47 mg, 29%**). ^{1}H-NMR δ (300MHz, CDCl$_3$) 3.78 (3H, s, Hc), 3.98 (2H, t, J = 1.8 Hz, Cp*), 4.18 (5H, s, Cp), 4.48 (2H, b, Cp*), 4.66 (2H, s, Hb), 6.11 (1H, s, Ha). ^{13}C-NMR δ (75MHz, CDCl$_3$) 51.3, 59.8, 60.1, 61.3, 63.5, 64.8, 68.2, 68.6, 68.7, 93.9, 151.8, 167.9 - includes 3 small impurity peaks. IR (KBr)ν (cm^{-1}) 3319, 1758 (*C*OOMe), 1714 (NH*C*O), 1558 (*NH*CO), 1486, 1436, 1417, 1390, 1261, 1207, 1116, 1002, 933, 810, 772, 720, 652. ** = reduced by trace amounts of impurities

Methyl (3-ferrocenyl-carbamoylsulfonyl)ethanoate 65
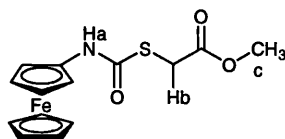
To a purged round-bottom flask was added *azide* **21** (100 mg, 0.39 mmol, 1.00 equiv.), 1,4-dioxane (10 mL) and crushed 4 Å molecular sieves under nitrogen. The reaction mixture was stirred for 20 minutes to allow traces of water to be removed. Methylmercaptoacetate **63** (180 μL, 1.95 mmol, 5.00 equiv.) and Hunig's base **45** (100 μL, 0.59 mmol, 1.5 equiv.) were added under nitrogen and the flask was heated in a 100 °C bath for 2 hours and then allowed to cool to room temperature. Gravity filtration was used to remove the molecular sieves. Ethyl acetate (100 mL) was added to the solution and this was washed with saturated brine solution (3x 150 mL). The organic phase was dried with anhydrous magnesium sulfate and filtered. The solution was concentrated *in vacuo* and purified using flash chromatography with ethyl acetate 70/ petroleum ether (bp 40-60 °C) 30 eluent. This yielded the *ester* **65** as light orange crystals (149 mg, 115% impure yield). ^{1}H-NMR δ (300MHz, CDCl$_3$) 3.59 (3H, s, Hc), 3.76 (2H, b, Hb), 4.02 (2H, b, Cp*), 4.02 (5H, s, Cp), 4.49 (2H, b, Cp*), 4.66 (2H, s, Hb), 6.69 (1H, s, Ha). IR (KBr)ν (cm^{-1}) 3318, 1746 (*COO*), 1654 (*NHCO*), 1543 (*NH*CO), 1474, 1436, 1360, 1299, 1157, 992, 933, 875, 690. MS (FAB+) *m/z* 333.1 [M].

(Ferrocenoyl amino)ethanoic acid 68
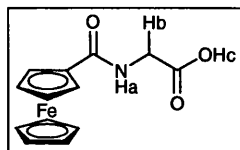
To a round-bottom flask was added ferrocene carboxylic acid **1** (350 mg, 14.9 mmol, 1.00 equiv.), anhydrous N,N-dimethylforamide (36 mL) and 1-hydroxybenzotriazole (403 mg, 29.8 mmol, 2.00 equiv.). The mixture was stirred under nitrogen, until the solid dissolves. Glycine benzylester hydrochloride (300 mg, 14.9 mmol, 1.00 equiv.) and triethylamine (2.1 mL, 15 mmol, 1.0 equiv) were added to the flask, which was then cooled to -4 °C and stirred under nitrogen. 1-(3-dimethylaminopropyl)-3-ethylcarbodiimide hydrochloride (583 mg, 29.8 mmol, 2.00 equiv) was added to the flask in 3 equal portions, at 15 minute intervals. The reaction mixture was allowed to warm to 4 °C over 2 hours and then to room temperature overnight (17 hours). Water (72 mL) was added to the flask, followed by diethylether (144 mL), which precipitated brown solid. The solid was isolated by Buchner filtration, washed with diethylether (100 mL) and then dissolved in ethylacetate (100 mL). The solution was purified through a silica plug and eluted with ethylacetate. The solution was concentrated *in vacuo* to give benzyl (ferrocenoyl amino)ethyloate, *ester* **67**, as an orange solid (281 mg, 52%). *Ester* **67** (86mg, 0.235 mmol, 1.00 equiv.) was added to a round-bottom flask with chloroform (6 mL), methanol (4 mL) and 1M sodium hydroxide (aq.) (0.38 mL). The reaction mixture was stirred at ambient temperature for 3 hours. The solution was acidified to pH = 1 with 1M hydrochloric acid and chloroform (10 mL), methanol (10 mL) and 1M hydrochloric acid (10 mL) were added. The chloroform layer was separated and the aqueous layer was extracted with chloroform (2x20 mL). The chloroform layers were combined, dried with anhydrous magnesium sulphate and concentrated *in vacuo* to give a fine orange solid. Purification was obtained using silica flash chromatography with a gradient system from ethyl acetate 50/ Petroleum ether (bp 40-60 °C) 50 to ethyl acetate, then methanol. The column was washed clean with methanol. The product was further dried *in vacuo* at 50 °C to yield the *acid* **68** as a yellow/orange oil (47 mg, 70% step, 36% overall). R_f (1:1 ethyl acetate / petroleum ether (bp 40-60 °C) = 0.11. ^{1}H-NMR δ (300MHz, d6-DMSO), 3.82 (2H, b, Hb), 4.24 (5H, s, Cp), 4.35 (2H, b, Cp*), 4.79 (2H, b, Cp*), 8.15 (1H, b, Ha), 12.8 (1H, s, Hc). IR

114

(KBr) ν (cm^{-1}) 3423, 1746 (COO), 1603 (CONH), 1549 (CONH), 1419, 1303, 1219, 1180, 815. HRMS (FAB+) m/z: $C_{13}H_{13}FeNO_3$ requires 287.0245 found 287.0247 [M].

2.8.3 Synthesis of activated linker molecules

Ferrocene carboxylic acid *N*-succinimide ester 2
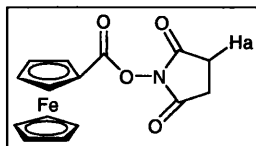
To a purged round-bottom flask was added ferrocene carboxylic acid **1** (2.00 g, 8.69 mmol, 1.0 equiv.), *N*-hydroxysuccinimide (1.14 g, 9.91 mmol, 1.14 equiv.) and anhydrous 1,4-dioxane (80 mL). Dicyclohexylcarbodiimide (2.04 g, 9.91 mmol, 1.14 equiv.) was dissolved in 1,4-dioxane and added over 5 minutes. The solution was stirred at room temperature for 22.5 hours. A small amount of light orange solid was removed by Buchner filtration and the solution was concentrated *in vacuo* to afford the crude product as an orange solid. The product was purified using silica flash chromatography with chloroform solvent. Drying *in vacuo* at 50 °C yielded the *ester* **2** as orange crystals (1.83g 74%). ^{1}H-NMR δ (400MHz, CDCl$_3$) 2.89 (4H, d, J = 5.1 Hz, Ha), 4.39 (5H, s, Cp), 4.57 (2H, t, J = 1.8 Hz, Cp*), 4.95 (2H, t, J = 1.8 Hz, Cp*).

Known compound (Takenaka et al. 1994).

116

4-(3-ferrocenyl-ureido)-benzoic acid *N*-succinimide ester 70
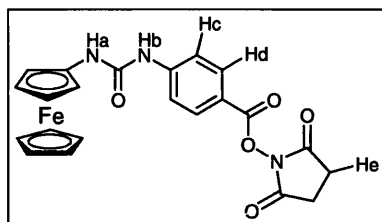
Dicyclohexylcarbodiimide (194 mg, 0.939 mmol, 1.14 equiv.) was dissolved in anhydrous 1,4-dioxane (2 mL) and added to a purged round-bottom flask, under nitrogen. *N*-hydroxysuccinimide (108 mg, 0.939 mmol, 1.14 equiv.) was added. *Acid* **32** (300 mg, 0.823 mmol 1.0 equiv.) was dissolved in anhydrous 1,4-dioxane (13 mL) and added dropwise to the flask. The solution was stirred at room temperature for 23 hours. A small amount of light brown solid was removed from the red/orange reaction mixture by Buchner filtration. Water (100 mL) and ethyl acetate (50 mL) were added to the reaction mixture. The ethyl acetate phase was separated and the aqueous was extracted with ethyl acetate (100 mL). The ethyl acetate phases were combined, dried with sodium sulphate and concentrated *in vacuo* to afford the crude product as an orange oil, which was purified using silica flash chromatography with a gradient system from ethyl acetate 60/ petroleum ether (bp 40-60 °C) 40 to ethyl acetate. Drying *in vacuo* at 50 °C yielded the *ester* **70** as fine orange crystals (237 mg, 66%). R_f (5:1 ethyl acetate / petroleum ether (bp 40-60 °C) = 0.41 ^{1}H-NMR δ (300MHz, d6-DMSO) 2.88 (4H, s, He), 3.98 (2H, t, J = 1.8 Hz, Cp*), 4.16 (5H, s, Cp), 4.55 (2H, t, J = 1.8 Hz, Cp*), 7.68 (2H, m, Hc), 8.00 (2H, m, Hd), 8.11 (1H, s, Ha), 9.16 (1H, s, Hb). ^{13}C-NMR δ (75.5MHz, d$_6$-DMSO) 25.9, 61.1, 64.2, 69.1, 117.7, 131.9, 170.9 - 5 tertiary carbons are not seen. IR (KBr)ν (cm^{-1}) 3379 (NH), 2928 (ArH), 2851 (ArH), 1762 (*COO*), 1734 (CO succinimide), 1718 (CO succinimide), 1600 (NH*CO*NH), 1540 (*NH*CO), 1487, 1416, 1363, 1328, 1243, 1202, 1176, 1073, 995, 851, 755, 689, 653. HRMS (ES+): C$_{13}$H$_{18}$O$_2$ requires 462.0747 [M+H] found 462.0748.

3,5-di(3-ferrocenyl-ureido)benzoic acid *N*-succinimide ester 71
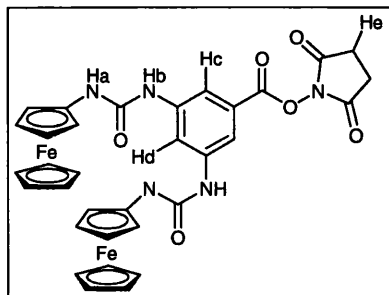
N-hydroxysuccinimide (23 mg, 0.193 mmol, 1.17 equiv.) was added to a purged round-bottom flask, under nitrogen. Dicyclohexylcarbodiimide (40 mg, 0.192 mmol, 1.16 equiv.) was dissolved in anhydrous 1,4-Dioxane (1 mL) and added. *Acid* 37 (100 mg, 0.165 mmol 1.0 equiv.) was dissolved in anhydrous 1,4-Dioxane (4 mL) and added dropwise to the flask. The solution was stirred at room temperature, under nitrogen, for 21 hours. Water (150 mL) and ethyl acetate (100 mL) were added to the orange reaction mixture. The ethyl acetate phase was separated and the aqueous was extracted with ethyl acetate (100 mL). The ethyl acetate phases were combined, dried with sodium sulphate and concentrated *in vacuo* to afford the crude product as an yellow/orange oil. This was purified using silica flash chromatography with a gradient system from ethyl acetate 50/ petroleum ether (bp 40-60 °C) 50 to ethyl acetate 70/ petroleum ether (bp 40-60 °C) 30. The product was concentrated *in vacuo* at 50 °C to yield the *ester* 71 as light yellow crystals (33 mg, 28%). R_f (4:1 ethyl acetate / petroleum ether (bp 40-60 °C) = 0.36 ^{1}H-NMR δ (300MHz, d6-DMSO), 2.90 (2H, s, He), 3.97 (2H, b, Cp*), 4.15 (5H, s, Cp), 4.54 (2H, b, Cp*), 7.82 (0.5H, s, Hd), 7.87 (1H, s, Hc), 7.92 (1H, s, Ha), 8.92 (1H, s, Hb). HRMS (FAB+) *m/z*: $C_{29}H_{26}Fe2N4O_4$ requires 607.0731 [M+H] found 607.0739 [M].

4-((3-ferrocenyl-ureido)methyl)benzoic acid *N*-succinimide ester 72
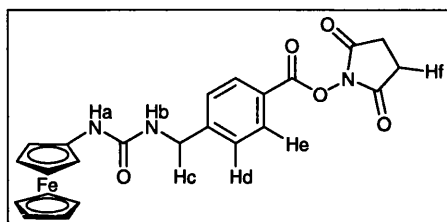
Dicyclohexylcarbodiimide (62.1 mg, 0.301 mmol, 1.14 equiv.) was dissolved in anhydrous 1,4-dioxane (2 mL) and added to a purged round-bottom flask, under nitrogen. *N*-hydroxysuccinimide (34.6 mg, 0.301 mmol, 1.14 equiv.) was added. *Acid* **49** (100 mg, 0.264 mmol 1.0 equiv.) was dissolved in anhydrous 1,4-dioxane (8 mL) and added dropwise to the flask. The solution was stirred at room temperature for 24 hours. Water (100 mL) was added to the flask and the small amount of light yellow solid which precipitated was removed, from the orange reaction mixture, by sinter filtration. The aqueous phase was extracted with ethyl acetate (100 mL), which was washed with water (3x 50 mL) and dried with anhydrous magnesium sulphate. The organic phase was concentrated *in vacuo* and recrystallised from ethyl acetate to yield the *ester* **72** as light yellow/orange crystals (34 mg, 27%). ^{1}H-NMR δ (300MHz, d$_6$-DMSO) 2.84 (1H, s, Hf), 3.89 (2H, t, J = 2.1Hz, Cp*), 4.09 (5H, s, Cp), 4.40 (2H, d, J = 5.7 Hz, Hc), 4.45 (2H, t, J = 1.8Hz, Cp*), 6.56 (1H, t, J = 6.5Hz, Hb), 7.54 (2H, app d, J = 8.7 Hz, Hd), 7.82 (1H, s, Ha), 8.07 (2H, app d, J = 8.4 Hz, He). MS (FAB+) *m/z* 475.1 [M].

(ferrocenoyl amino)ethanoic acid *N*-succinimide ester 73
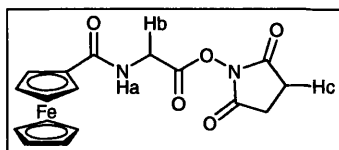
Dicyclohexylcarbodiimide (164 mg, 0.795 mmol, 1.14 equiv.) was dissolved in anhydrous 1,4-dioxane (2 mL) and added to a purged round-bottom flask, under nitrogen. *N*-hydroxysuccinimide (92.4 mg, 0.939 mmol, 1.28 equiv.) was added. *Acid* **68** (200 mg, 0.627 mmol 1.0 equiv.) was dissolved in anhydrous 1,4-dioxane (8 mL) and added dropwise to the flask. The solution was stirred at room temperature for 24 hours. A small amount of light brown solid was removed from the red/orange reaction mixture by Buchner filtration. The product was absorbed directly onto silica and purified using silica flash chromatography with a gradient system from ethyl acetate 80/ petroleum ether (bp 40-60 °C) 20 to ethyl acetate, then from dichloromethane to dichloromethane 50/ acetonitrile 50. The solvent was removed *in vacuo* and the orange oil produced crystallised on standing. Drying *in vacuo* at 50 °C yielded the *ester* **73** as fine orange crystals (24 mg, 10%). ^{1}H-NMR δ (300MHz, CDCl$_3$) 2.80 (4H, b, Hc), 4.19 (5H, s, Cp), 4.33 (2H, b, Cp*), 4.48 (2H, t, J = 5.4 Hz, Hb) 4.66 (2H, b, Cp*), 6.11 (1H, b, Ha). IR (KBr)ν (cm^{-1}) 3422, 1735 (*C*OO), 1707 (CO Succinimide), 1603 (*C*ONH), 1540 (CO*NH*), 1405, 1302, 1218, 1179, 1107, 1026, 1004, 816, 668.

2.8.4 Synthesis of phosphoramidite molecules

N-ferrocenoyl-6-amino-hexan-1-ol 27
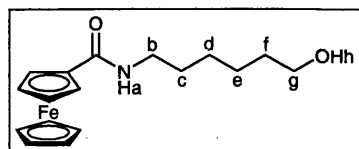
Oxalyl chloride (0.40 mL, 5.2 mmol, 2.4 equiv.) was added dropwise, to a stirred solution of ferrocene carboxylic acid (500 mg, 2.17 mmol, 1.0 equiv) in dry dichloromethane (DCM, 100 mL) at 0 °C under N_2. The reaction mixture was stirred for 1 hour and then allowed to warm to room temperature forming a dark red solution. The solvent and remaining oxalyl chloride was removed *in vacuo* to give the crude ferrocenyl chloride **24**. The ferrocenyl chloride was then taken up in dry, chilled (0 °C) DCM (100 mL) which was added dropwise, *via* a pressure equalised dropping funnel, to a stirred solution of 6-amino hexan-1-ol **74** (1.28 g, 10.9 mmol, 5.0 equiv) in dry DCM (200 mL) at 0 °C under N_2. The reaction mixture was stirred for 1 hour at 0 °C and allowed to warm to 10 °C over 30 minutes. The reaction mixture was concentrated to approximately 150 mL *in vacuo* and washed with saturated sodium bicarbonate (350 mL) and then saturated brine (100 mL). The organic layer was dried over magnesium sulphate and the solvent removed *in vacuo*. The crude mixture was purified using silica flash chromatography with a gradient system from ethyl acetate 50/ petroleum ether (bp 40-60 °C) 50 to ethyl acetate. Drying *in vacuo* at 50 °C yielded the *alcohol* **27** as fine orange crystals (382 mg, 53%). ^{1}H-NMR δ (300MHz, CDCl$_3$) 1.30-1.50 (4H, m, Hd and He), 1.50-1.65 (4H, m, Hc and Hf), 3.38 (2H, b, Hg), 3.66 (2H, b, Hb), 4.19 (5H, s, Cp), 4.33 (2H, b, Cp*), 4.65 (2H, b, Cp*), 5.73 (1H, b, Ha). ^{13}C-NMR δ (75.5MHz, CDCl$_3$) 25.7, 25.9, 31.0, 33.0, 39.7, 63.0, 66.4, 70.1, 70.7, 170.7.

Known compound (Beilstein, 2001)

N-Ferrocenoyl-6-aminohexan-1-(2-cyanoethyldiisoproylaminophoshoramidite) 28
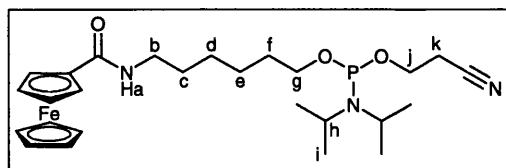
N,N-diisopropylethylamine (770 μL, 4.4 mmol, 4.0 equiv) was added to a stirred solution of the *alcohol* 27 (363 mg, 1.1 mmol, 1.0 equiv) in dry tetrahydrofuran (THF, 12 mL) under nitrogen. 2-cyanoethyldiisoproylchlorophosphoramidite (370 μL, 1.66 mmol, 1.5 equiv) was added dropwise and the reaction stirred for 15 minutes. Deionised water (200 μL) was added and the reaction stirred for a further 30 minutes. Diethylether-triethylamine (50/50, 15 mL) was added and a precipitate formed. The mixture was washed with saturated sodium bicarbonate (50 mL). The organic layer was separated, added with diethylether (20 mL), and washed with water (50 mL) and brine (50 mL). The organic layer was then dried over magnesium sulphate and the solvent removed *in vacuo*. The crude mixture was purified using silica flash chromatography (ethyl acetate 60/ petroleum ether (bp 40-60 °C) 40 + 1% triethylamine) and dried *in vacuo* to give the *phosphoramidite* 28 (582 mg, 61% yield) as a bright orange powder. ^{1}H-NMR δ (300MHz, CDCl$_3$) 5.76 (4H, b, Ha), 4.65 (2H, t, J = 1.8 Hz, Cp*), 4.32 (2H, t, J = 1.8 Hz, Cp*), 4.19 (5H, s, Cp), 3.83 (2H, m, Hj), 3.58 – 3.62 (4H, m, Hg and Hh), 3.33 – 3.39 (2H, m, Hb), 2.64 (2H, t, J = 6.3 Hz and Hk), 1.52 – 1.70 (4H, m, Hc and Hf), 1.35 – 1.49 (4H, m, Hd and He), 1.12 – 1.20 (12H, m, Hi). ^{13}C-NMR δ (75.5MHz, CDCl$_3$) 20.8, 25.0, 26.1, 27.1, 30.3, 31.6, 39.9, 43.3, 43.4, 58.5, 64.0, 68.4, 70.1, 70.7, 118.2, 170.4. ^{31}P-NMR δ (300MHz, CDCl$_3$) 106.9. IR (CDCl$_3$ film)ν (cm^{-1}) 3331, 2962, 2934, 2861, 1633, 1537, 1461, 1362, 1295,1183, 1025, 976, 896, 696. (FAB+) *m/z* 529.2 [M].

Known compound (Beilstein, 2001)

N-Ferrocenoyl-6-aminohexan-1-ferrocenylmethanoate 75
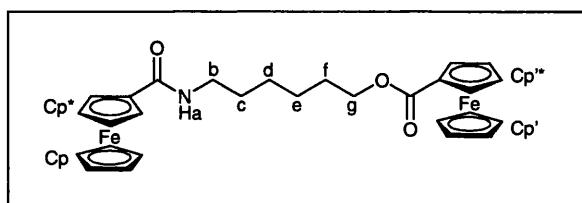
Oxalyl chloride (0.66 mL, 7.7 mmol, 3.5 equiv.) was added dropwise, to a stirred solution of ferrocene carboxylic acid **1** (500 mg, 2.17 mmol, 1.0 equiv) in dry dichloromethane (100 mL) at 4 °C under N_2. The reaction mixture was stirred for 1 hour and then allowed to warm to room temperature forming a dark red solution. The solvent and remaining oxalyl chloride was removed *in vacuo* to give the crude ferrocenyl chloride **24**. The ferrocenyl chloride was then taken up in dry, chilled (4 °C) DCM (75 mL) and was added dropwise, *via* a pressure equalised dropping funnel, to a stirred solution of 6-amino hexan-1-ol (1.28 g, 10.9 mmol, 5.0 equiv) in dry dichloromethane (25 mL) at 4 °C under N_2. The reaction mixture was stirred for 1 hour at 4 °C and allowed to warm to room temperature over 1 hour. The reaction mixture was washed with water (100 mL). The aqueous was extracted with DCM (50 mL) and the organic phases were combined. The organic layer was dried over magnesium sulfate and the solvent removed *in vacuo*. The crude mixture was purified using silica flash chromatography with a gradient system from ethyl acetate 50/ petroleum ether (bp 40-60 °C) 50 to ethyl acetate. Drying *in vacuo* at 50 °C yielded orange crystals. Further purification was required. The solid was dissolved in ethyl acetate (100 mL) and extracted with 2M sodium hydroxide (100 mL). The organic layer was dried over magnesium sulfate and the solvent was removed *in vacuo*. The *dimer* **75** was yielded as orange crystals (303 mg, 52%). ^{1}H-NMR δ (300MHz, CDCl$_3$) 1.38-1.58 (4H, m, Hd and He), 1.58-1.71 (2H, m, Hc), 1.71-1.81 (2H, m, Hi), 3.35-3.45 (2H, m, Hb), 4.18-4.22 (10H, 2s, Cp and Cp'), 4.23 (2H, t, J = 6.9 Hz, Hg), 4.34 (2H, b, Cp*), 4.39 (2H, t, J = 1.8 Hz, Cp'*), 4.66 (2H, b, Cp*), 4.81 (2H, t, J = 1.8 Hz, Cp'*), 5.64-5.81 (1H, m, Ha). ^{13}C-NMR δ (75.5MHz, CDCl$_3$) 26.1, 27.0, 29.3, 30.4, 39.8, 64.4, 69.1, 70.1, 70.5, 70.7, 71.7, 71.8, 120.2, 172.22. IR (KBr) v (cm^{-1}) 3084, 2934, 2871, 1701, 1639, 1526, 1457, 1374, 1277, 1152, 1105, 1027, 999, 962, 826, 774, 729, 510. HRMS (FAB+) *m/z*: $C_{28}H_{31}Fe_2NO_3$ requires 541.1003 [M] found 541.1010 [M].

2.9 Electropotential determination

Protocol 1 – Determination of electropotentials

Assay

A 10 mM solution of the ferrocenylated linker in DMSO was prepared and was diluted to 1 mM in 0.1M sodium acetate. The dilution should be done sufficiently slowly to prevent precipitation of the linker.

DPV analysis

Initial and end potential were varied for individual samples (approximately 500 mV range) so that the electropotential occurred in the centre of the DPV trace.

The electropotential is determined by DPV at 20 $^{\circ}$C: DPV 1, shown in Table 2.1.
WE Electrode: gold

	Pretreatment	Measurement		Potentials		
Protocol	Conditioning Potential	Modulation time (s)	Interval time (s)	Step potential (mV)	Modulation Amplitude (mV)	Standby Potential
DPV1	Initial potential / 5s	0.04	0.1	0.3	49.95	Final potential

Table 2.1 – DPV protocol.

2.10 Biological assays and analysis

2.10.1 Oligonucleotide sequences

The sequences of the oligonucleotides used in this chapter are given here.

By convention all oligonucleotide sequences are written 5' to 3'. [CX] indicates an alkyl spacer X carbon atoms long. The grey shaded sections on the target oligonucleotides indicated the complementary region to the probe oligonucleotides. Mismatched bases are shown in dark grey

S1 Digestion work

ACTB gene (beta actin) (Josefsson et al. 2000)

Probe (BAPR): [C6] ATG CCC TCC CCC ATG CCA TCC TGC GT (26mer)

FVR4 Oligonucleotide from Molecular Sensing PLC

Oligonucleotide: TGA AAG GTT ACT TCA AGG ACA AAA T (24mer)

T7 Digestion Work

C282Y (Human hemochromatosis gene) (Ugozzoli et al. 2002)

Probe (C282Y): [C12] ATATACGTGCCAGGTGGA (18mer)

Hairpin (C282YPR HP):

[C12] ATATACGTGCCAGGTGGGCCCACCTGGCACGTATAT

Synthetic Target (C282YST):

GAGGGGCTGATCCAGGCCTGGGTGCTCCACCTGGCACGTATATCTCTGCTCT

TCCCCAGG (60mer)

Dual Labelled Probe (C282Y): FAM-ATATACGTGCCAGGTGGA-TAMRA

CtrA gene (Meningococcal meningitis) (Guiver et al. 2000)

Probe (CTR044): CATTGCCACGTGTCAGCTGCACAT (24mer)

Synthetic Target (CTRA comp):

TGTGCAGGATACGAATGTGCAGCTGACACGTGGCAATGTAGTACGAACTG

(50mer)

ACTB gene (beta actin) (Josefsson et al. 2000)

Probe (BAPR): [C6] ATG CCC TCC CCC ATG CCA TCC TGC GT (26mer)

Synthetic Target (BAST):

CCAGCCAGGTCCAGACGCAGGATGGCATGGGGGAGGGCAGACCCCTCGTA

(50mer)

ACADM gene (medium chain acyl-CoA dehydrogenase) (Fujii et al. 2000)

Probe (MC11PR): CTAGAATGAGTTACCAGAGAGCAGCTTGG (29mer)

Synthetic Target (MC11ST 5'CC):

CCAGAATCAACCTCCCAAGCTGCTCTCTGGTAACTCATTCTACCTAGTTC

(50mer)

2.10.2 Experimental procedures

This section details the experimental protocols used in the chapter for both the assay work. Several of the experimental protocols use the same DPV protocol, so these methods are given at the end of the section.

Protocol 2 – Oligonucleotide labelling and digestion

C6 amino modified oligonucleotide (20 nmol) dissolved in 50 μL of 500 mM potassium carbonate buffer (pH = 9.0) was added to a solution of *ester* **70** (0.46 mg, 1 μmol) in 50 μL anhydrous DMSO. The mixture was shaken at 25 °C, wrapped in foil, for 15 hours. The conjugate was purified from unconjugated ferrocene and other low molecular weight species using a Sephadex™ G-25 column (Sigma). The column was conditioned with 0.1M ammonium acetate (15 mL) and the sample was diluted with 0.1M ammonium acetate (910 μL) to give a 1 mL sample volume. The sample was added to the column and allowed to drain. The column was eluted with 0.1M ammonium acetate (1.5 mL) and the first 1 mL was collected. A second column was conditioned with MilliQ (15 mL) and the collected oligonucleotide solution was charged to this and allowed to drain. The column was eluted with MilliQ (1.5 mL) and the eluent (1.5 mL) was collected.

Protocol 3 – S1 endonuclease digestion

Assays

Digest assay (200 μL): *ester* **70** labelled oligonucleotide (5 μM), S1 Buffer* (1X), S1 Nuclease 0.25 U / μL in MilliQ

Control assay (200 μL): as Digest assay with enzyme omitted

* The S1 enzyme buffer (Promega, USA) contains a high concentration of chloride ions, which would swamp the electrochemical response. A replacement buffer of 0.25M

127

ammonium acetate and 45mM zinc acetate (pH = 6.5) [1X concentration] is used instead.

The assays are both incubated at 37 °C for 1 hour.

Analysis

The digestion is followed by DPV: *DPV 2*; -100 mV to 400 mV (Protocol 14)
Working Electrode: glassy carbon

Protocol 4 – Agarose gel electrophoresis

Prepare 2 wt% agarose gel in 0.5X TBE buffer, pour into an electrophoresis tank and allow it to set.

The S1 Digest assay (Protocol 3) is prepared, omitting the enzyme. Chill the assay to 4 °C, add the enzyme and vortex. Incubate the assay at 37 °C, in 50 µL aliquots. Remove aliquots after the appropriate incubation times (2, 4, 6, 8, 10, 15 and every further 5 minutes until 60 minutes) and immediately chill to 4 °C.

Charge bromophenol blue loading buffer (New England Biolabs) (6X, 10 µL) to each time-course aliquot. This primarily contains glycerol to ensure that the sample remains in the well and SDS to ensure that the DNA remains single stranded, with no secondary structure. Centrifuge the samples and load onto the agarose gel (15 µL aliquot). The gel is covered by 0.5X TBE buffer (TBE buffer contains Tris buffer, boronic acid and EDTA). Also load a 100 bp DNA ladder (100 bp signifies the increase in fragment size). Run the electrophoresis at 10 V / cm for 30 minutes. Empty the buffer from the tray and add SYBR Gold solution (Molecular Probes). After 20 minutes wash the gel and visualise under UV light.

Protocol 5 – T7 digestion of hairpin oligonucleotides

Assays

Digest assay: C282Y hairpin oligonucleotide **81** (10 µM), 1X T7 buffer (NEBuffer 4: 50 mM potassium acetate; 20mM Tris-acetate; 10 mM magnesium acetate; 1 mM DTT; pH 7.9 @ 25 °C) and T7 exonuclease 0.1U / µL

Control assay: as Digest assay with enzyme omitted

End-point: the assays are both incubated at 25 °C for 1 hour.

Time-course: the assays are both incubated at 25 °C and sampled consecutively (after a 10 second delay) with DPV.

Analysis

The digestion was analysed by DPV: *DPV 2*; -100 mV to 300 mV (Protocol 14)

Working Electrode: glassy carbon

Protocol 6 – T7 digestion of duplex: post-labelled probe

Assays

Complementary Digest assay: C282Y oligonucleotide **80** (8.0 µM), C282YST target (6.0 µM), 1X PCR buffer (50 mM KCl; 10 mM Tris.HCl; 1.5 mM $MgCl_2$) and T7 exonuclease (0.05U/ µL)

Complementary Control assay: as Complementary Digest assay with T7 exonuclease omitted

Mismatch Digest and Control assays: as Digest and Control assays above with a CTRA comp target.

All the assays are hybridised at 25 °C/ 15 minutes, without the enzyme. The enzyme was then added (if required) and the assay was then incubated at 37 °C for 1 hour.

Analysis

The digestion was analysed by DPV: *DPV 2*; -100 mV to 300 mV (Protocol 14)

Working Electrode: glassy carbon

Protocol 7 – Determination of amidite labelling efficiency

Assays

Digest Assay: amidite labelled oligonucleotide (10 μM), Buffer* (1X), S1 Nuclease 0.25 U/ μL in MilliQ

Control Assay: as Digest assay with enzyme omitted

* The buffer is described in Protocol 3.

The assays are both incubated at 37 °C for 1 hour.

Analysis

The digestion is followed by DPV: *DPV 3*; -100 mV to 550 mV (Protocol 14)

Working Electrode: both gold and glassy carbon

Protocol 8 – Amidite labelled C282YP gene sensor

Assays

Complementary Digest assay: ferrocenylated C282Y oligonucleotide **78** (1.0 μM), C282YST target (1.2. μM), 1X PCR buffer, $MgCl_2$ (2.5 mM) and T7 exonuclease (0.1U/ μL)

Complementary Control assay: as Digest assay with T7 exonuclease is omitted

Mismatch Digest and Control assays: as Digest and Control assays above with a CTRAcomp target

All the assays are hybridised at 20 °C/ 15 minutes, without the enzyme. The enzyme was then added (if required) and the assay was then incubated at 37 °C for 1 hour.

Analysis

The digestion was analysed by DPV: *DPV 3*; -100 mV to 550 mV (Protocol 14).
Working Electrode: glassy carbon

Protocol 9 – Time-course: amidite labelled C282YP gene sensor

Assays

Complementary Digest assay: ferrocenylated C282Y oligonucleotide **78** (10.0 μM), C282YST target (12.0 μM), 1X PCR buffer, $MgCl_2$ (2.5 mM) and T7 exonuclease (0.1U/ μL)
Complementary Control assay: as Digest assay with T7 exonuclease omitted

All the assays are hybridised at 20 °C/ 15 minutes, without the enzyme. The enzyme was then added, if required, and the assays were then incubated at 25 °C for 1 hour. This was repeated with incubation at 37 °C.

Analysis

The digestion was analysed by DPV: *DPV 2*. 150 mV to 550 mV
Working Electrode: glassy carbon

Protocol 10 – Low concentration amidite labelled gene sensor

Assays

The combinations of probe and target are given in the text, in section 6.3.2.

Complementary Digest assay: amidite labelled oligonucleotide (0.55 μM), target (0.5 μM), 1X PCR buffer, $MgCl_2$ (2.5 mM) and T7 exonuclease (0.1U/ μL).

Complementary Control assay: as Digest assay with T7 exonuclease omitted

Mismatch Digest and Control assays: as Digest and Control assays above with a mismatched target

All the assays are hybridised at 37 °C / 15 minutes, without the enzyme. The enzyme was then added, if required, and the assays were then incubated at 37 °C for 1 hour.

Analysis

The digestion was analysed by DPV: *DPV 4*; -100 mV to 550 mV (Protocol 14).
Working Electrode: both glassy carbon and gold.

Protocol 11 – LightCycler assay

Assays

Complementary Digest assay: C282Y dual labelled probe (1.0 μM), C282YST (1.2 μM), 1X T7 buffer, BSA 1X and T7 exonuclease (0.01 U/ μL).

Complementary Control assay: as Digest assay with T7 exonuclease omitted

Mismatch Digest and Control assays: as Digest and Control assays above with a CTRAcomp target

Analysis

Mix all the assays, omitting the enzyme. Heat to 95 °C to denature the assay. Cool to 4 °C and then add the enzyme. Add 20 μL aliquot of each assay to a chilled LightCycler capillary. Centrifuge the sample and analyse in LightCycler. Ensure that the search temperature is at 20 °C.

Protocol 12 – Amperometry

Assays

S1 Digest assays: amidite labelled oligonucleotide (10 μM), S1 Buffer (1X), S1 endonuclease 0.25 U/ μL in MilliQ
Incubate 37 °C for 1 hour.

T7 Digest assay: Fc-amidite-oligonucleotide (10 μM), target (12 μM), 1X PCR buffer, $MgCl_2$ (2.5 mM) and T7 exonuclease (0.1 U/ μL).
Hybridise at 20 °C / 15minutes, without enzyme. Add enzyme and incubate at 37 °C/ 1 hour.

Probe Assays: the enzyme and target (if present) are omitted

Buffer Assays: contain the appropriate buffer and enzyme

Analysis: amperometry

The amperometry potential steps are given in Table 2.2, followed by the protocol used in Table 2.3. Analysis was undertaken at 25 °C.

Probe	Initial potential (mV)	Final potential (mV)
C282Y	250	550
CTR	120	420
BAPR	120	420

Table 2.2 – Amperometry voltage steps.

Pretreatment	Measurement	Potentials		
Conditioning Potential	Interval time (s)	Step potential (mV)	Step potential duration (s)	Standby Potential
Initial potential / 120s	0.1	Final potential	10	Final potential

Table 2.3 – Amperometry protocols.

Protocol 13 – Analysis of PCR amplicons

Assay

PCR was performed on 100 µL scale. The PCR assay details are given in Table 2.4, followed by the gene, primer and probe sequences. All components, except the probe and T7 exonuclease enzyme, were added and the assay was cycled at 95 °C for 10 minutes, followed by 40 cycles of 95 °C for 15 seconds and 60 °C for 1 minute. On completion the probe was added and samples were heated to 95 °C for 1 minute and then immediately cooled to 37 °C for 15 minutes. T7 exonuclease was added and sample incubated for a further 30 minutes.

Component	PCR	T7 Digest
T7 Buffer	1.1X	1.0X
MgCl$_2$	3.7 mM	3.5 mM
dNTPs	0.17 mM	0.20 mM
Primers	0.53 µM	0.50 mM
BSA	0.11 mg/mL	0.10 mg/mL
Taq	0.1 U / µL	0.1 U / µL
Human genomic DNA	0.4 ng / µL	0.4 ng / µL
Probe oligonucleotide **79**		0.45 µM
T7 Exonuclease		0.1 U / µL

Table 2.4 – PCR end point assay.
With the addition of the probe and enzyme for the T7 end-point digestion, the concentrations of the components in the assay change.

Matched PCR

Gene: ACTB (beta actin) (Josefsson et al. 2000)

Forward Primer (BAF): CAGCGGAACCGCTCATTGCCAAT G

Reverse Primer (BAR): TCACCCACACTGTGCCCATCTACGA

Probe (BAPR): ATGCCCTCCCCCATGCCATCCTGCGT

Mismatched PCR

Gene: ACADM (medium chain acyl-CoA dehydrogenase)

Forward Primer (MC11w): GCTGGCTGAAATGGCAATGA

Reverse Primer (MC11com): CTGCACAGCATCAGTAGCTAACTGA

Analysis

The digestion was analysed by DPV: *DPV 2*; 0 mV to 500 mV (Protocol 14).

Working Electrode: glassy carbon.

Protocol 14 – Detail of DPV analysis

For the end-point analysis experiments the analysis should always be done with the first DPV trace, as electrode fouling can affect the response of subsequent traces. The 3 DPV protocols are given in Table 2.5.

Protocol	Pretreatment	Measurement		Potentials		
	Conditioning Potential	Modulation time (s)	Interval time (s)	Step potential (mV)	Modulation Amplitude (mV)	Standby Potential
DPV 2	Initial potential / 10s	0.04	0.1	0.3	49.95	Final potential
DPV 3	None	0.04	0.1	1.05	49.95	Final potential
DPV 4	None	0.04	0.9	1.05	49.95	Final potential

Table 2.5 – DPV protocols.

2.11 Surface modification experimental

2.11.1 Oligonucleotide sequences

Fluorescence work (n = 8 or 20)

Capture probes:

Biotin-T_8 and Biotin-T_{20}

Reporter oligonucleotides:

Fluor-A_n: Fluorescein-A_n

Fluor-A_n-C282Y: Fluorescein-A_n-ATATACGTGCCAGGTGGA

Mismatched reporter oligonucleotide:

Fluor-T_n-C282Y: Fluorescein-T_n-ATATACGTGCCAGGTGGA

Dual labelled probe:

Dual labelled probe (A_8-C282Y): FAM-A_8-ATATACGTGCCAGGTGGA-TAMRA

Electrochemical work (n = 8 or 20)

Amidite labelled reporter oligonucleotide:

FcCONH$(CH_2)_6$-O-A_n

Amidite labelled mismatched reporter oligonucleotide:

FcCONH$(CH_2)_6$-O-T_n

Capture probes:

HS-T_n

2.11.2 Experimental procedures

This section details the experimental protocols used for the surface modification work.

Protocol 15 – Functionalisation and analysis of streptavidin plates

Immobilisation of biotinylated oligonucleotide capture probes

Plates: 96-well streptavidin coated plates (SigmaScreen™, Sigma-Genosys, UK).

Wash wells with PBS buffer (1X, 100 µL) containing Tween (0.05%). Add biotinylated oligonucleotide (1.0 µM) in PBS buffer (1X) containing Tween (0.05%). Allow to bind for 30 minutes at 37 °C. To remove any unbound oligonucleotides wash the wells with PBS buffer (1X, 100 µL) containing Tween (0.05%), followed by TE buffer (pH = 7.6, 3 x 100 µL). [Note: TE buffer is 10 mM Tris.HCl and 1 mM EDTA].

Hybridisation of reporter oligonucleotide

Reporter assay: fluorescein-oligonucleotide (1.0 µM), TE buffer (pH = 7.6, 25 °C) and NaCl (1.0 M).

Add the reporter assay (200 µL) to the well and allow to stand overnight for the specified time at room temperature (20 °C). Wash the wells (3x) with 100 µL TE buffer (pH = 7.6, 25 °C), NaCl (1.0M). Add TE buffer (pH = 7.6, 25 °C, 100 µL) containing NaCl (1.0 M) to each well and analyse using a plate fluorimeter (FARCyte, Tecan).

Experimental Note: pH of TE buffer varies with temperature. Buffer is prepared at 25 °C (pH = 7.6). Hybridisation occurs at 20 °C (pH = 7.0). This is equivalent to Tarlov's hybridisation conditions which are detailed in section 7.3.3.

Fluorescent analysis: plate fluorimeter (FARCyte, Tecan)

Measurement mode: fluorescence

Fluorescein setting (Excitation wavelength 485 nm, emission wavelength 535 nm)

Mirror: dichroic 4

Plate: GRE96fb

Number of flashes 10, no lag time, 40 integration time

Gain 64*

Z-Position 6.2mm*

* = both set as standard after initial experiments to improve comparison of data.

Protocol 16 – Evaluation of hybridisation conditions

Protocol 15 was followed with the assays detailed in Table 2.6.

Hybridisation conditions: 20 °C/ 11 hours 20 minutes.

Assay	Capture probe	Reporter oligonucleotide	
	Biotin- T_{20}	Fluor-A_{20}	Fluor-T_{20}
Match	X	X	
Mismatch	X		X
Control		X	

Table 2.6 - Evaluation of hybridisation conditions.

Protocol 17 – Evaluation of reporter oligonucleotides

Protocol 15 was followed with the assays given below in Table 2.7. Hybridisation conditions: 5 °C/ 17 hours 30 minutes.

Wash the wells with the TE buffer at 5 °C. After analysis wash the wells with buffer at room temperature 22 °C and then with warm buffer 40 °C.

Assay	Capture probe		Reporter oligonucleotide		
	Biotin -T$_8$	Biotin- T$_{20}$	Fluor-T$_8$	Fluor-A$_8$	Fluor-A$_{20}$
1- Match	X			X	
2 - Mismatch	X		X		
3 - Match		X		X	
4 - Mismatch		X	X		
5- Standard					5 nM

Table 2.7 - Evaluation of reporter molecules.

Protocol 18 – Generation and evaluation of long reporter oligonucleotides

The composition of the digestion assays is given in Table 2.8. The assays contain: Fluor-A$_{20}$-C282YPR probe oligonucleotide (1.0 μM); target (1.2 μM); 1X PCR buffer; MgCl$_2$ (2.5 mM) and T7 exonuclease (0.1U / μL).

Enzymatic digestion

The assays were hybridised at 20 °C/ 15 minutes, without the enzyme. The enzyme was then added (if required) and the assay was then incubated at 37 °C for 1 hour. The assay was then heated to 90 °C for 3 minutes to denature the enzyme.

Hybridisation detection

The streptavidin plates were prepared with the capture probe as above (Protocol 15). Hybridisation conditions: 20 °C/ 9 hours after which the wells were washed as normal.

Assay	Probe		Target		Enzyme	Capture probe
	Fluor-A_{20}-C282Y	Fluor-A_{20}	C282YST	CTRAcomp	T7	Biotin- T_{20}
1- Match	X		X		X	X
2 - Mismatch	X			X	X	X
3 - Duplex	X		X			X
4 - Probe	X					X
5 - Standard		5 nM				

Table 2.8 – Enzymatic digestion of Fluor-A_{20}-C282Y duplex.

Protocol 19 – Generation and evaluation of short reporter oligonucleotides

The composition of the digestion assays is given below in Table 2.9. The assays contain: Fluor-A_8-C282YPR oligonucleotide (1.0 µM), target (1.2. µM), 1X PCR buffer, $MgCl_2$ (2.5 mM) and T7 exonuclease (0.1 U/ µL).

Enzymatic digestion

The assays were hybridised at 20 ^{o}C/ 15 minutes, without the enzyme. The enzyme was then added, if required, and the assay was then incubated at 37 ^{o}C for 1 hour. The assay was then heated to 90 ^{o}C for 3 minutes to denature the enzyme.

Hybridisation detection

The streptavidin plates were prepared with the capture probe as above (Protocol 15). Hybridisation conditions: 4 ^{o}C/ 17 hours after which the wells were washed with chilled (4 ^{o}C) TE buffer.

Assay	Probe		Target		Enzyme	Capture probe	
	Fluor-A_8-C282Y	Fluor-A_{20}	C282YST	CTRAcomp	T7	Biotin-T_{20}	Biotin-T_8
1 - Match	X		X		X	X	
2 - Match	X		X		X		X
3 - Mismatch	X			X	X	X	
4 - Mismatch	X			X	X		X
5 - Duplex	X		X			X	
6 - Duplex	X		X				X
7 - Probe	X					X	
8 - Probe	X						X
9 - Standard		5 nM					

Table 2.9 - Enzymatic digestion of Fluor-A_8-C282Y/C282YST duplex.

Protocol 20 – Digestion of dual labelled probes

Assays

Complementary Digest assay (Match): A_8-C282Y dual labelled probe (1.0 µM), C282YST (1.2 µM), 1X PCR buffer, BSA 1X and T7 exonuclease (0.01 U/ µL).

Mismatch Digest assay (Mismatch): as Match assay (above) with a CTRAcomp target.

Complementary Control assay (Duplex): as Match assay (above) with T7 exonuclease omitted.

Probe Assay: A_8-C282Y dual labelled probe (1.0 µM).

Analysis

Mix all the assays, omitting the enzyme. Heat to 95 °C to denature the assay and then cool to 20 °C and add the enzyme (if required). Add 20 μL aliquot of each assay to a LightCycler capillary. Centrifuge the sample and analyse in LightCycler. Ensure that the search temperature is at 20 °C.

Protocol 21 – Electrochemical analysis of modified sensor surface

Overview

Step 1 - Hybridisation

Step 2 - Surface Immobilisation

Step 3 - Addition of blocking layer

Step 4 - Activation of surface

Step 5 – Sensing: surface capture and electrochemical (DPV) interrogation.

Hybridisation

Assay: $FcCONH(CH_2)_6$-O-A_8 1.0 μM, TE Buffer (10 mM Tris, 1 mM EDTA, pH = 7.0), 1M NaCl, 5'-SHT_8 1.0 μM.

Hybridise at 3 °C/ 1 hour 50 minutes.

Surface Immobilisation of duplex

Allow electrode to stand in solution at 3 °C for 1 hour.

Addition of MCH blocking layer

Immerse electrode in 1.0 mM MCH (aq.) for 1 hour. Wash electrode with chilled (3 °C) hybridisation buffer (see above).

Activation of surface

Heat to 25 °C/ 5 minutes. Wash with hybridisation buffer (see above).

Sensing: surface capture

Assay: as for hybridisation but without the target. Allow to hybridise in solution at 3 °C for 15 hours.

Sensing: electrochemical interrogation of assay

The digestion was analysed by DPV at 3 °C: *DPV 5*; -100 mV to 550 mV, as shown in Table 2.10.

Moving average baseline correction (step = 0.001V).

WE Electrode: surface modified gold electrode.

Protocol	Pretreatment	Measurement		Potentials		
	Conditioning Potential	Modulation time (s)	Interval time (s)	Step potential (mV)	Modulation Amplitude (mV)	Standby Potential
DPV5	Initial potential / 60s	0.04	0.1	0.3	49.95	Initial potential

Table 2.10 - DPV protocol.

Chapter 3: Theory and rationale behind linker design

3 Theory and rationale behind linker design

3.1 Overview

The first stage in the development of novel DNA hybridisation probes is the synthesis of novel ferrocenylated linker molecules, which are then used to label the probe oligonucleotide.

The established methods of labelling oligonucleotides with ferrocene are described. These methods involve: post-labelling; incorporation of nucleobases and phosphoramidite labelling. Synthesis of novel ferrocenylated linker molecules to allow the post-labelling and phosphoramidite approaches to be undertaken are then discussed. Detail is given for four synthetic routes. The first two approaches synthesise linker molecules for post-labelling using an isocyanate based route and the third approach uses an amide based route. The final approach synthesises a phosphoramidite label. In each case the approach is justified and then described, with literature examples. Finally, the specific plans for the synthetic work are summarised.

3.1.1 Specific aims

The overall aim of this chapter is the synthesis of novel ferrocenylated linker molecules for the labelling of probe oligonucleotides.

It is desirable that several novel linker molecules can be synthesised which have a variation in the ferrocene electropotential between them. If this variation is sufficiently large, the different linkers can be potentially used for multiplexing: in context, this is the ability to detect different gene sequences simultaneously using different probe sequences labelled with different linker molecules.

To realise these aims the ferrocenylated linker molecules must fulfil similar requirements to the overall electrochemical probe, which were introduced in section 1.10.2, and must be readily coupled to the oligonucleotide sequence. The most efficient approach for synthesising a library of ferrocenylated linker molecules is to develop a

robust and reliable synthetic route, in which the variation in one of the reagents gives variation in the final linker structure.

3.1.2 Ferrocene electrochemistry

The redox couple between ferrocene (Fc) and the ferrocenium ion (Fc$^+$) is shown below in Figure 3.1.
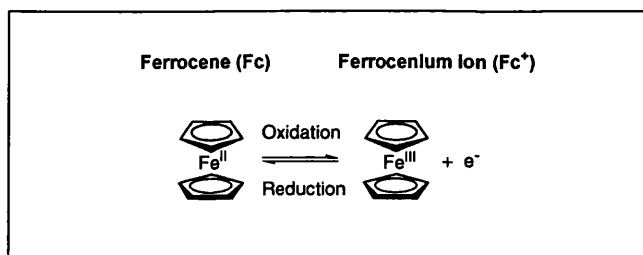
Figure 3.1– Ferrocene redox couple.

The ferrocenylated linker molecules will be analysed by Differential Pulse Voltammetry (DPV), a sensitive electrochemical detection technique described in section 2.5.7. As the reduced form of ferrocene (Fe^{II}) is the most stable, for all the molecules considered in this work, DPV is used to oxidise the ferrocene species to its ferrocenium ion and determine its characteristic oxidation electropotential (subsequently called electropotential).

3.1.3 Substituents on ferrocene: electropotential variation

The oxidation electropotential of ferrocene is affected by the introduction of substituents onto one, or both, of the cyclopentadienyl (Cp) rings, or by the use of ligands, which chelate with the iron atom. These modifications can affect the relative stability of both the ferrocene species and its ferrocenium ion and therefore the electropotential.

The cyclopentadiene rings of ferrocene are conjugated ring systems, which can be subjected to both inductive and mesomeric effects, shown in Figure 3.2. Inductive effects are short range and involve the pull on the electrons in the σ-bond, depending on

the electropotential of the substituent atom relative to the substituted carbon atom. Mesomeric effects can be longer range and concern the movement of π-electrons in a conjugated system.

	Inductive	Mesomeric
Donating (+) (stabilising)	⟨◯⟩—I	⟨◯⟩—M
Withdrawing (-) (destablising)	⟨◯⟩—I	⟨◯⟩—M
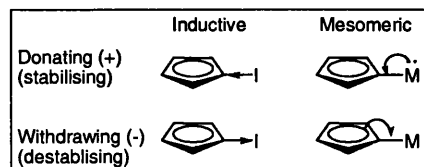
Figure 3.2 - Ferrocenium ion stability.
The stabilising and destabilising effect of inductive and mesomeric substituents on the cyclopentadienyl ring is shown.

The inductive and mesomeric effects can be both electron donating, Figure 3.2, top, which stabilises the ferrocenium ion, or electron withdrawing, Figure 3.2, bottom, which destabilises the ferrocenium ion. The movement of the electrons is shown by the direction of the arrows.

If electron withdrawing groups are introduced electron density is withdrawn from the ferrocene species. This does not favour the formation of the positive ferrocenium ion and hence it is more difficult to remove the electron and a higher potential is required to oxidise the ferrocene. The electropotential of a substituted ferrocene species containing electron withdrawing groups is therefore high (positive).

The electropotential of a ferrocene label is therefore dependent on the structure of the linker molecule which attaches it to the oligonucleotide. The manipulation of the ferrocene electropotential through the variation of electron donating and withdrawing groups on the ferrocene has been comprehensively reviewed by Pombeiro (Silva et al. 1991; Silva et al. 1994).

3.2   Labelling oligonucleotides with ferrocene: existing methods

3.2.1   Introduction

There are two main approaches for attaching ferrocene moieties to oligonucleotides: post-labelling and nucleobase incorporation, which are shown in Figure 3.3.

The post-labelling approach involves the synthesis of the probe oligonucleotide sequence and then attachment of the ferrocenylated linker molecule onto the 5' end. In the nucleobase incorporation approach, a nucleobase is synthesised which is ferrocene labelled. This base is then used during the probe oligonucleotide synthesis, allowing any number of labelled bases can be incorporated at the desired positions in the oligonucleotide.
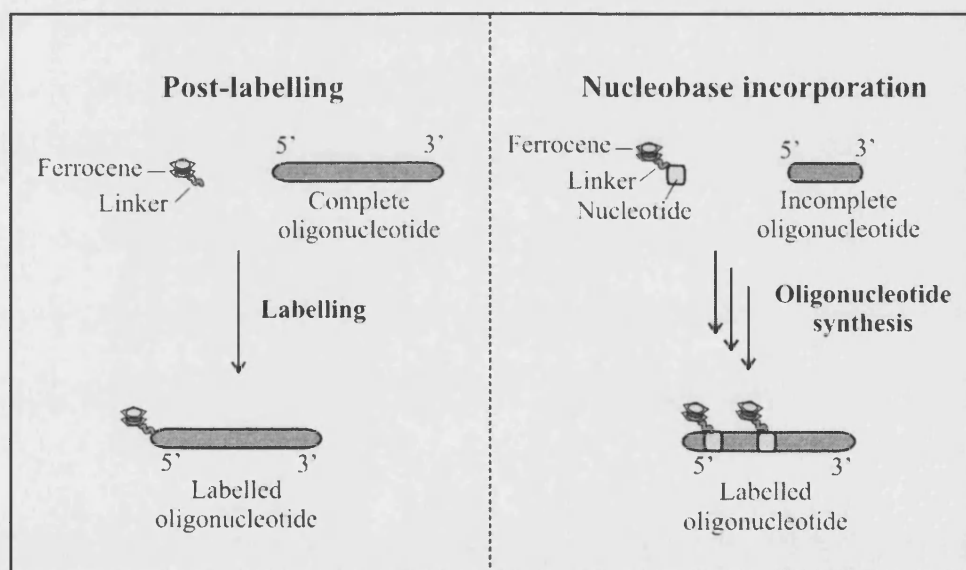
Figure 3.3 – Oligonucleotide covalent labelling.
The post-labelling approach (left hand side) involves the synthesis of the oligonucleotide sequence (dark grey strand), followed by its attachment to the ferrocenylated linker molecule at its 5' end. In the nucleobase incorporation approach (right hand side) a ferrocene labelled nucleobase (light grey square) is synthesised. This base is then used during the oligonucleotide synthesis, allowing any number of labelled bases to be incorporated at the desired positions in the probe (two are shown here).

Both approaches are now discussed in detail.

3.2.2 Post-labelled probes

Synthetic post-labelling

The original work was undertaken by Takenaka (Takenaka et al. 1994), in which ferrocene carboxylic acid **1** was derivatised to its *N*-succinimide ester **2**, as shown in Scheme 3.1. *Ester* **2** was then used to label the oligonucleotide.
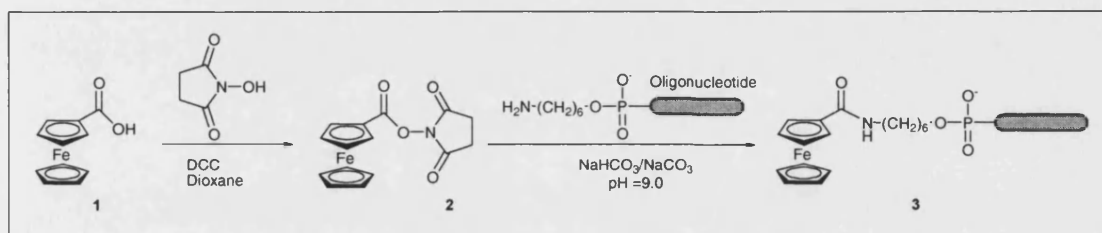
Scheme 3.1 – Takenaka's oligonucleotide labelling approach
Ferrocene *N*-succinimide ester 2 is synthesised and coupled to the oligonucleotide (grey strand) which has been 5' modified with a C6 alkyl amine. The labelled probe 3 was purified by NAP column and HPLC chromatography.

This labelled probe was originally used as a solution based DNA hybridisation sensor, described in Figure 3.4. Initially the ferrocene labelled probe is added to a solution containing complementary target DNA. The two sequences are allowed to hybridise and then the assay is injected into a HPLC instrument equipped with an electrochemical detector (ECD). Appropriate column selection was used to ensure that only hybridised DNA could be eluted and ssDNA was retained at the head of the column. The ECD is an electrochemical cell held at a potential above the oxidation potential of the ferrocene, which oxidises any ferrocene present and measures the resultant oxidation current. The technique can be calibrated using known concentrations of a ferrocene analogue of the label, to give quantitative analysis.
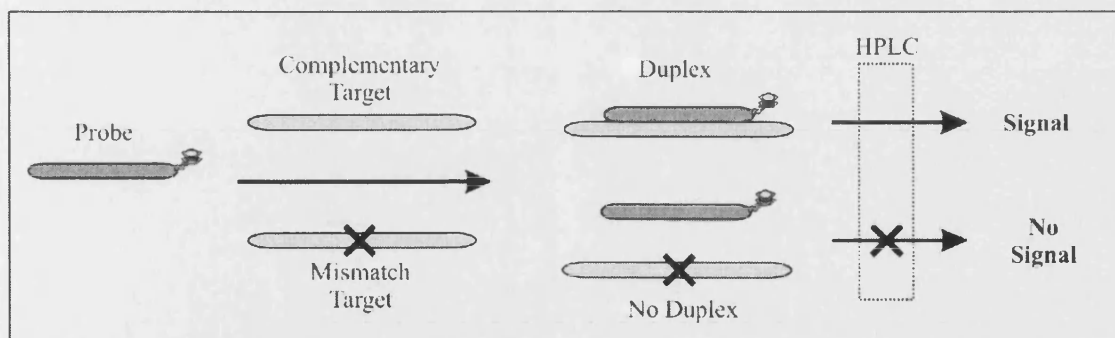
Figure 3.4- Hybridisation sensor with HPLC analysis.
The ferrocene labelled probe oligonucleotide (dark grey strand) is hybridised with a complementary target (light grey strand, top) or a mismatched target (light grey strand, X is the mismatch, bottom) under low stringency conditions. The matched target hybridises and forms a duplex, whilst the mismatched target does not. HPLC purification (dotted box) allows the duplex (top) to be eluted (arrow) and detected through ECD. The unhybridised probe from the mismatched assay (bottom) is retained on the column (crossed arrow) and no signal is observed by ECD.

Ihara adapted this approach to allow unlabelled duplex formation to be detected (Ihara et al. 1996). It was shown that at low temperatures (5 °C) a triplex could be formed between the duplex and a ferrocenylated probe, which was complementary to one strand of the duplex. This labelled triplex could then be detected by ECD after HPLC in the manner described above. This is not, however, practical for a sensor system.

Oligonucleotides labelled in the way described in Scheme 3.1, have also been used for surface modified work (Long et al. 2003; Mukumoto et al. 2003). Surface modification is described in Chapters 7 and 8.

In 2000 Xu used a different approach to covalently label ssDNA with ferrocene (Xu, C. et al. 2000). Free phosphate groups on the end of the ssDNA are functionalised by reaction with imidazole and then ethylene diamine, as shown in Scheme 3.2. The resultant DNA-amine **6** can then be labelled using EDCI coupling (for detail see section 3.3.2). The authors report the use of ferrocene carboxyaldehyde for labelling but this is not thought to be feasible and ferrocene carboxylic acid **1** was potentially used instead. The mode of action of the sensor is straightforward. Complementary ssDNA was adsorbed onto a carbon electrode and when the labelled ssDNA was introduced, specific hybridisation of complementary sequences occurred, which was detectable by differential pulse voltammetry (DPV). No signal is obtained for completely mismatched sequences.
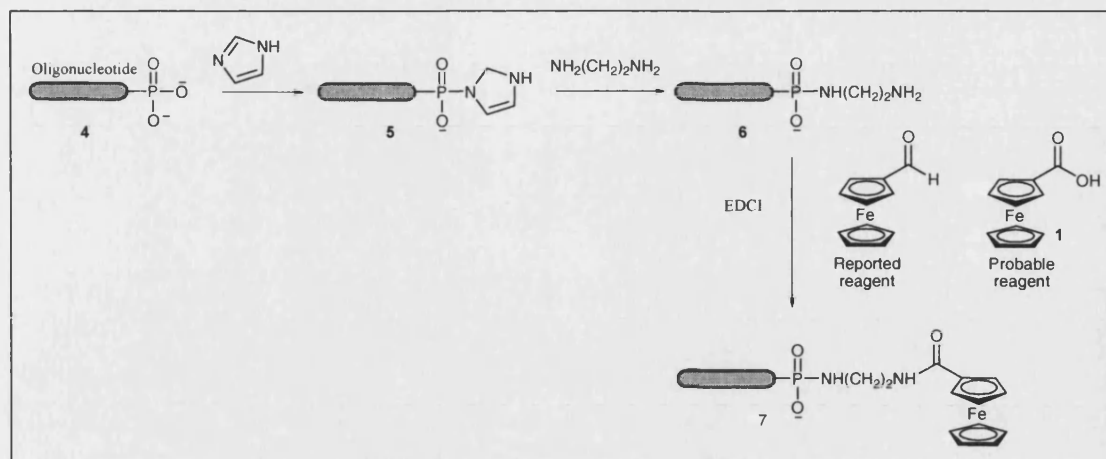
Scheme 3.2 – Xu's oligonucleotide labelling approach.
The oligonucleotide (grey strand, 4) is functionalised twice, before being ferrocene labelled using EDCI coupling. Ferrocene carboxyaldehyde is the reported reagent, but its use is not thought to be feasible. It is proposed that ferrocene carboxylic acid 1 was used instead.

Enzymatic post-labelling

It is also possible to enzymatically post-label on the 3' end of an oligonucleotide using a ferrocene labelled dideoxynucleotide (Fc-ddUTP), shown in Figure 3.5, and a terminal deoxynucleotidyl transferase enzyme (Anne et al. 2001). The author stresses that ferrocene analogues, which have different electropotentials, can also be used. This approach has also been used successfully to label oligonucleotides with ruthenium labels (Weizman et al. 2002).
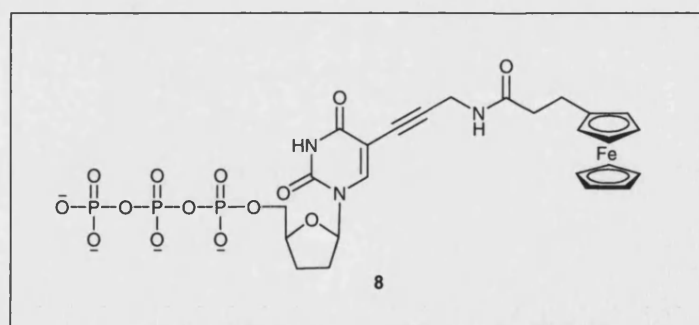
Figure 3.5 - 3' labelling reagent: Fc-ddUTP

3.2.3 Incorporated nucleobase probes

Solid supported synthesis

Oligonucleotide synthesis is a routine procedure whereby oligonucleotides are synthesised sequentially on a solid support and then cleaved off after the addition of the final base. This custom synthesis is now widely commercially available. The technique is summarised below, in Figure 3.6, and uses phosphoramidite nucleobase building blocks (Beaucage et al. 1981; Gait 1984; Khan et al. 1999).
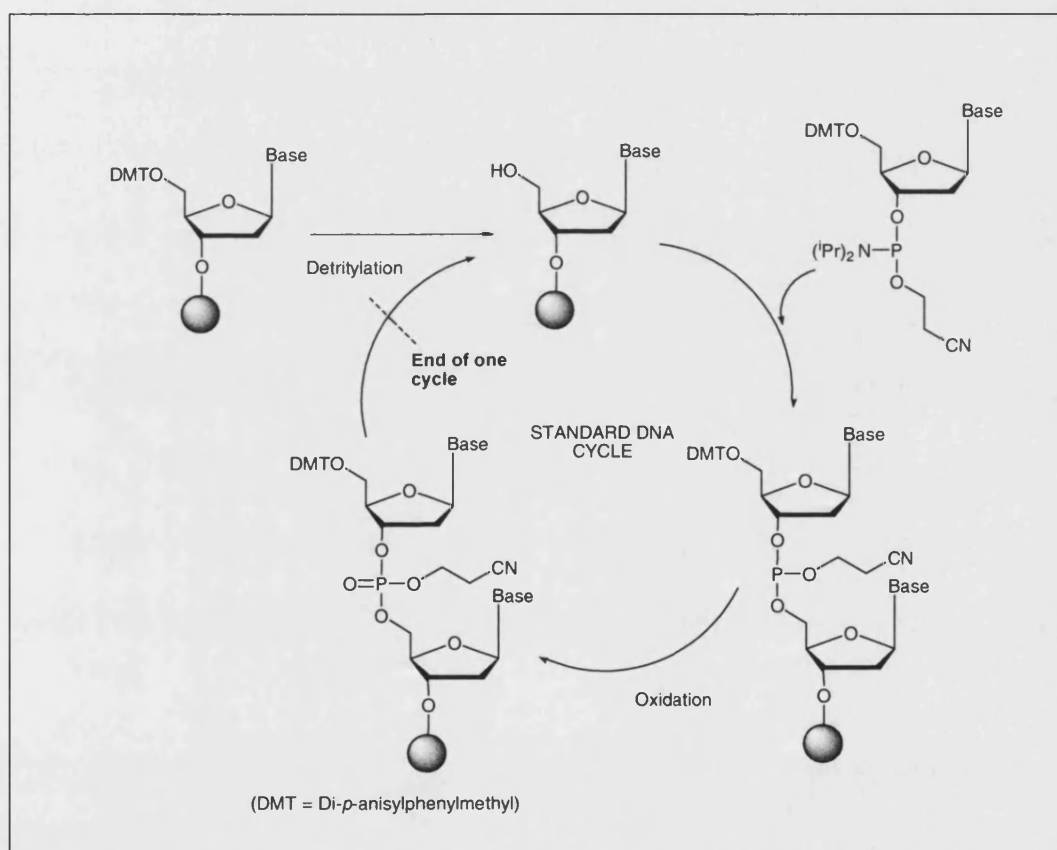
Figure 3.6 - Solid phase oligonucleotide synthesis.
The initial oligonucleotide (top left) is immobilised on a solid support (grey circle) the DMP (Di-p-anisylphenylmethyl) protection group on the 5' alcohol is initially removed through detritylation. The desired phosphoramidite nucleobase (A, C, G or T) is then coupled to the 5' alcohol. The primary amines of the nucleobases are already protected: A and C (benzoyl) and G (isobutyryl). This is followed by an oxidation step which completes the cycle. To add the next base the 5' alcohol is again detritylated. When the oligonucleotide sequence has been completed the final 5' alcohol is deprotected, the internucleotide alkyl esters are removed and the oligonucleotide is then cleaved from the support, in a step which also deprotects the amines in the bases. The full details are given elsewhere (Gait 1984).

By labelling the nucleobases with ferrocene, the ferrocene labels can be inserted at any desired point in an oligonucleotide sequence. This approach has been widely exploited in the literature with many variations in the design of the linker. The most prominent work has been done by the CMS group from Motorola (Yu et al. 2000; Umek, R.M 2001; Yu et al. 2001) and others (Beilstein et al. 2001; Pike et al. 2002). A similar route has also been applied to non-ferrocene redox labels (Khan et al. 1999; Hu et al. 2000; Tierney et al. 2000b; 2000a).

The work by the CMS group has been described in section 1.9.3, in the context of DNA chips and surface modification. Phosphoramidite nucleobases containing different ferrocene derivatives were also synthesised, which exhibited varying electropotentials. This allowed the authors to achieve the multiplexing they required in their technology i.e. the detection of two different target sequences. Two different derivatives of adenine, **9** and **10**, are shown in Figure 3.7. Importantly the derivativised bases do not affect the stability of duplex formation.
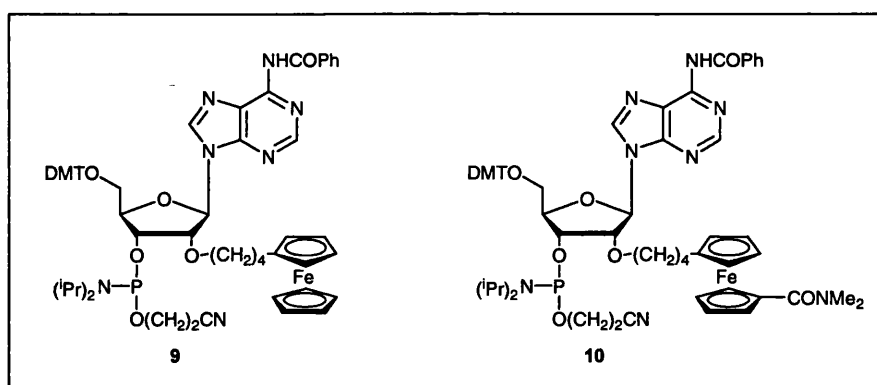
Figure 3.7 – Ferrocenylated adenine phosphoramidite nucleobases.

This work has been further developed by Kuhr (Brazill et al. 2001), whereby four different labels are used for multiplexing. Kuhr worked in collaboration with the CMS group and used the two phosphoramidites (**9** and **10**) to end label an oligonucleotide via nucleobase incorporation, resulting in the labelled oligonucleotides, **11** and **12**, shown in Figure 3.8. They also end labelled the same oligonucleotide using post-labelling with two of Ihara's labels, giving the labelled oligonucleotides, **13** and **14**, shown in Figure 3.8 (Ihara et al. 1996; Ihara 1997).
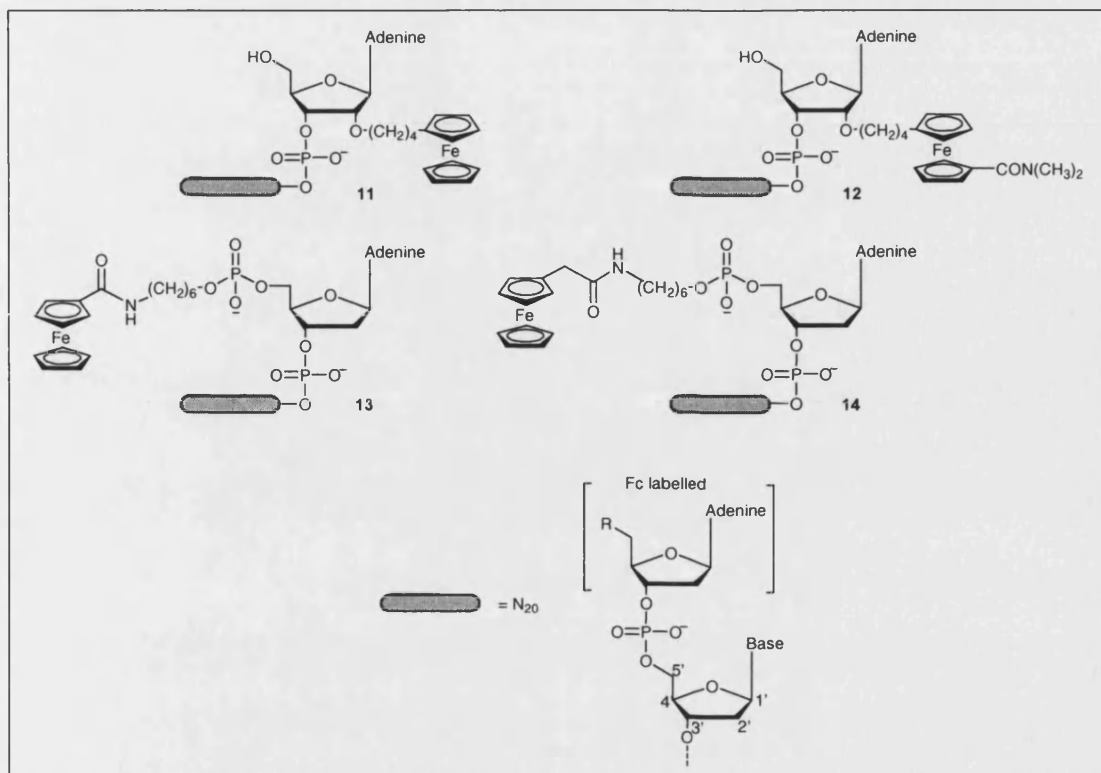
Figure 3.8 – Oligonucleotides labelled with ferrocenylated adenine nucleotides.
The four ferrocene labelled adenine (A) nucleotides are shown, after they have been used to 5' label a 20 bp oligonucleotide (grey strand). The ferrocenylated nucleobases (11 and 12, top) have a free 5' alcohol and further oligonucleotide synthesis would be possible if desired. The use of covalent ferrocene labels (13 and 14, bottom) does not leave a free 5' alcohol, so no further oligonucleotide synthesis would be possible.

The electropotentials of the labels were initially studied using Cyclic Voltammetry (CV) and displayed reasonable resolution, as shown in Figure 3.9. The authors then applied the technology to capillary electrophoresis and achieved good resolution with voltammetric detection (Brazill et al. 2001).

155
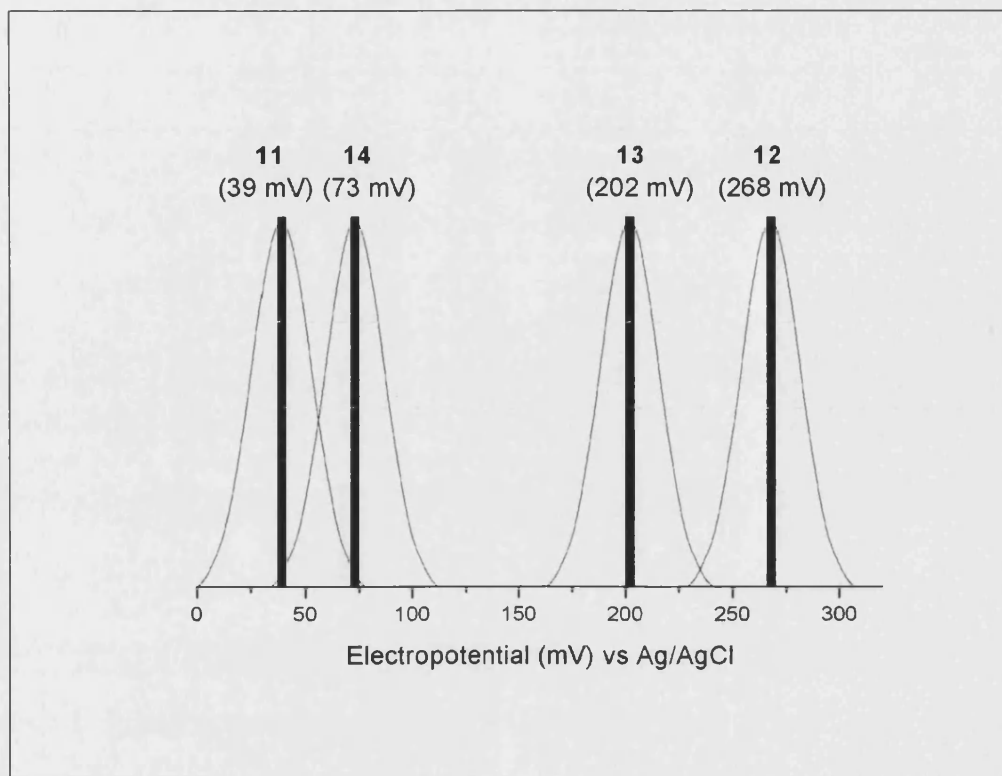
Figure 3.9 - Comparison of electropotentials.
The labelled oligonucleotides, illustrated in Figure 3.8, have resolvable electropotentials by Cyclic Voltammetry (CV). The figure is representative and not actual data.

Column labelling

The oligonucleotide can also be labelled on the column. This is done by incorporating the commercially available 5-iodo-2'-deoxyuridine phosphoramidite **15** (Glen Research) into the oligonucleotide sequence and then labelling it, using palladium cross-coupling, as shown in Figure 3.10 (Beilstein et al. 2000).

156
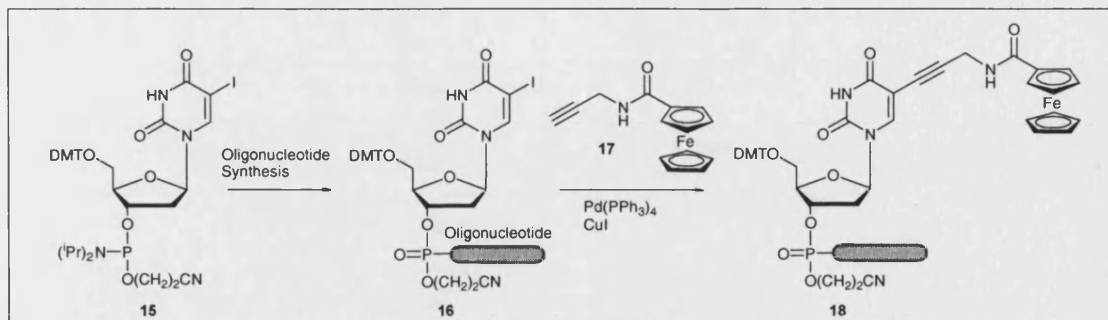
Figure 3.10 - On-column oligonucleotide labelling.
The overall mechanism for oligonucleotide synthesis has been given in Figure 3.6. The modified phosphoramidite nucleobase 15 is coupled to the oligonucleotide being synthesised to form oligonucleotide 16. This is labelled with ferrocenoyl propargylamide 17, to give the ferrocene labelled oligonucleotide 18. 18 is considered "end of cycle" in Figure 3.6 and normal oligonucleotide synthesises can be resumed or terminated.

3.2.4 Phosphoramidite labelling

Phosphoramidite labelling is a technique which combines aspects of the two above approaches (Beilstein et al. 2001). A ferrocenylated phosphoramidite molecule, described below in Figure 3.11, is used to end label the oligonucleotide, as in section 3.2.2. However, it is a linker molecule, not a nucleobase and the labelling is done at the end of the solid phase synthesis, as in section 3.2.3, under the same conditions. This labelling is commercially available (TibMol Biol, Germany).
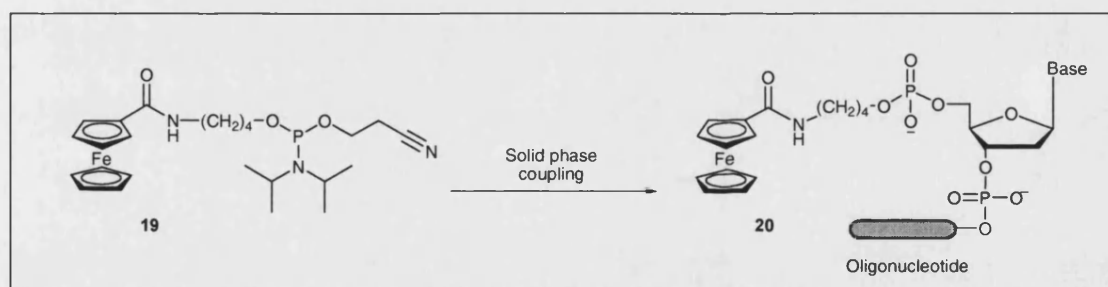
Figure 3.11 – Phosphoramidite labelling.
The ferrocene labelled phosphoramidite 19 is used to label the 5' end of the oligonucleotide (grey strand) after the solid phase oligonucleotide synthesis has finished. The labelled oligonucleotide is then cleaved from the solid support.

3.2.5 Evaluation of labelling approaches

All three labelling approaches: nucleobase labelling; post-labelling and phosphoramidite labelling have been shown to be effective for introducing a ferrocene label onto an oligonucleotide sequence and would be able to introduce a ferrocene label at the 5' end of the oligonucleotide. The approaches all require the initial synthesis of the ferrocenylated linker or nucleobase. Oligonucleotide synthesis is then followed by labelling with the ferrocenylated moiety, during or after oligonucleotide synthesis has been completed.

The post-labelling approach is most straight forward as it can be done easily with no specialist equipment and with commercially synthesised oligonucleotides. However, if the oligonucleotide synthesis equipment is available then the labelling, both nucleobase and phosphoramidite, is routine and the full synthesis can be done *in house*. Alternatively this labelling is available commercially if the nucleobase or phosphoramidite is supplied to the appropriate company.

3.3 Synthesis of novel ferrocenylated linker molecules

The synthesis of novel ferrocenylated linker molecules is now discussed. Since the discovery of the structure of ferrocene (Woodward 1952), many literature methods have been applied to its derivatisation. This ranges from comprehensive early work (Plesske 1962b; 1962a) to more recent work, which is well reviewed (Deeming 1982; Rockett et al. 1991; Kerber 1995)[1] and includes the synthesis of chiral compounds (Bildstein et al. 1997; Balavoine et al. 1998). Subsequently there is a large scope for linker design. Three routes for the synthesis of novel linker molecules are then discussed. The first two approaches synthesise ferrocenylated linker molecules for post-labelling oligonucleotides, through isocyanate and amide routes respectively. The final approach synthesises phosphoramidite linker molecules for end labelling oligonucleotides. Each approach is justified and then described, with literature examples. These examples are contrasted and potential routes for the synthesis of novel linkers are selected.

---

[1] Rockett published annual reviews on ferrocene chemistry in the Journal of Organic Chemsitry from 1981-1989.

3.3.1 Synthesis of linker molecules: isocyanate approach

Justification

Takenaka's approach to oligonucleotide labelling is well established (Ihara 1997; Takenaka 2001; Mukumoto et al. 2003), low cost and practical. The scope for potential novel ferrocenylated molecules is very high; as the only constraint is that they require a free carboxylic acid functionality, which can be activated allowing the molecule to be used as a label, as shown in Scheme 3.1, in section 3.2.2. These molecules could be stored in the activated ester form and then used in the straightforward labelling step (which simply requires agitation, with the coupling reagents, overnight).

Takenaka's ferrocenylated linkers potentially fulfil all the criteria given in section 3.1.1, except for novel design. Variation of linker structure, should not only afford novel linker molecules, but it can be designed to give control over the ferrocene electropotential as well. It was envisaged that the relatively high oxidation potential of ferrocene carboxylic acid based labels from Takenaka's work (ca. 0.4 V vs. Ag|AgCl)(Takenaka 2001) could be reduced. Lower operating potentials make electrochemical chips more efficient to run (Brazill et al. 2001) and avoids potential problems, such as the formation of gold chloride on the electrode surface, as described in section 5.7.1 (Pouradier et al. 1965; Bard et al. 1985).

Approach

The manipulation of the redox properties of ferrocene could best be realised by short range electronic effects through the linker, as shown in section 3.1.3. Once a test reaction is shown to be effective, analogues of the product can be swiftly synthesised to provide a range of potential probes. The probes will contain a free carboxylic acid (or analogue), which will allow the easy conversion into the activated ester.

Literature: synthetic route

A versatile route for the synthesis of novel ferrocenylated linker molecules involves the exploitation of the versatile reagent azido(ferrocenyl)methanone, *azide* **21**. The existing literature work will be discussed.

Initial work by Arimoto (Arimoto 1955) reported the synthesis of ferrocene benzylurethane **23** from *azide* **21**, as shown in Scheme 3.3.
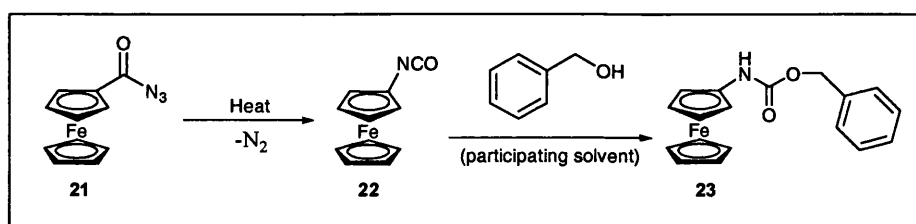
Scheme 3.3 – Synthesis of ferrocene benzylurethane 23.

This work was adapted by Schlogl (Schlogl et al. 1958) and more recently by Van Berkel and co-workers (Van Berkel et al. 1998; Quirke et al. 2000). Van Berkel applied the reaction to a range of alcohols, for both small scale mechanistic studies and for some preparative work, shown in Scheme 3.4.
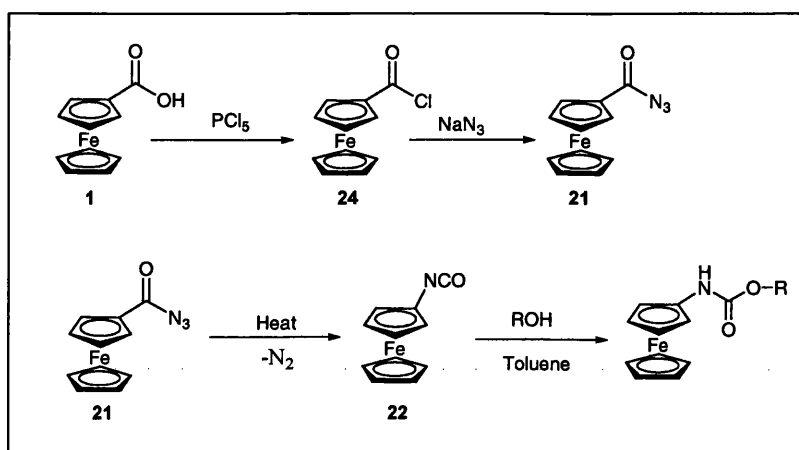
Scheme 3.4 – Synthesis of ferrocene carbamates.
A range of different alcohols (ROH) are used in the final step.

The *azide* **21** intermediate is initially synthesised from ferrocene carboxylic acid **1** and isolated. On heating (90 °C) in toluene for 10 to 30 minutes, *azide* **21** rapidly loses

nitrogen and undergoes the Curtius rearrangement, described in Figure 3.12 (Clayden et al. 2001; Smith et al. 2001) to ferrocene isocyanate **22**.
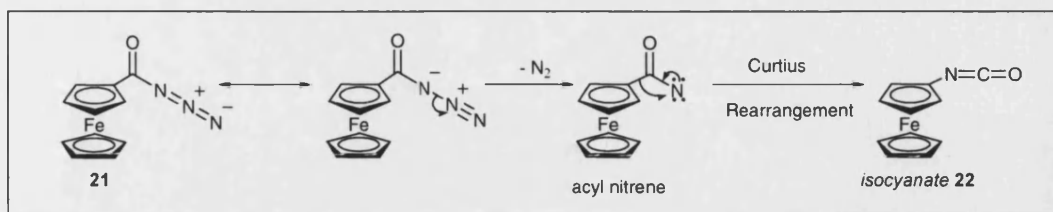
Figure 3.12 – Curtius rearrangement.

The isocyanate subsequently undergoes a nucleophillic substitution reaction with the alcohol to give the carbamate, shown in Figure 3.13 (Van Berkel et al. 1998).
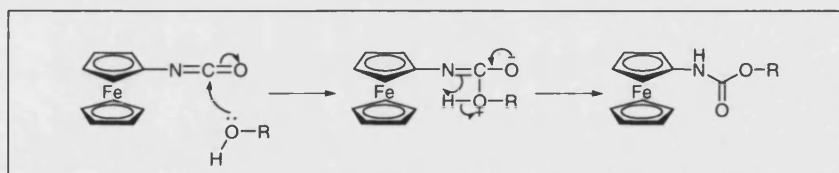
Figure 3.13 - Carbamate formation.

The results and recrystallised yields for the preparative work are given below in Table 3.1. The reaction is given in Scheme 3.5 for clarity.

Alcohol (ROH)	R group	Yield (%)
ethanol	CH_3CH_2OH	82
benzyl alcohol	$PhCH_2OH$	84
2-propanol	$CH_3CHOHCH_3$	77
methanol	CH_3OH	69
tert-butanol	$C(CH_3)_3OH$	81
p-nitrophenol	pNO_2PhOH	85
cholesterol	$C_{27}H_{29}OH$	73
stigmasterol	$C_{32}H_{46}OH$	75

Table 3.1– Ferrocene carbamate formation (Van Berkel et al. 1998).
The products were purified through a pad of silica gel and recrystallised from toluene. Both cholesterol and stigmasterol are 5 ring heterocyles.
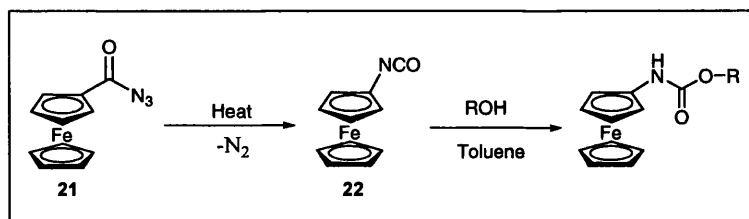
Scheme 3.5 - Carbamate formation.

A range of ferrocenyl carbamates have been successfully synthesised.

Scope for novel linker molecules

Isocyanates readily undergo nucleophillic substitution. The *isocyanate* **22** intermediate has the potential to react with alcohols, amines and thiols to form carbamates, ureas and *S*-thiocarbamates respectively, shown in Scheme 3.6 (Smith et al. 2001). The sulfur substitution (*S*-) must be specified as thiocarbamates are a different class of compounds.
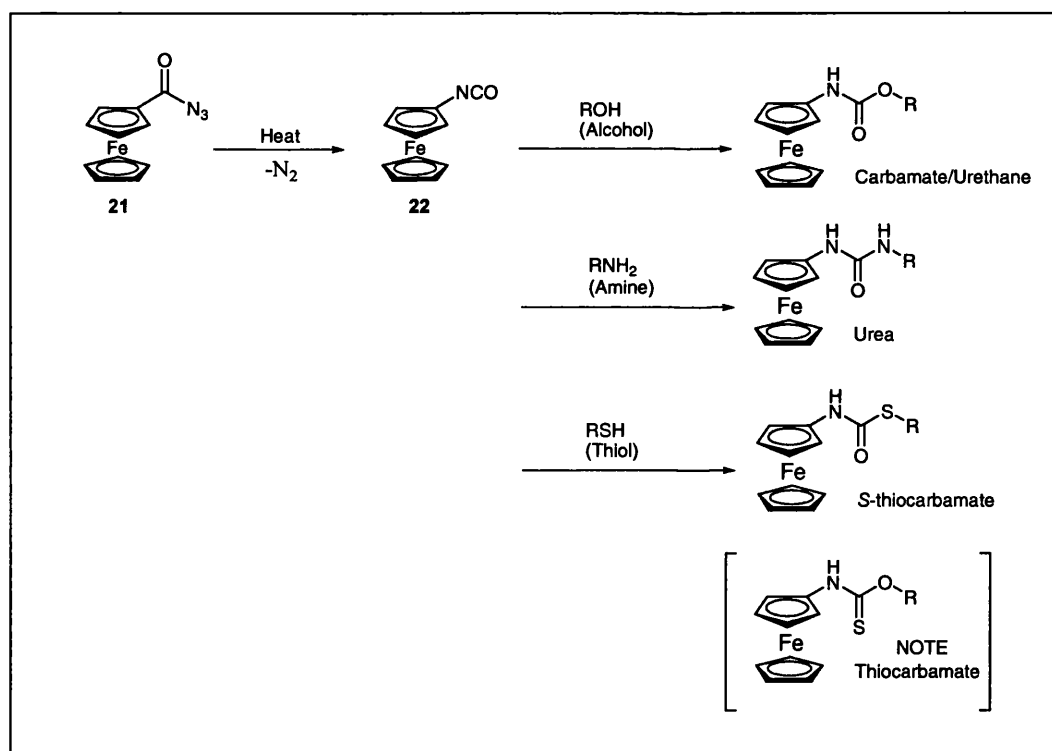
Scheme 3.6 – Synthetic options.
Isocyanate **22** has the potential to react with alcohols, amines and thiols to form carbamates, ureas and *S*-thiocarbamates respectively

The synthesis of carbamates by this route has been discussed above. Schlogl applied the reaction to the synthesis of ureas (Schlogl et al. 1958) and this was reviewed by Plesske (Plesske 1962a). There is no direct literature precedent for the synthesis of *S*-

162

thiocarbamates known to the author, however, work has been done using phenyl isocyanate (PhNCO), with both phenylthiol (PhSH) (Ricci 1977; Bourne et al. 1984; Satchell et al. 1992) and alkylthiols (AlkSH) (Ulrich 1967). This is described in Figure 3.14.

Figure 3.14 - *S*-Thiocarbamate synthesis.

Potential substrates are given below, in Figure 3.15, and in more detail later, in section 3.4.1. Aromatic acids have the potential for all three analogues (amine, thiol and alcohol), which can be substituted onto the ring, either directly or with a spacer group. There are a wide range of amino acids (natural or synthetic) can be potentially used in the reaction, which gives access to a large number of potential linker molecules. The structural variation of the amino acids may also give a variation in the ferrocene electropotential. Many of the amino acid analogues are also commercially available.

Figure 3.15 - Potential substrates.

3.3.2 Synthesis of linker molecules: amide approach

The use of amide coupling reactions as an alternative route for the synthesis of novel linker molecules was considered. This approach does not use ferrocene isocyanate.

Justification

Amide couplings are a very well established and robust protocol, which are commonly used in all areas of organic synthesis and have good procedures for use with ferrocenylated compounds (Gross et al. 1979; Bodansky et al. 1984). The general reaction scheme is given below, in Scheme 3.7.
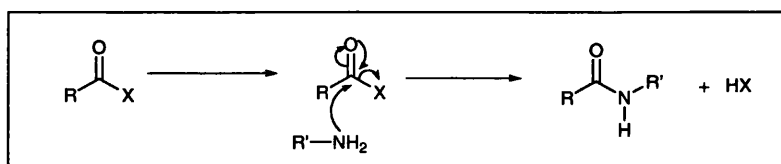
Scheme 3.7 – Amide coupling reaction.
The carbonyl group of the reactant (RCOX) undergoes nucleophillic attack from amine (R'NH$_2$), eliminating the leaving group (X) and forming an amide bond.

Approach

The coupling works with acids, but better leaving groups (X) are often used (Clayden et al. 2001). Two of the most common approaches are the use of acid chloride and the use of coupling reagents. These will be discussed here.

Acid chlorides

Acid chlorides are very reactive and can be reacted directly with amines to prepare amides, as shown in Scheme 3.8 (Gross et al. 1979).
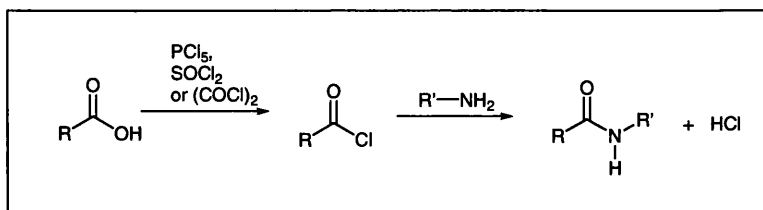
Scheme 3.8 –Amide synthesis from acid chlorides.

This approach, whilst effective, has several limitations. The high reactivity of the acid chloride can produce by-products and the chlorinating agents: phosphorous pentachloride; thionyl chloride or oxalyl chloride, are very harsh and can cause additional chlorination of many reagents and products.

Coupling reagents

Several coupling reagents have been developed which allow much more control over amide synthesis (Gross et al. 1979), the most common of which are carbodiimides. In the presence of a hindered base, the acid is activated and reacts *in situ* in a simple, one-pot, procedure, shown in Scheme 3.9. The most widely used carbodiimide is dicyclohexylcarbodiimide (DCC) (Konig 1970), although the DCU by-product can be problematic to remove in purification. 1-(3-dimethylaminopropyl)-3-ethylcarbodiimide hydrochloride (EDCI) is more expensive, but is now commonly used as it gives a water soluble urea by-product, EDCU, which is much more easily removed. The activated ester is, however, very reactive and can give rise to the acyl transfer side reaction which reduces the yield and causes purification problems.
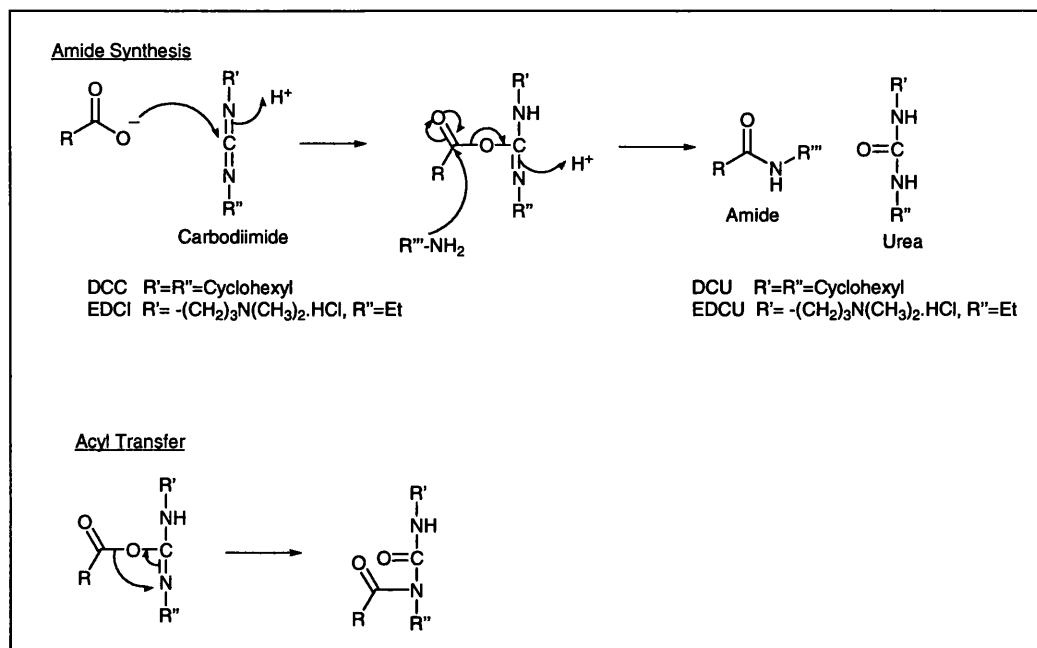
Scheme 3.9 – Amide synthesis with coupling reagents.
In the amide synthesis (top) the carbodiimide readily undergoes nucleophillic attack from the acid. The ester then undergoes nucleophillic attack from the amine resulting in synthesis of the amide. If the attack of the amine is not rapid, it is possible for the acyl group to transfer down the carbodiimide (bottom), which prevents further reaction.

This problem of acyl transfer is negated by using a nucleophile, which reduces the reactivity of the ester intermediate, as shown in Scheme 3.10. N-Hydroxysuccinimide was initially used (Wunsch 1966), but 1-hydroxybenzotriazole (HOBt) is now commonly used instead (Konig 1970).
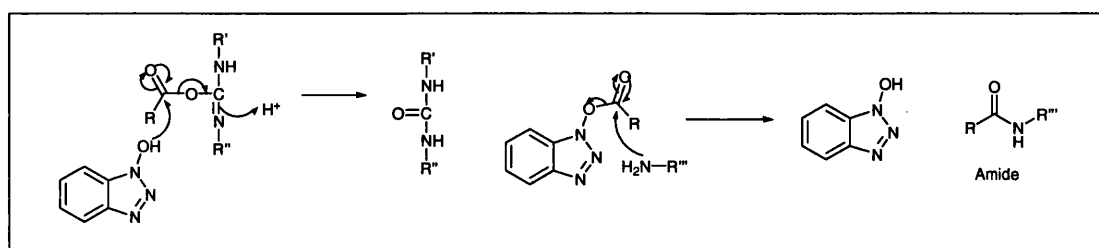
Scheme 3.10 – Preventing acyl transfer.
1-hydroxybenzotriazole (HOBt) attacks the ester intermediate (initial step) producing a less reactive HOBt-ester and the urea. The HOBt-ester then reacts with the amide, which produces the amide product and regenerates the HOBt.

Carbonyl Diimidazole (CDI) is also commonly used, as it gives no urea by-product and uses mild reaction conditions, as shown in Scheme 3.11.
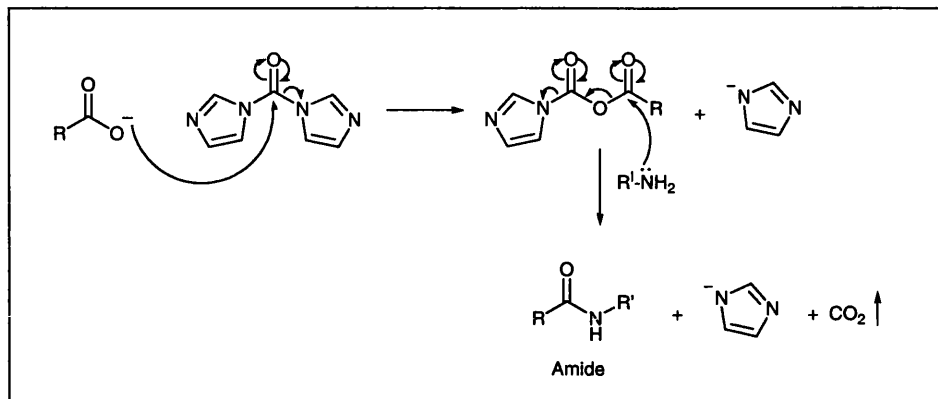
Scheme 3.11 – CDI coupling
CDI undergoes nucleophillic attack from the acid, resulting in an activated ester intermediate. This is then attacked by the amine to produce the amide product. Carbon dioxide (CO_2) is liberated, which is the driving force for the reaction, together with imidazole anions. The imidazole has a low boiling point and is easily removed.

Scope

The synthesis of ferrocene based amide linker molecules was considered *via* the acid chloride and amide coupling reagent routes, shown in Scheme 3.12.
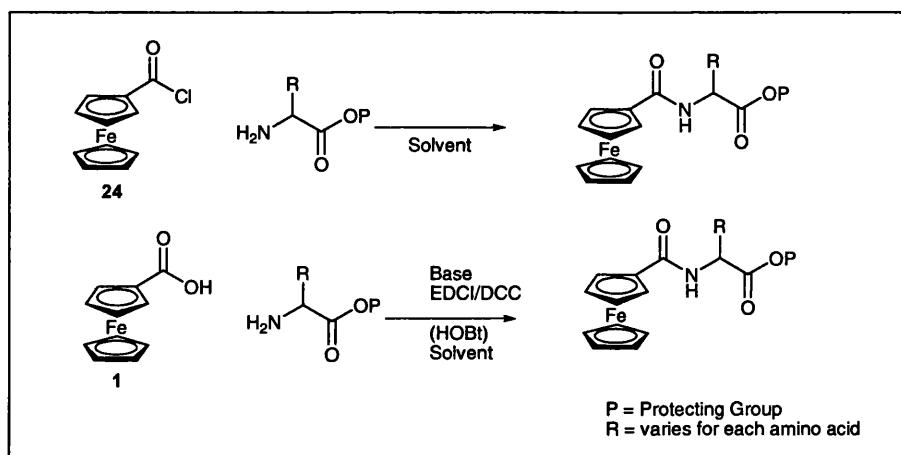
Scheme 3.12 – Proposed amide synthesis.

The coupling reagent route was favoured due to the improved control over the reaction. The use of the carbodiimide coupling reagents was chosen due to the availability of established protocols (Neises 1987) and reagents. The use of amino acids as reagents will give a large scope for potential linker molecules.

3.3.3 Synthesis of linker molecules: phosphoramidite approach

Justification

The synthesis of ferrocene labelled, phosphoramidite linker molecules affords an alternative labelling approach. This has been introduced in section 3.2.4. The synthetic work to produce the linker is more complex than the approach detailed above, in section 3.3.1, due to potential problems with the oxidation of phosphoramidite, which are discussed below. It is also more expensive in terms of reagents and the requirement for the labelling to be done by a commercial company, as oligonucleotide synthesis equipment was not available. The additional expense can be justified as the oligonucleotides are supplied purified and high labelling efficiency is guaranteed.

The nucleobase labelling approach, detailed in section 3.2.3, was dismissed as it is synthetically more complex. It was thought sufficient to only 5' end label the oligonucleotide with a ferrocene moiety mainly due to the mechanism of enzymatic digestion: the oligonucleotide probe is digested from the 5' end, therefore a 5' labelled fragment would be the first to be released on enzymatic digestion and should not cause any problems.

Phosphoramidite synthesis

A phosphoramidite label has been synthesised by Beilstein (Beilstein et al. 2001) and is detailed below in Figure 3.16.
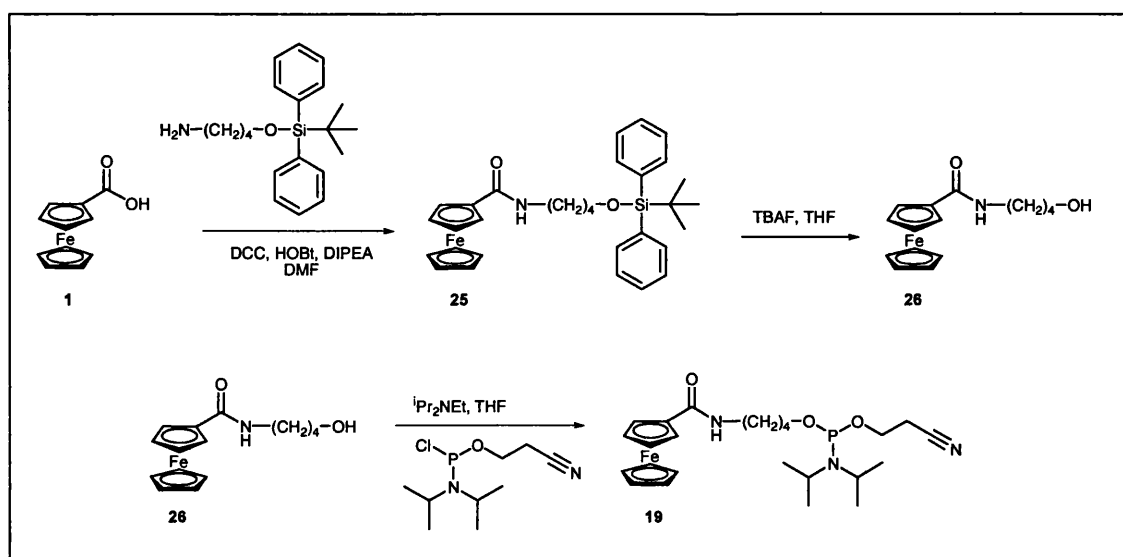
Figure 3.16 - *Phosphoramidite* 19 synthesis.

The post-labelling work, described in section 3.2.2, involves the ferrocene moiety being attached to the oligonucleotide using a $(CH_2)_6$ linker. This is commonly abbreviated to C6. It was proposed to adapt the above route, as shown in Scheme 3.13, to synthesise the C6 phosphoramidite linker (instead of C4), whilst making the synthesis more straightforward. Initially ferrocene carboxylic acid 1 is derivatised to an alkyl alcohol 27 and this is then converted to the *phosphoramidite* 28.
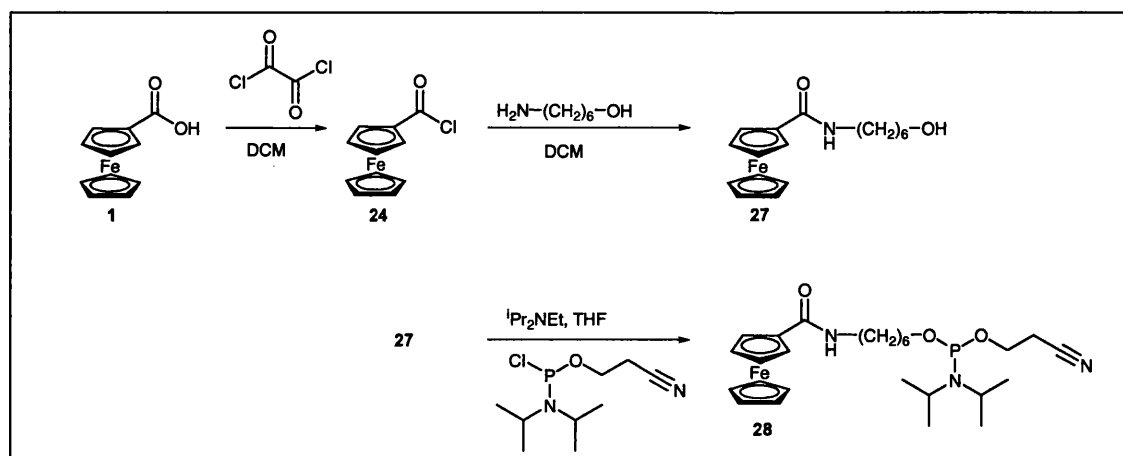
Scheme 3.13 - Synthesis of *phosphoramidite* 28.

Care must be taken during the synthesis and purification of the *phosphoramidite* **28** as the phosphorous (P^{III}) will readily oxidise to the phosphorous oxide (P^{V}), as shown in Scheme 3.14. This oxidation would make the molecule unsuitable for use in oligonucleotide synthesis.
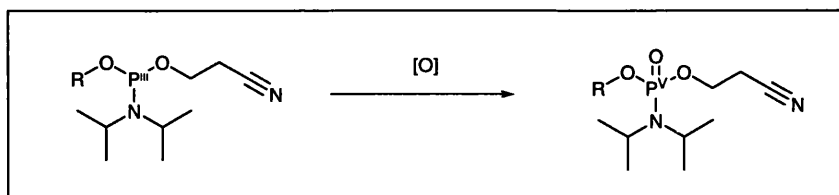
Scheme 3.14 - Phosphoramidite oxidation.
The phosphorous will readily oxidise from P(III) to P(V) in air, which cannot easily be reversed. R = alkyl ferrocene, as in Scheme 3.13.

3.4   Summary: experimental plan

The experimental plan is intended to:

- Clearly and concisely describe the experimental work in Chapter 4, using specific detail.

- Give clarity to the structure of Chapter 4 and to be a reference point for it.

3.4.1 Novel ferrocenylated linker molecules

The main focus of the synthetic work is on the synthesis of novel ferrocenylated linker molecules for post-labelling. The starting material, *azide* **21**, is synthesised, allowing a range of novel ferrocenylated linker molecules to be synthesised. The electropotentials of these molecules are determined by DPV, described in section 2.5.7, and a select number of them are converted to activated esters.

Azide starting material

The large scale synthesis of the *azide* **21** starting material is undertaken and optimised.

Synthesis of azide based ferrocenylated linker molecules

The azide route, detailed in section 3.3.1, is then used to synthesise the following novel ferrocenylated linker molecules:

1) Aromatic acids, both mono- and di- substituted, shown in Figure 3.17.
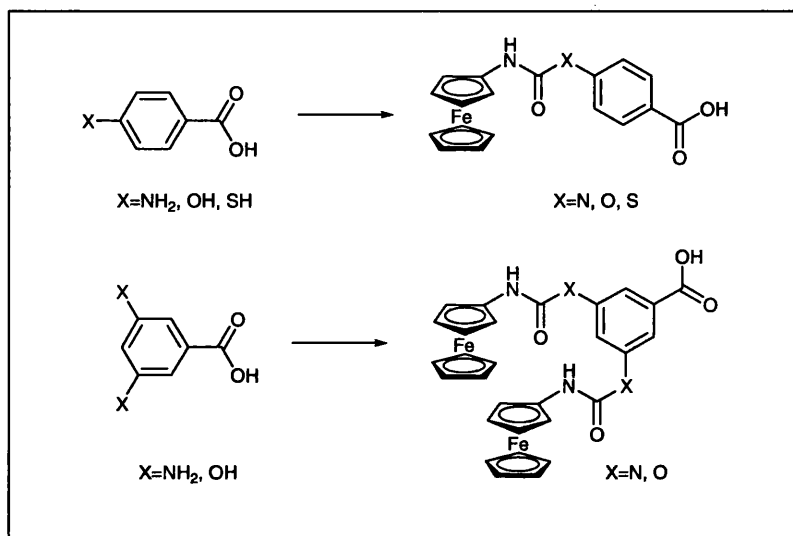
Figure 3.17 – Synthetic plan: aromatic acids.

2) Alkyl aromatic acids, shown in Figure 3.18.
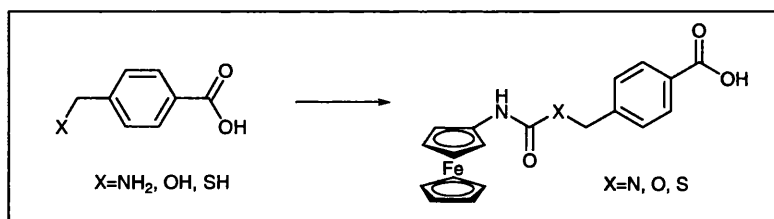
Figure 3.18 – Synthetic plan: alkyl aromatic acids.

3) Amino acids , shown in Figure 3.19.
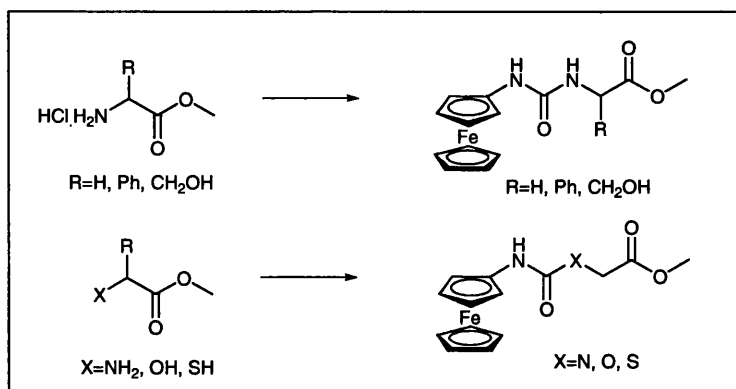
Figure 3.19 – Synthetic plan: amino acids.

Synthesis of amide based ferrocenylated linker molecules

Test reactions are undertaken with glycine, shown in Figure 3.20, as detailed in section 3.3.2.
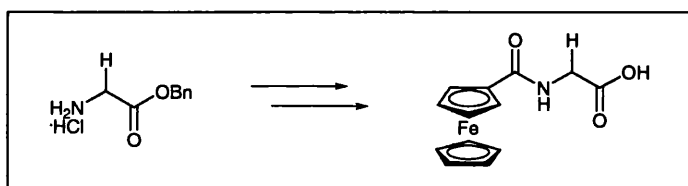
Figure 3.20 – Synthetic plan: amide approach.

Synthesis of activated linker molecules

Selected linker molecules are converted to the activated ester form, as described in section 3.2.2, to allow them to be used for post-labelling oligonucleotides.

3.4.2 Phosphoramidite linker molecule

A known phosphoramidite linker molecule is synthesised, shown in Figure 3.21, as detailed in section 3.3.3. This allows the alternative oligonucleotide labelling approach to be used in Chapter 6.
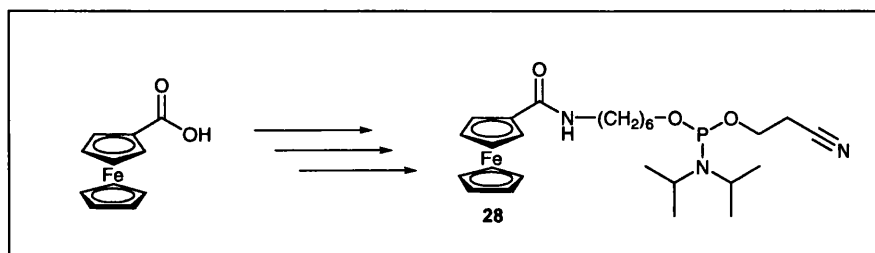
Figure 3.21 –Synthetic plan: phosphoramidite linker.

173

Chapter 4: Results
Synthesis and characterisation of linker molecules

4 Results: Synthesis and characterisation of linker molecules

4.1 Introduction

This chapter concerns the synthesis of novel ferrocenylated linker molecules. The justification for the approaches used has been given in Chapter 3, together with an overall synthetic plan in section 3.4. The results for the synthesis of the linker molecules are given, together with their characterisation and activation.

This chapter is split into two parts. Part A details the synthesis of linker molecules for covalent labelling. The main focus of this work is on the synthesis of the novel linker molecules. Synthetic variation was undertaken, where necessary, to synthesise the desired compound. Whilst a high yield is desirable, limited optimisation of the yields has been undertaken, as this is not the main priority and could be achieved with future work. Part B details the synthesis of a phosphoramidite linker molecule.

The structure of the chapter is as follows:

Part A

- Synthesis of the *azide* 21 starting material (section 4.2)
- Synthesis of novel linker molecules (sections 4.3 and 4.4)
- Electrochemical characterisation of the linker molecules (section 4.5)
- Activation of selected linker molecules for labelling (section 4.6)

Part B

- Synthesis of phosphoramidite linker molecule (section 4.8)

The results will be evaluated in conclusions for each part.

The experimental detail for the synthetic products is given in section 2.8.

175

PART A: Synthesis of linker molecules for covalent labelling

4.2   Synthesis of *azide* 21

A robust synthesis of *azide* 21 was required to allow the synthetic work to progress. The literature preparation (Van Berkel et al. 1998) is shown, in Scheme 4.1, and is reported to give a good synthetic yield (Entry 1, Table 4.1). Reproducing this result was not possible (Entry 2, Table 4.1) due to problems with the chlorination step.
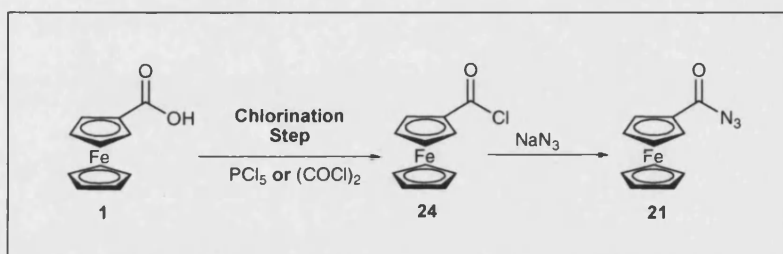
Scheme 4.1 - Synthesis of *azide* 21

The use of oxalyl chloride as an alternative chlorination agent, using a variation of Chu's method (Chu et al. 1999), improved the yield and reduced the reaction time (Entries 3 and 4, Table 4.1).

Entry	Chlorinating Agent	Time (h)	Yield (%)
1[†]	Phosphorous Pentachloride	3	67
2	Phosphorous Pentachloride	3.5	11
3	Oxalyl chloride	1.25	75
4	Oxalyl chloride	1	83

Table 4.1 - Synthesis of *azide* 21.
[†]Entry 1 is the reported literature yield (Van Berkel et al. 1998).

4.3   Synthesis of azide based ferrocenylated linker molecules

4.3.1 Scope of synthetic route

The scope of the linker synthesis from *azide* **21**, shown in Scheme 3.6, has been introduced in section 3.3.1. The route is applied to 3 different groups of reagents: aromatic acids; alkyl aromatic acids and amino acids. The results for this work are discussed in turn.
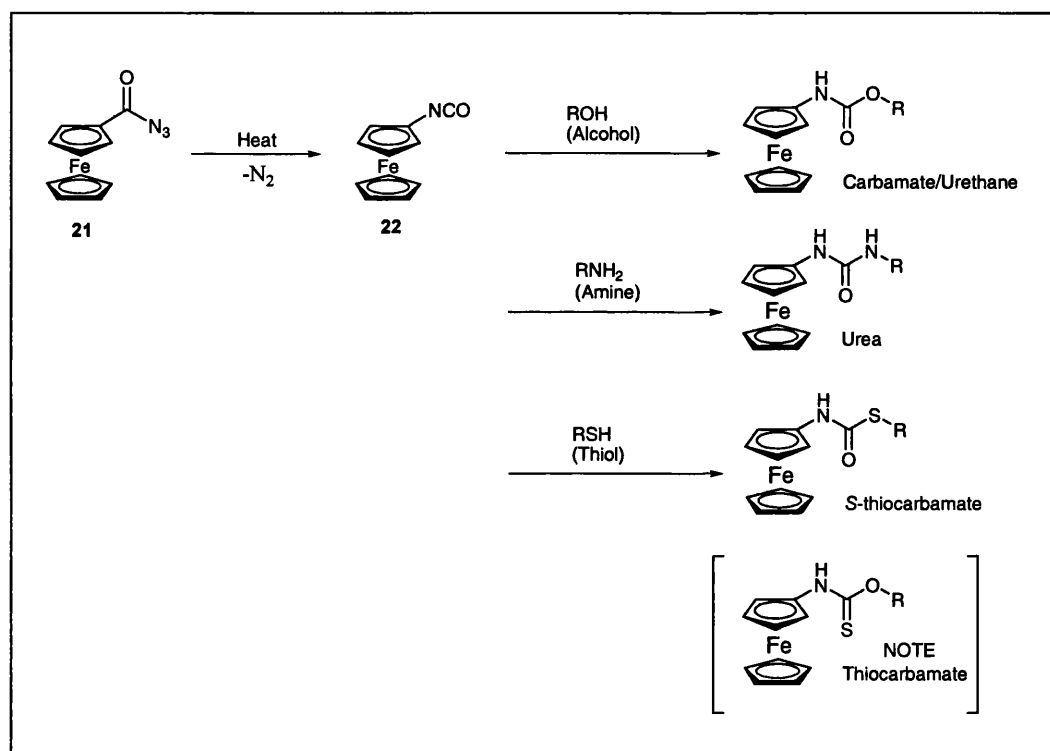
Scheme 4.2 – Synthetic options.
Isocyanate **22** has the potential to react with alcohols, amines and thiols to form carbamates, ureas and *S*-thiocarbamates respectively

4.3.2 Synthesis with aromatic acids

Reaction overview

The synthetic plan for the aromatic acids is summarised below in Figure 4.1.
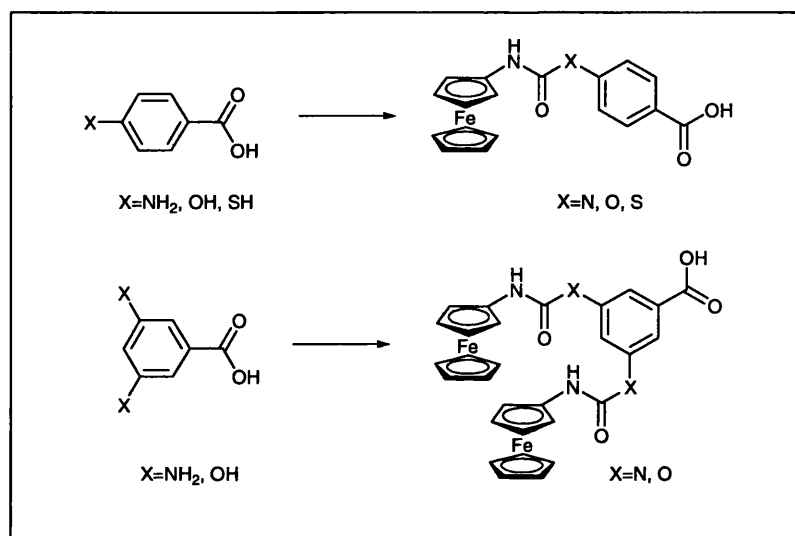
Figure 4.1 – Synthetic plan: aromatic acids.

The substrates described above were selected due to the commercial availability of the analogues and the opportunity to expand the work to the dual substituted substrates. The substrates also had a free carboxylic acid group, to allow easy activation and oligonucleotide labelling.

Reaction detail

For each experiment the substrates were dissolved in 1,4-dioxane and heated, under nitrogen, at 100 °C until all the *azide* **21** was consumed, as determined by TLC, see Scheme 4.3. This was typically 1 to 4 hours. The results are given below in Table 4.2.
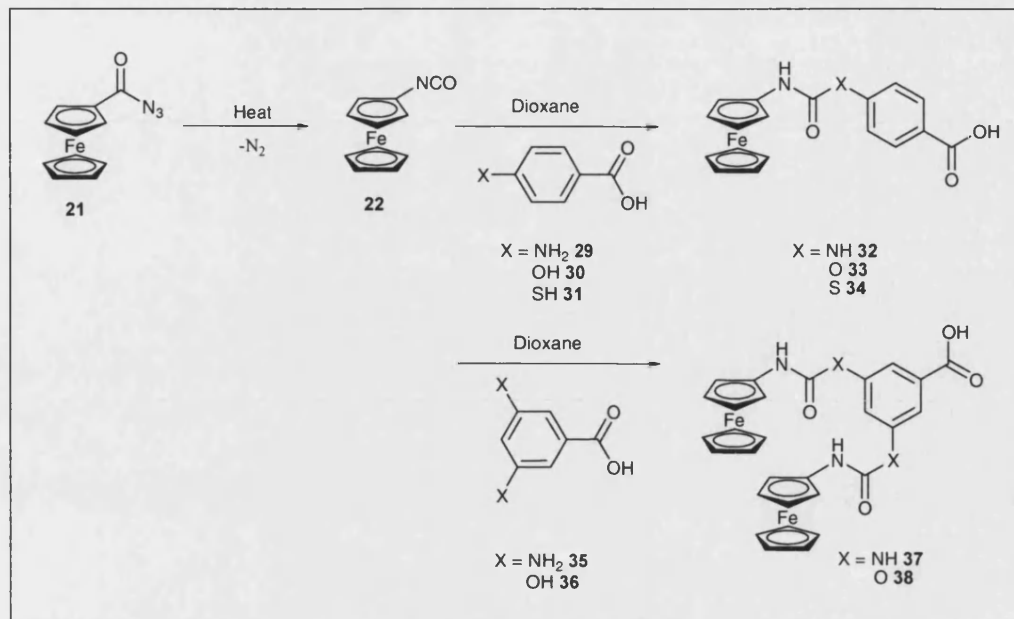
Scheme 4.3 – Synthesis using aromatic acid analogues.

Entry	Substrate	Substituent (X)	Product	Yield (%)
1	29	NH$_2$	32	96%
2	30	OH	33	Fail
3	31	SH	34	Fail
4	35	NH$_2$	37	27%
5	36	OH	38	Fail

Table 4.2 – Synthesis of linker molecules.

Results

The two reactions using the amine substrates, **29** and **35**, are successful. The other three reactions fail, producing only very low yields (<2%) of unknown ferrocenylated products.

Discussion

The success of the amine reagents over the others can be explained as they are stronger nucleophiles than alcohols, which in turn are generally stronger than thiols. Due to this amines should react more readily with the isocyanate.

The nucleophillic strength of the alcohol on 4-hydroxybenzoic acid **30** is low due to stabilisation by π electron delocalisation, shown in Figure 4.2. This cannot occur for the 3,5-dihydroxybenzoic acid **36** which should be more nucleophillic and therefore more reactive.
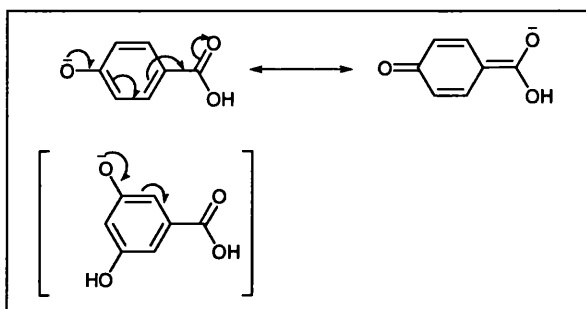
Figure 4.2 – Stabilisation of *acid* 30 by delocalisation.

Although phenols are poorly reactive, Van Berkel reports the synthesis of carbamate products from *p*-nitrophenol (Van Berkel et al. 1998) and phenol (Quirke et al. 2000). He also states that "phenols" have been derivatised in his laboratory, although this is on the very small scale used to derivatise the molecules before their analysis in Electrospray Mass Spectrometry (ES-MS).

Carbamate formation is known to be catalysed by bases, including DABCO **39** (Erner 1960) and triethylamine **40** (Griffin et al. 1996) (Figure 4.3), which activate the alcohol through hydrogen bonding.
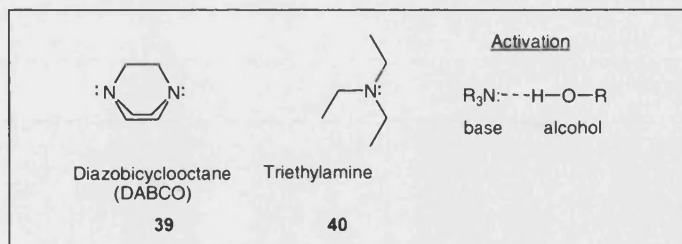
Figure 4.3 – Basic catalysts.

Repeating the reaction with the alcohol substrates, **30** and **36**, together with the addition of DABCO or triethylamine, failed to activate the reactions and no yield was obtained. The work was not pursued further with alcohol substrates.

Thiols readily react with isocyanates on heating (Bourne et al. 1984) or when treated with catalysts, shown in Figure 4.4, such as dibutyltin dilaurate **41**, dibutyltin di(2-ethylhexanoate) **42**, dibutyltin dibutanethiolate **43** (Noomen et al. 1995) trimethyl(phenylthio)silane **44** (Ricci 1977) and triethylamine **40** (Noomen et al. 1995).
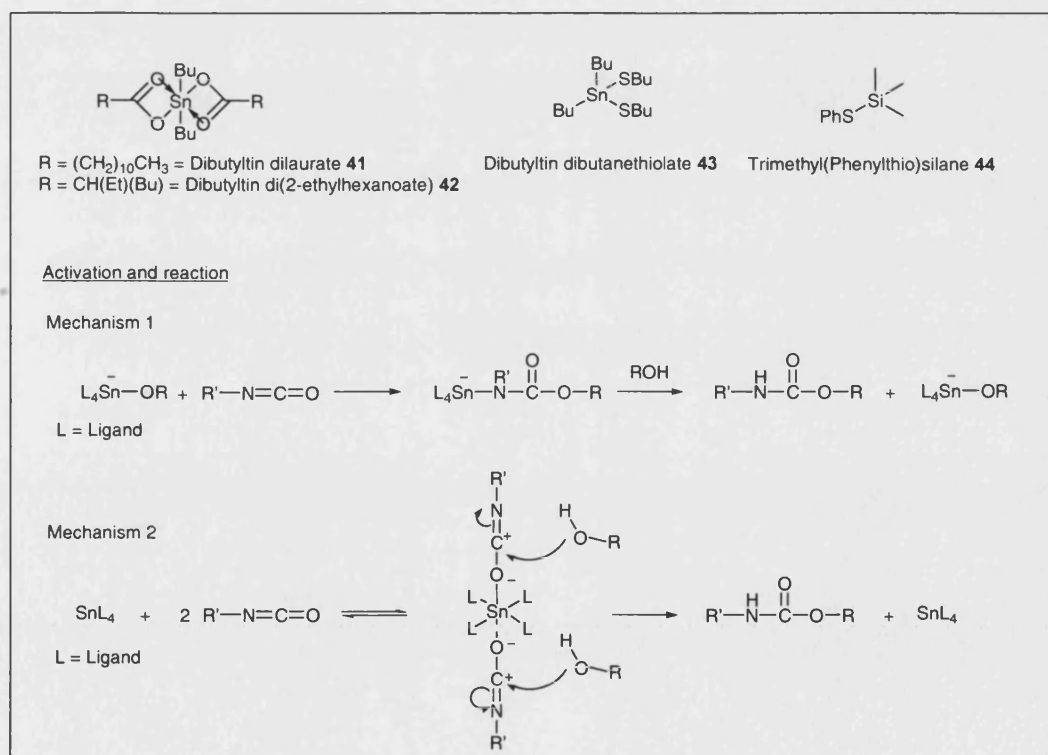
Figure 4.4 – Catalysts for carbamate formation.
The tin and silicon catalysts act as Lewis acid catalysts (Herrington et al. 1991). In Mechanism 1, the alcohol (ROH) forms a complex which can then react with the isocyanate. In Mechanism 2, the isocyanate forms a complex with the catalyst, which can then react with the alcohol.

As for the carbamate formation, heat may not be sufficient to drive the reaction and basic catalysis should be attempted. Repeating the reaction using triethylamine, the strongest base mentioned above, failed. The failure of the reaction to proceed under these conditions is postulated to be due to the low nucleophillicity of the thiol. The work was not pursued further with thiol substrates.

Summary

The more reactive amine substrates successfully produced urea products. Reactions with the less reactive alcohol and thiol substrates failed. Basic catalysis of the unsuccessful reaction was also unsuccessful, but could be hampered by the free acid groups on the substrates, which necessitate the use of excess base and may cause side reactions and solubility problems.

Future work should consider the use of reagents with protected acid groups. Tin catalysts could also be used to catalyse the substrate/isocyanate transition state (Houghton et al. 1996).

4.3.3 Synthesis using alkyl aromatic acids

Reaction overview

The synthetic plan for the alkyl aromatic acids is summarised below in Figure 4.5.
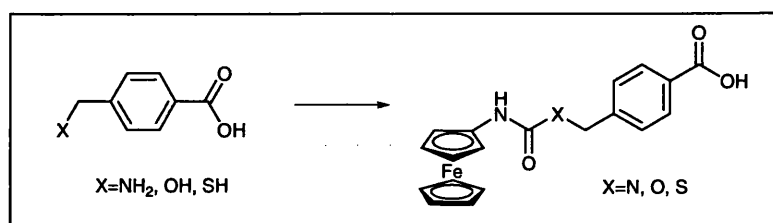
Figure 4.5 - Synthetic plan: alkyl aromatic acids.

The introduction of an alkyl group between the functional group and the aromatic ring (Table 4.3) eliminates the possibility of deactivation by stabilisation and makes the substrates more reactive.

Reaction detail

For each experiment the substrates were dissolved in 1,4-dioxane and heated, under nitrogen, at 100 °C until the *azide* **21** had been completely consumed, as determined by TLC (typically 2 to 5 hours). The alcohol and thiol substrates both required the addition of Hunig's base (^{i}Pr$_2$EtN, **45**) to promote the reaction, which is described in Scheme 4.4. 4-(Aminomethyl)benzoic acid **46** was sparingly soluble in 1,4-dioxane, so anhydrous dimethylsulfoxide (DMSO) was added to the reaction mixture. The results are given below in Table 4.3.
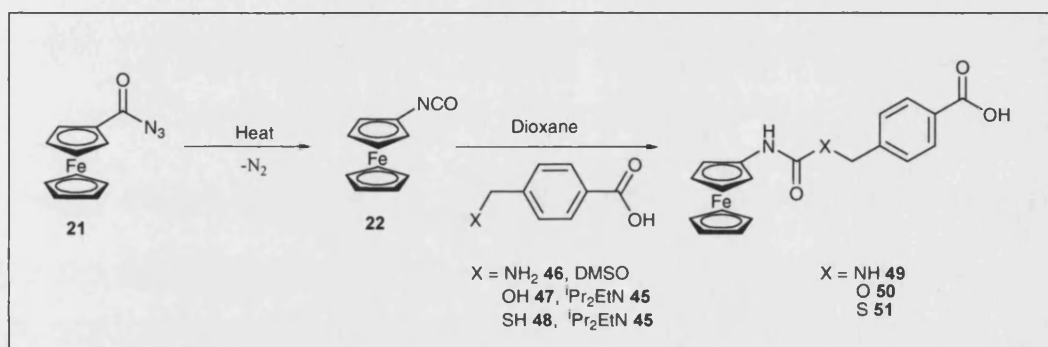
Scheme 4.4 – Synthesis of ferrocenylated alkyl aromatic acids.

Results

Entry	Substrate	Substituent (X)	Product	Yield (%)
1	**46**	NH$_2$	**49**	21%
2	**47**	OH	**50**	60%
3	**48**	SH	**51**	62%

Table 4.3 – Synthesis of ferrocenylated alkyl aromatic acids.

Discussion

The *carbamate* **50** and *S-thiocarbamate* **51** are synthesised in a reasonable yield. The yield of the *urea* **49** is significantly lower, but the reaction is still successful.

The low yield of the *urea* **49** is caused, in part, by the nucleophillic substitution of the amide onto the *azide* **21** to form an amide by-product, shown in Figure 4.6.
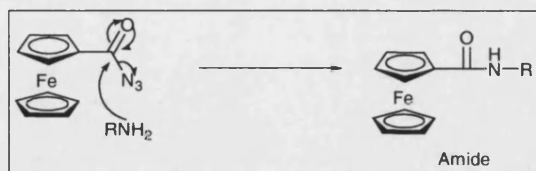
Figure 4.6 – Mechanism of amide formation.

Optimisation of the synthesis of the *urea* **49** proved to be problematic. For clarity only limited examples will be discussed. Variation of the solvent system influenced the ratio of the products obtained, with the more polar solvent system (DMSO) favouring the *urea* **49** product, as shown in Table 4.4. The reaction scheme is given in Scheme 4.5.
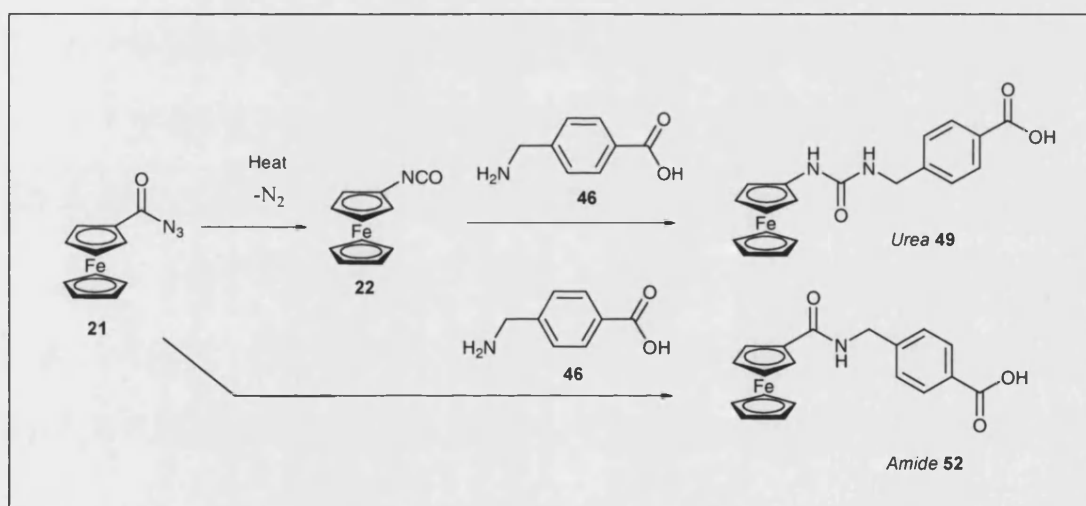
Scheme 4.5 - Formation of *urea* 49 and *amide* 52 products.

Entry	Solvent volume (mL)		Yield (%)		Ratio
	DMSO	Dioxane	*Urea* 49	*Amide* 52	*Urea* 49: *Amide* 52
1	100	10	21	2	93: 7
2	40	10	12	2	88: 12
3	60	0	2	18	9: 91

Table 4.4 – Optimisation of the *urea* 49 yield.

The low yields for the urea formation are not satisfactory. It was not possible to effectively separate the reaction products using flash chromatography or crystallisation

(mixed crystals formed). The use of HPLC purification was not viable as preparative HPLC equipment (large scale) was not available.

Heating the *azide* **21** starting material to ensure full conversion to isocyanate, before the addition of the amine substrate also did not improve the yields. This may be due to the diferrocene urea formation, discussed below.

The use of DMSO solvent may also be detrimental to the urea synthesis. DMSO is a strong electron donor and the degradation of ferrocenium ions (Fc^+) by DMSO, through ligand exchange, is well known and described in Scheme 4.6 (Prins et al. 1972). The iron (Fe^{II}) ion is considered to be strongly bound to the two cyclopentadiene (Cp) groups in ferrocene itself. However, it may be possible that if the ferrocene substituents are sufficiently electron withdrawing, the ferrocene complex may be sufficiently destabilised for the ligand exchange to occur at the high reaction temperature.

$$2FeCp_2^+ + 6DMSO \rightarrow FeCp_2 + Fe(DMSO)_6^{2+} + 2Cp$$

Scheme 4.6 – Ferrocenium ion degradation.
The ferrocenium ion (Fc^+, $FeCp^+$) undergoes ligand exchange with DMSO producing ferrocene (Fc, $FeCp_2$), $Fe(DMSO)_6^{2+}$ and free cyclopentadiene (Cp).

There is also anecdotal evidence for the instability of ferrocenylated compounds in DMSO. If a DMSO solution, or solution containing DMSO, of any of the ferrocenylated compounds prepared in this section is left exposed to light, it discolours and a brown/black residue is precipitated. This process is slowed, but not prevented, if the sample is protected from light. If the samples are frozen in a dark freezer many of them will still discolour over time.

The yield of all these experiments detailed above, in Table 4.3, was affected by the formation of diferrocene urea **54**. This is thought to occur through hydrolysis of the isocyanate, by any water present in the reaction mixture, forming a reactive amine capable of reacting with further isocyanate, as shown Scheme 4.7. This dimer has previously been reported (Van Berkel et al. 1998).
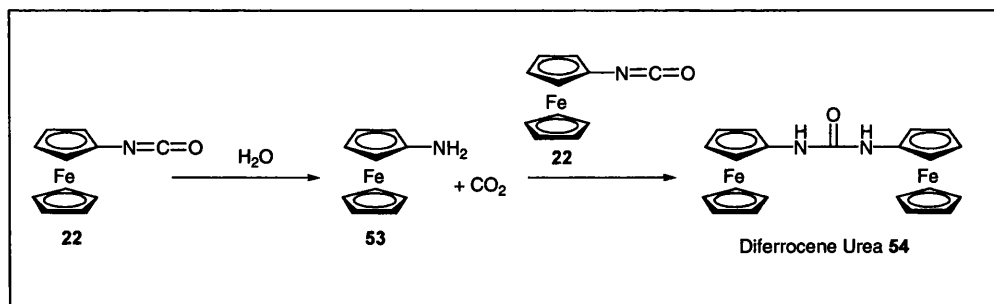
Scheme 4.7 – Diferrocene urea 54 formation.

Repeated efforts to improve the yield of the *urea* **49** by improving the solvent dryness or by varying the reaction times were unsuccessful.

Summary

The use of alkyl aromatic substrates afforded the successful synthesis of three novel analogues **49**, **50** and **51**. The synthesis of the *urea* **49** was problematic and optimisation of the reaction, particularly the reaction solvent is required in the future. The production of the diferrocene urea by-product **54** should also be investigated so that it can be eliminated.

4.3.4 Synthesis using amino acids

Reaction overview

The synthetic plan for the amino acids is summarised below in Figure 4.7.
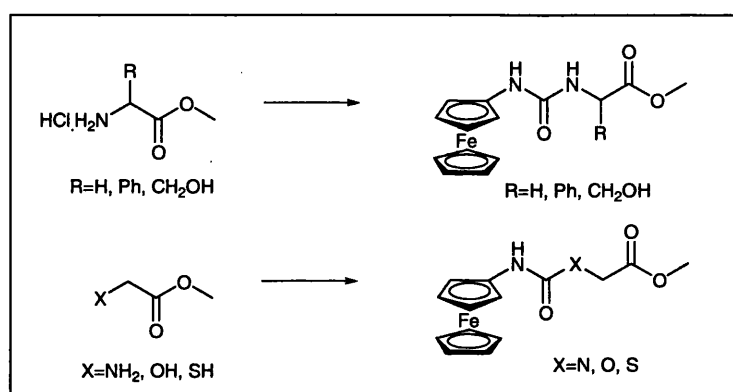
Figure 4.7 – Synthetic plan: amino acids.
Amino acid methyl ester hydrochloride salts are used (top scheme), together with glycine analogues (bottom scheme).

The high polarity of the free amino acids restricts the reaction solvent to water or methanol, which typically contains water. The presence of water would probably hydrolyse any ferrocene isocyanate **22** to *amine* **53**, as described in section 4.3.3. This problem was avoided by using the less polar amino acid methyl ester hydrochloride salts. Alcohol and thiol analogues are commercially available for many of the amino acid methyl esters.

Reaction detail

For solubility reasons the substrates were used directly in DMSO with no base present, as described in Scheme 4.8. The results are given below in Table 4.5. For optimisation basic catalysis was then used.
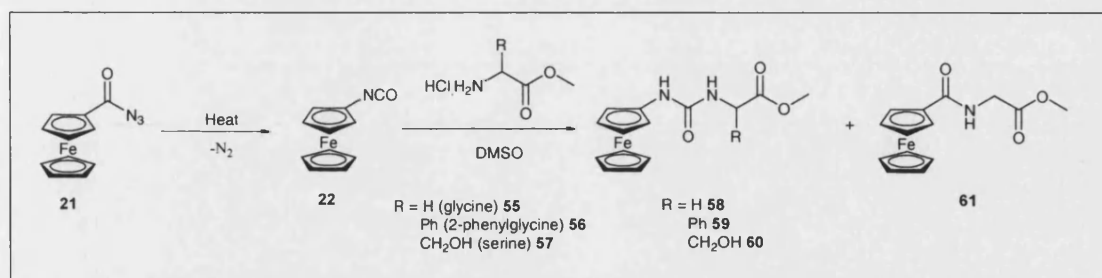
Scheme 4.8 – Synthesis of ferrocenylated amino acids.

Entry	Substrate	R	Catalyst	Product	Yield (%)
1	glycine **55**	H	None	**58**	31
2	2-phenyl glycine **56**	Ph	None	**59**	12
3	serine **57**	CH$_2$OH	None	-	-
4	glycine **55**	H	DABCO **39**	**58**	28
5	glycine **55**	H	^{i}PrEt$_2$N **45**	**61**	74

Table 4.5 – Synthesis of ferrocenylated amino acids.

Results

The initial reactions (entries 1, 2 and 3, Table 4.5) gave low yields with glycine **55** (31%) and 2-phenyl glycine **56** (12%). No product was isolated for serine **57**. Basic catalysis was used with DABCO **39** (entry 4) and Hunig's base **45** (entry 5). DABCO does not improve the yield and Hunig's base produces the *amide* **61** by-product, in high yield (74%).

Discussion

Using the uncatalysed approach, two of the amino acid substrates were successful with glycine **55** and 2-phenyl glycine **56** giving moderate yields. The reaction with serine **57** was unsuccessful. DMSO is not an ideal reaction solvent, due to the possible degradation of the ferrocene species, as described in section 4.3.3. Poor solubility of all

three substrates in this solvent, combined with the necessary aqueous extraction of the DMSO, which produces significant amounts of an unidentified black oil, could account for a large amount of the product loss.

The substrates were used as tertiary amine salts, which will reduce their reactivity. To increase the reactivity attempts were made to debase the glycine methylester hydrochloride **55**, using aqueous bases, but this failed due to solubility problems. The alternative use of basic catalysis was ineffective at improving the synthesis of the urea (entries 4 and 5, Table 4.5); with the use of the stronger Hunig's base promoting the synthesis of an *amide* **61** by-product (entry 5, Table 4.5). *Amide* **61** is formed due to the elimination reaction introduced in section 4.3.3.

Additional work

The alcohol and thiol analogues of glycine methyl ester were synthesised, as detailed in Scheme 4.9 and the results are given in Table 4.6. These two substrates had improved solubility in organic solvents, allowing 1,4-dioxane to be used instead of DMSO. This has a lower water content and improved long term stability of the ferrocenylated compounds. In addition both Hunig's base and 4Å molecular sieves (to remove water) were used.
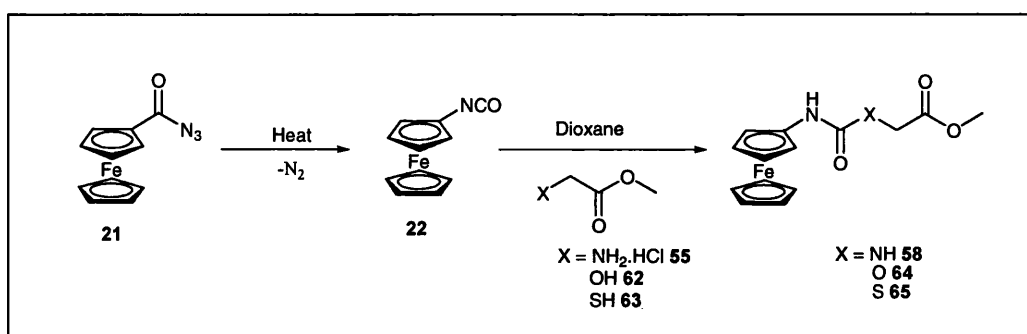
Scheme 4.9 – Synthesis using glycine methyl ester analogues.

Entry	Substrate	Substituent (X)	Product	Yield (%)
1	55	NH$_2$.HCl	58	31*
2	62	OH	64	29
3	63	SH	65	115% crude

Table 4.6 – Glycine methyl ester analogue synthesis.
* = This has been reported in Table 4.5, Entry 1.

Summary

The use of amino acid esters afforded the successful synthesis of five novel molecules (four intended products and a by-product) in low to moderate yield. If further work shows that these molecules are desirable, the synthetic routes can be optimised.

4.4 Synthesis of amide based ferrocenylated linker molecules

Reaction overview

The synthetic plan for the amide coupling reaction with glycine is summarised below in Figure 4.8.
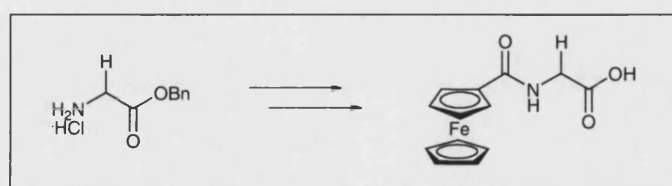
Figure 4.8 – Synthetic plan: amide approach.

Glycine was used as a simple model substrate for the synthesis; it was protected for solubility reasons. It should be emphasised that this linker molecule was synthesised without using the ferrocene isocyanate approach.

190

Reaction detail

The peptides were synthesised following the literature procedure of Neises and co-workers (Neises 1987). Glycine benzylester hydrochloride **66** was coupled with ferrocene carboxylic acid **1** and then deprotected, as shown in Scheme 4.10.
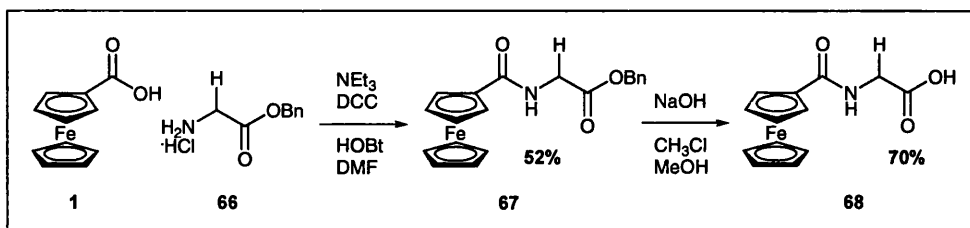
Scheme 4.10 – Ferrocene amide synthesis.

Results

The protected intermediate *amide* **67** is synthesised in reasonable yield (52%). It was then deprotected to form *amide* **68** in good yield (70%).

Discussion

The reaction was successful as the amino acid **66** was coupled to ferrocene carboxylic acid **1** in reasonable yield and then deprotected. Evidently there is a wide scope for this synthesis to be applied to a wide range of protected amino acids.

4.5 Measurement of electropotentials

The electropotential of a redox active species, such as ferrocene, can be defined as the potential at which the maximum differential current response occurs in a Differential Pulse Voltammetry (DPV) trace, as illustrated in Figure 2.21. This has been thoroughly described in section 2.5.7.
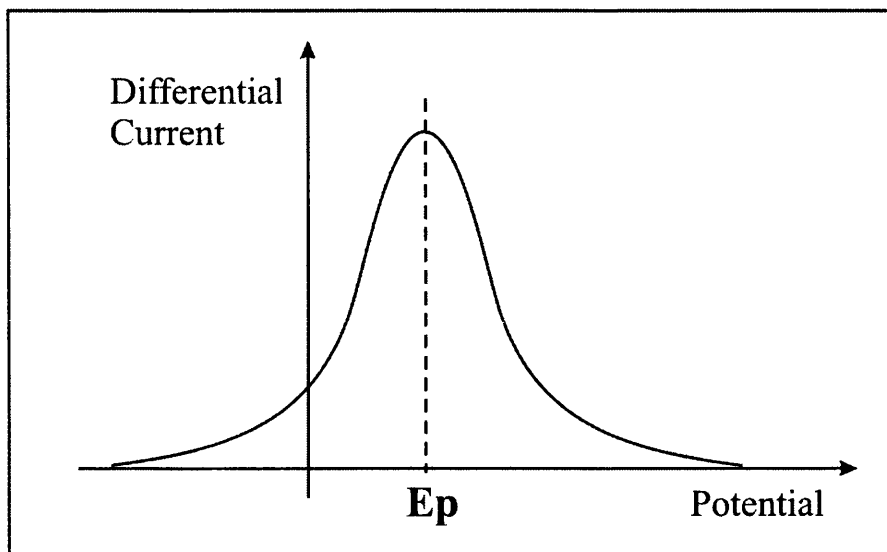
Figure 4.9 - DPV: determination of Ep.
Plotting the differential current (δi) against potential for the DPV traces allows the electropotential (Ep) to be determined.

The electropotentials of the ferrocenylated linker molecules produced in sufficient yield will be measured. The electropotentials are expected to vary depending on the substituents on the ferrocene cyclopentadiene rings, as described in section 3.1.3.

4.5.1 Measurement of electropotentials

The electropotentials of the linker molecules are measured before they have been activated or used to label oligonucleotides. It is possible that the electropotential of each molecule could vary between all three states and this variation may not be the same for different molecules. However, measuring the electropotential of the acids, or analogues, is of value as variation of the electropotential is primarily due to short range effects, discussed in section 3.1.3, and therefore it is proposed that differences observed in electropotentials of the acids should be roughly retained after labelling. The exception would be if the linker is very short, such as ferrocene carboxylic acid, where the ferrocene is in close proximity to the acid group.

The electrochemical cell and electrodes have been described in section 2.5.8, together with the practical theory in section 2.5.7. The measured electropotentials will be comparable if the assay, electrochemical cell and conditions remain constant. A gold working electrode and standard, low volume, BAS cell were used.

A 10 mM solution of each ferrocenylated linker in DMSO was prepared and was diluted to 1 mM in 0.1 M sodium acetate. The electropotential was then measured: full experiment details are given in section 2.9, Protocol 1.

The electropotentials are given below in Figure 4.10 and in Table 4.7. The electropotential of the commercially available ferrocene carboxylic acid, which Takenaka activated and used for labelling (Takenaka et al. 1994), was also measured for comparison.
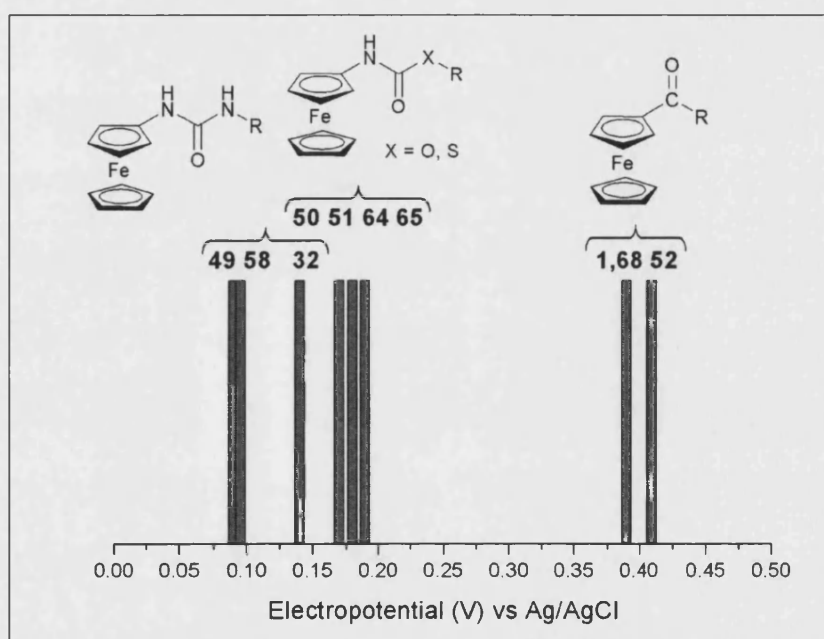
Figure 4.10 - Comparison of electropotentials.
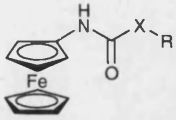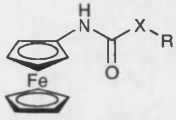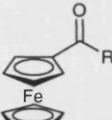
Linker molecule	Substituent (X)	Name	Number	Electropotential (V)
	N	4-((3-ferrocenyl-ureido)methyl)benzoic acid	*Acid* **49**	0.09
	N	Methyl (3-ferrocenyl-ureido)ethanoate	*Ester* **58**	0.10
	N	4-(3-ferrocenyl-ureido)-benzoic acid	*Acid* **32**	0.14
	O	4-((ferrocenyl-carbamoyl)methyl)benzoic acid	*Acid* **50**	0.14
	S	4-((ferrocenyl-carbamoyl-sulfonylmethyl)benzoic acid	*Acid* **51**	0.17
	O	Methyl (3-ferrocenyl-carbamoyl)ethanoate	*Ester* **64**	0.18
	S	Methyl (3-ferrocenyl-carbamoylsulfonyl)ethanoate	*Ester* **65**	0.19
	-	Ferrocene carboxylic acid	*Acid* **1**	0.39
	-	(Ferrocenoyl amino)ethanoic acid	*Acid* **68**	0.39
	-	4-((3-ferrocenoyl-amino)methyl)benzoic acid	*Acid* **52**	0.41

Table 4.7 – Electropotentials of linker molecules.

4.5.2　Discussion of electropotentials

General overview

It can be seen in section 4.5 that the linker molecules have a range of electropotentials. If the electropotentials of different linker molecules are sufficiently different, they will be resolvable by DPV and therefore could be used simultaneously in a detection system and multiplexing would be possible.

The majority of the labels also have a significantly lower electropotential than ferrocene carboxylic acid, which Takenaka activated and used for labelling (Takenaka et al. 1994). This is also desirable as it would require less power, due to lower voltages, in a detection system.

The oxidation electropotential can be considered in terms of the ease with which the ferrocene moiety is oxidised. Hence, if the electropotential is low oxidation can readily occur and the ferrocenium ion can be thought of as being stabilised, relative to the ferrocene.

Trends

The trends in the data should now be discussed. Initially the high electropotential molecules with a carbonyl group in the α position will be discussed. After this the low electropotential molecules synthesised by the *azide* **21** route, with an amide group in the α position, will be discussed.

Trends: high electropotential molecules

The high electropotential molecules have a carbonyl group (Fc*CO*R) in the α position. The carbonyl group destabilises the aromatic ring by mesomeric withdrawal giving a high electropotential, as illustrated in Figure 4.11. The presence of hetero atoms in the β position, such as amide (CO*NH*) and acid (CO*OH*) are able to reduce the effect of the carbonyl by mesomeric stabilisation. In this case the effect of the amide and acid groups on the stability of the ferrocenium ion are similar and the resultant electropotentials of all three molecules are similar.
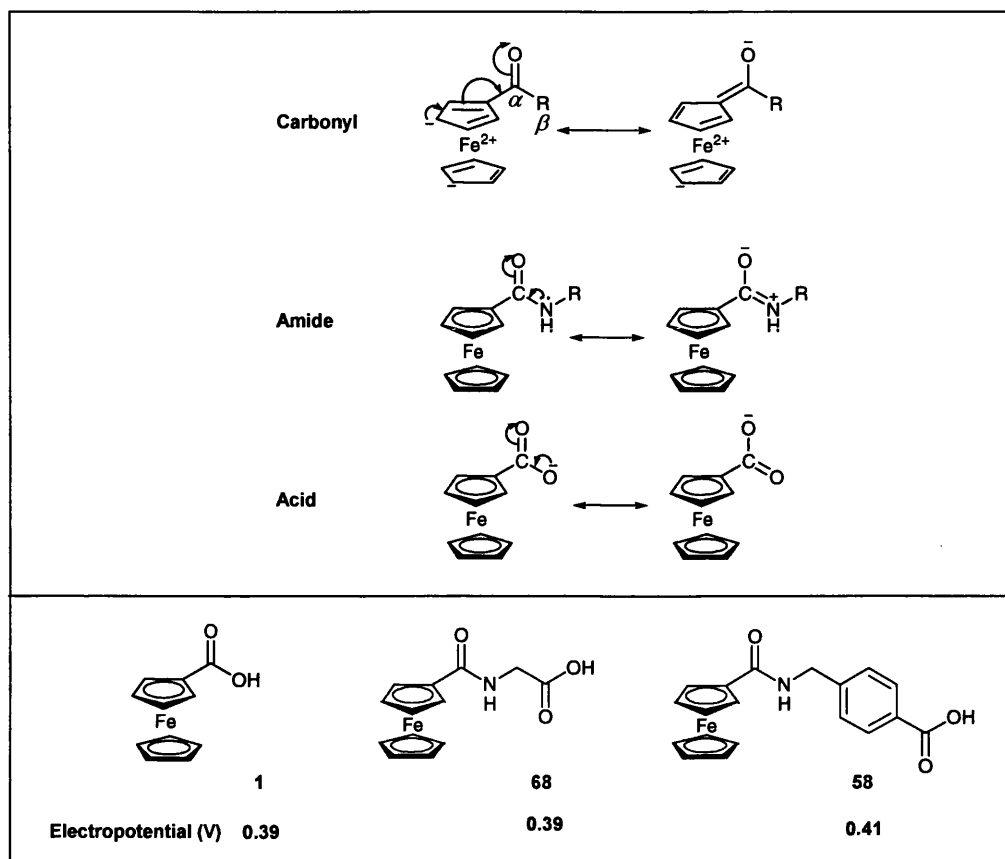
Figure 4.11 - Alpha carbonyl compounds.
The presence of a carbonyl substituent in the α position on the cyclopentadiene ring (top diagram, carbonyl) destabilises the Fe^{2+} ion through mesomeric withdrawal of electron density (the illustration of the ring using double bonds is equivalent to the lower diagrams which use a circle). Hetero atoms in the β position (top diagram, amide and acid) donate electron density to the carbonyl, reducing its destabilising effect. The electropotentials of ferrocene carboxylic acid and the two novel linker molecules (bottom diagram) are similar.

Trends: low electropotential molecules

If the amide group is "reversed" and the nitrogen atom is in the α position the electropotentials are significantly lower. Nitrogen can either be electron withdrawing (through induction) as a quaternary amine ($-N^+R_3$) or donating (through mesomeric donation) as tertiary amine ($-NR_2$). For a neutral amide group ($-NHCOR$) the donation is the dominant effect, although this effect, shown in Figure 4.12 (a) is dramatically weakened by the alternative delocalisation onto the carbonyl, shown in Figure 4.12 (b).

196
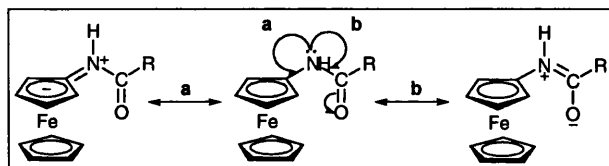
Figure 4.12 – Stabilising effects of the amide group.
There is competition for the electron density of the nitrogen atom in the ferrocene amide (centre). The lone pair electrons can stabilise either (a) the ferrocene (left hand side) or (b) the carbonyl (right hand side) through mesomeric donation.

The electropotentials of the two structural series of linker molecules are given in Figure 4.13. For both series it can be seen that the urea (NH) has the lowest electropotential (most stabilisation), followed by the carbamate (O) and then the S-thiocarbamate (S) has the highest electropotential (least stabilisation). The S-thiocarbamate electropotentials are close to those of the carbamate, but will be treated as significantly different as the trend is reproducible.
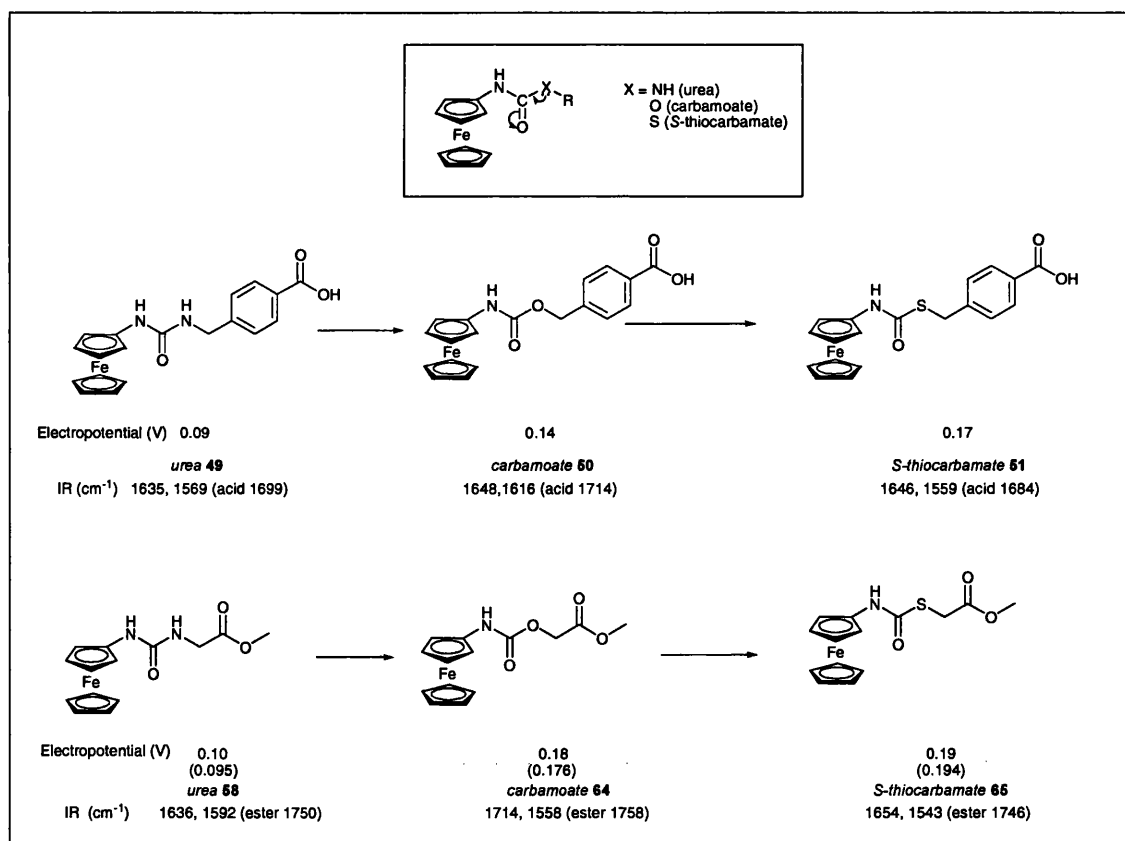
Figure 4.13 - Comparison of homologous series.
The effect of the hetero atom on mesomeric stabilisation of the carbonyl group is shown (top box). The two structural series are given below. These are shown in order of increasing electropotential (left to right). This trend is urea (NH) carbamate (O) and S-thiocarbamate (S) in both cases. The IR carbonyl stretches are also given.

In an attempt to explain this trend the mesomeric effects will first be considered. It is thought that the stabilising effect of the "amide group" will remain high if further π electron delocalisation is possible from the hetero atom, as shown in Figure 4.14, which reduces the delocalisation of the amide nitrogen lone pair to the carbonyl, as in Figure 4.12, b.
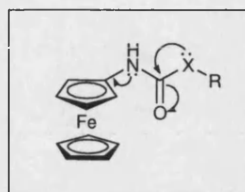
Figure 4.14 - Delocalisation of lone pair electrons from the hetero atom.

As shown in Figure 4.15, all the atoms in the "amide group" (NCO) are sp^2 hybridised (i.e. trigonal planar with a p orbital out of the plane) which gives good p orbital overlap and hence favourable conditions for π-bond formation. For molecules containing the urea group, the additional nitrogen (N) is sp^2 hybridised, allowing good overlap. In contrast the hetero atoms of the carbamate (O) and S-thiocarbamate (S) groups are sp^3 hybridised and the overlap with the π-bonding p orbitals is poor and may even be negligible due to bond rotation. Thus the urea groups will afford the most stability for oxidation (low ferrocene electropotential), whilst the carbamate and S-thiocarbamate groups afford less stabilisation (higher ferrocene electropotential).
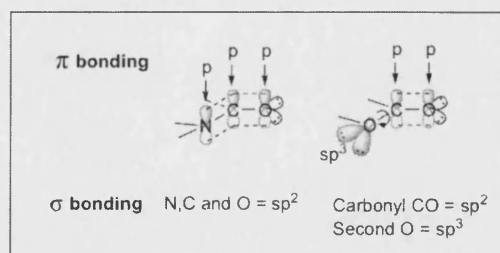
Figure 4.15 – Potential electron delocalisation from the hetero atoms onto the carbonyl group. Detail of the π-bonding electron orbitals and their hybridisation are shown for the urea (left hand side) and carbamate (right hand side) groups. For the urea all of the σ-bonding electron orbitals on the atoms (for N, C and O) are sp^2 hybridised, allowing good and overlap (dotted line) and therefore π-bonding though the p orbitals. For the carbamate the additional oxygen atom is sp^3 hybridised, which gives no free p orbital and restricts the π-bonding to the carbonyl group.

The S-thiocarbamate molecules have a slightly higher electropotential than the carbamate groups and this should be discussed. If delocalisation onto the carbonyl group is considered as above, it could be proposed that the larger 3sp^3 π orbitals of the

sulfur atom overlap less efficiently than the smaller $2sp^3$ π orbitals of the oxygen O, allowing less delocalisation and less stabilisation. A complicating factor is the issue that the oxygen and sulphur atoms do not have true sp^3 tetrahedral shape as this is distorted by repulsion between the bulky lone pairs and the other bonds and this will affect the π bonding interaction between their electrons and those on the carbonyl. Nevertheless, the above theory would explain the electropotential trend.

However, analysing the carbonyl stretches of the molecules by IR spectroscopy suggests that this may not be the case. Comparative graphs are given, in Figure 4.16 and Figure 4.17, for the two series of molecules, showing their IR stretches and electropotentials.
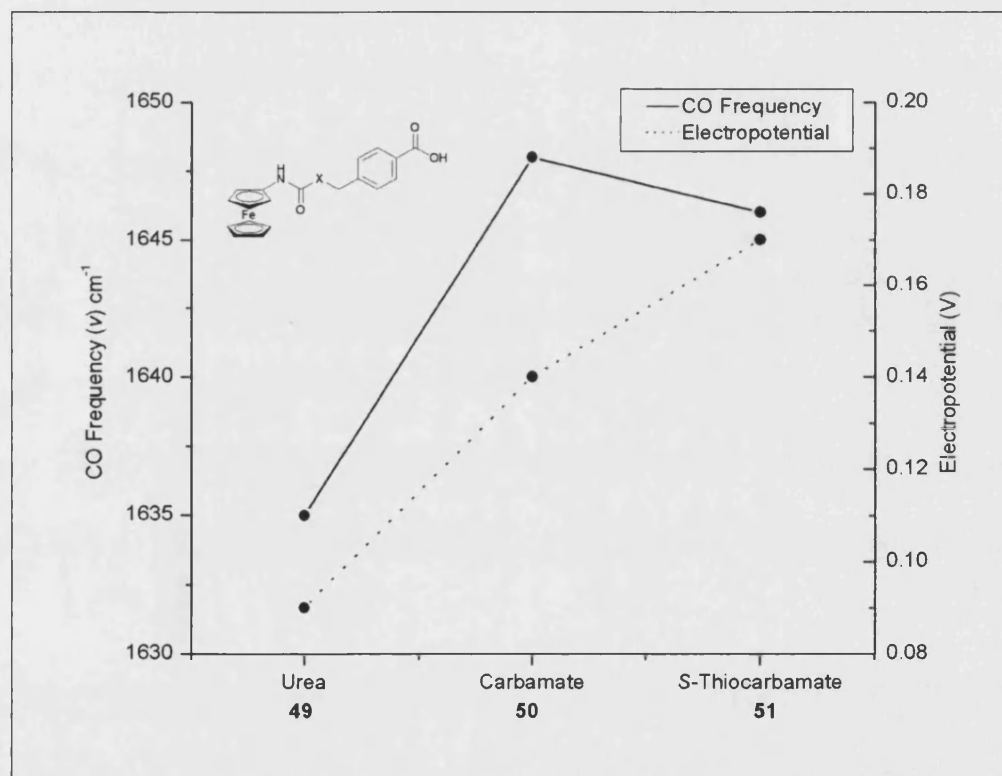
Figure 4.16 - Comparison between electropotential and carbonyl strength for the alkyl aromatic analogues.
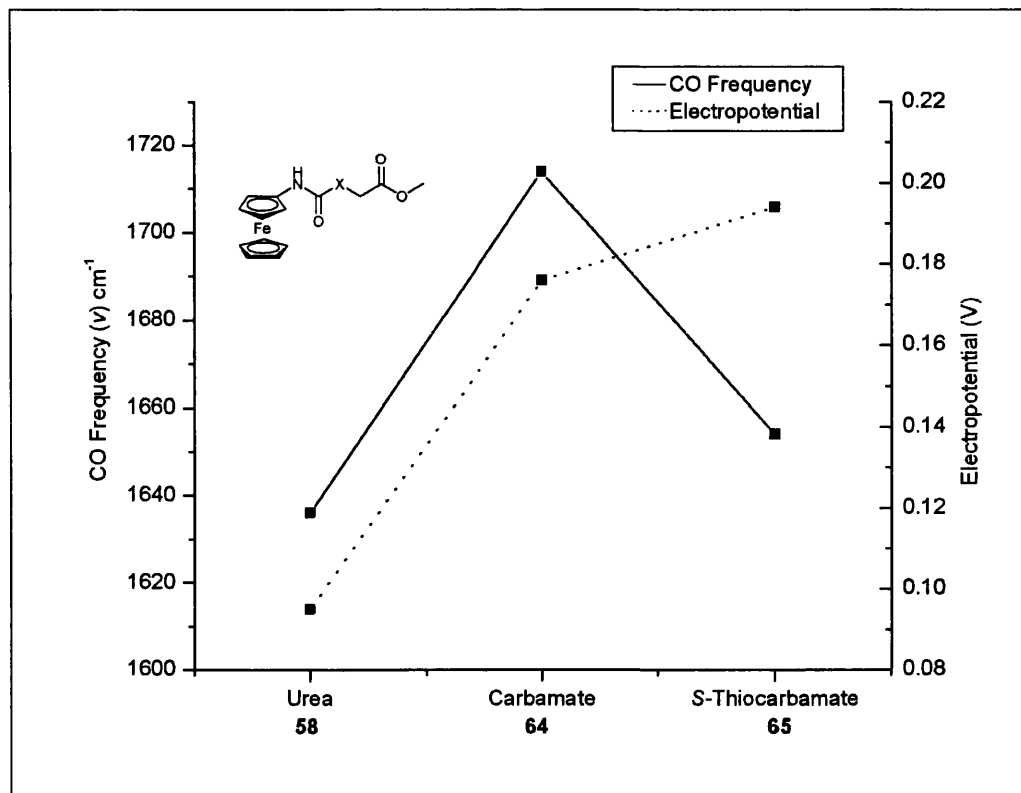
Figure 4.17 - Comparison between electropotential and carbonyl strength for the glycine methyl ester analogues.

As expected the urea molecules have the lowest IR carbonyl stretch, which corresponds to a weak carbonyl bond and high amounts of electron delocalisation from the hetero (N) atom. The carbamate molecules, however, showed higher carbonyl stretches and therefore stronger carbonyl bonds, than the S-thiocarbamate molecules. This was the reverse of what was expected. This trend could tentatively be explained if the sulfur does not delocalise any electron density to the carbonyl, as shown in Figure 4.18, and all the delocalisation comes from the nitrogen. In contrast there may be a degree of competition between the delocalisation of the oxygen and nitrogen in the carbamate, which results in less delocalisation and a longer carbonyl bond.
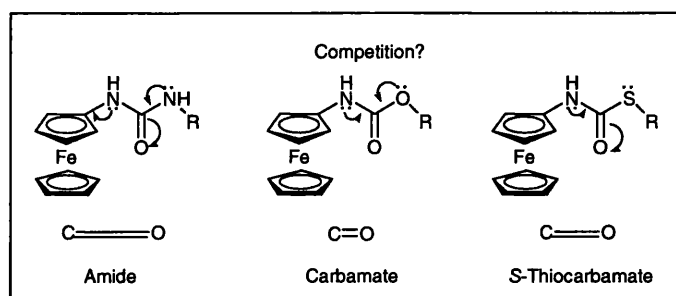
Figure 4.18 – Proposed explanation of carbonyl bond length.

The electronegativities and hence inductive effects of the hetero atoms have not yet been considered in relation to the electropotential trend. The electronegativity, and therefore the strength of the electron withdrawing inductive effect (− I), of the hetero atoms varies (O>N>S = C). It would be expected that the electronegative oxygen would pull more electron density from the carbonyl carbon, causing it to become more electropositive and therefore shortening and strengthening the carbonyl bond, as shown in Figure 4.19. This does not agree with the IR measurements and therefore induction may not have a significant effect on the electropotential.
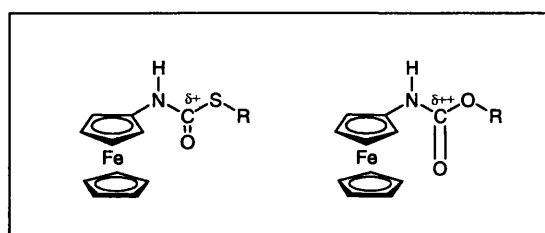
Figure 4.19 - Comparison of carbonyl groups.
The *S*-thiocarbamate molecules (left hand side) have a shorter carbonyl bonds than the carbamate molecules (right hand side), by IR. The carbamate oxygen is more electronegative than sulfur and therefore the carbonyl carbon should be more electronegative (δ++).

Although the electropotential variation has been explained in terms of mesomeric stabilisation, the steric arrangement of the molecules should also be considered. It is possible that there could be a direct stabilising interaction between the carbonyl oxygen and the ferrocenium ion, which could decrease the electropotential.

4.6 Synthesis of activated linker molecules

Selected linker molecules are now derivatised from acids to activated esters so that they can be used for post-labelling oligonucleotide probes.

The activated esters were synthesised using the literature procedure of Takenaka (Takenaka et al. 1994), shown in Scheme 4.11. Ferrocene carboxylic acid **1** was derivatised, together with four selected linker molecules, which had been synthesised in good yield. The results are given below in Table 4.8.
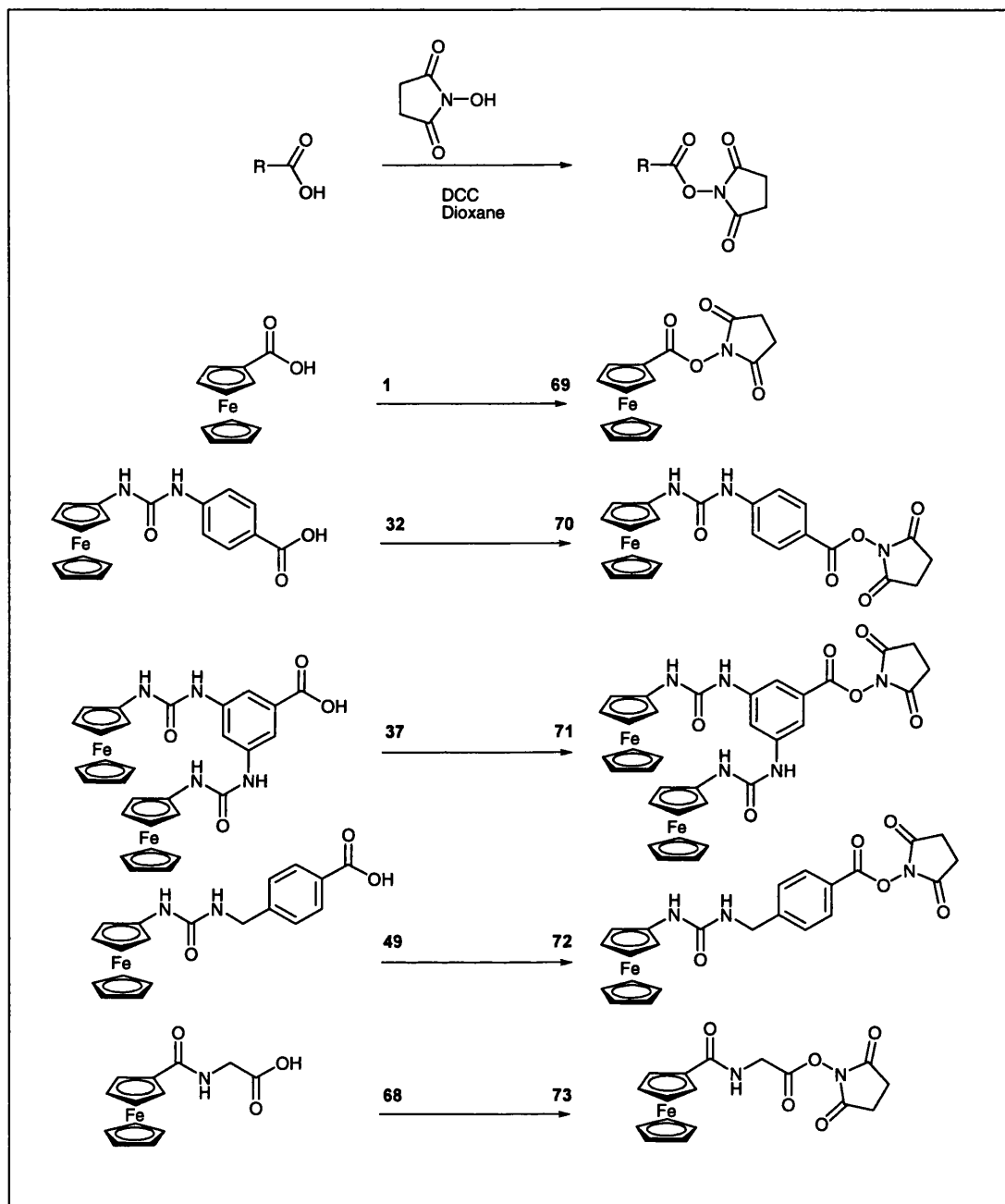
Scheme 4.11 – Activation of linker molecules as the *N*-succinimide ester.

Entry	Reagent (acid)	Product (ester)	Yield (%)
1	1	69	74
2	32	70	66
3	37	71	28
4	49	72	27
5	68	73	10

Table 4.8 –Activation of linker molecules.
All of the products have been purified by silica flash chromatography.

The yields were good for ferrocene carboxylic acid **1** (*ester* **69**, 74%) and *urea* **32** (*ester* **70**, 66%), but poor for the other three linker molecules (*ester* **37** 28%, *ester* **49** 27% and *ester* **68** 10%).

None of the above reactions or purifications have been optimised and therefore the yields can probably be improved. All of the products were purified using silica flash chromatography, however, as silica is very nucleophillic, it is thought that the products may degrade during the purification. Due to this direct purification by crystallisation should be developed. An alternative approach would be to simplify the work-up using polymer (polystyrene) bound HOBt (Dendrinos et al. 1998) or EDCI (Desai et al. 1993; Adamczyk et al. 1995), described in Figure 4.20, which should allow flash chromatography to be omitted.
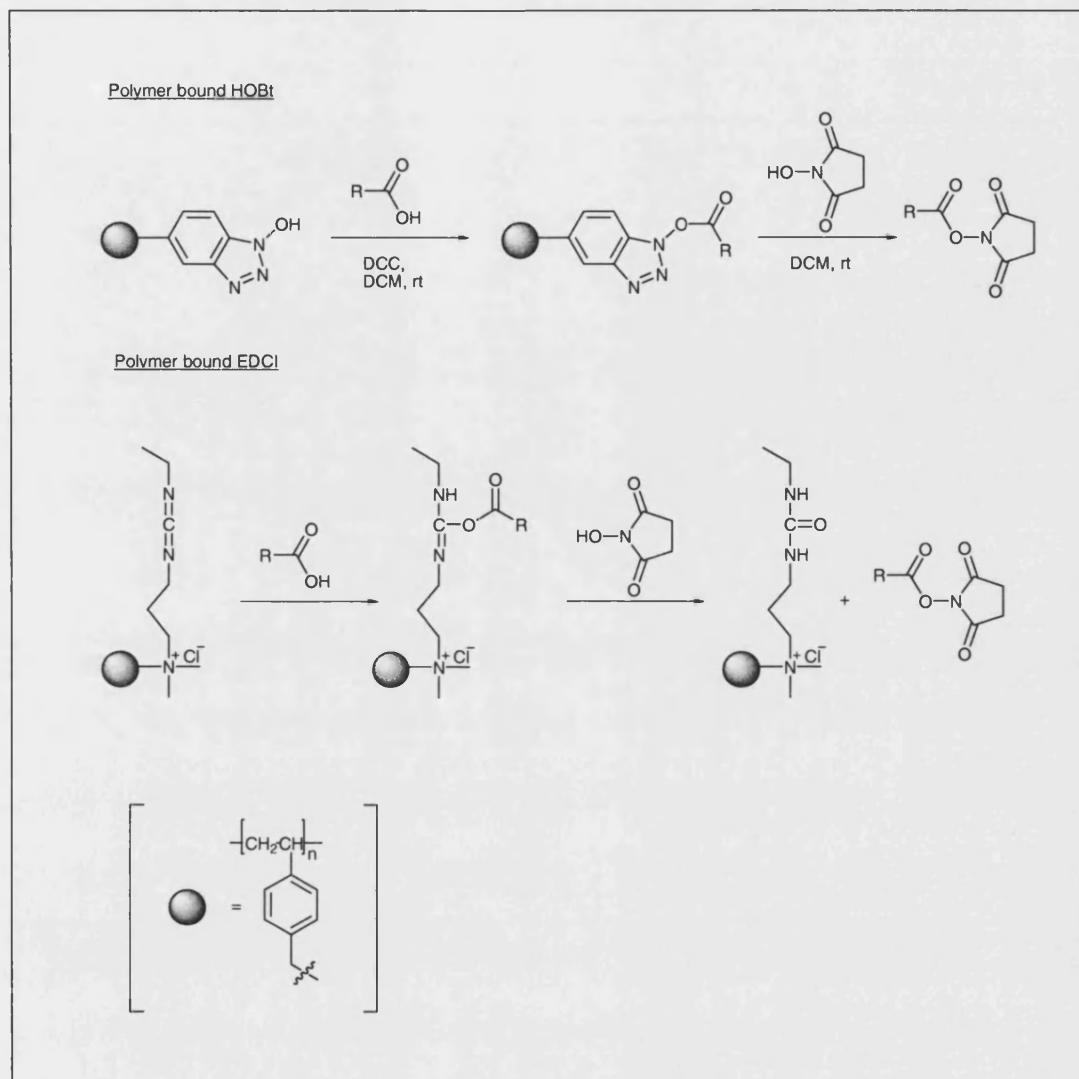
Figure 4.20 - Use of polymer (polystyrene) bound coupling reagents.
Polymer supported coupling reagents: HOBt (top) and EDCI (bottom) are shown. These could be used to improve the work-up of the coupling reaction.

4.7   Conclusions (Part A)

Linker synthesis

In the sections 4.3 and 4.4 a range of novel ferrocenylated linker molecules have been synthesised, which have either free carboxylic acid groups or protected acid groups. All of these linker molecules could be derivatised to activated esters and used for the covalent labelling of oligonucleotide probes.

The potential for further synthesis has been illustrated, although not exploited and careful adjustment of the experimental conditions should allow the yield of the successful reactions to be improved and optimised. It should also allow the synthetic problems from the unsuccessful approaches to be overcome. Although high yields are preferable, the primary aim was to synthesise novel linker molecules in isolatable yields, which can then have their electropotentials measured. This has been achieved.

Electropotential analysis

The electropotentials of the novel ferrocenylated linker molecules have been determined by DPV in section 4.5. They exhibit a range of different electropotentials. There is sufficient difference in electropotential for some of these linkers, that discrimination could be achieved between the electrochemical signals (DPV), which would allow the linkers to be utilised in technologies requiring multiplexing.

As expected the atoms on the substituents closest to the cyclopentadiene ring of the ferrocene have the greatest effect on the electropotential. The linker molecules with carbonyl groups in the alpha position have a similar electropotential to the ferrocene carboxylic acid standard, whilst those with a urea, carbamate or S-thiocarbamate group are significantly lower. For these molecules ascending electropotentials are obtained from urea to carbamate to S-thiocarbamate.

The most valuable further work would be to synthesise another structural series of urea, carbamate and S-thiocarbamate linker molecules to determine if the electropotential trend is retained. The use of X-ray crystallography to determine the conformational structure of the linker molecules, would be very useful as it would highlight any steric factors which may affect the electropotential of the ferrocene moiety. Attempts to crystallise the linker molecules for X-ray analysis proved problematic, so this analysis has not been currently undertaken.

Activation of linker molecules

Four ferrocenylated linker molecules and ferrocene carboxylic acid have been derivatised to activated esters. These can now be used for post-labelling the oligonucleotide probes.

Choice of linker molecule

The *ester* **70** was selected for use in oligonucleotide labelling as its electropotential (140 mV) was significantly different to that of ferrocene carboxylic acid (390 mV) and the oligonucleotide labelled with ferrocene carboxylic acid activated ester (approx 400 mV) (Takenaka et al. 1994). The synthesis of *ester* **70** and its precursor, *acid* **32**, were also straightforward and high yielding.

PART B: Synthesis of phosphoramidite linker molecules

4.8 Synthesis of phosphoramidite label

The synthesis of *phosphoramidite* **28**, via the *alcohol* **27** intermediate, is reported.

4.8.1 Reaction overview

The synthetic route for the production of *phosphoramidite* **28** is summarised below in Figure 4.21.
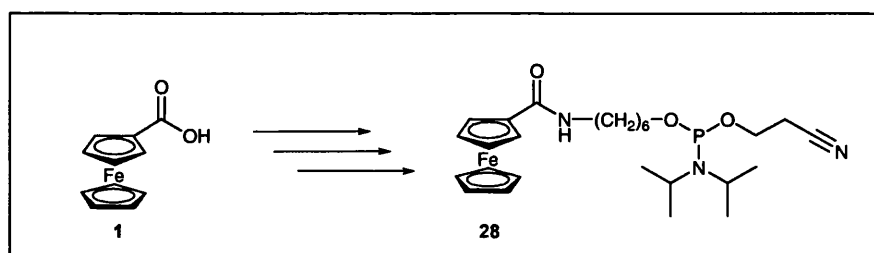
Figure 4.21 – Synthetic plan: Phosphoramidite linker.

Phosphoramidite **28** is a known molecule (Beilstein et al. 2001), but an alternative route is used to synthesise it. The rationale behind this has been given in section 3.3.3.

4.8.2 Reaction detail

Initially ferrocene carboxylic acid **1** is derivatised to *alcohol* **27** which is purified and this is then converted to *phosphoramidite* **28**, as shown in Scheme 4.12.
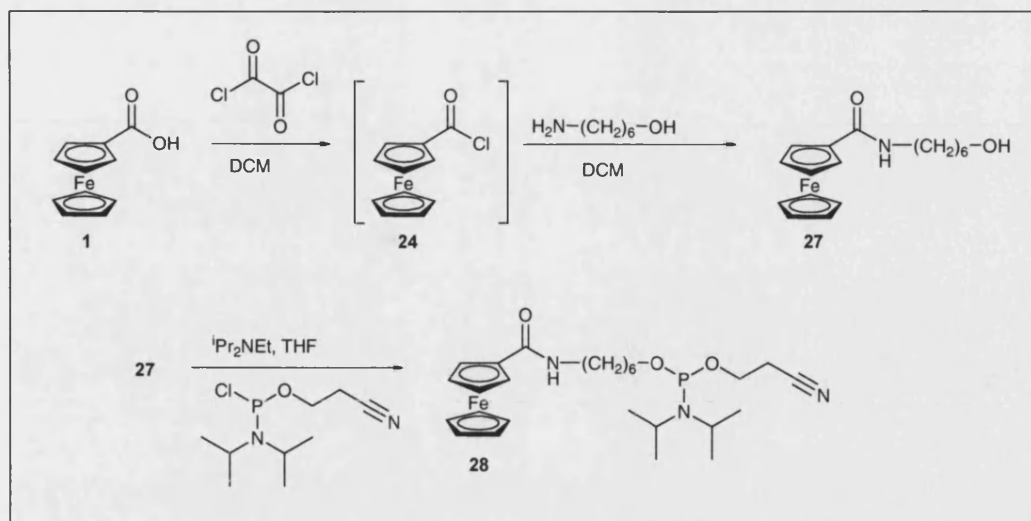
Scheme 4.12 - Synthesis of *phosphoramidite* 28.

4.8.3 Synthesis of *alcohol* 27

The synthesis of *alcohol* **27** is detailed in Scheme 4.13 and the results are given in Table 4.9. Problems arose as it is possible for the *alcohol* **27** to react further with the ferrocene acid chloride **24** and form the *dimer* **75** by-product (Table 4.9, entry 1).
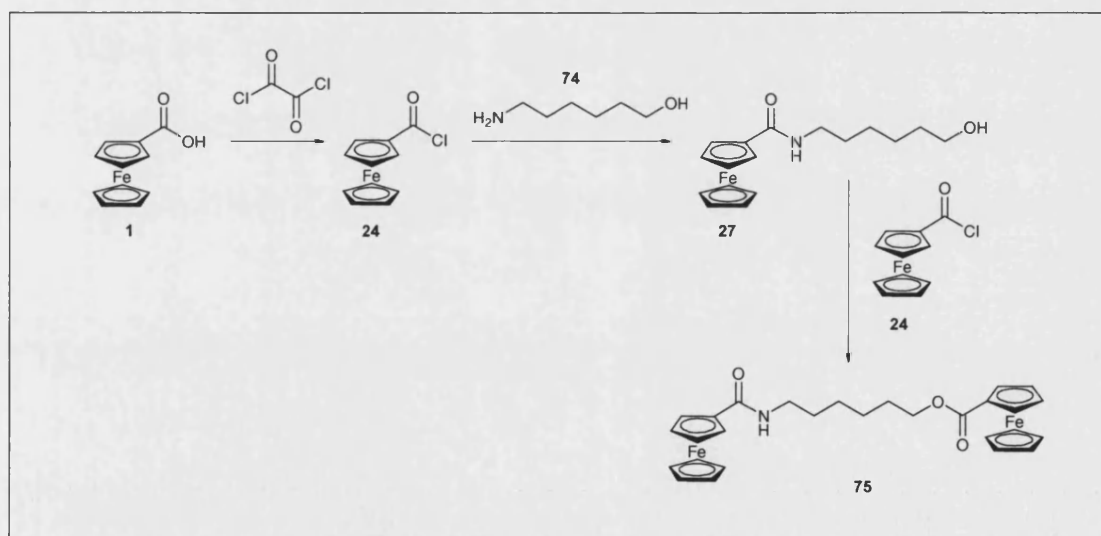
Scheme 4.13 – Production of *dimer* 75.

Entry	Mol. Equivalents			Yield (%)		Comments		
	Acid 1	Oxalyl Chloride	*Alcohol* 74	*Alcohol* 27	*Dimer* 75	ROH → R'CO$_2$Cl	R'CO$_2$Cl → ROH	Temp (°C)
1	1.0	4.0	1.2	-	52	✓		4
2	1.0	2.4	1.2	-	48	✓		0
3	1.0	2.4	5.0	42	-		✓	0
4	1.0	2.4	5.0	53	-		✓	0

Table 4.9 - Synthesis of *alcohol* 27.
The left hand side of the table gives the molar equivalents of the reagents which were used. In the comments section (right hand side) a tick signifies if 6-aminohexan-1-ol was added to a solution of ferrocene acid chloride (ROH → R'CO$_2$Cl) or if this was reversed.

To promote the formation of *alcohol* **27** the amount of the oxalyl chloride and the temperature were reduced, but this did not prevent the side reaction (Table 4.9, entry 2). Subsequently the excess of the *alcohol* **74** reagent was increased and the order of addition was changed so that the acid chloride was added to the *alcohol* **74**. This approach proved to be successful and the *alcohol* **27** was reproducibly produced in reasonable yield (Table 4.9, entries 3 and 4).

4.8.4 Synthesis of *phosphoramidite* 28

The synthesis of *phosphoramidite* **28** is detailed below, in Scheme 4.14.
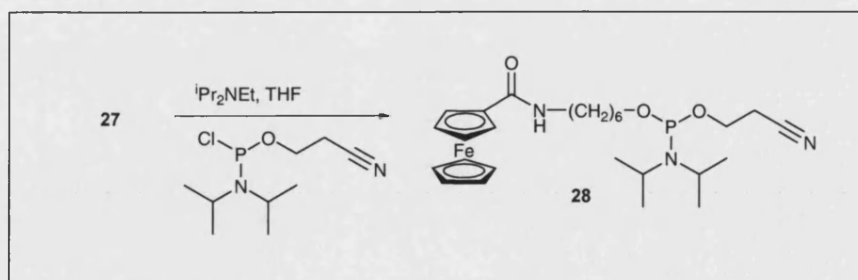
Scheme 4.14 – Synthesis of *phosphoramidite* 28.

The phosphoramidite was then synthesised in an acceptable yield (61%).

Care must be taken during the synthesis and purification of *phosphoramidite* **28** as the phosphorous (P^{III}) will readily oxidise to the phosphorous oxide (P^{V}), as shown in Scheme 4.15. This oxidation would make the molecule unsuitable for use in oligonucleotide synthesis.
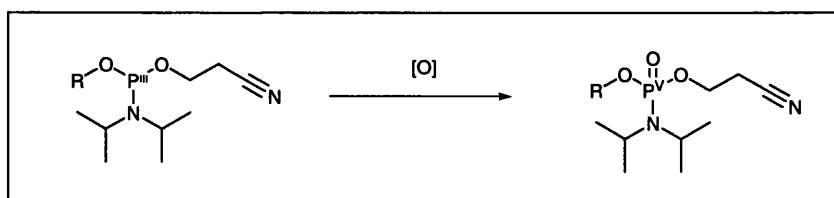
Scheme 4.15 – Phosphoramidite oxidation.

4.9   Conclusions (Part B)

Phosphoramidite **28** was successfully synthesised in acceptable yield (61%). It can now be used to label probe oligonucleotides.

Chapter 5: Theory and rationale behind electrochemical DNA hybridisation probes

5 Theory and rationale behind electrochemical DNA hybridisation probes

5.1 Introduction

This chapter gives the specific theory and rationale behind the design of a novel, ferrocene based, DNA hybridisation gene sensor. This gene sensor is ultimately designed for use with PCR products and potentially *in situ* PCR analysis, but will be developed using simpler systems.

The integral aspects of the work: oligonucleotide labelling and enzymatic digestion, are discussed in detail, together with the mode of action of all the enzymes which will be used: S1 endonuclease; T7 exonuclease and Taq. DNA hybridisation probes are then discussed in the context of gene sensing, based on enzymatic digestion. Gene sequence selection, stringency of the assay and electrochemical detection are all covered. Experimental issues, including the potential problems that the enzyme buffers can cause for electrochemical analysis, are highlighted. The specific uses of the complementary techniques, which can be used to validate the DPV results, are given. These included the use of fluorescence, gel electrophoresis and potential step amperometry.

The proposed experimental work is given at the end of the chapter in detail. To the author's knowledge there is no direct literature precedent for this work, although aspects of the work has been published by the author (Hillier, S. C. et al. 2004a; Hillier, S.C. et al. 2004b) and have been patented (Molecular Sensing 2004).

5.2 Aims

The aim of this chapter is to detail the development of an electrochemical DNA hybridisation gene sensor. The aims are summarised diagrammatically in Figure 5.1. The development requires that different aspects of the hybridisation probes are addressed sequentially:

- Effective oligonucleotide labelling

The ferrocenylated linker molecules, both covalent labels and phosphoramidite labels, must be shown to be efficient at labelling oligonucleotides, to produce ferrocenylated probe oligonucleotides. The success of the labelling is most readily ascertained through S1 enzymatic digestion of the labelled oligonucleotide.

- Successful enzymatic digestion

It must be shown that enzymatic digestion of the ferrocenylated probe oligonucleotide can be followed by electrochemical detection. This is achieved if the digested ferrocenylated probe fragments, give a higher electrochemical response, by Differential Pulse Voltammetry (DPV), than the undigested oligonucleotide. The most straightforward way to test this is to digest a ssDNA probe oligonucleotide, with a ssDNA specific enzyme, such as S1 endonuclease.

A DNA hybridisation probe would require that a DNA duplex (matched ferrocenylated probe and target) is digested with a dsDNA specific enzyme, whilst an unhybridised probe (mismatched ferrocenylated probe and target) is not. The most straightforward way to determine if a dsDNA specific enzyme is suitable is to initially use it with a ferrocenylated hairpin oligonucleotide. The oligonucleotide is self complementary and forms a duplex with itself, which eliminates the requirement for hybridisation with a complementary target.

- Development of DNA hybridisation gene sensor

If discrimination has been obtained between a ferrocenylated hairpin oligonucleotide, before and after digestion with a dsDNA specific enzyme, this enzyme can be applied to the digestion of a complementary probe/target duplex. To minimise the number of different components in the assay, the target oligonucleotide will be custom synthesised.

The aim is then to achieve discrimination between a matched ferrocenylated probe and gene target (duplex formation, enzymatic digestion and high DPV response) and a

mismatched ferrocenylated probe and target (no duplex formation, no enzymatic digestion and low DPV response). If discrimination is obtained, the approach can be used as a DNA hybridisation gene sensor.

- Application of gene sensor to PCR product and PCR analysis

A successful PCR synthesises a high concentration of a desired DNA target sequence (amplicon). The presence of this amplicon can be determined, as for the synthetic target, after the PCR has been completed. The aim of a gene sensor is to show that gene amplification (correct primers) gives an increase in electrochemical response, whilst the failure of gene amplification (incorrect primers or lack of target) does not.

Finally *in situ* analysis of PCR could be possible. Introducing the ferrocenylated probe oligonucleotide into the PCR mixture would allow it to be digested by the Taq polymerase enzyme and allow the progress of the PCR to be followed.
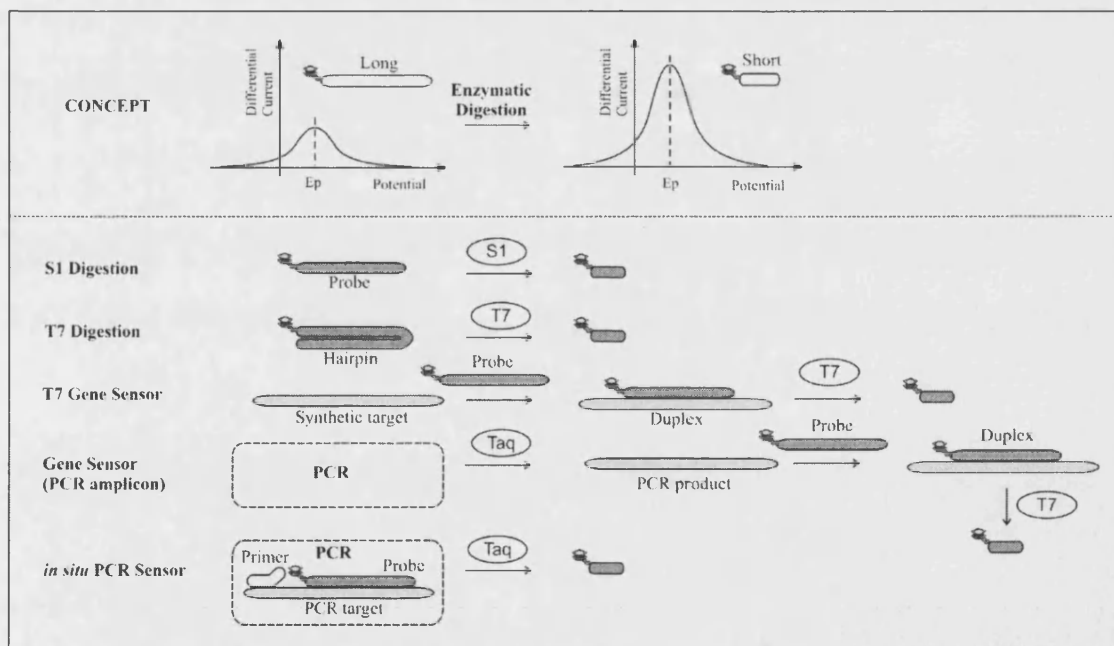
Figure 5.1– Aims: development of gene sensor.
The concept behind the work is summarised (top diagram). A large ferrocenylated oligonucleotide (left hand side) gives a low DPV response (low differential current at the electropotential, Ep). The DPV response increases when enzymatic digestion affords a smaller ferrocenylated oligonucleotide fragment (right hand side). The assays required for the development of the gene sensor are described here (bottom diagram). For each assay a large ferrocenylated moiety (oligonucleotide, hairpin oligonucleotide or duplex) is enzymatically digested (white circle: S1 endonuclease; T7 exonuclease or Taq polymerase) to generate a small ferrocenylated probe fragment (short, dark grey strand). The fragment size can differ depending on the enzyme. Full details of the assays are described in the chapter and the figure is fully described in the Experimental plan (section 5.9).

The work will be undertaken using unmodified electrode surfaces as surface modification introduces a layer of complexity to the work, which may be unnecessary. Whilst sensitivity is ultimately very important the focus of this work is on "proof of concept" rather than optimisation of sensitivity. The commercialisation of the work, involving the optimisation of sensitivity and electrodes, has been undertaken by Dr. S. Flower (University of Bath, UK) on a 2 year Post Doctoral project which will conclude in 2006. His work will not be discussed here.

5.3 Oligonucleotide labelling

Oligonucleotide labelling with ferrocenylated linker molecules has been broadly introduced in section 3.2. The specific post-labelling and phosphoramidite labelling methods for covalently labelling probe oligonucleotides are given below. **A fold-out reference page for the labelling can be found in the "labelling oligonucleotides" section at the end of the thesis.**

5.3.1 Post-labelling

Based on work by Takenaka (Takenaka et al. 1994) ferrocene based N-succinimide ester linker molecules can be used to post-label synthetic oligonucleotides, as shown in Scheme 5.1.
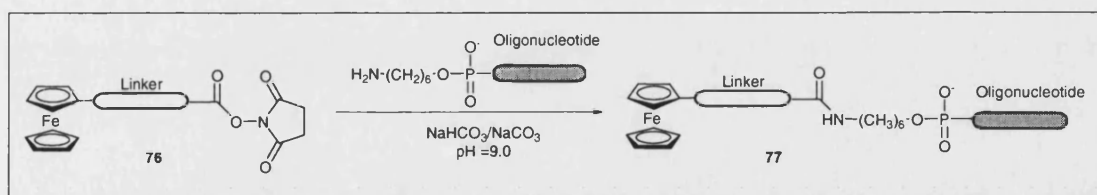
Scheme 5.1- Oligonucleotide labelling.
The N-succinimide ester of the ferrocenylated linker molecule 76 is coupled to the oligonucleotide (grey strand) which has been 5' modified with a C6 alkyl amine. This gives the labelled oligonucleotide 77.

The full experimental details are given in section 2.10.2.

5.3.2 Phosphoramidite labelling

Phosphoramidite labelling end labels an oligonucleotide, using solid phase coupling with a ferrocenylated *phosphoramidite* **28**, as shown in Figure 5.2. This is based on work by Beilstein (Beilstein et al. 2001) and was done commercially (TibMol Biol, Germany). The labelled oligonucleotides were supplied after purification by reverse phase HPLC.
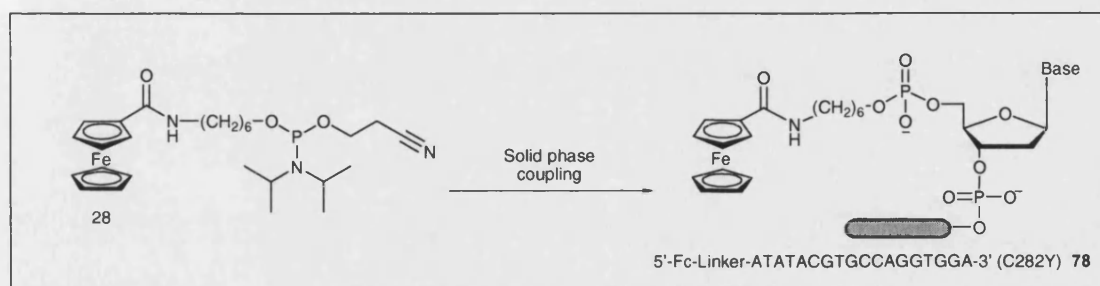
Figure 5.2 – Phosphoramidite labelling.
The ferrocene labelled *phosphoramidite* 28 is used to 5' label the oligonucleotide (grey strand) after the solid phase oligonucleotide synthesis has finished. The labelled oligonucleotide is then cleaved from the solid support. The phosphoramidite incorporates a C6 alkyl chain in contrast to the C4 chain used by Beilstein (Beilstein et al. 2001). This gives consistency with the post-labelling approach in section 5.3.1.

5.3.3 Labelling efficiency

The efficiency of a labelling technique describes the proportion of oligonucleotides which are successfully labelled. A high labelling efficiency, preferably 100%, is desired as the presence of any number of unlabelled oligonucleotides in an assay will decrease the sensitivity of the detection technique. The commercial labelling company, TibMol Biol, state that the efficiency of their phosphoramidite labelling is very high.

The concentration of the probe oligonucleotides in solution can be readily determined using UV/Vis spectrometry, detailed in section 2.4, but the efficiency of a labelling process is much more difficult to absolutely determine. This would rely on the measurement of the electrochemical response from the ferrocene labels and the comparison of this response against results from a series of calibration experiments. However, this also relies on the availability of a standard of known concentration, which must be a ferrocenylated oligonucleotide of the same sequence, as the

oligonucleotide sequence can affect the electrochemical response. Relative efficiencies could be determined between samples.

To determine if the labelling efficiency of a labelling approach in this work is sufficiently high, the labelled probe will be subjected to S1 endonuclease digestion and electrochemical response is then measured.

5.4   Enzymatic digestion

The fundamental principle behind the work is that a ferrocene labelled probe oligonucleotide gives a higher electrochemical response (by DPV) after enzymatic digestion, which generates a smaller oligonucleotide fragment. This has been introduced in Figure 5.1.

Three different enzymes are used in the work: S1 endonuclease; T7 exonuclease and Taq. Their modes of action are described here.

5.4.1 S1 endonuclease

S1 nuclease (Promega, USA) is an endonuclease that digests single stranded nucleic acids by cleavage of the phosphodiester bond to yield 5' phosphorylated products, mononucleotides or short oligonucleotides (Vogt 1973). This is shown in Figure 5.3. As the linker is not affected by the enzyme, ferrocene labelled oligonucleotides will be digested in the same way and therefore some of the fragments will be ferrocene labelled.
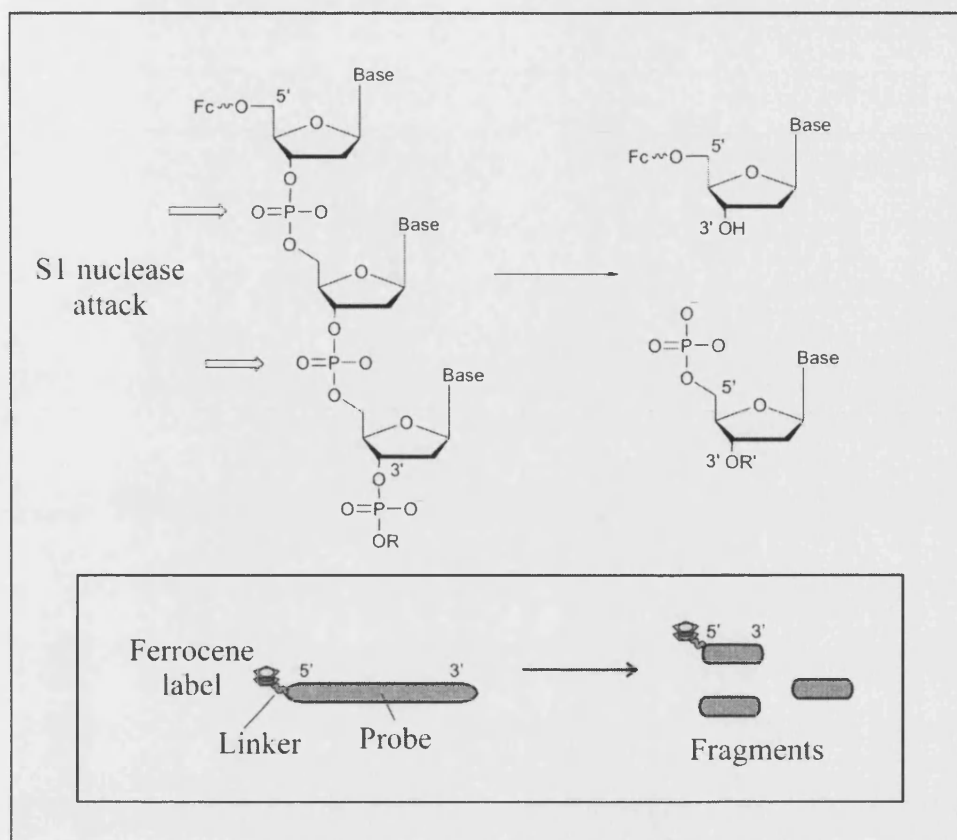
Figure 5.3 - S1 nuclease digestion.
The probe oligonucleotide (left hand side) is 5' labelled with a ferrocenylated linker molecule (Fc~).
The S1 enzyme digests ssDNA (left hand side) at the phosphodiester bonds (white arrows) to yield
5' phosphorylated products (mononucleotides or short oligonucleotides, right hand side), some of
which retain the ferrocene label. The R groups (R and R') signify either further oligonucleotides or
the end of the chain (R, R' = H).

5.4.2 T7 exonuclease

The T7 enzyme is a double strand specific exonuclease which reads along double strand
DNA (5' to 3') sequentially removing the terminal 5' nucleotides of the duplex DNA, as
described in Figure 5.4 (Kerr 1971b; 1971a). Both ends of a DNA duplex can be
attacked and the enzyme uses random exonucleolytic attack.
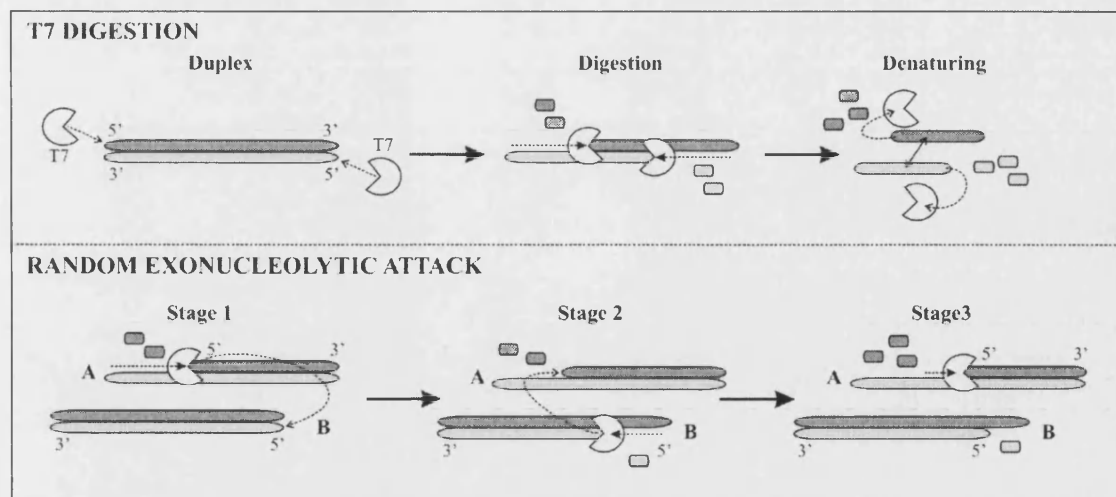
Figure 5.4 – T7 exonuclease: mode of action.
For a fully complementary DNA duplex (dark grey and light grey strands, top diagram) the DNA can be attacked simultaneously at both 5' ends (open head dotted arrow), by different T7 enzymes (white circles). Digestion: both T7 exonuclease enzymes digest the dsDNA in the 5' to 3' direction (closed head dotted arrow), liberating mononucleotides (a dinucleotide is initially liberated if the DNA has a 5' terminal hydroxyl group). Denaturing: when only a small length of duplex DNA remains, the DNA strands will denature and move apart (doubled headed arrow). The T7 exonuclease will not digest ssDNA and releases the strand and moves away (open head dotted arrow). The T7 mechanism has been illustrated (top diagram) as a progressive mechanism, whereby the enzyme starts digesting a strand and moves along the strand until it is finished. This is not typically the case and random exonucleolytic attack occurs (bottom diagram), although the overall results are the same. Only one enzyme is considered for clarity. The enzyme digests duplex A (stage 1) before moving to a second duplex B, after digesting a few bases. After digesting some of duplex B (stage 2), it can move back to the original strand (or any other) and continue digestion (stage 3).

The enzyme will attack at 5' strands of duplex DNA which have either terminal hydroxyl or phosphoryl groups at equal rates (Kerr 1971a), but its action at substituted 5' groups is not known. As it is ineffective at digesting ssDNA, the proposed action of T7 exonuclease on a probe/target duplex is illustrated in Figure 5.5. The probe/target duplex contains both a 5' ferrocenylated linker group (probe) and a 5' hydroxyl terminated ssDNA sequence (target). It is hoped that the enzyme will favour digestion of the probe and generate ferrocenylated fragments. Even if the digestion of the initial ferrocenylated probe sequence is slow and there is competition for the T7 enzyme, the random nature of the enzyme's exonucleolytic attack should ensure that it has numerous chances to digest the ferrocenylated probe sequence.
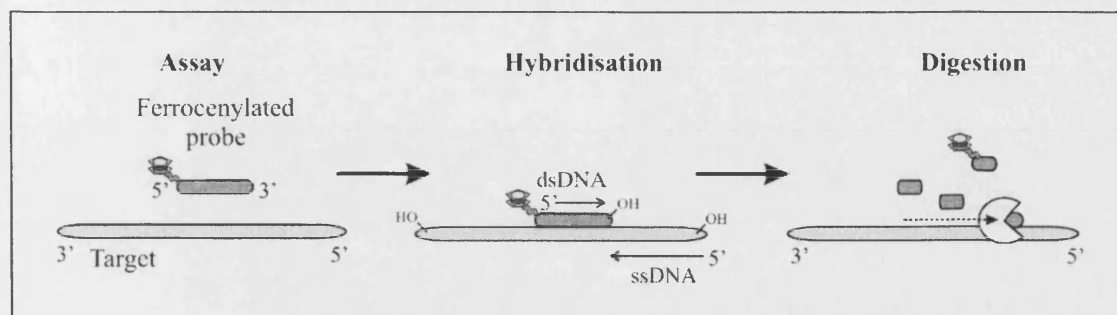
Figure 5.5 - T7 exonuclease: sensor application.
The ferrocenylated probe sequence (dark grey strand) and complementary target (light grey strand) in the assay hybridise to form a duplex. The synthetic target has a 5' hydroxyl group, whilst the probe has a 5' ferrocenylated linker molecule. The T7 exonuclease can attack at either 5' end, but will not attack the target sequence due to the section of ssDNA. It is hoped that the enzyme will tolerate the ferrocenylated label and attack the probe oligonucleotide, generating ferrocenylated fragments in the digestion step.

5.4.3 Taq polymerase

DNA polymerase has been introduced in biological DNA replication, in section 1.2.2, and in PCR, in section 2.2. The DNA polymerase most commonly used in PCR is obtained from the thermophilic bacterium *Thermus Aquaticus (Taq)* (Saiki et al. 1988).

The PCR assay contains the target sequence, ferrocenylated probe molecule, primer molecules, DNA polymerase enzyme, dNTP building blocks and buffer components. Under these conditions, both primer and probe anneal to the complementary target when the temperature is reduced, as shown in Figure 5.6. The DNA polymerase enzyme (Taq) then digests the probe whilst synthesising a new complementary strand (5' to 3' direction) from the primer. This produces the ferrocenylated digestion fragments.
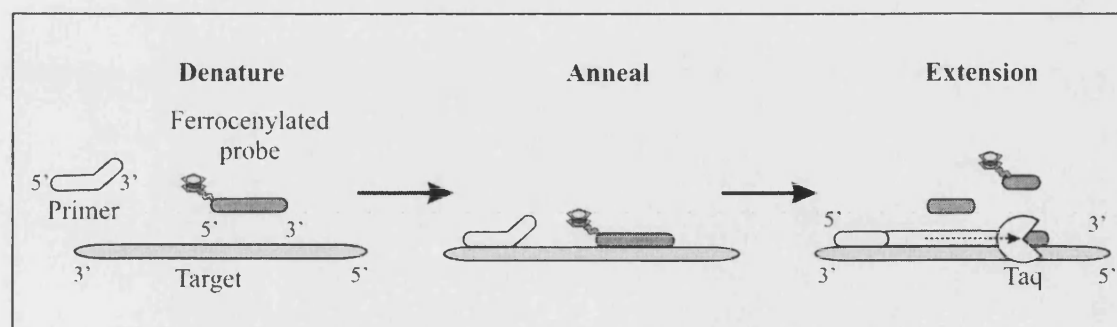
Figure 5.6 - Proposed electrochemical PCR probe.
The PCR cycle has been described earlier (Chapter 2). At the denature step (left hand side) the primer (white strand), target (light grey strand) and ferrocenylated probe (dark grey strand) are free in solution. Other components of the assay are not shown. On cooling the primer and probe anneal to complementary sections on the target oligonucleotide. In the extension stage (right hand side) the enzyme extends the complementary strand from the primer and digests the ferrocenylated probe, generating oligonucleotide fragments (short, dark grey strands; only two are shown) one of which contains the ferrocene label.

5.5 DNA hybridisation probe: gene sensor

The use of T7 exonuclease as a hybridisation sensor has been introduced in section 5.4.2. The use of this enzyme in a gene sensor is now detailed.

5.5.1 Electrochemical gene sensor detection

Gene sensor

The theory relating to the selectivity of the electrochemical DNA hybridisation gene sensors is now discussed. In the match assay where a ferrocenylated probe is used which is fully complementary to the target gene sequence, illustrated in Figure 5.7, the fully matched duplex will be stable and have a high melting temperature (Tm). In the mismatch assay where the target gene sequence is mutated (contains mismatched base pairs) the resultant duplex will be less stable, with a lower Tm. Under low stringency conditions only the fully matched probe and gene target will hybridise and therefore only this duplex will be digested by the T7 exonuclease. If the gene sequence is absent and the target sequence is completely mismatched, and low stringency conditions will be easy to obtain. Gene recognition (match) results in the generation of ferrocenylated oligonucleotide fragments, whilst no recognition (mismatch) results in no digestion of the probe oligonucleotide.
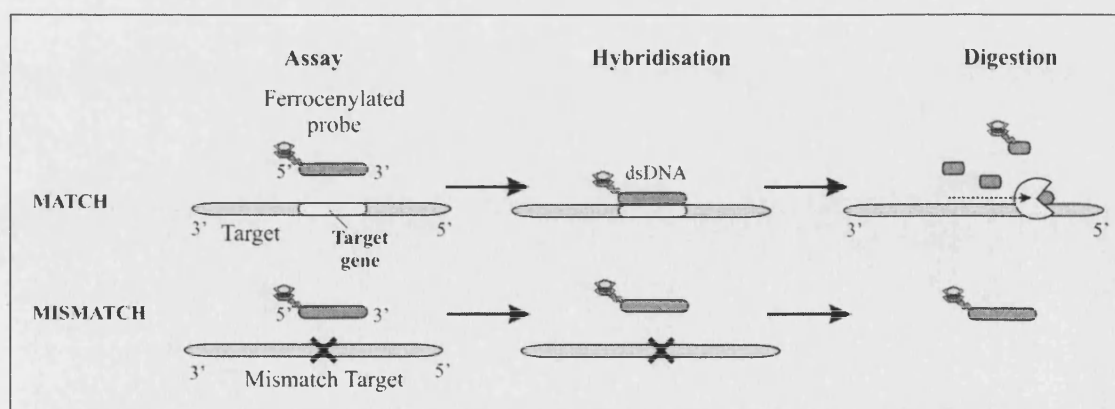
Figure 5.7 - T7 exonuclease: gene sensor.
Under low stringency conditions the matched target (Match assay), containing the target gene, will hybridise with the ferrocenylated probe oligonucleotide and T7 enzymatic digestion will occur. The mismatched target (Mismatch assay) will not hybridise with the probe and enzymatic digestion will not occur.

Electrochemical detection

DPV analysis is used to analyse the Match and Mismatch assays. It is proposed that the short digested oligonucleotide fragments will give a higher DPV differential peak current than the undigested oligonucleotides, as shown in Figure 5.8. This would allow discrimination to be obtained between the digested and undigested oligonucleotides and hence the matched and mismatched assays in the gene sensor. Such discrimination would allow gene sensing.
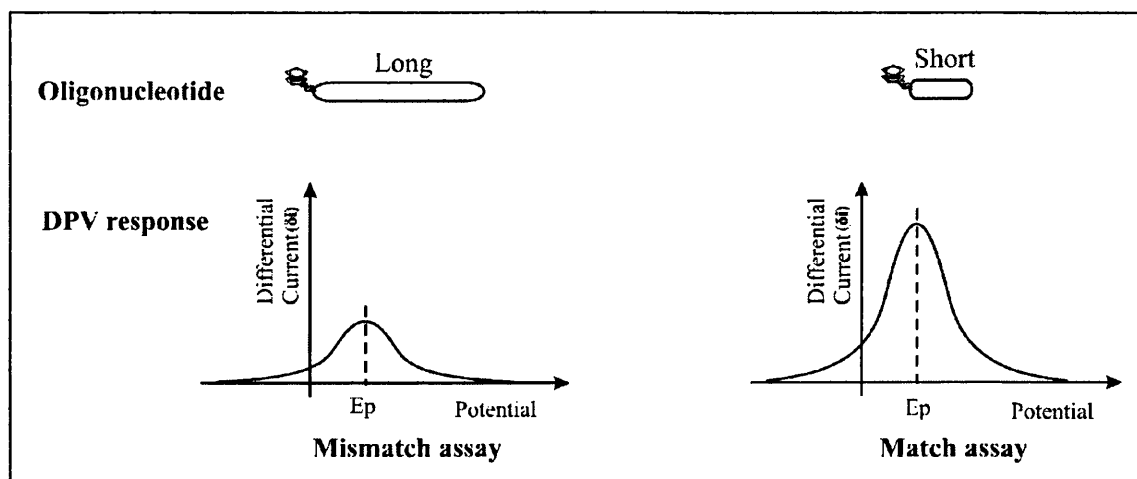
Figure 5.8 – Electrochemical detection of enzymatic digestion.
A long ferrocenylated oligonucleotide (left hand side) gives a low DPV response (low differential current at the electropotential, Ep). The DPV response increase when enzymatic digestion affords a shorter ferrocenylated oligonucleotide (right hand side). The size difference between the digested and undigested oligonucleotides is generally much bigger than illustrated.

It is suggested that discrimination in DPV response between the long (undigested) probe oligonucleotide and the short digested probe fragment would be primarily due to differences in diffusion coefficients (D, the rate at which a species diffuses through the solution) between the two species. It has been shown, in section 2.5.7, that in a diffusion controlled system the differential peak current (δi) is proportional to $D^{1/2}$. The smaller oligonucleotide fragment should have a larger D and diffuse more quickly to the electrode surface, hence its peak current should be higher than the undigested oligonucleotide.

Other, less well defined, factors may also improve the discrimination between the response of the digested and undigested ferrocenylated oligonucleotide. The

ferrocenylated label must be able to reach the electrode surface (or be close enough to the electrode surface that electron transfer can be readily mediated to it). If the much longer, undigested probe oligonucleotide adopts a coiled structure in solution, it could reduce access of the ferrocene label to the surface, as illustrated in Figure 5.9. Equally the electrode surface could be partially blocked through fouling by the components of the assay. This may affect the smaller ferrocenylated fragment significantly less than the undigested probe.
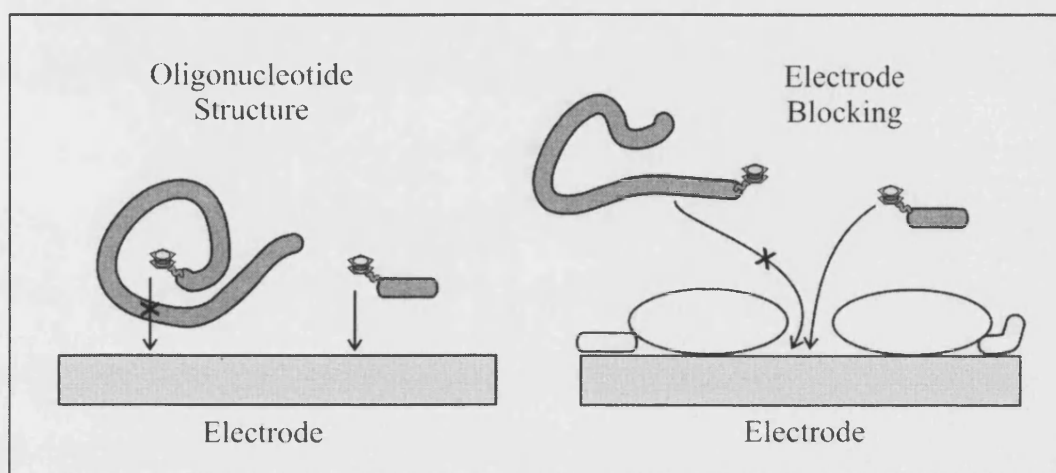
Figure 5.9 – Proposed discrimination at the electrode surface.
The structure of the undigested probe oligonucleotide could block the access of the ferrocene label to the electrode surface, whilst the digested fragment is unhindered (left hand side). Components of the assays such as the enzyme (white circle) or oligonucleotides, including oligonucleotide fragments (white strands) could block the electrode surface to the larger probe oligonucleotide (right hand side).

The electrodes could be surface modified to improve selectivity between the undigested and digested probe, which should also improve sensitivity. Surface modification was not proposed for this work to keep the system as straightforward and inexpensive as possible.

5.5.2 Gene sequence selection

The gene sequence studied and hence the complementary sequence used for the oligonucleotide probe, is not restricted by the T7 exonuclease as its digestion is not sequence specific.

223

A suitable gene sequence to study is the C282Y SNP mutation of the human haemochromatosis gene (HFE), which results in hereditary haemochromatosis (HH). This condition causes iron overload in parenchymal cells in critical organs including the liver, pancreas and heart and results in organ malfunction (Ugozzoli et al. 2002). This gene mutation is well characterised and has been studied using the fluorescent TaqMan® PCR approach (Ugozzoli et al. 2002) and with the successful electrochemical gene sensor developed by the CMS Motorola group (Umek, R. M. et al. 2000; Umek, R.M 2001), as described in section 1.9.3.

A small number of other oligonucleotides were used during the development of the gene sensor. These are summarised below and will be discussed where they are introduced. The sequence details are given in section 2.10.1.

ACTB gene (beta actin): BAPR probe sequence (Josefsson et al. 2000)

FVR4: oligonucleotide from Molecular Sensing PLC

CtrA gene (Meningococcal meningitis): CTR044 probe sequence (Guiver et al. 2000)

5.6   DNA hybridisation probe: PCR sensor

The action of the Taq polymerase enzyme in a PCR, described in section 5.4.3, produces ferrocenylated fragments as the reaction progresses. It is proposed that discrimination can be achieved between the undigested probe (gene not present, PCR amplicon not produced) and digested probe (gene present, PCR amplicon produced) for the same reasons as discussed in section 5.5.1. This should also allow the progress of a successful PCR to be followed *in situ.*

5.7   Detection issues

5.7.1   Enzyme buffer

All three enzymes (S1, T7 and Taq) are supplied with buffers which contain chloride (Cl^-) counter ions. This can potentially cause problems in the DPV analysis of the assays with gold electrodes.

Work by Pouradier (Pouradier et al. 1965) showed that insoluble metallic gold from the electrode can react to form both auric chloride ($Au^{III}Cl_4^-$) and aurous chloride ($Au^ICl_2^-$), which are soluble. This process is described with three reduction potentials in Figure 5.10.

$$
\begin{array}{llll}
 & & & E^{\ominus}\,(25\ ^{\circ}C) \\
E_{1\text{-}3} & Au^{III}Cl_4^- + 2e^- \longrightarrow Au^ICl_2^- + 2Cl^- & & 0.921 \\
E_{0\text{-}3} & Au^{III}Cl_4^- + 3e^- \longrightarrow Au^0 + 4Cl^- & & 0.995 \\
E_{0\text{-}1} & Au^ICl_2^- + e^- \longrightarrow Au^0 + 2Cl^- & & 1.418 \\
\end{array}
$$

Equilibrium

$$Au^{III}Cl_4^- + 2Au^0 + 2Cl^- \rightleftharpoons 3Au^ICl_2^- \quad K = 4 \times 10^8$$

Figure 5.10 – Gold chloride formation.
Gold chloride formation is described by three reduction potentials. $E_{1\text{-}3}$ signifies a reduction from Au^{III} (3) to Au^I (1). All three reduction potentials are in equilibrium and the overall equilibrium is also given (bottom).

Overall an equilibrium is established which lies strongly on the right, favouring metallic gold (Au^0) oxidation and solubilisation. This oxidation is only possible if auric chloride ($Au^{III}Cl_4^-$) and chloride ions are present. Under standard conditions the formation of auric chloride ($Au^{III}Cl_4^-$) from metallic gold ($E_{0\text{-}3}$) is not favoured as the reduction potential is positive.

However, a gold electrode in the electrochemical cell is not under standard conditions and a low applied potential at the start of a DPV oxidation trace, can allow metallic gold to be oxidised and solubilised. This can be rationalised if the Nernst equation, discussed in section 2.5.7, is considered for E_{0-3}, as shown in Equation 5.1.

$$Ep = Ep^{\theta} + \frac{RT}{nF} \ln \frac{[AuCl_4^-]}{[Au^0][Cl^-]^4} \qquad (5.1)$$

Nernst equation for E_{0-3}: Ep = electropotential, Ep^{θ} = standard potential, R = gas constant, T = temperature, n = the number of electrons exchanged = 3, F = Faraday constant, [x] = concentration of x.

As metallic gold Au^0 is a solid its concentration is considered to be very high and invariant. Initially the concentration of auric chloride $[AuCl_4^-]$ will be very low, approximately zero, as E_{0-3} favours the elemental gold Au^0. The electropotential (Ep) will therefore be dependent on the chloride ion concentration $[Cl^-]$, with higher concentrations of chloride ion reducing the electropotential ($\ln x$ is negative if $x < 1$). Once auric chloride ($Au^{III}Cl_4^-$) is produced it quickly (due to the equilibrium) reacts to form aurous chloride ($Au^ICl_2^-$), solubilising more gold. Depending on the surface concentrations of the aurous chloride ($Au^ICl_2^-$) and chloride ions it is possible that this species can be oxidised in the DPV trace (E_{1-3}) and potentially so can metallic gold (E_{0-3} and E_{0-1}).

These redox processes are important, since if they occur they will produce a detectable response with DPV, which will give a large background signal. Equally if the reaction occurs and gold is solubilised, this will roughen the electrode surface and increase the capacitive charging current which flows, see section 2.5.4. This will also increase the background signal and decrease the sensitivity of the DPV analysis.

5.7.2 Electrode choice

Three working electrodes are available: glassy carbon (GC, 3.0 mm diameter, BAS, UK); gold (Au, 1.6 mm diameter, BAS, UK) and boron doped diamond (BDD, 3.0 mm diameter, Windsor Scientific, UK). These have been introduced in section 2.5.8.

The different electrodes inherently have different surface characteristics and may give appreciably different responses for the same sample, for reasons that may not be clear without extensive further study. It is common practice to use different electrodes in exploratory work

Molecular Sensing (sponsoring CASE company) indicated a preference for the use of gold electrodes as these are easier to miniaturise and have better thermal stability in PCR buffer. However, exploratory work (not reported) showed that the DPV response for the electrode for several ferrocenylated species is proportional to its area and therefore the response of the larger GC electrode is higher.

5.8 Validation of results

The electrochemical gene sensor, described in section 5.5.1, is based on enzymatic digestion of ferrocenylated probe oligonucleotides, which is proposed to give a higher DPV response.

The simplicity of the DPV response (peak on a baseline) means that the origin of the peak must be confirmed. The peak can be generated in different ways:

- Ferrocene oxidation after the proposed enzymatic digestion mechanism.
- Ferrocene oxidation after an alternative or competitive mechanism.
- Experimental factors, including: electrode issues; equipment issues; buffer problems or impurities.

Whilst the experimental factors can be negated by good experimental practice, the validity of the DPV results must be confirmed by using complementary techniques to support the enzymatic digestion mechanism.

The enzymatic digestion can be supported by the use of fluorescence and gel electrophoresis experiments. The diffusion coefficients of the digested and undigested oligonucleotides can be determined using potential step amperometry.

5.8.1 Fluorescence

The work in this thesis aims to develop an electrochemical sensor based on established fluorescent sensors. It is therefore appropriate to use fluorescent sensors to validate the results obtained from the electrochemical sensor assays.

For the electrochemical assay the actual rate of enzyme activity towards the hybridised duplex is masked by the necessary requirement of the ferrocenylated oligonucleotide fragment to diffuse to the electrode and overcome any surface effects before it can be oxidised and detected. This is not the case for fluorescence, which can be measured in solution and therefore gives an insight into the absolute digestion.

Hybridisation probes

The well established fluorescent TaqMan® PCR probe technology, discussed in Chapter 3, uses a dual labelled fluorescent probe. Detection of the C282Y mutation has been studied by Ugozzoli (Ugozzoli et al. 2002). The same dual labelled probe can be used to follow T7 exonuclease digestion of the probe/target duplex as shown in Figure 5.11. As the T7 enzymatic digestion occurs the quencher and fluorophore become spatially separated, resulting in an increase in fluorescence.
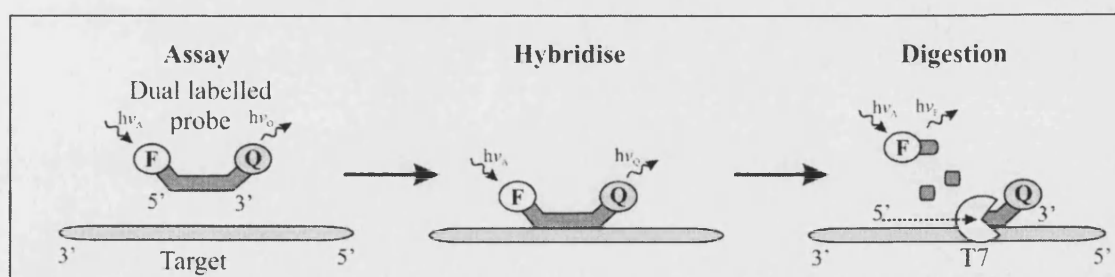
Figure 5.11 - Use of dual labelled probe to follow T7 exonuclease digestion.
The dual labelled probe (dark grey) has a fluorophore (F) and quencher (Q) at separate ends. The F and Q of the dual labelled probe are close enough together for FRET quenching to occur (see section 2.6.2) and the fluorescence of F is quenched. The probe hybridises to a complementary sequence on the target oligonucleotide (light grey strand). The T7 exonuclease enzyme (white circle) digests the probe oligonucleotide in the 5' to 3' direction (direction of dotted arrow), generating oligonucleotide fragments (short, dark grey strands) and separating F and Q. As F and Q are no longer covalently joined and can move apart. F is no longer quenched by Q and its fluorescence is detected. Hence the hybridisation event is detected.

The dual labelled probe was commercially labelled (Sigma Genosys, UK) 5' with the fluorophore 6-FAM (6-carboxy fluorescein) and 3' labelled with the quencher 6-TAMRA (6-carboxytetramethylrhodamine), as shown in Figure 5.12.
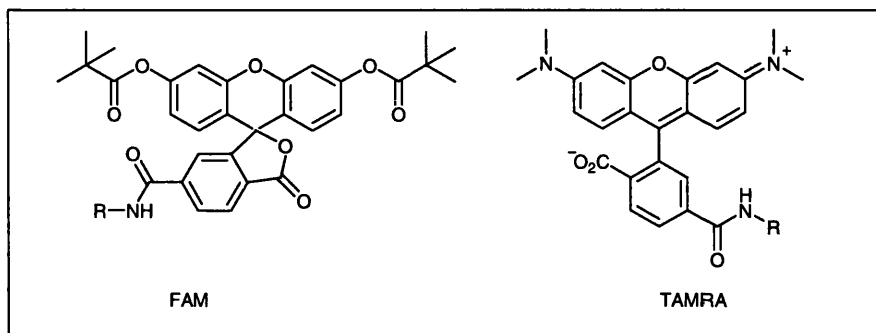
Figure 5.12 - FAM and TAMRA fluorescent labels.
The dual labelled probe is 5' labelled with 6-FAM and 3' labelled with 6-TAMRA. R = a C6 linker to the oligonucleotide. The fluorophore 6-FAM is excited at 494 nm and without quenching emits at 525 nm.

The fluorescent measurements were made on a Roche LightCycler, introduced in section 2.6.2.

5.8.2 Gel electrophoresis

Gel electrophoresis is a technique, described in section 2.3, which has the ability to separate DNA sequences by size and then to quantify the length of these sequences (Alberts et al. 1994; Brown 1995a). This technique, shown in Figure 5.13, can therefore be used to follow enzymatic digestion of the relatively large probe oligonucleotide, which generates much smaller digested fragments.
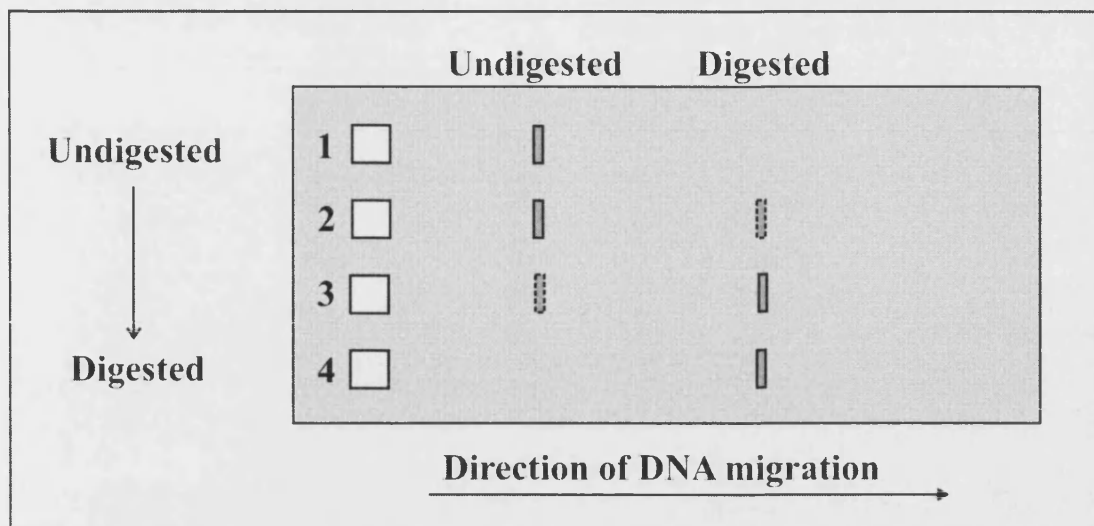
Figure 5.13 - Determination of enzymatic digestion with gel electrophoresis.
Smaller DNA oligonucleotides migrate more rapidly through the gel (left to right). An enzymatic digestion is sampled 4 times, from the beginning (well 1) to the end (well 4). The undigested oligonucleotide (well 1) is relatively large and will run relatively slowly in the gel (band is visualised on left hand side). As enzymatic digestion occurs (wells 2, 3 and 4) much smaller oligonucleotide fragments are generated, which run quickly in the gel (band is visualised on right hand side). As the digested fragments are very small, the visualisation of the digested band may be difficult as the DNA binding dye may have a poor affinity to them.

The technique is also routinely used to determine if a PCR has been successful.

5.8.3 Determination of diffusion coefficient

It has been proposed, in section 5.5.1, that the small (digested) ferrocenylated probe oligonucleotide fragments have larger diffusion coefficients (D) than the larger (undigested) ferrocenylated probe oligonucleotides and this may allow discrimination between the two assays on DPV analysis. This proposal must be validated by determining the diffusion coefficients for the digested and undigested oligonucleotides, for both the T7 and S1 assays.

To accurately determine the diffusion coefficients for any species, the initial concentration of the labelled oligonucleotide must be accurately known. For the post-labelled work the efficiency of the labelling and hence the concentration can vary, therefore only the calculation of relative results would be possible. The phosphoramidite labelling method is more efficient and coupled with HPLC purification gives as high as possible guarantee of probe concentration. This will allow the accurate determination of absolute diffusion coefficients.

The diffusion coefficients will be determined using potential step amperometry which is introduced in section 2.5.5. This technique has high sensitivity and can be used in the low volume cell with a static electrode (Bard et al. 2001). The potential step and resultant current are summarised below in Figure 5.14.
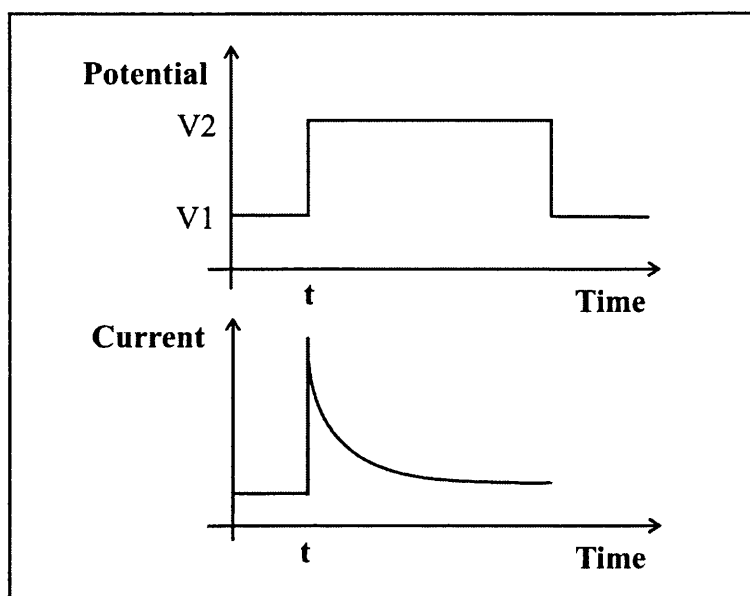
Figure 5.14 – Summary: potential step amperometry.
The potential step (top graph) and resultant current flow (bottom graph) are shown. This is a reproduction of Figure 2.15.

The voltages used in the potential step (V1 and V2, Figure 5.14) are chosen, which are either side of the DPV peak. At V1 all the ferrocenylated species is reduced and at V2 it is all oxidised.

When the potential step is applied to a solution under diffusion control an observed current will flow, which is the combination of the capacitive charging current and Faradaic current, see section 2.5.5. After a short time delay the measured current will be entirely due to the Faradaic current, as illustrated in Figure 5.15.
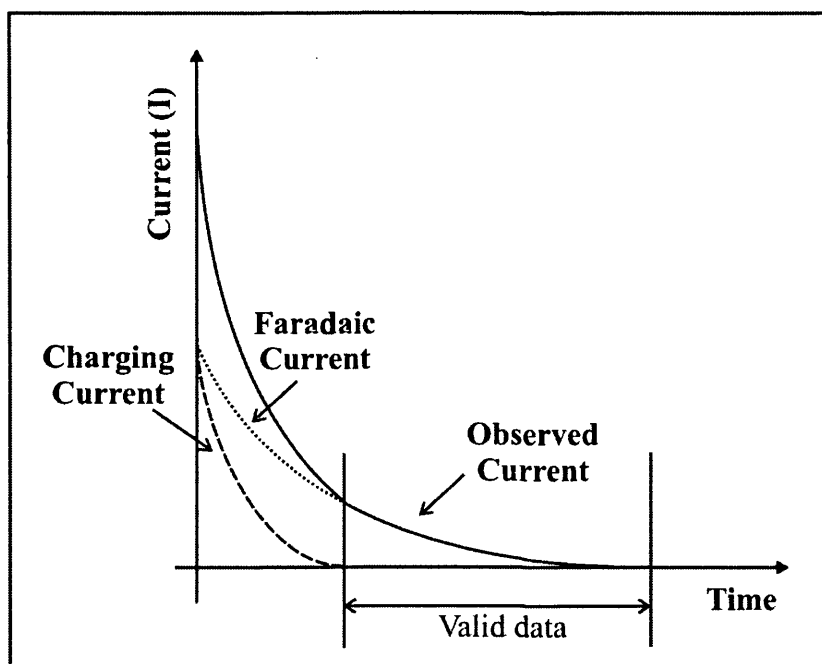
Figure 5.15 – Potential step amperometry.
The figure shows the observed current (full line) which is generated after the potential pulse. This is a combination of the charging current (dashed line) and Faradaic current (dotted line). After a time delay the charging current has decayed to zero, leaving only the Faradaic current. The valid data for the determination of the diffusion coefficient is indicated.

The diffusion coefficient can therefore be determined by using the data for the Faradaic current, shown as "valid data" in Figure 5.15. The Faradaic current decays according to Equation 5.2, the Cottrell equation.

$$|i| = \frac{nFA\sqrt{D}C_\infty}{\sqrt{\pi.t}}$$

(5.2)

Cottrell Equation: i = current, n = number of electrons transferred in redox couple, F = Faraday constant, A = electrode area, D = diffusion coefficient, C_∞ = bulk concentration of reactant and t = time.

Rearrangement of the Cottrell equation, given in Equation 5.3 and then Equation 5.4, shows that a graph of $|1/i|^2$ against t will allow D to be determined from the gradient.

$$|1/i|^2 = \frac{\pi.t}{(nFAC_\infty)^2 D}$$

(5.3)

$$D = \frac{\pi}{(nFAC_\infty)^2 .gradient}$$

(5.4)

As the time taken for the charging current to decay to zero is unknown and must be estimated, it is also possible to obtain the valid data for the Faradaic current, by running a buffer trace containing the enzyme (totally charging current) and subtracting this from the observed current, shown as the full line in Figure 5.15.

Practical considerations

DPV traces should be run before each amperometry measurement. This ensures that the electropotential is well known, so that the step parameters can be chosen accordingly. The step should be as small as possible to limit the charging current, but must encompass the entire DPV peak to ensure that the entire ferrocene label is oxidised. A good peak shape indicates that the electrode is working well and that the results can be trusted.

To measure the true diffusion coefficient of a species, you require a clean electrode, which is not affected by fouling (i.e. there is no physical barrier to any of the electroactive species which are moving toward the electrode to be oxidised). As discussed before assays containing other components (oligonucleotide and enzyme) will foul the electrode and this may influence the amperometry measurements. However, although this is unavoidable it may actually be beneficial as it could give insights into the condition of the electrode surface. The GC electrode, used for most of the DPV, would therefore be ideally used for the amperometry measurements.

5.9   Summary: experimental plan

The experimental plan is intended to:

- Clearly and concisely describe the experimental work in Chapter 6, using specific detail, and give the rationale behind choices which were made.

- Give clarity to the structure of Chapter 6 and to be a reference point for it.

The overall plan is described in section 5.9.1, after which the component parts are described in more detail. Bullet points throughout this section give experiment results which must have been obtained before the next stage in the development can be undertaken.

5.9.1   Introduction

The work detailed here describes the development of the DNA hybridisation probes and their validation. The mode of action of the enzymes involved is studied as the work progresses.

Oligonucleotide labelling

The focus of the synthetic work described in Chapter 3 is on the synthesis of novel ferrocenylated linker molecules, for post-labelling oligonucleotides through Takenaka's labelling protocol. The probe oligonucleotides for this work are post-labelled with the ferrocenylated linker molecule, *ester* **70**. The effectiveness of this labelling is evaluated through S1 endonuclease digestion, as discussed in section 5.3.3. Oligonucleotides are commercially labelled with the *phosphoramidite* **28** label in later work.

Assay development

The experimental work involves a progressive series of work towards electrochemical hybridisation gene sensors for PCR products. The progression of the work is

undertaken to allow technical and sensitivity issues to be highlighted and overcome. If successful the work can be applied to *in situ* PCR probes. The work is summarised below, in Figure 5.16.
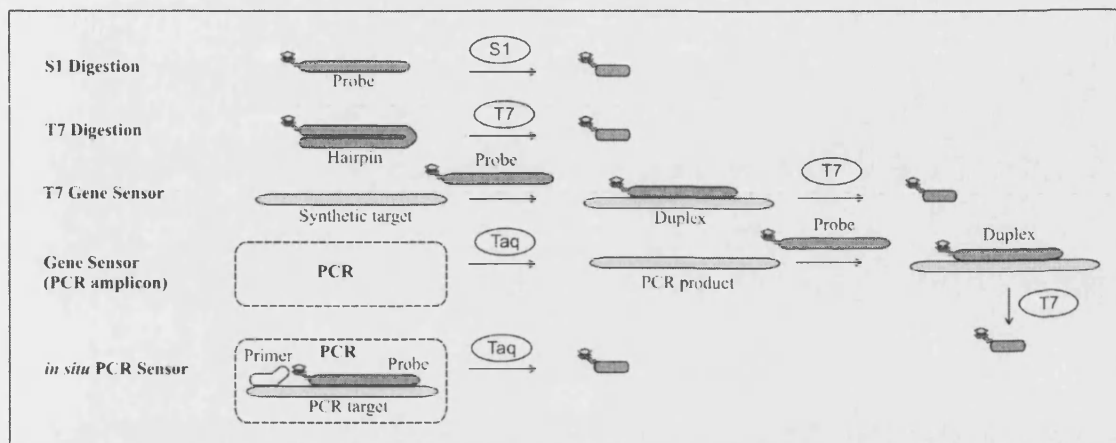
Figure 5.16 – DNA hybridisation probes: work plan.
There are five stages to the work plan which will be discussed in sequence. Each stage produces a short ferrocenylated fragment (short, dark grey strand). S1 digestion: the ferrocene labelled probe (long, dark grey strand) is digested by the S1 enzyme (white circle) to produce the fragment. T7 digestion: the ferrocene labelled hairpin oligonucleotide (folded, dark grey strand) in digested by the T7 enzyme (white circle) to produce the fragment. T7 gene sensor: the ferrocene labelled probe oligonucleotide hybridises with a synthetic target (light grey strand) to form a duplex. This is then digested by the T7 enzyme, as above. Gene sensor (PCR amplification): the PCR reaction uses the Taq enzyme to synthesise the desired PCR product (light grey strand). The product hybridised with the ferrocenylated probe (dark grey strand) to form a duplex, which is digested by the T7 enzyme, as above. *In situ* PCR sensor: the PCR reaction, see section 2.2, includes primer (white strand) PCR target (light grey strand) and ferrocenylated probe (dark grey strand). On the extension step all the probe and primer are annealed to the target. The Taq enzyme digests the probe on the synthesis of the complementary strand (not shown), generating the ferrocenylated fragment. In all approaches other (unlabelled) oligonucleotide fragments are produced on digestion, but these are not shown.

Digesting a labelled oligonucleotide with the ssDNA specific S1 endonuclease enzyme allows the level of discrimination between the DPV response for the digested and undigested labelled oligonucleotides, to be determined. Labelling a hairpin oligonucleotide and digesting it with the dsDNA specific T7 exonuclease enzyme, allows the effectiveness of this enzyme to be determined, without having to consider hybridisation. The T7 exonuclease is then used with a hybridisation product (duplex), which is formed from a probe and a synthetic target. This is repeated using a target (amplicon) produced by PCR and also *in situ* in a PCR. In the PCR the Taq enzyme does the digestion. Throughout the work, the analysis gives an insight into the mode of action of the enzymes used.

5.9.2   S1 digestion

The work is based on the digestion of probe oligonucleotides by S1 endonuclease, shown in Figure 5.17. The actual sequence of the oligonucleotide used does not matter as the S1 nuclease is non-specific. The oligonucleotide used was BAPR (beta actin, probe).
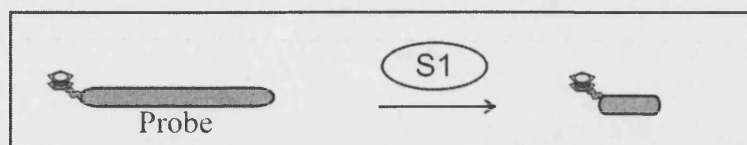
Figure 5.17 – Summary: S1 digestion.

Oligonucleotide labelling and evaluation

The BAPR oligonucleotide is post-labelled with the *ester* **70**, which is described in Figure 5.18.

5'-Fc-Linker-ATGCCCTCCCCCATGCCA TCCTGCGT-3' (BAPR) **79**
5'-Fc-Linker-ATATACGTGCCAGGTGGA-3' (C282Y) **80**
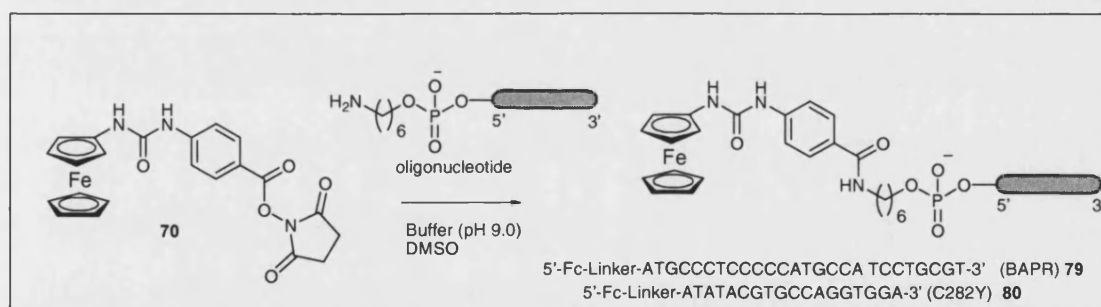
Figure 5.18 - Oligonucleotide labelling.
The probe oligonucleotide (grey strand) is labelled with *ester* 70, producing a ferrocenylated BAPR probe oligonucleotide 79.   The C282Y sequence is labelled for later work, producing a ferrocenylated BAPR probe oligonucleotide 80.

The labelling is evaluated by subjecting the labelled probe to digestion by S1 endonuclease, shown in Figure 5.17.   The labelling is considered successful if discrimination is obtained between the probe oligonucleotide and the digested fragments, illustrated in Figure 5.19.   The DPV measurements are taken when the enzymatic digestion had gone to completion (after incubation for 1 hour) for a Digest assay and a Control assay, which omits the enzyme. This is described as end-point analysis.
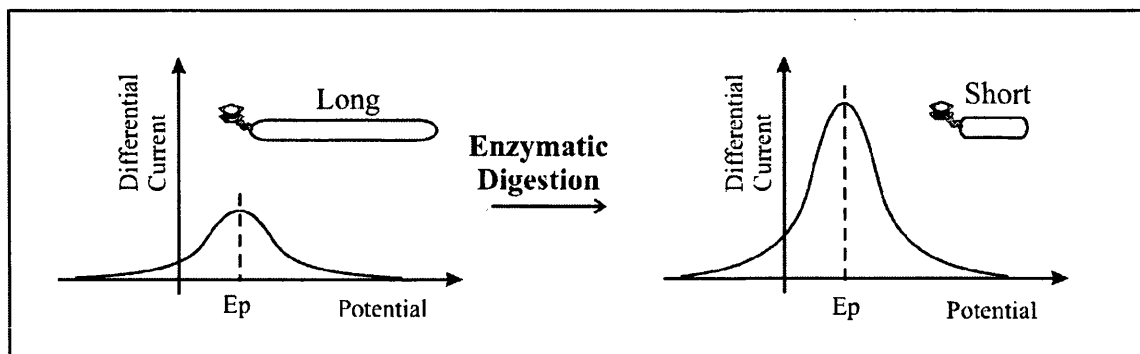
Figure 5.19 – Evaluation of labelling.
The labelling is considered successful if the DPV response of the undigested probe oligonucleotide (left hand side) increases significantly after enzymatic digestion (right hand side).

The buffer solution supplied with the S1 enzyme contained a high concentration of chloride ions (sodium chloride) which causes problems with the DPV baseline when used with gold electrodes, presumably due to the formation of gold chloride species, detailed in section 5.7.1. A replacement, acetate based, buffer had been shown to work effectively for S1 digestion (Braven 2002) and was adopted for this work.

S1 time-course

Taking consecutive DPV measurements allows the progress of the S1 digestion to be followed. This is described as time-course analysis. The results of the time-course analysis are compared with those obtained from gel electrophoresis, see section 5.8.2, to determine if the DPV results are supported. This real-time analysis of enzymatic digestion is very important as it is integral to *in situ* PCR analysis.

Electrode fouling

The effect of electrode fouling on the electrochemical response in the time-course analysis is assessed by repeating the time-course analysis, whilst washing the electrode with MilliQ deionised water before every measurement.

5.9.3 T7 exonuclease work

- Discrimination must have been achieved between the DPV responses of the digested and undigested ssDNA in the S1 endonuclease work.

It is expected that comparable results can be obtained for the digestion of dsDNA with the T7 enzyme. As the fouling of the electrode surface is thought to have a prominent role in the selectivity and sensitivity of the system, the working electrodes of different materials (gold and glassy carbon) are evaluated.

The T7 digestion work is undertaken in three sections: hairpin assay; hybridisation assay and PCR end-point assay.

5.9.4 T7 hairpin assay

Although the hybridisation between fully complementary probe and target oligonucleotide should be straightforward, initial studies are undertaken using a labelled hairpin oligonucleotide, which is self complementary and therefore allows the controlled study of the action of a double strand specific enzyme, without the uncertainty of efficient hybridisation (Figure 5.20).
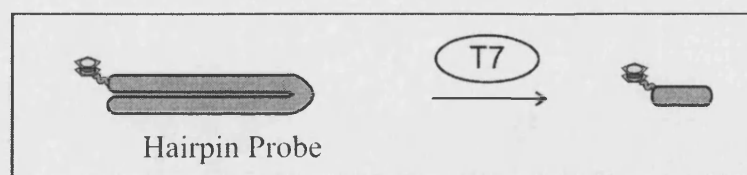
Figure 5.20 - Summary: T7 hairpin digestion.

Oligonucleotide labelling and evaluation

The C282Y hairpin oligonucleotide is post-labelled with *ester* **70**, following the protocol of Takenaka (Takenaka et al. 1994), see section 3.2.2. The labelling is summarised below, in Figure 5.21.
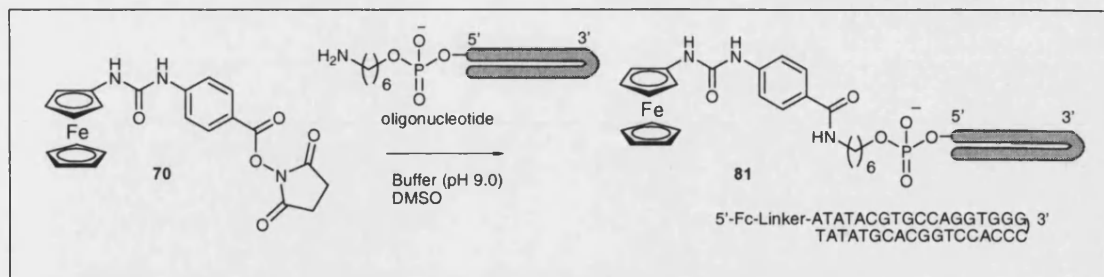
Figure 5.21 - Oligonucleotide labelling.
The probe oligonucleotide (grey strand) is labelled with *ester* 70, producing a ferrocenylated C282Y hairpin probe oligonucleotide 81.

The labelled *oligonucleotide* **81** is subjected to T7 exonuclease digestion. If discrimination is obtained between the digested and undigested hairpin oligonucleotides, then both the labelling and the T7 digestion of dsDNA are shown to be successful.

The glassy carbon (GC) and gold (Au) electrodes are compared and contrasted in this work to determine which is most effective for the hybridisation work.

T7 time-course

Taking consecutive DPV measurements allows the progress of the T7 digestion to be followed. This is described as time-course analysis.

The glassy carbon (GC) and gold (Au) electrodes are compared and contrasted in this work to determine which is most effective for the future hybridisation work.

5.9.5 T7 Hybridisation Assay: gene sensor

- T7 exonuclease must have been shown to effectively digest dsDNA.

The development of the DNA hybridisation gene sensor, detailed below in Figure 5.22, is undertaken.
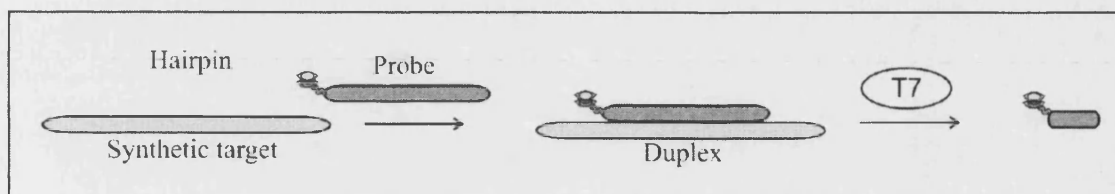
Figure 5.22 - Summary: T7 hybridisation probe.

Exploratory work

In a mimic of gene sensing the C282Y probe oligonucleotide (18 bp) is labelled with *ester* **70** and hybridised with a larger 60 bp target (C282YST). This is a custom synthesised oligonucleotide (ST: Synthetic Target), with the same sequence as the amplicon which would be produced by the PCR reaction (Ugozzoli et al. 2002). After hybridisation (25 °C) the duplex is subjected to T7 exonuclease digestion (37 °C) and the end-point response is measured by DPV. The probe has a Tm of 59 °C (under standard conditions, see Chapter 2) and therefore will readily hybridise at 25 °C and will remain hybridised at 37 °C. Three control assays will be used: Complementary Control (complementary target, no enzyme); Mismatched Digest (mismatched target sequence, with enzyme) and Mismatched Control (mismatched target sequence, without enzyme).

Determination of reproducibility

The reproducibility of the work is considered. If problems are encountered with reproducibility all aspects of the assay and analytical system, particularly the electrode and oligonucleotide labelling are addressed. Oligonucleotide labelling is a critical issue and improved labelling efficiency can be achieved by using phosphoramidite labelling. The labelling efficiency of any probe oligonucleotide is evaluated, as above, by the use of S1 endonuclease digestion, using the two different electrodes and different

phosphoramidite labels are evaluated. If the phosphoramidite labelling is shown to be effective, the labelled oligonucleotide is then used as a hybridisation gene sensor.

Hybridisation time course: digestion of duplex DNA

To better understand the enzymatic digestion of the duplex in a successful, reproducible, hybridisation gene sensor, this digestion is analysed with time-course analysis, whereby consecutive DPV traces are taken during the enzymatic digestion.

Further gene sensing

If the hybridisation gene sensor is shown to be effective with the C282Y probe (Human hemochromatosis gene) it can then be used to interrogate further gene sequences: BAPR (beta actin); CTR044 (meningococcal meningitis) and MC11 (medium chain acyl-CoA dehydrogenase).

5.9.6 Validating the gene sensor work

The DNA hybridisation gene sensor is based on enzymatic digestion of the complementary duplex. This enzymatic digestion is corroborated by using complementary analysis using a dual labelled fluorescent probe and fluorescent detection (section 5.8.1). Differences in the diffusion coefficients of digested and undigested probe sequences are thought to be one of the major factors behind the electrochemical discrimination between these assays. The diffusion coefficients are measured and quantified for both S1 and T7 enzymatic digestion.

Fluorescent analysis: enzymatic digestion

The enzyme digestion is followed using a dual labelled fluorescent probe (5' 6-FAM labelled and 3' 6-TAMRA labelled), with the C282Y sequence. The theory behind this approach has been introduced, in section 5.8.1, and is summarised below in Figure 5.23. The enzymatic digestion will is followed using a Roche LightCycler.
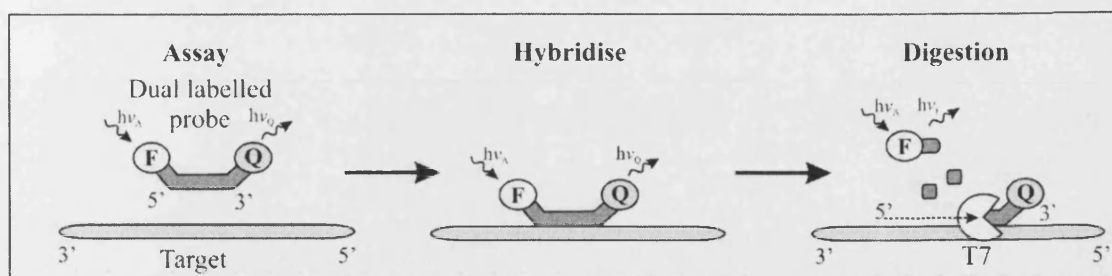
Figure 5.23 – Summary: use of dual labelled probe to follow T7 exonuclease digestion.

Determination of diffusion coefficients.

Potential step amperometry, described in section 5.8.3, is used to measure the diffusion coefficients of the ferrocenylated probe assays. For the diffusion coefficient work to be valid there must be a significant difference between the response of the assay sample and a buffer control.

Exploratory work is done both with GC and BDD electrodes to determine which gives the best discrimination between the amperometry traces for the Digest and Control assays. These use the *phosphoramidite* **28** labelled C282Y oligonucleotide **78** for S1 endonuclease digestion and the fully complementary hybridisation duplex for T7 exonuclease digestion.

The diffusion coefficient for the ferrocenylated species in the S1 assay (Digest and Control) will then be determined by measuring potential step amperometry traces for the Digest, Control and buffer assays. This is initially undertaken with the C282Y oligonucleotide. If successful the alternative BAPR and CTR oligonucleotides are used in comparable assays.

The diffusion coefficients for the ferrocenylated species in the T7 assays (Digest and Control) are determined for assays containing C282Y, BAPR and CTR probe oligonucleotides. The following amidite probes are used; mono ferrocenylated C282Y and diferrocenylated BAPR and CTR044. The dual ferrocene moiety in the BAPR and CTR044 labels should be emphasised, as the two electron transfers must be accounted for in the diffusion coefficient calculations.

242

5.9.7 PCR end point detection

- After the T7 exonuclease based gene sensor, must have been shown to effective with synthetic oligonucleotide target sequences.

The sensor can be used with PCR amplicons, detailed below in Figure 5.24.
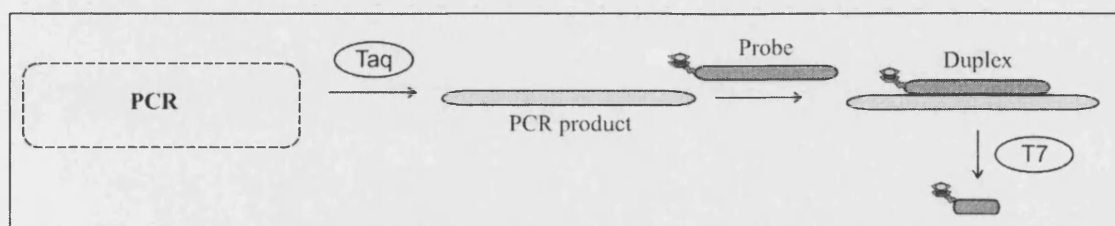
Figure 5.24 – Summary: PCR end point analysis
The PCR (described in section 2.2) synthesises a PCR product which is a complementary target for the probe oligonucleotide.

Gene sensing with PCR amplicons

In this work the target sequence is amplified by PCR, through the selection of the appropriate primers. The PCR amplicon is then heated (to denature it) in the presence of the ferrocenylated oligonucleotide probe. On cooling the probe will form a duplex with the ssDNA amplicon and this duplex can be digested with the T7 exonuclease , as shown in Figure 5.25. The beta actin gene is amplified from human genomic DNA, using primers developed by Josefsson (Josefsson et al. 2000). The amplicon is then interrogated by the post-labelled BAPR probe oligonucleotide **79.**
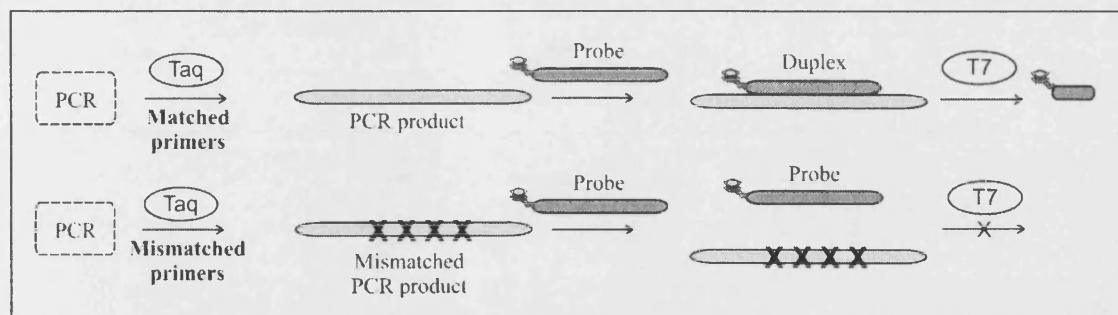
Figure 5.25 - End-point PCR analysis.

PCR was performed on 100 μL scale to amplify the beta actin gene from human genomic DNA. Using matched primers (top scheme), developed by Josefsson (Josefsson et al. 2000), a matched PCR product (light grey strand) is synthesised. After the PCR was completed, the BAPR probe oligonucleotide 79 (dark grey strand) is then added to the assay and hybridises to the amplicon. This can then be digested with T7 exonuclease (1 hour, 37 °C) to generate small ferrocenylated fragment. Using mismatched primers for the ACADM (medium chain acyl-CoA dehydrogenase) gene (Fujii et al. 2000), and fully mismatched amplicon (light grey strand, X mismatches) is synthesised (bottom scheme) which doesn't hybridise with the ferrocenylated probe. The probe is therefore not digested by the T7 exonuclease.

5.9.8 *In situ* PCR analysis

- The PCR end point analysis must have been successful.

The technology can be applied to *in situ* PCR detection, as shown in Figure 5.26.
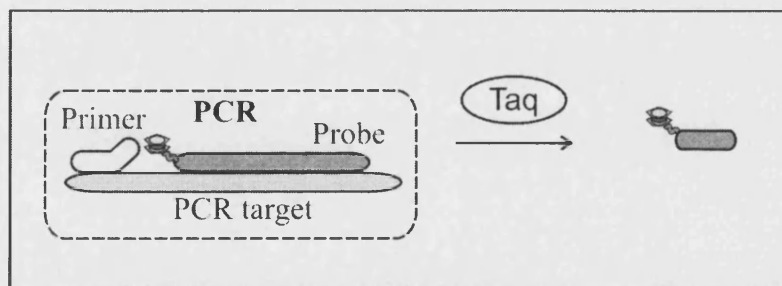
Figure 5.26 - Summary: PCR *in situ* analysis.

Chapter 6: Results

Development of an electrochemical DNA hybridisation gene sensor

6 Results: Development of an electrochemical DNA hybridisation gene sensor

6.1 Introduction

This chapter reports the experimental results for the development of electrochemical DNA hybridisation gene sensors.

Enzymatic digestion of the C282Y ferrocenylated probe with S1 endonuclease is analysed by electrochemical detection (DPV) to determine if this digestion can be followed. The digestion of a hairpin dsDNA ferrocenylated oligonucleotide, with a dsDNA specific enzyme, T7 exonuclease, is then undertaken to determine if electrochemical detection (DPV) allows the digestion of duplex DNA to also be followed. The original ferrocenylated probe can then be used as a hybridisation gene sensor, with a gene target. To address reproducibility issues, phosphoramidite labelling of the probe oligonucleotide is also be used. To determine the effectiveness of the sensor system, sensor work is undertaken with different gene sequences and with different electrodes. The DPV results are validated by the use of a complementary fluorescent approach, using dual labelled probes, and by the measurement of diffusion coefficients for the probe oligonucleotide, before and after digestion. After the work with synthetic gene targets, the gene sensor is then used with PCR products. Potentially this approach could be applied to *in situ* PCR analysis.

The general detail for the experimental work is given in Chapter 2, including the electrochemical cell set-up in section 2.5.8 and the oligonucleotide sequences in section 2.10.1. The specific details concerning DPV analysis, oligonucleotide labelling and biological assays are given as Protocols in section 2.10.2. The theory concerning enzymatic digestion is given in section 5.4.

6.2 Development of S1 work

Oligonucleotide labelling is undertaken and its success is determined by subjecting the oligonucleotide to S1 endonuclease digestion: if discrimination between the digested and undigested oligonucleotide is possible, then the labelling (and the detection technique, DPV) is considered successful. The progression of the S1 enzymatic digestion over time is then analysed in more detail using a time-course measurement. This allows the mode of enzymatic digestion to be corroborated, by gel electrophoresis, and the effect of fouling on the electrode to be examined.

6.2.1 Oligonucleotide labelling

The BAPR oligonucleotide is post-labelled with *ester* **70** following the method of Takenaka (Takenaka et al. 1994) detailed in section 3.2.2. The labelling is summarised below in Figure 6.1) and full details are given in section 2.10.2, Protocol 2.
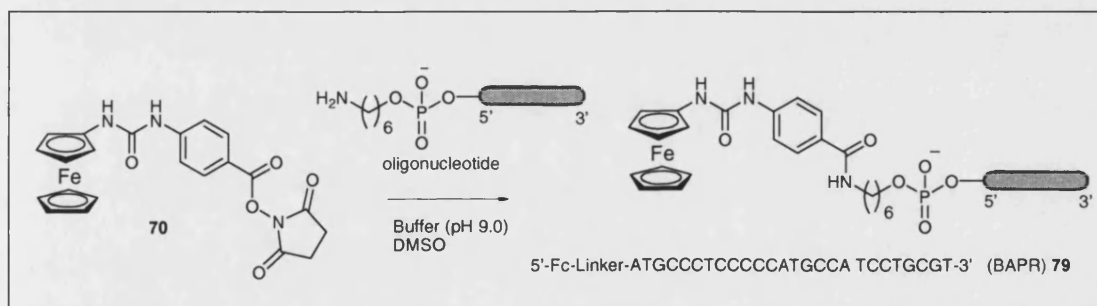
Figure 6.1 - Oligonucleotide labelling.
The probe oligonucleotide (grey strand) was custom synthesised (Sigma Genosys) with a free amine group attached to the 5' end via a C6 alkyl chain. It is labelled with the *ester* 70, producing a ferrocenylated BAPR probe oligonucleotide 79.

6.2.2 S1 digestion

After labelling, the ferrocenylated BAPR oligonucleotide **79** was subjected to S1 digestion.

The S1 nuclease digestion is detailed in section 2.10.2, Protocol 3. The Digest sample contained the oligonucleotide and enzyme, whilst the Control sample omitted the

enzyme. The samples were incubated at 37 °C for 1 hour, after which DPV measurements of both the assays were made, also at 37 °C. The standard BAS low volume electrochemical cell was used with a glassy carbon working electrode, as this afforded the best results. The acetate buffer was retained for consistency.

The DPV traces, given in Figure 6.2, show that there is a reasonable (50%) increase in ferrocene oxidation current, between the undigested oligonucleotide (Control assay) and the oligonucleotide after enzymatic digestion (Digest assay). The discrimination between the peak areas is better, with a 70% increase on digestion.
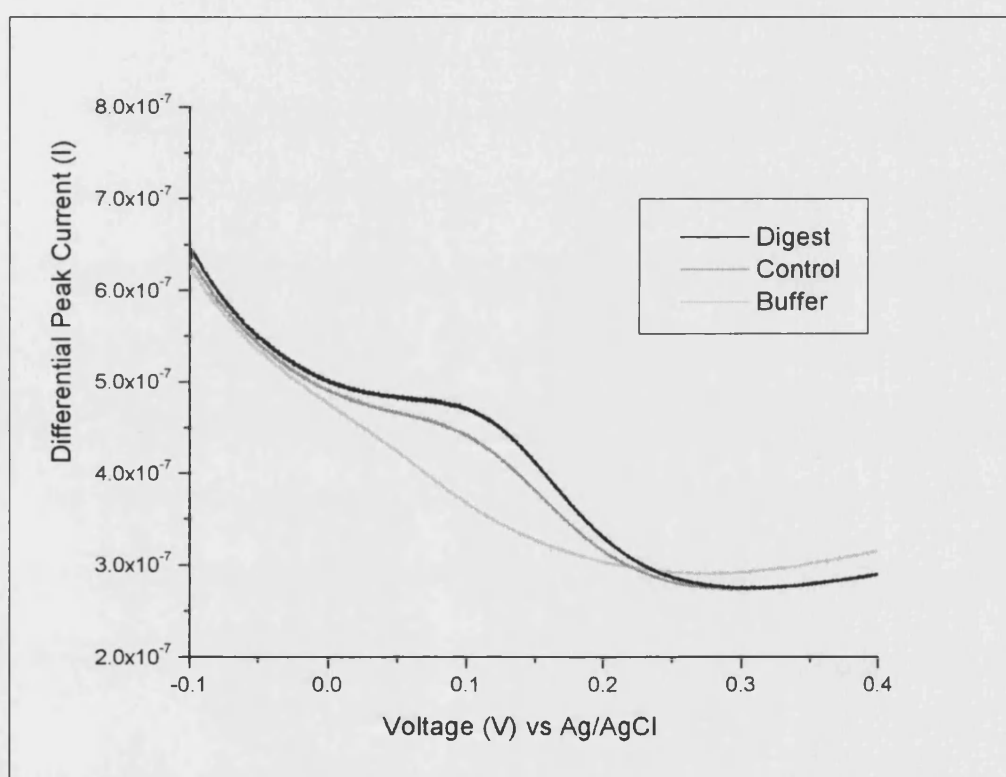
Figure 6.2- S1 Digestion of ferrocenylated BAPR oligonucleotide 79.
The Digest assay was run with 5 µM oligonucleotide, 0.25 U / µL S1 nuclease and a buffer consisting of 0.25 M ammonium acetate and 4.5 mM zinc acetate dihydrate (pH = 6.5). The Control assay omitted the enzyme. The assays were analysed by DPV after digestion (1hr / 37 °C). The Digest assay (black line, top) has a 50% higher differential peak current than the Control assay (grey line, middle). A DPV trace of the buffer (light grey line, bottom) shows no peak.

For ease of interpretation this, and all future graphs, will be reported after the baseline has been smoothed using the "moving average" baseline correction feature on the Autolab software. This correction technique is described in section 2.5.7 and the graph is given in Figure 6.3.
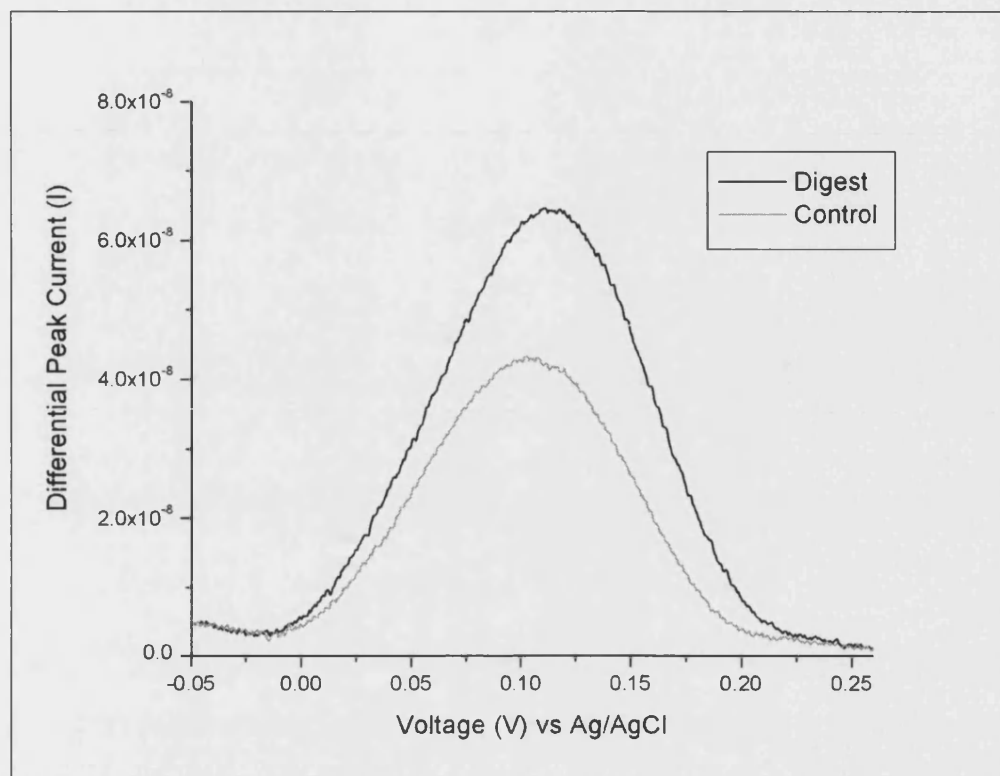
Figure 6.3 - S1 Digestion graph after baseline correction.
The S1 digest graph, shown in Figure 6.2, was subjected to "moving average" baseline correction. The Digest (black line, top) and Control (grey line, bottom) DPV traces are shown.

The difference in the electrochemical response (discrimination) between the labelled oligonucleotide before and after enzymatic digestion (Figure 6.3) is attributed to both differences in the diffusion coefficient of the free probe compared to the labelled oligonucleotide and the possibility that the response of the larger, undigested oligonucleotide can be reduced if the conformation it adopts in solution blocks access of the ferrocene label to the electrode.

The labelling of the BAPR probe has been successful, but the actual labelling efficiency is not known. To avoid issues arising from differences in labelling efficiency, future experiments should be done with the same batch of oligonucleotide, so that the results are relative and can be directly compared.

The success of all future oligonucleotide labelling experiments will be determined by subjecting each newly labelled batch to S1 enzymatic digestion.

6.2.3 S1 time-course

Consecutive DPV measurements during the course of the S1 enzymatic digestion allows real-time electrochemical analysis of the digestion. These measurements were taken approximately every 8 minutes up to 90 minutes and are reported in Figure 6.4. Repeating the experiment using automated measurements, every 3 minutes, gave comparable results.
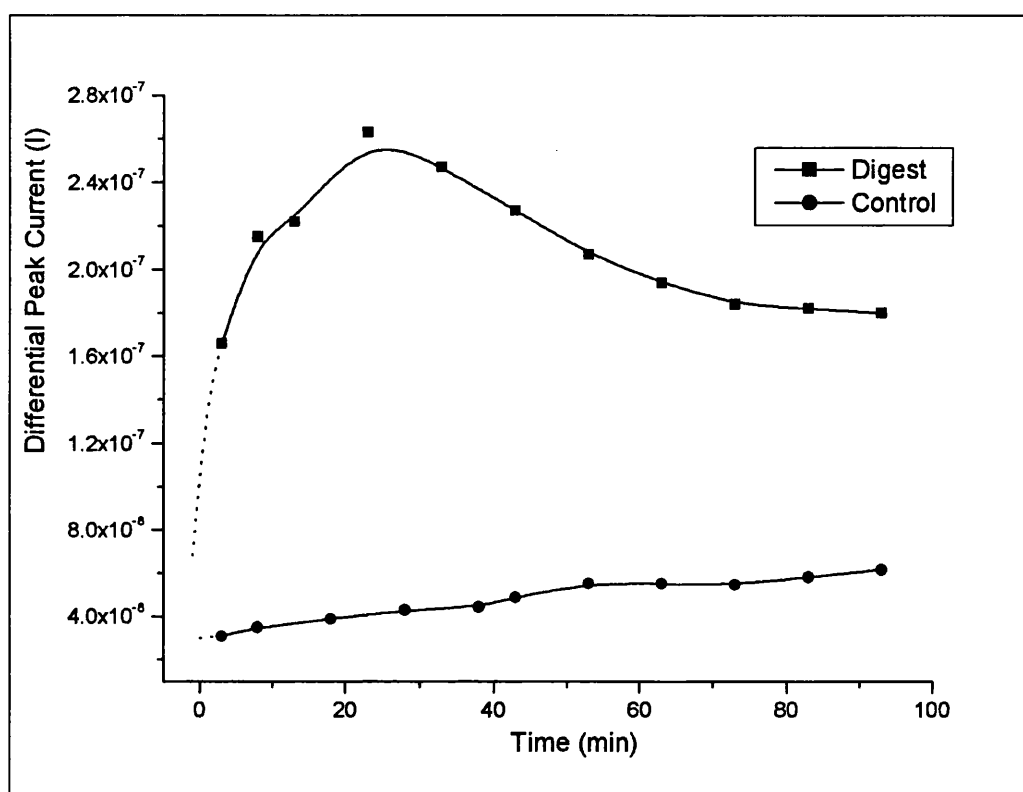
Figure 6.4 - S1 time-course.
Consecutive DPV traces were taken during the S1 time-course experiments for the Digest and Control assays. The DPV peak current is plotted against analysis time for the Digest (square data points, top graph) and Control (circular data points, bottom graph) assays.

The discrimination between the Digest and Control assays is quantified by taking a ratio between the two traces, as shown in Figure 6.5. The shape of the graph will be discussed shortly.
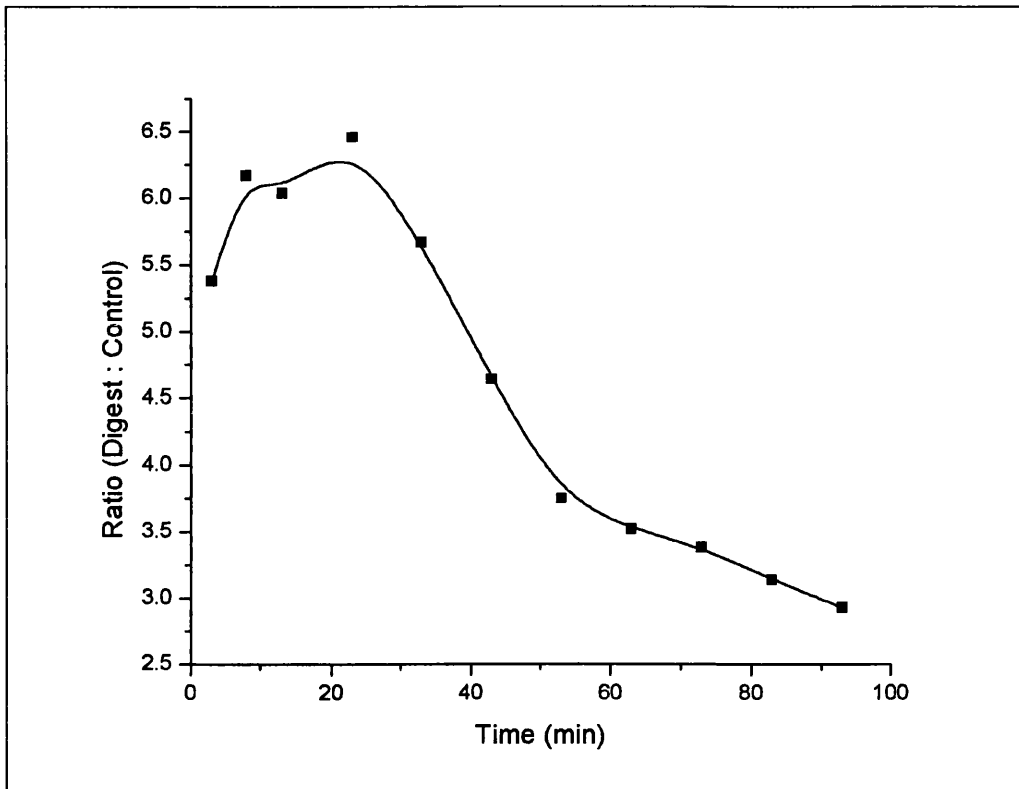
Figure 6.5 - Discrimination between time course results.
A ratio is taken between the differential peak current for the Control and Digest assays from the time-course analysis, shown in Figure 6.4.

The peak shapes of the individual DPV traces are as expected for the diffusion controlled system (Bard et al. 2001) and comparable to that of the end-point measurement. The actual trace for 63 minutes is given, in Figure 6.6, to allow a direct comparison to be drawn between the end-point and time-course experiments. The discrimination is increased from 1.5: 1 (Digest: Control) for the end-point to 3.5: 1 for the time-course, which is a large improvement.
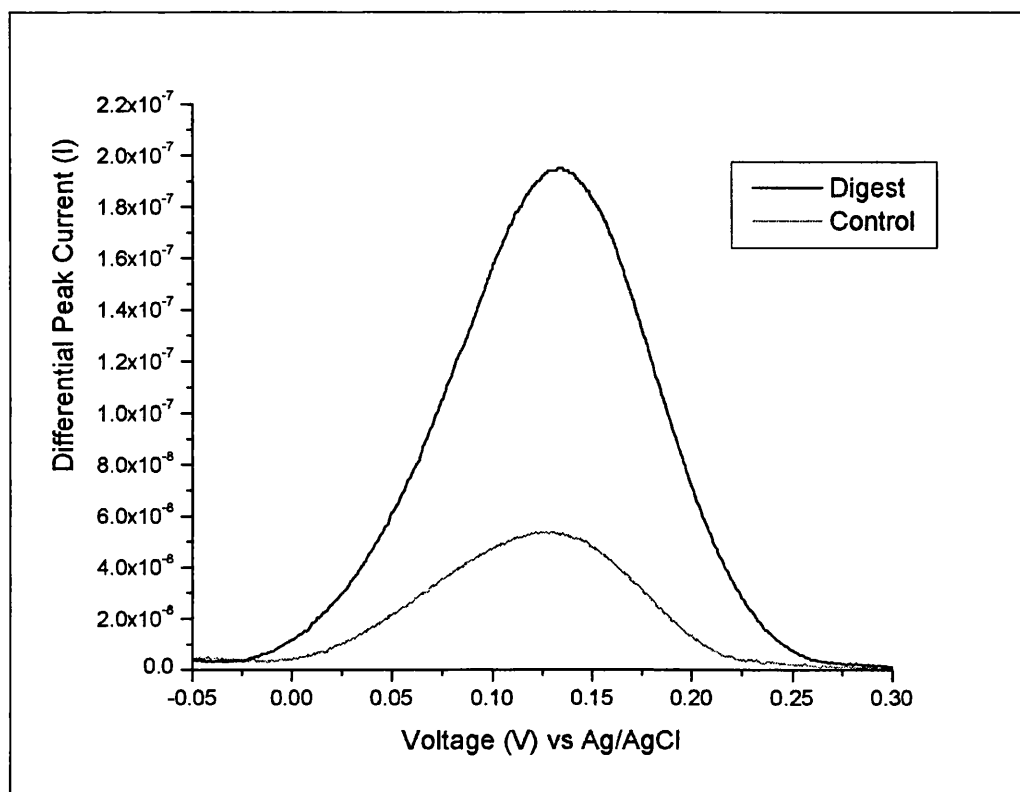
Figure 6.6 – Individual DPV traces from the time-course experiment.
The DPV traces after 63 minutes from the time-course experiment, reported in Figure 6.4, are given for the Digest (solid line) and Control (dotted line) assays.

To address the improved discrimination the shape of the time-course graph, shown in Figure 6.4, must first be discussed. The Digest assay gives a current maximum shortly after 25 minutes, which then decays. It is probable that the initial rapid increase of signal is due to the enzymatic digestion and liberation of the small ferrocene labelled fragments, which are able to readily diffuse to the electrode surface. The rate of increase slows to the maximum and then decays, probably due to the effect of electrode fouling from the enzyme and oligonucleotide fragments. In contrast, when the enzyme is omitted in the Control assay the much weaker response increases linearly with time. Although the origin of this behaviour is not entirely clear, one possibility is that this is indicative of non-specific absorption of the ferrocene labelled oligonucleotide probe, which creates an electroactive film that slowly thickens with time, giving a gradual increase of background signal. The highest discrimination between the two samples occurs at the Digest assay maximum, around 20 minutes.

To determine if the digestion conclusion is reasonable, it is important to visualise the digestion using an absolute, established method. For this reason a time-course was run

combined with agarose gel electrophoresis, the detail of which is given in section 2.10.2, Protocol 4. Gel electrophoresis is a standard molecular biology technique, introduced in see section 2.3, which separates DNA fragments by size. Unfortunately it was not possible to use the same oligonucleotide, but, as S1 digestion is non specific, any oligonucleotide of comparable length can be used. A 24 base oligonucleotide, FVR4, was used.

Digest assays were run at 37 °C for a range of times from 0 to 60 minutes (Figure 6.7). The undigested oligonucleotide is itself quite small and runs quickly through the gel. The full method is reported in the experimental.
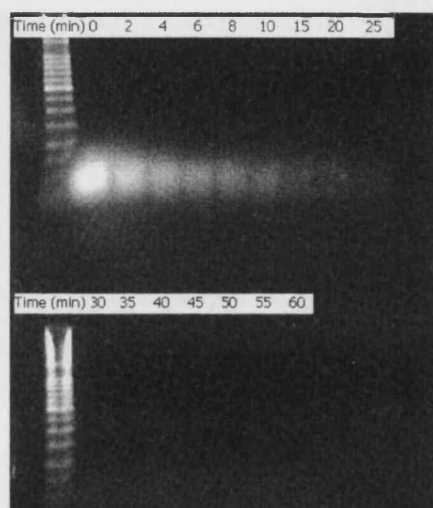
Figure 6.7 - Electrophoresis gel for S1 digestion time-course.
S1 digest assays were run for different times from 0 to 60 minutes (shown on the white band) and then run (downwards) on a 2% agarose gel, against a 100bp DNA ladder (left hand side). The initial sample wells are just below the white band, below the number. The oligonucleotide bands were visualised with SYBR Gold dye (Molecular Probes, UK).

The undigested oligonucleotide was visualised with a non-specific dye (SYBR Gold, Molecular Probes), as more oligonucleotide is digested, the intensity of the spot falls, until none is seen. The digested fragments are not visualised. For this oligonucleotide the digestion is virtually complete after 25 minutes, which is consistent with the above work.

Investigation into electrode fouling

The time-course was repeated, but the working electrode was removed and rinsed with MilliQ water for 10 seconds between measurements. The results are given in Figure 6.8.
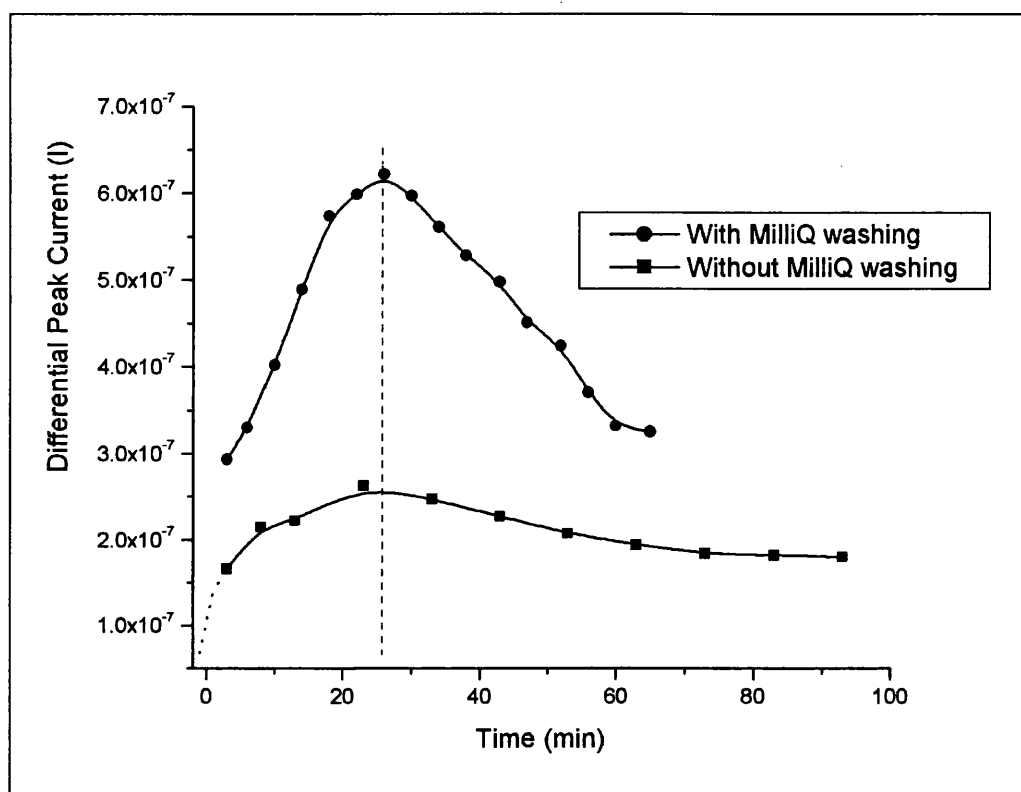
Figure 6.8 - S1 time-course with MilliQ water washing.
A S1 Digest time-course (top graph, circular data points) was run and the electrode was washed with water after every measurement. This is compared with the Digest time-course (bottom graph, square data points, from Figure 6.4). The time at which the maximum peak height occurs for the two graphs is shown (dotted line).

The above analysis shows that by introducing the wash step, a much higher current response is obtained at the current maximum (2.5: 1). This increased response suggests that there is significant fouling of the electrode during the experiment, from non-specific binding of the oligonucleotides, fragments or enzyme. The cleaning of the electrode therefore improves access of the digested fragments to the surface increasing the signal. However, the true situation is more complicated than this as the DPV response for the washed experiment falls from the maximum, indicating that some persistent fouling still occurs. Also crucially if the washing was completely effective (i.e. it generates a clean electrode) the response after 1 hour should equate to the original end-point response, as shown in Figure 6.3. In reality, the time-course response

is nearly 5 times greater. It may be the case that the washing step allows a more tightly packed, or favourably ordered, fouling layer to form which contains a greater amount (and possibly a higher proportion) of ferrocene labelled fragments. The proposed interaction between the response due to fouling and the response due to diffusion is shown below in Figure 6.9.
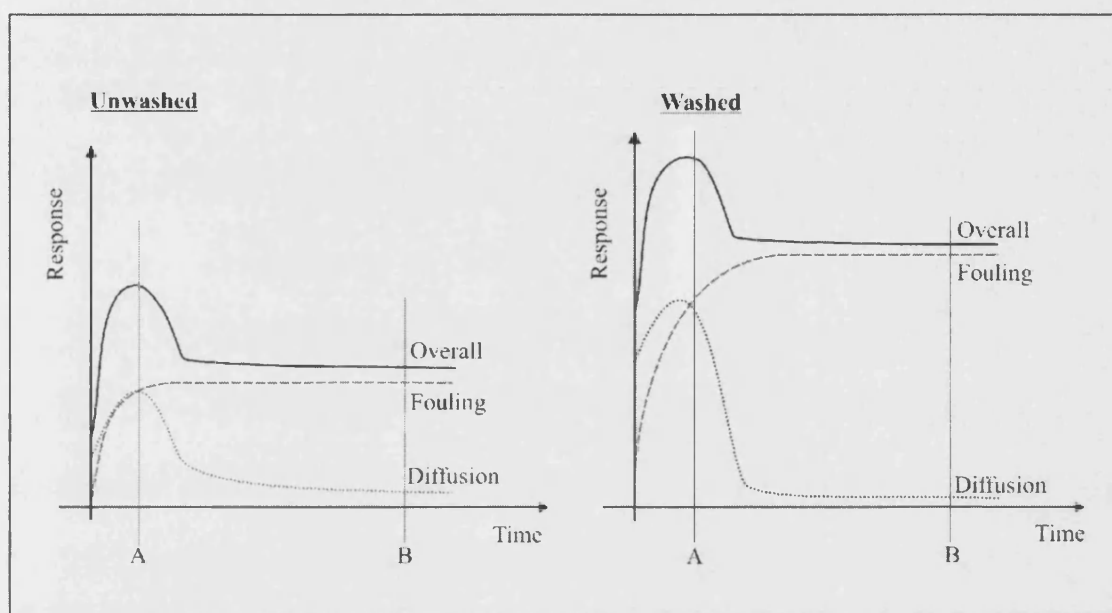
Figure 6.9 – Proposed explanation of time-course response.
The contribution to the overall DPV peak current (solid line) from the fouling layer (dashed line) and diffusion from ferrocenylated species from solution (dotted line) during a S1 digestion time-course is described. The overall response is the sum of the fouling and diffusion components. This description is given for an electrode without washing (left hand side) and with washing before analysis (right hand side).

In both cases the initial Faradaic current is due to the diffusion of the undigested labelled oligonucleotide to the surface, followed by its oxidation. This current initially increases primarily due to the generation of small digested ferrocene labelled fragments, which can readily diffuse to the surface, before this response is limited by surface fouling and begins to fall, shown in Figure 6.9 (point A). Without washing the equilibrium current, shown in Figure 6.9 (left hand side, point B), comes from a combination of the high current from the fouling layer and perhaps a small contribution from diffusion. With washing, shown in Figure 6.9 (right hand side), the initial contribution from diffusion is higher, due to the removal of some of the loose, non-specific fouling layer, but falls to a low value when the ordered fouling layer has been generated. The current from this fouling layer, and hence the equilibrium current, is high due to the access of many ferrocene moieties in the fouling layer to the surface.

These proposed models fit with the experimental data (Overall response), but the relative contributions from the diffusion and fouling currents to the overall response could actually be different, particularly for the final equilibrium current.

Whilst the washing with MilliQ gives a possible insight into the behaviour at the electrode, it would be impractical for a final small scale application. However, if a small scale flow cell could be developed, this could give improved over the use of a static solution.

A further complication arises because it has been assumed that the oxidation of the ferrocene is perfectly reversible. It is possible that in some cases the ferrocenium ion could be stabilised by negatively charged DNA phosphate backbone at the electrode surface, thus preventing its oxidation on the next DPV trace. This would cause the same reduction of peak current as described above for the physical fouling (i.e. blocking) of the electrode. This cannot be substantiated.

S1 endonuclease has been used to digest ferrocenylated oligonucleotides and good discrimination has been shown between the digested fragments and the undigested oligonucleotide, using DPV and a standard electrochemical cell. This can be used to determine the success of ssDNA oligonucleotide labelling. The time resolved work gives an insight into the enzymatic digestion of the oligonucleotide and the behaviour of the electrode surface, particularly the effect of fouling, showing that the fouling actually increases the discrimination between the digested and undigested samples. The exact nature of the fouling is unknown.

6.3 Development of the hybridisation gene sensor

This work details the development and use of T7 exonuclease for DNA hybridisation sensing and is primarily based on the C282Y sequence. Initially a hairpin oligonucleotide is post-labelled with *ester* **70**. This oligonucleotide is then subjected to end-point enzymatic digestion, followed by time-course analysis of the digestion. The hybridisation gene sensing hybridisation assay is then developed. Exploratory hybridisation assays are run to prove that discrimination is possible and then reproducibility issues are addressed. Reproducibility issues are shown to necessitate the use of oligonucleotides labelled with a ferrocene amidite. The labelling efficiency of the amidite labelling was assessed through S1 digestion and then the probe was used in a gene sensor assay, which undergoes end-point analysis. A time-course analysis of the digestion of the hybridised duplex was undertaken to gain a better understanding of the system. The gene sensor was then applied to the detection of other gene sequences, using alternative ferrocene amidite labelled probe oligonucleotides. This allowed the robustness of the system to be tested.

6.3.1 Hairpin assay

The dsDNA specific T7 exonuclease is initially evaluated to determine if discrimination is possible between digested and undigested hairpin oligonucleotides.

Oligonucleotide labelling

The C282Y hairpin oligonucleotide was post-labelled with the *ester* **70**, following the protocol of Takenaka. Full details are given in section 2.10.2, Protocol 5.

T7 digestion of hairpin oligonucleotides

The ferrocenylated hairpin oligonucleotide **81** was digested at 25 °C for 1 hour, using the T7 buffer supplied with the enzyme and the DPV measurements were also done at this temperature, details are given in section 2.10.2, Protocol 5. The Control assay

omits the enzyme as this has been shown to be equivalent to using a heat denatured enzyme (Braven 2002).

The change in electrochemical response of the *oligonucleotide* **81** is reported before and after enzyme digestion. Both the GC electrode, results shown in Figure 6.10, and gold electrode, results shown in Figure 6.11, were used to measure the same sample, making the results directly comparable. These graphs clearly show the large increase in ferrocene oxidation current, measured by DPV, following exonuclease action compared to the *oligonucleotide* **81** without enzymatic digestion.
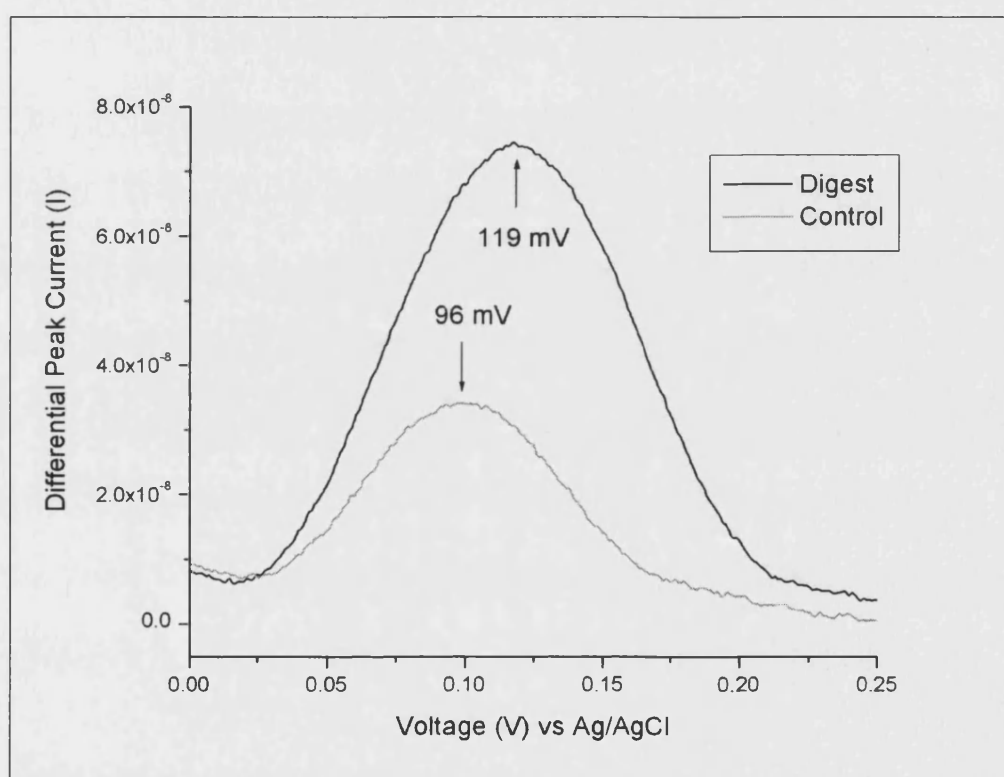
Figure 6.10 – T7 digestion of hairpin oligonucleotide 81: GC electrode.
The DPV traces for the Digest assay (black line, top) and Control assay (grey line, bottom) are shown. The electropotentials for each trace are given. The ratio between the peak heights is 1: 2.4 (Control: Digest).
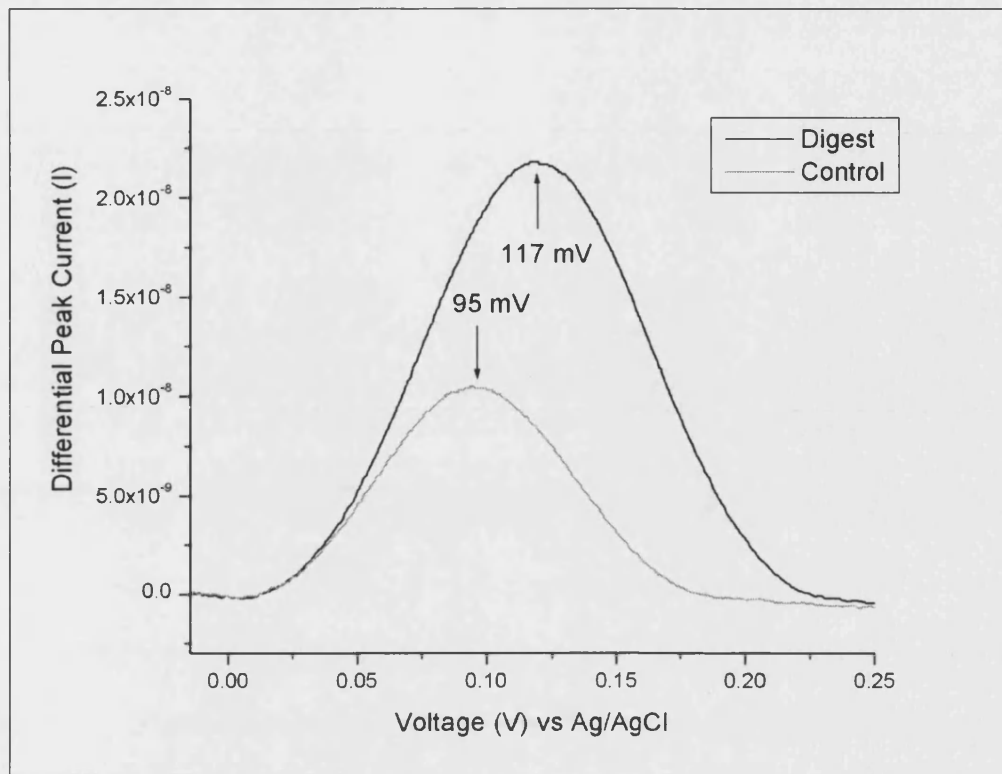
Figure 6.11 - T7 digestion of hairpin oligonucleotide 81: Au electrode.
The DPV traces for the Digest assay (black line, top) and Control assay (grey line, bottom) are shown. The electropotentials for each trace are given. The ratio between the peak heights is 1: 2.1 (Control: Digest).

The above data is directly compared in Figure 6.12. The GC electrode gives a slightly better discrimination than the gold electrode and a higher response.
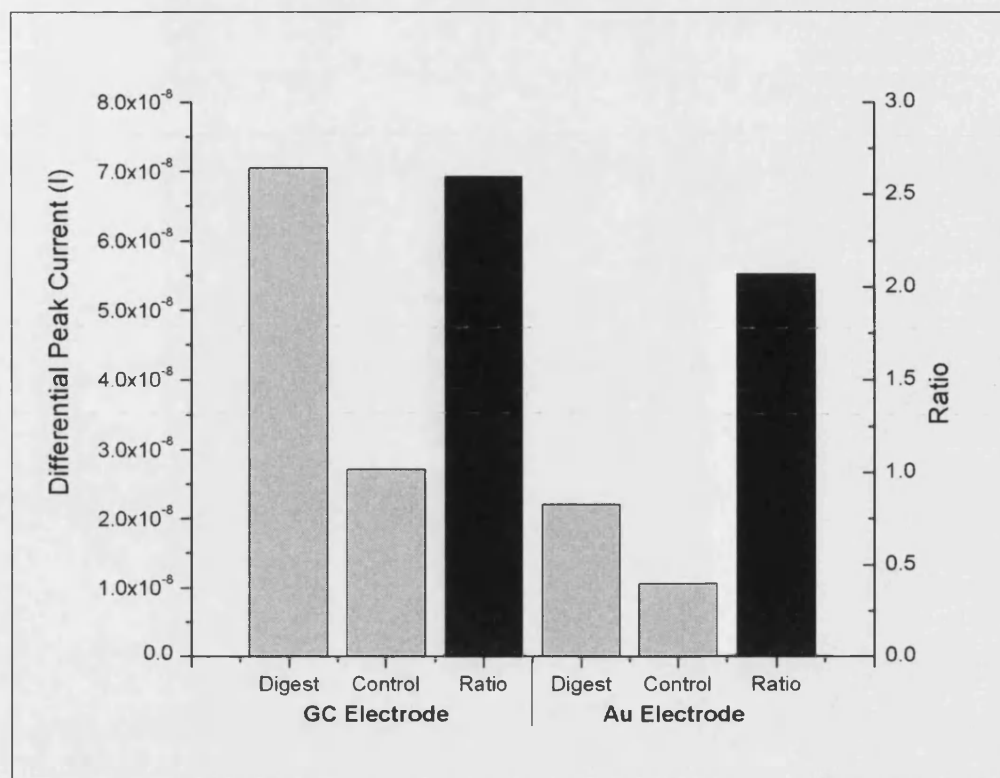
Figure 6.12 – T7 digestion of hairpin oligonucleotide 81: comparison between electrodes.
This figure details the differential peak currents, from the DPV analysis of the C282Y hairpin oligonucleotide, for both the GC electrode (DPV trace in Figure 6.10) and Au electrode (DPV trace in Figure 6.11). Ratios (black bars) are given between the Digest and Control responses in each case.

The improved responses of the GC electrode can be rationalised if the ratios between the responses of the Digest and Control assays, on the different electrodes, are considered in Figure 6.13. For the Digest assay the ratio is 3.2: 1 (GC: Au) and for the Control 2.6: 1.

The explanation for the higher response of the GC electrode is that it has a higher surface area. It has been discussed, in section 2.5.3, that electrode surface area is directly proportional to current response in an ideal case. The gold electrode has a 1.6 mm diameter (area = 2.6π), whilst the glassy carbon electrode has 3.0 mm diameter (area = 9.0π), hence the expected response should be 3.5 times bigger for the GC electrode. This is approximately true for the Digest assay (3.2 times increase) and is actually true if the electrodes are used with standard solutions of ferrocene carboxylic acid. The ratio is lower for the Control assay (2.5 times increase) and must be due to either the surface condition or behaviour of the electrodes in this assay. The consequence of this low ratio is that discrimination (between the Digest and Control responses) is higher for the GC electrode (Figure 6.12).
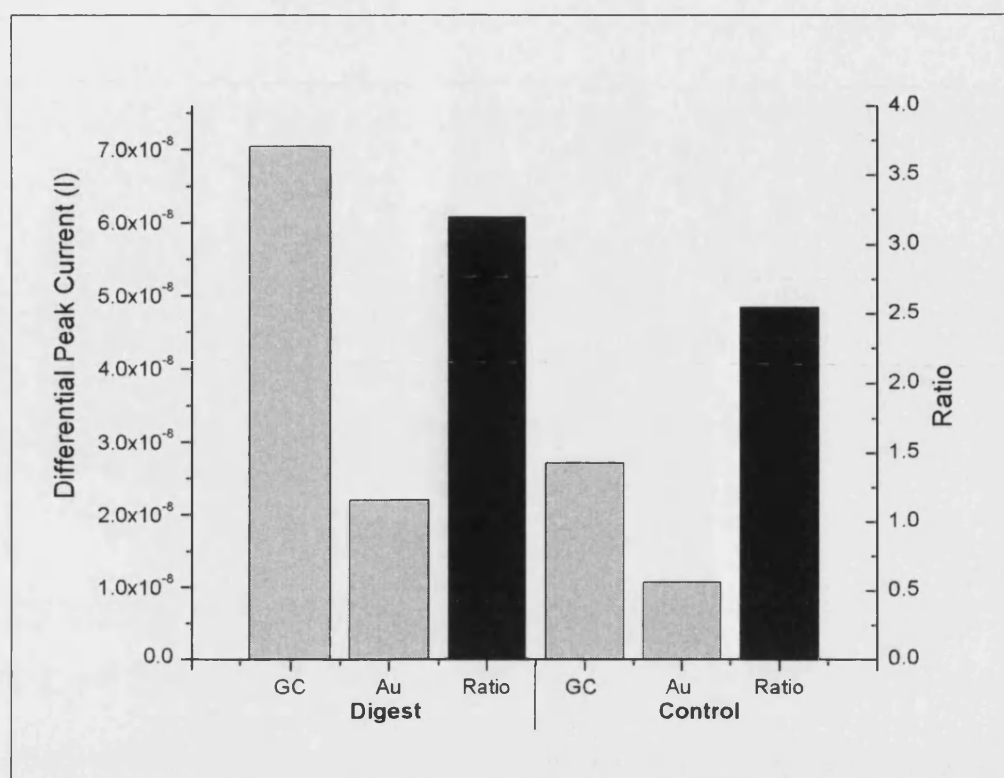
Figure 6.13 - T7 digestion of hairpin oligonucleotide 81: comparison of Digest and Control assays.
This figure details the differential peak currents, from the DPV analysis of the C282Y hairpin
oligonucleotide, for both the Digest and Control assays. Ratios (black bars) are given between the
response of the GC and Au electrodes for the two assays.

If the electropotentials of the ferrocenylated oligonucleotides are considered before and
after digestion (Figure 6.10 and Figure 6.11) it can be seen that there is an increase in
electropotential on enzymatic digestion of 23-24 mV for both electrodes. If the Au
electrode is considered, the ferrocenylated linker molecule, *ester* **70**, has an
electropotential of 140 mV, which is reduced to 95 mV on labelling, but increases to
117 mV on digestion. In other words, the ferrocene moiety is stabilised on labelling and
destabilised on digestion. The differences in the assay in which the electropotential is
measured for the linker and labelled oligonucleotide, will slightly affect the
electropotential, but the trend should still be valid.

The change in electropotential is unlikely to be due to the inductive and mesomeric
effects, introduced in section 3.1.3 and discussed in section 4.5.2, as the structure of the
linker molecule close to the ferrocene moiety is retained in the labelling and digestion.
In the labelling process the oligonucleotide is introduced on a C6 alkyl spacer chain, so
inductive effects from the oligonucleotide will be insignificant and mesomeric effects

cannot occur due to the lack of conjugation. The stabilisation must therefore be due to some interaction between the ferrocenium ion (Fc^+) and the negatively charged oligonucleotide sequence, whereby the linker is sufficiently flexible that the ferrocene moiety can be spatially close to the rigid DNA hairpin duplex. On digestion this effect is diminished.

The clearest example of stabilisation of the ferrocene moiety, through interaction with the oligonucleotide is reported by Ihara (Ihara et al. 1996). The hybridisation of a ferrocenylated oligonucleotide does not affect its electropotential, but the introduction of further bases on the target sequence lowers the electropotential of the ferrocene indicating stabilisation of the ferrocenium ion (Fc^+) and therefore an interaction between the ferrocenium ion overlapping oligonucleotide bases. This is illustrated in Figure 6.14.
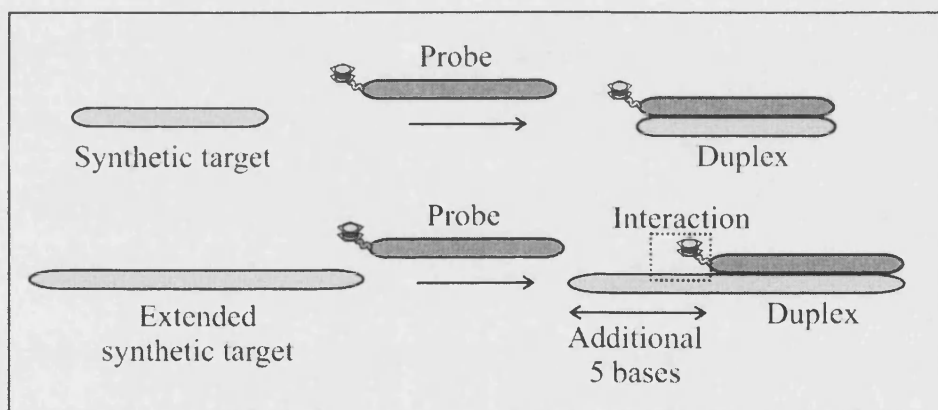
Figure 6.14 - Ferrocene interaction with additional oligonucleotide bases.
The ferrocenylated probe (dark grey strand) readily hybridises to its fully complementary target (light grey strand, top scheme). If the target has an overlap of additional bases (bottom scheme), the ferrocene label can readily interact with these bases (dotted box) and therefore the ferrocenium ion can be stabilised.

Time-course of T7 digestion of hairpin oligonucleotide

Real-time analysis of T7 enzymatic digestion of the hairpin oligonucleotide was undertaken at 25 °C, by measuring consecutive DPV traces using automated sampling. This work was done with both the GC electrode, results shown in Figure 6.15, and the gold electrode, results shown in Figure 6.16.
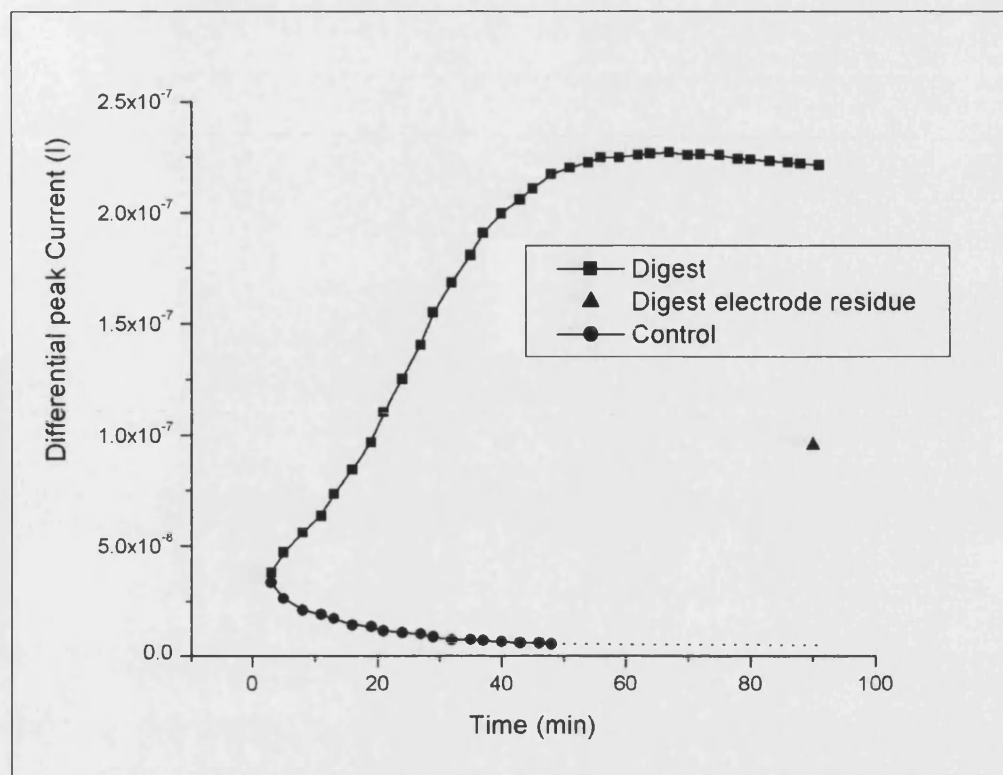
Figure 6.15 – Time-course of T7 Digestion of hairpin oligonucleotide 81: GC electrode.
A T7 Digest time-course (top graph, square data points) and a Control time-course (bottom graph, circular data points) were run. After 50 minutes the Control response was not resolved from the baseline and it is extrapolated (dotted line). Measuring the Digest electrode in fresh buffer solution, without cleaning the surface, gives a response (triangular data point).
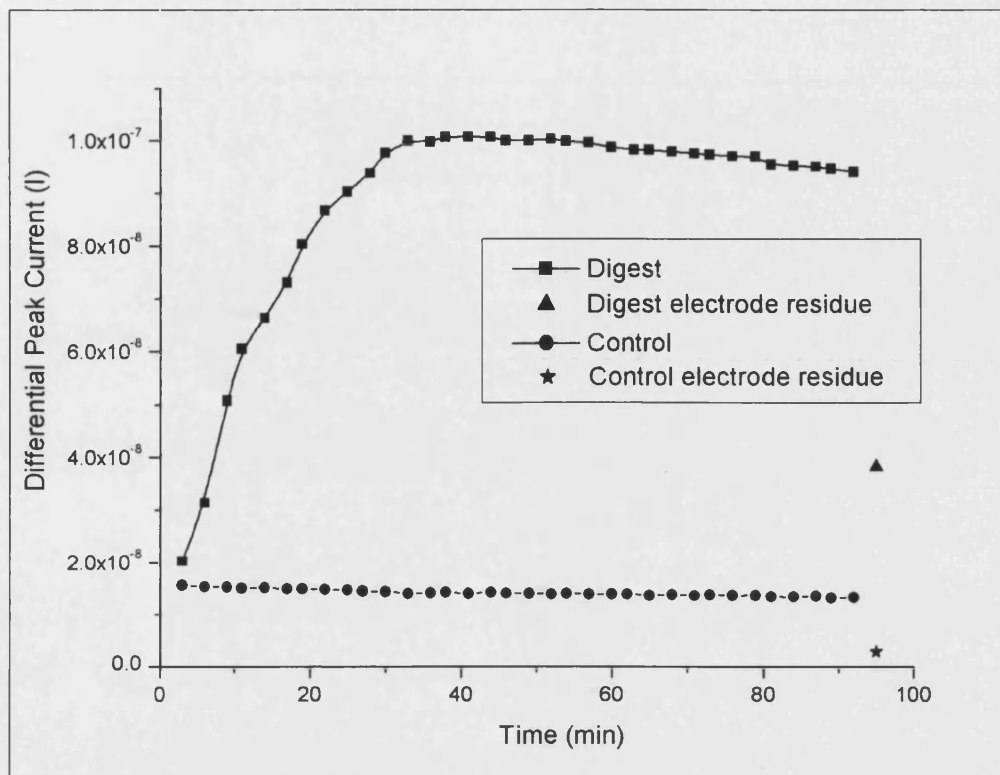
Figure 6.16 - Time-course of T7 Digestion of hairpin oligonucleotide: Au electrode.
A T7 Digest time-course (top graph, square data points) and a Control time-course (bottom graph, circular data points) were run. Measuring the Digest electrode in fresh buffer solution, without cleaning the surface, gives a response (triangular data point) as does the Control electrode (star data point).

Both time-course graphs have a similar shape. The response for the Digest sample rapidly increases to a current maximum, after which a plateau occurs. This plateau effect occurs more quickly on the gold electrode (35 minutes) than on the GC electrode (50 minutes). In contrast the response for the Control sample is initially low and either remains constant (Au electrode) or falls slightly before the plateau occurs (GC electrode). The explanation appears to be more straightforward than for the S1 work. The undigested hairpin oligonucleotide gives a low response which could be due to either slow diffusion of the duplex to the surface and hence a low diffusion limited current, or quicker fouling of the electrode, where the fouling layer is poorly electroactive and blocks the surface. The combination of these two effects is the most likely situation.

In contrast for both Digest assays, the rapid increase in signal must be due to the fast access of the small fragments to the surface. Again the nature of the blocking layer is

264

unknown, but the larger, rigid hairpin DNA may be less effective at blocking the surface to the small fragments than the ssDNA. The response plateau is either due to the response of the fouling layer or a diffusion controlled steady state, through a partially fouled electrode as mentioned above. Interestingly if the electrodes are removed from the cell and then a DPV trace is measured for the buffer, as shown in Figure 6.15 and Figure 6.16, there is still a reasonable response from the Digest electrode (approximately 40%), which must be due to the fouling layer. As an unknown amount of the fouling layer will be lost when the electrode is moved between solutions, the only conclusion that can be drawn is that in the final DPV trace fouling accounts for at least 40% of the signal whilst diffusion accounts for a maximum of 60%.

The discrimination between the Control and Digest samples should be discussed. If the trace at 40 minutes is considered (before the resolution of the Control trace of the GC sample is lost) the discrimination for the GC electrode is 29: 1 (Digest: Control) and for the gold electrode it is 7.2: 1. Both of these are a big improvement on the earlier end-point analysis (i.e. analysis after 1 hour when the digestion has gone to completion, Figure 6.10 and Figure 6.11), with the GC electrode having a discrimination which is over an order of magnitude higher. This situation is ideal for a sensor, with high constant discrimination being obtained after digestion of the hairpin oligonucleotide has been finished.

Conclusions for the T7 digestion of the hairpin oligonucleotide

It has been shown that the C282Y hairpin oligonucleotide has been successfully covalently labelled using *ester* 70 and that T7 exonuclease successfully digests hairpin dsDNA. Discrimination can be obtained between the hairpin oligonucleotide before and after T7 enzymatic digestion using DPV end point analysis. The GC electrode gives a higher response and improved discrimination over the Au electrode. Following the enzymatic digestion, using a time-course experiment with consecutive DPV traces, is also successful and the discrimination between the Digest and Control samples is improved. The time-course experiment also gives an indication as to when the enzymatic digestion has been completed. Again the GC electrode gives a higher

response and improved discrimination over the Au electrode. The GC electrode is the preferred candidate for further work.

6.3.2 Hybridisation gene sensor

It has been shown that discrimination has been achieved between the digested and undigested hairpin oligonucleotide, using the T7 exonuclease enzyme. The work can now be applied to the development of a DNA hybridisation gene sensor, whereby genes on the target oligonucleotide are detected by hybridisation with a ferrocene labelled probe oligonucleotide and the duplex is then digested by T7 exonuclease.

Exploratory hybridisation work

In a mimic of gene sensing *oligonucleotide* **80**, the 18 bp C282Y probe labelled with *ester* **70**, was hybridised with a larger 60 bp target (C282YST). This is a custom synthesised oligonucleotide (ST: Synthetic Target), with the same sequence as the amplicon which would be produced by the PCR reaction. Using this approach reduces the complexity of the assay and guarantees the oligonucleotide concentration. After hybridisation the assays were then subjected to end-point T7 digestion, the results of which are shown in Figure 6.17. Full experimental details are given in section 2.10.2, Protocol 6. The results from this initial work, with GC electrode, are very encouraging. Good discrimination was seen between the Control sample, with no enzymatic digestion (low response) and the Digest sample (high response). The assay was also run using a 50 bp mismatch target sequence (CTRAcomp). Both of these assays (with and without enzyme) gave an equivalent low response.
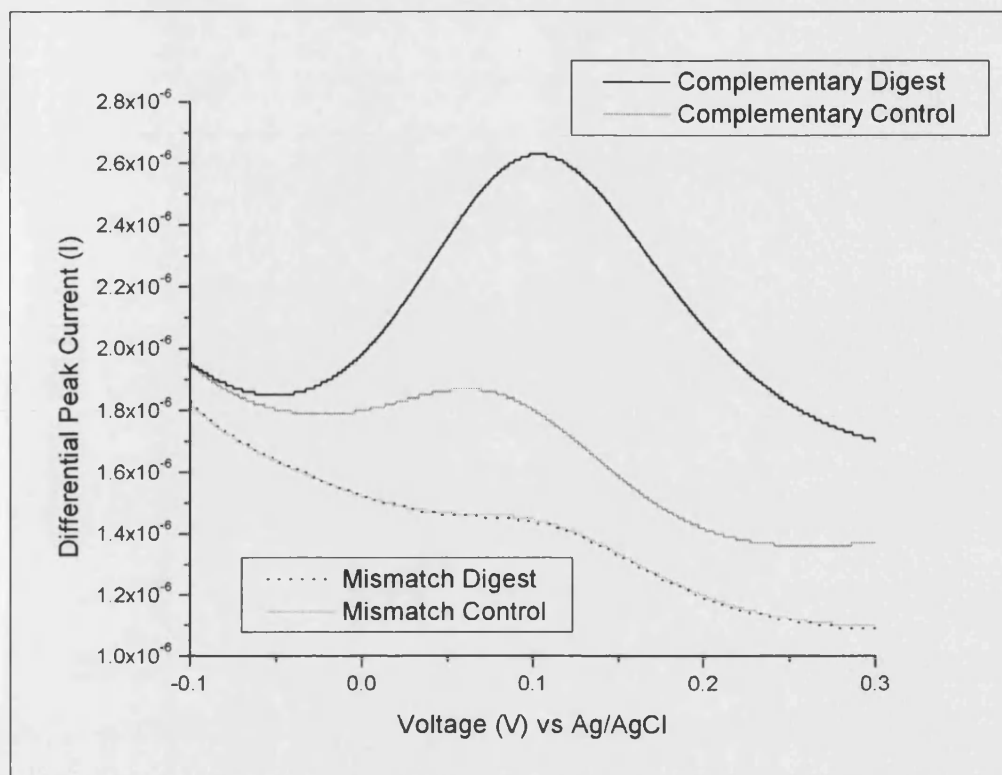
Figure 6.17 – T7 digestion of the C282Y hybridised duplex.
Ferrocenylated C282Y probe oligonucleotide 80 is hybridised (25 °C for 15 minutes) with its complementary target (C282YST) and then subjected to T7 digestion for 45 minutes. End-point DPV analysis was run for the assay (Complementary Digest, black line, top graph), using GC electrode. Three control assays were also analysed: Complementary Control (complementary target, no enzyme, dark grey graph); Mismatched Digest (mismatched target sequence, with enzyme, dotted black graph) and Mismatched Control (mismatched target sequence, without enzyme, light grey graph). The Mismatched Digest and Control graphs are very similar and overlap.

The discrimination is good with a ratio between Digest and Control of 3.4: 1, shown in Figure 6.18. This is comparable to the results obtained from the digestion of the hairpin oligonucleotide, which has a ratio between Digest and Control of 2.4: 1, shown in Figure 6.12. This comparability suggests that these results are real and can be explained with the same theory: the large hybridised duplex (Complementary Control) is assumed to have a lower diffusion coefficient (D) than the digest fragment (Complementary Digest) and therefore slower access to the surface and lower diffusion limited current. The fouling issues are also the same: the small digested fragments are not blocked as much at the surface and possibly form a more electroactive layer.
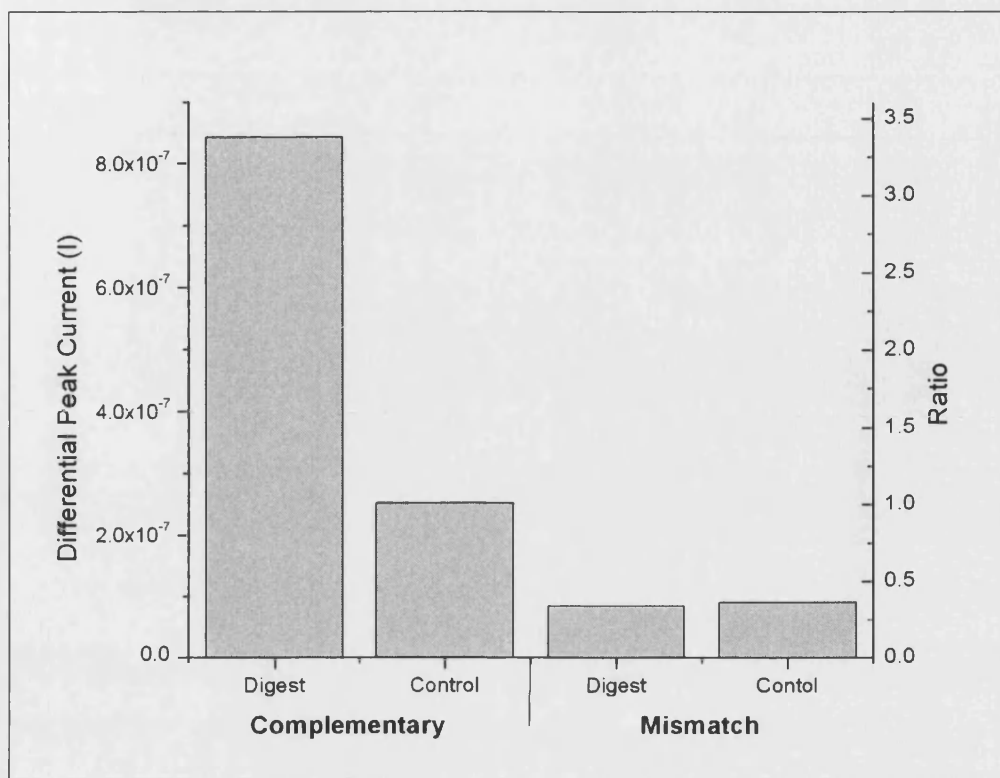
Figure 6.18 – T7 digestion of the C282Y hybridised duplex: ratios of peak height.
The peak heights of the T7 digestion work, shown in Figure 6.18, are reported as ratios against the
response of the Complementary Control assay (second column on left, ratio = 1.0).

The Complementary Control response is more than three times higher than the Mismatch responses with or without the enzyme. This can be explained as most of the oligonucleotides in the Complementary Control assay will be hybridised, producing a relatively rigid, conformationally constrained, duplex. In contrast there will be no hybridisation and therefore no steric restriction for the Mismatch oligonucleotide, tand so it is proposed that they will be able to block the surface much more effectively than the duplex, as illustrated in Figure 6.19.
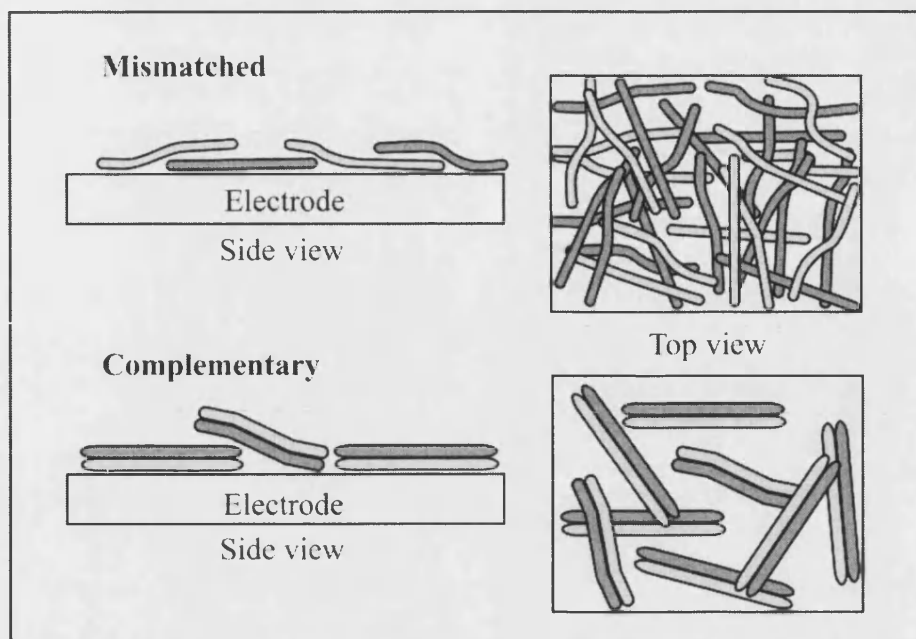
Figure 6.19 - Electrode fouling of oligonucleotides on the electrode surface.
The unhybridised oligonucleotides from the mismatched assays (top) have a high degree of flexibility and can effectively block the electrode surface.   The duplex DNA from the complementary control assay (bottom) is much less effective at blocking the surface.   The probe oligonucleotide (dark grey) and complementary target (light grey) are shown. The contribution of the enzyme is ignored in this model.

The unhybridised oligonucleotides may also be able to block the access of the ferrocene label to the surface much more effectively, as illustrated in Figure 6.20.
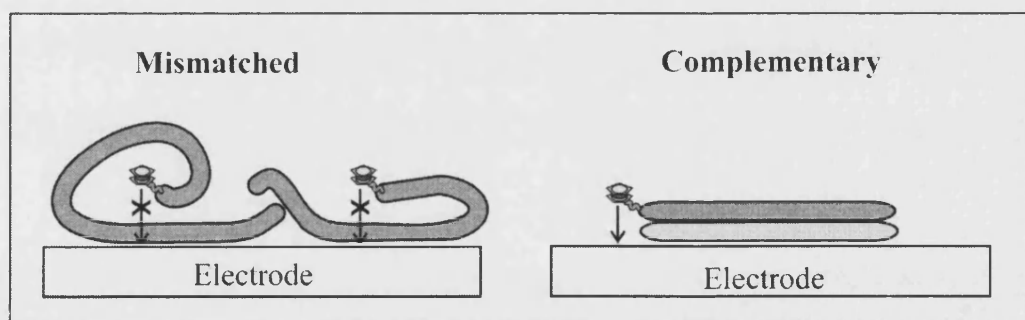
Figure 6.20 – Blocking of the electrode by the oligonucleotide structure.
The ferrocene labels on the unhybridised oligonucleotides in the mismatched assay (left hand side) can be blocked from the electrode surface by the structure of the oligonucleotide (crossed arrow). The ferrocene labels the duplex of the complementary control assay (right hand side) are not blocked from the surface (arrow).

Gene sensor reproducibility issues

It was now necessary to validate the results for the hybridisation gene sensor, illustrated in Figure 6.17, but this was not straightforward and problems were encountered. Direct repetition of the sensor assay, illustrated as Assay 1 in Figure 6.21, was undertaken using the same batches of labelled oligonucleotide, Assay 2, and a second batch of labelled oligonucleotide, Assay 3. Whilst discrimination of 1.3 and 1.4: 1 was obtained between the Digest and Control responses for these assays, it was significantly lower than that of Assay 1 and the magnitude of the differential peak current responses were also much lower.
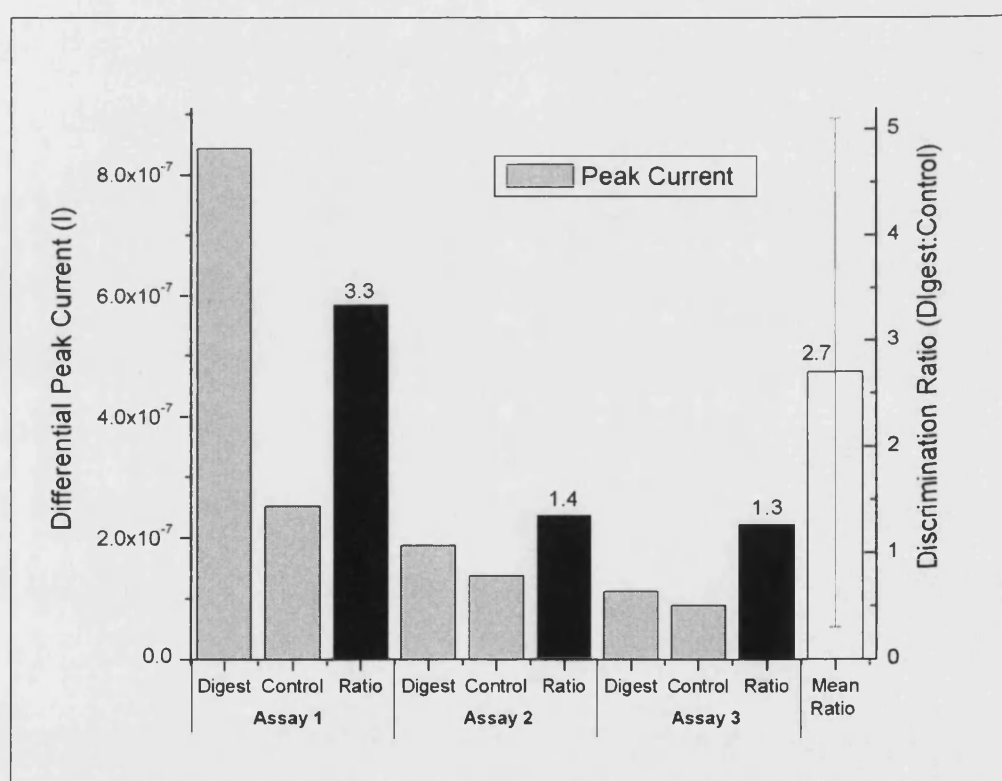
Figure 6.21 – Examining the reproducibility of the C282Y gene sensor assay.
Three hybridisation assays were analysed and their DPV differential peak currents are shown (grey bars). The discrimination between the peak currents is given as a ratio (Digest: Control, black bars). The sample mean ratio and its 95% interval of confidence are shown (white bar).

If the three assays are considered together, then the mean discrimination ratio of the sample, shown in Figure 6.21, is reasonable at 2.7: 1. However, confidence in this result is low, as the 95% interval of confidence is large, due to the large differences in discrimination and small number of samples. Hence, by this analysis, the Assay 1 result is poorly reproducible.

Before dismissing the highly desirable initial result for Assay 1, the possible reasons behind the poor reproducibility should be considered. The sensor assay is complex and relies on: effective labelling, effective enzymatic digestion and reproducible electrochemical detection. If any of these variables is poorly reproducible or ineffectively controlled, then the final electrochemical analysis will not be reproducible.

A prime reason for not dismissing the Assay 1 result is the aforementioned correlations with the hairpin oligonucleotide work, which achieved comparable discrimination (2.4: 1, Digest: Control) using the same labelling and purification protocol together with the same enzymatic digestion assay (i.e. the same enzyme and buffer).

An investigation into the effectiveness of the labelling of the oligonucleotide, with *ester* 70, was undertaken by subjecting fresh batches of labelled oligonucleotide to S1 endonuclease digestion and analysing the assays by DPV. The results for this work are given in Figure 6.22. Only 3 out of 8 oligonucleotide assays gave a positive discrimination for the Digest response and of these, a good discrimination was achieved once (4.5: 1, Assay 2) with lower discriminations for the other assays (1.5: 1, Assay 5 and 1.2: 1, Assay 7). Misleadingly if the 8 assays are considered as a sample, then the sample mean, see Figure 6.22, is skewed by the one high result and shows positive discrimination, albeit with a very large 95% confidence interval. The high result can be excluded as an out-lying point using a 95% confidence Q test ($Q = 0.819 > Q_{95} = 0.526$, 8 data points), described in section 2.7.2. Subsequently the sample mean is reduced to 1.0, with a large 95% confidence interval, suggesting that there is no significant discrimination across the assays in the sample.
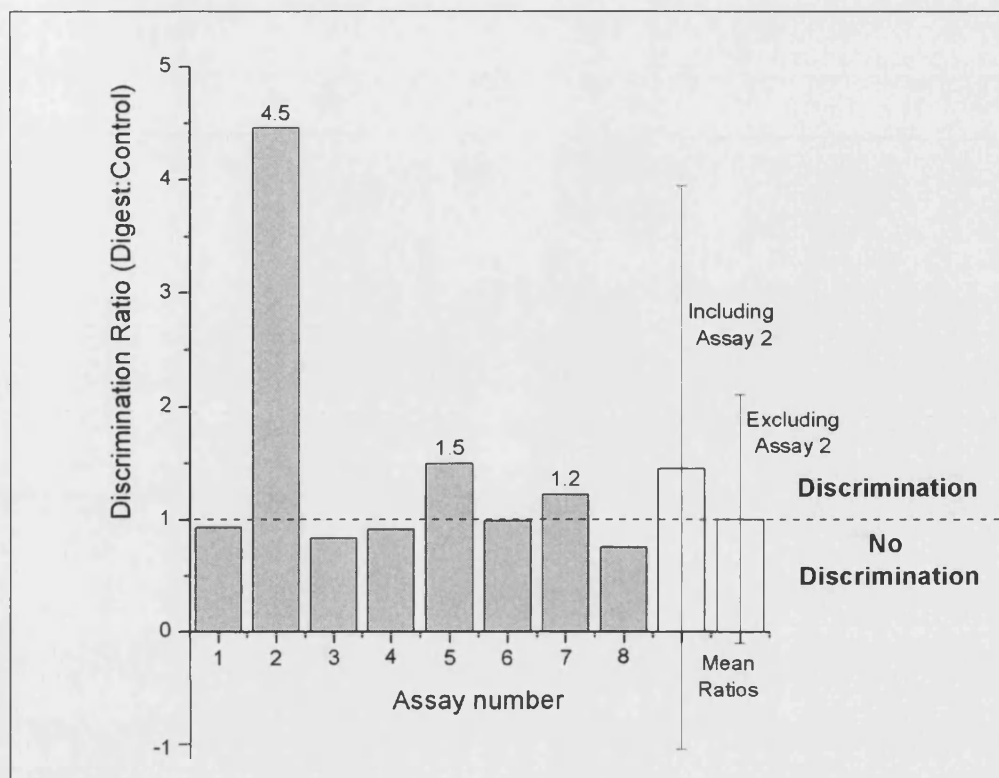
Figure 6.22 – Evaluation of C282Y oligonucleotide labelling.
Eight post-labelled C282Y oligonucleotide samples were subjected to S1 endonuclease digestion. The discrimination between the DPV differential peak currents for each assay is shown as a ratio (Digest: Control). The sample mean discrimination is given, together with 95% interval of confidence for the sample (white bars), with Assay 2 both included and excluded.

The work, described in Figure 6.22, was unable to show that the covalent post-labelling of the oligonucleotide sequences was effective. However, the problems in achieving discrimination, and the variability of discrimination when it was obtained, do not necessarily indicate poor labelling and could be due to problems with the electrochemical detection, specifically the condition of the electrodes.

The condition and roughness of the electrode surface, described in sections 2.5.7 and 2.5.8, is thought to directly affect the DPV response of the electrode, with rougher or fouled surfaces giving lower sensitivities. The recommended cleaning protocol, to prepare the electrode for use, is to initially polish the electrode using coarse alumina slurry and then progressively use finer slurries until the electrode is visually smooth and shiny (Bott 1997). The choice of the grade of the coarsest slurry is dependent on the initial roughness of the electrode. The assays used here are quite benign towards the electrode, so the coarse slurries were omitted and only the fine (0.05 μm) slurry was used. The use of just water was not sufficient to effectively clean and polish the

electrode and did not increase sensitivity. The electrode surface was polished to be as reproducibly smooth as possible, but as the polishing was undertaken by hand, there would always be some variation of the electrode surface. This variation could not be quantified.

With uncertainty surrounding the efficiency of the oligonucleotide labelling and the reproducibility of the condition of the electrode surface, investigation of other parameters which could affect the assay results was not a priority. However, all the assay components were replaced by new solutions and fresh batches, to ensure contamination or degradation of a component had not occurred. Preliminary work to vary the parameters for the DPV trace, specifically the step potential, was undertaken, but did not afford any improvement. Optimisation of the DPV parameters should be undertaken as the final step, after reproducibility has been obtained.

Amidite labelled hybridisation probes

The sensitivity of the sensor system could only be addressed, by reducing the number of variables in the system. As the post-labelling approach has an unknown labelling efficiency and purity, the amidite labelling of the oligonucleotide, together with HPLC purification, was adopted in an effort to eliminate this uncertainty. The labelling was done commercially by TibMol Biol, Germany.

Amidite labelling efficiency

The labelling efficiency and purity of the oligonucleotide, labelled using the ferrocenylated amidite is guaranteed to be very high (approximately 100%) after their HPLC purification. The suitability of the label for use in the enzymatic digestion assay, should still, however, be routinely determined by analysing the S1 digest, which is a simple technique to determine if the electrode based discrimination is satisfactory, without the complicating factor of hybridisation.

A C282Y oligonucleotide labelled with the ferrocenylated *amidite* 28 was not immediately available, therefore exploratory work was undertaken with an alternative amidite which had been used to label two oligonucleotide sequences. These were

BAPR (as for the S1 work) and the meningitis sequence CTR044 (Guiver et al. 2000). This novel *diferrocene amidite* **82** was synthesised by Dr Steve Flower, University of Bath and is illustrated in Figure 6.23.

5'-Fc-Linker-ATGCCCTCCCCCATGCCA TCCTGCGT-3' (BAPR) **83**
5'-Fc-Linker-CATTGCCACGTGTCAGCTGCACAT-3' (CTR044) **84**
5'-Fc-Linker-CTAGAATGAGTTACCAGAGAGCAGCTTGG (MC11PR) **85**
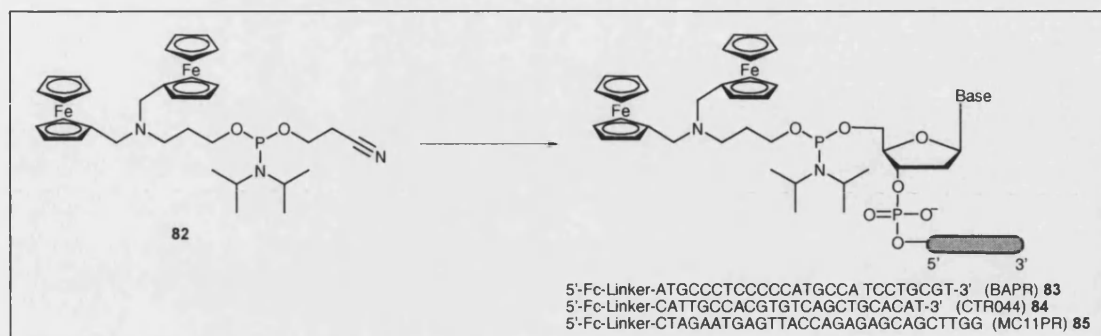
Figure 6.23 – Oligonucleotide labelling with *diferrocene amidite* 82.

The assays were run at high concentration of oligonucleotide (10 µM) to ensure that a signal was seen for the undigested ferrocenylated oligonucleotide. The Control samples omit the enzyme. Full assay details are given in section 2.10.2, Protocol 7. The Digest and Control samples were analysed using DPV with both the Au and GC electrodes. This allows them to be compared for both sensitivity and selectivity with a S1 assay.

The DPV peak currents for the CTR044 probe, *oligonucleotide* **84**, are compared in Figure 6.24. The GC electrode gives a higher response for the Digest peak, but poorer discrimination from the Control sample. As for the T7 digestion of the hairpin oligonucleotides, the higher response is expected due to the increased surface area of the CG electrode.
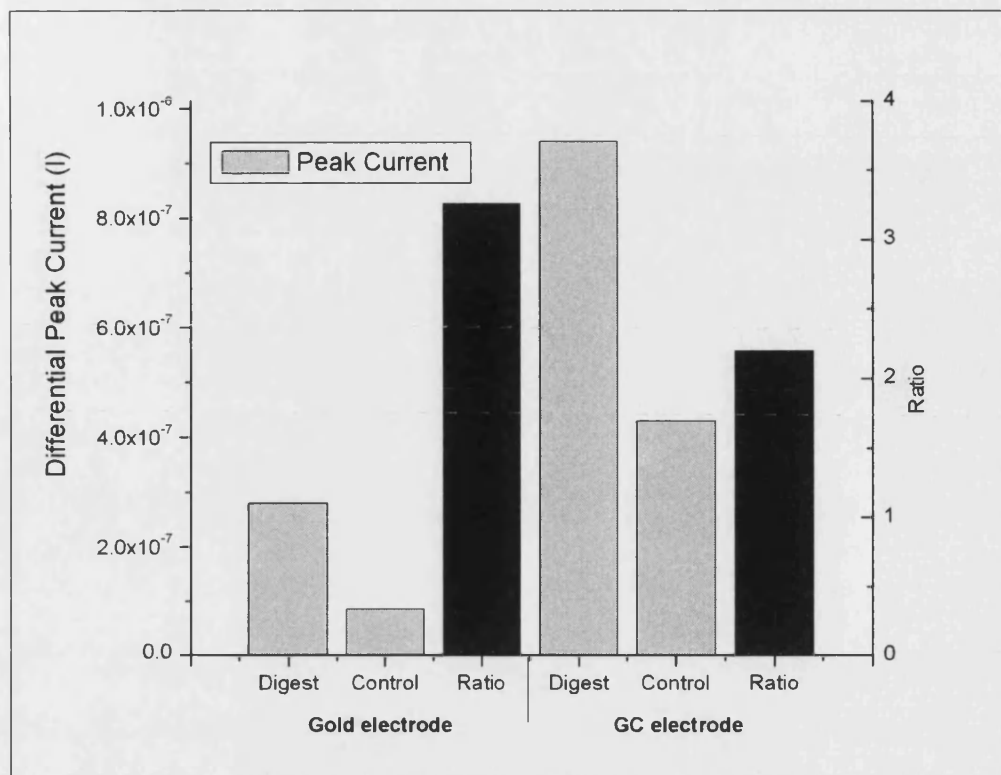
Figure 6.24 – S1 digestion of the CTR044 probe.
Digest and Control assays were run for S1 endonuclease digestion of ferrocenylated CTR044 probe, *oligonucleotide* 84. The assays were analysed using a gold electrode (left hand side) and a glassy carbon electrode (right hand side). The differential peak currents are given (grey bars). The ratio between the peak currents (Digest: Control) is also given (black bars).

The DPV peak currents for the BAPR probe, *oligonucleotide* 83, are given below in Figure 6.25.
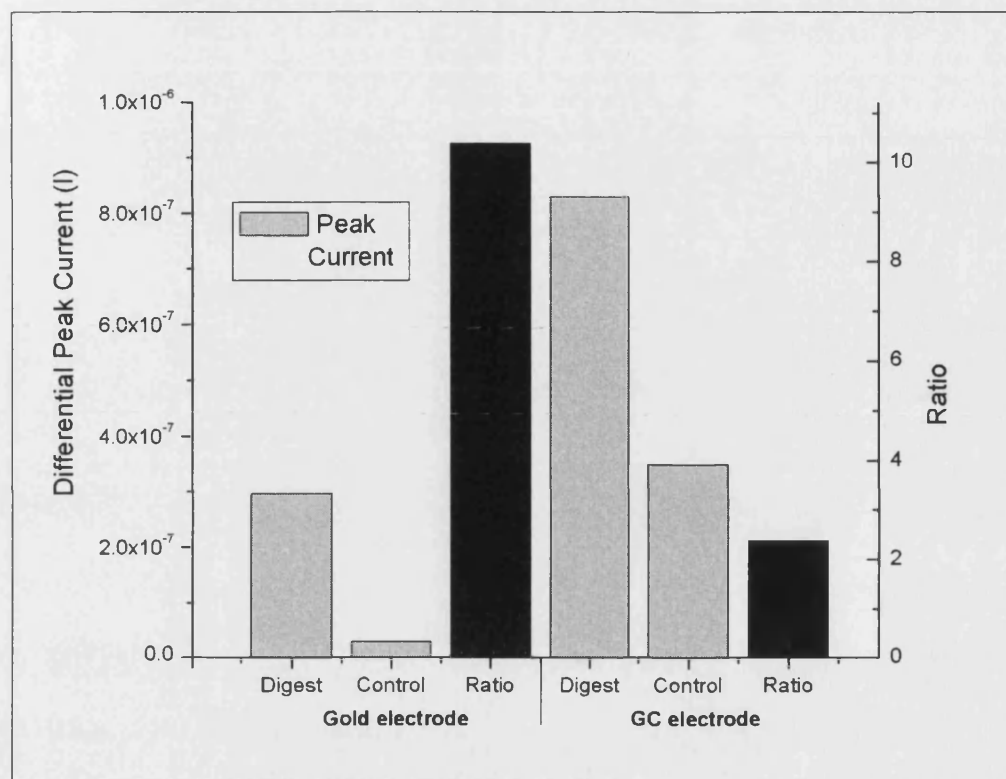
Figure 6.25 - S1 digestion of the BAPR probe.
Digest and Control assays were run for S1 endonuclease digestion of ferrocenylated BAPR probe, *oligonucleotide* 83. The assays were analysed using a gold electrode (left hand side) and a glassy carbon electrode (right hand side). The differential peak currents are given (grey bars). The ratio between the peak currents (Digest: Control) is also given (black bars).

Both assays (i.e. both oligonucleotides) give a higher response for the digested oligonucleotide, over the undigested probe (Control sample, no enzyme). This suggests that the labelling was successful and the probes can be used as hybridisation probes. The very good discrimination for the gold electrode with the BAPR probe is not mirrored in the CTR044 work and is probably misleading as the response for the control sample is low and on the sensitivity limit. If the experiment was repeated at normal (1 μM) concentration the low response of the digest sample would cause problems. The higher response and reasonable discrimination of the GC electrode makes it more useful.

This work shows that enzymatic digestion does give discrimination between the phosphoramidite labelled oligonucleotides and this can be achieved for different sequences, with the gold and GC electrodes. Phosphoramidite labelled oligonucleotides should be suitable for use in hybridisation experiments.

Amidite labelled C282YP end-point digestion

The C282Y oligonucleotide was labelled with *phosphoramidite* **28** to yield *oligonucleotide* **78**, by TibMol Biol and this is detailed below in Figure 6.26.
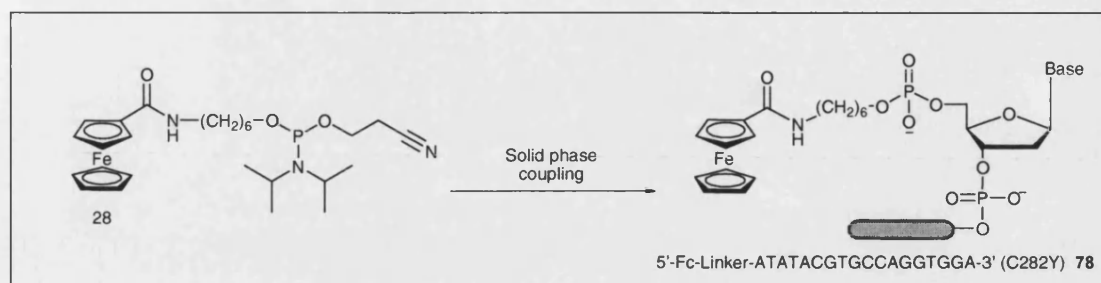
Figure 6.26 – Phosphoramidite labelling of C282Y oligonucleotide.

The T7 digestion assay uses a low concentration of probe oligonucleotide (1.0 μM) with the target in slight excess (1.2 μM), in an attempt to obtain the best possible selectivity (i.e. it ensures that all the probe oligonucleotides hybridise and are digested). Chloride based PCR buffer was also used, which will gives directly comparable results to the T7 buffer (acetate based). Mismatch assays were also run using the non-complementary target CTRAcomp. The full details are given in 2.10.2, Protocol 8. Each assay was allowed to hybridise at 20 °C for 15 minutes and then incubated at 37 °C for 1 hour to allow enzymatic digestion to go to completion. The assay is directly comparable to the later dual labelled probe work in section 6.4.1.

A GC electrode was used to get good sensitivity. Very good discrimination is obtained between the Digest and Control assays, shown in Figure 6.27, as the Control assay gives no peak. The two fully mismatched assays give comparable low results. These results and the explanation for them are directly comparable to those for the *ester* **70** labelled work, given in Figure 6.17, and this was the first time that those results had been replicated. The only difference is that the Control response is lower than that for the mismatched assays, this is postulated to be due to different fouling behaviour at the electrode surface, potentially due to the change in buffer solution.
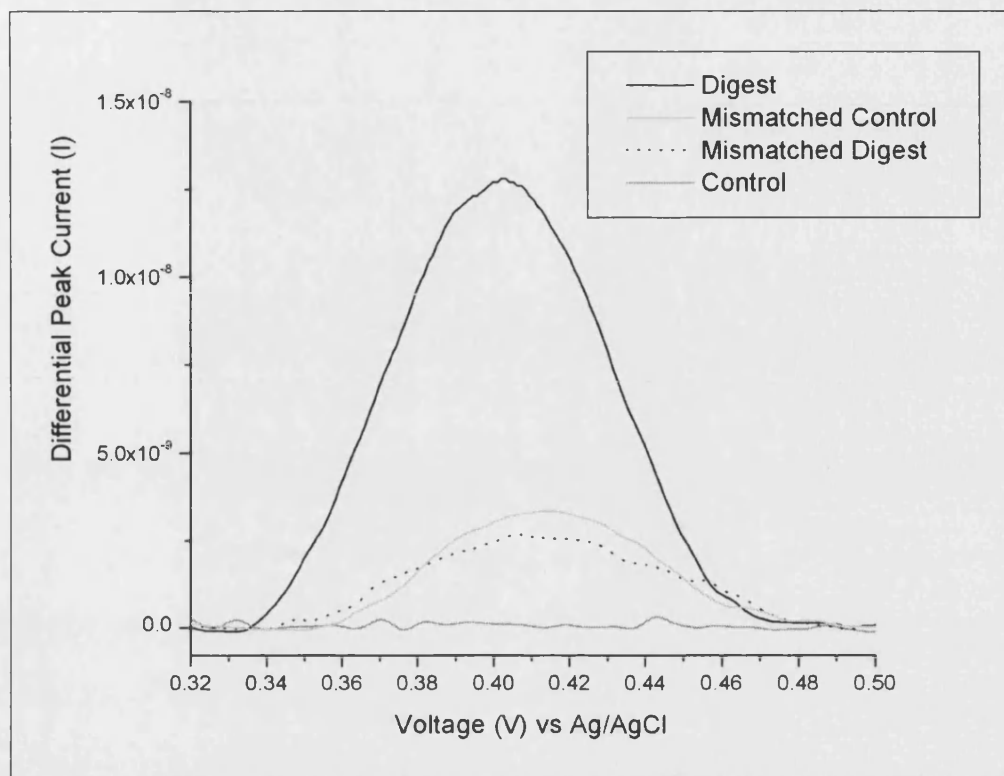
Figure 6.27 – T7 digestion of the amidite labelled C282Y duplex.
The amidite labelled C282Y probe, *oligonucleotide* **78**, is hybridised (15 minutes/ 25 °C) with its complementary target (C282YST) and then subjected to T7 digestion for 45 minutes. End-point DPV analysis was run for the assay (Digest, black line, top graph), using GC electrode. Three control assays were also analysed: Mismatched Control (mismatched target sequence, without enzyme, light grey graph); Mismatched Digest (mismatched target sequence, with enzyme, dotted black graph) and Control (complementary target, no enzyme, dark grey graph).

The result shown in Figure 6.27 is reproducible, whereby repetition of the experiment gave a reasonable Digest response (76% of original) and a zero Control response. Further repetition of the experiment would allow the errors and confidence in the result to be absolutely determined.

C282Y hybridisation time-course

A time-course was run using the same low concentration (1 μM probe) with a 15 minute hybridisation at 25 °C, followed by enzymatic digestion at 37 °C for 1 hour. After this time DPV with a GC electrode surprisingly gave no response. The lack of response may be due to electrode fouling, with the high proportion of enzyme to oligonucleotide perhaps causing the problem. The time-course was repeated using the higher 10 μM oligonucleotide concentration, at both 25 °C and 37 °C. The assay details are given in section 2.10.2, Protocol 9.

The responses for the Digest assays are reported in Figure 6.28. A Control assay, without enzyme, was run at 37 °C, but no significant response was obtained. The graphs are summarised in Table 6.1.
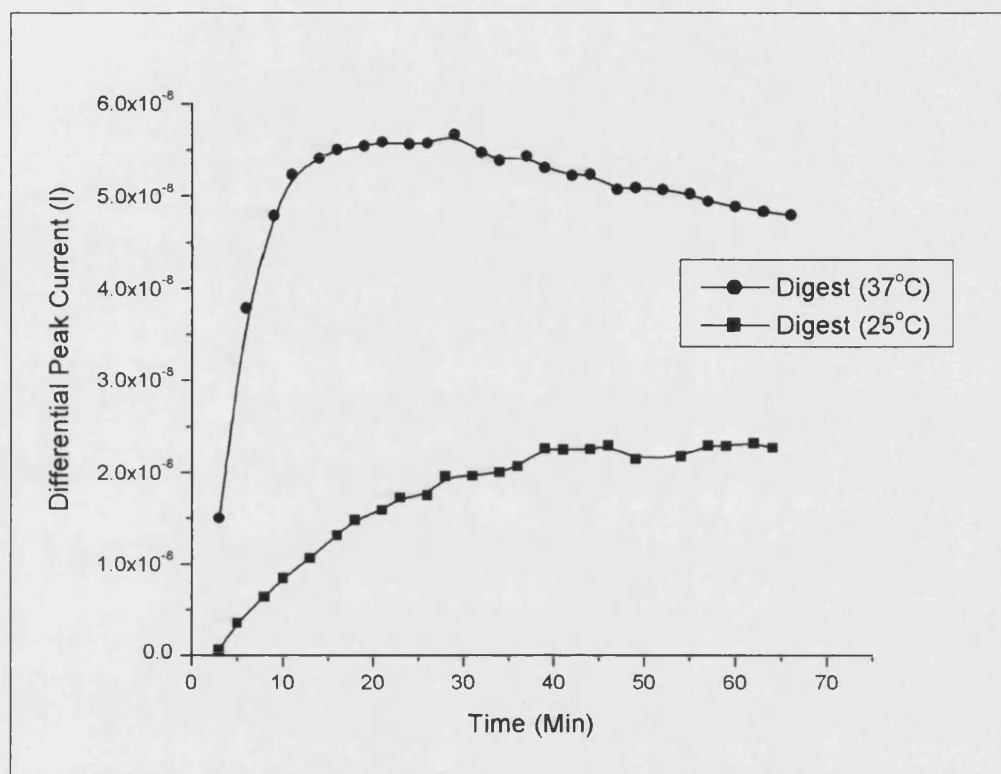
Figure 6.28 - T7 time-course graphs.
The T7 digestion of Digest assays with the C282Y probe, *oligonucleotide* 78, was undertaken at 37 °C (top graph, circular data points) and 25 °C (bottom graph, square data points).

Temperature	Maximum current time (min)	Final current (I)	Ratio
37 °C	50-60	4.8×10^{-8}	1.0
25 °C	20	2.4×10^{-8}	0.5

Table 6.1 - T7 time-course graphs.
Comparision of the Digest time-course graphs shown in Figure 6.28.

The shape of the time-course graph for 37 °C is very similar to that for the S1 digests. The maximum current is thought to occur after the majority of the probe has been digested and then decay due to electrode fouling. At 25 °C the time-course takes longer to reach a lower maximum current and does not have the early maximum. This can be explained if both enzyme action and fouling are considered. The T7 enzyme works much less efficiently at 25 °C hence, whilst the mechanism of fouling is unknown, the rate of fouling is assumed to decrease at a much slower rate. Subsequently at the lower

temperature by the time the T7 enzyme has digested all the hybridised duplex there is lots of material (including some of the enzyme) fouling the electrode. In terms of sensors these results are very good due to the low (zero) response for the Control sample.

Further amidite labelled hybridisation assays

To determine the applicability of the gene sensor it must now be shown that discrimination between the Digest and Control assays is possible for different gene sequences. Hybridisation assays were run using three amidite labelled oligonucleotide probes and with both the glassy carbon and gold electrode, to allow a comparison to be drawn between them. The details of the oligonucleotide probes and gene targets are given in Table 6.2. The full oligonucleotide sequences are given in section 2.10.1. These are labelled with the *diferrocene amidite* **82** as described in section 6.3.2.

Oligonucleotide probe	Gene target
BAPR **83**	BAST
CTR044 **84**	CTRAcomp
MC11PR **85**	MC11ST 5'CC

Table 6.2 – Detail of the hybridisation probes and their complementary targets.

The oligonucleotide concentrations were reduced to half of that used previously, due to stock limitations, however, this is not thought to cause a problem. The ratios of the components in the assay are comparable to the C282Y work and PCR buffer was used instead of T7 buffer. The full details of the assay are given in Chapter 2,

Protocol 10. The results for the three assays are given in Figure 6.29, Figure 6.30 and Figure 6.31. As expected a greater response is obtained for the glassy carbon electrode.
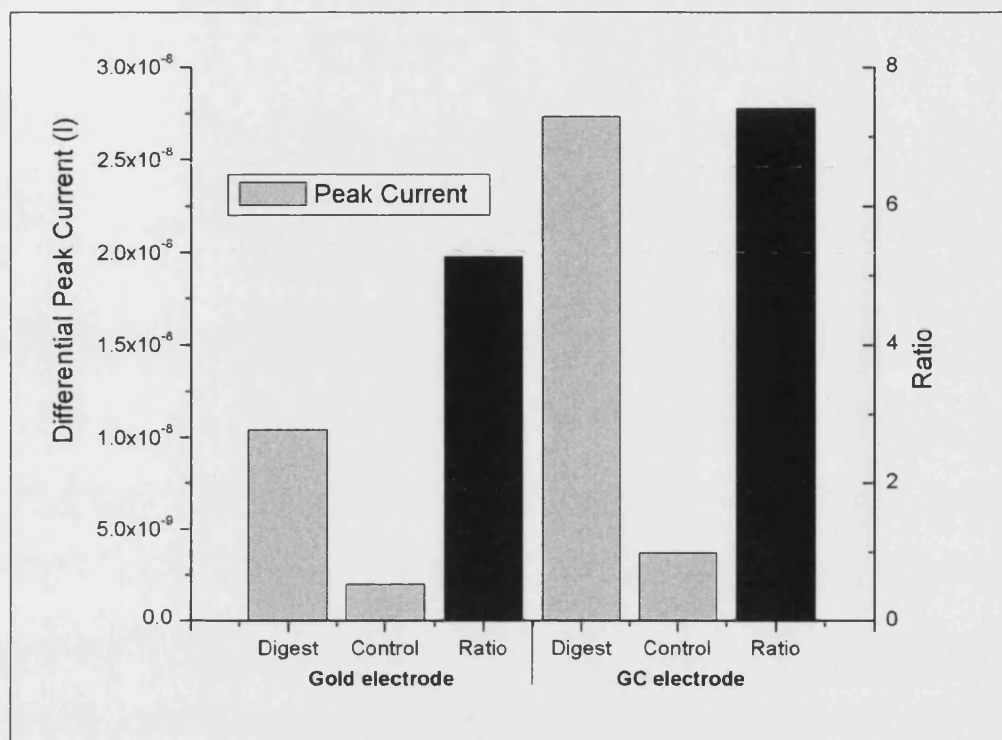
Figure 6.29 – BAPR hybridisation assays.
The DPV differential peak currents (grey bars) are given for the Digest and Control assays with the BAPR probe, *oligonucleotide* 83. The gold electrode (left hand side) and glassy carbon electrode (GC, right hand side) were used for analysis. A ratio is given (black bars) between the response of the Digest and Control assays for each electrode.
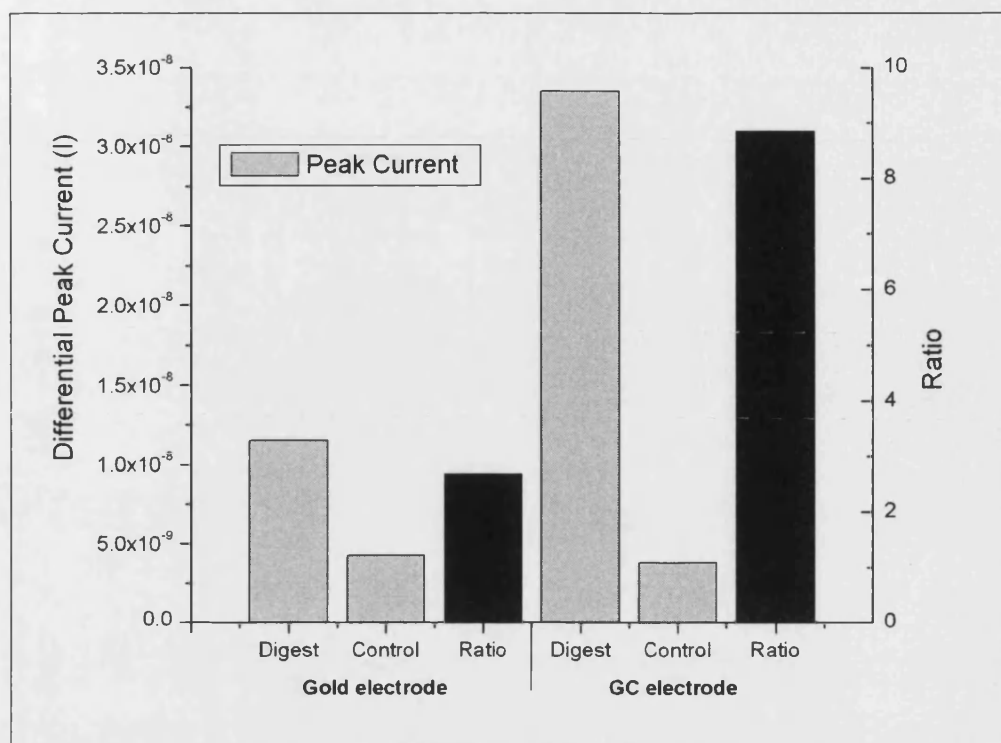
Figure 6.30 – CTR044 hybridisation assays.
The DPV differential peak currents (grey bars) are given for the Digest and Control assays with the CTR044 probe, *oligonucleotide* 84. The gold electrode (left hand side) and glassy carbon electrode (GC, right hand side) were used for analysis. A ratio is given (black bars) between the response of the Digest and Control assays for each electrode.
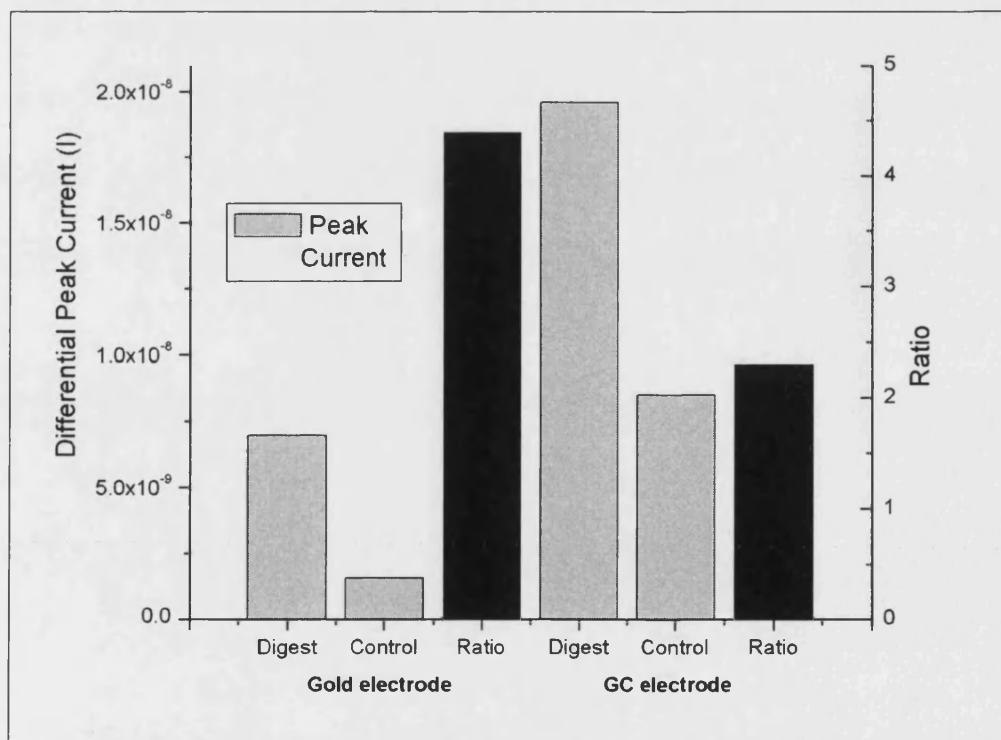
Figure 6.31 – MC11 hybridisation assays.
The DPV differential peak currents (grey bars) are given for the Digest and Control assays with the MC11 probe, *oligonucleotide* 85. The gold electrode (left hand side) and glassy carbon electrode (GC, right hand side) were used for analysis. A ratio is given (black bars) between the response of the Digest and Control assays for each electrode.

The discrimination for the different assays and varies between 2.3: 1 to 8.9: 1 (Digest: Control) for the GC electrode. This shows improved discrimination over the gold electrode for the BAPR probe, shown in Figure 6.29, and for the CTR044 probe, shown in Figure 6.30, and maintains reasonable discrimination for the MC11 assay, shown in Figure 6.31, although the discrimination for the gold electrode is better. To understand the discrimination, ratios are taken between the responses for the two electrodes (GC: gold) for the three gene probe assays (Digest and Control), which is shown in Figure 6.32. It can be seen that the key variable in the discrimination is the strength of the Control signal, with the Digest response maintaining a consistent ratio between the electrodes. The results suggest that there is variation in the formation and character of the fouling layer in the Control assay, with different oligonucleotides and surfaces, whilst the Digest assay generates small labelled fragments, which give an approximately constant response.
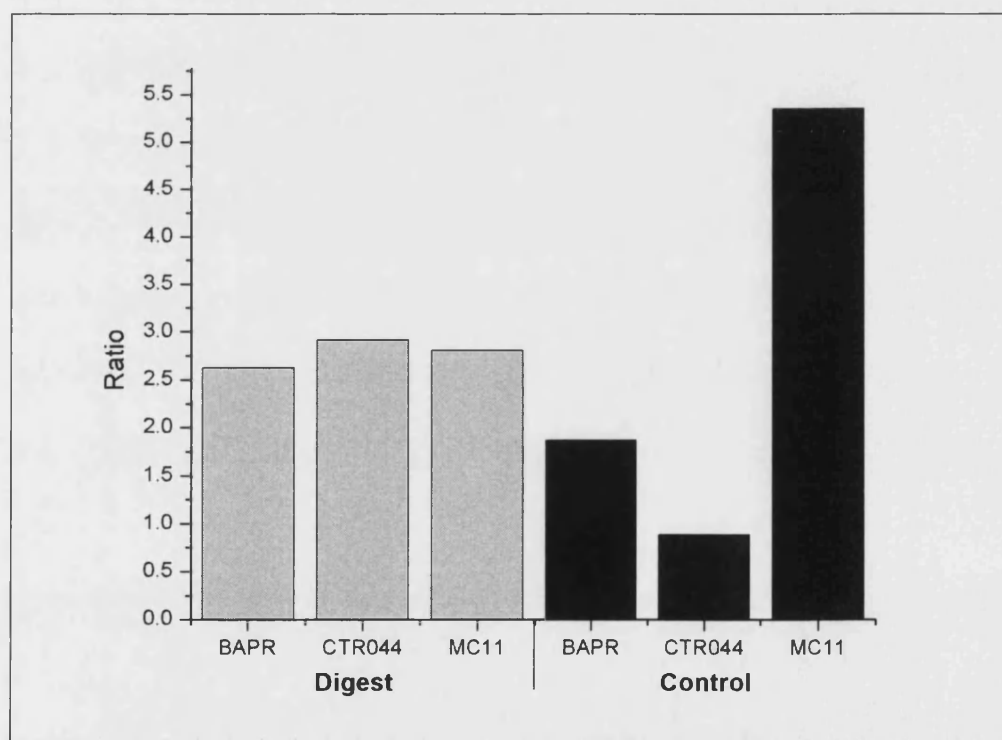
Figure 6.32 - Comparison between the DPV responses for the GC and gold electrodes. Ratios are given (GC response: Gold response) for the Digest (left hand side, grey bars) and Control (right hand side, black bars) assays. This allows the consistency of the response to be seen for the Digest and Control assays. The assay data has been reported above: BAPR probe (Figure 6.29); CTR044 probe (Figure 6.30) and MC11 probe (Figure 6.31).

T7 digestion of hybridised oligonucleotides is effective for different gene sequences and different phosphoramidite ferrocene probe labels. The response of the Digest assay is significantly higher than the Control assay, however, the key to high discrimination

appears to be the magnitude of the Control response. Both electrodes, GC and gold, have shown effective discrimination.

It must also be shown that discrimination is possible when the oligonucleotide probe is used with matched (complementary) and mismatched (non-complementary) target sequences. The matched sequences will be able to form a duplex, which can be digested by the T7 enzyme, whilst the mismatched sequences are unable to form a duplex and the probe oligonucleotide will not be digested. The assays used are given below, Table 6.3.

Probe	Complementary Target	Mismatched Target
BAPR **83**	BAST	CTRAcomp
CTR044 **84**	CTRAC	BAST

Table 6.3 – Mismatch assay work.
The complementary and mismatched targets are given for the two probes used

Both assays were analysed with DPV using a GC electrode. For both the assays the response from the Match sample is high, whilst the Mismatch sample gives no response. There is ideal discrimination between the Mismatch and Match assays and the actual traces are given below to emphasise this, in Figure 6.33 and Figure 6.34.
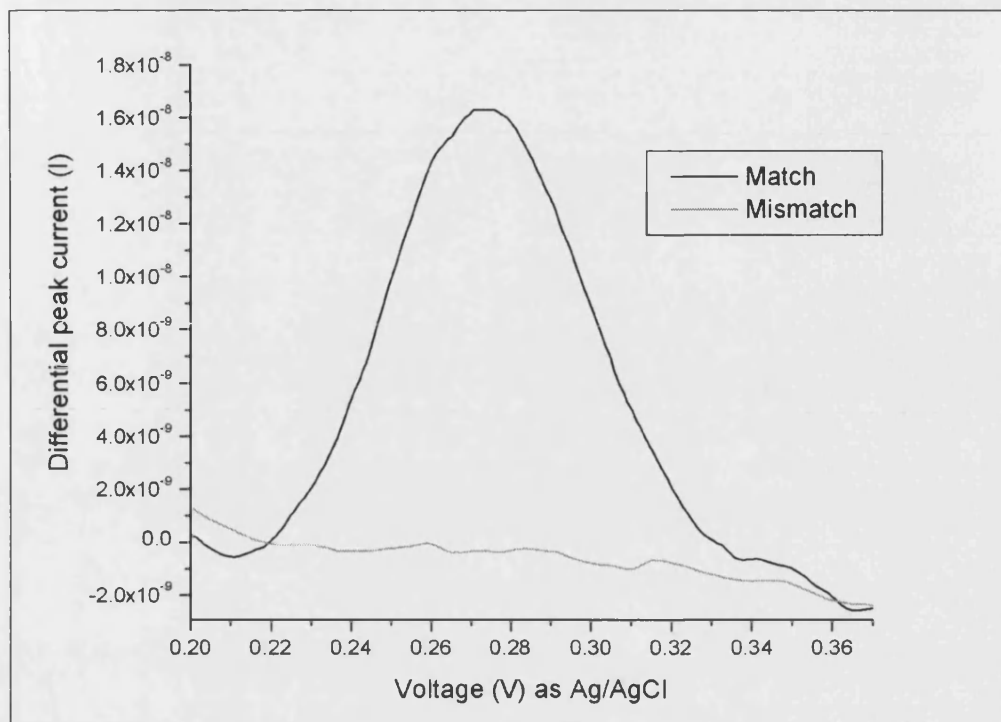
Figure 6.33 – DPV analysis of BAPR assays.
The BAPR probe, *oligonucleotide* 83, in a matched assay (fully complementary target) and mismatched assay (mismatched target) were subjected to T7 enzymatic digestion. The matched assay (black line, top) gives a good response. The mismatched assay (grey line, bottom) gives no response.
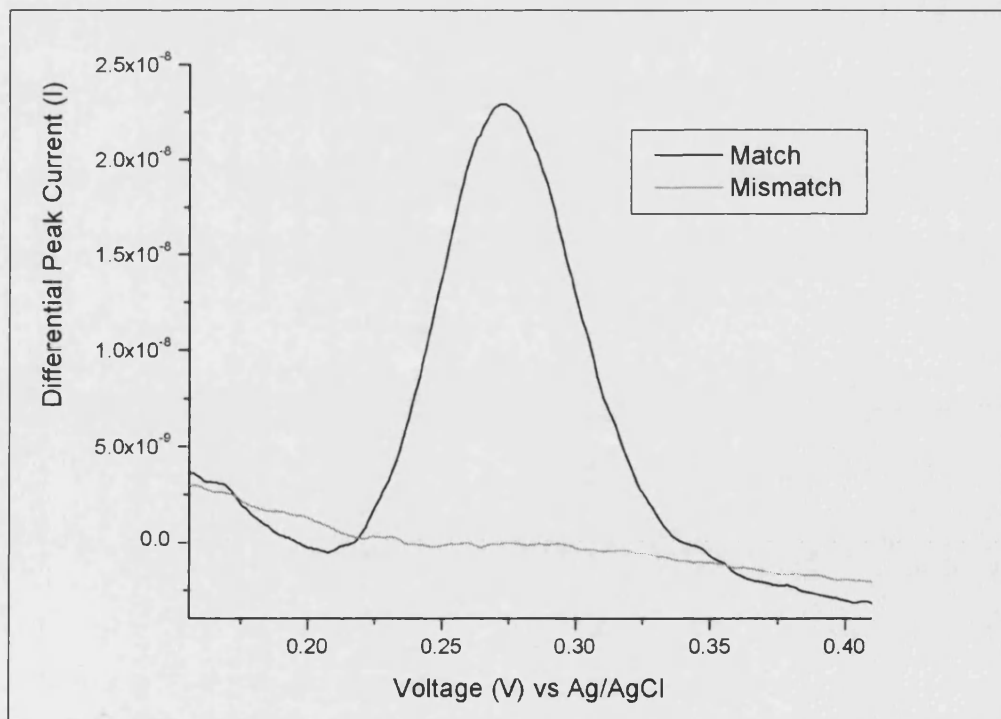
Figure 6.34 – DPV analysis of CTR044 assays.
The CTR044 probe, *oligonucleotide* 84, in a matched assay (fully complementary target) and mismatched assay (mismatched target) were subjected to T7 enzymatic digestion. The matched assay (black line, top) gives a good response. The mismatched assay (grey line, bottom) gives no response.

It has been shown that the use of a ferrocenylated probe oligonucleotide, in combination with T7 exonuclease digestion, is an effective electrochemical probe for gene detection. Discrimination has been obtained between the DPV response of the Digest and Control (no enzyme) samples for three different gene sequences, probe and target. Discrimination has also been shown between Match (complementary gene target) and Mismatch (mismatched target) assays. This discrimination is detectable with both GC and Au electrodes. It is proposed that the DPV Faradaic response from the assays is a combination of the current from the diffusion of the ferrocenylated species to the electrode surface and the action of a fouling layer, which often has an electrochemical response of its own. The fouling has not been explicitly investigated here.

The scope of the above results, which use different electrodes and probe sequences, strongly suggests that the measurements are real and valid; however, the absolute peak current values are affected by a range of factors, the most important of which is the surface condition of the electrode. The absolute peak currents must be treated with caution until further work can be undertaken to determine the reproducibility and error in the results. Ideally this would be achieved by preparing and using multiple electrodes. Consecutive measurements cannot be taken on the same electrode as the response always falls.

6.4   Validating the T7 hybridisation gene sensor

The DNA hybridisation gene sensor is based on enzymatic digestion of a complementary duplex. This enzymatic digestion will be corroborated by using complementary analysis using a dual labelled fluorescent probe and fluorescent detection.

Differences in the diffusion coefficients of digested and undigested probe sequences are thought to be one of the major factors behind the electrochemical discrimination between these assays. Potential step amperometry will be used to measure the diffusion coefficients of the ferrocenylated probes, before and after S1 and T7 enzymatic digestion.

6.4.1 Fluorescent analysis of enzymatic digestion

The enzymatic digestion is followed using a dual labelled fluorescent probe. This oligonucleotide has the C282Y sequence and it is 5' labelled with 6-FAM labelled and 3' labelled with 6-TAMRA. T7 exonuclease digestion of the probe/target duplex is summarised below in Figure 6.35.
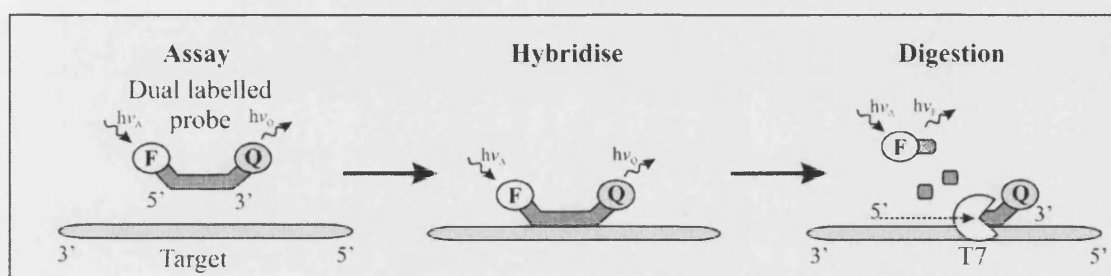
Figure 6.35 – Summary: use of dual labelled probe to follow T7 exonuclease digestion. This is a reproduction of Figure 5.11.

A time-course was run to follow the T7 enzymatic digestion of the C282Y probe/target duplex at 25 °C, using the Roche LightCycler. Full experimental details are given in section 2.10.2, Protocol 11. It should be noted that the assay concentration were a factor of 10 less than with the electrochemical assay, detailed in section 2.10.2, Protocol 9, as the high concentration of the dual labelled probe saturated the response for the fluorescence detection. The time-course is reported below in Figure 6.36.
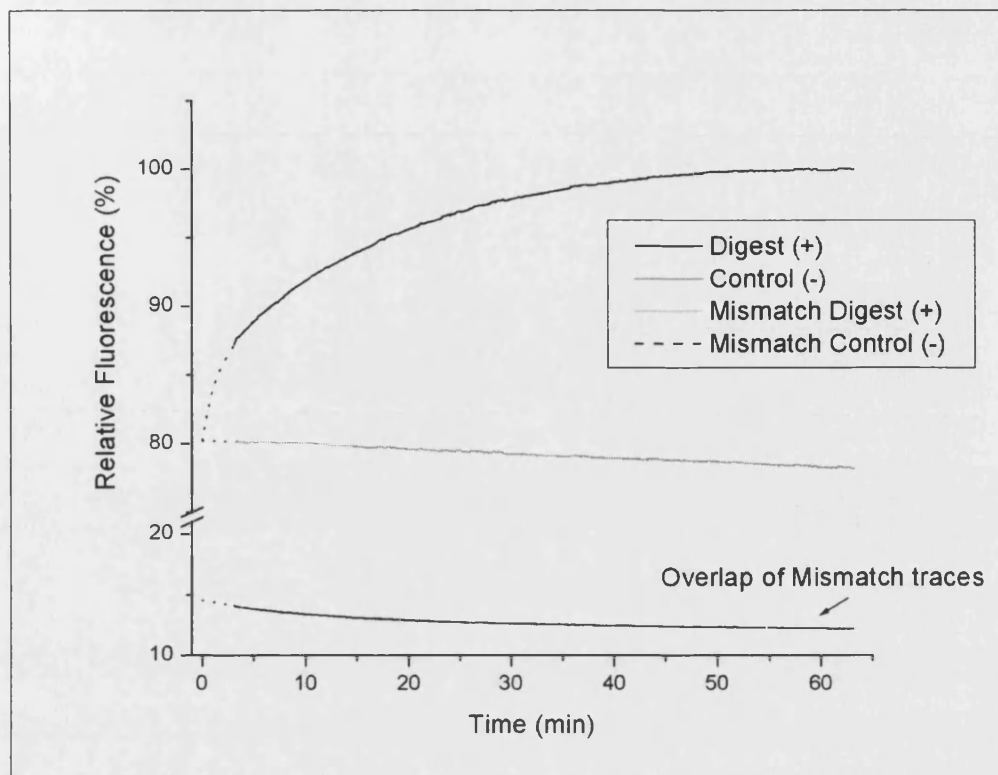
Figure 6.36 – LightCycler time-course: T7 digestion of C282Y duplex.
The fluorescent response is measured over time at 25 °C. The fluorescence values are relative to 100% fluorescence for the final Digest assay reading. The complementary Digest assay (black line, top) contains: C282Y Dual Labelled Probe (1.0 μM); complementary target (C282YST, 1.2 μM); T7 buffer; BSA and T7 exonuclease (0.01U / μL). The complementary Control assay (dark grey line, middle) omits the enzyme. The Mismatch Digest (light grey line, bottom) and Mismatch Control (dashed line, bottom) assays duplicate the other assays, but use a mismatched CTRAcomp target.

The fluorescence of the Digest assay increases with time (80% to 100% fluorescence), whilst that of the Control assay actually decreases slightly from the initial 80%. This strongly supports the enzymatic digestion theory and it is the only realistic way, by which the fluorophore (6-FAM) and quencher (6-TAMRA) can become spatially separated, leading to an increase in fluorescence. The assays with the mismatched target sequences (Mismatched Digest and Mismatched Control) both give a much lower fluorescent response. In these assays, the probe oligonucleotides do not hybridise with the mismatched targets and remain single stranded and flexible. The coiling of the oligonucleotides will bring the fluorescent labels closer together and aid FRET quenching. In contrast the Control assay forms a rigid dsDNA duplex where the fluorescent labels are further apart and therefore the FRET quenching is less efficient.

Analysing the graph in more detail shows that the enzymatic digestion in the Digest assay is virtually (95%) complete after 33 minutes, this is relative to the initial 80% fluorescence of the Control sample. Comparing these time-course results to those for electrochemical detection (ferrocenylated oligonucleotides, 25 °C trace, Figure 6.28) shows that the time-courses (at 25 °C) are very similar in shape and both reach their maximum value after 60 minutes. The electrochemical response takes slightly longer to reach this maximum. The fluorescent time-course was repeated at 37 °C, but the digest was at a maximum, constant value as soon as the analysis started. This was after an unavoidable 3 minute delay, which is integral to the operation of the LightCycler. Absolute comparisons between the two graphs must be done with caution, primarily due to differences in component concentration of the two assays. The labels also have inherent structural differences between them, which may effect the action of the exonuclease enzyme. However, it is reasonable to assume that the small labelling groups do not particularly inhibit the enzyme (FAM/TAMRA dual labelled probes are specifically designed for use in PCR with exonuclease enzymes). A potentially more significant issue is the physical differences between the two analysis cells. The LightCycler cell is a thin glass capillary, with a much higher surface to volume ratio than the electrochemical cell, which may affect the overall behaviour of the assay if a significant amount of the enzyme becomes surface supported.

In summary, the results of the fluorescence time-course show that hybridisation only occurs between the probe and the fully complementary target (shown by an increase in fluorescence) and that T7 enzymatic digestion results in the digestion of the probe oligonucleotide (shown by a further gradual increase in fluorescence). It is probable that this will occur through the expected mechanism of enzymatic digestion.

6.4.2 Determination of diffusion coefficients

The steps required in determining the diffusion coefficient of a ferrocenylated oligonucleotide species are:

- Run DPV to determine the position of the electropotential. A voltage step can then be chosen which encompasses the DPV peak.

- Run potential step amperometry with Digest, Control and buffer assays. The Digest and Control assays must be resolvable from the buffer for the determination of D to be possible.

- Determine D, by applying the Cottrell equation to the valid data. The observed (overall) current generated in the potential step amperometry is due to Faradaic current and charging current. The Faradaic current is determined by subtracting the buffer trace from the assay trace. The initial data (high rate of change, high error) and final data (low rate of change, high proportion of error due to noise) are omitted.

Electrode evaluation

Exploratory work was undertaken with the amidite labelled C282Y probe, *oligonucleotide* 78, using the GC electrode to determine if discrimination could be obtained between amperometry traces for the Digest and Control assays for both the S1 endonuclease digestion of the labelled oligonucleotide and T7 exonuclease digestion of the hybridisation duplex. These assays were run at high concentration (10 µM probe). Assay details and the protocol for the potential step amperometry are given in section 2.10.2, Protocol 12. These traces were not reported as no discrimination was obtained between them.

Repeating the analysis with the BDD electrode did give discrimination between the Digest and Control traces.

Determination of S1 diffusion coefficients

The S1 digestion was undertaken for three amidite labelled probes: mono ferrocenylated C282Y, *oligonucleotide* **78,** and diferrocenylated BAPR and CTR044, *oligonucleotides* **83** and **84**. Potential step amperometry traces for the Control (undigested probe), Digest and buffer (buffer with enzyme) were measured. Details are given in section 2.10.2, Protocol 12.

The calculation of the diffusion coefficient will be illustrated for the S1 assay with the ferrocenylated C282Y oligonucleotide. The raw data for the S1 assay is given in Figure 6.37. The buffer trace is then subtracted from the probe and Digest traces to give two graphs, which are similar in appearance (not shown).
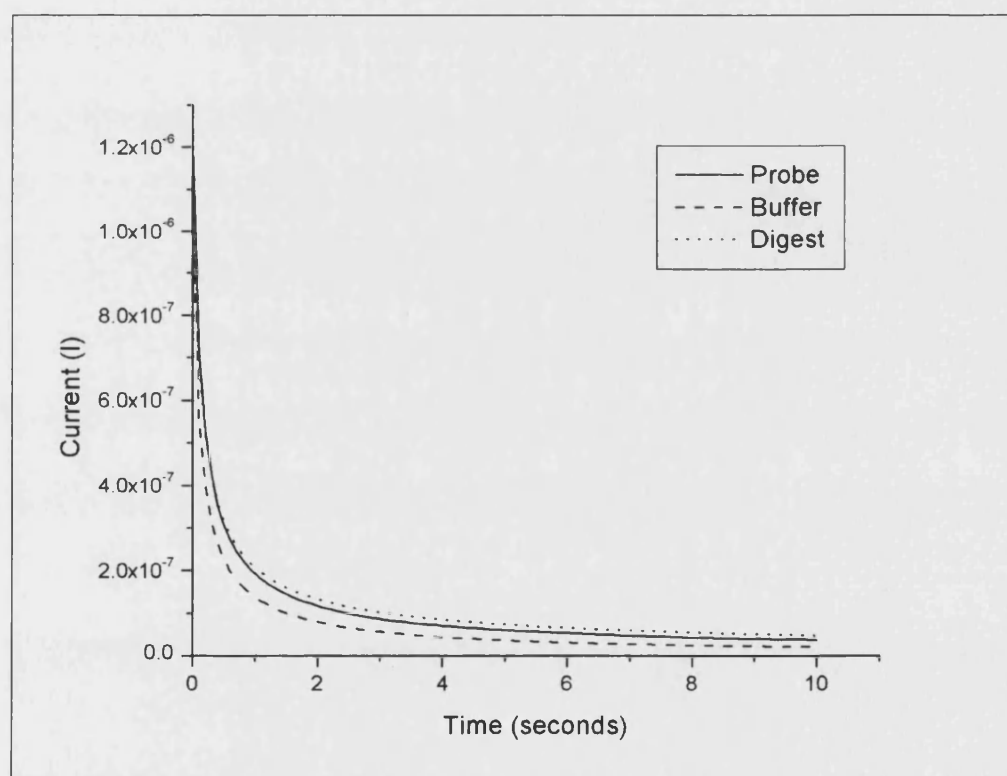
Figure 6.37 – Potential step amperometry: S1 digestion of C282Y probe, *oligonucleotide* 78.
The potential step amperometry traces for the buffer (dashed line, bottom), probe assay (full line, middle) and Digest assay (dotted line, top) are shown.

The diffusion coefficients will be determined, by utilising the rearranged Cottrell equation, described in section 5.8.3. The data from the amperometry graphs is plotted as $|1/i|^2$ against t, as shown in Figure 6.38 and Figure 6.39. The R^2 value is good for

both graphs, due to the high number of data points and reasonable fit. It is reasonable to omit the very early data points (very rapid change in current and therefore high error) and the later data points (very little change in current and therefore a high contribution of noise). Both graphs have a kink at about 4 seconds, which is probably due to an artefact of the system. Even if this was absent the graphs begin to curve slightly after about 3.5 seconds, so the data after this point was omitted.
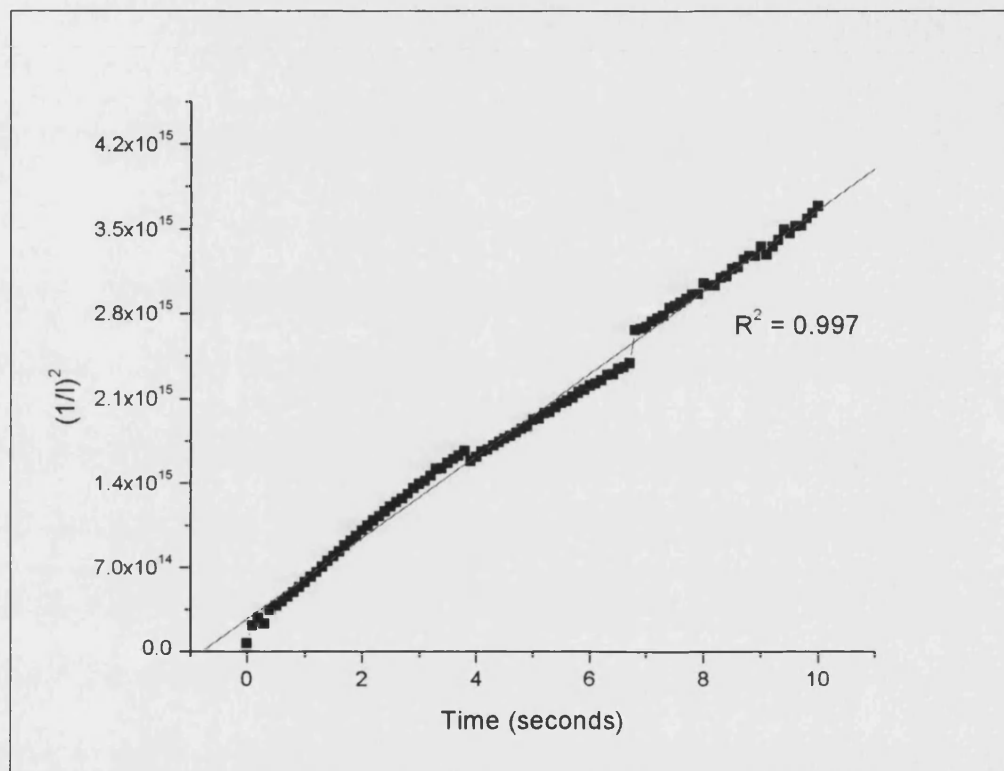
Figure 6.38 – Determination of D: probe assay.
The potential step amperometry data for the Control assay containing the C282Y probe,
oligonucleotide **78, is plotted as** $\left|1/i\right|^2$ **against t.**
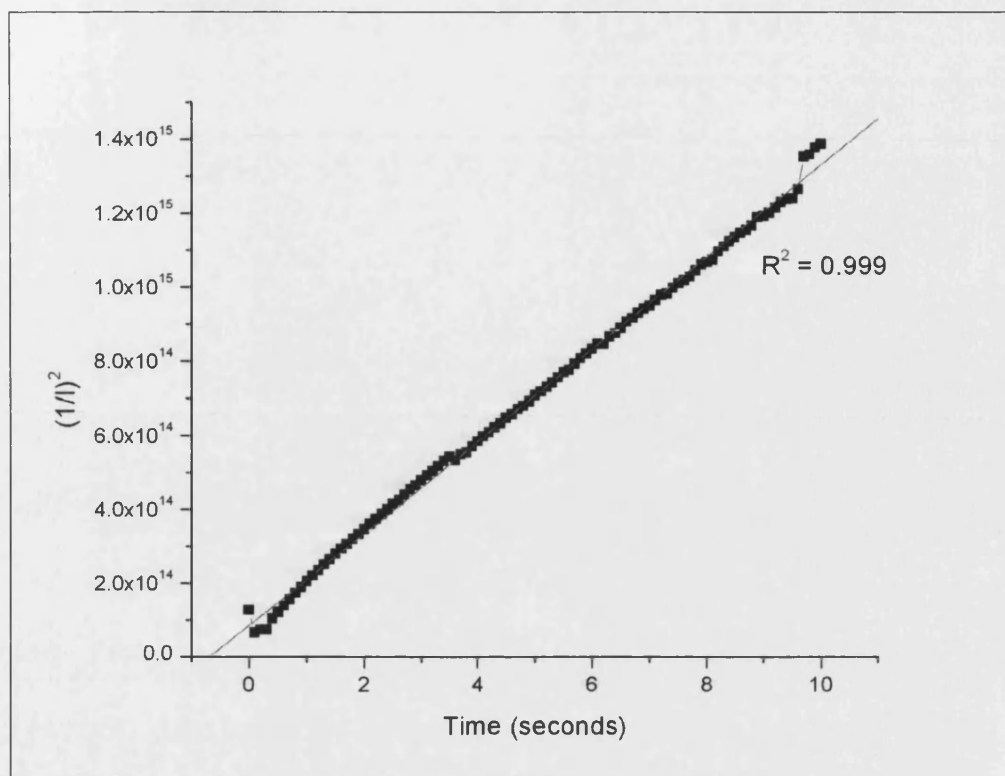
Figure 6.39 - Determination of D: Digest assay.
The potential step amperometry data for the S1 Digest assay of the C282Y probe, *oligonucleotide* 78, is plotted as $\left|1/i\right|^2$ against t.

The above graphs were replotted using the data points between 0.4 and 3.5 seconds (not shown). The gradients were; Probe = 4.0×10^{14} (2 s.f.), $R^2 = 0.999$ and Digest = 1.4×10^{14} (2 s.f.), $R^2 = 0.999$. The calculation of the diffusion coefficient for the digest fragments, based on Figure 6.39, is given below:

$$D = \frac{\pi}{(nFAC_\infty)^2 . gradient}$$

Where: $n = 1e^-$
             $F = 9.64853 \times 10^4 \ Cmol^{-1}$

$$A = \pi . \left(\frac{1.5 \times 10^{-3}}{2}\right)^2 = 1.8 \times 10^{-6} m^2$$

C_∞ = Bulk conc. of reactant = 10 μM = 0.01 molm^{-3}
$D = 7.4 \times 10^{-9} \ m^2 s^{-1}$ (2 s.f.).

The diffusion coefficients for the other S1 assays were calculated in an identical way and are compared in Figure 6.40.

293
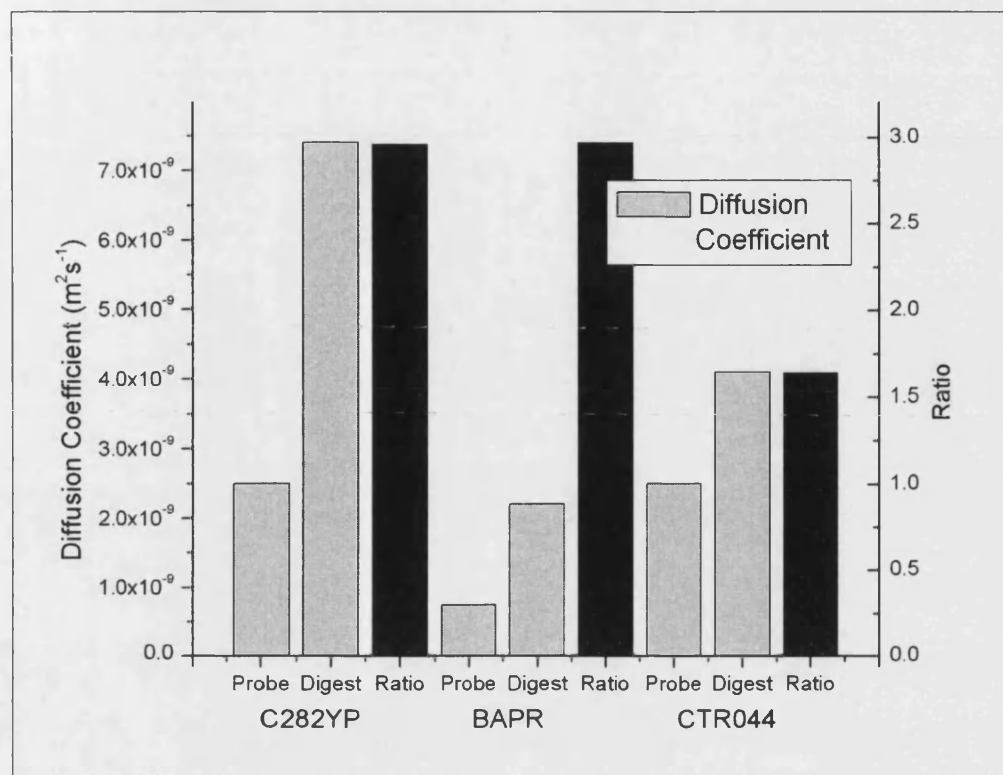
Figure 6.40 – Comparison of diffusion coefficients for S1 assays.

For all three of the assays, the digested fragments have higher diffusion coefficients which range from 1.5 to 3 times that of the undigested probes. These results are very significant. As discussed before, these measured diffusion coefficients may not be absolute, but the speed of the measurement limits the fouling as much as possible and substantial fouling would be required to totally prevent the ferrocene electron transfer. It is very likely that this difference in the diffusion coefficients is the basis for some of the discrimination in the peak height between the Control and Digest assays, in the gene sensor. The observed difference in diffusion coefficients is attributed to the different sizes of the digested and undigested oligonucleotides and perhaps the structure they adopt in solution. Evidently if enzymatic fouling of the electrode occurs, which blocks electron transfer in the Digest assay, the value of the absolute diffusion coefficient would be higher than calculated.

The fact that larger diffusion coefficients are calculated for the digested oligonucleotide than for the probe for all three probe sequences suggests that the results are real and that there is significant discrimination between them (multiple repeats would be required to mathematically prove this). Confidence in the validity of these experimental results is

increased by comparing the diffusion coefficient to a known complex. Ferricyanide (III) ions [Fe(CN)$_6^{3-}$] have a diffusion coefficient of 6.3×10^{-9} m^{2}s^{-1} (Adams 1969) which is in the same order of magnitude as all the results obtained.

Determination of T7 diffusion coefficients

The T7 digestion was undertaken for the duplexes of three amidite labelled probes: mono ferrocenylated C282Y, *oligonucleotide* **78,** and diferrocenylated BAPR and CTR044, *oligonucleotides* **83** and **84**. Potential step amperometry traces for the Control (undigested probe), Digest and buffer (buffer with enzyme) were measured. Details are given in section 2.10.2, Protocol 12. The results are given in Figure 6.41.
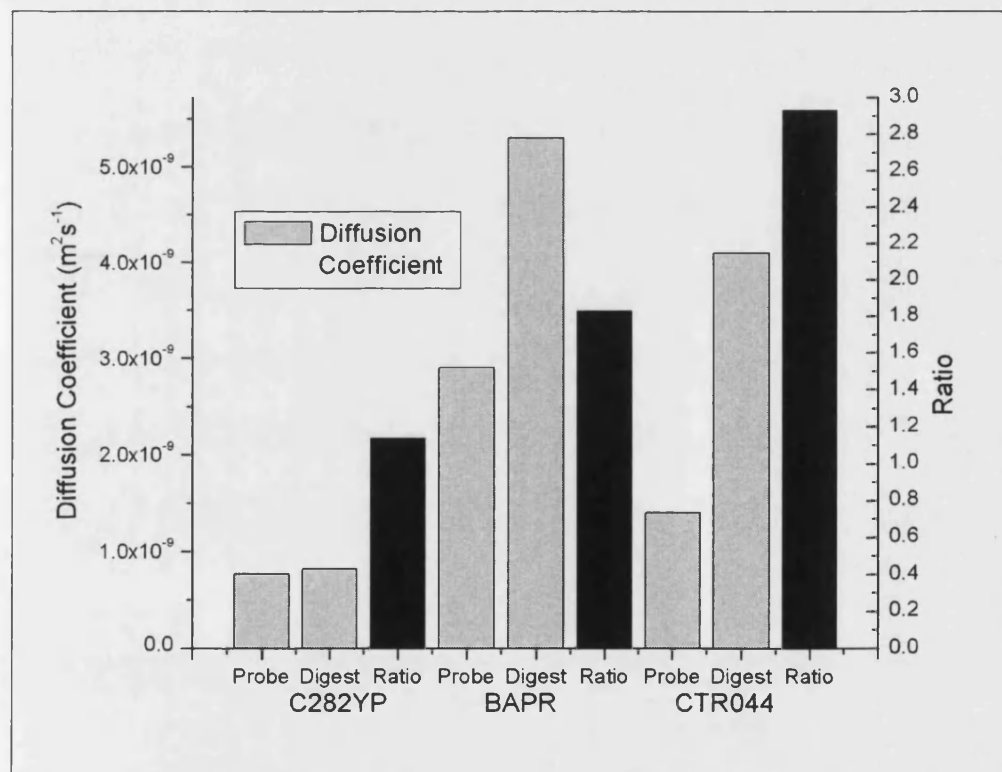
Figure 6.41 – Comparison of T7 Diffusion coefficients.

In this case both the BAPR and CTR assays show good discrimination between the diffusion coefficients of the digest and control assays, whilst the C282Y assay (reproducibly) does not. The C282Y either does not have an absolute difference in diffusion coefficients between the digested and undigested oligonucleotide or fouling

effects (which were in evidence in the DPV traces) affect the response. This might be a factor in the poor discrimination in the initial C282Y work.

Comparison of diffusion coefficients

The calculated diffusion coefficients can be compared between the S1 and T7 assays for each probe , in Figure 6.42.
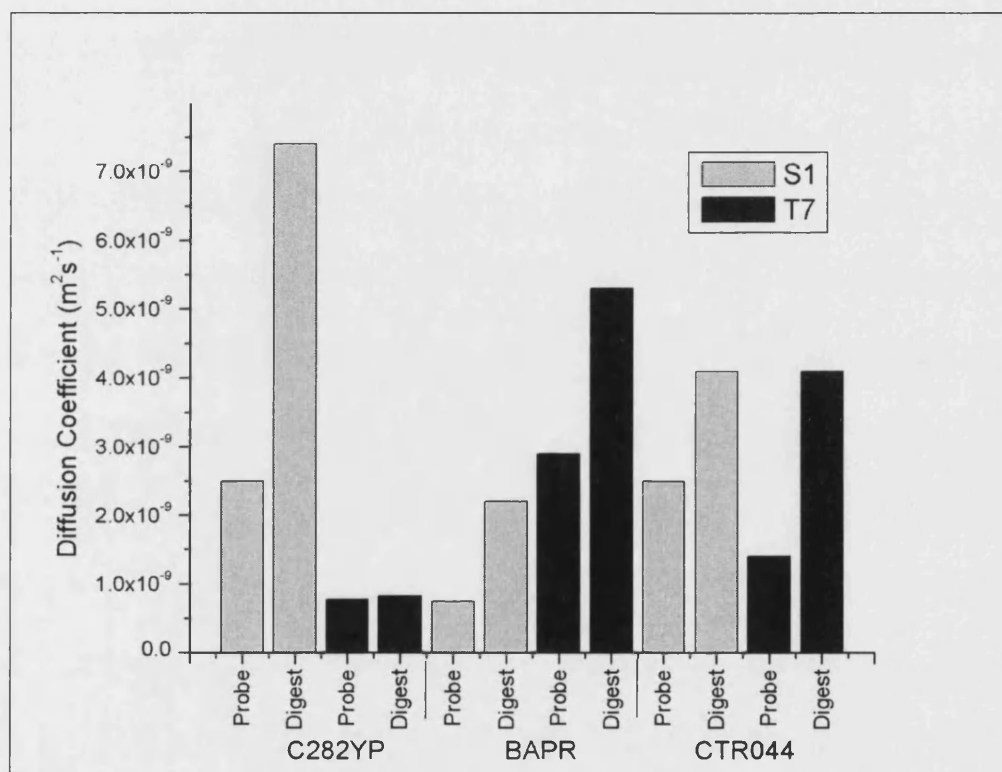
Figure 6.42 - Comparison between S1 and T7 diffusion coefficients for different assays.

It would have been interesting to find a trend (i.e. significant differences) between the diffusion coefficients of the digest fragments after either S1 or T7 digestion, which might highlight different enzyme behaviour towards the substrates i.e. different sized fragments are produced on enzymatic digestion. However, this is not the case. Attention should be drawn to the difference in the diffusion coefficients for the probe assays for each oligonucleotide as they would have been expected to be more comparable. The only difference between these assays is the type of buffer being used and this would not be expected to influence the diffusion coefficients dramatically, unless it significantly affects the preferred orientation of the oligonucleotide in solution.

With a view to this, direct comparisons should not be made between these results, until multiple repeats have been done to confirm their validity, which would eliminate the potential effects of electrode surface variation. This caution is advised as small differences in gradient of the amperometry graph can have a large effect on the calculated value of D.

In summary, initial measurements of the diffusion coefficients of the probe oligonucleotides, before and after digestion, showed that digestion of the large probe oligonucleotides (either directly by S1 endonuclease or after hybridisation by T7 exonuclease) gives smaller ferrocenylated fragments with higher diffusion coefficients. As a ferrocenylated species with a higher diffusion coefficient gives a higher DPV response, as detailed in section 2.5.7, this is seen as one of the major factors in discrimination between the digested and undigested assays.

6.4.3 Gene sensor with PCR amplicon

It has been shown that discrimination can be obtained between synthetically produced matched and mismatched oligonucleotide gene sequences, using a ferrocenylated probe oligonucleotide. This probe oligonucleotide shall now be applied to the detection of a gene sequence on a PCR amplicon, which is produced in a PCR.

The target sequence is amplified by PCR, through the selection of the appropriate primers. The PCR amplicon is then heated (to denature it) in the presence of the ferrocenylated oligonucleotide probe. On cooling the probe will form a duplex with the ssDNA amplicon and this duplex can be digested with the T7 exonuclease. This is summarised in Figure 6.43.
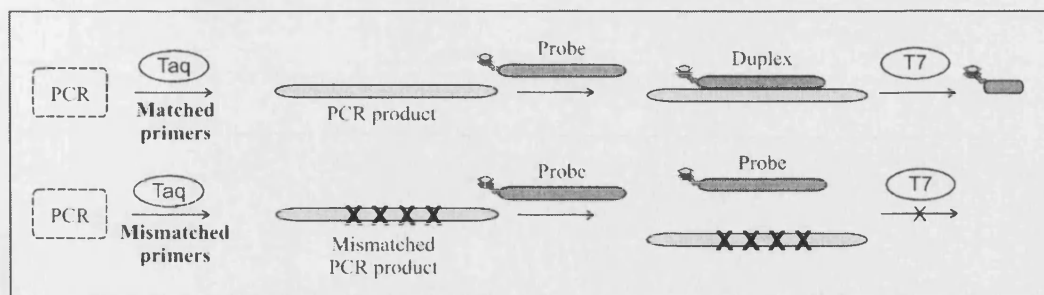
Figure 6.43 – Summary of end-point PCR analysis.
This is a reproduction of Figure 5.25, which is given in the experimental plan, section 5.9.

Matched primers are used to synthesise the beta actin gene from human genomic DNA, which has a fully complementary sequence to the BAPR probe. Mismatched primers are used to synthesise the ACADM (medium chain acyl-CoA dehydrogenase) gene, which is fully mismatched to the probe sequence. The full assay details are reported in section 2.10.2, Protocol 13. After PCR, both assays are interrogated using an *ester* **70** labelled BAPR probe, *oligonucleotide* **79**. The assays are analysed by DPV, using a GC electrode, and the results are shown in Figure 6.44.
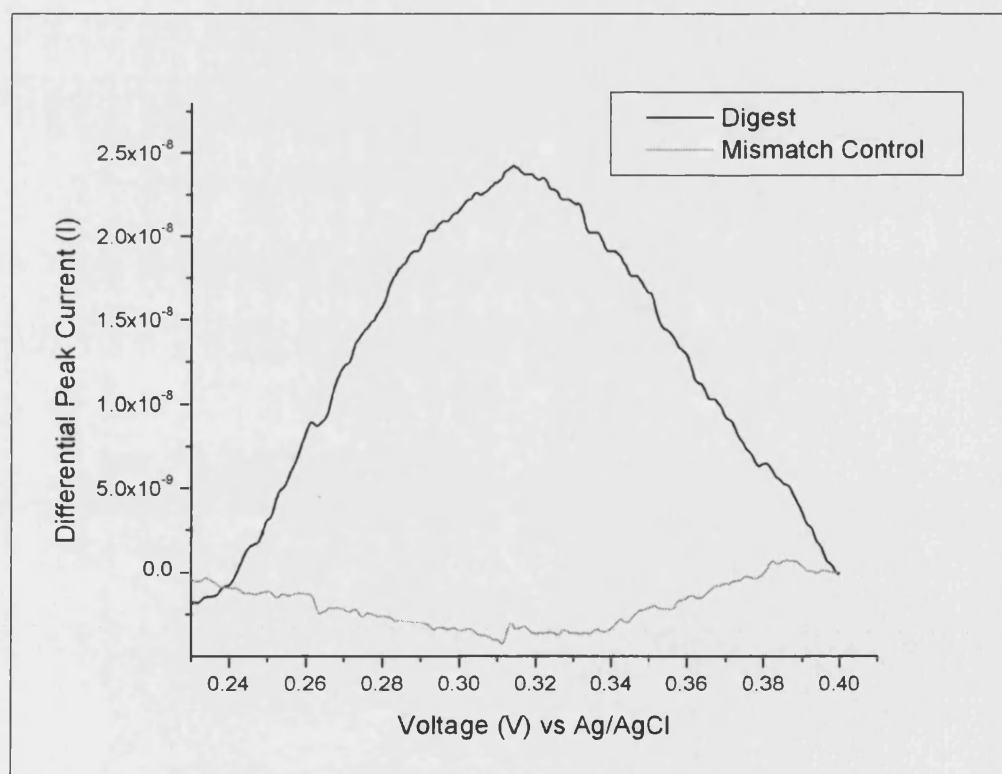
Figure 6.44 – DPV end-point analysis of PCR amplicons.
The DPV analysis is shown for interrogation of PCR amplicons with a BAPR probe, *oligonucleotide* **79**. The response for the matched amplicon (Digest sample, solid line) shows a peak, whilst the response for the mismatched amplicon (Mismatch Control sample, dotted line) does not show a peak. Analysis was done with a GC electrode.

The matched amplicon gives a positive response by DPV, whilst the mismatched amplicon gives no response. The detection of the PCR amplified gene sequence has been successful.

6.4.4 *In situ* PCR analysis

In situ PCR detection, summarised in Figure 6.45, was successfully undertaken by co-workers at Molecular Sensing PLC, UK. This was done using ferrocene amidite labelled oligonucleotide probes.
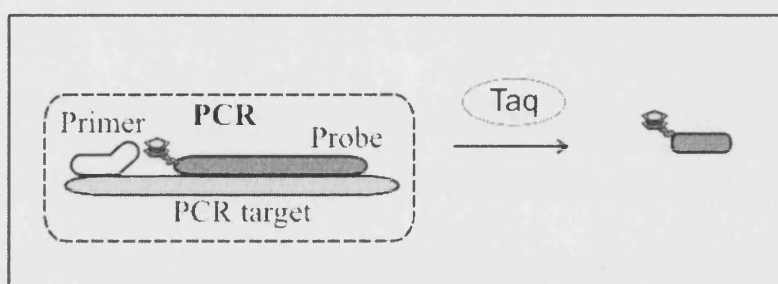
Figure 6.45 - Summary: PCR *in situ* analysis.

This work is subject to patent applications (Molecular Sensing 2004) and will not be discussed here.

6.5   Conclusions and further work

6.5.1 Conclusions

The overall aim of this work was to illustrate that an electrochemical DNA gene sensor could be developed, based on a ferrocene labelled probe oligonucleotide, which would allow gene sensing to be realised. After the recognition event (hybridisation) it was envisaged that enzymatic digestion of the duplex would increase the electrochemical response of the assay (by DPV), thereby giving discrimination between the duplex (gene recognition) and probe (no gene recognition). This has emphatically been achieved using a simple, unmodified electrode, a widely available method of electrochemical detection (DPV) and a standard (BAS) electrochemical cell. The sensor work is successful with both synthetic gene targets and PCR amplicons. The work is

currently being applied to *in situ* PCR detection. The development of the work gave valuable information on the action of the enzymes (S1 and T7), together with a practical understanding of the system. The important detail from this will now be highlighted.

Work using the S1 enzyme, given in section 6.2, showed that DPV could be used to detect a significant increase of the electrochemical response of labelled ssDNA after enzymatic digestion. The use of gel electrophoresis then showed that these results were directly related to the enzymatic digestion. Using time-course measurements and repeating them with a wash step, allowed it to be inferred that the condition of the electrode surface is crucial to the sensitivity of the system and is significant factor in the observed discrimination. The discrimination between Control and Digest assays is much higher after a time-course measurement than after one end-point measurement.

T7 digestion of an equivalent ferrocene labelled hairpin oligonucleotide, described in section 6.3.1, showed that discrimination of the electrochemical response was also possible for the digestion of dsDNA. The time-course analysis highlighted the significant role that the electrode surface plays in the discrimination and improved the discrimination.

The success of the T7 enzyme enabled the approach to be applied to the digestion of DNA hybridisation duplexes, detailed in section 6.3.2, and therefore to the development of a gene sensor. If the target oligonucleotide was not complementary to the ferrocenylated probe oligonucleotide no duplex would form and digestion would not be possible. Although good discrimination was obtained between the Match (complementary) and Mismatch (non-complementary) assays, for the initial experiment, this discrimination fell when the work was repeated. The oligonucleotide labelling and condition of the electrode surface were identified as key variables in the sensor assay, however, investigation into the oligonucleotide labelling using S1 endonuclease digestion gave poor discrimination, which could be attributed to either poor labelling or problems with the electrode surface. To ensure high labelling efficiencies and purity, the labelling protocol was changed to the more expensive use of ferrocenylated amidite linker molecules. The use of amidite labelled probes enabled the initial gene sensor results to be replicated.

The suitability of ferrocenylated oligonucleotides as hybridisation probes was then determined and good discrimination was obtained between the Matched sequence and Mismatch sequences. The earlier discrimination between Digest and Control (no enzyme) assays was also retained. Different oligonucleotide probe sequences were successfully used, as were different ferrocenylated labels. The success of these assays allowed different electrode materials to be evaluated. Both glassy carbon and gold electrodes gave good discrimination between assays, although glassy carbon had a larger electrode area and therefore a higher DPV response. For this reason it was more widely used. In both cases the condition of the electrode surface was very important and care had to be used with the polishing protocol.

Complementary techniques were used, in section 6.4, to gain a better understanding of the assay and validate the results. The use of fluorescent labels in a dual labelled probe allowed the enzymatic digestion to be followed using a LightCycler (Roche), without any mass transport to an electrode, and comparable results were obtained to the electrode time-course experiments.

The high labelling efficiency of the amidite label allowed potential step amperometry to be applied to the system and for diffusion coefficients to be calculated for the oligonucleotides before and after enzymatic digestion. This was done for both S1 endonuclease with a ferrocenylated probe and for T7 exonuclease with a ferrocenylated probe, hybridised to a complementary target. Although further, precise work is required to accurately determine the absolute values and their errors, discrimination was obtained for each oligonucleotide before and after enzymatic digestion. The smaller digested fragments each had a larger diffusion coefficient and therefore could diffuse more quickly to the electrode surface.

The characteristics of the fouling layer of the electrode surface have been debated primarily for the S1 assay, in section 6.2.3, and also for the T7 assay, section 6.3.2. Depending on how the species in the assay adsorb onto the surface, it is proposed that this layer can block the access of ferrocenylated oligonucleotides and digested fragments to the surface, whilst at the same point generating its own electrochemical response from the ferrocene labels in its constituent parts. The large enzyme could be

integral to this behaviour. The exact nature of the surface fouling is not, however, known.

The use of ferrocenylated probe oligonucleotides was shown to be successful as hybridisation gene sensors with synthetic oligonucleotide targets. They were also successfully used to interrogate targets generated from a PCR reaction (amplicons). Co-workers have also undertaken the study of the ferrocenylated labels to follow PCR *in situ* for pathogen detection.

6.5.2 Further work

The work has potential as a cheap, effective gene sensor, for the detection of pathogens or genetic disease. Whilst sensitivity is ultimately very important, the focus of the work in this thesis has always been on "proof of concept" rather than optimisation of sensitivity. The commercialisation of the work, involving the optimisation of sensitivity and the design of new electrodes, has been untaken by Dr. S. Flower (University of Bath) on a 3 year Post Doctoral project which will conclude in 2006. This work also has future application to the *in situ* monitoring of PCR.

In direct relation to this project several issues which must be addressed to achieve better reproducibility through a better understanding of the system. These are: the condition and fouling of the electrode surface; the labelling efficiency of the probe oligonucleotide and the characteristics of the labelled fragment produced on digestion. These will be addressed in turn.

Electrode surface

The reproducibility of the DPV results, using the current system, is affected by the surface condition of the electrode used, which in turn determined by the polishing protocol. For this work all the polishing was done by hand, which inherently leads to some surface variation. It is essential to repeat all the work, using multiple equivalent electrodes which have been polished using a semi-automated system. Such approach is

currently employed by Takenaka and would allow the accuracy (and errors) of all the results to be determined.

To improve the discrimination of the assay it would be very valuable to gain an understanding of the electrode surface. As this is in a delicate equilibrium a non-invasive, sensitive technique is ideally required. Techniques available include: Surface Plasmon Resonance (SPR); Quartz crystal microbalance (QCM) and Electrochemical Impedance Spectroscopy (EIS). SPR is an optical technique for detecting the adsorption of species onto a gold surface. Its use is described by Schuck (Schuck 1997) for biosensing and by Peterlinz (Peterlinz et al. 1997) for DNA sensing. QCM measures the change of mass at the electrode surface (Han et al. 2001). EIS is a technique which allows equivalent electrochemical circuits to be determined for modified electrodes. In this case electrode fouling can be modelled as a capacitance. EIS involves the interrogation of a system by a applying a weak alternating current to a system and measuring how this is affected by the system. The measured impedance (Z) value can be thought of a combination of resistance and capacitance (Bard et al. 2001).

It should be noted that all three of these techniques work with very smooth surfaces and SPR and QCM require relatively large gold surfaces which are generally specific to that technique and not well suited to use as electrodes. Ecochemie (Autolab supplier, Holland) are in the process of developing a dual SPR and electrochemical cell with a separate gold surface and electrode, which may be suitable.

Alternatively the surface could be modified, to reduce the fouling, whilst maintaining the discrimination. Common methods include the use of alkyl thiols, which is introduced in section 1.4.5 and described in detail in section 7.3. This does, however, introduce further complexity to the system. If the technology was applied to *in situ* PCR detection any surface modification would have to maintain its integrity under the rapidly changing PCR conditions, see section 2.2.

Probe oligonucleotide labelling

The focus of the synthetic work (Chapter 3 and 4) was on the synthesis of novel ferrocenylated linker molecules. Reproducibility issues concerning the oligonucleotide post-labelling led to use of phosphoramidite labelling for a significant portion of the work. To overcome these problems the post-labelled oligonucleotides should be purified by the use of HPLC, to remove the unlabelled oligonucleotides and other impurities. The relative labelling efficiency can then be determined by using electrochemical detection (DPV) calibrated against ferrocenylated oligonucleotides, labelled through the amidite route.

Analysis of the ferrocenylated fragment

The actual size of the ferrocenylated fragment (or fragments) which are generated on enzymatic digestion could have a significant effect on the DPV response of the assay, although the exact relationship between fragment size and response is not known. This relationship can be determined by synthesising ferrocenylated fragments of different lengths and measuring their DPV response, as shown in Figure 6.46. The effect of fouling on the DPV response can then be determined. Initially the effect of enzymatic fouling would be determined through the addition of the enzyme (T7 or denatured S1) to the oligonucleotide samples. The overall effect of fouling of the component parts of the hybridisation gene sensor assay could then be determined through the addition of Digest or Control assays, completed using unlabelled probe oligonucleotides, to the ferrocenylated oligonucleotide solutions. This final approach may allow the calibration of the DPV response against oligonucleotide length, in a mimic of the Digest assay. If this was possible, the length of the actual ferrocenylated fragments generated with enzymatic digestion could potentially be determined. Alternatively, purification of the ferrocenylated fragments from a labelled Digest assay could allow the fragment length to be determined by calibration against the results from the labelled oligonucleotides, provided the concentration of the ferrocenylated fragments could be accurately determined.
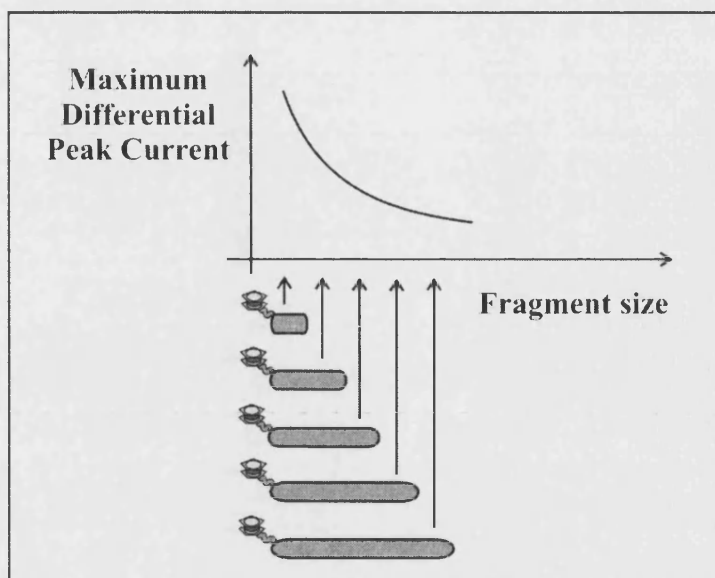
Figure 6.46 - Proposed effect of oligonucleotide length on DPV response.
Variation of oligonucleotide length could affect the maximum DPV peak current, allowing a trend to be established. The actual trend could vary from this prediction.

Extended work

The effectiveness of the hybridisation gene sensor may be improved if the system is modified.

The ferrocenylated probe oligonucleotide has been used as a hybridisation probe under reasonably high stringency conditions (low temperature, typically 37 °C), under which several mismatches would be tolerated in duplex formation. Discrimination has, however, been possible as the probes hybridise with the fully complementary targets and do not hybridise with the fully mismatched targets. Ideally the sensor would be able to discriminate between matched and SNP mismatched sequences, which would require low stringency conditions. As increasing the digest temperature may be detrimental to action of the enzyme, the most straight forward approach would be to shorten the length of the probe oligonucleotide until low stringency is obtained at 37 °C. The position of the mismatch may also be important, as a mismatch in the middle of the hybridisation duplex causes maximum destabilisation (Yamashita et al. 2000; Sato et al. 2003), whilst a mismatch at the 5' end may inhibit the action of the T7 exonuclease, if hybridisation with the SNP mismatched target does occur.

Many alternative enzymes, such as restriction enzymes, are available (New England Biolabs, USA) which digest specific oligonucleotide sequences to generate specific fragments. Their action is described in Figure 6.47. The use of restriction enzymes should give no variation in the size and type of the ferrocenylated fragments, which may improve the DPV response (different fragments, with different responses could reduce sensitivity and broaden the peak). For a specific gene sequence SNP mismatch detection may be possible, if the restriction site includes, or is disrupted by, the mismatch.
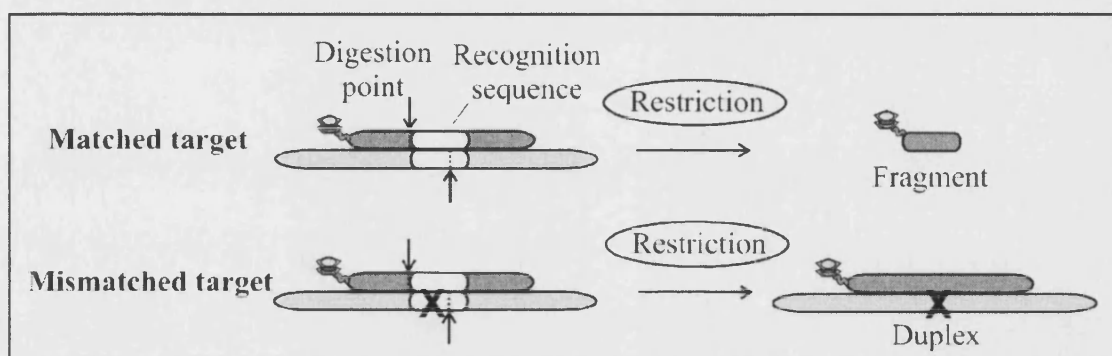
Figure 6.47 - Use of restriction enzymes.
A ferrocenylated probe/target duplex is shown (grey strands). For the matched target (top scheme) the restriction enzyme recognises the recognition sequence (shown as white strands) and cleaves the duplex at the digestion points (arrows). This generates a ferrocenylated fragment of known size. If the SNP mismatched target is allowed to hybridise under low stringency conditions, the mismatch (X) in the recognition sequence prevents enzymatic recognition and no digestion occurs. The mismatched duplex remains. The recognition sequence can incorporate the digestion points (as illustrated) or be several bases away. The digestion points on the duplex can be offset (as illustrated) or adjacent to each other.

An alternative approach is to adapt Umek's work (Yu et al. 2000; Umek, R.M 2001; Yu et al. 2001) and use phosphoramidite labelling to produce a probe oligonucleotide with multiple ferrocene labels, as detailed in Figure 6.48. These do not affect the digestion of the duplex. It is reasonable to assume that although the response for the undigested probe at the electrode may increase, some of the ferrocene labels may be blocked from the surface, limiting the signal. In contrast multiple small ferrocenylated digest fragments would be generated when each duplex is digested, so the Digest response should increase much more.
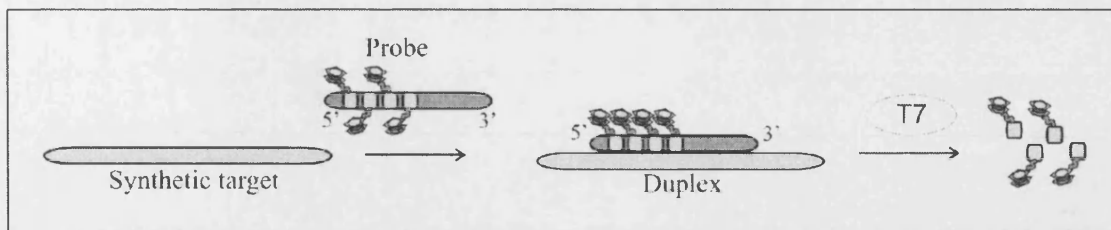
Figure 6.48 - Multiple ferrocene labelled probe.
A probe (dark grey strand) containing multiple ferrocene labels (4 are shown) hybridises with the synthetic target (light grey strand) to form the duplex. T7 exonuclease digests the probe releasing multiple ferrocenylated fragments. The labels are at the 5' end of the probe, so that they will be digested before the duplex becomes sufficiently short that it melts.

For the gene sensor approaches discussed, particularly the approach with multiple ferrocene labels (above), the discrimination between the matched (hybridisation) and mismatched (no hybridisation) assays could be significantly improved by the addition of a large excess of additional target sequences to the assay before analysis. This is either this is done at reduced temperature or after denaturing or inactivating the enzyme. The undigested probe in the mismatched assay would hybridise, resulting in a rigid duplex with some of the ferrocene moieties blocked, or held away from the surface, which would reduce its response. The additional target would also block access of the duplex to the surface. In contrast, the ferrocenylated fragments may only be blocked to a limited extent. Other approaches, such as removing the undigested probe using immobilised target sequences (for example: supported on polystyrene beads, which can be introduced and then discarded) introduce increasing complexity to the system and are therefore not ideal.

Chapter 7: Theory and rationale behind surface supported electrochemical DNA hybridisation probes

7 Theory and rationale behind surface supported electrochemical DNA hybridisation probes

7.1 Introduction

This chapter introduces the concept of electrode surface modification to improve the sensitivity of electrochemical DNA hybridisation sensors, based on enzymatic digestion of ferrocenylated probes, which have been developed in the preceding chapters.

Surface immobilisation of the probe oligonucleotides has been introduced in section 1.4.5, whereby the probe oligonucleotide hybridises with a target sequence from the solution and the hybridisation (recognition event) is then detected electrochemically. The use of surface based hybridisation in electrochemical detection is considered to give improved sensitivity and selectivity over the use of unmodified electrodes (Peterson et al. 2002) and the immobilisation of different probe sequence at different positions on the surface has been used to develop microarray (chip) based sensors.

In contrast, the work in this chapter aims to exploit the improved sensitivity of surface immobilisation, using an electrode surface optimised to detect a specific ferrocenylated oligonucleotide sequence. This specific sequence will be generated in solution, when the labelled probe oligonucleotide hybridises in solution (recognition event) and is enzymatically digested which generates a specific ferrocenylated oligonucleotide sequence. It should be emphasised that the sequence generated is relatively long (8-20 bp) and capable of hybridisation with a complementary sequence. This is in contrast with the preceding work where the ferrocenylated fragment is a mono- or di- nucleotide. For convenience the exploratory experimental work described in this chapter will use established fluorescent detection, to prove the concept.

7.2 Aims

The overall aim of this work is to utilise surface modification to improve the sensitivity of the solution based electrochemical DNA hybridisation sensor developed previously.

The proposed system is detailed below in Figure 7.1. After hybridisation of the ferrocenylated probe with the target oligonucleotide, enzymatic digestion produces a medium sized ferrocenylated oligonucleotide, which is captured at the electrode surface by a complementary capture probe. This surface hybridisation is detected by electrochemistry (DPV).
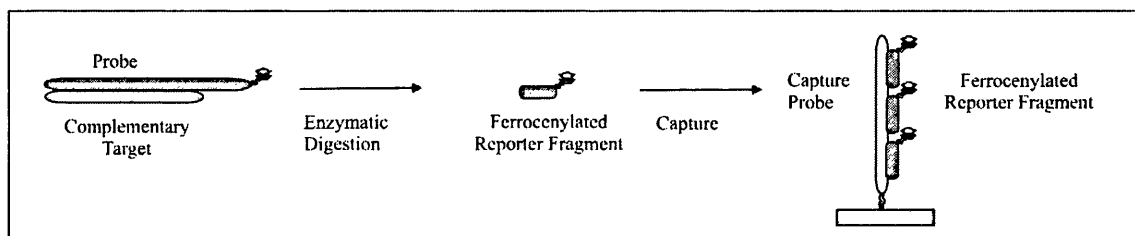
Figure 7.1 – Improving sensor sensitivity with surface modification.
The ferrocenylated probe (dark grey strand) hybridises with the complementary target (light grey strand) in solution (left hand side). The probe overlaps the target. Enzymatic digestion generates a ferrocenylated reporter molecule (middle), which is complementary to a surface immobilised capture probe (white strand, right hand side) and can hybridise to it. The immobilised ferrocenylated probe can then be detected by electrochemistry (DPV).

This work will be developed sequentially and the aims are given below:

- Determination of a suitable reporter fragment and development of the hybridisation conditions.

Variation is possible in the length of the probe overlap and hence the size of the ferrocenylated reporter fragment produced on enzymatic digestion. A suitable reporter fragment sequence and length must be determined, using labelled oligonucleotides of known sequence, and hybridised with a suitable probe sequence. Effective assay conditions must also be established. This can be achieved using established fluorescence based technology.

- Electrochemical detection of ferrocenylated reporter oligonucleotides.

With hybridisation established, the hybridisation event must be followed using ferrocenylated reporter oligonucleotides and electrochemical detection (DPV).

- Electrochemical DNA hybridisation sensors.

The ferrocenylated fragments have been synthetically produced in the preceding work. The detection must be shown to be effective with ferrocenylated fragments generated from the enzymatic digestion of hybridised probe/target duplex (gene sensor). If the probe and target are mismatched hybridisation would not occur, the enzymatic digestion would not occur and reporter fragments would not be generated.

7.3   Surface supported electrochemical hybridisation probes

The use of thiolated, probe oligonucleotides, immobilised onto a gold surface as a hybridisation sensor has been widely studied (Herne et al. 1997; Peterson et al. 2002; Yamashita et al. 2002) and will be discussed.

Whilst the immobilisation of the probe oligonucleotide is reasonably straightforward, the nature of the surface must be well controlled for it be an effective hybridisation sensor. The following aspects will be discussed: the use of blocking layers; the optimisation of surface coverage and practical details concerning the surface modification.

7.3.1   Immobilisation and blocking layers

When the capture probe is introduced to the gold surface a strong covalent bond is formed between the thiol and the gold surfaces, however, the orientation is not controlled and the negatively charged oligonucleotide backbone can also have non-specific (electrostatic) interactions with the gold surface, illustrated in Figure 7.2. This reduces the hybridisation efficiency and therefore an alkyl thiol is typically introduced to negate the problem. The probe oligonucleotide is usually modified with a C6 alkyl thiol and therefore mercaptohexanol (MCH) is typically used for the blocking layer, as

its alkyl chain is the same length. It is also cheap, commercially available and water soluble (Herne et al. 1997).
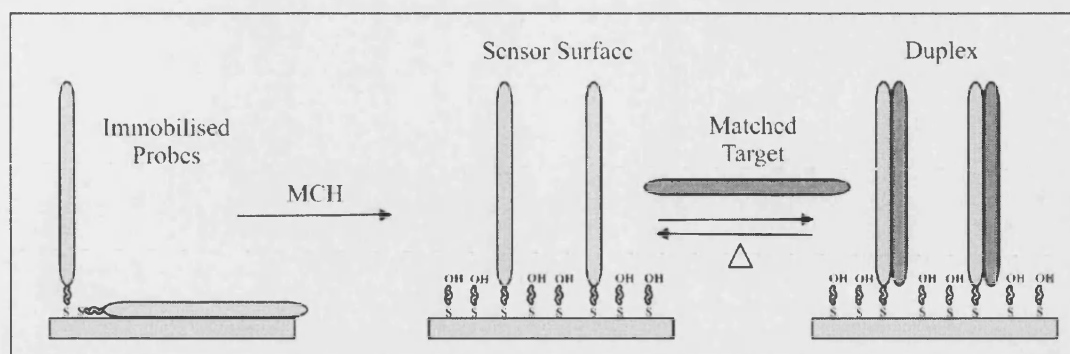
Figure 7.2 - Surface hybridisation.
The thiolated probe oligonucleotides (light grey strand) can covalently bond to the gold electrode surface (left hand diagram) through the terminal thiol linkage (vertical probe in solution), or non specifically bind to the surface (horizontal probe on electrode surface).   The addition of mercaptohexanol (MCH, illustrated as S~OH) eliminates the non specific interactions, orientating the probes into the solution (middle diagram).   The probes can then hybridise with the matched target (dark grey strand) to form a duplex (right hand diagram).   Heating the duplex (delta) melts the duplex and regenerates the probe surface (middle).

It is possible to take the alternative approach and hybridise the thiolated capture probe in solution with its complementary target and then use the duplex for surface modification (Peterson et al. 2001), as shown in Figure 7.3. MCH is then used, as before, to reduce the none specific interactions between the duplex and the gold surface. The immobilised duplex can then be denatured by heating above its Tm point or by washing the surface with a solution containing a reduced salt concentration. The use of warm water is highly effective and is not detrimental to the sensing surface.
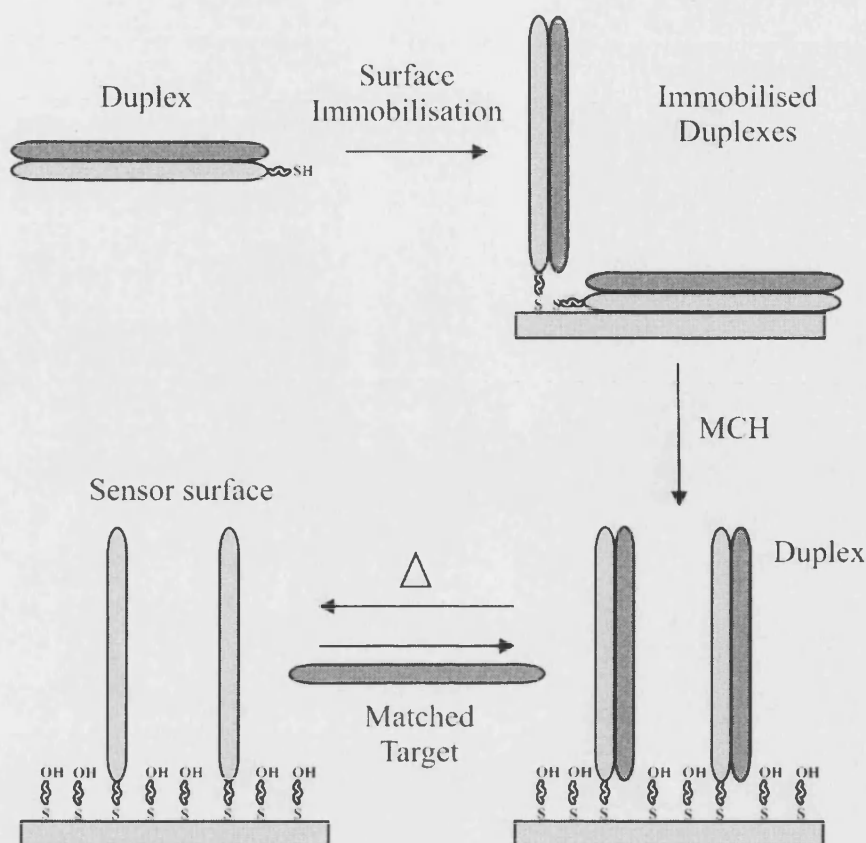
Figure 7.3 - Solution hybridisation and capture.
The thiolated probe oligonucleotide (light grey strand) is hybridised with its complementary target (dark grey strand) in solution to form a thiolated duplex (top left corner). This duplex can covalently bond to the gold electrode surface through the terminal thiol linkage (duplex in solution), or non specifically bind to the surface (horizontal duplex on electrode surface). The addition of mercaptohexanol (MCH, illustrated as S~OH) eliminates the non specific interactions, orientating the duplex into the solution (bottom right diagram). Heating the duplex (delta) melts the duplex and generates the probe surface (bottom left diagram). This probe surface is then ready to hybridise with the matched target oligonucleotide.

A comprehensive study by Tarlov's group (Herne et al. 1997) used X-Ray photoelectron spectroscopy (XPS) to show that MCH displaced unthiolated oligonucleotides from a gold surface. He was also able to show that the thiolated oligonucleotide surface was stable to the thermal heating required to denature the duplex DNA on the surface. Subsequent workers have all used a MCH blocking layer (Steel et al. 1999; Takenaka et al. 2000; Peterson et al. 2002; Wolf et al. 2004) or MCE (mercaptoethanol) (Yamashita et al. 2002).

7.3.2 Surface coverage and hybridisation efficiency

The surface concentration of immobilised probe oligonucleotides can be controlled in two ways and will be discussed in relation to the immobilisation of ssDNA probes. It is important as it affects the hybridisation efficiency of the surface, which is discussed later.

Firstly, Tarlov (Herne et al. 1997) varied the surface coverage, by varying the exposure time of the gold surface to thiolated DNA, whilst keeping the subsequent exposure to MCH constant. The actual surface coverage was determined using SPR and radioactive (^{32}P) labelled oligonucleotides were used to determine hybridisation efficiency.

Secondly, the surface coverage is affected by the immobilisation buffer. The salt content of the buffers is important, as higher salt concentrations decrease the electrostatic repulsion between the oligonucleotides, allowing higher surface densities of immobilised probes. Tarlov *et al.* have shown this with varying concentrations of potassium dihydrogen phosphate (KH_2PO_4) (Herne et al. 1997) and by doubling the concentration of cations in solution (by changing buffer from KH_2PO_4 to K_2HPO_4), which increased the coverage by 50% (Petrovykh et al. 2003). The use of buffers containing divalent cations (Ca^{2+} or Mg^{2+}) increased the coverage by over 100%.

It might be expected that, for a given buffer, the use of the dsDNA approach would reduce the probe density by half as the dsDNA has twice the amount of anionic charge and therefore twice the amount of electrostatic repulsion. In fact the maximum probe density is less than half so other factors, such as conformation and flexibility are important. The dsDNA does, however, reach its maximum coverage much more rapidly than the ssDNA (Peterson et al. 2001).

When the surface has been prepared the target oligonucleotide is then introduced and the hybridisation event can occur. To obtain the best possible sensitivity there is a trade off between the probe surface coverage and hybridisation efficiency. This is due to the electrostatic repulsion between the highly charged immobilised oligonucleotides (due to the negatively charged phosphate groups of the backbone) and also the steric problems

which the complementary target oligonucleotide encounters before it can hybridise at the surface. Work by Georgiadis (Peterson et al. 2001; Peterson et al. 2002; Wolf et al. 2004) and Tarlov (Levicky et al. 1998) using Surface Plasmon Resonance (SPR) estimates that the optimal surface coverage to maximise hybridisation for 25 bp oligonucleotide probes is approximately 10% of the monolayer area.

7.3.3 Practical details

Immobilisation approach

Importantly, in terms of sensor development, the study (Peterson et al. 2001) also found that if ssDNA and dsDNA were immobilised at a comparable probe density, the sensing surface generated from denaturing the dsDNA behaved in an identical way to that generated directly from ssDNA. This work is done on a flat gold surface and analysed by SPR, without the use of labels. The main advantage of using dsDNA is that it could give rise to films that have a more optimum packing (i.e. the density is not too high) and this could be very useful if the sensing work was transferred to a surface (such as an electrode) where the surface coverage could not be easily measured before use.

Hybridisation buffer

Different hybridisation buffers were used by different workers and these are compared in Table 7.1. Tarlov's work is recognised as "the benchmark" by others (Aqua et al. 2003).

Reference	Year	Hybridisation Buffer	Duplex length	Hybridisation Conditions
Tarlov (Herne et al. 1997)	1997	10 mM Tris.HCl (pH = not reported), 1 mM EDTA, 1M NaCl	25 bp	24 °C/ 90 minutes
Tarlov (Levicky et al. 1998)	1998	10 mM Tris.HCl (pH = 7), 1 mM EDTA, 1M NaCl	25 bp	37 °C/ 90 minutes
Ihara (Nakayama et al. 2002)	2002	5 mM Tris (pH = 8) buffer, 5 °C), 100 mM KCl. *Note: pH = 8 buffer, 5 °C is pH = 7.4, 25°C*	7 bp	5 °C/ 24 hours

Table 7.1 – Comparison of hybridisation buffers.

The established methods for modifying a gold electrode have been introduced. To be of practical use the sensing surface must be easily produced robust and stable. The binding efficiency (i.e. duplexes formed per unit area with the target sequence) should be as high as possible and preferably this hybridisation should be reversible and reproducible enabling multiple use of the sensor. High binding efficiencies should give the highest sensitivity for the sensor surface.

7.4 Development of surface supported hybridisation probes

7.4.1 Established work by Friz Biochem

Friz Biochem (Germany) have developed a surface supported DNA hybridisation sensor for use in chip based sensing, called EDDA^{TM} (Electrically Detected Displacement Assay). This work has been patented (FrizBiochem 1999), but not published. Probe oligonucleotides are immobilised on a gold surface and exposed to the biological assay as shown in Figure 7.4. If complementary target oligonucleotides are present in solution hybridisation occurs. If no complementary targets are present, duplex formation does not occur. The surface is then washed and small ferrocenylated reporter

oligonucleotides are introduced, which hybridise to any unhybridised probes. Hence, mismatched probes give a positive electrochemical (DPV) response.
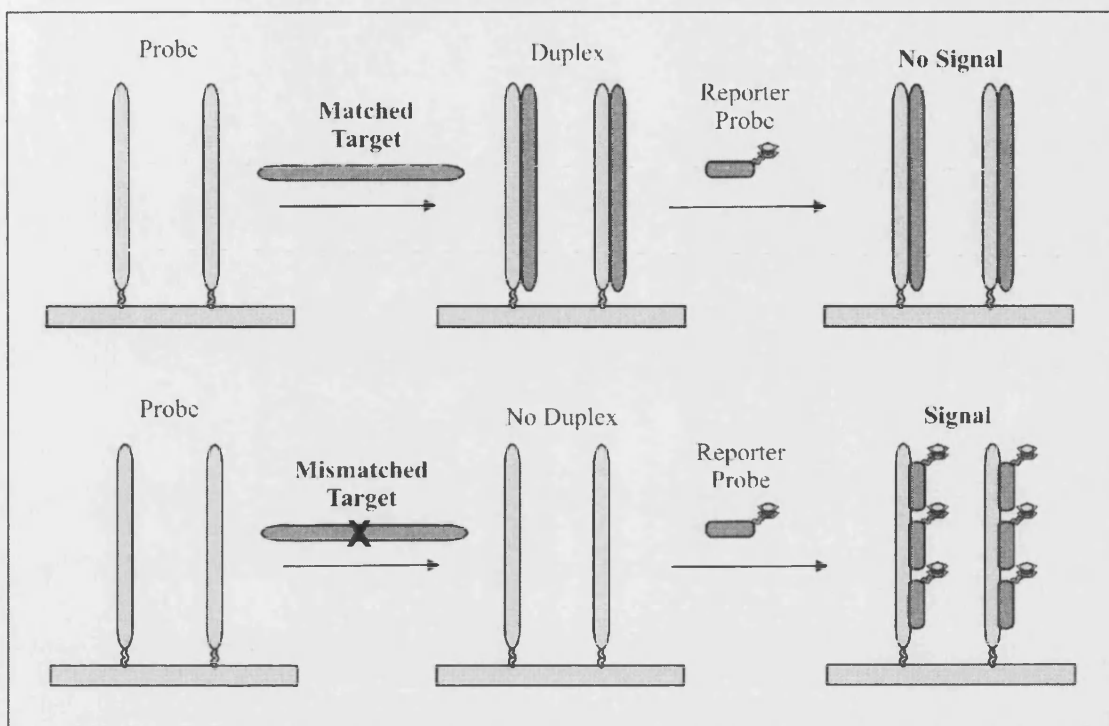
Figure 7.4 - EDDA technology (Friz Biochem).
The immobilised probe oligonucleotides (light grey strands, left hand side) hybridise with a matched target oligonucleotide (dark grey strand, top) but not a mismatched target oligonucleotide (dark grey strand, X shows mismatch, bottom). Reporter oligonucleotides (small, dark grey strands) are introduced which contain a ferrocene moiety on a random 4 bp oligonucleotide sequence. The ferrocenylated reporter probe can hybridise with the unhybridised probe (bottom), but not the duplex (top). Hence, a matched target (top) gives no DPV electrochemical response, whilst a mismatched target (bottom) gives a high DPV response.

Evidently this approach is well suited to chip technology, where a range of immobilised probe oligonucleotides are used to interrogate a mixed biological assay. If there is sufficient diversity in the reporter oligonucleotide random sequences, all unhybridised probes will generate a signal. The major concern with this technology is that it generates positive responses when hybridisation does not occur. Careful calibration and selection of hybridisation conditions would be required to avoid errors and ensure that all the matched targets in the sample hybridise and are detected through their low (zero) response.

In an alternative approach for SNP detection Friz Biochem have adapted their technology to a displacement assay as shown in Figure 7.5 (Hillebrant 2003). In this case both a fully matched and SNP mismatched capture probe are allowed to hybridise

with the fully matched target. An electrochemically labelled reporter oligonucleotide is then introduced which is fully complementary to the SNP. SNP detection is possible as the reporter probe is able to displace the target from the SNP probe sequence and give a response for that strand.
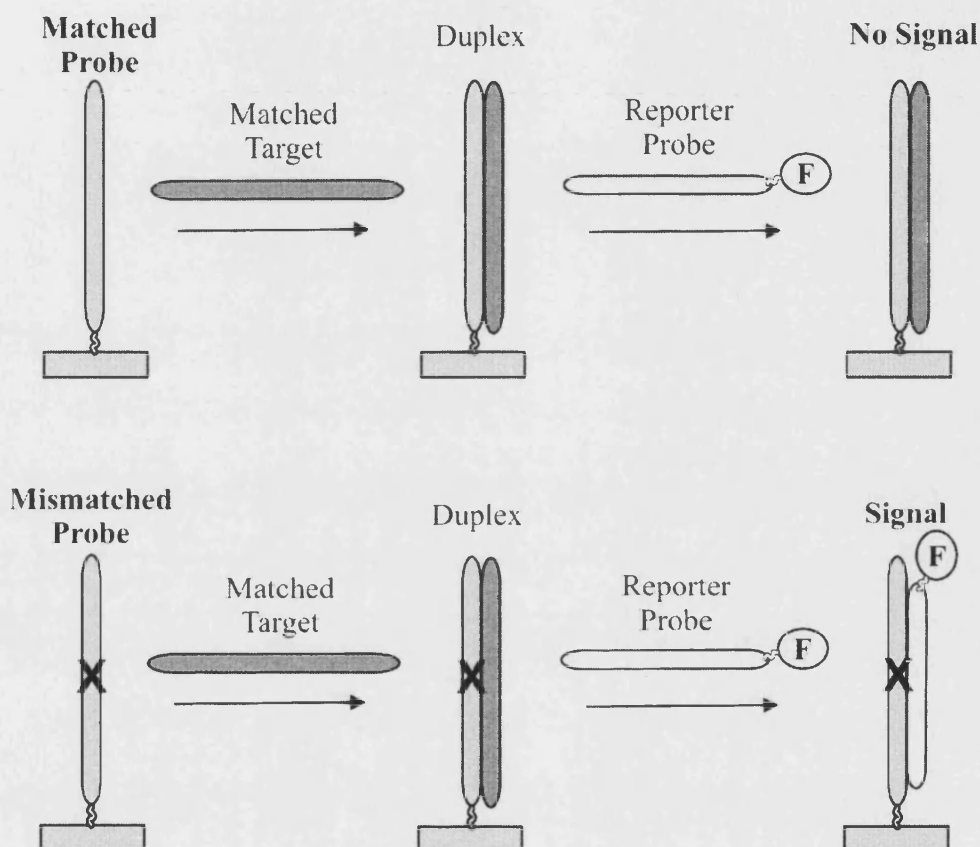
Figure 7.5 - EDDA SNP detection.
Matched (top scheme) and mismatched (bottom scheme) probe oligonucleotides (light grey strands) are immobilised on a surface. Under low stringency conditions the matched target (dark grey strand) hybridises with both probe sequences to form duplexes. A reporter fluorescent probe (white strand) is introduced which is fully complementary to the mismatched probe sequence and can exchange with the target sequence in the mismatched duplex and displace it (bottom scheme). On fluorescent analysis the mismatched probe sequence is detected.

Again careful calibration and selection of hybridisation conditions would be required as the matched and SNP mismatched duplexes will have similar thermodynamic stabilities and Tm, so care must be taken to prevent the reporter probe displacing a matched duplex.

318

7.4.2 Proposed work

The overall approach will be described, followed by a discussion of: the development of the sensor surface; the effectiveness of hybridisation; the choice of enzyme; the evaluation of enzymatic digestion and finally the evaluation of the electrochemical sensor surface.

Overall approach

The approach developed by Friz Biochem can be adapted for pathogen specific gene detection, by combining it with the solution based DNA hybridisation and enzymatic digestion work described in the preceding chapters. After the recognition event, the hybridisation of the ferrocenylated probe with the complementary target oligonucleotide, enzymatic digestion produces a medium sized ferrocenylated oligonucleotide, which is captured at the electrode surface by a complementary capture probe. This is illustrated in Figure 7.6. The surface captured reporter fragments are detected by electrochemistry (DPV).
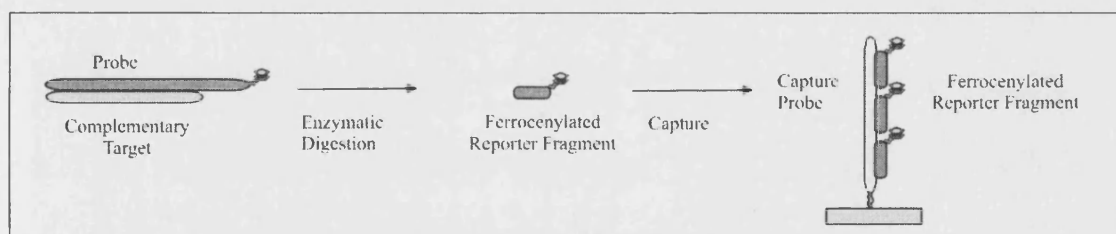
Figure 7.6 - Surface modification.
The ferrocenylated probe (dark grey strand) hybridises with the complementary target (light grey strand) in solution (left hand side). The probe overlaps the target. Enzymatic digestion generates a ferrocenylated reporter molecule (middle), which is complementary to a surface immobilised capture probe (white strand, right hand side) and can hybridise to it.   The immobilised ferrocenylated probe can then be detected by electrochemistry (DPV).

This approach has a number of advantages over the Friz Biochem approach. The sensor generates a positive response for a positive match (hybridisation event). Also the probe sequence, which hybridises with the Target, could be varied for detection of different pathogens, whilst the additional sequence for the reporter fragment can remain constant. Due to this, once a surface modified sensor has been developed, for a given

ferrocenylated reporter oligonucleotide, the same sensor can be used irrespective of which target gene sequence is being detected.

Development of the sensor surface

There are two integral parts to this work. The first is the selection of the capture probe (length and sequence) and the validation that hybridisation is possible between the probe and a reporter fragment of a selected length. The second is to ensure that the sensor surface, containing the capture probe, can be produced effectively and reproducibly.

Effectiveness of hybridisation

The most straightforward way to assess the effectiveness of the hybridisation of short oligonucleotide fragments is to use biotinylated probe oligonucleotides, which are immobilised on the surface by affinity binding with streptavidin. This is shown in Figure 7.7. The immobilisation technique is well established and guarantees good surface immobilisation of the probe oligonucleotide (Prozyme 2004), as described in section 1.4.5. The use of fluorescent labelling ensures effective detection, using a plate fluorimeter, see section 2.6.2.
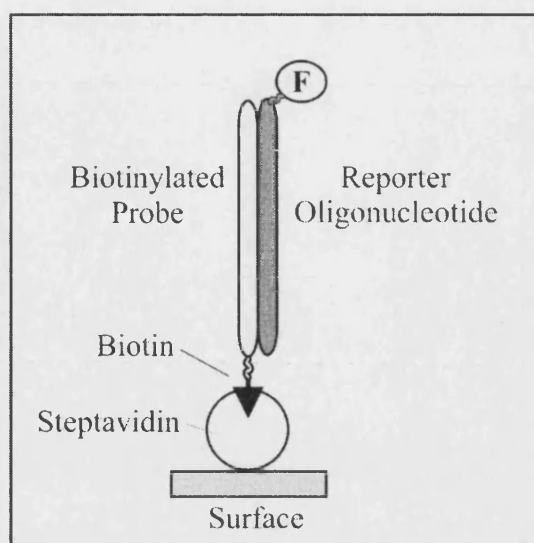
Figure 7.7 – Affinity binding using surface immobilised streptavidin.
Streptavidin (white circle) is bound to the surface. The biotin labelled probe oligonucleotide (white strand) is immobilised on the surface due to the strong biotin/streptavidin binding. The probe hybridises with the complementary fluorescent labelled reporter oligonucleotide (dark grey strand). Streptavidin is a biotin binding protein with the ability to bind up to four moles of biotin per mole (only one is illustrated for simplicity and this may be the realistic case for bound streptavidin). The binding affinity is one of the strongest known is biology (the equilibrium dissociation constant, Kd $\approx 10^{-15}$).

The use of this technology should ensure that a reproducible capture probe surface is generated.   Using target oligonucleotides labelled with fluorescein (cheap and convenient) allows fluorescence detection to be used, eliminating any surface or sensitivity issues which may arise from electrochemical detection

Evidently this strategy involves a different surface to the proposed electrochemical work. The most significant difference is that the capture probes should be well spatially separated due to the physical size of the streptavidin, which makes the two surfaces not directly comparable.   However, optimising the electrochemical approach would probably involve controlling the surface density of the capture probe, rather then changing the hybridisation buffer.

If short reporter probes can be shown to hybridise with longer capture probes the sensitivity of the system can be increased, as shown in Figure 7.8. Shorter reporter probes will also be cheaper to synthesise than longer probes.
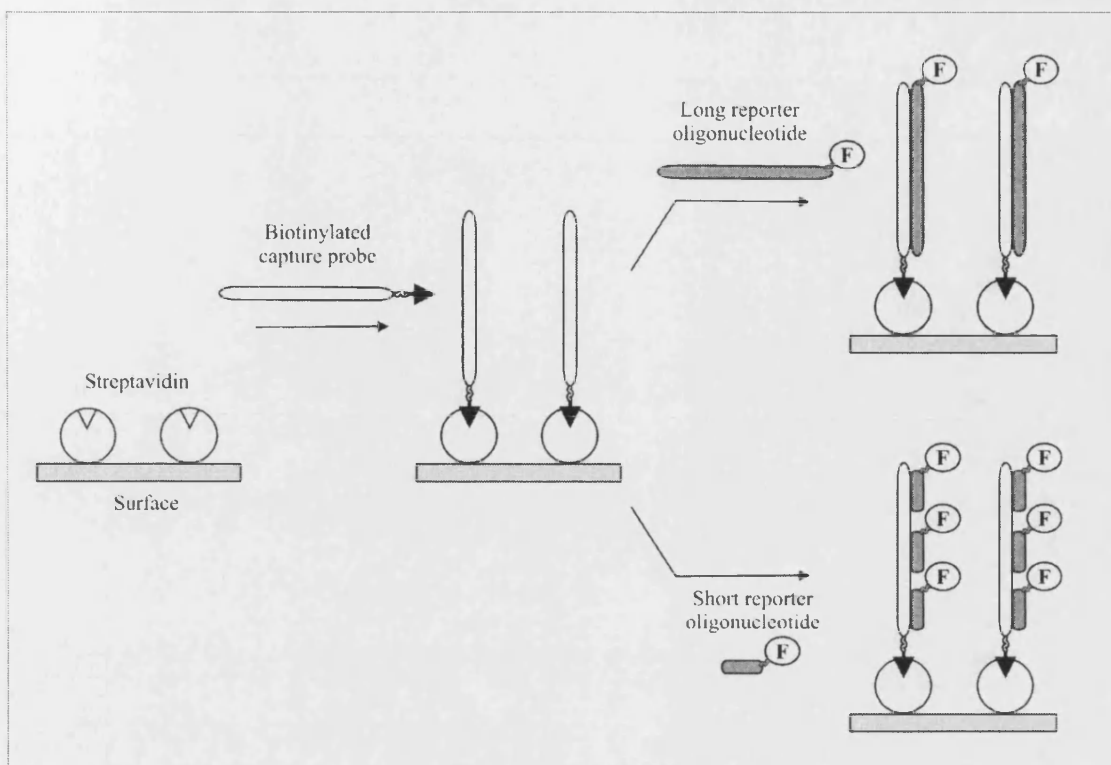
Figure 7.8 – Variation of reporter oligonucleotide length.
The streptavidin modified surface (white circles) is modified with a biotinylated capture probe (white strand, biotin is shown as arrow head). The capture probe is hybridised with a complementary, fluorescent labelled, reporter oligonucleotide (grey strand, Fluorescent labels are shown as F). If a long reporter oligonucleotide is used (top) only one reporter oligonucleotide can hybridise per probe. If smaller reporter oligonucleotides are used (bottom) multiple reporter oligonucleotides can hybridise.

Choice of enzyme

The reporter probe fragments will be generated on enzymatic digestion; the mechanism of this enzymatic action has been introduced in section 5.4.2. It was proposed to initially attempt this using T7 exonuclease as detailed in Figure 7.9. The duplex is not ideally suited for T7 exonuclease digestion as both 5' ends are ssDNA overlaps. However, digestion may be still be possible, despite being inefficient.
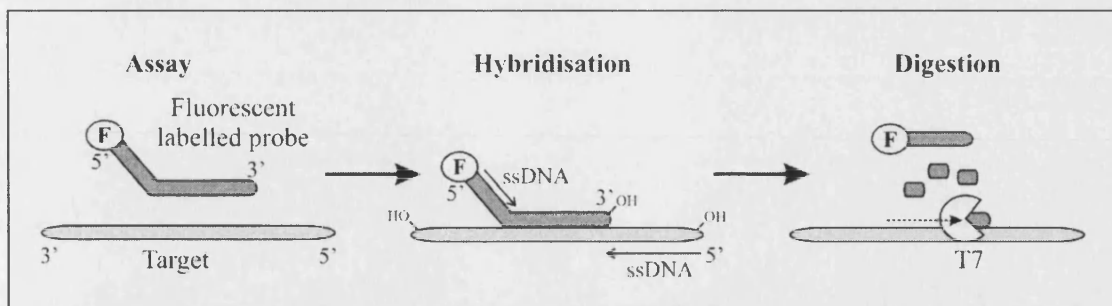
Figure 7.9 – T7 exonuclease digestion.
The 5' fluorescent labelled probe (dark grey strand) hybridises with the complementary target (light grey strand), forming a duplex. Despite the 5' ssDNA overlap at both ends of the duplex it is potentially possible for the T7 exonuclease (white circle) to digest the probe in the 5' to 3' direction (dotted arrow), liberating the fluorescent labelled reporter fragment (short, dark grey strand).

The TaqMan® enzyme could also be used to generate labelled fragments, if it can also tolerate the 5' overlap, as shown in Figure 7.10. This can be achieved with the appropriate primers or in PCR, resulting in its use as an *in situ* PCR probe.
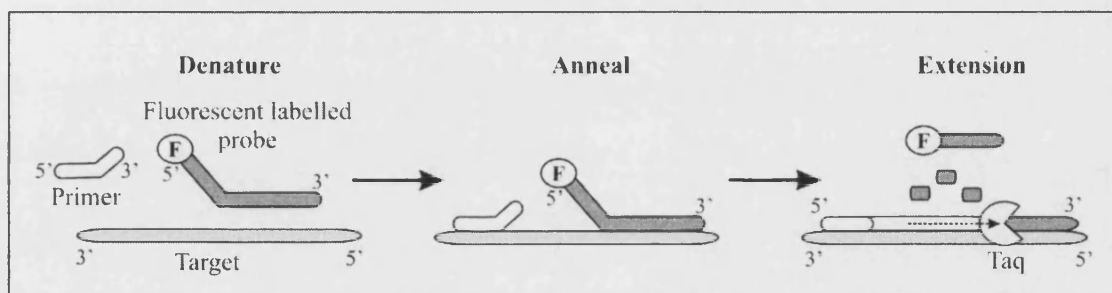
Figure 7.10 - Taq enzymatic digestion
The 5' fluorescent labelled probe (dark grey strand) and primer (white strand) hybridise with the complementary target (light grey strand). Despite the 5' ssDNA overlap of the hybridised probe it is potentially possible for the Taq enzyme (white circle) to digest the probe in the 5' to 3' direction (dotted arrow), liberating fluorescent labelled reporter fragment (short, dark grey strand).

Evaluation of enzymatic digestion

The most straight forward approach is to run a Digest assay (complementary probe and target, with enzymatic digestion) and compare the fluorescent response with that of three Control assays (Mismatch; Mismatched target; Duplex, with the enzyme omitted from Digest assay, and Probe, with no target or enzyme). This is shown in Figure 7.11. It is hoped that the steric hindrance, due the additional oligonucleotides in the two Control assays will hinder the hybridisation of these oligonucleotides and give rise to selective binding for the digested fragment from the Match assay.
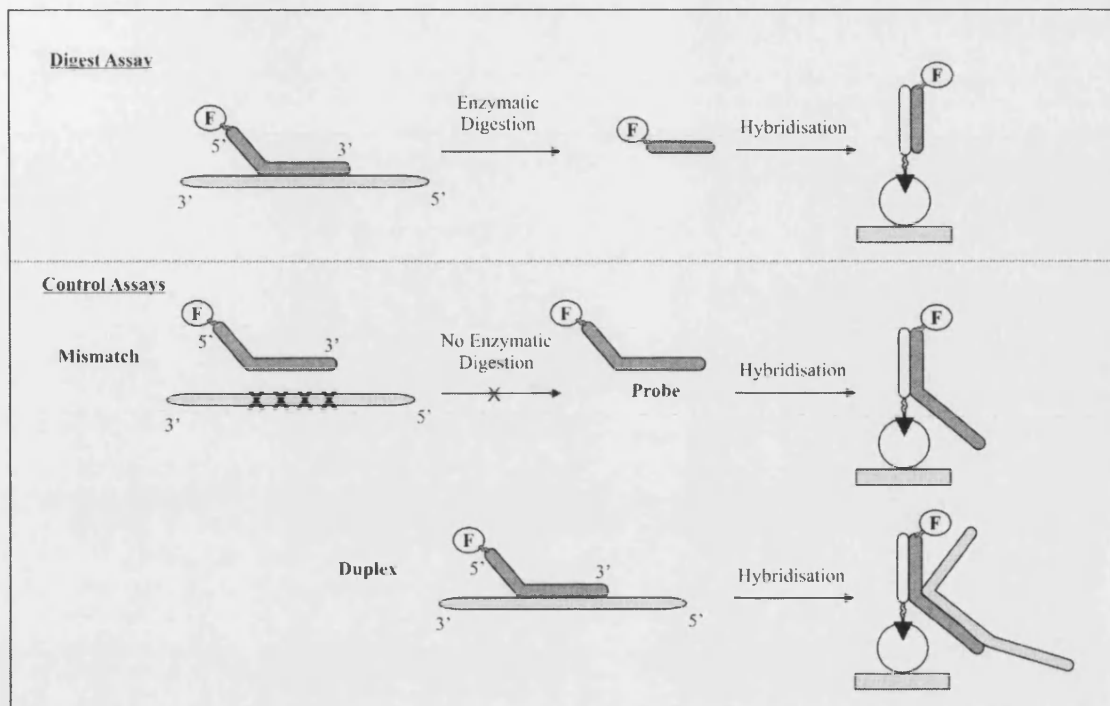
Figure 7.11 – Enzymatic digestion assays.
In the Digest assay (top), complementary probe (dark grey strand) and target (light grey strand) hybridise and undergo enzymatic digestion producing the smaller reporter oligonucleotide (short grey strand), which can readily hybridise to the surface immobilised capture probe (white strand). This is followed by fluorescent detection.   In contrast Control assays (bottom) do not undergo enzymatic digestion and the hybridisation of the large probe or duplex to the capture probe will be sterically hindered and should occur much less readily.   The three Control assays are Mismatch: Mismatched target; Probe, no target or enzyme, and Duplex, enzyme omitted from Digest assay.

To determine if absolute enzymatic digestion is occurring, a dual labelled fluorescent probe is used, as illustrated in Figure 7.12.   Dual labelled probes have been utilised before in section 6.4.1.   As the T7 enzymatic digestion occurs the quencher and fluorophore become spatially separated, resulting in an increase in fluorescence.   The dual labelled probes are commercially available (Sigma Genosys, UK).
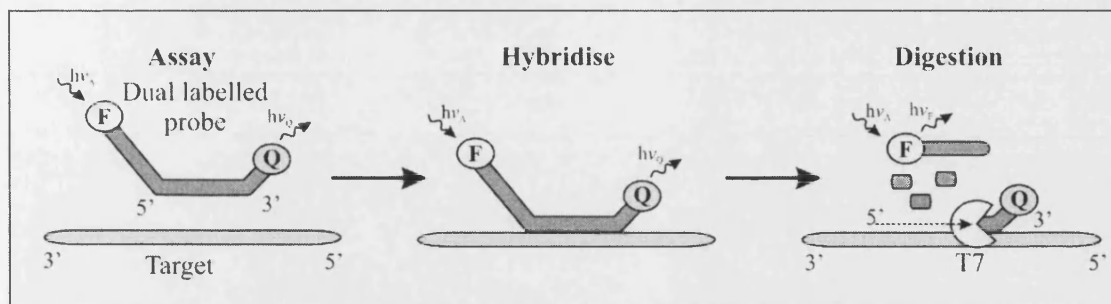
Figure 7.12 - Use of dual labelled probe to follow T7 exonuclease digestion.
The dual labelled probe (dark grey) has a fluorophore (F) and quencher (Q) at separate ends. The F and Q of the dual labelled probe are close enough together for FRET quenching to occur (see section 2.6.1) and the fluorescence of F is quenched. The probe hybridises to a complementary sequence on the target oligonucleotide (light grey strand). The T7 exonuclease enzyme (white circle) digests the probe oligonucleotide in the 5' to 3' direction (direction of dotted arrow), generating oligonucleotide fragments (short, dark grey strands) and separating F and Q. As F and Q are no longer covalently joined and can move apart. F is no longer quenched by Q and its fluorescence is detected. Hence the hybridisation event is detected.

Evaluation of electrochemical sensor surface

A gold electrode surface can be modified with ssDNA capture probe through either the immobilisation of thiolated probe oligonucleotides or immobilisation of thiolated duplexes, as described in section 7.3.1. The use the BAS gold electrode prohibits the determination of surface coverage, using techniques such as SPR, discussed in section 7.3.2, therefore it is preferable to modify the surface with a capture probe by first immobilising a thiolated duplex at the surface, adding the MCH blocking layer and then heating to remove the target oligonucleotide. This is shown in Figure 7.13.
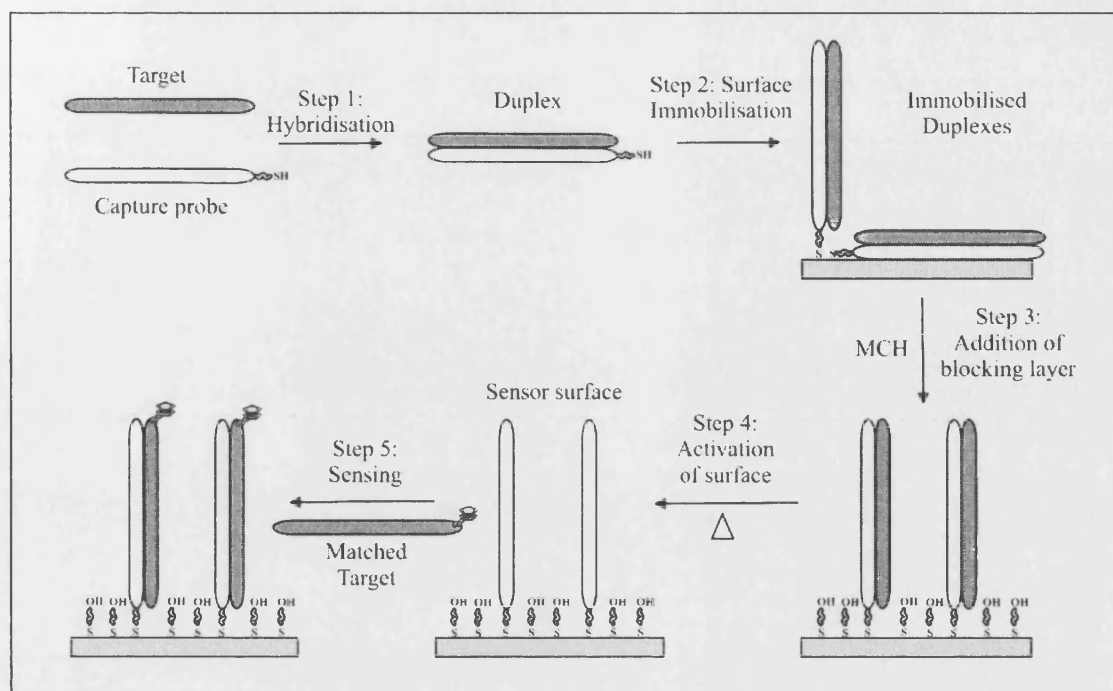
Figure 7.13 – Production and use of modified probe sensor surface.
The process involves 5 discrete steps. Step 1: hybridisation between thiolated probe and complementary target to form duplex. Step 2: immobilisation of duplex onto gold surface. The orientation of the duplex is not controlled. Step 3: addition of a blocking layer. Addition of MCH blocks the electrode surface and orientates the thiolated duplex into solution. Step 4: activating of the surface. Heating denatures the duplex resulting in a capture probe modified surface. Step 5: sensing. Hybridisation can occur between the capture probe surface and the ferrocenylated complementary targets from solution. This event can be detected electrochemically (DPV). If a ferrocenylated target is used in the initial hybridisation (Step 1) the progress of the surface preparation could be followed electrochemically (DPV).

As direct parallels cannot be drawn between the fluorescence work and the electrochemical detection due to the inherent differences in the surface, work will initially be undertaken to prepare a gold surface modified with a T_8 capture probe.

The surface will be used to detect a ferrocenylated A_8 reporter oligonucleotide (Match assay), before being activated again and used to detect a ferrocenylated T_8 reporter oligonucleotide (Mismatch). With only one BAS gold electrode available, the reuse of the sensor surface is considered to be the best way to obtain meaningful, comparable results.

7.4.3 Terminology

Throughout the DNA hybridisation probe work, described in Chapters 5 and 6, the target sequence is the DNA sequence of interest which is detected through hybridisation to its complementary Probe sequence, in the recognition event. However, in the case of the proposed work there are two hybridisation events so the terminology must be defined, which is done in Figure 7.14. The solution based recognition event retains the terms probe and target, whilst the ferrocenylated oligonucleotide fragment generated by the digestion is the reporter fragment, which is able to hybridise to a surface immobilised capture probe.
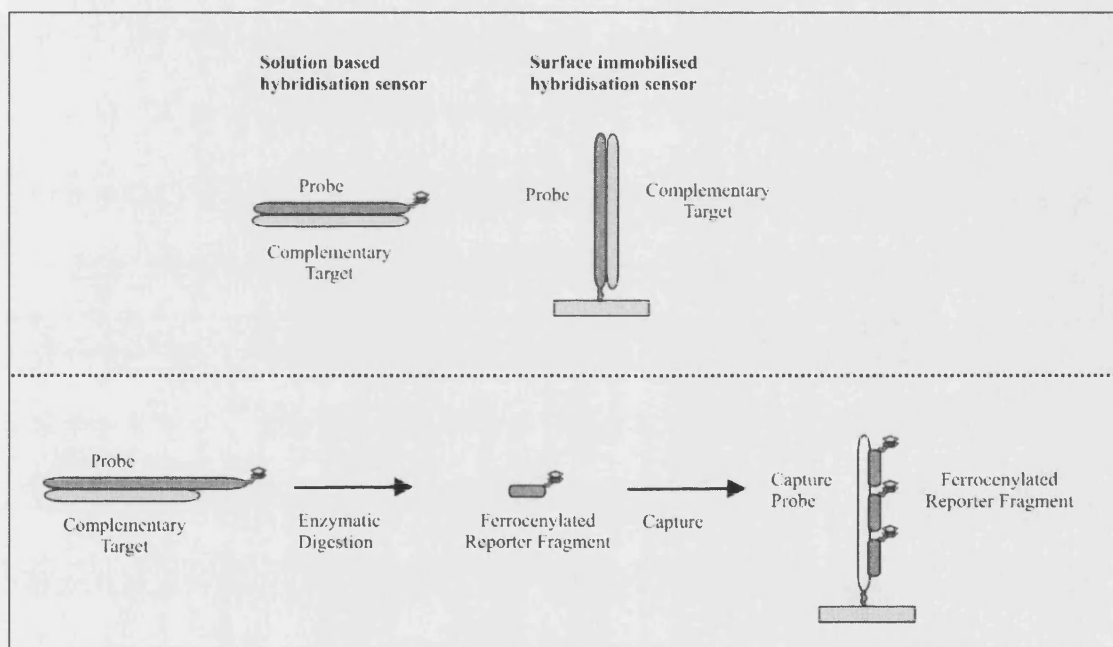
Figure 7.14 – Terminology.

7.5   Summary: experimental plan

The experimental plan is intended to:

- Clearly and concisely describe the experimental work in Chapter 8, using specific detail, and give the rationale behind choices which were made.
- Give clarity to the structure of Chapter 8 and to be a reference point for it.

The aims for the work have been given in section 7.2. The overall aim of this work is to utilise surface modification to improve the sensitivity of a solution based electrochemical DNA hybridisation probe.   Bullet points in this section give experimental results which must have been obtained before the next stage in the development can be undertaken.

7.5.1   Fluorescent work

Fluorescence detection is used in combination with biotin labelled, surface immobilised, capture probes (see section 7.4.2) to determine suitable hybridisation conditions for the work.   It is also used to evaluate the effect of the length of the reporter oligonucleotides and the capture probes have on the fluorescent response and to evaluate enzymatic digestion, which produces the ferrocenylated reporter molecules.   The fluorescein labelled reporter probes are custom synthesised (Sigma-Genosys, UK), together with the biotinylated oligonucleotides.   The streptavidin coated plates (96-well) are also commercially available (SigmaScreen^{TM}, Sigma-Genosys, UK).

The oligonucleotides used for the work are 5' fluorescein labelled reporter probes (T_8 and T_{20}) with complementary 5' biotinylated capture probes (A_8 and A_{20}).

Evaluation of hybridisation conditions

Initial work assess the hybridisation of the larger, T_{20}, fluorescein labelled reporter fragment with its complementary biotinylated capture probe (A_{20}), to determine the

effectiveness of Tarlov's buffer, described in section 7.3.3. The speed of this hybridisation is followed using a time-course experiment. Tarlov states that most hybridisation occurs relatively quickly and should be complete in less than 2 hours (Levicky et al. 1998).

Evaluation of reporter oligonucleotide

The hybridisation of the A_8 synthetic reporter fragment (5' labelled with fluorescein) to the T_8 and T_{20} biotinylated capture probes is evaluated, using the assays detailed in Table 7.2. The hybridisation of multiple short (A_8) reporter fragments with the large, T_{20}, capture probe would allow improved sensitivity to be achieved.

Assay	Reporter fragment	Capture probe	Predicted fluorescence
1	Fluor-A_8	T_8	1X
2	Fluor-A_8	T_{20}	2X

Table 7.2 - Evaluation of reporter fragments.

Evaluation of enzymatic digestion

In the full sensor system the reporter probes are generated by enzymatic digestion of the probe target duplex. Two fluorescence based techniques, described in section 7.4.2, are used to evaluate the effectiveness of this digestion.

In the first approach a 5' fluorescein labelled probe oligonucleotide (Fluor-A_n-C282Y, n = 8 or 20) is hybridised with its complementary target (C282YST) and digested with T7 exonuclease in PCR buffer. This is the Digest assay. After T7 digestion the assay is heated to 90 °C for 3 minutes to denature the enzyme. The assay is then interrogated with the capture probe sensor as has been described above. Three control assays are also run: Mismatch, mismatched target and no hybridisation; Duplex, enzyme omitted from Digest assay and Probe, no target or enzyme.

In the second approach a dual labelled probe (FAM-A_8-C282Y-TAMRA) will be hybridised with its complementary target (C282YST) and digested with T7 exonuclease

in PCR buffer. The same assays will be used as for the first approach. Enzymatic digestion would result in an increase in fluorescence.

7.5.2 Electrochemical work

- The fluorescence work, in section 7.5.1, must have shown that discrimination is possible between the digested fragment produced from the Digest assay and the Control assays.

Work can be undertaken to develop an electrochemical sensor, based on surface modification.

A gold electrode surface is modified with a T_8 capture probe, as in section 7.4.2, then used to detect a ferrocenylated A_8 reporter oligonucleotide (Match), before being activated again and used to detect a ferrocenylated T_8 reporter oligonucleotide (Mismatch). Both the probe sequences are 5' labelled with *amidite* 28. Using a ferrocenylated target in the formation of the initial duplex, as shown in Figure 7.13 in section 7.4.2, will allow the preparation of the sensor surface and the hybridisation to be followed electrochemically with DPV.

Chapter 8: Results

Surface supported electrochemical DNA hybridisation probes

8 Results: Surface supported electrochemical DNA hybridisation probes

8.1 Introduction

This chapter reports the experimental results for the development of surface supported electrochemical DNA hybridisation probes.

Understanding of the sensor surface is developed using a streptavidin surface, modified with biotin labelled capture probe oligonucleotides. These are initially hybridised with custom synthesised, fluorescent labelled reporter oligonucleotides, and analysed with a fluorimeter. The work progresses to using reporter oligonucleotides produced from enzymatic digestion. The system is then applied to electrochemical detection using ferrocenylated reporter oligonucleotides.

The general detail for the experimental work is given in Chapter 2, including electrochemical cell set-up in section 2.5.1, oligonucleotide sequences in section 2.11.1, and fluorescent detection in section 2.6. The specific details concerning DPV analysis, oligonucleotide labelling, and biological assays are given as Protocols in section 2.11.2.

8.2 Fluorescent work

Fluorescence detection of fluorescein labelled reporter oligonucleotides is used in combination with biotin labelled, surface immobilised, capture probes to develop the senor assay. This work is then applied to electrochemical detection.

332

8.2.1 Experimental details: fluorescent analysis

The work was undertaken using 5' biotinylated T_8 or T_{20} capture probes, which were used to modify wells on a streptavidin plate. These were hybridised with either A_8 or A_{20} reporter oligonucleotides, 5' labelled with fluorescein (abbreviated to Fluor-A_x). Analysis was undertaken using a fluorescent plate reader, the specific details are given in section 2.11.2, Protocol 15.

8.2.2 Evaluation of hybridisation conditions

Initial experiments were required to determine if Tarlov's hybridisation conditions (buffer: 10 mM Tris.HCl (pH = 7), 1 mM EDTA, 1M NaCl and hybridisation time: 90 minutes) are suitable for the streptavidin based system.

An initial experiment was conducted to determine if the hybridisation conditions were effective for the long (20 mer) capture probe. The Match assay used the T_{20} probe and A_{20} reporter oligonucleotide, whilst the Mismatch assay used an A_{20} probe. The assays are given in section 2.11.2, Protocol 16.

Good discrimination was obtained between the Match and Mismatch assays on fluorescent analysis, which is shown in Figure 8.1. A low response was obtained when the biotinylated probe was omitted (Control assay). The melting point of the duplex was estimated at 52 $^\circ$C (Sigma-Genosys datasheet). Washing the wells with warm (60 $^\circ$C) buffer removed virtually all of the bound target. Repeating the experiment with no salt (NaCl) gave a low response for both match and mismatch assays and no discrimination between them.
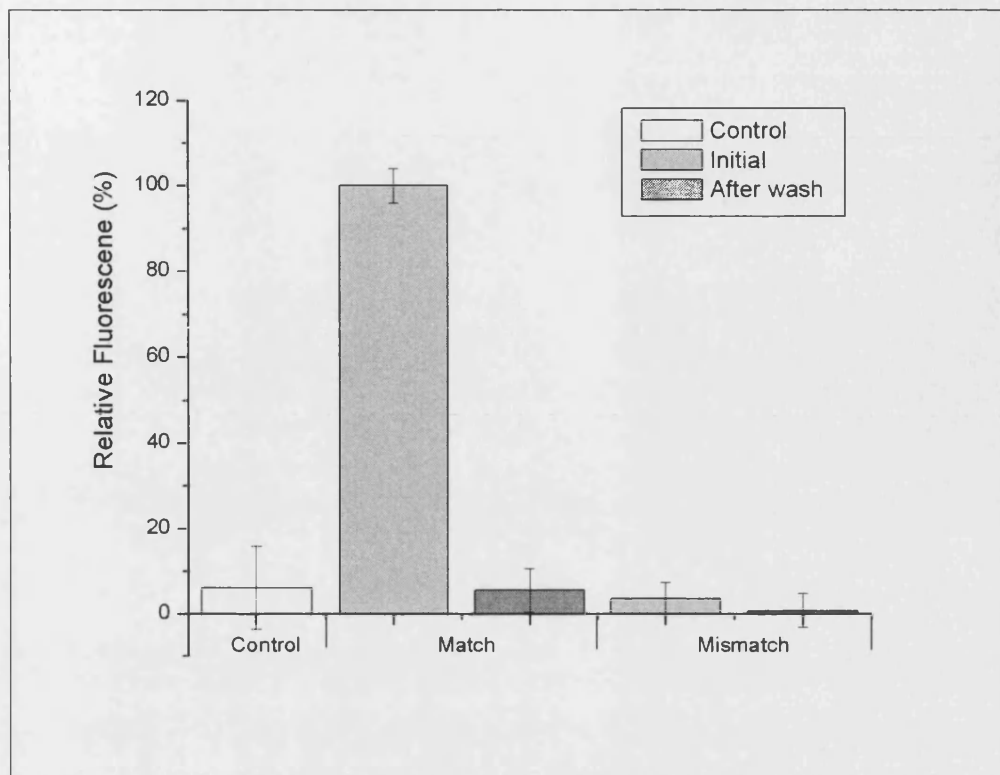
Figure 8.1 - Evaluation of hybridisation conditions.
The Fluor-A_{20} reporter oligonucleotide was allowed to hybridise with a surface immobilises T_{20} capture probe (Match) and an A_{20} probe (Mismatch). For comparison the capture probe was omitted (Control). The fluorescent response was measured initially (after washing with buffer, 5 °C, light grey bar) and after further washing (buffer wash 60 °C, dark grey bar). 95% intervals of confidence.

To determine the optimum time required for hybridisation (Fluor-A_{20} reporter oligonucleotide with the T_{20} capture probe) a time-course was run and the results are given in Figure 8.2. Leaving the sample overnight (10 hours 45 minutes) ensures that the maximum amount of hybridisation (assigned as 100%) occurs. Virtually all the hybridisation (>90%) has been obtained after two hours, which agrees with Tarlov's work.
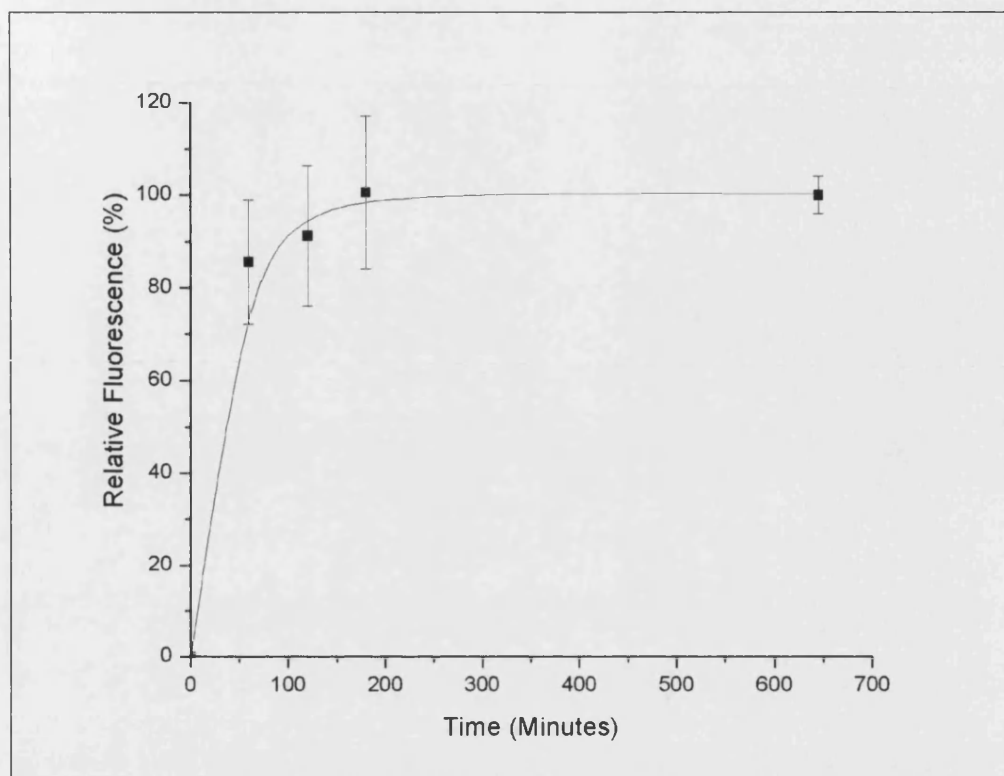
Figure 8.2 - Hybridisation time-course.
The Fluor-A_{20} reporter oligonucleotide was hybridised with the T_{20} capture probe for varying amounts of time under standard conditions. After washing the cells with buffer the fluorescence was measured (all details are given in **section 2.11.2**, Protocol 15). 95% intervals of confidence levels are shown.

The buffer conditions allow effective hybridisation of the long (20 bp) reporter oligonucleotide with its complementary target. The hybridisation is sufficiently rapid.

8.2.3 Evaluation of reporter oligonucleotide

Hybridisation experiments were undertaken for the short reporter oligonucleotide (Fluor-A_8). Matched assays were run using both short (T_8) and long (T_{20}) fully complementary capture probes; this is illustrated diagrammatically in Figure 8.3. Mismatched assays were run using a mismatched reporter oligonucleotide (Fluor-T_8). A Standard was also run using a known concentration (5 nM) of Fluor-A_{20}. The assays were allowed to hybridise at 5 °C overnight (17 hours 30 minutes) and were analysed at this temperature. The full experimental detail is given in section 2.11.2, Protocol 17.

335
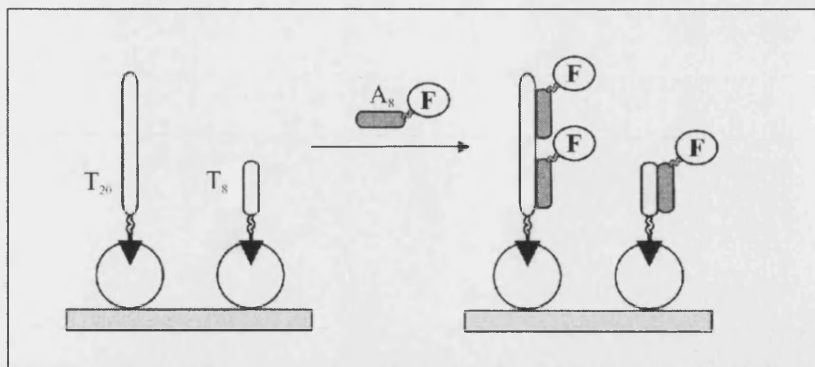
Figure 8.3 – Summary: illustration of the effect of variation in capture probe length.
The short reporter oligonucleotide (Fluor-A_8, short grey strand) was allowed to hybridise with two lengths (long T_{20} and short T_8) of capture probe (white strands). It is possible for multiple reporter oligonucleotides to hybridise to the longer capture probe.

The results of the fluorescent analysis are given in Figure 8.4. The Standard solution gives an indication of the amount of reporter oligonucleotide at the surface in the other assays.
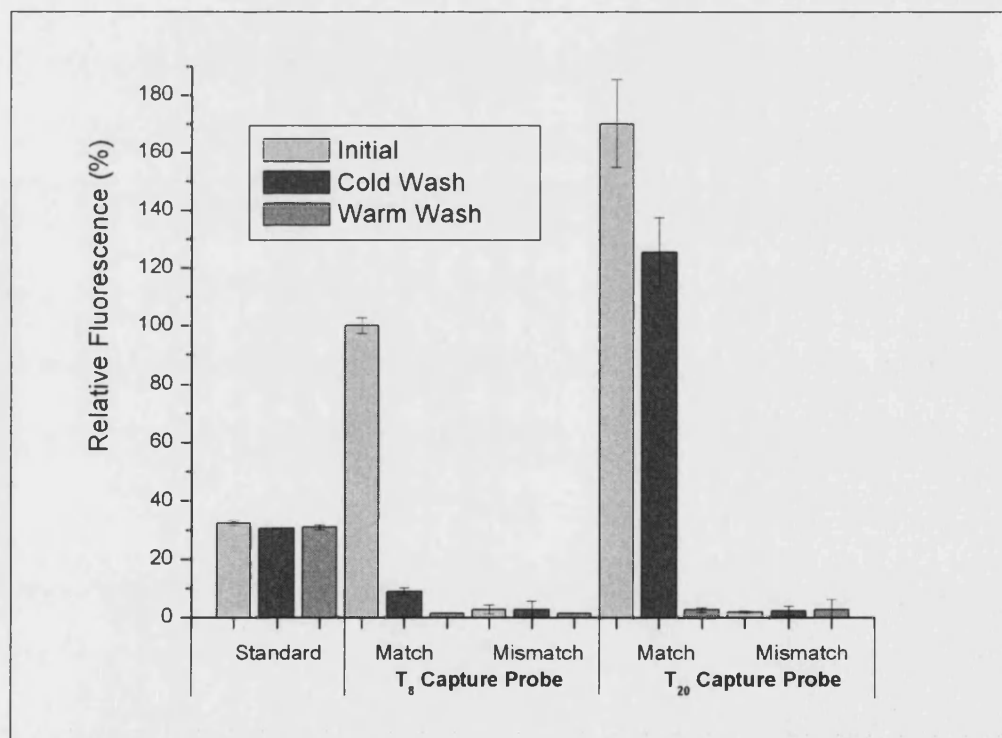
Figure 8.4 – Evaluation of short (Fluor-A_8) reporter oligonucleotide.
Match assays: the short, fluorescent labelled reporter oligonucleotide (Fluor-A8) is hybridised with the surface immobilised complementary capture probes (T_8 and T_{20}). Mismatch assays: the mismatched, fluorescent labelled reporter oligonucleotide (Fluor-T_8) is used. The fluorescent response is measured after buffer washes (3 x 100 µL, 5 °C, light grey bar). The fluorescence is given relative to T_8 capture probe match assay (100%). The wells were washed with buffer (3 x 100 µL) and the fluorescent response was re-measured after each: cold wash (22 °C, black bar) and Warm wash (40°C, dark grey bar). The fluorescence of a standard solution was (5 nM, Fluor-A_{20}) was measured at each stage. 95% intervals of confidence are shown.

In the initial analysis there is very good discrimination between the Match and Mismatch assays for both lengths of reporter oligonucleotide. For the short (8 bp) capture probe the Mismatch assay has a 3% response, relative to the Match, which decreases to 2% for the long (20 bp) capture probe. Significantly, if the two Matched assays are compared, increasing the length of the capture probe (8 bp to 20 bp) increases the response by 70%, as up to two target oligonucleotides can bind to it.

The strength of the reporter oligonucleotide binding at the surface was investigated by washing each well with buffer at a cold temperature, 22 °C, and then at a warm temperature, 40 °C. It was expected that the cold wash would remove virtually all the reporter sequence from both capture probes (Tm = 8 °C in solution), but whilst most of the signal was lost from the 8 bp capture probe only a quarter was lost from the longer (20 bp) sequence. This improved stabilisation with the longer capture probe must be due to different surface characteristics of the capture films, possibly due to improved ordering of the longer capture oligonucleotides. Using the warm wash removed virtually all the target from both capture probes.

Summary

The short reporter oligonucleotide (Fluor-A_8) has been shown to give good discrimination between the Match and Mismatch assays, when hybridisation is undertaken at 5 °C. When this reporter oligonucleotide is used in conjunction with the longer (T_{20}) capture probe, multiple reporter oligonucleotides can hybridise to the probe increasing the sensitivity.

8.2.4 Evaluation of enzymatic digestion

The effectiveness of enzymatic digestion to generate reporter fragments will be investigated. The work is summarised, in Figure 8.5, and is undertaken with both a large probe oligonucleotide (Fluor-A_{20}-C282Y, hence large reporter oligonucleotide) and a smaller probe oligonucleotide (Fluor-A_8-C282Y, hence small reporter oligonucleotide).
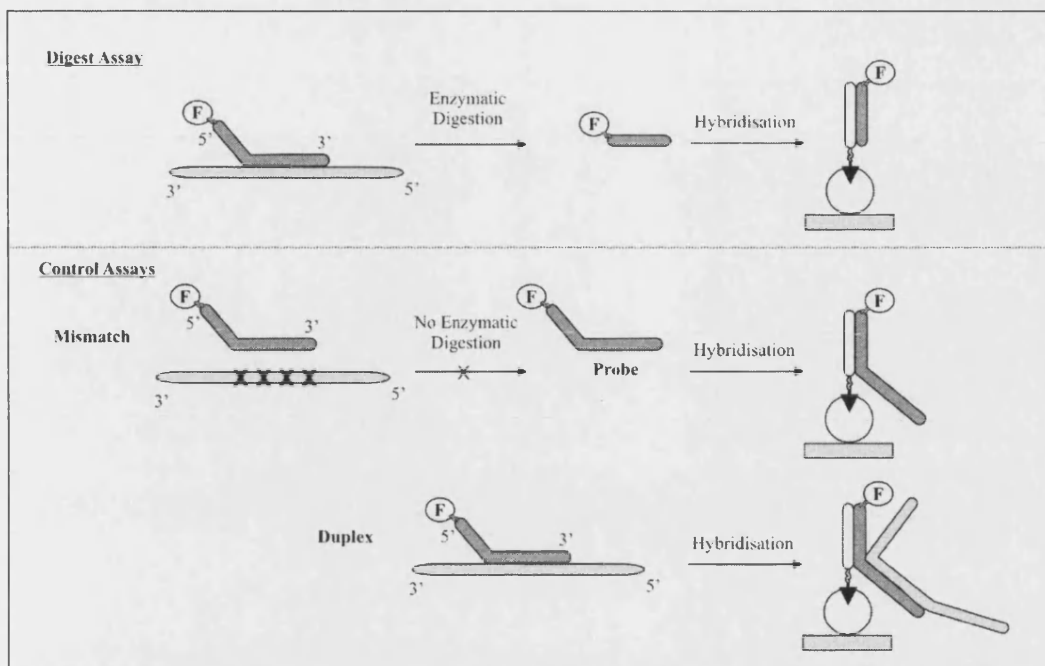
Figure 8.5 – Summary: enzymatic digestion assays.
This is a reproduction of Figure 7.11, which is given here for clarity.

Generation and evaluation of large reporter oligonucleotide

The long probe oligonucleotide (Fluor-A_{20}-C282Y) was used in the four different enzymatic digestion assays described above, in Figure 8.5. The full details are given in section 2.11.2, Protocol 8.

After incubation with the T7 enzyme the assays were allowed to hybridise with the complementary capture probe (T_{20}) on the surface. The fluorescent results are given in Figure 8.6.
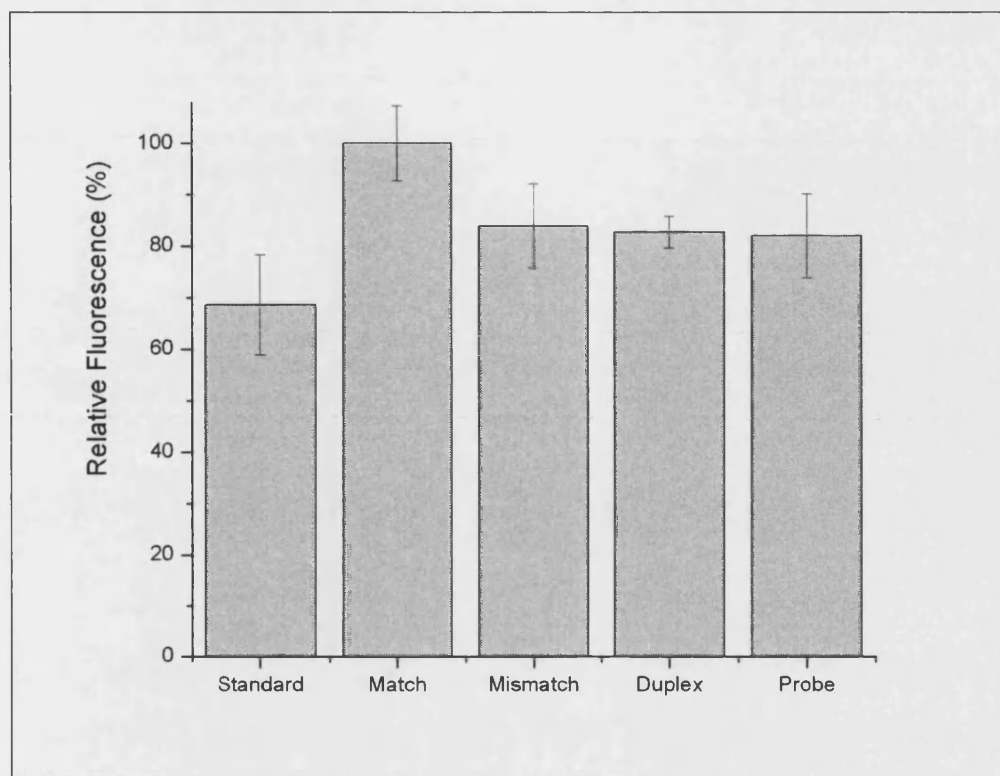
Figure 8.6 - Enzymatic digestion: large reporter oligonucleotide.
All assays use the Fluor-A_{20}-C282Y probe. Match assay: complementary C282YST target,
Mismatch assay: mismatched CTRAcomp target, Duplex assay: no enzyme, Probe assay: only
probe in buffer. Assays interrogated by the complementary capture probe (T_{20}) immobilised on the
surface (9 hours at 20 °C). The fluorescence, analysed by plate fluorimeter, is reported relative to
the Match assay (100%). 95% intervals of confidence levels are shown.

The Match assay gives a response which is 20% higher than the three control
experiments. This discrimination is positive, but not very high.

If enzymatic digestion was successful in the Digest assay, this should produce the
desired small reporter fragments which should be able to readily hybridise to the capture
probe. In contrast, it was thought that steric hindrance could limit the hybridisation of
the fluorescent species, which is the probe in the Control assays, Mismatch and Probe,
and the probe/ target duplex, in the Duplex assay. Limiting the hybridisation would
decrease the observed fluorescence.

The low discrimination could be due to the relatively large size of the reporter
fragment/capture probe duplex (20 bp), which may not be sufficiently destabilised by
steric effects in this system. If the size of this duplex was reduced there could be much
better sensitivity. Equally, in a system with more tightly packed capture probe
oligonucleotides, as can be achieved with thiolated oligonucleotides on a gold surface,

339

the discrimination could be improved. The discrimination could also be reduced if the wash steps are inefficient at removing any fluorescein labelled probe oligonucleotides which are non-specifically bound to the streptavidin.

The discrimination has been illustrated. Optimisation is not undertaken as this is not the electrochemical system. Clearly optimisation could be achieved by increasing the hybridisation temperature, from 20 °C, and by reducing the hybridisation time, from 9 hours.

Generation and evaluation of short reporter oligonucleotide

The short probe oligonucleotide (Fluor-A_8-C282YPR) was used in the four different enzymatic digestion assays described above in Figure 7.11. Each assay can be analysed with two different lengths of capture probe. The full details are given in section 2.11.2, Protocol 19.

The plate was analysed by a fluorimeter and the results are given in Figure 8.7. If the use of the different capture probes for each assay is contrasted, the use of the longer (T_{20}) capture probe gives a higher response for every assay (Digest and Control).
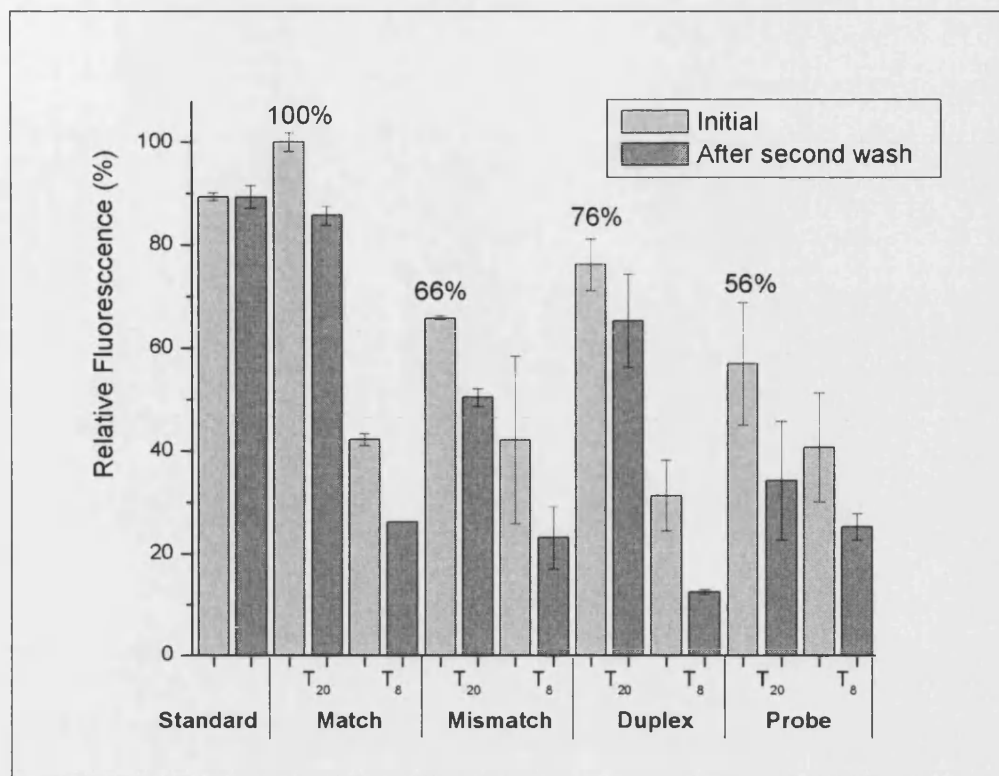
Figure 8.7 – Enzymatic digestion: short reporter oligonucleotide.
All assays use the Fluor-A_8-C282Y probe. Match assay: complementary C282YST target, Mismatch assay: mismatched CTRAcomp target, Duplex assay: no enzyme, Probe assay: only probe in buffer. Assays each interrogated by two complementary capture probes (T_{20} and T_8) immobilised on the surface (17 hours at 5 °C). The fluorescence, analysed by plate fluorimeter, is reported relative to the Match assay, with T_{20} capture probe (100%). 68% intervals of confidence are shown.

In this work, which uses short reporter probes and the long (T_{20}) capture probes, there is some discrimination between the response for the Match sequence and the Control samples (Mismatch 66%, Duplex 76%, Probe 56%). This is an improvement on the earlier work which used long reporter probes for which the Control assays had approximately 80% of the Match assay response. A room temperature (20 °C) buffer wash of the wells reduces the response of the assays but the ratios remain the same. This supports the theory that the response is from specific hybridisation.

No discrimination is observed between the four assays which use the short (T_8) capture probe sequences. This may be due to a lack of order at the surface, which would severely compromise any steric or hybridisation based discrimination. Whilst long immobilised oligonucleotides tend to align themselves in straight lines from the electrode surface to minimise the electrostatic repulsions, there may not be sufficient repulsion for the short probe sequences to do this.

Dual labelled probe approach

The absolute T7 enzymatic digestion was investigated by using an A_8-C282Y Dual Labelled Probe (5' labelled with 6-FAM 3' labelled with a quencher 6-TAMRA) and fluorescent detection. The Dual Labelled Probe was used in the four different enzymatic digestion assays described above in Figure 7.11. Full details are given in section 2.11.2, Protocol 20. The relative fluorescence of each assay is given below in Figure 8.8.
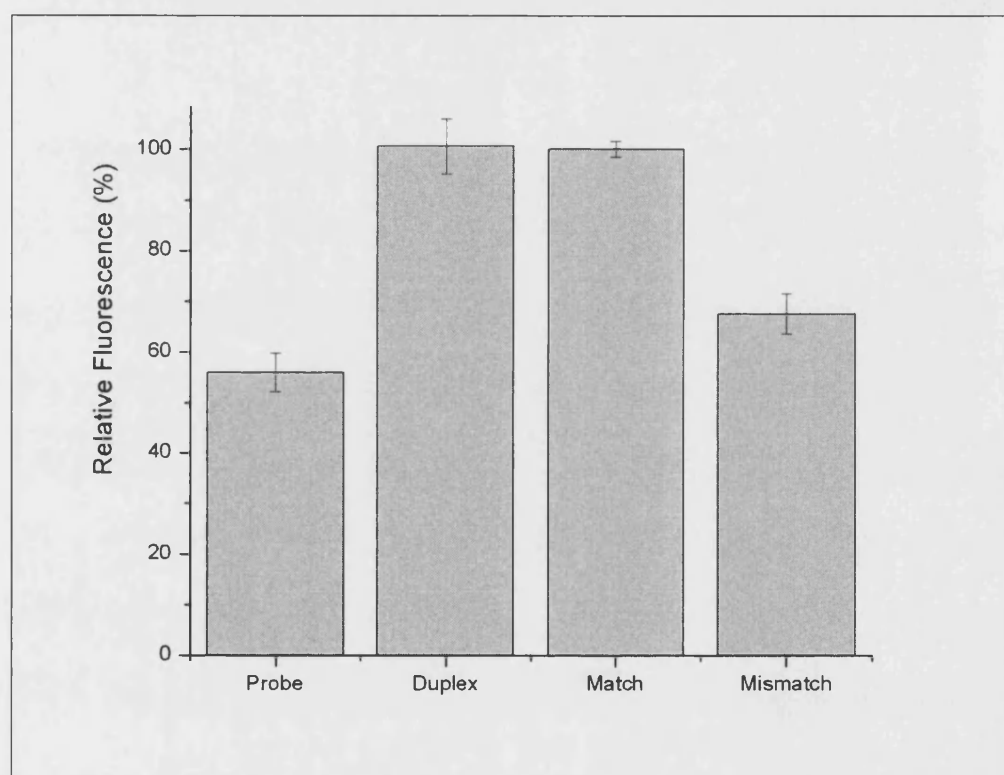
Figure 8.8 - LightCycler analysis of duplex digestion.
The fluorescent response is measured for assays which contain the A_8-C282Y dual labelled probe. Duplex assay: complementary C282Y target, Match assay: complementary target and T7 enzyme and Mismatch assay: mismatched CTRAcomp target and T7 enzyme. 95% intervals of confidence are shown.

The dual labelled probe (Probe assay) is able to reasonably efficiently quench its fluorescent emission through FRET, as the ssDNA is flexible and the two labels can be reasonably close together as shown in Figure 8.9. The fluorescent response is comparable to that of the Mismatch assay which also only contains the unhybridised dual labelled probe. When the complementary target is introduced (Duplex assay) the relative fluorescence approximately doubles as the rigid duplex keeps the two labels

342

further apart and therefore reduces the efficiency of the quenching. When the T7 exonuclease is introduced and the sample is incubated at 37 °C for 1 hour there is no increase in fluorescent response. There are two possible explanations for this result. Firstly the enzymatic digestion could be inefficient or may not occur at all and hence the duplex remains undigested. Alternatively the digestion is successful, but the experiment cannot follow this as the duplex holds the two labels sufficiently far apart that the quenching falls to the level that would be seen for digested label fragments in solution, as shown in Figure 8.9. The fluorescent results in Figure 8.8 do, however, show that the T7 exonuclease does not digest complementary target in the probe target duplex, regenerating the probe oligonucleotide.
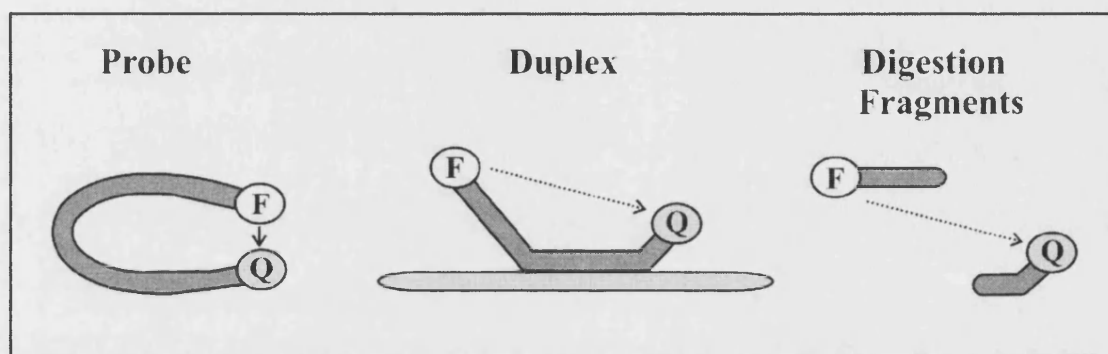
Figure 8.9 – Spatial influences on FRET in the dual labelled probe.
The unhybridised dual labelled probe (left hand side) can coil in solution bringing the fluorophore (F) and quencher (Q) spatially close together, enabling effective quenching (arrow). When the probe hybridises to the target (Duplex) the fluorophore and quencher are spatially separated and the effectiveness of quenching is reduced (dotted arrow). If the FRET quenching in the Duplex is sufficiently poor it may be equivalent to the very low interaction between the digested fragments in solution (right hand side).

Summary

The results from the initial surface supported work suggest that enzymatic (T7) digestion of the probe/target duplex generates fluorescein labelled fragments, which can be captured on a modified surface and detected with fluorescence. Discrimination has been obtained between the response for the fully complementary matched probe/target and assay consisting of the undigested duplex, a mismatched target and probe and the probe in isolation. The discrimination is not high but the sensing protocol has not been optimised. Time was not spent on optimisation as the sensor surface is not directly comparable to the surface which would be used in the electrochemical sensor and proof of concept is sufficient. Discrimination in favour of the hybridisation of the small

digested reporter probe to the capture probe (which should have the highest Tm) could be improved by using a using a higher hybridisation temperature, decreasing the hybridisation time or decreasing the salt concentration in the assay.

The results from the dual labelled probe work are inconclusive. The experiment either shows failure of the T7 enzymatic digestion, which contradicts the observed results for the surface supported work, or then results are constrained by the dual labelled probe assay, whereby ineffective FRET quenching of the duplex results in a fluorescent increase not being observed on digestion.

8.3   Electrochemical work

The preparation and use of the electrochemical sensor surface is illustrated below in Figure 8.10. The gold surface was modified with a thiolated capture probe (T_8) and then used to detect an A_8 ferrocenylated reporter oligonucleotide (Match), before being activated again and used to detect a ferrocenylated T_8 reporter oligonucleotide (Mismatch). Full details are given in section 2.11.2, Protocol 21.
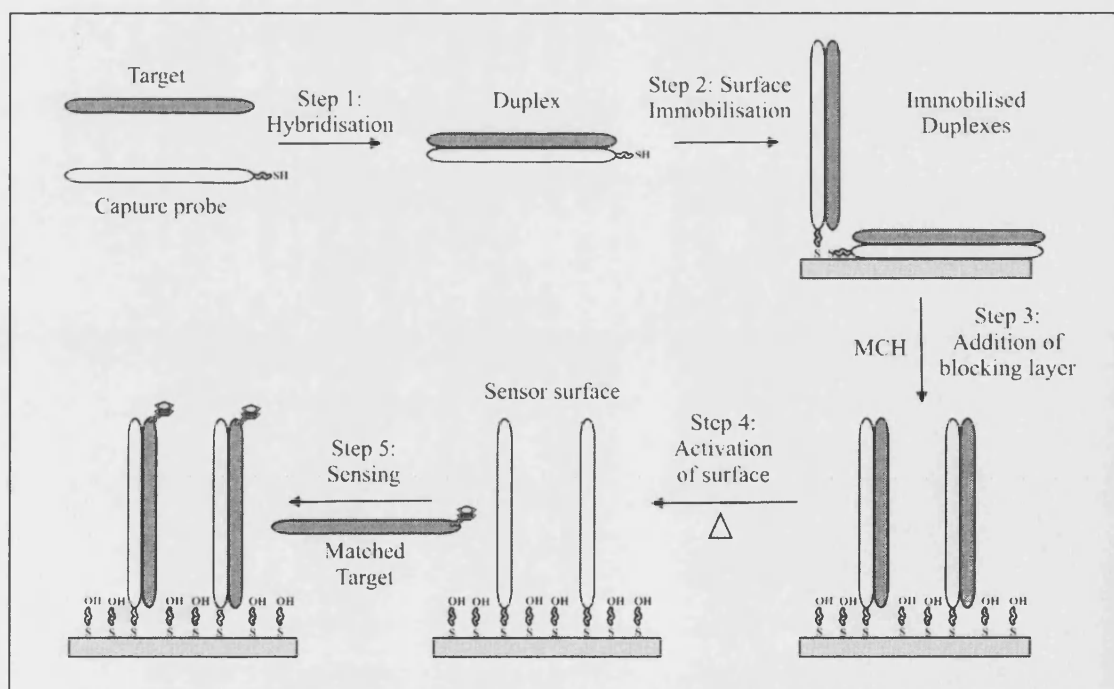
Figure 8.10 – Summary: production and use of modified probe sensor surface.
This is a reproduction Figure 7.12, which is given here for clarity.

344

Although it is not illustrated in the experimental scheme, Figure 8.10, for clarity, the complementary target (used in Step 1) was ferrocene labelled in the exploratory work so that duplex immobilisation and probe activation could be electrochemically verified. The electrochemical detection was done using DPV, with moving average baseline correction. The experimental set-up used is described section 2.5.8.

The electrochemical response (DPV) was measured at each stage of the sensor development, and the results are given in Figure 8.11. The steps directly relate to those in Figure 8.10.
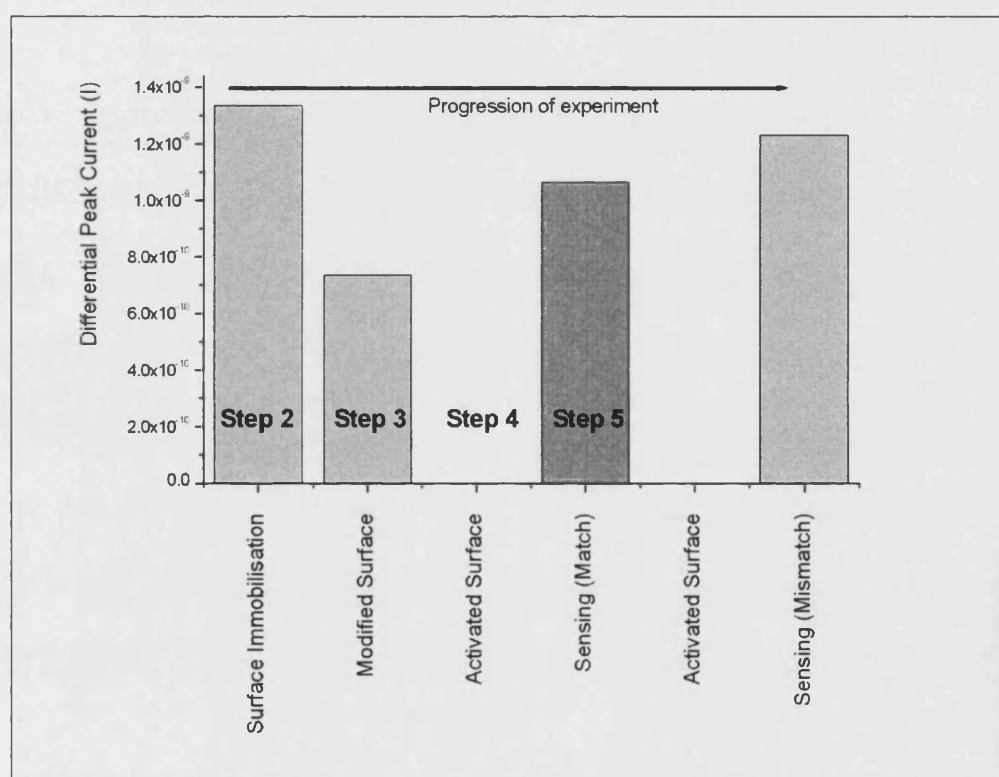
Figure 8.11 - Development of sensor surface.
The DPV response (light grey bars) is given for the different stages of the sensor development (Figure 7.13). Step 2: surface immobilisation of duplex. Step 3: modification of surface with MCH. Step 4: denaturing of surface by heating. Step 5: sensing; addition of ferrocenylated complementary target (dark grey bar). The surface is then denatured by heating and a ferrocenylated mismatched target is added.

Encouragingly a high response was obtained after the duplex was immobilised on the surface, which decreased when the MCH was added. This would be expected as the MCH would reduce the amount of non-specific DNA interactions with the surface and spatially remove some of the ferrocene reporter molecules from the surface. Activating the sensor surface, by melting the target from the duplex is also successful as the

response falls and no DPV response is seen. A positive DPV response is obtained when the complementary ferrocenylated reporter probe is introduced. This would be significant, but the subsequent activation of the surface and introduction of the non-complementary (mismatched) reporter probe also gave a high response. The mismatch response must be due to non-specific interaction between the mismatched reporter probe and the surface rather than hybridisation. This could also be the case for the matched reporter probe.

The most reasonable explanation for the results is that structural integrity of the immobilised probe surface is lost. The loss of bound capture probe is not thought to be a problem as Gerorgiadis (Peterson et al. 2001) routinely activates the probe surface with hot (no specific temperature is given) water washes and her earlier work, with Tarlov (Peterlinz et al. 1997) shows that heating the immobilised sample to 80 °C in buffer, denatures the duplex with no reduction in the surface density of the bound oligonucleotides. It may, however, be the case that the density of the capture probe at the surface is low and insufficient to block the small ferrocenylated reporter probes from reaching the surface. Alternatively, the density may be reasonable but the length of the oligonucleotides is not sufficient for them to form an ordered film which would act as a barrier to the reporter probes. A third alternative is that even if the density and orientation of the probes is reasonable, the act of analysing the surface with DPV may affect the integrity of the surface. Kelley has shown that applying a positive potential to an oligonucleotide film changes the orientation of the immobilised oligonucleotides until at a sufficiently high (positive) potential the film lies flat to the electrode (Kelley et al. 1998). In reality the explanation could be a combination of all three explanations. The experiment should be repeated using longer (T_{20}) capture probes and the DPV analysis should only be done once the reporter molecule has been introduced.

The initial development of an electrochemical sensor based on a surface immobilised capture probe has been unsuccessful.

8.4   Conclusions and further work

8.4.1   Conclusions

The exploratory work towards the development of an electrochemical sensor based on a surface immobilised capture probe has been undertaken.

Fluorescent labelling has been used to show that short complementary reporter oligonucleotides (Fluor-A_8) will hybridise with the immobilised capture probe at the surface. Good discrimination was shown between the response for the complementary and mismatched reporter probes, as illustrated by the Match and Mismatch assays in section 8.2.3. Using longer (T_{20}) capture probes allowed multiple reporter oligonucleotides to hybridise with the probe increasing the sensitivity.

The enzymatic digestion of the complementary probe/target duplex to produce fluorescent labelled reporter molecules, which were detected at the surface appears to have been successful. However, this was not substantiated when a fluorescent dual labelled probe was used to determine of enzymatic digestion could generate the reporter fragments. In this experiment, the undigested probe/target duplex gave the same fluorescent response before and after the addition of the enzyme, which suggests that T7 enzymatic digestion may not occur.

Initial work to translate the work from fluorescent detection to electrochemical detection was unsuccessful, but this highlights the potential route for further work.

8.4.2 Further work

To successfully develop the sensor further work must be done in two categories: fragment generation and surface modification.

Fragment generation

It is not absolutely known if T7 exonuclease digestion is successful. The fluorescent analysis of the FAM-A_8-C282Y-TAMRA dual labelled probe, discussed in section 8.2.4, should be repeated with both Taq and restriction enzyme digestion. Whilst the system is not ideal for the Taq enzyme (due to oligonucleotide overlap, see section 5.4.3) there is no theoretical reason why a restriction enzyme should not be successful. If fragment generation is successful with fluorescent labels, it is expected that it will be successful with an electrochemical (ferrocene) label.

Surface modification

Successful, robust surface modification is vital to the development of the electrochemical sensor. It is crucial that mechanical polishing of multiple gold electrodes is used to give a reproducibly flat electrode surface.

If surface modification through immobilisation of a thiolated duplex is considered, as in section 8.3, then the length of the capture probe can be increased together with the length of the reporter fragment. This should give a more ordered robust sensing surface.   Surface coverage of the duplex and hence the immobilised probe oligonucleotide can be controlled by varying the time for which the modified surface is exposed to the MCH blocking layer (more exposure, less coverage) or varying the salt concentration of the immobilisation buffer (higher salt concentration, higher coverage). Electrodes with a range of surface coverage can then by activated (initial target is removed though heating) and used as a hybridisation sensor for synthetically produced ferrocenylated reporter oligonucleotides. The hybridisation time should be as short as possible to reduce non-specific binding to the electrode surface.   In this work the

surface is only interrogated electrochemically (DPV) once to minimise the destabilising effect of the voltage sweep on the sensor layer.

If problems still exist with the integrity of the modified surface (as indicated by a high response for the Mismatched assay), the modification can be undertaken in an analogous way using the thiolated capture probe. This approach allows higher surface coverage to be obtained (although if the coverage is too high hybridisation efficiency will be reduced) which should reduce the access of mismatched reporter oligonucleotides to the surface. This approach does not require an activation step (heating) of the surface, which may be disruptive to the integrity of the surface in the duplex immobilisation.

When a robust surface has been developed which gives reproducible discrimination between matched and mismatched reporter probes, the surface can be used to interrogate reporter fragments generated through enzymatic digestion. If positive results are obtained from this work, the technology will have been shown to be an effective gene sensor.

Further sensor development

Once the sensor system has been proven as a gene sensor, it can be applied to further sensor systems including PCR and SNP detection.

If the Taq digestion of the duplex DNA is successful the technology could be used for *in situ* analysis of PCR, as illustrated in Figure 8.12. The progression of the PCR generates ferrocenylated reporter fragments which are captured on the electrode surface and detected electrochemically (DPV).
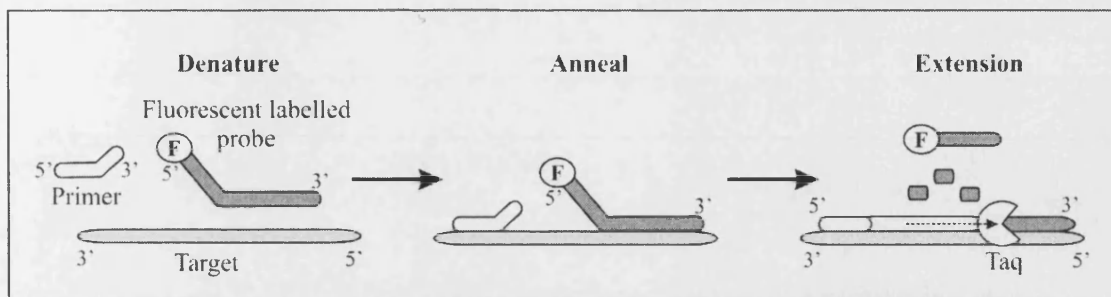
**Figure 8.12 – Summary: PCR generation of ferrocenylated reporter fragments.
This is a reproduction of Figure 7.10, which is given here for clarity.**

The concept of using dsDNA restriction enzymes for specific SNP detection or specific gene sequence detection has been introduced in section 6.5.2 and is summarised below in Figure 8.13. Surface modification could increase the sensitivity of this work.
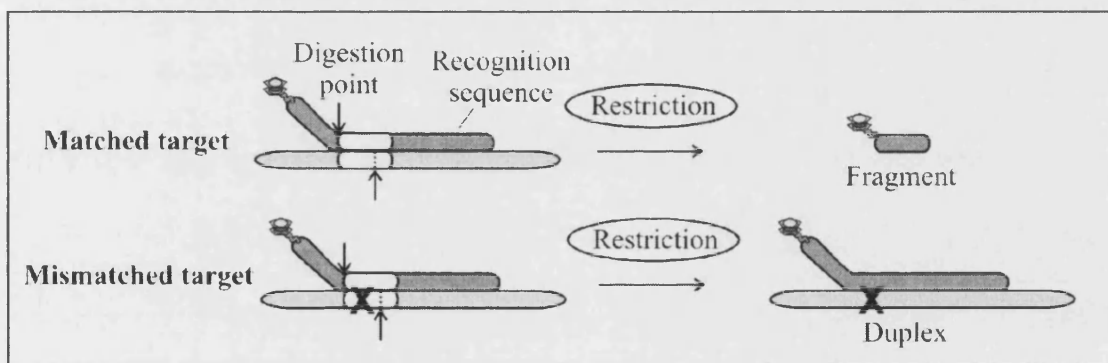
Figure 8.13 – Summary: restriction enzyme SNP sensor.

Chapter 9: Overall conclusions

9 Overall conclusions

The aim of this work has been the development of a novel electrochemical DNA gene sensor, based on enzymatic digestion. This has been achieved.

The development work was undertaken in three distinct parts. The full conclusions and further work are given in the respective results chapters. The principle conclusions from those studies are summarised here.

9.1 Synthesis of novel ferrocenylated linker molecules

The synthesis, activation for labelling and characterisation of novel ferrocenylated linker molecules was undertaken (theory **Chapter 3**, results **Chapter 4**).

- Ten novel ferrocenylated linker molecules have been synthesised. Each molecule has the potential to be derivatised to activated ester, which would allow it to be used for the covalent labelling of oligonucleotide probes.

- The synthetic routes utilised here have the potential to be developed further, which will allow the synthesis of additional novel linker molecules.

- Through synthetic variation, structural control affords variation of the ferrocene electropotential of the linker molecule. These electropotentials have been measured and the trends discussed. There is sufficient variation of the electropotential that resolvable DPV traces would be obtained for different molecules. This facilitates potential multiplexing.

- Four novel molecules have been derivatised to activated esters and can therefore be used for post-labelling probe oligonucleotides.

- A ferrocenylated phosphoramidite molecule was successfully synthesised which allowed the alternative phosphoramidite labelling approach to be undertaken.

9.2 Development of the gene sensor assay

Probe oligonucleotides were labelled with ferrocenylated linker molecules and used in gene sensor assays, in combination with enzymatic digestion (theory **Chapter 5**, results **Chapter 6**).

- Digestion of probe oligonucleotide with ssDNA specific S1 endonuclease showed discrimination was possible between the digested and undigested probe using DPV. The enzymatic digestion was validated using gel electrophoresis.

- The S1 endonuclease digestion assay can straightforwardly determine the success of probe oligonucleotide labelling.

- Hybridisation gene sensors based on T7 exonuclease enzymatic digestion were shown to be effective using both post-labelled and phosphoramidite labelled probes, with both glassy carbon and gold electrodes. Higher labelling efficiency is thought to give more reliable results for the phosphoramidite approach.

- It is proposed that the discrimination in the gene sensors is primarily due to the generation of small ferrocenylated fragments from the complementary assays on enzymatic digestion. The enzymatic digestion has been shown to occur using fluorescent dual labelled probes. The ferrocenylated fragments have been shown to have higher diffusion coefficients than the undigested probes, which directly results in a higher DPV response.

- A fouling layer, of undetermined physical character, has been shown to be formed on the electrodes during time-course experiments. This layer exhibits an electrochemical response and has been shown to improve the discrimination of the sensor time-course measurements.

- Gene sensing was successfully demonstrated for the following genes: Human hemochromatosis; beta actin; meningococcal meningitis and medium chain acyl-CoA dehydrognase. This work was done using synthetic gene sequences.

- Gene sensing was also successful for beta actin, using a PCR amplicon gene target.

9.3   Development of surface supported DNA hybridisation probes

Surface modification of the electrode was undertaken to improve the sensitivity of the gene sensor (theory **Chapter 7**, results **Chapter 8**).

- A sensor surface was shown to selectively bind fluorescent labelled reporter probes. Experimental results show discrimination for the gene sensing assay and suggest that enzymatic digestion could generate the reporter probe fragments. The enzymatic digestion was not substantiated using dual labelled probe digestion, but could be absolutely determined by using restriction enzymes.

- The methodology for translating this work to electrochemical detection has been described, although exploratory work was unsuccessful. It is envisaged that this will be possible and the necessary development work is described.

Labelled oligonucleotides

Label

Labelled oligonucleotide

70

5'-Fc-Linker-ATGCCCTCCCCCATGCCA TCCTGCGT-3' (BAPR) 79
5'-Fc-Linker-ATATACGTGCCAGGTGGA-3' (C282Y) 80
5'-Fc-Linker-ATATACGTGCCAGGTGGG 3' 81
TATATGCACGGTCCACCC

28

5'-Fc-Linker-ATATACGTGCCAGGTGGA-3' (C282Y) 78

82

5'-Fc-Linker-ATGCCCTCCCCCATGCCA TCCTGCGT-3' (BAPR) 83
5'-Fc-Linker-CATTGCCACGTGTCAGCTGCACAT-3' (CTR044) 84
5'-Fc-Linker-CTAGAATGAGTTACCAGAGAGCAGCTTGG (MC11PR) 85

References

Adamczyk, M., Fishpaugh, J. R., Mattingly, P. G. **1995**. "An easy preparation of hapten active esters via solid supported EDAC." Tetrahedron Letters 36: 8345-8346.

Adams, R. N. in A. J. Bard and M. Dekker (Eds.) **1969**. Electrochemistry at solid electrodes. New York, Wily: 19-42.

Alberts, B., Bray, D., Lewis, J., Raff, M., Roberts, K., Watson, J. D. **1994**. "Molecular biology of the cell." Garland Publishing.

Aleksandrovskii, Y. A., Bezhikina, L. V., Rodionov, Y. V. **1981**. "Comparative study of reactions cataylzed by glucose oxidase in the presence of different electron-acceptors." Biochemistry Moscow 46 (4): 593-599.

Alfonta, L., Singh, A. K., Willner, I. **2001**. "Liposomes labeled with biotin and horseradish peroxidase: A probe for the enhanced amplification of antigen-antibody or oligonucleotide-DNA sensing processes by the precipitation of an inoluble product on electrodes." Analytical Chemistry 73: 91-102.

Anne, A., Blanc, B., Moiroux, J. **2001**. "Synthesis of the first ferrocene-labeled dideoxynucleotide and its use for 3 '-redox end-labeling of 5 '-modified single-stranded oligonucleotides." Bioconjugate Chemistry 12 (3): 396-405.

Aoki, H., Buhlmann, P., Umezawa, Y. **2000**. "Electrochemical detection of a one-base mismatch in an oligonucleotide using ion-channel sensors with self-assembled PNA monolayers." Electroanalysis 12: 1272-1276.

Applied Biosystems, Applera Corporation U.S. Patents 5,723,591 5,801,155 and 6,084,102

Aqua, T., Naaman, R., Daube, S. S. **2003**. "Controlling the adsorption and reactivity of DNA on gold." Langmuir.

Arimoto, F. S. **1955**. "Derivatives of dicyclopentadienyliron." Journal of the American Chemical Society: 6295.

Atkins, P. W. **1990**. "Physical chemistry." Oxford University Press.

AutoLab **2001**. "AutoLab user manual GPES, version 4.9."

Balavoine, G. G. A., Daran, J. C., Iftime, G., Manoury, E., Moreau-Bossuet, C. **1998**. "Selective synthesis of ferrocenes." Journal of Organometallic Chemistry 567 (1-2): 191-198.

Bard, A. J., Parsons, Jordan **1985**. "Standard potentials in aqueous solution." Marcel Dekker Inc.

Bard, A. J., Faulkner, L. R. **2001**. "Electrochemical methods." John Wiley & Sons, Inc.

BAS **2004**. "Working electrodes." http://www.bas.com.

Bassler, H. A., Flood, S. J. A., Livak, K. J., Marmaro, J., Knorr, R., Batt, C. A. **1995**. "Use of a fluorgenic probe in a PCR-based assay for the detection of listeria monocytogenes." Applied and Environmental Microbiology 61 (10): 3724-3728.

Beaucage, S. L., Caruthers, M. H. **1981**. "Deoxynucleoside phosphoramidites - a new class of key intermediates for deoxypolynucleotide synthesis." Tetrahedron Letters 22 (20): 1859-1862.

Beilstein, A. E., Grinstaff, M. W. **2000**. "On-column derivatisation of oligodeoxynucleotides with ferrocene." Chemical Communications: 509-510.

Beilstein, A. E., Grinstaff, M. W. **2001**. "Synthesis and characterization of ferrocene-labeled oligodeoxynucleotides." Journal of Organometallic Chemistry 637: 398-406.

Bildstein, B., Hradsky, A., Kopacka, H., Malleier, R., Ongania, K. H. **1997**. "Functionalized pentamethylferrocenes: synthesis, structure, and electrochemistry." Journal of Organometallic Chemistry 540 (1-2): 127-145.

Blackburn, G. M., Gait, M. J. **1996**. "Nucleic acids in chemistry and biology." Oxford, Oxford University Press.

Bodansky, M., Bodansky, A. **1984**. "The practice of peptide synthesis." Springer-Verlag.

Bott, A. W. **1997**. "Practical problems in voltammetry: 4. Preparation of working electrodes." Current Separations 16: 79.

Boujtita, B., El Murr, N. **2000**. "Ferrocene-mediated carbon paste electrode modified with D-fructose dehydrogenase for batch mode measurement of D-fructose." Applied Biochemistry and Biotechnology 89 (1): 55-66.

Bourne, N., Williams, A., Douglas, K. T., Penkava, T. R. **1984**. "The E1cb mechanism for thiocarbamate ester hydrolysis - equilibrium and kinetic-studies." Journal of the Chemical Society-Perkin Transactions 2 (11): 1827-1832.

Braven, H. **2002**. "Molecular Sensing PLC, unpublished work."

Brazill, S. A., Kim, P. H., Kuhr, W. G. **2001**. "Capillary gel electrophoresis with sinusoidal voltammetric detection: a strategy to allow four color DNA sequencing." Analytical Chemistry 73 (20): 4882-4890.

Breslauer, K. J., Frank, R., Blocker, H., Marky, L. A. **1986**. "Predicting DNA duplex stability from the base sequence." Proceedings of the National Academy of Sciences of the United States of America 83: 3746-3750.

Brett, C. M. A., Brett, A. M. O., Serrano, S. H. P. **1993**. "On the adsorption and electrochemical oxidation of DNA at glassy carbon electrodes." J. Electroanalytical Chem. 366: 225-231.

Brown, T. A. **1995a**. "Gene cloning: an introduction." Cheltenham, Stanley Thornes Ltd.

Brown, T. A. **1995b**. "DNA sequencing." Oxford, Oxford University Press.

Bustamante, C., Bryant, Z., Smith, S. B. **2003**. "Ten years of tension: single-molecule DNA mechanics." Nature 421: 423 - 427.

Cai, H., Xu, C., He, P., Fang, Y. **2001**. "Colloid Au-enhanced DNA immobilization for the electrochemical detection of sequene-specific DNA." Journal of Electroanalytical Chemistry 510: 78-85.

Cai, H., Wang, Y., He, P., Fang, Y. **2002**. "Electrochemical detection of DNA hybridization based on silver-enhanced gold nanoparticle label." Analytica Chimica Acta 469: 165-172.

Cass, A. E. G., Davis, G., Francis, G. D., Hill, H. A. O., Aston, W. J., Higgins, I. J., Plotkin, E. V., Scott, L. D. L., Turner, A. P. F. **1984**. "Ferrocene-mediated enzyme electrode for amperometric determination of glucose." Analytical Chemistry 56: 667-671.

Cass, A. E. G., Davis, G., Green, M. J., Hill, H. A. O. **1985**. "Ferricinium ion as an electron acceptor for oxido-reductases." Journal of Electroanalytical Chemistry 190: 117-127.

Christian, G. D. **1994**. "Analytical chemistry." New York, John Wiley and Sons.

Chu, Y. Y., Yu, C. S., Chen, C. J., Yang, K. S., Lain, J. C., Lin, C. H., Chen, K. M. **1999**. "Novel camphor-derived chiral auxiliaries: significant solvent and additive effects on asymmetric reduction of chiral alpha- keto esters." Journal of Organic Chemistry 64 (19): 6993-6998.

Clayden, J., Greeves, N., Warren, S., Wothers, P. **2001**. "Organic chemistry." Oxford, Oxford University Press.

Collins, F. S., Morgan, M., Patrinos, A. **2003**. "The Human Genome Project: lessons from large scale biology." Science 300: 286-290.

Creager, S., Yu, C. J., Bamdad, C., O'Connor, S., MacLean, T., Lam, E., Chong, Y., Olsen, G. T., Luo, J. Y., Gozin, M., Kayyem, J. F. **1999**. "Electron transfer at electrodes through conjugated "molecular wire" bridges." Journal of the American Chemical Society 121 (5): 1059-1064.

Cygan, M. T., Dunbar, T. D., Arnold, J. J., Bumm, L. A., Shedlock, N. F., Burgin, T. P., Jones, L., Allara, D. L., Tour, J. M., Weiss, P. S. **1998**. "Insertion, conductivity, and structure of conjugated organic oligomers in self-assembled alkanethiol monolayers on Au{111}." Journal of the American Chemical Society 120: 2721-2732.

de Castro, C. S. P., SouzaDe, J. R., Bloch, C. **2003**. "Investigations on the binding of mercury ions to albumins employing differential pulse voltammetry." Protein and Peptide Letters 10 (2): 155-164.

de-los-Santos-Alvarez, P., Lobo-Castanon, M. J., Miranda-Ordieres, A. J., Tunon-Blanco, P. **2002**. "Voltammetric determination ofunderivatised oligonucleotides on graphite electrodes based on their oxidation products." Analytical Chemistry 74: 3342-3347.

de-los-Santos-Alvarez, P., Lobo-Castanon, M. J., Miranda-Ordieres, A. J., Tunon-Blanco, P. **2004**. "Current strategies for electrochemical detection of DNA with solid electrodes." Analytical and Bioanalytical Chemistry 378 (1): 104-118.

Deeming, A. J. in G. Wilkinson, F. G. A. Stone and E. W. Abel (Eds.) **1982**. Ferrocene compounds. Comprehensive Organometallic Chemistry. Oxford, Pergammon Press. 4: 475.

deLumley, T., Campbell, C. N., Heller, A. **1996**. "Direct enzyme-amplified electrical recognition of a 30-base model oligonucleotide." Journal of the American Chemical Society 118 (23): 5504-5505.

Dendrinos, K. G., Kalivretenos, A. G. **1998**. "Synthesis of N-hydroxysuccinimide esters using polymer bound HOBT." Tetrahedron Letters 39 (11): 1321-1324.

Desai, M. C., Stramiello, L. M. **1993**. "Polymer bound EDC (P-EDC): a convenient reagent for formation of an amide bond." Tetrahedron Letters 34 (48): 7685-7688.

Drummond, T. G., Hill, M. G., Barton, J. K. **2003**. "Electrochemical DNA sensors." Nature Biotechnology 21 (10): 1192-1199.

Epstein, J. R., Biran, I., Walt, D. R. **2002**. "Fluorescence-based nucleic acid detection and microarrays." Analytica Chimica Acta 469: 3-36.

Erdem, A., Kerman, K., Meric, B., Akarca, U. S., Ozsoz, M. **2000**. "Novel hybridisation indicator methylene blue for the electrochemcial detection of short DNA sequences related to the hepatitis B virus." Analytica Chimica Acta 422: 139-149.

Erner, W. E. **1960**. Modern Plastics 37: 107.

Fan, C., Plaxco, K. W., Heeger, A. J. **2003**. "Electrochemical interrogation of conformational changes as a reagentless method for the sequence-specific detection of DNA." Proceedings of the National Academy of Sciences of the United States of America: 9134-9137.

Farkas, D. H. **1999**. "Bioelectric detection of DNA and the automation of molecular diagnostics." J. Assoc. Lab Automation 4: 20-24.

Fisher, A. C. **1996**. "Electrode dynamics." Oxford Chemistry Primers.

Foreman, J., Walton, I. D., Stern, D., Rava, R. P., Trulson, M. O. **1998**. "Thermodunamics of duplex formation and mismatch discrimination on

photolithographically sythesized oligonucleotide arrays." ACS symposium series: Molecular modelling of nucleic acids: 206-228.

FrizBiochem DE 19901761A1

Fryer, R. M. **2002**. "Global analysis of gene expression: Methods, interpretation, and pitfalls." Exp. Nephrol 10: 64-74.

Fujii, K., Matsubara, Y., Akanuma, J., Takahashi, K., Kure, S. **2000**. "Mutation detection by TaqMan-allele specific amplification: application to molecular diagnostics of glycogen storage disease type 1a and medium-chain acyl-CoA dehydrogenase deficiency." Human mutation 15: 189-196.

Gait, M. J. **1984**. "Oligonucleotide synthesis: a practical approach." Oxford, IRL Press.

Gau, J., Lan, E. H., Dunn, B., Ho, C. M., Woo, J. C. S. **2001**. "A MEMS based amperometric detector for E. Coli bacteria using self-assembled monolayers." Biosens. Bioelectron. 16: 745-755.

Georgiadis, R., Peterlinz, K. P., Peterson, A. W. **2000**. "Quantitative measurements and modeling of kinetics in nucleic acid monolayer films using SPR spectroscopy." Journal of the American Chemical Society 122 (13): 3166-3173.

Ghica, M. E., Brett, C. M. A. **2005**. "Development of a carbon film electrode ferrocene-mediated glucose biosensor." Analytical Letters 38 (6): 907-920.

Gleria, K., Hill, H. A. O., McNeil, C. J., Green, M. J. **1986**. "Homogenous ferrocene-mediated amperometric immunoassay." Analytical Chemistry 58: 1203-1205.

Griffin, R. J., Evers, E., Davison, R., Gibson, A. E., Layton, D., Irwin, W. J. **1996**. "The 4-azidoberazyloxycarbonyl function; Application as a novel protecting group and potential prodrug modification for amines." Journal of the Chemical Society-Perkin Transactions 1 (11): 1205-1211.

Gross, E., Meienhofer, J. **1979**. "The peptides." New York, Academic Press Inc.

Guiver, M., Borrow, R., Marsh, J., Gray, S. J., Kaczmarski, E. B., Howells, D., Boseley, P., Fox, A. J. **2000**. "Evaluation of the Applied Biosystems automated Taqman polymerase chain reaction system for the detection of meningococcal DNA." FEMS Immunology and Medical Microbiology 28: 173-179.

Hagan, M. F., Chakraborty, A. K. **2004**. "Hybridization dynamics of surface immobilised DNA." Journal of Chemical Physics 120 (10): 4958-4968.

Halperin, A., Buhot, A., Zhulina, E. B. **2004**. "Sensitivity, specificity, and the hybridisation isotherms of DNA chips." Biophysical chemistry 86: 718-730.

Han, S. B., Lin, J. Q., Satjapipat, M., Baca, A. J., Zhou, F. M. **2001**. "A three-dimensional heterogeneous DNA sensing surface formed by attaching oligodeoxynucleotide-capped gold nanoparticles onto a gold-coated quartz crystal." Chemical Communications (7): 609-610.

Hashimoto, K. **1994**. "Novel DNA sensor for electrochemical gene detection." Anal.Chim.Acta. 286: 219-224.

Hashimoto, K., Ito, K., Ishimori, Y. **1998**. "Microfabricated disposable DNA sensor for detection of hepatitis B virus DNA." Sensors and Actuators B-Chemical 46: 220-225.

Herne, T. M., Tarlov, M. J. **1997**. "Characterization of DNA probes immobilized on gold surfaces." Journal of the American Chemical Society 119 (38): 8916-8920.

Herrington, R., Hock, K., (Eds.) **1991**. Flexible polyurethane foams. Midland, The Dow chemical company.

Hillebrant, H. **2003**. Friz Biochem sensing technologies. Bioelectrochemistry. Florence.

Hillier, S. C., Flower, S. E., Frost, C. G., Jenkins, A. T. A., Keay, R., Braven, H., Clarkson, J. **2004a**. "An electrochemical gene detection assay utilising T7

exonuclease activity on complementary probe-target oligonucleotide sequences." Electrochemistry Communications 6: 1227-1232.

Hillier, S. C., Frost, C. G., Jenkins, A. T. A., Braven, H., Keay, R., Flower, S. E., Clarkson, J. **2004b**. "An electrochemical study of enzymatic oligonucleotide digestion." Bioelectrochemistry 63: 307-310.

Houghton, R. P., Mulvaney, A. W. **1996**. "Mechanism of tin(IV)-catalysed urethane formation." Journal of Organometallic Chemistry 518 (1-2): 21-27.

Hu, X., Smith, G. D., Sykora, M., Lee, S. J., Grinstaff, M. W. **2000**. "Automated solid phase synthesis and photophysical properties of oligodeoxynucleotides labeled at 5' aminothymidine with $Ru(bpy)_2(4\text{-}m\text{-}4'\text{-}cam\text{-}bpy)^{2+}$." Inorganic Chemistry 39: 2500-2504.

Ihara, T., Maruo, Y., Takenaka, S., Takagi, M. **1996**. "Ferrocene-oligonucleotide conjugates for electrochemical probing of DNA." Nucleic Acids Research 24 (21): 4273-4280.

Ihara, T. **1997**. "Gene sensor using ferrocenyl oligonucleotide." Chemical Communications 17: 1609.

Jimenez-Sanchez, G., Childs, B., Valle, D. **2001**. "Human disease genes." Nature 409: 853-855.

Johnston, D. H., Glasgow, K. C., Thorp, H. H. **1995**. "Electrochemcial measurement of the solvent accessibility of nucleobases using electron transfer between DNA and metal complexes." Journal of the American Chemical Society 117: 8933-8938.

Josefsson, A. M., Magnusson, P. K. E., Ylitalo, N. **2000**. "Viral load of human papilloma virus 16 as a determinant for development of cervical carcinoma in situ: a nested case-control study." Lancet 355: 2189-2193.

Kelley, S. O., Barton, J. K., Jackson, N. M., McPherson, L. D., Potter, A. B., Spain, E. M., Allen, M. J., Hill, M. G. **1998**. "Orienting DNA helices on gold using applied electric fields." Langmuir 14 (24): 6781-6784.

Kelley, S. O., Boon, E. M., Barton, J. K., Jackson, N. M., Hill, M. G. **1999a**. "Single-base mismatch detection based on charge transduction through DNA." Nucleic Acids Research 27 (24): 4830-4837.

Kelley, S. O., Jackson, N. M., Hill, M. G., Barton, J. K. **1999b**. "Long-range electron transfer through DNA films." Angewandte Chemie-International Edition 38 (7): 941-945.

Kerber, R. C. in E. W. Abel, F. G. A. Stone and G. Wilkinson (Eds.) **1995**. Ferrocene. Comprehensive organometallic chemistry II (A review of the literature 1982 - 1994). Oxford, Pergamon Press. 7: 185.

Kerr, C. **1971a**. "Gene 6 Exonuclease of Bacteriaphage T7 (II)." Journal of Biological Chemistry 247 (1): 311-318.

Kerr, C. **1971b**. "Gene 6 Exonuclease of Bacteriaphage T7 (I)." Journal of Biological Chemistry 247 (1): 305-310.

Kertesv, V. **2000**. "Electrochemical detection of surface hybridization of oligodeoxynucleotides bearing antraquinone tags at gold electrodes." Electroanalysis 12: 889-894.

Khan, S. I., Beilstein, A. E., Grinstaff, M. W. **1999**. "Automated solid phase synthesis of site-specifically labeled ruthenium-oligonucleotides." Inorganic Chemistry 38 (3A): 418-419.

King, H. C., Sinha, A. A. **2001**. "Gene expression profile analysis by DNA microarrays." The Journal of the American Medical Association 286: 2280-2288.

Konig, K. R. G. **1970**. "Eine neue methode zur synthese von peptiden." Chemische Berichte 103: 788-798.

Kwiatkowski, R. W., Lyamichev, V., de Arruda, M., Neri, B. **1999**. "Clinical, genetic, and pharmacogenetic applications of the Invader assay." Molecular Diagnosis 4 (4): 353-364.

Lenigk, R., Liu, R. H., Athavale, M., Chen, Z., Ganser, D., Yang, J., Rauch, C., Liu, Y., Chan, B., Yu, H., Ray, M., Marrero, R., Grodzinski, P. **2002**. "Plastic biochannel hybridisation devices: a new concept for microfluidic DNA arrays." Analytical Biochemistry 311: 40-49.

Letowski, J., Brousseau, R., Masson, L. **2004**. "Designing better probes: effect of probe size, mismatch position and number on hybridization in DNA oligonucleotide microarrays." Journal of Microbiological Methods 57: 269-278.

Levicky, R., Herne, T. M., Tarlov, M. J., Satija, S. K. **1998**. "Using self-assembly to control the structure of DNA monolayers on gold: A neutron reflectivity study." Journal of the American Chemical Society 120 (38): 9787-9792.

Li, J., Xue, M., Wang, H., Cheng, L., Gao, L., Lu, Z., Chan, M. **2003**. "Amplifying the electrical hybridisation signals of DNA array by multilayer assembly of Au nanoparticle probes." Analyst 128: 917-923.

Liu, S., Ye, J., He, P., Fang, Y. **1996**. "Voltammetric determination of sequence-specific DNA by electroactive intercalator on graphite electrode." Analytica Chimica Acta 335: 239-243.

Livak, K. J., Flood, S. J. A., Marmaro, J., Giusti, W., Deetz, K. **1995**. "Oligonucleotides with fluorescent dyes at oppostite ends provide a quenched probe system useful for detecting PCR product and nucleic-acid hybridisation." PCR-Methods and Applications 4 (6): 357-362.

Long, Y., Li, C., Sutherland, T. C., Chahma, M., Lee, J. S., Kraatz, H. **2003**. "A comparision of electron-transfer rates a ferrocenoyl-linked DNA." Journal of the American Chemical Society 125: 8724-8725.

Mao, Y., Luo, C., Ouyang, Q. **2003**. "Studies of temperature-dependant electronic transduction on DNA hairpin loop sensor." Nucleic Acids Research 31 (18): e108-e114.

Maxam, A., Gilbert, W. **1977**. "A new method of sequencing DNA." Proceedings of the National Academy of Sciences of the United States of America 74: 560-564.

Meric, B., Kerman, K., Ozkan, D., Kara, P., Ozsoz, M. **2002**. "Indicator-free electrochemical DNA biosensor based on adenine and guanine signals." Electroanalysis 14: 1245-1250.

Mikkelesen, S. R. **1996**. "Electrochemical biosensors for DNA sequence detection." Electroanalysis 8: 15-19.

Millan, K. M., Mikkelesen, S. R. **1993**. "Sequence-selective biosensor for DNA based on electroactive hybridization indicators." Analytical Chemistry 65: 2317-2323.

Millan, K. M., Saraullo, A., Mikkelesen, S. R. **1994**. "Voltammetric DNA biosensor for cystic fibrosis based on a modified carbon paste electrode." Analytical Chemistry 66: 2943-2948.

Miyahara, H., Yamashita, K., Kanai, M., Uchida, K., Takagi, M., Kondo, H., Takenaka, S. **2002**. "Electrochemical analysis of single nucleotide polymorphisms of p53 gene." Talanta 56 (5): 829-835.

Mizutani, F., Yabuki, S., Katsura, T. **1994**. "Amperometric glucose-sensing electrodes with the use of modified enzymes." ACS symposium series: Diagnostic biosensor polymers 556: 41-46.

Molecular Probes **2004**. http://www.probes.com.

Molecular Sensing WO 03/074731 A2

Morris, J. G. **1987**. "A biologist's physical chemistry." Bristol, Edward Arnold.

Mukumoto, K., Nojima, T., Furuno, N., Takenaka, S. **2003**. "Development of a novel genosensor based on ferrocenyl oligonucleotides." Nucleic Acids Research Supplement 3: 43-44.

Mullis, K., Faloona, F., Scharf, S., Saiki, R., Horn, G., Erlich, H. **1986**. "Specific enzymatic amplification of DNA invitro. The polymerase chain-reaction." Cold Spring Harbour Symposia on Quantitative Biology 51: Part 1: 263-273.

Mullis, K., Ferre, F., Gibbs, R. A. **1994**. "The polymerase chain reaction." Boston, Birkhauser.

Nakayama, M., Ihara, T., Nakano, K., Maeda, M. **2002**. "DNA sensors using a ferrocene-oligonucleotide conjugate." Talanta 56 (5): 857-866.

Napier, M. E., Loomis, C. R., Sistare, M. F., Kim, J., Eckhardt, A. E., Thorp, H. H. **1997**. "Probing biomolecule recognition with electron transfer: electrochemical sensors for DNA hybridization." Bioconjugate Chemistry 8: 906-913.

Neidle, S. **2002**. "Nucleic acid structure and recognition." New York, Oxford University Press.

Neises, B. S., W **1987**. "Esterification of carboxylic acids with dicyclohexyl-carbodiimide/4-Dimethylaminopyridine." Organic Synthesis Collection 5: 183-187.

Nojima, T., Yamashita, K., Takagi, A., Takagi, M., Ikeda, Y., Kondo, H., Takenaka, S. **2003**. "Direct detection of single nucleotide polymorphism (SNP) with genomic DNA by the ferrocene diimide-based electrochemcial hybridisation asssay (FND-EHA)." Analytical Sciences 19: 79-83.

Noomen, S. N., Breel, G. J., Winkel, C. **1995**. "The synthesis of pure amadori rearrangement products." Recueil Des Travaux Chimiques Des Pays-Bas-Journal of the Royal Netherlands Chemical Society 114 (7): 321-324.

Olivier, M., Chuang, L., Chang, M., Chen, Y., Pei, D., Ranade, K., Witte, A., Allen, J., Tran, N., Curb, D., Pratt, R., Neefs, H., Indig, M., Law, S., Neri, B., Wang, L., Cox, D. R. **2002**. "High-throughput genotyping of single nuleotide polymorphisms using new biplex invader technology." Nucleic Acids Research 30 (12): e53.

Ozkan, D., Kara, P., Kerman, K., Meric, B., Erdem, A., Jelen, F., Nielsen, P. E., Ozsoz, M. **2002**. "DNA and PNA sensing on mercury and carbon electrodes by using methylene blue as an electrochemical label." Bioelectrochemistry 58: 119-126.

Ozsoz, M., Erdem, A., Kerman, K., Ozkan, D., Tugrul, B., Topcuoglu, N., Ekren, H., Taylan, M. **2003**. "Electrochemical genosensor based on colloidal gold nanoparticles for the detection of factor V lleiden mutation using disposable pencil graphite electrodes." Analytical Chemistry 75: 2181-2187.

Padeste, C., Steiger, B., Grubelnik, A., Tiefenauer, L. **2003**. "Redox labelled avidin for enzyme sensor architectures." Biosensors and Bioelectronics 19 (3): 239-247.

Palecek, E. **1960**. "Oscillographic polarography of highly polymerized deoxyribonucleic acid." Nature 188: 656-657.

Palecek, E., Fojta, M. **2001**. "Detecting DNA hybridization and damage." Analytical Chemistry 73 (3): 74A-83A.

Palecek, E. **2002**. "Past, present and future of nucleic acids electrochemistry." Talanta 56 (5): 809-819.

Palecek, E., Billova, S., Havran, L., Kizek, R., Miculkova, A., Jelen, F. **2002**. "DNA hybridisation at microbeads with cathodic stripping voltammetric detection." Talanta 56: 919-930.

Park, S. J., Taton, T. A., Mirkin, C. A. **2002**. "Array-based electrical detection of DNA with nanoparticle probes." Science 295: 1503-1506.

Peterlinz, K., Tarlov, M. **1997**. "Observation of hybridisation and dehybridisation of thiol-tethered DNA using two-color surface plasmon resonance spectroscopy." Journal of the American Chemical Society 119: 3401-3402.

Peterson, A. W., Heaton, R. J., Georgiadis, R. M. **2001**. "The effect of surface probe density on DNA hybridization." Nucleic Acids Research 29 (24): 5163-5168.

Peterson, A. W., Wolf, L. K., Georgiadis, R. M. **2002**. "Hybridization of mismatched or partially matched DNA at surfaces." Journal of the American Chemical Society 124 (49): 14601-14607.

Petrovykh, D. Y., Kimura-Suda, H., Whitman, L. J., Tarlov, M. J. **2003**. "Quantitative analysis and characterization of DNA immobilized on gold." Journal of the American Chemical Society 125 (17): 5219-5226.

Pike, A. R., Ryder, L. C., Horrocks, B. R., Clegg, W., Elsegood, M. R. J., Connolly, B. A., Houlton, A. **2002**. "Metallocene-DNA: synthesis, molecular and electronic structure and DNA incorporation of C5-ferrocenylthymidine derivatives." Chemistry. A European Journal 8 (13): 2891-2899.

Plesske, K. **1962a**. "Ring substitutions and secondary reactions of aromatic-metal pie-complexes, Part II." Angewandte Chemie-International Edition 1 (7): 394-399.

Plesske, K. **1962b**. "Ring substitutions and secondary reactions of aromatic-metal pie-complexes, Part I." Angewandte Chemie-International Edition 1 (6): 312-327.

Popovich, N. D., Eckhardt, A. E., Mikulecky, J. C., Napier, M. E. **2002a**. "Electrochemical sensor for detection of unmodified nucleic acids." Talanta 56: 821-828.

Popovich, N. D., Thorp, H. H. **2002b**. "New strategies for electrochemcial nucleic acid detection." Interface 11 (4): 30-34.

Pouradier, M., Gadet, M. C., Chateau, H. **1965**. "Electrochime des sels d'or." Journal de Chimie Physique 62: 203-216.

Prins, R., Korswagen, A. R., Kortbeek, A. G. T. G. **1972**. "Decompostion of the ferrocenium cation by nucleophilic reagents." Journal of Organometallic Chemistry 39: 335-344.

Prozyme **2004**. http://www.prozyme.com.

Quirke, J. M. E., Hsu, Y. L., Van Berkel, G. J. **2000**. Journal of Natural Products 63 (2): 230-237.

Rendell, D. **1987**. "Fluorescence and phosphorescence spectroscopy." New York, John Wiley and Sons.

Ricci, A. **1977**. "Organomettalic reactions. Addition reactions of benzenethiol to unsaturated systems catalysed by trimethyl(phenylthio)-silane or -stannane." Journal of the Chemical Society-Perkin Transactions 1: 1069-1073.

Roberts, L. **2001**. "A history of the human genome project." Science 291 (5507): 1195.

Rockett, B. W., Marr, G. **1991**. "Annual survey of ferrocene chemistry 1989." Journal of Organometallic Chemistry 416: 327-398.

Saiki, R. K., Gelfand, D. H., Stoffel, S., Scharf, S. J., Higuchi, R., Horn, G. T., Mullis, K. B., Erlich, H. A. **1988**. "Primer-directed enzymatic amplification of DNA with a thermostable DNA polymerase." Science 239: 487-91.

Sakakida, M., Nishida, K., Shichiri, M., Ishihara, K., Nakabayashi, N. **1993**. "Ferrocene-mediated needle-type glucose sensor covered with newly designed biocompatible membrane." Sensors and Actuators B-Chemical 13 (1-3): 319-322.

Sanger, F. **1977**. "DNA sequencing with chain-terminating inhibitorts." Proceedings of the National Academy of Sciences of the United States of America 74: 5463-5467.

Satchell, D. P. N., Satchell, R. S., Wassef, W. N. **1992**. "The kinetics and mechanism of the thallium(Iii) ion-promoted hydrolysis of thiolurethanes in aqueous solution - a metal ion promoted elimination." Journal of the Chemical Society-Perkin Transactions 2 (7): 1199-1202.

Sato, S., Meada, Y., Nojima, T., Kondo, H., Takenaka, S. **2003**. "SNP analysis by using ferrocenyl naphthalene diimine (FND)-based electrochemical hybridisation assay (EHA)." Nucleic Acids Research Supplement No. 3: 169-170.

Schlapfe, P., Mindt, W., Racine, P. **1974**. "Electrochemical measurement of glucose using various electron acceptors." Clinica Chimica Acta.

Schlogl, K., Seiler, H. **1958**. "Ferrocenoyl-isocyanat." Naturwissenshaften 45: 337.

Schuck, P. **1997**. "Use of surface plasmon resonance to probe the equilibrium and dynamic aspects of interactions between biological macromolecules." Annual Review of Biophysics and Biomolecular Structure 26: 541-566.

Sha, X. Z., Huo, J. W., Wang, X. Z. **1993**. "Amperometric determination of glucose with a ferrocence-mediated glucose-oxidase electrode." Sensors and Actuators B-Chemical 12 (1): 33-36.

Sigma Genosys **2004**. "Determination of Tm." http://www.genosys.com.

Silva, M. E. N. P. R. A., Pombeiro, A. J. L., Dasilva, J., Herrmann, R., Deus, N., Castilho, T. J., Silva, M. **1991**. "Redox potential and substituent effects at ferrocene Derivatives - Estimates of Hammett sigma-p and Taft polar sigma substituent constants." Journal of Organometallic Chemistry 421 (1): 75-90.

Silva, M. E. N. P. R. A., Pombeiro, A. J. L., Dasilva, J., Herrmann, R., Deus, N., Bozak, R. E. **1994**. "Redox potential and substituent effects in ferrocene derivatives 2." Journal of Organometallic Chemistry 480 (1-2): 81-90.

Smith, M. B., March, J. in (Eds.) **2001**. The Curtius rearrangement. March's Advanced Organic Chemistry, John Wiley & Sons, Inc: 1412.

Steel, A. B., Herne, T. M., Tarlov, M. J. **1999**. "Electrostatic interactions of redox cations with surface- immobilized and solution DNA." Bioconjugate Chemistry 10 (3): 419-423.

Steemers, F. J., Ferguson, J. A., Walt, D. R. **2000**. "Screening unlabelled DNA targets with randomly ordered fibre-optic gene array." Nature Biotechnology 18: 91-94.

Steitz, T. A. **1999**. "DNA polymerases: structural diversity and common mechanisms." The Journal of Biological Chemistry 274: 17395-17398.

Sun, X., He, P., Liu, S., Ye, J. **1998**. "Immobilisation of single-stranded deoxyribose acid on gold electrode with self-assembled aminoethanethiol monolayer for DNA electrochemcial sensor applications." Talanta 47: 487-495.

Takenaka, S., Uto, Y., Kondo, H., Ihara, T., Takagi, M. **1994**. "Electrochemically active DNA probes. Detection of target DNA sequences at femtomole level by High-Performance Liquid Chromatography with electrochemical detection." Analytical Biochemistry 218 (2): 436-443.

Takenaka, S., Takagi, M., Uto, Y., Kondo, H. **1998**. "Construction of a polyferrocene array with ferrocenyl napthalene diimide intercalated to the double stranded DNA." Nucleic Acids Symposium Series 39: 107-108.

Takenaka, S., Yamashita, K., Takagi, M., Uto, Y., Kondo, H. **2000**. "DNA sensing on a DNA probe-modified electrode using ferrocenylnaphthalene diimide as the electrochemically active ligand." Analytical Chemistry 72 (6): 1334-1341.

Takenaka, S. **2001**. "Highly sensitive probe for gene analysis by electrochemical approach." Bulletin of the Chemical Society of Japan 74 (2): 217-224.

The Celera Genomics Sequencing Team **2001**. "The sequence of the human genome." Science: 1304-1351.

The Human Genome Project **2005**. http://www.doegenomes.org/.

The International Human Genome Mapping Consortium **2001**. "A physical map of the human genome." Nature 409: 934-941.

The International SNP Map Working Group **2001**. "A map of human genome sequence variation containing 1.42 million single nucleotide polymorphisms." Nature 409: 928-933.

Tierney, M. T., Grinstaff, M. W. **2000a**. "Synthesis and characterization of fluorenone-, anthraquinone- and phenothiazine labeled oligodeoxynucleotides: 5' probes for redox chemistry." Journal of Organic Chemistry 65: 5355-5359.

Tierney, M. T., Grinstaff, M. W. **2000b**. "Sythesis and stability of oligodeoxynucleotides containing C8-labeled 2'-deoxyadenosine: novel redox nucleobase probes for DNA-mediated charge transfer studies." Organic Letters 22: 3413-3416.

Tyagi, S., Kramer, F. R. **1996**. "Molecular beacons: probes that fluoresce upon hybridisation." Nature Biotechnology 14: 303-308.

Tyagi, S., Bratu, D. P., R., K. F. **1998**. "Mulitcolur molecular beacons for allele discrimination." Nature Biotechnology 16: 49-53.

Ugozzoli, L. A., Chinn, D., Hamby, K. **2002**. "Fluorescent multicolor multiplex homogeneous assay for the simultaneous analysis of the two most common hemochromatosis mutations." Analytical Biochemistry 307 (1): 47-53.

Ulrich, H. **1967**. "Base catalysed reactions of isocyanates." Journal of Organic Chemistry 32: 3938-3941.

Umek, R. M., Lin, S. S., Chen, Y., Irvine, B., Paulluconi, G., Chan, V., Chong, Y., Cheung, L., Vielmetter, J., Farkas, D. H. **2000**. "Bioelectronic detection of point mutations using discrimination of the H63D polymorphism of the Hfe gene as a model." Molecular Diagnostics 5 (4): 321-328.

Umek, R. M. **2001**. "Electronic detection of nucleic acids." Journal of Molecular Diagnostics 3 (2): 74-84.

Urban, M., Moller, R., Fritzsche, W. **2003**. "A paralleled readout system for an electrical DNA-hybridization assay based on a microstructured electrode array." Review of Scientific Instruments 74: 1077-1081.

Van Berkel, G. J., Quirke, J. M. E., Tigani, R. A., Dilley, A. S., Covey, T. R. **1998**. "Derivatization for electrospray ionization mass spectrometry. 3. Electrochemically ionizable derivatives." Analytical Chemistry 70 (8): 1544-1554.

Verheijen, J. C., van der Marel, G. A., van Boom, J. H., Metzler-Nolte, N. **2000**. "Transition metal derivatives of Peptide Nucleic Acid (PNA) oligomers. Synthesis, characterization and DNA binding." Bioconjugate Chemistry 11: 741-743.

Vet, J. A., Majithia, A. R., Marras, S. A., Tyagi, S., Dube, S., Poiesz, B. J., Kramer, F. R. **1999**. "Multiples detection of four pathogenic retroviruses using molecular beacons." Proceedings of the National Academy of Sciences of the United States of America 96: 6394-6399.

Vogt, V. M. **1973**. "Purification and further properties of single-strand-specific nuclease from Asperillus Oryzae." European Journal of Biochemistry 33: 192-200.

Wallace, R. B., Shaffer, J., Murphy, R. F. **1979**. Nucleic Acids Research 6: 3543.

Wang, D., Coscoy, L., Zylberberg, M., Avila, P. C., Boushey, H. A., Ganem, D., DeRisi, J. L. **2002a.** "Microarray-based detection and genotyping of viral pathogens." Proceedings of the National Academy of Sciences of the United States of America 99 (24): 15687-15692.

Wang, J., Cai, X., Wang, J., Jonsson, C. **1995.** "Trace measurements of RNA by potentiometric stripping analysis at carbon paste electrodes." Analytical Chemistry 67: 4065-4070.

Wang, J., Cai, X., Jonsson, C., Balakrishan, M. **1996a.** "Adsorptive stripping potentiometry of DNA at electrochemcially pretreated carbon paste electrodes." Electroanalysis 8 (1): 20-24.

Wang, J., Cai, X. H., Tian, B. M., Shiraishi, H. **1996b.** "Microfabricated thick-film electrochemical sensor for nucleic acid determination." Analyst 121 (7): 965-969.

Wang, J., Palecek, E., Nielsen, P. E., Rivas, G., Cai, X., Shiaishi, H., Dontha, N., Luo, D., Farias, P. A. M. **1996c.** "Peptide nucleic acid probes for sequence-specific DNA biosensors." Journal of the American Chemical Society: 7667-7670.

Wang, J., Rivas, G., Cai, X., Chicharro, M., Parrado, C., Dontha, N., Begleiter, A., Mowat, M., Palecek, E., Nielsen, P. E. **1997.** "Detection of point mutation in the P53 gene using a peptide nucleic acid biosensor." Analytica Chimica Acta 344: 111-118.

Wang, J. **1998.** "DNA biosensors based on Peptide Nucleic Acid (PNA) recognition layers." Biosens Bioelectron 13: 757-762.

Wang, J., Rivas, G., Fernandes, J. R., Paz, J. L. L., Jiang, M., Waymire, R. **1998.** "Indicator-free electrochemcial DNA hybridization biosensor." Analytica Chimica Acta 375: 197-203.

Wang, J. **1999.** "Towards genoelectronics: electrochemical biosensing of DNA hybridization." Chemistry. A European Journal 5 (6): 1681-1685.

Wang, J., Jiang, M., Mukherjee, B. **2000.** "On-demand electrochemcial release of DNA from gold surfaces." Bioelectrochemistry 52: 111-114.

Wang, J., Kawde, A. **2001.** "Pencil-based renewable biosenesor for label-free electrochemcial detection of DNA hybridization." Analytica Chimica Acta 431: 219-224.

Wang, J. **2002.** "Electrochemical nucleic acid biosensors." Analytica Chimica Acta 469 (1): 63-71.

Wang, J., Kawde, A. B. **2002b.** "Amplified label free electrical detection of DNA hybridization." Analyst 127: 383-386.

Wang, J., Liu, G., Merkoci, A. **2003.** "Electrochemcial coding technology for simultaneous detection of multiple DNA targets." Journal of the American Chemical Society 125: 3214-3215.

Watson, J. D., Crick, F. H. C. **1953.** "Molecular structure of nucleic acids: A structure for deoxyribose nucleic acid." Nature 171: 737-734.

Watson, J. D., Gilman, M. **1992.** "Recombinant DNA." New York, Scientific American Books.

Watterson, J. H., Piunno, P. A. E., Krull, U. J. **2002.** "Practical physical aspects of nterfacial nucleic acid oligomer hybridisation for biosensor design." Analytica Chimica Acta 469: 115-127.

Weizman, H., Tor, Y. **2002.** "Redox-active metal containing nucleotides: synthesis, tunability, and enzymatic incorporation into DNA." Journal of the American Chemical Society 124 (8): 1568-1569.

Whitcome, D., Theaker, J., Guy, S. P., Brown, T., Little, S. **1999**. "Detection of PCR products using self-probing amplicons and fluorescence." Nature Biotechnology 17: 804-807.

Willner, I., Patolsky, F., Weizman, Y., Willner, B. **2002**. "Amplified detection of single-base mismatches in DNA using microgravimetric quartz-crystal-microbalance transduction." Talanta 56: 847-856.

Wingard, L. B. **1983**. "Immobilized enzyme electrodes for glucose determination for the artificial pancreas." Federation Proceedings 42: 288-291.

Wojciechowski, M., Sundseth, R., Moreno, M., Henkens, R. **1999**. "Multichannel electrochemcial detection system for quantitative mointoring of PCR amplifiaction." Clinical Chemistry 45: 1690-1693.

Wolf, L. K., Gao, Y., Georgiadis, R. M. **2004**. "Sequence-dependent DNA immobilization: specific versus nonspecific contributions." Langmuir 20 (8): 3357-3361.

Woodward, R. B. **1952**. "A new aromatic system." Journal of the American Chemical Society 74: 3458-3459.

Wunsch, E. **1966**. Chemische Berichte 99: 110-120.

Xu, C., He, P. G., Fang, Y. Z. **2000**. "Electrochemical labeled DNA probe for the detection of sequence-specific DNA." Analytica Chimica Acta 411 (1-2): 31-36.

Xu, J., Zhu, J., Huang, Q., Chen, H. **2001**. "A novel DNA-modified indium tin oxide electrode." Electrochemistry Communications 3: 665-669.

Yamashita, K., Takagi, M., Kondo, H., Takenaka, S. **2000**. "Electrochemical detection of base pair mutation." Chemistry Letters: 1038-1039.

Yamashita, K., Takagi, M., Kondo, H., Takenaka, S. **2002**. "Electrochemical detection of nucleic base mismatches with ferrocenyl naphthalene diimide." Analytical Biochemistry 306 (2): 188-196.

Yang, I. V., Thorp, H. H. **2001a**. "Modification of indium tin oxide electrodes with repeat polynucleotide: Electrochemcial detection of trinucleotide repeat expanstion." Analytical Chemistry 73: 5316-5322.

Yang, I. V., Thorp, H. H. **2001b**. "Oxidation of 7-dezaguanine by one-electron and oxo-transfer oxidants: Mismatch-dependant electrochemistry and selective strand scission." Inorganic Chemistry 40: 1690-1697.

Yang, I. V., Ropp, P. A., Thorp, H. H. **2002a**. "Toward electrochemcial resolution of two genes on one electrode: using 7-deaza analogues of guanine and adenine to prepare PCR products with differential redox activity." Analytical Chemistry 74: 347-354.

Yang, W., Ozsoz, M., Hibbert, D. B., Gooding, J. J. **2002b**. "Evidence for the direct interaction between methylene blue and cuanine bases using DNA-modified carbon paste electrodes." Electroanalysis 14: 1299-1302.

Yu, C. J., Yowanto, H., Wan, Y. J., Meade, T. J., Chong, Y., Strong, M., Donilon, L. H., Kayyem, J. F., Gozin, M., Blackburn, G. F. **2000**. "Uridine-conjugated ferrocene DNA oligonucleotides: unexpected cyclization reaction of the uridine base." Journal of the American Chemical Society 122 (28): 6767-6768.

Yu, C. J., Wan, Y. J., Yowanto, H., Li, J., Tao, C. L., James, M. D., Tan, C. L., Blackburn, G. F., Meade, T. J. **2001**. "Electronic detection of single-base mismatches in DNA with ferrocene-modified probes." Journal of the American Chemical Society 123 (45): 11155-11161.

Zhao, Y., Pang, D., Wang, Z., Cheng, J., Qi, Y. **1997**. "DNA-modified electrodes. Part 2. Electrochemcial characterization of gold electrodes modified with DNA." Journal of Electroanalytical Chemistry 431: 203-209.

Publications

The following publications resulted from work reported in this thesis.

The copyright for the following papers lies with the respective publishers.
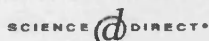
ELSEVIER

An electrochemical study of enzymatic oligonucleotide digestion

Stephen C. Hillier[a], Christopher G. Frost[a], A. Toby A. Jenkins[a,*], Helen T. Braven[b], Russell W. Keay[b], Stephen E. Flower[b], John M. Clarkson[b]

[a]Department of Chemistry, University of Bath, Bath BA2 7AY UK
[b]Molecular Sensing PLC, Challeymead Business Park, Melksham, Wiltshire SN12 8LH UK

Abstract

This paper describes the synthesis and application of a novel ferrocene (Fc) label that can be efficiently attached to oligonucleotides. We demonstrate how pulse electrochemical methods can be used to measure very low concentrations of ferrocene label and, importantly, show good electroanalytical discrimination between a labelled oligonucleotide and an enzyme digested labelled oligonucleotide, in which the ferrocene label nucleotide conjugate has been released. Real time in situ analysis gives a much greater understanding of the process. Potential applications include the detection of specific nucleic acid sequences and measurement of nuclease activity.
© 2004 Elsevier B.V. All rights reserved.

Keywords: Ferrocene; Oligonucleotide; Sensor; Enzymatic digestion

1. Introduction

The use of electrochemical probes to rival fluorescence in DNA and oligonucleotide interrogation has recently attracted attention [1,2]. Typically, ferrocene (Fc) or other electro-active moities such as ruthenium and osmium inorganic complexes [3] are used as the reporter molecule as they have well-understood electrochemistry, good stability and convenient synthetic chemistry [4]. In electrochemical studies of DNA, ferrocene-labelled intercalators and other transition metal complexes have been used as intercalators predominately for hybridisation detection [5]. A review of the use of electrochemistry to study both DNA hybridisation (for base sequence determination), as well as the presence of point mutations and damaged DNA is given by Palecek and Fojta [6] and complemented by Wang's biosensing review [7]. In an alternative approach, several workers [8–10] have ferrocene labelled a base phosphoramidite and then incorporated it into the oligonucleotide by synthesis. We report a ferrocene-based electrochemical label that allows the enzymatic digestion of oligonucleotides to be easily detected using Differential Pulse Voltammetry (DPV). Van Berkel et al. [11] have reported the detection of the ferrocene dimer (FcNHCONHFc) during derivatisation experiments to form

ferrocene urethanes. Ferrocene carboxylic acid based labels have been used previously, but have relatively high oxidation potentials (ca. 0.4 V vs. Ag | AgCl) [1]. The advantage of ferrocene urea compounds is that the urea stabilises the oxidised ferrocene, thus giving a lower oxidation potential. Hence, potential problems from interferants such as peroxides can be avoided.

2. Experimental

4-(3-Ferrocene-ureido)-benzoic acid 5 was synthesised by a variation of the method of Van Berkel et al. [11]. Ferrocene acyl chloride 2 was reacted with sodium azide to form the ferrocenoyl azide 3. This was heated to form 4 which was coupled to 4-aminobenzoic acid to yield 5. The acid was converted to the N-hydroxysuccinimide ester 6 using standard coupling conditions (Scheme 1).

The oligonucleotide coupling followed the method of Takenaka [12]. Compound 6 (0.46 mg, 1 μmol) in 50 μl anhydrous DMSO was added to C6 amino modified oligonucleotide (20 nmol) dissolved in 50 μl of 500 mM potassium carbonate buffer (pH 9.0). The mixture was shaken at 25 °C for 15 h. The conjugate 7 was purified from unconjugated ferrocene and other low molecular weight species using a sephadex G-25 column (Sigma) (Scheme 2).
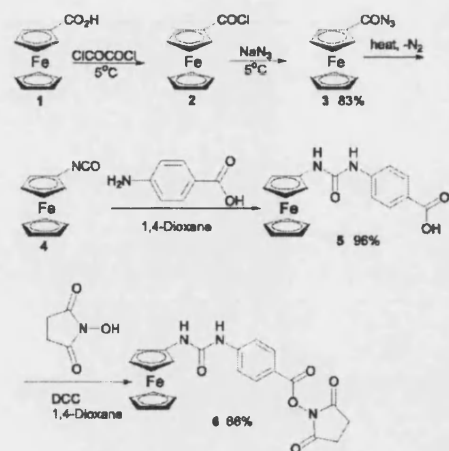

Scheme 1. Synthesis of 4-(3-ferrocene-ureido)-benzoic acid 5 and conversion to the N-hydroxysuccinimide ester 6.

The S1 nuclease digestion used 5 μM oligonucleotide, 0.25 U/μl S1 nuclease and a buffer consisting of 0.25 M ammonium acetate and 4.5 mM zinc acetate dihydrate (pH 6.5). The control sample omitted the enzyme, which gives the same result as using a heat-denatured enzyme (data not shown). The samples were incubated at 37 °C with electrochemical measurements of both a control system (without enzyme) and the digest being made in situ approximately every 8 min up to 90 min (Fig. 3).

The control and digest samples were electrochemically measured using DPV with an Ecochemie Autolab. The electrochemical cell consisted of a 200 μl low volume cell (BAS), glassy carbon working electrode, a silver/silver chloride (3M KCl) reference electrode and a platinum wire counter electrode.

3. Results and discussion

We report the change in electrochemical response of the labelled conjugate 7, before and after enzyme digestion. This single-stranded Fc-labelled oligonucleotide is digested by the

5'-Fc-Linker-ATATACGTGCCAGGTGGA-3'

7
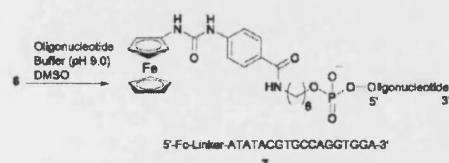
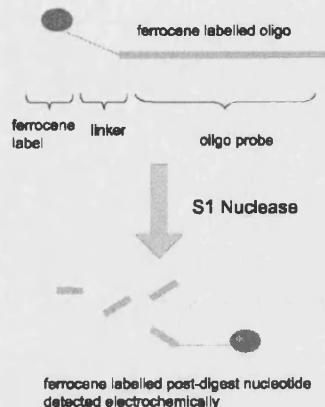Scheme 2. Attachment of the oligonucleotide to 6 to form conjugate 7

Fig. 1. Schematic of experimental procedure. Labelled oligonucleotide 7 has very low electrochemical oxidation current. Following endonuclease action, Fc probe cleaved and detected by differential pulse voltammetry.

S1 nuclease enzyme, as detailed above (Fig. 1). This enzyme is an endonuclease that degrades single-stranded nucleic acids by cleavage of the phosphodiester bond to yield 5' phosphorylated products (mononucleotides or short oligonucleotides). As the linker is not affected by the enzyme, some of these fragments will be ferrocene labelled. Fig. 2 clearly shows the large increase in ferrocene oxidation current (measured by DPV) following endonuclease action compared to the labelled oligo before enzyme digestion.

DPV is a pulse technique which allows much higher sensitivity than conventional sweep techniques when detecting very low concentrations of a redox probe [13]. This is achieved by applying a small voltage pulse superimposed
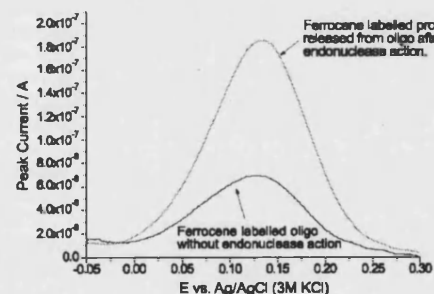

Fig. 2. Differential Pulse Voltammogram of the labelled oligonucleotide before enzyme digestion and following enzyme digestion following 90 min incubation at 37 °C. The area of the glassy carbon electrode is 0.07 cm². Voltammetric parameters are as follows. Scan rate, 3 mV s⁻¹; modulation time, 40 ms; interval time, 100 ms; step potential, 0.3 mV; modulation amplitude 50 mV.
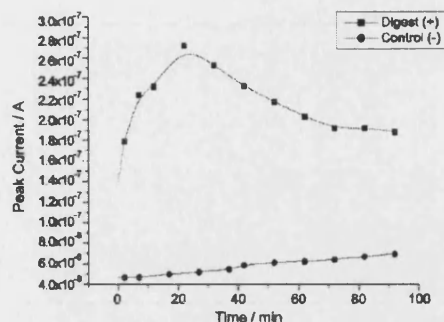
309

Fig. 3. Comparison of the Digest (+) and Control (−) samples, during S1 nuclease digestion.

on the linear voltage sweep, and sampling the differential current at a short time after the pulse. Hence, the measured current is only a product of the Faradaic process, with the capacitive charging current eliminated.

The difference in the electrochemical response of the labelled oligonucleotide before and after endonuclease action shown in Fig. 2, is attributed to both differences in the diffusion coefficient of the free probe compared to the labelled oligo and the possibility that the oligonucleotide assumes a secondary structure that may hinder access of the ferrocene label to the electrode.

A time course of the S1 digestion, using gel electrophoresis, showed the digestion to be virtually complete after 25 min. Real time analysis of the digestion at 37 °C, by measuring consecutive DPV traces (Fig. 3), gives a current maximum for the digest (+) shortly after 25 min, which then decays. We propose that the initial rapid increase of signal is due to the enzymatic digestion and liberation of small ferrocene-labelled fragments, which are able to readily diffuse to the electrode surface. The rate of increase slows to the maximum and then decays probably due to the effect of electrode fouling from the enzyme and oligo fragments. In contrast when the enzyme is omitted, the control (−), the much weaker response increases linearly with time. Although the origin of this behaviour is not entirely clear, one possibility is that this is indicative of nonspecific absorption of the ferrocene-labelled oligo probe, which creates an electroactive film that slowly thickens with time, giving a gradual increase of background signal. Further work is underway to determine the exact nature of this adlayer.

In conclusion, we have shown that using our ferrocene-labelled probe gives us good discrimination between digested and undigested oligonucleotide, using DPV and a standard electrochemical cell. The time resolved work gives a good understanding of the digestion and the behaviour of the electrode surface, particularly the effect of fouling. Moreover, the good correlation between the gel electropho-

resis time course measurement and the time at which the maximum current was observed is of interest. Further applications of these (and related) probes are currently being investigated, a potential application being homogeneous, nuclease-based assays for the sequence specific detection of DNA.

Appendix A. Notes and references

This work is the subject of patent applications.

Synthesis of 4-(3-ferrocene-ureido)-benzoic acid N-succinimide ester 6. Further synthetic detail is available form the authors on request.

DCC (194 mg, 0.939 mmol, 1.14 equiv.) was dissolved in anhydrous 1,4-dioxane (2 ml) and charged to a purged flask, under nitrogen. N-Hydroxysuccinimide (108 mg, 0.938 mmol, 1.14 equiv.) was charged. The 4-(3-ferrocene-ureido)-benzoic acid 5 (300 mg, 0.824 mmol 1.0 equiv.) was dissolved in anhydrous 1,4-dioxane (13 ml) and charged dropwise to the flask. The solution was stirred at room temperature for 23 h. A small amount of light brown solid was removed from the red/orange reaction mixture by Buchner filtration. Water (100 ml) and ethyl acetate (50 ml) were charged to the reaction mixture. The ethyl acetate phase was separated and the aqueous was extracted with ethyl acetate (100 ml). The ethyl acetate phases were combined, dried with sodium sulphate and concentrated in vacuo to afford the crude product as an orange oil, which was purified using silica flash chromatography with a gradient system from ethyl acetate 60/petroleum ether (bp 40–60 °C) 40 to ethyl acetate. Drying in a vacuum oven yielded 6 as fine orange coloured crystals (237 mg, 66%). ^{1}H-NMR δ (300 MHz, d6-DMSO) 2.88 (4H, s, CH_2CO), 3.98 (2H, t, $J = 1.8$ Hz, Cp*), 4.16 (5H, s, Cp), 4.55 (2H, t, $J = 1.8$ Hz, Cp*), 7.68 (2H, m, ArH), 8.00 (2H, m, ArH), 8.11 (1H, s, CpNH), 9.16 (1H, s, ArNH). ^{13}C-NMR δ (100 MHz, d6-DMSO) 25.9 (Ar), 60.7 (CH, Cp*), 63.8 (CH, Cp*), 68.7 (Cp), 95.8 (C, Cp*), 116.0 (CCO_2N), 117.2 (Ar), 131.4 (Ar), 146.4 (Ar), 152.0 (CONH), 161.0 ($COCH_2$), 170.2 (CO_2N). IR (KBr) v (cm-1) 3379, 2928, 2851, 1762, 1734, 1718, 1600, 1560, 1540. MS (FAB + m/z) 462.0 [M + H]. HRMS (ES+): $C_{22}H_{20}FeN_3O_5$ [M + H] requires 462.0747 found 462.0748.

References

[1] S. Takenaka, Highly sensitive probe for gene analysis by electrochemical approach, Bulletin of the Chemical Society of Japan 74 (2001) 217–224.

310   *S.C. Hillier et al. / Bioelectrochemistry 63 (2004) 307–310*

[2] T. Ihara, Gene sensor using ferrocenyl oligonucleotide, Chemical Communications 17 (1997) 1609.

[3] X.H. Xu, A.J. Bard, Immobilization and hybridization of DNA on an aluminum(III) alkanebisphosphonate thin-film with electrogenerated chemiluminescent detection, Journal of the American Chemical Society 117 (1995) 2627–2631.

[4] C.J. Yu, H. Yowanto, Y.J. Wan, T.J. Meade, Y. Chong, M. Strong, L.H. Donilon, J.F. Kayyem, M. Gozin, G.F. Blackburn, Uridine-conjugated ferrocene DNA oligonucleotides: unexpected cyclization reaction of the uridine base, Journal of the American Chemical Society 122 (2000) 6767–6768.

[5] S. Takenaka, K. Yamashita, M. Takagi, Y. Uto, H. Kondo, DNA sensing on a DNA probe-modified electrode using ferrocenylnaphthalene diimide as the electrochemically active ligand, Analytical Chemistry 72 (2000) 1334–1341.

[6] E. Palecek, M. Fojta, Detecting DNA hybridization and damage, Analytical Chemistry 73 (2001) 74A–83A.

[7] J. Wang, Electrochemical nucleic acid biosensors, Analytica Chimica Acta 469 (2002) 63–71.

[8] C.J. Yu, Y.J. Wan, H. Yowanto, J. Li, C.L. Tao, M.D. James, C.L. Tan, G.F. Blackburn, T.J. Meade, Electronic detection of single-base mis-matches in DNA with ferrocene-modified probes, Journal of the American Chemical Society 123 (2001) 11155–11161.

[9] A.E. Beilstein, M.W. Grinstaff, Synthesis and characterization of ferrocene-labeled oligodeoxynucleotides, Journal of Organometallic Chemistry 637 (2001) 398–406.

[10] A.R. Pike, L.C. Ryder, B.R. Horrocks, W. Clegg, M.R.J. Elsegood, B.A. Connolly, A. Houlton, Metallocene-DNA: synthesis, molecular and electronic structure and DNA incorporation of C5-ferrocenylthymidine derivatives, Chemistry-A European Journal 8 (2002) 2891–2899.

[11] G.J. Van Berkel, J.M.E. Quirke, R.A. Tigani, A.S. Dilley, T.R. Covey, Derivatization for electrospray ionization mass spectrometry. 3: Electrochemically ionizable derivatives, Analytical Chemistry 70 (1998) 1544–1554.

[12] S. Takenaka, Y. Uto, H. Kondo, T. Ihara, M. Takagi, Electrochemically active DNA probes: Detection of target DNA sequences at femtomole level by HPLC with electrochemical detection, Analytical Biochemistry 218 (1994) 436–443.

[13] C.S.P. de Castro, J.R. SouzaDe, C. Bloch, Investigations on the binding of mercury ions to albumins employing differential pulse voltammetry, Protein and Peptide Letters 10 (2003) 155–164.

An electrochemical gene detection assay utilising T7 exonuclease activity on complementary probe–target oligonucleotide sequences

Stephen C. Hillier [a], Stephen E. Flower [a], Christopher G. Frost [a], A. Toby A. Jenkins [a,*], Russell Keay [b], Helen Braven [b], John Clarkson [b]

[a] *Department of Chemistry, University of Bath, Bath BA2 7AY, UK*
[b] *Molecular Sensing PLC, Challeymead Business Park, Melksham, Wiltshire SN12 8LH, UK*

Abstract

This communication describes the synthesis of an electrochemically active oligonucleotide probe and its application in sensing complementary oligonucleotides sequences using a T7 exonuclease enzyme. Target oligonucleotides are detected by hybridisation with a ferrocene labelled probe oligonucleotide followed by addition of T7 exonuclease. The T7 enzyme is a double strand specific exonuclease that removes the terminal 5′ nucleotide of the probe sequence. The 5′ nucleotide is attached to a ferrocene label, which is subsequently detected at an electrode using differential pulse voltammetry. Time and temperature resolved measurements were performed and an associated study using dual labelled fluorophore–quencher labelled probes was performed to confirm the validity of the electrochemical assay.
© 2004 Published by Elsevier B.V.

Keywords: DNA; Electrochemistry; T7 exonuclease

1. Introduction

Fast and accurate detection of DNA is becoming an important sensing methodology for a wide range of biological systems, especially pathogens. The technology has largely grown from the requirements for rapid parallel screening of genomic DNA in the Human Genome Project, with technologies based on fluorescence plate analysis being developed by companies such as Affymetrix [1]. With rapid screening of DNA now possible, the possibility of creating gene sensors for specific viral or bacterial pathogens is now being realised [2]. Although existing DNA sensor technology is largely based on flu-

orescence detection, other sensor transduction paradigms are starting to be investigated including quartz crystal microbalance [3] and electrochemistry. Comprehensive reviews on the recent developments in electrochemical DNA sensing have been written by Drummond et al. [4] and by de-los-Santos-Alvarez et al. [5].

The detection of specific gene fragments using electrochemistry has some advantages and some challenges compared with the more widely used fluorescence assays. The principal advantages are: optical sample transparency is not necessary; direct signal read-out; potential for ease of miniaturisation and device manufacture. Potential challenges are the lower general sensitivity of electrochemistry compared with fluorescence (whereby single molecule detection is in principle possible).

* Corresponding author. Tel.: +44 1225 386118; fax: +44 1225 386231.
E-mail address: a.t.a.jenkins@bath.ac.uk (A. Toby A. Jenkins).

Much of the current electrochemical DNA hybridisation sensing work is based on the surface modification of a gold electrode with a probe sequence, and usually a blocking layer. The hybridisation event occurs and is then detected in a range of ways, with or without the use of labels. Much careful work has to be done, often very specifically, to achieve a reproducible sensing layer [6–8]. In the typical case of a labelled target assay, the capture probe is first immobilised on the surface, a blocking layer is introduced to reduce the non-specific response and then the hybridisation event is allowed to occur. To obtain the best possible sensitivity there is a trade off between the probe surface coverage and hybridisation efficiency, with the blocking layer introducing a further layer of complexity. The use of unmodified electrode surfaces is often overlooked, due to the perceived limited sensitivity, particularly due to electrode fouling. However, we combine the very efficient hybridisation of a solution based sensor system with the simplicity of an unmodified electrode surface and show that the sensitivity issue has been overcome.

This paper describes an oligonucleotide detection assay based on an electrochemistry detection methodology. Additionally, results from a complementary fluorescence assay are also given as a further proof of principle. The basis of the assay detailed in this communication is that the T7 exonuclease exhibits 5'–3' exonuclease activity on double strand (ds) DNA and in doing so cleaves the terminal nucleotide at the 5' end of the probe. The higher diffusion mobility and enhanced access of the enzymatically cleaved ferrocene la-bel to the electrode surface, results in an increase in ferrocene oxidation current at an electrode. This work concerns the C282Y sequence, which is a mutation on the human heamochromatosis gene (HFE) [9]. An oligonucleotide probe, with a sequence complementary to the synthetic target (C282YST), was developed which contained a ferrocene label attached to the 5' end of the probe oligonucleotide [10]. The C282Y sequence is a convenient model, which exemplifies the assay. However, the importance of this approach is that it could be used for recognition of any oligonucleotide sequence. Currently, we are carrying out research to use this assay for detection of genes which are identifiers for bacterial meningitis and methicillin resistant *Staphylococcus aureus*.

2. Experimental

2.1. Probe synthesis

The ferrocene probe was synthesised according to the steps shown in Scheme 1. The coupling reagent, 2-cyanoethyldiisopropylchlorophosphoramidite, (Sigma–Adrich, U.K.) was added to (1) to form *N*-Ferrocenoyl-6-aminohexan-2-cyanoethyldiisoproylamino phosphoramidite (2) [11]. This was then attached to the 5' end of the 18mer oligonucleotide recognition sequence using standard solid phase coupling and reverse phase HPLC purification (Tibmol Bio, Germany), to afford the ferrocene labelled probe oligonucleotide (3).
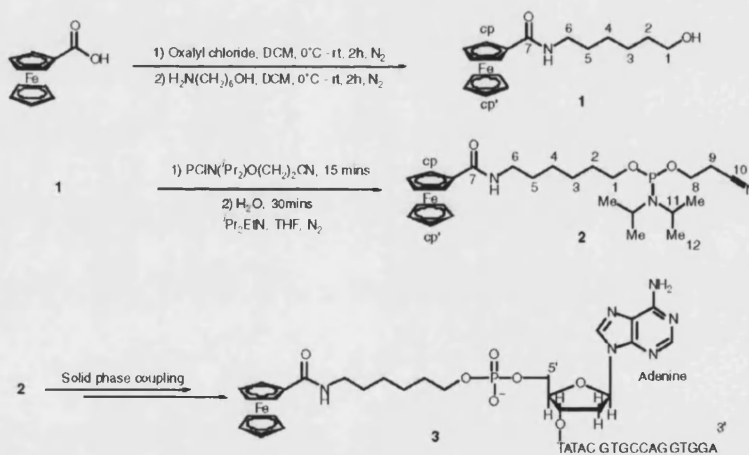
Scheme 1. Synthesis of *N*-ferrocenoyl-6-aminohexan-2-cyanoethyldiisoproylamino phosphoramidite.

2.2. Structural and synthetic data

### 2.2.1. N-Ferrocenoyl-6-amino-hexan-1-ol (1)

Oxalyl chloride (0.89 ml, 10.32 mmol) in dry DCM (2 ml) was added dropwise, using a pressure equalising dropping funnel, to a stirred suspension of ferrocene carboxylic acid (1 g, 4.3 mmol) in dry DCM (100 ml) at 0 °C under N_2. The reaction mixture was allowed to warm to room temperature and stirred for 2 h forming a dark red solution. The solvent and remaining oxalyl chloride was carefully removed in vacuo to give the crude ferrocenyl chloride. The ferrocenyl chloride was then taken up in dry DCM (75 ml) and 6-amino hexan-1-ol (0.62 g, 5.16 mmol) in dry DCM (75 ml) was added dropwise via a pressure equalised dropping funnel at 0 °C under N_2. The reaction mixture was stirred for 2 h whilst warming to room temperature. The reaction mixture was washed with saturated $NaHCO_3$ (1×100 ml), then 1.0 M HCl (1×100 ml). The organic layer was dried over $MgSO_4$ and the solvent removed in vacuo. The crude mixture was taken up in 50% EtOAc in petrol and filtered through a short silica pad in a sintered Büchner funnel capped with filter paper. The pad was then washed with 500 ml of 50% EtOAc in petrol to remove any starting materials. The pure product was then eluted from the pad using EtOAc to give the amidoalcohol (1) (700 mg, 50% yield) as an orange powder; v_{max} (thin film) 3436, 3367, 2924, 2846, 2752, 1634, 1538, 1450, 1282, 1082, 1048, 873, 821; δ_H (300 MHz; $CDCl_3$) 6.15 (1H, br m, NH), 4.69 (2H, ap. s, H-cp), 4.31 (2H, ap. s, H-cp), 4.17 (5H, s, H-cp'), 3.62 (2H, t, J 6.3, H-1), 3.34 (2H, q, J 6.3, H-6), 2.57 (1H, br. s, OH), 1.57 (4H, m, H-2, 5), 1.40 (4H, m, H-3, 4); δ_C (75 MHz; $CDCl_3$) 170.6 (C-7), 70.7 (C-cp), 70.1 (C-cp'), 68.4 (C-cp), 39.7 (C-1), 33.0 (C-6), 30.4 (C-2), 26.9 (C-5), 25.7 (C-3); m/z (FAB+) 329.1 ($M+$), 212.9, 185.0, 150.0, 129.0, 113.0, 81.9.

2.2.2. N-Ferrocenoyl-6-aminohexan-1-(2-cyanoethyldiisoproylaminophoshoramidite) (2)

N,N-Diisopropylethylamine (1.5 ml, 8.4 mmol) was added to a stirred solution of the amidoalcohol (1) (700 mg, 2.1 mmol) in dry THF (25 ml) under argon. 2-Cyano ethyldiisopropylchlorophosphoramidite (700 µl, 3.15 mmol) was added dropwise and the reaction stirred for 15 min. Deionised water (200 µl) was added and the reaction stirred for a further 30 min. Ether–triethylamine (50/50, 25 ml) was added and a precipitate formed. The mixture was washed with saturated $NaHCO_3$ (25 ml), then water (225 ml). The organic layer was then dried over $MgSO_4$ and the solvent removed in vacuo. Purification by flash chromatography (SiO_2, 60% EtOAc/petrol + 1% Et_3N, rf 0.7) gave the phosphoramidite (2) (600 mg, 54% yield) as a bright orange powder. δ_H (300 MHz; $CDCl_3$) 6.06 (1H, br. m, NH), 4.66 (2H, ap. s, H-cp), 4.27 (2H, ap. s, H-cp), 4.14 (5H, s, H-cp'), 3.83 (2H, m, H-8), 3.57 (4H, m, H-1, 11), 3.28 (2H, dd, J 13.2, 6.9, H-6), 2.65 (2H, t, J 6.4, H-9), 1.56-1.00 (20H, m, H-2, 3, 4, 5, 12); δ_C (75 MHz; $CDCl_3$) 170.5 (C-7), 118.2 (C-10), 70.6 (C-cp), 70.0 ($2 \times$ C-cp), 68.5 (C-cp'), 64.0 (C-1), 58.7 (C-8), 43.4 (C-11), 39.8 (C-6), 31.5 (C-2), 30.3 (C-5), 27.0 (C-4), 26.1 (C-3), 25.0 (C-12), 14.6 (C-9); δ_P (121.5 MHz; $CDCl_3$) 147.9 (s); m/z (FAB+) 529.3 ($M+$), 459.2, 429.1, 375.1, 358.0, 212.9, 201.0, 102.0.

2.3. Hybridisation assay

The complementary target sequence was the C282YST (a 60-mer) [12]. The probe was hybridised with the target for 15 min at 20 °C, with a probe concentration at 1.0 µmol dm^{-3} and target concentration at 1.2 µmol dm^{-3} (Scheme 2). The first experiments involved measuring the oxidation current of the probe–target du-
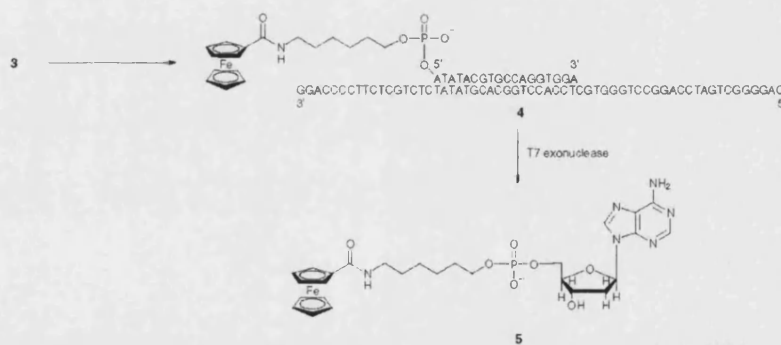
Scheme 2. Hybridisation of the ferrocene-labelled probe oligonucleotide (3) with a target oligonucleotide. A ferrocene-labelled, nucleotide is released following T7 digestion.

plex prior to T7 exonuclease action and after T7 digestion for 1 h at 37 °C. Two control measurements were performed using a non-complementary target sequence and without adding the enzyme.

2.4. Detection of probe–target hybridisation

2.4.1. Electrochemical measurements

The electrochemical oxidation of the ferrocene label was measured in a low volume 200 μl cell separated from a platinum counter electrode and a Ag|AgCl reference electrode by a Vycor polymer frit. A freshly polished 6 mm diameter glassy carbon working electrode was used. All electrodes and cells came from BAS, UK. Differential pulse measurements (DPV) were performed using an Autolab PGstat12 (Windsor Scientific, UK). Pulse conditions used in the experiments are detailed in the captions of Figs. 1 and 2. DPV measurements allow the current due to electrode charging to be subtracted, leaving only the Faradaic current, which makes measurements of electroactive molecules possible at very low concentrations [13]. Probe–target hybridisation and measurement was in standard PCR buffer: 10 mM Tris–HCl, 50 mM, KCl, 2.5 mM $MgCl_2$, pH 8.5.

2.4.2. Fluorescence

In order to further substantiate the fundamental validity of the assay, fluorescence experiments were performed to study the exonuclease activity of T7 enzyme on both
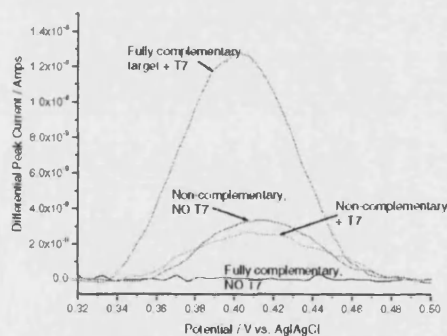

Fig. 1. DPV response showing peak currents after 15-min probe target hybridisation and 60 min incubation with (or without) T7 exonuclease enzyme. The fully complementary sequence shows large increase in current compared with control measurements. Enzyme concentration was 0.1 IU μl⁻¹. *Note:* DPV response is base-line corrected, and peak area magnified for clarity of results. Start potential, −0.1 V; end potential, 0.55 V vs. Ag|AgCl; step potential, 1 mV; modulation amplitude, 50 mV; modulation time, 0.04 s; interval time, 0.9 s.
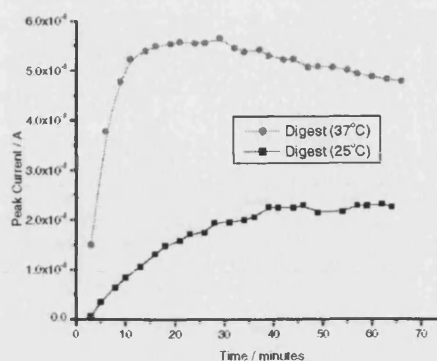

Fig. 2. Time course measurement of change in differential pulse peak current as a function of T7 exonuclease action on fully complementary probe target duplexes at 25 and 37 °C. Start potential, 0.15 V; end potential, 0.55 V vs. Ag|AgCl; step potential, 3 mV; modulation amplitude, 50 mV; modulation time, 0.04 s; interval time, 0.1 s.

fully complementary probe–target duplexes and non-complementary sequences. A dual labelled probe approach was used which is well described by Ugozzoli et al. [9]. Measurements were made on a Roche Lightcycler™. The 5′ end of the probe was labelled with a fluorophore 6-FAM (6-carboxy fluoroscein) and the 3′ end of the probe was labelled with a quencher 6-TAMRA (6-carboxytetramethylrhodamine), both via a C6 linker. As digestion by T7 takes place, the quencher and fluorophore become spatially separated, resulting in an increase in fluorescence. A lower concentration of T7 enzyme (0.01 IU μl⁻¹) was used, as the higher sensitivity of fluorescence resulted in a rapid saturation of signal. 6-FAM is excited at 494 nm and emits at 525 nm. This approach has been used by Kelemen et al. [14] to study RNAase activity. The purpose of this experiment was not to compare kinetics of enzyme exonuclease action, but to confirm that the fundamentals of the assay were reproducible using a different instrumentation methodology.

3. Results and discussion

3.1. Electrochemical assay

The DPV results in Fig. 1 show how the relative size of the labelled fragments correlates with peak height: Maximum current is observed for post-digest, fully complementary probe–target duplex (small nucleotide fragment), with lower currents for non-hybridised probe and no current peak being observed for probe–target duplexes in the absence of T7.

3.2. Time and temperature resolved electrochemistry

Having established that it was possible to determine an end-point measurement for exonuclease digestion of the hybridised duplex, the next step was to determine the time dependent response of T7 digestion, following hybridisation. This was done by making sequential DPV measurements at 3 min intervals over the course of 65 min. Measurements were performed at both 37 °C (optimum enzyme working temperature) and at 25 °C, to compare response at sub-optimal temperature. The results are shown in Fig. 2. It can be clearly seen that at 37 °C, rapid digestion of the probe–target duplex occurs, resulting in a maximum current being measured at around 25 min. In order to enhance the measured signal, higher concentrations of oligonucleotides were used in the time course measurement, with 10 μmol dm^{-3} probe and 12 μmol dm^{-3} target. An enzyme concentration of 0.1 International Units (IU) μl^{-1} was used. The subsequent decrease in current is attributed to partial blocking of the electrode with oligonucleotides and enzyme. Various factors may contribute to this decrease in current: Adsorption at the electrode surface may inactivate the enzyme, leading to a reduction in the rate of probe digestion, and cause partial blocking of the electrode surface. Surface Plasmon Resonance measurements on gold electrodes for this system confirm that material does adsorb on the electrode and the time course trend also fits with previous measurements made on single strand oligonucleotides [15]. Although care should be taken when extrapolating from measurements made on gold electrodes to glassy carbon, these results do at least suggest that electrode fouling may have a significant effect on assay sensitivity and moreover, DNA absorption onto carbon has been shown to occur by Xu et al. [16]. For this reason, it will be necessary to incorporate internal controls of electroactive species with a known concentration, but different oxidation potential, into any potential biosensor application of this assay. [1]

3.3. Fluorescence assay using fluorophore–quencher labelled probes

Fig. 3 shows the change in fluorescence (normalised to maximum measured fluorescence) for four systems: fully complementary probe–target with and without enzyme, and mismatch probe–target also with and without T7 enzyme. Maximum fluorescence is measured after ca. 40 min T7 nuclease digestion of fully complementary probe–target duplex. The relative conformational flexibility of the non-complementary single strand se-

[1] After repeated washing of the glassy carbon electrode in buffer, DPV analysis still shows a residual ferrocene peak.
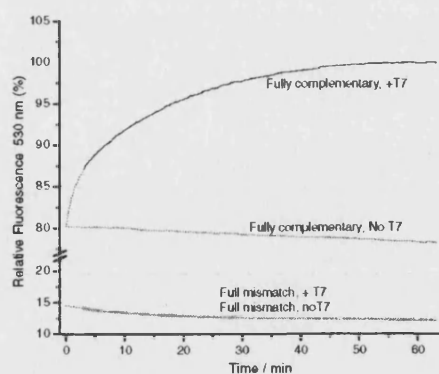

Fig. 3. Change in fluorescence for dual labelled (quencher fluorophore) probes as a function of time of T7 exonuclease action. Maximum intensity normalised to 100%. Fully complementary probe target shows large change in fluorescence after T7 digestion.

quences, compared to the fully complementary duplex, account for the greater extent of fluorescence quenching in these systems.

3.4. Discussion

The basis of the assay described in this communication is that it is possible to discriminate electrochemically between a ferrocene-labelled probe oligonucleotide–target duplex and a post T7 digest nucleotide labelled with a ferrocene phosphoramidite.

The results raise the question: what is the basis for the difference in oxidation current between the post-digest labelled nucleotide and the ferrocene-labelled probe–target duplex before T7 action? Two possible mechanisms for this discrimination present themselves: The first simply relies on the difference in diffusion coefficient of the small post-digest ferrocene-labelled nucleotide and the labelled probe and probe–target duplex. The diffusion coefficients have been determined using chronocoulometry and found to be 8.2×10^{-9} m^2 s^{-1} for the post-digest label-nucleotide and 7.7×10^{-9} m^2 s^{-1} for the ferrocene-labelled probe [13]. This difference is not very large, but when the probe is hybridised with its complement target (a 60-mer), the diffusion coefficient will be very much smaller. However, this is hard to measure because the hybridisation efficiency of the probe–target duplex (and therefore duplex concentration) is difficult to determine. Moreover, it is likely that steric effects due to restricted access of the ferrocene attached to the probe–target duplex to the electrode, compared with a single nucleotide-ferrocene label, may also be very important – this is a subject of ongoing investigation.

A relatively simple, potentially widely applicable assay for detecting DNA targets based on hybridisation of a ferrocene-labelled probe with a target, subsequent exonuclease action by T7 enzyme and detection using electrochemistry has been presented. No surface modification is required. Time and temperature resolved measurements have been shown, together with a comparison measurement using fluorescence, illustrating the way in which T7 exonuclease discriminates between complementary duplex ds DNA and non-complementary oligonucleotides.

Acknowledgements

References

[1] H.C. King, A.A. Sinha, J. Am. Med. Assoc. 286 (2001) 2280.
[2] D. Wang, L. Coscoy, M. Zylberberg, P.C. Avila, A. Homer, A. Boushey, D. Ganem, J.L. DeRisi, Proc. Natl. Acad. Sci. USA 99 (2002) 15687.
[3] S. Han, J. Lin, M. Satjapipat, A.J. Baca, F. Zhou Chem. Commun. (2001) 609.
[4] T.G. Drummond, M.G. Hill, J.K. Barton, Nat. Biotech. 21 (2003) 1192.
[5] P. de-los-Santos-Alvarez, M.J. Lobo-Castanon, A.J. Miranda-Ordieres, P. Tuñón-Blanco, Anal. Bioanal. Chem. 378 (2004) 104.
[6] A.W. Peterson, L.K. Wolf, R.M. Georgiadis, J. Am. Chem. Soc. 124 (2002) 14601.
[7] T.M. Herne, M.J. Tarlov, J. Am. Chem. Soc. 119 (1997) 8916.
[8] K. Yamashita, M. Takagi, H. Kondo, S. Takenaka, Anal. Biochem. 306 (2002) 188.
[9] L.A. Ugozzoli, D. Chinn, K. Hamby, Anal. Biochem. 307 (2002) 47.
[10] Patent ref-WO 03/074731 A2 (Molecular Sensing).
[11] M.J. Gait (Ed.), Oligonucleotide Synthesis: A Practical Approach, IRL Press, Oxford, 1984.
[12] C282YP Probe: Fc label-ATATACGTGCCAGGTGGA; C282YST Target (complementary): GAGGGGCTGATCCA-GGCCTGGGTGCTCCACCTGGCACGTATATCTCTGCTC-TTCCCCAGG; Non-complementary control sequence: TGTGCAGGATACGAATGTGCAGCTGACACGTGGCAAT-GTAGTACGAACTG.
[13] A.J. Bard, L.R. Faulkner, Electrochemical Methods   Fundamentals and Applications, second ed., Wiley, New York, 2001.
[14] R.A. Kelemen, T.A. Klink, M.A. Behlke, S.R. Eubanks, P.A. Leland, R.T. Raines, Nucleic Acids Res. 27 (1999) 3696.
[15] S.C. Hillier, C.G. Frost, A.T.A. Jenkins, H.T. Braven, R.W. Keay, S.E. Flower, J.M. Clarkson, Bioelectrochem. 63 (2004) 307.
[16] C. Xu, P.G. He, Y. Fang, Anal. Chim. Acta 411 (2000) 31.